



Simwela, Nelson Victor (2020) *Drug action and resistance in malaria parasites: experimental genetics models and biochemical features of fast acting novel antimalarials*. PhD thesis.

<http://theses.gla.ac.uk/81876/>

Copyright and moral rights for this work are retained by the author

A copy can be downloaded for personal non-commercial research or study, without prior permission or charge

This work cannot be reproduced or quoted extensively from without first obtaining permission in writing from the author

The content must not be changed in any way or sold commercially in any format or medium without the formal permission of the author

When referring to this work, full bibliographic details including the author, title, awarding institution and date of the thesis must be given

Enlighten: Theses

<https://theses.gla.ac.uk/>
research-enlighten@glasgow.ac.uk

**Drug action and resistance in malaria parasites:
experimental genetics models and biochemical features of fast
acting novel antimalarials**

Nelson Victor Simwela,
BSc (Hons), MSc

October, 2020

Thesis submitted in fulfilment of the requirements for the
Degree of Doctor of Philosophy
Institute of Infection, Immunity and Inflammation
College of Medical, Veterinary and Life Sciences
Wellcome Centre for Integrative Parasitology
University of Glasgow



University
of Glasgow

Abstract

Resistance to antimalarial drugs inevitably follows their deployment in malaria endemic parts of the world. For instance, current malaria control efforts which significantly rely on artemisinin combination therapies (ACTs) are being threatened by the emergence of resistance to artemisinins and ACTs.

Understanding the role of genetic determinants of artemisinin resistance is therefore important for implementation of mitigation strategies. Moreover, elucidating the mode of action for drugs that are in advanced stages of development is specifically critical as drug resistance mechanisms can be prospectively predicted and possible means of surveillance put in place.

In the present work, CRISPR-Cas9 genome editing has been used to engineer candidate artemisinin resistance mutations (Kelch13 and UBP-1) in the rodent malaria parasite *Plasmodium berghei*. The role of these mutations in mediating artemisinin (and chloroquine) resistance under both *in vitro* and *in vivo* conditions has been assessed which up until now, has either remained unvalidated (UBP-1) or debated (Kelch13, under *in vivo* conditions) in human infecting *Plasmodium falciparum*. The results have provided an *in vivo* model for understanding and validating artemisinin resistance phenotypes which just like their *Plasmodium falciparum* equivalents do not just mediate resistance phenotypes, but also carry accompanying fitness costs.

In addition to the above findings, biochemical and drug inhibition studies have been carried out to demonstrate that small molecule inhibitors targeting ubiquitin hydrolases (to which UBP-1 is a class member) display activity in human and rodent infecting malaria parasites *in vitro* and *in vivo*. These inhibitors also show evidence of ability to potentiate artemisinin action which can be exploited to overcome the emerging resistance as combination partner drugs. Untargeted metabolomic screens have also been used to characterize the mode of action of lead antimalarial drug candidates that are emerging from the Novartis Institute of Tropical Diseases drug discovery pipeline. A common biochemical and metabolic profile of these compounds which display a very fast parasite killing rate is presented and can hopefully be used to identify compounds that can achieve a similar feat. Moreover, these profiles have

pointed to possible mode of action for novel drugs whose mechanistic mode of parasite killing is still unknown or disputed.

Author's declaration

I declare that this is my own work except where stated otherwise and that this work has not been submitted for any degree at any other institution.

Nelson Victor Simwela

Acknowledgments

When I embarked on a >7500 miles journey from Malawi to Glasgow four years ago, little did I know of what an incredible scholarly and scientific endeavour it will turn out to be. I am extremely grateful to my supervisor Prof. Andy Waters for allowing me to join his lab and for his supervision, support and advice over the years. I was warned that graduate school can be hard. However, his infectious passion for his work and attention to detail, were just “too contagious” to propel me across the finish line. I would also like to thank my second supervisor Prof. Mike Barrett for his expertise in metabolomics, data discussions and proofreading part of this thesis. I also thank my assessors Dr. Lisa Ranford-Cartwright, Dr. Karl Burgess (now at the University of Edinburgh) and Prof. Andrew Tobin for their continued advices, independent oversight and guidance.

Of course, this would not have been possible if it weren't for the enormous support from the Waters lab. Special thanks to Katie Hughes who was my direct mentor in the lab and for her overall critical insights into the data/experimental procedures as well as helping in proofreading this thesis. I would also like to thank Michael Rennie for helping me in setting up the *P. berghei* flow cytometry medium throughput drug susceptibility assays. I wish to further thank Alexa Brett Roberts who introduced me into the CRISPR-Cas9 world with over the head ideas which always worked the magic. A special mention to Sebastian Kirchner and Scott Miller who were always around in the lab to bounce off ideas as well as offer help and support wherever needed. I also thank Farzana Khaliq for “those transfections”, and specifically her flexibility to help with the sometimes “off the rail” experiments. A very special thank you to the lab manager of the Waters group, Julie Martin, who always made sure I had, or I could get everything I needed. Above all, to all the Waters group, thank you for putting up with my little (if not a bit more) social awkwardness. I truly couldn't have imagined of a better lab to do my PhD.

I would also like to thank staff at the University of Glasgow Polyomics for LC-MS processing of metabolomics samples. Specifically, thanks to Erin Manson, Gavin Blackburn and Clement Regnault for those IDEOM and PiMP data analysis trainings. Let me also thank the JRF (past) and CRF biological services staff as

well as the iii-core flow cytometry staff (specifically Diane and Alana) for technical assistance over the years. Special thanks to Amit Mahindra and Dr. Andrew Jamieson at the University of Glasgow School of Chemistry who carried out HPLC analysis of the DUB inhibitors. I also thank the UK Commonwealth Scholarship Commission for funding my PhD studentship.

Over the course of my PhD, I have had the privilege to collaborate with numerous scientists across the world, who have significantly contributed to the outputs of this thesis. Firstly, let me thank Dr. Thierry Diagana at the Novartis Institute of Tropical Diseases (NITD) in California, USA who through the Novartis global health fellowship allowed me to spend time in his labs between June and August 2018. His permission to screen NITD compounds for mode of action characterisation using metabolomics are indeed the basis of Chapter 6 of this thesis. At NITD, I would also like to thank Armand Guiguemde who guided me in the lab during the visit as well as Judith Straimer and Vida Ahyong for meaningful discussions. Let me also thank Prof. David Fidock and Barbara Stokes at Columbia University in New York, with whom we have extensively collaborated for the Kelch13 work. I also express my gratitude to Prof. Mathew Bogoy and Erin Yo at Stanford University, California who kindly provided the proteasome inhibitor which has been used in part of this work.

More importantly, a huge thank you to my family back in Malawi who don't see me very often but have been a strong tower of support. To mum and dad, yes, I am technically still in school! To my big brothers Sam, Gib, Francis; my sisters Salome and Victoria, and my little brother Augustine, thank you for everything.

Lastly, I would like to dedicate this work to our brother and first born in the family, Wilson N. Simwela who passed away in 1999 in his second year of secondary school. I have no doubt you would have been the family's first-generation graduate student. Alas, death had other plans!

Nelson Victor Simwela
01/10/2020

List of abbreviations

$^{\circ}\text{C}$	Degree Celsius
μ	Micro
μg	Microgram
μl	Microliter
μM	Micromolar
3' UTR	Three Prime Untranslated Region
5' UTR	Five Prime Untranslated Region
3' Cam	Three Prime UTR of Calmodulin gene
3' P48/45	Three Prime UTR of P48/P45 gene
6-Cys	Six Cysteine
AAA+	ATPases Associated with diverse cellular Activities
<i>aat</i>	Amino Acid Transporter
ACT	Artemisinin based Combinational Therapies
ADP	Adenosine Diphosphate
AMA-1	Apical Membrane Antigen 1
AMP	Adenosine Monophosphate
AM	Artemether
ANOVA	Analysis of Variance
AP2-G	Apetala 2 - Gametocyte
AP2-O	Apetala 2 - Ookinete
APIAP2	Apicomplexan AP2
AQ	Amodiaquine
ARMED	Accelerated Resistance to Multiple Drugs
ART	Artemisinin
AS	Artesunate
ATP	Adenosine Triphosphate
bp	base pairs
BTB/POZ	Broad-Complex, Tramtrack Bric a brac; POxvirus and Zinc Finger
CAS-9	CRISPR associated protein 9
CDPK	Calcium Dependent Protein Kinase
cGMP	Cyclic Guanosine Monophosphate
CITH	CAR-I and fly Trailer Hitch
COPII	Coat Proteins II
CPSII	Carbamoyl Phosphate Synthase II,

CQ	Chloroquine
CRISPR	Clustered Regularly Interspaced Short Palindromic Repeats
CSP	Circumsporozoite prorein
CYP	Cytochrome P450
DBL	Duffy Binding Like
DDT	Donor DNA templates
DDX6	Dead-box Helicase 6
DHA	Dihydroartemisinin
DHFR/TS	Dihydrofolate Reductase-Thymidylate Synthase
DHODH	Dihydroorotate Dehydrogenase
DMSO	Dimethyl Sulfoxide
DNA	Deoxyribonucleic Acid
DOZI	Development of Zygote Inhibited
DUBs	Deubiquitinating Enzymes
DV	Digestive Vacuole
EBA	Erythrocyte Binding Antigen
EBL	Erythrocyte Binding Like
ECP	Egress Cysteine Protease
EDTA	EthyleneDiamineTetraacetic Acid
EF-1 α	Elongation Factor 1 Alpha
ER	Endoplasmic Reticulum
ERM	ER Membrane
ESP15	Endocytosis Protein 15
EXP2	Exported Protein 2
FACS	Fluorescence Activated Cell Sorting
FIC	Fractional Inhibitory Concentrations
FPIX	Ferriprotoporphyrin IX
g	grams
g	Relative Centrifugal Force
GAP	Gliding Associated Proteins
GC	Guanylyl Cyclase
GC-MS	Gas Chromatography Mass Spectrometry
GCS	Generative Cell Specific 1
GDP	Guanosine Diphosphate
GDV	Gametocyte Development 1

GEP1	Gametogenesis Essential Protein 1
GEST	Gamete Egress and Sporozoite Traversal
GFP	Green Fluorescent Protein
GOI	Gene of Interest
GPI	GlycoPhosphotidylInositol
GST	Glutathione S Transferases
GTP	Guanosine Triphosphates
HAUSP	Herpesvirus Associated Ubiquitin Specific Protease
HDA-2	Histone Deacetylase 2
hDHFR	Human derived DHFR
HEPES	4-(2-Hydroxyethyl)-1-Piperazineethanesulfonic Acid
HILIC	Hydrophilic Interaction Liquid Lhromatography
HP-1	Heterochromatin Protein 1
HPLC	High Performance Liquid Chromatography
HSP	Heat Shock Protein
IC ₅₀	Half Inhibitory Concentrations
IDC	Intraerythrocytic Developmental Cycle
IP	Intra-Peritoneal
IRS	Indoor Residual Spraying
IV	Intra-Venous
JAMM	JAB1/MPN/Mov34 Metalloenzyme
kb	Kilobases
KEGG	Kyoto Encyclopaedia of Genes and Genomes
LB	Lysogeny Broth
LC-MS	Liquid Chromatography Mass Spectrometry
LCCL	Litmus Clotting Factor C, Cochlin and and Lgl1
LLIN	Long Lasting Insecticidal Bed Nets
m	Meters
m	Milli
M	Molar
MDH	Malate Dehydrogenase
mg	Milligram
MDV-1/PEG3	Male Development Protein 1/Protein of Early Gametocyte 3
MgCl ₂	Magnesium Chloride
min	Minute

ml	Millilitre
MLC1	Myosin Light Chain 1
mM	Millimolar
MMV	Medicines for Malaria Venture
MOA	Mode of Action
MOR	Mode of Resistance
MSI	Metabolomics Standards Initiative
MSPs	Merozoite Surface Proteins
N	Nano
NaCl	Sodium Chloride
NAI	Naturally Acquired Immunity
NEK	NIMA Related Kinase
ng	Nanograms
NIMA	Never In Mitosis A
nm	Nanometer
nM	Nanomolar
NMR	Nuclear Magnetic Resonance
NPP	New Permeability Pathways
N-terminal	Amino Terminal
ORPP	Orotate Phosphoribosyltransferase
OTU	Ovarian Tumour
PABA	Para-AminoBenzoic Acid
PAM	Protospacer Adjacent Motif
PBS	Phosphate Buffered Saline
PCA	Principal Component Analysis
PCE	Parasite Clearance Estimator
PCR	Polymerase Chain Reaction
PDB	Protein Data Bank
PEXEL	<i>Plasmodium</i> Export Element
PfCARL	<i>P. falciparum</i> Cyclic Amine Resistance Locus
PfCRT	<i>P. falciparum</i> Chloroquine Resistance Transporter
PfEMP1	<i>P. falciparum</i> Erythrocyte Membrane Antigen 1
PfMDR1	<i>P. falciparum</i> Multidrug Resistance Transporter 1
PfMDR2	<i>P. falciparum</i> Multidrug Resistance Protein 2
PfSUB1	<i>P. falciparum</i> SUBtilisin-like protease

Phz	Phenylhydrazine
PKG	Protein Kinase G
PLP	Perforin Like Proteins
PNEP	PEXEL Negative Exported Proteins
PPM	Parasite Plasma Membrane
PPQ	Piperaquine
PQ	Primaquine
PRR	Parasite Reduction Ratios
PSOP	Putative Secreted Ookinete Proteins
PTEX	<i>Plasmodium</i> Translocon of Exported Proteins
PV	Parasitophorous Vacuole
PVM	Parasitophorous Vacuole Membrane
RBC	Red Blood Cell
RFLP	Restriction Fragment Length Polymorphism
RFP	Red Fluorescent Protein
RH	Reticulocyte like binding Homologue
RING	Really Interesting New Gene
RLU	Relative Luminescence Units
RNA	RiboNucleic Acid
RON	Rhoptry Neck Proteins
RPM	Revolutions Per Minute
RPMI	Roswell Park Memorial Institute
RSA	Ring stage Survival Assay
scRNA	Cas9 binding scaffold
SDH	Succinate DeHydrogenase
SDM	Site Directed Mutagenesis
SEA	South East Asia
sec	Seconds
SENP	SENtrin-specific Protease
SERA	Serine-Rich Antigen
sgRNA	Short Guide RNA
SM	Selectable Marker
SNP	Single Nucleotide Polymorphism
SOC	Super Optimal broth with Catabolite repression
spp.	species

SPP	Signal Peptide Peptidase
TBV	Transmission Blocking Vaccines
TCA	Tri-Carboxylic Acid cycle
TLC	Thin Layer Chromatography
TO	Theilers Original
TRAP	Thrombospondin Related Anonymous Protein
UBP-1	Ubiquitin Carboxyl Terminal Hydrolase 1
UCH	Ubiquitin Carboxyl Hydrolases
UDP	Uridine DiPhosphate
UPR	Unfolded Protein Response
UPS	Ubiquitin Proteasome System
USP	Ubiquitin Specific Protease
UTP	Uridine TriPhosphate
VAR2CSA	Variant Surface antigen 2 Chondroitin Sulfate A
v/v	Volume per volume
w/v	Weight per volume
WHO	World Health Organisation
WT	Wild-type
WWARN	Worldwide Antimalarial Resistance Network
XA	Xanthurenic Acid
YIR	<i>Yoelii</i> Interspaced Repeats
ZFN	Zinc Finger Nucleases

Table of contents

Abstract	i
Author's declaration.....	iii
Acknowledgments	iv
List of abbreviations	vi
Table of contents.....	xii
List of figures	xix
List of tables	xxi
1 Introduction.....	1
1.1 Introduction outline.....	1
1.2 Malaria	2
1.3 Life cycle of <i>Plasmodium</i> spp.	3
1.3.1 Sporozoite inoculation and pre-erythrocytic stages	3
1.3.2 The Intra-erythrocytic developmental cycle.....	6
1.3.2.1 Getting in, essential first steps of malaria parasites invasion.....	6
1.3.2.2 Ring, trophozoite and schizont stages	10
1.3.2.3 Merozoite egress in mature schizonts	10
1.3.2.4 Parasite RBC remodelling and immune evasion: an intricate renovation and escape	12
1.3.3 Sexual developmental stages: adaptive plasticity or hedging the bets? ..	15
1.3.3.1 A molecular switch to sexual differentiation	16
1.3.3.2 Environmental players of sexual commitment.....	18
1.3.3.3 Gene regulation during commitment and gametocyte development ..	19
1.3.3.4 Gamete formation and zygote development.....	20
1.3.3.5 Ookinete-oocyst to sporozoite differentiation.....	23
1.4 Malaria prevention and control	26
1.4.1 Insecticides in malaria control	26
1.4.2 Malaria vaccines	28
1.5 Antimalarial drugs and resistance	31
1.5.1 Quinolines	32
1.5.2 Atovaquone.....	39
1.5.3 Antibiotics: tetracyclines and macrolides	40
1.5.4 Antifolates.....	40

1.5.5	Artemisinins	41
1.5.5.1	ARTs MOA: a glass half full?.....	42
1.5.5.2	Malaria parasite resistance to ARTs: a multifaceted trait	44
1.5.5.3	ART derived antimalarials.....	53
1.5.6	Antimalarial drugs in the pipeline	54
1.6	Approaches to characterising antimalarial drugs MOA	56
1.6.1	Forward genetic approaches.....	56
1.6.2	Metabolomics	56
1.6.2.1	Metabolomic approaches.....	57
1.6.2.2	Metabolomic platforms	58
1.6.2.3	Metabolomic data analysis.....	59
1.7	Genome editing strategies for validating genetic determinants of antimalarial drug resistance	61
1.7.1	The Bxb1 integrase system.....	62
1.7.2	Zinc finger nucleases	62
1.7.3	CRISPR-Cas9	63
1.8	Animal models of malaria and antimalarial drug resistance.....	65
1.8.1	Rodent models and antimalarial drug resistance.....	65
1.8.1.1	Sulfadoxine and pyrimethamine	66
1.8.1.2	ART resistance	70
1.8.1.3	Atovaquone.....	73
1.8.1.4	Mefloquine.....	73
1.8.1.5	CQ.....	74
1.8.2	Non-human primates, humanized mouse models and antimalarial drug resistance.....	76
1.8.3	Precise genome editing: a new era to revive rodent models of malaria for genetic validation of candidate drug resistance markers <i>in vivo</i> ?	77
1.9	Aims and objectives.....	78
1.9.1	Using genome editing to test orthologous ART resistance mutations in <i>P. berghei</i>	78
1.9.2	Profiling the activity of ubiquitin hydrolase inhibitors as candidate antimalarial agents with potential to overcome ART resistance	78
1.9.3	Metabolomics profiling of NITD drug candidates to characterise their MOA	79
2	Materials and methods.....	80
2.1	<i>P. berghei</i> general methods	80

2.1.1	Maintenance of <i>P. berghei</i> parasites in rodents	80
2.1.2	<i>P. berghei</i> lines	80
2.1.3	Monitoring parasitaemia in infected mice	80
2.1.4	<i>In vitro</i> short-term culture of <i>P. berghei</i>	81
2.1.5	Isolation of mature schizonts	81
2.1.6	Parasite transfection and positive selection of transformants	82
2.1.7	Parasite cryopreservation	82
2.1.8	Cloning by limiting dilution	82
2.1.9	Genomic DNA extraction	83
2.2	Generation of <i>P. berghei</i> mutant parasites by CRISPR-Cas9	83
2.2.1	Sequence alignment and 3D structural homology modelling	83
2.2.2	Primary vectors	83
2.2.3	Site directed mutagenesis (SDM) and generation of secondary vectors ..	85
2.2.4	Preparation of plasmid DNA for transfection	88
2.2.5	Genotyping of mutant parasites	88
2.2.6	Asexual growth competitions of mutant and wild type parasites	88
2.3	<i>P. falciparum</i> culture and maintenance	90
2.4	Drug susceptibility assays	90
2.4.1	Drugs and inhibitors	90
2.4.2	HPLC analysis of DUB inhibitors	91
2.4.3	<i>P. berghei</i> short term <i>in vitro</i> asexual growth inhibition assays	91
2.4.4	Adapted <i>P. berghei</i> ring stage survival assay	92
2.4.5	<i>P. falciparum</i> SYBR Green I® assay for parasite growth inhibition	93
2.4.6	<i>P. falciparum</i> viability assays	94
2.4.7	<i>In vitro</i> drug combinations	94
2.4.8	<i>In vivo</i> drug assays: Peter's 4-day suppressive test and recrudescence ..	95
2.4.9	<i>In vivo</i> drug assays: Rane's curative test and parasite clearance	95
2.4.10	General statistical methods	96
2.5	Untargeted metabolomics using LC-MS for MOA studies	96
2.5.1	<i>P. falciparum</i> luciferase kill rate assay	96
2.5.2	Magnetic purification of trophozoites	97
2.5.3	Metabolite sample preparation	98
2.5.4	Metabolite extraction	98
2.5.5	LC-MS Metabolomics analysis	99
2.5.6	Mass spectrometry fragmentation	99
2.5.7	Data acquisition	99
2.5.8	Data processing, analysis and metabolite identification	100

3	UBP-1 mutations mediate reduced <i>in vivo</i> susceptibility to ARTs and CQ in <i>P. berghei</i>	101
3.1	Chapter aim	101
3.2	Introduction	101
3.3	Results	102
3.3.1	CRISPR-Cas9 introduction of UBP-1 mutations in <i>P. berghei</i>	102
3.3.2	Engineered mutations in UBP-1 confer <i>in vivo</i> selective advantage to ART and CQ pressure in <i>P. berghei</i>	104
3.3.3	The V2721F mutation confers observable reduced <i>in vivo</i> susceptibility to ARTs while the V2752F mutation confers resistance to CQ and low-level protection to ARTs in <i>P. berghei</i>	108
3.3.4	Growth of parasites carrying UBP-1 V2752F and V2721F mutations is impaired	112
3.3.5	Reversal of the V2752F mutation restores CQ sensitivity in the G1807 ^{V2752F} line while introduction of the V2721F in the same line appears to be lethal	115
3.4	Discussion	119
3.4.1	UBP-1 mutations carry ART and CQ cross-resistance traits in <i>P. berghei</i>	120
3.4.2	Fitness costs could possibly explain lack of expansion of UBP-1 mutations in <i>P. falciparum</i>	122
3.4.3	UBP-1 mutations could be impairing haemoglobin endocytosis in malaria parasites	122
3.4.4	Conclusion	124
4	<i>In vitro</i> and <i>in vivo</i> phenotypes of orthologous ART resistance Kelch13 mutations in <i>P. berghei</i>	125
4.1	Chapter aim	125
4.2	Introduction	125
4.3	Results	127
4.3.1	CRISPR-Cas9 mediated introduction of <i>P. berghei</i> orthologous Kelch13 mutations and <i>in vivo</i> mutant enrichment by AS	127
4.3.2	<i>P. berghei</i> Kelch13 mutants display reduced susceptibility to DHA in a standard 24-hour <i>in vitro</i> assay	132
4.3.3	<i>P. berghei</i> Kelch13 mutants display increased survival in an adapted RSA	133
4.3.4	<i>P. berghei</i> Kelch13 mutants mimic the delayed parasite clearance phenotype <i>in vivo</i> upon AS treatment	136

4.3.5	<i>P. berghei</i> Kelch13 mutants achieve faster recrudescence than wild type parasites at higher ART doses	140
4.3.6	<i>P. berghei</i> Kelch13 mutants are associated with an <i>in vivo</i> fitness cost but are preferentially selected for in the presence of AS or CQ	142
4.3.7	A <i>Plasmodium</i> -selective proteasome inhibitor is potent against <i>P. berghei</i> wild type and Kelch13 mutant parasites and synergizes DHA action.....	148
4.4	Discussion.....	152
4.4.1	Acquisition of certain Kelch13 mutations may require permissive genetic backgrounds.....	152
4.4.2	Some <i>P. berghei</i> Kelch13 mutations carry a pronounced fitness cost...	154
4.4.3	Proteasome inhibition off-sets ART resistance in <i>P. berghei</i> Kelch13 mutants	155
4.4.4	Conclusion	155
5	Small molecule inhibitors of mammalian deubiquitinating enzyme display activity in malaria parasites and show evidence of potentiating ART action	157
5.1	Chapter aim	157
5.2	Introduction	157
5.3	Results	159
5.3.1	<i>In vitro</i> activity of DUB inhibitors in malaria parasites.....	159
5.3.2	Different classes of DUB inhibitors can be combined to provide more effective blocking of malaria parasite growth <i>in vitro</i>	162
5.3.3	DUB inhibitors alone or in combination can potentiate DHA action in malaria parasites <i>in vitro</i>	163
5.3.4	A combination of DUB and 20s proteasome inhibitor can synergize with DHA	167
5.3.5	Pre-incubation of malaria parasites with UPS inhibitors efficiently mediates DHA potentiation	168
5.3.6	b-AP15 fails to block parasite growth but potentiates ART action <i>in vivo</i>	171
5.4	Discussion.....	174
5.4.1	DUB inhibitors inhibit malaria parasites IDC proliferation	175
5.4.2	<i>Plasmodium</i> UCH-L3 could be an even more attractive drug target	177
5.4.3	DUBs can be targeted to overcome ART resistance	177
5.4.4	Conclusion	179

6	A metabolic profile of fast acting antimalarial drugs and drug candidates	180
6.1	Chapter aim	180
6.2	Introduction	180
6.3	Results and discussion	182
6.3.1	ITDs display a fast killing rate relative to DHA and Spiroindolones.....	182
6.3.2	Atovaquone disrupts pyrimidine biosynthesis pathway in malaria parasites	185
6.3.3	KAE609a elicits a pleiotropic metabolic response in malaria parasites.	188
6.3.4	ITD series elicit minimal metabolic responses that suggest inhibition of haemoglobin catabolism as a possible MOA	193
6.3.5	KAF156a elicits a minimal non-specific metabolic response.....	196
6.3.6	Metabolomics time point resolution of fast acting compounds; DHA, ITD2a and KAE609a during early points of drug incubation	197
6.3.6.1	Global metabolomic responses to DHA, ITD2a and KAE609a are unique and respond to duration of drug exposure	198
6.3.6.2	KAE609a perturbation of choline, pyrimidine and purine metabolites at 2.5 hours is reflected in time dependent changes at earlier time points	200
6.3.6.3	Time dependent changes in peptide response for KAE609, DHA and ITD2a	203
6.4	Conclusions.....	206
7	Summary and future work	207
7.1	Drug resistance in rodent malaria parasites in the CRISPR-Cas9 era..	207
7.2	Targeting the upstream components of the UPS to overcome ART resistance.....	210
7.3	Capturing the metabolomic fingerprint of fast acting antimalarial drugs and drug candidates: any cues to the MOA?.....	211
7.4	Future work	212
7.4.1	Cellular localisation of UBP-1 and Kelch13 in <i>P. berghei</i>	212
7.4.2	Transmission competency and competitive release of drug resistance mutations in <i>P. berghei</i>	213
7.4.3	Phenotypic heterogeneity of drug resistance mutants in <i>P. berghei</i>	214
8	Appendix	216
8.1	Appendix figures for chapter 2.....	216

8.2	Appendix figures for chapter 3.....	217
8.3	Appendix figures for chapter 4.....	220
8.4	Appendix figures for chapter 5.....	230
8.5	Appendix tables	243
9	References	256
10	Publications	302

List of figures

Figure 1.1: Global malaria status between 2000 and 2018.	2
Figure 1.2: Life cycle of <i>Plasmodium</i> spp.	5
Figure 1.3: Structure of <i>P. falciparum</i> merozoite.....	7
Figure 1.4: Protein export in malaria parasites.	13
Figure 1.5: Sexual developmental switch in malaria parasites.	17
Figure 1.6: An illustrated life cycle progression of malaria parasites in the mosquito vector.	22
Figure 1.7: Chemical structure of common antimalarials in clinical usage.	35
Figure 1.8: Emergence and spread of CQ resistance.	39
Figure 1.9: Structure of artemisinin and its derivatives dihydroartemisinin, artemether and artesunate.	42
Figure 1.10: Artemisinin action, resistance and possible intervention points. ...	52
Figure 1.11: Structure of some of the second-generation ART-based antimalarials.	54
Figure 1.12: Schematic overview of genome editing strategies in malaria parasites.	64
Figure 1.13: selection strategies used to obtain <i>P. chabaudi</i> ART resistant lines and the causal genetic determinants.	72
Figure 2.1: Schematic of the ABR099 Cas9 plasmid.....	84
Figure 2.2: Overview of site directed mutagenesis by overlapping PCR.....	87
Figure 2.3: Schematic of donor templates supplied in Cas9 plasmids and example RFLP analysis.....	89
Figure 3.1: Introduction of UBP-1 mutations in <i>P. berghei</i>	104
Figure 3.2: Enrichment of UBP-1 mutant lines by drug challenges and cloning of mutant lines.....	108
Figure 3.3: ART and CQ in vitro and in vivo resistance profiles of the G1807 ^{V2752F} and G1808 ^{V2721F} lines.....	112
Figure 3.4: Growth kinetics of the 820, G1808 ^{V2721F} and G1808 ^{V2752F} relative to the 1804cl1 line.	114
Figure 3.5: Swapping of the V2752F to V2721F mutations and attempted generation of a double mutant in the G1807 ^{V2752F} line.	119
Figure 4.1: Introduction of orthologous Kelch13 nucleotide substitutions in <i>P. berghei</i>	131

Figure 4.2: DHA dose response curves and IC ₅₀ values for <i>P. berghei</i> Kelch13 mutant lines as compared to wild type 1804 ^{WT} and the UBP-1 G1980 ^{V2721F} mutant line.	133
Figure 4.3: RSA survival of <i>P. berghei</i> Kelch13 mutants.	135
Figure 4.4: <i>In vivo</i> clearance kinetics and microscopy analysis of <i>P. berghei</i> Kelch13 mutants upon AS treatment.	138
Figure 4.5: <i>In vivo</i> recrudescence rates of <i>P. berghei</i> Kelch13 mutants upon treatment with ART.	141
Figure 4.6: Relative fitness of <i>P. berghei</i> Kelch13 mutants in presence or absence of AS or CQ.	147
Figure 4.7: Activity and DHA synergy of proteasome inhibitor in <i>P. berghei</i> Kelch13 mutants.	151
Figure 5.1: <i>In vitro</i> interaction of different classes of DUB inhibitors in malaria parasites.	163
Figure 5.2: <i>In vitro</i> potentiation of DHA by DUB inhibitors.	166
Figure 5.3: A combination of DUB and 20s proteasome inhibitor improves synergy with DHA.	168
Figure 5.4: Pre-exposure of malaria parasites to UPS inhibitors alone or in combination enhances DHA action.	171
Figure 5.5: <i>In vivo</i> activity of b-AP15 alone and or in combination with ART. .	174
Figure 6.1: Killing kinetics of KAE609a, DHA, Atovaquone, ITD1a, ITD2a and KAF156a in the 3D7 luc line.	184
Figure 6.2: Metabolomics profile of atovaquone.	187
Figure 6.3: Pleiotropic metabolic response of malaria parasites after exposure to KAE609a for 2.5 hours.	192
Figure 6.4: Peptide metabolic responses of the ITD series compounds in malaria parasites.	195
Figure 6.5: KAF156a metabolomic response for selected metabolites.	197
Figure 6.6: Global volcano plots of all detected mass features in DHA, ITD2a and KAE609a treatments according to their fold change relative to DMSO treatments.	200
Figure 6.7: Time course comparisons of choline, pyrimidine and purine metabolites in DHA, KAE609a and ITD2a parasite treatments.	203
Figure 6.8: Time point resolution of global peptide responses in KAE609a, DHA and ITD2a treated parasites.	206

List of tables

Table 1.1: Classes of selected antimalarial drugs in clinical use...	38
Table 1.2: Comparison of life cycle and utility features of rodent malaria parasites	69
Table 2.1: PCR master mix components.	86
Table 2.2: PCR cycling conditions.	86
Table 5.1: <i>In vitro</i> activity of DUB inhibitors in rodent and human malaria parasites.	161
Table 6.1: <i>In vitro</i> growth inhibition of the <i>P. falciparum</i> 3D7 line for the compounds used in the metabolomics screen.	183

1 Introduction

1.1 Introduction outline

The introduction addresses the general context of malaria in terms of disease burden, causative agents (*Plasmodium* spp.), their life cycle, control and intervention strategies. A specific detail will focus on artemisinins, their mode of action and resistance mechanisms.

Specifically, each section of the introduction addresses the background literature as follows

- section 1.2: a general overview of malaria disease burden and its causative agents
- section 1.3: a detailed life cycle of *Plasmodium* spp. in the context of interventional points
- section 1.4: malaria prevention and control strategies
- section 1.5: antimalarial drugs and drug resistance
- section 1.6: approaches to studying antimalarial drugs mode of action
- Section 1.7: genome editing strategies for validating genetic determinants of antimalarial drug resistance
- Section 1.8: role of animal models in understanding drug action and resistance in malaria
- Section 1.9: outlines the aims and objectives of this thesis in context of the sections above.

1.2 Malaria

Malaria is a haematoprotzoan tropical disease resulting from infection by apicomplexan parasites of the genus *Plasmodium*. The disease is a serious global health problem with nearly half of the world population at risk, over 200 million cases and greater than 400 000 deaths in 2018 alone (WHO, 2019). Over 90% of malaria deaths occur in the WHO-defined African region, mostly in children of less than five years old (WHO, 2019). Since the dawn of new millennium in the early 2000s, substantial progress has been made in malaria control. For example, between 2010 and 2018, the incidence rates of malaria have declined by ~19% globally (WHO, 2019). By 2018, 49 countries have reported less than 10 000 cases up from 40 in 2010 while 27 countries reported fewer than 100 local cases as compared to 17 in 2010 (WHO, 2019), Figure 1.1. More importantly, between 2000-2016 the number of countries with endemic malaria has dropped from 106 to 86 while annual mortality rates have declined by over 60% (Feachem et al., 2019)

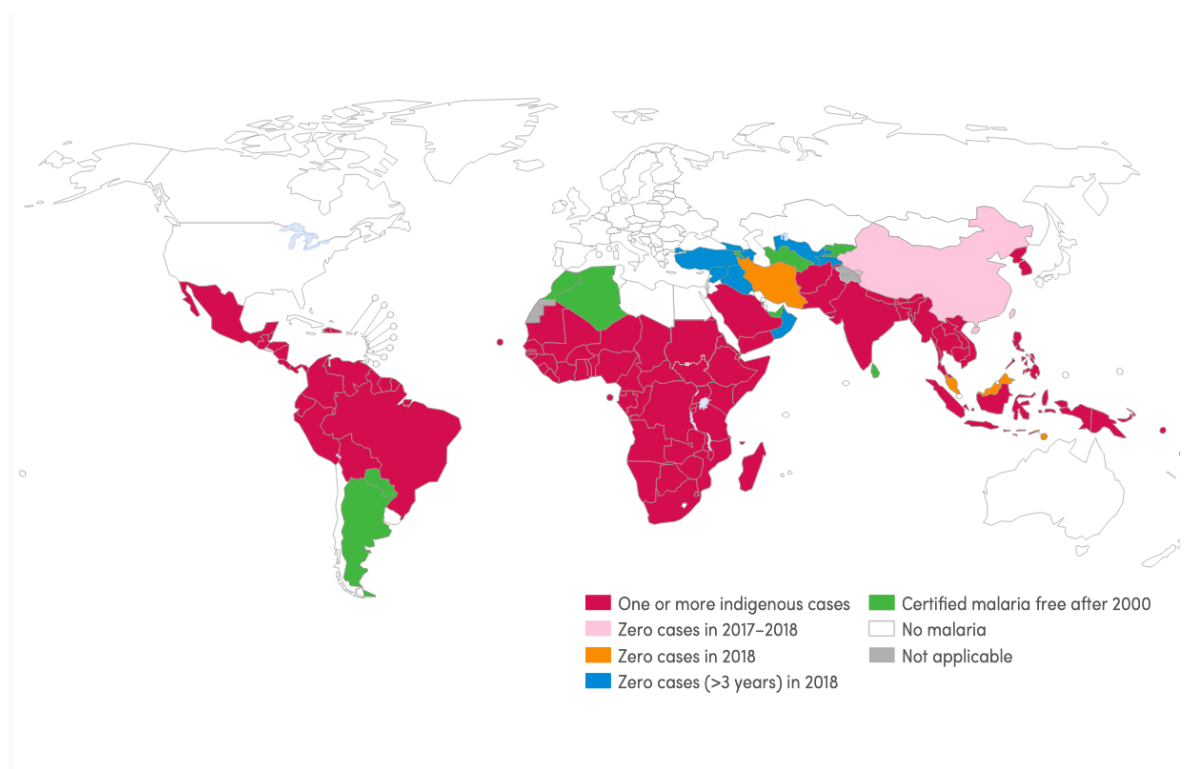


Figure 1.1: Global malaria status between 2000 and 2018.

Figure adapted from (WHO, 2019)

However, despite these remarkable feats, the disease continues to have a significant impact on people's health and daily livelihoods. This is being recently worsened by failure of effective control efforts like the emergence of resistance to frontline antimalarial drugs, resistance to insecticides used in vector control

and absence of effective vaccines in the near future (Feachem et al., 2019, Cui et al., 2015, Hemingway et al., 2016b). More worryingly and likely consequence of these threats, a global stall in malaria control has been recently reported with an observed increase in malaria cases from 2014 to 2016 which has remained at similar levels through to 2018 (WHO, 2019).

1.3 Life cycle of *Plasmodium* spp.

Malaria is caused by *Plasmodium* spp. which are obligate intracellular parasites of the *Protista* kingdom in the phylum Apicomplexa. There are five *Plasmodium* spp. that cause human malaria: *P. falciparum*, *P. vivax*, *P. ovale*, *P. knowlesi* and *P. malariae*. Of these, *P. falciparum* is responsible for the most severe and lethal forms of the disease and accounts for >99% of malaria cases in Sub-Saharan Africa (WHO, 2019). Malaria caused by *P. vivax* is also highly prevalent, which though not frequently associating with severe forms of the disease, accounts for more than half of all malaria cases in the WHO-defined South-East Asia and America regions (WHO, 2019). Meanwhile, *Plasmodium* spp. that infect rodents and cause rodent malaria (*P. berghei*, *P. yoelii*, *P. chabaudi*, *P. vinckei*) have also demonstrated remarkable utility in delineating the fundamental aspects of parasite biology because of their genetic similarity with human infecting counterparts, experimental tractability of all life cycle stages and their relative amenability to vast and powerful genetic manipulation systems (De Niz and Heussler, 2018).

1.3.1 Sporozoite inoculation and pre-erythrocytic stages

The basic life cycle features of *Plasmodium* spp. are conserved across the genus sharing almost all of the developmental stages, Figure 1.2. The cycle is initiated by the bite of a female anopheles' mosquito which can inject up to 100 sporozoites in experimental conditions. Injected sporozoites move by gliding motility through the extracellular matrix of the skin before eventually invading blood and lymphatic vessels (Menard et al., 2013). Consequently, sporozoites find their way to the liver where they invade hepatocytes aided by a sporozoite coat forming protein, the circumsporozoite protein (CSP) (Menard et al., 2013). Through a series of host cell invasions, traversal and exits, sporozoites invade a final hepatocyte where they develop to establish a parasitophorous vacuole (PV) (Menard et al., 2013, Prudencio et al., 2006). Thereafter, in an iterative series

of DNA replication and asexual proliferation, sporozoites differentiate into mature schizonts which contain tens of thousands of merozoites, a process which takes 2-16 days depending on the *Plasmodium* spp. Access of liver stage merozoites (in fully developed schizonts) to the blood stream to initiate the intraerythrocytic developmental cycle (IDC) is partly restricted as they are confined to the host hepatocytes and require an escape mechanism to exit the host cell, pass through the extracellular matrix and endothelium of liver blood vessels while at the same time evade constant surveillance from resident phagocytic cells. In an ingenious “stealth shuttle” mechanism, these late stage parasites allow hepatocytes to commit an unusual form of apoptosis by forming membrane enclosed structures that extrude from the infected host cell. These structures, called merozoites, act as shuttles that release merozoites into the blood stream while avoiding host defence mechanism (Sturm et al., 2006). Rudimentary details of merozoite formation, traversal across the liver matrix and eventual bursting in the bloodstream are still unknown. However, this process is thought to involve initial disintegration of the PV, possibly through the action of a *Plasmodium* phospholipase (Burda et al., 2015), which releases merozoites into the host RBC cytosol followed by an arrest of host cell processes such as protein synthesis and mitochondrial energy homeostasis. In a “Trojan horse strategy”, released merozoites in the host cytosol are wrapped with the host cell membrane to form a shield that protects them from the host immune system (Graewe et al., 2011). At the same time, parasites mediate a dissociation of actin cytoskeleton from the host cell membrane and destabilisation of plasma membrane integrity by altering protein and phospholipid composition (Burda et al., 2017). Formed merozoites traverse through sinusoids and endothelial cell barriers to reach the blood where they rupture (by unknown triggers) to release merozoites which invade RBCs to initiate the IDC.

Unlike in *P. falciparum*, the liver stage of other *Plasmodium* spp. particularly; *P. vivax* and *P. ovale* involves a small proportion of invading sporozoites developing into dormant non replicating forms called hypnozoites (Krotoski et al., 1982). Hypnozoites are characteristically persistent, refractory to killing by several antimalarial drugs (except primaquine) and are the frequent source of relapsing malaria caused by *P. vivax* (Wells et al., 2010). The mechanism behind hypnozoites formation and dormancy is unknown, with however, a distinct

variation between the length to relapse among various *P. vivax* strains which can range from days to years (Wells et al., 2010).

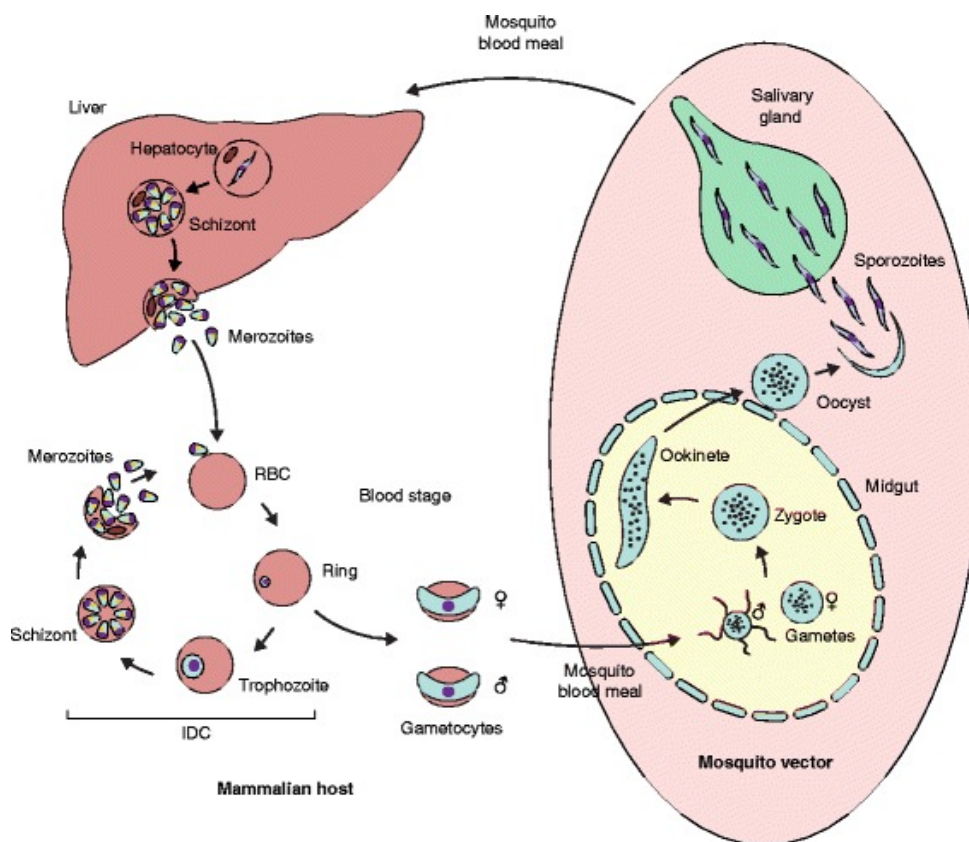


Figure 1.2: Life cycle of *Plasmodium* spp.

Upon a mosquito bite, sporozoites are injected at the base of skin where they migrate through the blood stream and lymph nodes to the liver. In the liver, sporozoites infect hepatocytes to initiate the exoerythrocytic liver stage. Depending on *Plasmodium* spp. (~2 days in *P. berghei* or 6.5 days in *P. falciparum*), sporozoites develop into fully formed mature schizonts containing 29000-90000 merozoites after several rounds of asexual proliferation. Upon rupture of the host cell, free merozoites invade RBCs to initiate the blood stage IDC. The IDC comprises of a series of asexual developmental transitions; from metabolically less active ring stages to highly active trophozoites which mature to schizonts after further rounds of asexual proliferation and DNA replication. Mature schizonts which produce a species-specific number of merozoites (15-30) rupture to release merozoites which invade new RBCs to re-initiate the cycle. This process usually takes ~48 hours in *P. falciparum* and half the time (~24 hrs) in the rodent malaria *P. berghei*. Meanwhile, during the IDC, a small proportion of ring stage parasites commit to a sexual developmental cycle which results in formation of male and female gametocytes for transmission. Gametocytes are taken up into a mosquito midgut after a new blood meal where they activate, fertilise and develop into a zygote. The zygote undergoes a

meiotic cell division and develops into motile ookinetes which traverse the mosquito midgut to form oocysts. Oocysts go through another round of asexual propagation to generate thousands of sporozoites which migrate to and colonize the mosquito salivary glands to re-initiate the cycle upon a mammalian bite. Figure adapted from, (Kirchner et al., 2016).

The liver stage of malaria parasites is mostly asymptomatic but provides unique opportunities to interrupt the parasite life cycle before the infection is established. A recent genome wide knockout screen in *P. berghei* has identified 461 genes which are required for efficient progression through the liver stage providing opportunities for novel drug and vaccine targets (Stanway et al., 2019). Targeting the liver stage through, for example, antibodies that elicit immune responses to sporozoites is also one of the lead vaccine initiatives aimed at achieving malaria eradication (Vaughan and Kappe, 2017).

1.3.2 The Intra-erythrocytic developmental cycle

Once released into the peripheral blood circulation, merozoites invade RBCs to initiate the blood stage IDC enclosed within a membranous PV. RBCs are terminally differentiated cells that lack a nucleus and more other important cellular and biochemical organelles that would promote intracellular survival of parasites such as *Plasmodium* spp., more so within a PV. To this, malaria parasites extensively remodel the host RBC to 1) ensure efficient acquisition of nutrients as nutrient transporters are lost during RBC differentiation 2) confer cytoadhesive properties to infected RBCs to minimise their splenic clearance 3) escape the immune system by exporting immunological variant proteins (Silvie et al., 2008, Gilson et al., 2017).

1.3.2.1 Getting in, essential first steps of malaria parasites invasion

Invasion of RBCs by merozoites, be it from hepatocyte derived or mature blood stage schizonts involves three distinct stages: 1) an initial merozoite RBC interaction that causes erythrocyte deformation, 2) merozoite apical end interactions with RBCs and subsequent invasion, 3) echinocytosis and RBC recovery stage.

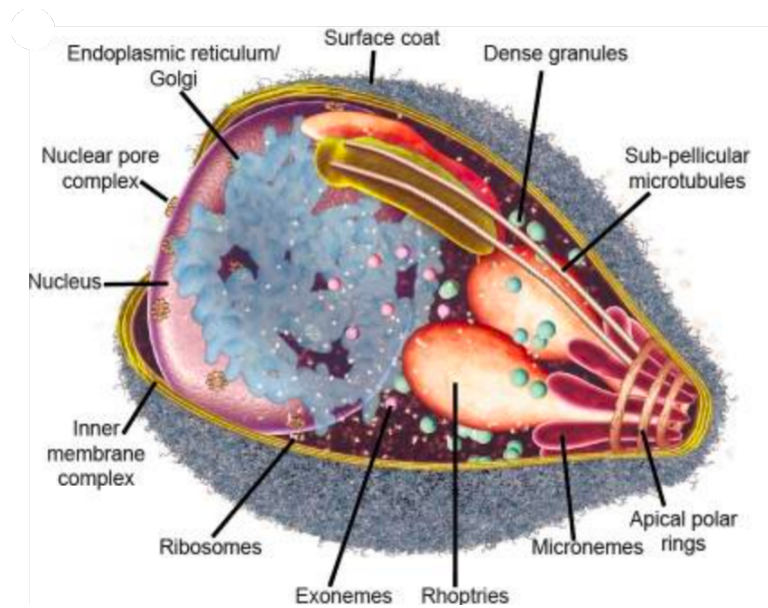


Figure 1.3: Structure of *P. falciparum* merozoite.

A three-dimensional sectioned merozoite highlighting the organelles and structures that are involved during invasion and egress. PfSUB1, a critical protease involved in merozoite egress, localises to the recently identified exonemes. Micronemes, rhoptry neck and rhoptry bulb are sites for adhesion and invasion proteins such as RON, AMA1, EBL and PfRH. Figure reproduced from (Cowman et al., 2012) with permission.

Immediately upon release into the bloodstream, merozoites (Figure 1.3) encounter low potassium levels which act as a signal to trigger a rise in intracellular concentration of calcium which in itself triggers the release of adhesins and invasins from the merozoites rhoptries and micronemes (Singh et al., 2010). When the activated merozoite encounters a RBC, low level affinity interactions occur with the RBC cell membrane and these interactions are thought to be primarily facilitated by membrane anchored glycoposphotidylinositol (GPI) merozoite surface proteins (MSPs) on the fibrillar merozoite surface. *P. falciparum* GPI anchored MSPs such as MSP1, MSP2, MSP3, MSP4, MSP5 and MSP5 as well as those belonging to the 6-cysteine domain protein family have all been predicted to play a role in initiating the early interactions with RBCs (Sanders et al., 2005, Ishino et al., 2005). Exact details on how MSPs mediate the initial contact and or facilitate the invasion processes remain unknown. For instance, even though MSP1 forms a complex with MSP3, MSP6 and MSP7 on the merozoite surface that appear to be involved in the invasion process (Kauth et al., 2006), parasites lacking MSP1 can still

invade RBCs downplaying the direct role of this protein in invasion or a potential functional redundancy (Das et al., 2015). Nevertheless, these initial merozoites RBC interactions are characterised by rapid movements of merozoites and a dramatic ruffling of the RBC membrane, all occurring within ~11 seconds (Gilson and Crabb, 2009).

After the initial contact, an irreversible interaction of the RBC and the parasite occurs at the apical end of the merozoites (Figure 1.3). This process is mediated by two protein families; the erythrocyte binding like (EBL) and reticulocyte binding-like homologues (PfRh), both of which localise to micronemes and neck rhoptries of merozoites, reviewed by (Cowman et al., 2012, Cowman et al., 2017). The PfRh family comprises of five key proteins; PfRh1, PfRh2a, PfRh2b, PfRh4 and PfRh5. Host RBC receptors have been identified for PfRh4 (complement receptor 1 (Tham et al., 2010)) and PfRh5 (basigin (Crosnier et al., 2011)). Due to the significant role these proteins play in the invasion process, antibodies raised against PfRh proteins block merozoite invasion and are indeed being actively pursued as vaccine targets (Tham et al., 2012). However, out of the five PfRhs, only PfRh5 appears to be essential during the IDC in gene knockout studies which could be due to a functional redundancy or compensatory invasion mechanisms (Tham et al., 2012). PfRh5 is a leading vaccine target as antibodies raised against this protein have been shown to neutralise a broad spectrum of lab and clinical isolates of *P. falciparum* (Crosnier et al., 2011). The EBL family consists of four identified redundant set of proteins in *P. falciparum* (PfEBA-175, PfEBA-140, PfEBA-181, and PfEBL-1) which contain unique single or double Duffy Binding like (DBL) domains. Even though PfEBA-181 and PfEBL-1 are not yet structurally characterised, PfEBA-175 and PfEBA-140 bind to host RBCs via glycophorin A and C respectively in a sialic-acid-dependent manner. Antibodies raised against DBL domains in EBL proteins also block merozoite invasion and are potential vaccine candidates, reviewed by (Tham et al., 2012). Crucially, attachment of these ligands to the host RBC receptors appear to be a critical “no turning back” commitment stage of merozoites to the invasion process (Riglar et al., 2011).

Downstream of the PfRh or EBL ligand host RBC receptor engagement, a high affinity interaction also known as the tight junction is formed at the interface of

the apical merozoite and host RBC membrane. At the centre of the junction are two proteins; rhoptry neck proteins (RON) and the apical membrane antigen 1 (AMA1). RON4 and possibly other RON proteins such as RON2 are translocated to the cytosolic side of the RBC membrane immediately after merozoites ligands engage their receptors on the host RBC. AMA1 which is present on the surface of the merozoite then complexes with RON proteins to form a complex which acts as a molecular seal of the tight junction (Riglar et al., 2011). The AMA1-RON complex has been a lead malaria vaccine candidate especially with observations that antibodies raised against these proteins can block merozoite invasion (Collins et al., 2009, Srinivasan et al., 2011). However, there still remain some controversies on the role of the AMA1-RON interaction in facilitating parasite invasion because knockout studies have shown that inactivation of AMA1 in *Plasmodium* and closely related apicomplexan *Toxoplasma* can be achieved with resultant parasites able to invade host cells despite displaying impaired host cell attachment (Bargieri et al., 2013). This suggests involvement of other uncharacterised proteins in the formation and function of the tight junction.

Formation of the tight junction and phosphorylation of adhesin proteins like AMA1 by a cAMP related protein kinase trigger the release of rhoptry bulb contents into the host RBC some of which include proteins and lipids required for the formation of the parasitophorous vacuole membrane (PVM) and PV (Leykauf et al., 2010, Riglar et al., 2011). At the same time, the parasite actinomyosin-based molecular motor complex (also called glideosome) powers the forced entry of the merozoite into the host RBC. The glideosome which is specifically conserved between *Plasmodium* and *Toxoplasma* spp. localises between the inner membrane complex and plasma membranes of the parasites and is thought to be composed of myosin A, an associated myosin light chain (MLC1) and three gliding-associated proteins, GAP40, GAP45 and GAP50 (Frénal et al., 2010, Green et al., 2017). Recent conditional deletion of GAP45 has indeed demonstrated that this component of the glideosome is critically essential for malaria parasite invasion (Perrin et al., 2018). It is believed that the glideosome connects to various cytoplasmic tails of adhesins which then propels the merozoite into the shear space generated when contents of the rhoptry bulb are released through into the RBC (Cowman et al., 2017).

In the final stage, the tight junction is pulled across the merozoite pulling in part of the host RBC membrane until the merozoite is fully internalised within a PV (Riglar et al., 2011). This is typified by a dehydration like RBC morphology (echinocytosis) ~30-40 seconds after invasion following which the RBC retains its normal morphology within 5-11 minutes (Gilson and Crabb, 2009).

1.3.2.2 Ring, trophozoite and schizont stages

The first morphological feature of malaria parasites upon successful invasion is the appearance of a signet ring structure in Giemsa stained thin blood smears which characteristically defines the “ring” stage (Bannister et al., 2000). The very early ring stage of the parasite, contained within a PV, is metabolically less active and acquires nutrients from host haemoglobin through cytotomes as well as flux of solutes (sugar, amino acids, vitamins) by the induction of new permeability pathways (NPP). As the ring stage progresses, transcription of ring stage specific genes occurs (Spielmann and Beck, 2000) some of which transcribe for virulence proteins that are exported into the host RBC and mediate adhesion of infected RBCs into host endothelial blood vessels (Pouvelle et al., 2000).

At approximately 22-24 hours post invasion (in *P. falciparum*), ring stage parasites have developed into trophozoites which are metabolically highly active and involve rapid growth differentiation as well as modification of the host RBC. In mid-late trophozoite stages, the parasite starts replicating its DNA (S-phase) and asexually divides its nucleus to enter the schizont stage. Typically, 10-30 nuclei (depending on the *Plasmodium* spp.) are generated and these migrate into merozoite buds in the schizont periphery. Upon full maturation, merozoites separate from the cytoplasmic residual bodies ready to re-initiate a new invasion cycle upon rupture of the infected cell (Bannister and Mitchell, 2003). This results in cyclic increase of infected RBCs that accompany the associated disease pathology seen in malaria.

1.3.2.3 Merozoite egress in mature schizonts

Egress of merozoites from RBCs in mature schizonts possess a unique challenge to the parasite as it requires a breach of at least three cellular structures; the PVM, host cytoskeleton and RBC membrane. Surprisingly, this stage is uniquely synchronous in *P. falciparum* characterised by a unified ending of the replicative

cycle and subsequent simultaneous rupture and release of merozoites (Singh and Chitnis, 2017). Even though the exact details of how merozoites egress from host RBCs remain to be fully unravelled, this process is believed to be mediated by a tightly regulated proteolytic cascade which breaches the PVM and host RBC membranes immediately before merozoite escape. Several proteases and perforin like proteins (PLP) have been identified as key players of egress in malaria parasites (Blackman, 2008, Garg et al., 2013). Specifically, a secreted subtilisin-like protease, PfSUB1, and the *P. falciparum* PLP (PfPLP); both of which localise in micronemes and exonemes of merozoites (Figure 1.3) mediate the critical events that precede disruption of the PVM, host membranes and cytoskeletons and the eventual release of merozoites (Arastu-Kapur et al., 2008, Yeoh et al., 2007, Garg et al., 2013).

PfSUB1 is refractory to deletion in blood stages of malaria parasites and is fully expressed in very late schizonts. Upon secretion into the PV from exonemes, PfSUB1 is thought to activate a secondary family of proteases, the serine-rich antigen 5 (SERA5) or other SERAs which upon activation lead to proteolysis of host cytoskeletal proteins which in turn mediates parasite egress (Arastu-Kapur et al., 2008, Yeoh et al., 2007). Recent work has demonstrated that SERA5 and SERA6 are both active proteases which cleave cytoskeletal membranes and results in RBC rupture while at the same time require activation by PfSUB1 (Collins et al., 2017, Thomas et al., 2018). More intriguingly, besides activating SERA5 and SERA6, PfSUB1 appears to mediate the initial PVM rupture while SERA6 disintegrates the host RBC membrane and cytoskeleton in a coordinated proteolytic cascade (Thomas et al., 2018). PfSUB1 activity is apparently regulated by signalling through a *Plasmodium falciparum* cGMP-dependent protein kinase (PfPKG) which is required not just for the discharge of PfSUB1 into the PV, but also other microneme proteins involved in merozoite invasion (Collins et al., 2013). Calcium dependent signalling of PfPLPs has also been shown to promote permeability and lysis of host RBC membranes during egress (Garg et al., 2013).

Nevertheless, these processes appear to occur in a highly organised and coordinated manner that, in the first place, ensures that all merozoites are fully matured before schizont rupture. PfPKG activation of PfSUB1 triggers its

proteolytic activation of SERA6 and possibly other SERA proteins while at the same time plays a role in disintegrating the PVM through its own protease activity or by activating PLPs. SERA6 and or SERA5 then accomplish the final step of RBC membrane rupture before merozoites are released (Thomas et al., 2018). Morphologically, just before rupture, the diameter of schizonts increases while merozoites become uniquely visible. A few seconds downstream, merozoites disaggregate and fill the RBC as the PVM ruptures. At this stage, merozoites become highly mobile which precedes rupture of the RBC membrane and their release into the blood stream to initiate a new invasion cycle (Gilson and Crabb, 2009).

1.3.2.4 Parasite RBC remodelling and immune evasion: an intricate renovation and escape

After invasion, the parasite activates a host RBC remodelling program that converts this terminally differentiated cell lacking proper organelles and transporters into a “viable home” in which the parasite can reside and thrive (Boddey and Cowman, 2013). This process is facilitated by hundreds of exported parasite proteins which upon synthesis are trafficked to the host cell cytosol via secretory pathways through the parasite plasma membrane, PV and PVM. Malaria parasites exported proteins play a significant role in parasite growth and survival. Over 20% of these exported proteins are refractory to deletion illustrating a crucial role they play in mediating parasite survival and virulence (Maier et al., 2008). Some of these proteins include the *P. falciparum* erythrocyte membrane protein 1 (PfEMP1) which is one of most extensively studied exported protein in *P. falciparum*. PfEMP1 export to the surface of RBC extensively remodels the RBC cytoskeleton into knob like multiprotein complexes that facilitate binding and cytoadherence of infected RBCs to surface ligands in the microvasculature (Maier et al., 2008, Nash et al., 1989). This is crucial for parasite survival as it limits splenic clearance, but can eventually clog vascular structures and is indeed a significant contributor to severe malaria pathogenesis (Storm and Craig, 2014). The display of PfEMP1 (encoded by *var* genes) on the RBC surface also results in exposure to host antibodies. Parasites switch PfEMP1 expression among antigenically distinct isoforms to avoid immune destruction in what is classically called antigenic variation. The expanded spectrum of *var* genes (~60), differences in PfEMP1 receptor binding selectivity

and the resulting ability of PfEMP1 expressing infected RBCs to sequester in various tissues and organs do indeed play a significant role in mediating parasite host immune escape and the associated disease pathology (Hviid and Jensen, 2015).

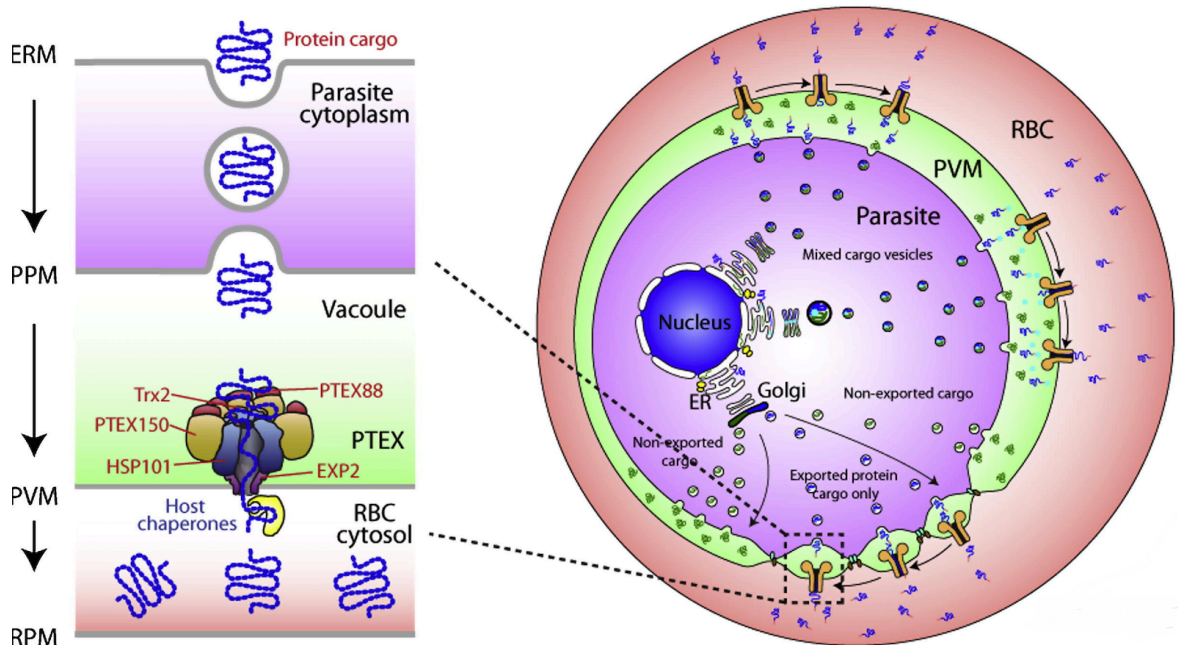


Figure 1.4: Protein export in malaria parasites.

PEXEL proteins or PNEPs are prepared for vesicular trafficking into the secretory pathway in the ER upon fusion and passage into the ER lumen through the ER membrane (ERM). Vesicular cargo proteins in ER fuse with the parasite plasma membrane (PPM) and release soluble proteins into the PV where they associate with a translocon, PTEX. The PTEX translocon unfolds cargo proteins and translocates them into the host cytosol where host chaperones facilitate their refolding and distribution to various destinations. Figure reproduced from (Crabb et al., 2010) with permission.

The voyage of exported proteins in malaria parasites begins in the ER, Figure 1.4. These processes are initially coordinated by vesicular transport coat proteins (COPII) which facilitate transfer of the exported proteins from the ER to the Golgi apparatus which at the same time require a signal sequence to enter into a network cascade of secretory pathways (Crabb et al., 2010, Gilson et al., 2017). Using GFP marker proteins, it has been demonstrated that chemical inhibition of COPII traps exported and secreted proteins into the ER (Wickham et al., 2001). Meanwhile, the signal sequence is cleaved from the exported proteins and recycled in the ER by a signal peptide peptidase (SPP) immediately before

the cargo enters the secretory pathway (Adisa et al., 2003). Since the secretory pathway is utilised by several other proteins whose destiny is within the PVM, a highly conserved motif consisting of five core amino acid residues RnLnE/Q/D (n is any uncharged amino acid) is required to specifically tag proteins which require export and traverse through the PVM to the RBC cytosol (Hiller et al., 2004, Marti et al., 2004). This motif, also called *Plasmodium* export element (PEXEL), is conserved in all *Plasmodium* spp. and occurs at the N-terminal of cargo proteins downstream of the signal sequence (Sargeant et al., 2006).

The PEXEL motif acts as a cleavage site for an aspartic protease, Plasmepsin V (Russo et al., 2010, Boddey et al., 2010) and a binding site for phosphatidylinositol 3-phosphate (PI3P) in the ER (Bhattacharjee et al., 2012). It has been proposed that PI3P concentrates in the ER and binds to the PEXEL motif with high affinity segregating cargo proteins into export competent vesicles (Bhattacharjee et al., 2012). However, recent work has challenged this, as it has been demonstrated that PI3P does not bind the PEXEL motif nor does it concentrate in the ER, rather in the apicoplast and food vacuole (Boddey et al., 2016). Nevertheless, PEXEL cleavage by Plasmepsin V and subsequent acetylation of the N-terminal is apparently critical for the cargo to be exported (Gruring et al., 2012, Gilson et al., 2017). How this links to the next stage of the trafficking pathway remains unclear. Moreover, an additional motif downstream of the PEXEL sequence has also been shown to play a role in the export process independent of PEXEL cleavage by Plasmepsin V and is thought to facilitate export of proteins that lack the PEXEL motif, PEXEL negative exported proteins (PNEPs), such as PfEMP1 (Gruring et al., 2012).

Upon fusion with the parasite plasma membrane, cargo vesicles release their contents into the PVM where they apparently associate with a *Plasmodium* translocon of exported proteins (PTEX) which pumps cargo proteins into the host RBC cytosol (de Koning-Ward et al., 2009). Translocation across the PVM requires unfolded proteins and energy in form of ATP, reviewed by (Gilson et al., 2017). Early characterisation of PTEX revealed that this protein consisted of five key constituents; an AAA+-ATPase heat shock protein 101 (HSP101) which belongs to a chaperone family of proteins and likely plays a role in protein unfolding, an exported protein-2 (EXP2) which would form a transmembrane complex,

PTEX150, thioredoxin (TRX2) and PTEX88 which are all conserved across the *Plasmodium* spp. (de Koning-Ward et al., 2009). Knockdown studies of HSP101 and PTEX150 as well as knockout of TRX2 significantly reduces export of both PEXEL positive as well PNEP proteins (Elsworth et al., 2014). A recent structural resolution of PTEX in *P. falciparum* has revealed that EXP2 and PTEX150 form a funnel shaped symmetric protein conductance channel spanning the PVM while HSP101 forms a spiral shape hexamer at the top of the funnel (Ho et al., 2018). Tellingly, TRX and PTEX88 could not be resolved with the PTEX structure which is suggestive of their transient association with the PTEX complex (Ho et al., 2018, de Koning-Ward et al., 2009).

Due to the significant role the parasite protein export machinery plays in mediating parasite virulence, transmission and survival, the pathway is actively being explored for novel antimalarial drug targets (Gilson et al., 2017). Inhibitors targeting the aspartyl protease SPP which is involved in the ER signal cleavage and recycling display potent activity against blood and liver stages of malaria parasites (Harbut et al., 2012). Moreover, the *P. falciparum* Plasmepsin V gene is refractory to deletion and compounds targeting the same inhibit protein export as well block ring-trophozoite stage transition during the IDC stage of malaria parasites (Sleebs et al., 2014). Plasmepsin V is also actively expressed in gametocyte stages and its chemical inhibition blocks formation of mature *P. falciparum* gametocytes and subsequent mosquito transmission (Jennison et al., 2019).

1.3.3 Sexual developmental stages: adaptive plasticity or hedging the bets?

Over the course of the parasite's IDC cycle in the mammalian host, a small proportion (<10%) of ring stage parasites commit to a sexual developmental cycle that produce transmissible forms of the parasite, male and female gametocytes. This process appears to be a conserved approach of evolutionary adaptation in which upon exposure to certain environmental cues, parasites can make a special investment in production of these transmissible forms which minimises their risk to extinction while at the same time maximises their fitness across generations (Ngotho et al., 2019). This could also be a finely tuned strategy of spreading the risk where due to multiple and diverse environments the parasites will more likely encounter, an evolutionary bet is spread by a

situational production of a small number of transmissible forms of the parasites in optimal proportions and numbers to ensure continued species survival in virtually all possible environmental encounters (Waters, 2016).

Generation of mature gametocytes (gametocytogenesis) in mammalian hosts varies significantly between *Plasmodium* spp., both in terms of duration to maturity and gametocyte morphology (Josling et al., 2018, Ngotho et al., 2019). In rodent malaria parasites *P. berghei* and *P. yoelii*, gametocytes maintain a spherical shape as they develop and take approximately 24-26 hours to mature (Josling et al., 2018, Mons, 1985). *P. falciparum* gametocytes take 9-12 days to mature and undergo five morphological distinguishable stages (stage I-V) over the course of development (Hawking et al., 1971). Typically, stage I gametocytes retain core structural features of trophozoites and cannot be morphologically distinguished. Stage II gametocytes attain a pointed end morphology with an oat grain or half-moon like shape. In stage III and IV, gametocytes attain a spindle shape that resemble blunt ends for the former and pointed ends for the latter. Mature, fully grown stage V gametocytes attain the signature falciform sickle shaped crescent shape (Figure 1.5).

1.3.3.1 A molecular switch to sexual differentiation

The underlying molecular mechanisms of switching from the asexual IDC to the sexual stage that generates transmissible forms of the parasite have for long been unknown. Meanwhile, forward genetic screens have recently been used to identify a key transcription factor that controls this intricate switch. As it is common for lab adapted *P. falciparum* isolates to lose the ability to produce gametocytes after an extended period of *in vitro* asexual propagation, sequencing of these *P. falciparum* gametocyte non-producers as well as *P. berghei* gametocyte non-producer lines which were generated by continuous blood passage in mice revealed that the lost ability to produce gametocytes was due to mutations in an ApiAP2 gene transcription factor, AP2-G (Sinha et al., 2014, Kafsack et al., 2014).

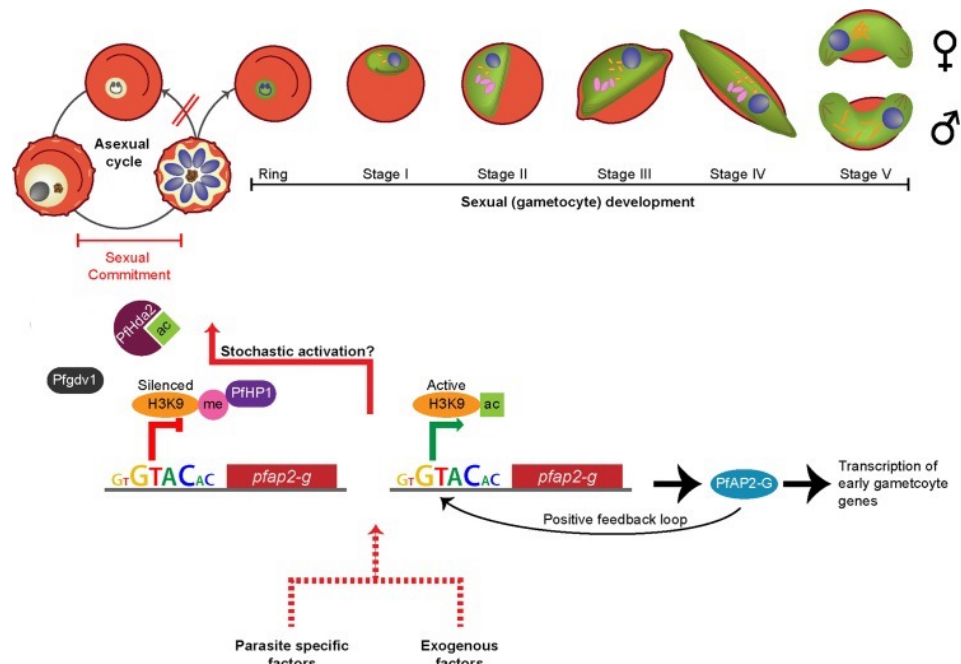


Figure 1.5: Sexual developmental switch in malaria parasites.

During the blood stage IDC, commitment to sexual differentiation occurs in a small proportion of the parasites during the previous asexual cycle that results in development of sexually committed schizonts to gametocyte stages even though artificial induction of sexual commitment in the same cycle has been reported. This sexual developmental switch is regulated by a master transcription factor AP2-G. AP2-G is epigenetically regulated by HP-1 and Hda-2 while at the same time regulates itself through a positive feedback loop mechanism. Other regulators of AP2-G include GDV-1 which evicts HP-1 from epigenetically repressed AP2-G which in turn enhances gametocytogenesis. Even though parasite or environmental exogenous factors influence gametocytogenesis, AP2-G could also be amenable to a stochastic activation which would allow baseline low level production of gametocytes for continued transmission. Induction of AP2-G leads to transcription of gametocyte specific genes that facilitate development and maturation of stage I-V gametocytes in *P. falciparum*. Figure adapted from (Nilsson et al., 2015).

Reverse genetics approaches confirmed the role of AP2-G in gametocytogenesis as deletion of this gene in both *P. berghei* and *P. falciparum* attenuates gametocyte production while allelic replacement of mutant AP2-G in gametocyte non-producer lines with wild type copies restores the gametocyte producing phenotype (Kafsack et al., 2014, Sinha et al., 2014). It has also been demonstrated in both *P. falciparum* and *P. berghei* that AP2-G recognizes a motif upstream of its own coding sequence, and deletion or mutation of this motif stops or impairs production of gametocytes in what would be an

autoregulatory positive feedback loop (Sinha et al., 2014, Josling et al., 2020). This level of sexual commitment appears to occur in a previous life cycle of the parasites where maturing schizonts in the ensuing cycle are already pre-committed to either producing asexual cell progenies or gametocytes (Bruce et al., 1990, Brancucci et al., 2018). Meanwhile, consistent with the hallmarks of a master regular, conditional overexpression of AP2-G in both *P. falciparum* and *P. berghei* in ring stage parasites can reprogram these stages into sexual forms in the same cycle which results in a dramatic rapid increase in production of gametocytes (Bancells et al., 2019, Kent et al., 2018). AP2-G is epigenetically controlled by heterochromatin protein 1 (HP-1) and a histone deacetylase 2 (Hda-2) (Coleman et al., 2014, Brancucci et al., 2014). Conditional depletion of both Hda-2 and HP-1 doesn't just regulate the epigenetic status of AP2-G, but also disrupts the monoallelic expression of virulence associated genes which are also amenable to epigenetic silencing (Brancucci et al., 2014, Coleman et al., 2014). More interestingly, a *P. falciparum* gametocyte development 1 (GDV-1) gene which was identified upon sequencing of other non-gametocyte producing lines (Eksi et al., 2012) appears to act upstream of the sexual commitment by evicting HP-1 from the epigenetically repressed AP2-G (Filarsky et al., 2018). Overexpression of GDV-1 results in markedly reduced occupancy of HP-1 at the AP2-G locus which in turn results in significant increase in gametocytogenesis (Filarsky et al., 2018).

1.3.3.2 Environmental players of sexual commitment

Several environmental factors that affect commitment to gametocytogenesis have been identified. Among these include the use of conditioned spent medium (Williams, 1999), presence of young RBCs “reticulocytes” (Trager and Gill, 1992) as well as antimalarial drugs (Buckling et al., 1999). The use of spent media relies on stressing parasites at high parasitaemia which is, indeed, the basis for most current lab methods used in inducing gametocytogenesis in *P. falciparum* *in vitro* (Brancucci et al., 2015). Nevertheless, how these environmental players link to molecular and genetic processes that regulate commitment remain unknown (Ngotho et al., 2019, Josling et al., 2018).

Only recently, it has been demonstrated that a component of human serum, lysophosphatidylcholine (LysoPC), can mediate different levels of commitment

to gametocytogenesis in the right parasite genetic background (Brancucci et al., 2017). Depletion of LysoPC in *in vitro* *P. falciparum* cultures results in increased production of gametocytes which, thus far, is the only defined environmental inhibitor to the production of gametocytes. This would also partly explain numerous previous observations of using conditioned spent media to stimulate gametocytogenesis which would indeed be deficient in LysoPC (Brancucci et al., 2017). Transcriptomic profiling of LysoPC treated and untreated parasites revealed that chromatin modifying enzymes are upregulated in LysoPC mediated sexual differentiation which would suggest a possible link between LysoPC and epigenetic de-repression of AP2-G (Brancucci et al., 2017). However, even though low LysoPC levels affect parasite growth and sexual differentiation in *P. falciparum*, these effects do not equally translate in *P. berghei* as despite influencing the schizont development stage, depletion of this factor does not affect gametocyte production in this parasite (Brancucci et al., 2017). This illustrates that differences in genetic and epigenetic makeup as well as diverse environmental cues can significantly influence how different *Plasmodium* spp. or parasite lineages in the same spp. commit to gametocytogenesis. Indeed, it has also been demonstrated that intensity of transmission can also influence different rates of commitment among field *P. falciparum* strains (Rono et al., 2018).

Nevertheless, even though it is clearly evident that environmental cues play a significant role in sexual commitment, it is more likely that basal levels of gametocytogenesis are an intrinsic feature of malaria parasites which through a stochastic and possibly bet hedged strategy allows for a production of low numbers of gametocytes that are ready for transmission during each IDC cycle. This could be due to various environment, genetic and epigenetic factors leading to stochastic expression of AP2-G (Waters, 2016, Ngotho et al., 2019, Josling et al., 2018), the molecular interplay of which require detailed characterisation.

1.3.3.3 Gene regulation during commitment and gametocyte development

Historical characterisation of transcription during gametocytogenesis has been challenging due to difficulties in isolating sufficient number of gametocytes at specific stages for transcriptomic profiling. However, recent identification of AP2-G and LysoPC has provided important genetic and environmental conditions

that can be manipulated to produce significant number of gametocytes for transcriptomic analysis.

Comparisons of AP2-G mutant parasites with non-mutants revealed that AP2-G activity specifically enriches for gametocyte specific genes among which include P27/25, P14.744, P16, P14.745 and P14.748; all of which are important for gametocyte development (Kafsack et al., 2014). On the contrary, genes that are involved in host cell remodelling and or virulence during the asexual IDC stages are epigenetically silenced in gametocytes (Fraschka et al., 2018). In what is a classic “just in time expression system”, gene expression in gametocytes is also regulated by translational repression where genes that are required for development in the mosquito vector are actively transcribed in gametocyte stages but are stored in translationally repressed mRNA bodies until activated in the vector (Mair et al., 2006). Comparisons of transcriptomes of parasites in which sexual commitment is inhibited by LysoPC to untreated parasites has also revealed gene transcripts that are upregulated during early stages of gametocytes, some of which include metabolism related genes of the Kennedy pathway that appear to be involved in regulation and or induction of sexual commitment (Brancucci et al., 2017). Meanwhile, an AP2-G overexpression system in *P. berghei* has been used to identify gene transcripts that define and or predominate in very early stages of sexual commitment (~6 hours), some of which include male gametocyte developmental gene 1 and nucleic acid binding proteins (Kent et al., 2018). This is also seemingly evident when AP2-G is overexpressed in *P. falciparum* as up to 90% sexual conversion can be achieved despite the resultant gametocytes failing to transmit (Llorà-Batlle et al., 2020).

1.3.3.4 Gamete formation and zygote development

Mature gametocytes circulating in the mammalian host are taken up by a mosquito vector during a blood meal into the midgut where an active escape from RBCs leads to the formation of gametes in a process that is called gametogenesis. Within 10 minutes of ingestion, male and female gametocytes activate and differentiate into eight flagellate microgametes (exflagellation) and a single spherical macrogamete respectively (Aly et al., 2009).

Upon encountering the mosquito's microenvironment in the midgut, three distinct environmental signals have been identified to play a crucial role in differentiation of gametocytes to gametes. These include a 5°C temperature drop which is critical for gametocyte activation (Sinden et al., 1996), a pH rise from 7.3 to 8 (Kawamoto et al., 1991) and the presence of a mosquito derived intermediate of tryptophan catabolism, xanthurenic acid (XA) (Billker et al., 1998, Garcia et al., 1998). Even though detailed signalling mechanisms involved are yet to be fully characterised, a XA triggered increase of intracellular calcium (Ca^{2+}) is thought to activate a calcium dependent protein kinase, CDPK4, which upon activation mediates cell cycle progression and exflagellation of male gametocytes (Billker et al., 2004). XA can also enhance the activity of a guanylyl cyclase (GC) in gametocyte membrane fractions which increases the levels of a second messenger cGMP (Muhia et al., 2001). In *Plasmodium*, only 2 GCs (GC α and GC β) have been identified, of which GC α is possibly central in cGMP synthesis as deletion of GC β is readily achievable and results in viable gametocytes that are able to exflagellate and fertilise (Moon et al., 2009). Increase in intracellular levels of cGMP activates a cGMP-dependent protein kinase (PKG) which acts as a master regulator of the signalling cascade during gametogenesis (McRobert et al., 2008). Indeed, chemical inhibition of PKG prevents rounding up of gametocytes and prevents male gametocyte exflagellation (McRobert et al., 2008). More recently, an intracellular membrane protein; gametogenesis essential protein 1 (GEP1) has been shown to play a critical role in regulating XA mediated gametogenesis in the rodent malaria parasite *P. yoelii*. Disruption of GEP1 blocks XA mediated synthesis of cGMP and downstream effects such as Ca^{2+} mobilisation and gamete formation. GEP1 also co-localises with GC α further illustrating that this parasite protein acts as a crucial XA-cGMP-PKG axis link in the gametogenesis signalling cascade and could thus be a crucial vaccine or drug target to block malaria transmission (Jiang et al., 2020).

Activation of gametocytes is thus a rapid stage conversion which within 10 minutes results in rounding up of gametocytes (in *P. falciparum*), egress from RBCs and transformation into male microgametes and female macrogametes. Activated male gametocytes replicate their genome three times into an octaploid which produces eight microgametes in a round of mitotic cell division

(Janse et al., 1986). Mediated by serine or cysteine proteases, egress of activated gametes from RBCs involves a rapid (seconds) multisite rupture of the PVM which is followed by a disintegration of subpellicular membrane and eventual rupture of the RBC (Sologub et al., 2011). Electron dense membrane vesicles (osmiophilic bodies) which predominantly associates with female gametocytes, but have also been observed in males, accumulate underneath the PVM immediately before rupture (Olivieri et al., 2015). Osmiophilic bodies carry several gametocyte specific proteins such as Pg377, MDV-1/Peg3 and the gamete egress and sporozoite traversal (GEST) which are released into the PV immediately after gametocyte activation, reviewed by (Bennink et al., 2016). Pg377 is involved in gamete egress in *P. berghei* (Olivieri et al., 2015), but this function is not conserved in *P. falciparum* (Suaréz-Cortés et al., 2014). Gene disruption of MDV-1/Peg3 or GEST impairs egress of male and female gametes in the rodent malaria parasite *P. berghei* (Ponzi et al., 2009, Talman et al., 2011).

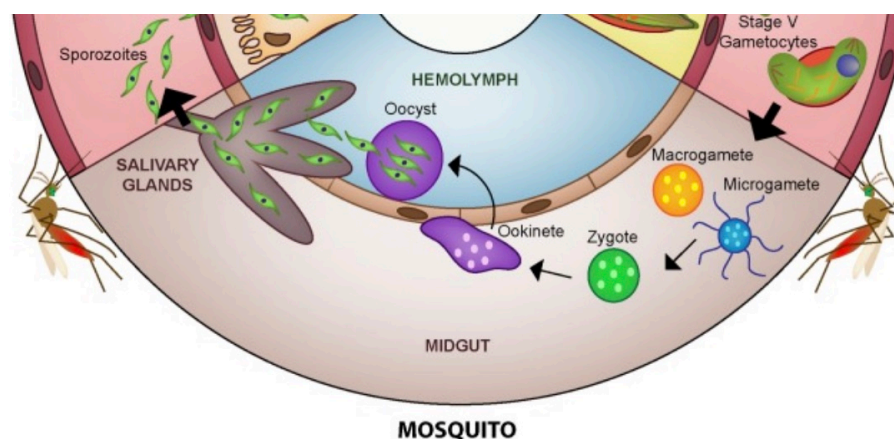


Figure 1.6: An illustrated life cycle progression of malaria parasites in the mosquito vector.

Uptake of mature stage V gametocytes (in *P. falciparum*) by a mosquito vector leads to their activation in the midgut. This is environmentally triggered by a drop in temperature, increase in pH and the mosquito derived factor, XA. Activated gametocytes egress from RBC as male gametes (microgametes) and female gametes (macrogametes). Micro and macrogametes fertilise upon contact to form a zygote which differentiates into an ookinete. The ookinete escapes the mosquito midgut into basal laminal epithelial cells where it develops into a mature oocyst carrying fully developed sporozoites in 10-12 days. Sporozoites bud off from the oocyst into the haemolymph where they migrate to the salivary glands. Once in the salivary glands, they can be taken up by a mosquito and re-injected in a mammalian host. Figure adapted from (Nilsson et al., 2015).

For fertilisation to take place, emerged microgametes and macrogametes come into contact with each other and fuse their membranes. Just before this occurs, a calcium dependent protein kinase 1 (CDPK1) mediates a specific activation of some of the translationally repressed mRNAs in macrogametes (Sebastian et al., 2012) which are silenced during the mammalian stage of gametocyte maturation by the DDX6 class RNA helicase, DOZI (development of zygote inhibited) and the Sm-like factor, CITH (homolog of worm CAR-1 and fly Trailer Hitch) (Mair et al., 2006, Mair et al., 2010). Motile microgametes actively seek macrogametes until an attachment is established. Proteins involved in microgamete attachment to macrogametes include LCCL-domain family of proteins as well as the 6-cysteine motif family of proteins, most notably the P48/45 and P230, reviewed by (Bennink et al., 2016). P48/45, which is expressed on the surface of both micro and macrogametes, is essential for fertilisation to occur as disruption of this gene greatly impacts zygote formation (van Dijk et al., 2001). P48/45 and P230 are indeed lead vaccine targets for potential transmission blocking vaccines as antibodies targeting these proteins inhibit development of zygotes (Acquah et al., 2019).

Fusion of microgametes and macrogametes plasma membranes initiates fertilisation which is preceded by entry of the microgamete's nucleus and axonemes into the macrogamete. A microgamete-specific plant like reproduction factor, generative cell specific 1 (GCS1) also known as HAP2, plays a crucial role in these membrane fusions as it has been demonstrated that knockout of this gene leads to total male sterility and unsuccessful fertilization (Liu et al., 2008, Hirai et al., 2008). Nuclear fusion follows the plasma membrane fusion which then undergoes meiotic cell division producing a tetraploid zygote (Janse et al., 1986). A family of NIMA-related protein kinases, NEK-2 and NEK-4, play a critical role in this stage of meiotic division as disruption of these genes results in dysregulated DNA synthesis, blocks genome replication to tetraploid level and abolishes zygote differentiation into ookinetes (Reininger et al., 2005, Reininger et al., 2009).

1.3.3.5 Ookinete-oocyst to sporozoite differentiation

In the mosquito midgut, zygotes mature over 18-24 hours into motile forms of parasites called ookinetes which are characterised by an elongated and polarised

morphology and exhibit a tight gene expression cascade. Controlled by the APiAP2 transcription factor AP2-0 (Yuda et al., 2009), over 500 genes which are important for ookinete development have been identified in malaria parasites (Kaneko et al., 2015). Some of these genes include components of the glideosome GAP40, GAP45 and GAP50 which would play an important role in ookinete motility, putative ookinete secreted proteins PSOP-1, PSOP-2, PSOP-6, PSOP-7 and PSOP-12, putative ookinete surface proteins 1-10, P25 and P28 (Kaneko et al., 2015). The ookinete surface proteins P25 and P28 are indeed potential transmission blocking vaccine targets as simultaneous knockout of these genes prevents the transition of ookinetes to oocysts by blocking traversal through the mosquito midgut epithelium (Tomas et al., 2001). Meanwhile, downregulation of GAP45 results in zygotes which fail to mature and transform into ookinetes (Sebastian et al., 2012). cGMP-PKG signalling also appears to play a role in regulating ookinete motility as PKG inhibitors blocks ookinete gliding (Moon et al., 2009).

Mature motile ookinetes traverse the mosquito midgut into the basal lamina of the epithelial midgut where oocyst development takes place (Figure 1.6). Even though exact details of traversal are not clearly understood, several microneme proteins have been implicated some of which include the five members of the *Plasmodium* PLPs and the cell-traversal protein for ookinetes and sporozoites (CelTOS), reviewed by (Bennink et al., 2016). Just before exit from the midgut lumen, the ookinete releases a chitinase which facilitates the breakdown of a chitin polysaccharide rich membrane which lines the mosquito midgut and provide protection to the host from food particles as well as bacterial or viral infections (Vinetz et al., 1999, Shahabuddin et al., 1993). Chemical inhibition of chitinase and or gene disruption of the *P. falciparum* chitinase gene impairs ookinete traversal of the midgut and prevents oocyst development (Tsai et al., 2001, Shahabuddin et al., 1993). Oocysts develop at the basal lamina of the mosquito immediately after ookinete traversal from the midgut with the sole aim of producing viable transmissible forms of the parasites, sporozoites. Oocyst development takes approximately 10-12 days and results in 50-60 μm diameter sized parasite stages making it the longest as well as largest life cycle stages of malaria parasites (Canning and Sinden, 1973). During the initial stages of sporozoite formation in the oocysts, the plasma membrane retracts to form

cytoplasmic lobes while at the same time the nucleus undergoes multiple rounds of division to produce thousands of haploid nuclei (Canning and Sinden, 1973). This process (called sporogony) which is partly aided by CSP, results in formation of sporoblasts which are precursor sporozoites marked with CSP on the membrane and nuclei localisation to the periphery (Thathy et al., 2002). CSP plays a critical role in formation of sporoblasts as disruption of this gene attenuates sporozoite development within oocysts (Ménard et al., 1997). After developmental maturation, sporozoites bud from sporoblasts into the oocyst and attain a crescent shape before escaping the oocyst into the mosquito haemolymph. It remains to be determined the exact molecular events that precedes sporozoite release. However, a cysteine protease “egress cysteine protease 1” (ECP-1) is likely essential during this process as deletion of ECP-1 in *P. berghei* traps mature sporozoites in the oocysts (Aly and Matuschewski, 2005). Sporozoite escape also seems to be aided by region II plus of CSP as substitution of this region with alternative amino acids (alanine residues) prevents exit of sporozoites from oocysts (Wang et al., 2005). More recently, gene deletion of newly identified oocysts rupture proteins (ORPs) 1 and 2 has been shown to prevent oocyst rupture and release of sporozoites (Currà et al., 2016).

Thousands of sporozoites are released from each oocyst which migrate throughout the mosquito's tissues aided by haemolymph circulation. While passing through the salivary glands, specific parasite ligands recognise host cell receptors in the basal lamina allowing a specific capture of sporozoites into the mosquito's salivary glands. This process is highly inefficient as >75% of sporozoites are lost and degraded in circulation while less than a quarter make it to the salivary glands (Baton and Ranford-Cartwright, 2005). Several parasite ligands that facilitate sporozoite attachment into the salivary glands have been identified. Specifically, region I of the CSP is apparently a ligand for receptors on the luminal surface of mosquito vectors and facilitates sporozoite attachment (Sidjanski et al., 1997). A thrombospondin-related anonymous protein (TRAP) also plays an important role in salivary gland invasion of sporozoites as deletion of this gene in *P. berghei* attenuates sporozoites gliding motility and blocks sporozoites infection of salivary glands (Sultan et al., 1997). The CSP multifunctional role in facilitating mammalian hepatocyte invasion of sporozoites as well as development and progression through the mosquito oocyst

to sporozoite stages has made it a very promising vaccine candidate. Indeed, a malaria vaccine which is currently under pilot rollout, RTS-S, is based on a recombinant CSP (Rts, 2015). When a mosquito bites a mammalian host, around 100 sporozoites are injected into the blood stream in experimental conditions which can be as few as <50 in natural infections initiating the cycle again (Menard et al., 2013).

1.4 Malaria prevention and control

Despite the complicated life cycle of malaria parasites and several possible intervention points, there is a relatively small set of tools for malaria control and prevention. These mainly evolve around integrated vector management and effective malaria therapeutics even though malaria vaccines are slowly becoming an option.

1.4.1 Insecticides in malaria control

Malaria vector control is of special focus as it offers a direct interruption of the malaria parasite life cycle (Figure 1.2) by directly blocking transmission to humans (and zoonotic reservoirs). Major interventions which are being employed in mosquito vector control programs include the use of long-lasting insecticidal bed nets (LLINs) and indoor residual spraying (IRS) of insecticides. LLIN and IRS programs have been massively implemented in malaria endemic regions of the world and have accounted for 78% of the 663 million malaria cases averted since the early 2000s (Bhatt et al., 2015). As of 2018, over 50% of the population at risk in Sub-Saharan Africa was protected from malaria by LLINs interventional programs (WHO, 2019). Despite these significant gains, the use of insecticides in vector control has recently become under threat as mosquito vectors are increasingly becoming resistant to pyrethroids which are the primary insecticides currently in use in both LLIN and IRS programs (Hemingway et al., 2016a).

Resistance to pyrethroids was first reported in the early 1970s in Sudan and subsequently spread to West Africa in the 1990s (Brown, 1986, Elissa et al., 1993). Since the beginning of the 21st century, pyrethroid resistance has significantly spread and is now endemic in almost all parts of Africa with active malaria transmission (Ranson, 2017). As of 2016, 77% of countries monitoring

pyrethroid effectiveness have reported some form of vector resistance to this class of insecticides (WHO, 2018b). Four genetic bases of insecticide resistance have been described in mosquito vectors. Of these, the best characterised are target site point mutations which alter the voltage gated sodium channels (direct target of pyrethroids) by reducing their affinity to the compounds. In the African mosquito vector *Anopheles gambiae*, knock down resistance alleles in the same codon position of the sodium channel (1014F and 1014S) strongly associate with pyrethroid resistance and are indeed the basis of multiple on-site field molecular diagnostics for monitoring resistance (Donnelly et al., 2009, Wang et al., 2015c). A second form of pyrethroid resistance is “metabolic” based as decreased susceptibility to insecticides is conferred by elevating the activities of cytochrome P450s or glutathione transferases (GSTs) which results in sequestration and detoxification of the compounds (Ranson, 2017). Even though the genetic mechanism underlying this form of resistance is yet to be characterised in detail, amino acid substitutions and or overexpression of the GST gene have been used to associate some pyrethroid metabolic resistance phenotypes to genotypes (Lumjuan et al., 2005, Riveron et al., 2014). Meanwhile, in *Anopheles funestus*, directional selection through mutations in a regulatory element close to the *CYP9P9* gene of the cytochrome P450 family have been shown to drive pyrethroid resistance in field vector populations (Riveron et al., 2013). However, even though experimental transgenic expression of the *CYP9P9* gene in *Drosophila* confers resistance to pyrethroids (Riveron et al., 2013) and many other studies have reported candidate cytochrome P450 enzymes involved in driving metabolic resistance, identification of specific loci that drive overexpression of these genes has so far remained elusive (Ranson, 2017).

Besides the above major determinants of pyrethroid resistance, cuticular (or reduced penetrance) and behavioural resistance are other forms of resistance, which though minor, are seemingly evolving in Africa. Cuticular resistance involves thickening of the mosquito’s cuticle which reduces uptake and penetration of insecticides. Thickening of the cuticle has indeed been attributed to pyrethroid resistance in *Anopheles funestus* (Wood et al., 2010).

Environmental use of LLINs and IRS programs could also force a behavioural adaptive evolution of mosquitos. Success of LLINs and IRS programs rely on

indoor transmission behaviour of mosquito's and these have indeed been successfully exploited as despite intensive use of LLINs and IRS over the past decade, malaria transmission in Africa appear to still occur indoors (Bayoh et al., 2014). However, these behaviour's require constant surveillance and monitoring as evolution to outdoor transmission would be a further catastrophe to ITN and IRS programs in Africa as seems to be the current case in South America and Asia (Gryseels et al., 2015, Santos et al., 2009).

1.4.2 Malaria vaccines

Besides vector control, development of an effective malaria vaccine has remained a key priority in global malaria control programs especially in the current era of accelerated eradication efforts. Modern pursuits of a malaria vaccine have largely been based on early seminal work which demonstrated a protective immunity in mice upon injection with irradiated sporozoites of the rodent malaria *P. berghei* (Nussenzweig et al., 1967). This was also later replicated in humans as experimental challenge with radiation-attenuated sporozoites resulted in protection against *P. falciparum* infection (Rieckmann et al., 1979). However, over five decades down the line, a highly effective malaria vaccine is still elusive despite some strides that have seen a malaria vaccine, RTS, S, entering pilot rollout in the malaria endemic regions of the world (Rts, 2015, Draper et al., 2018, WHO, 2019). Research efforts towards malaria vaccines have focussed on targeting liver stages (pre-erythrocytic) to prevent establishment of infection, blood stages (erythrocytic) to prevent clinical disease and mosquito stages to block transmission.

Pre-erythrocytic or sporozoite based vaccines have thus far been the most promising and extensively tested vaccine candidates with the lead RTS, S vaccine now entering pilot rollout (Draper et al., 2018, WHO, 2019). The RTS, S developed by GlaxoSmithKline is a virus like particle consisting of a recombinant C-terminal of CSP fused to the hepatitis B virus surface antigen (HBsAg) with a liposomal adjuvant system. So far, the RTS, S remains the only malaria vaccine that has shown clinical efficacy in Phase III clinical trials. However, efficacy of this vaccine appears to be modest as despite offering protection to clinical disease by up to 51% in three vaccination formulations for children aged between 5-17 months, this seems to be relatively lower in young infants aged 6-

12 weeks (~26%). Moreover, this vaccine induced immunity appear to wane over time (Rts, 2015). Nevertheless, pilot rollout of the RTS, S vaccine is currently ongoing in Malawi, Ghana and Kenya (WHO, 2019, WHO, 2016). Besides subunit sporozoite vaccines, whole sporozoite vaccines made up of irradiated sporozoites (PfSPZ) have been actively pursued despite underlying challenges in isolating enough quantities of purified sporozoites for clinical trials in humans and the requirement of subcutaneous mosquito bites for delivery. However, recent technology advances have been used to successfully isolate and cryopreserve these irradiated sporozoites as well as use alternative intravenous administration to elicit robust immune responses (Seder et al., 2013, Hoffman et al., 2010). More encouragingly, exploratory clinical trials of the PfSPZ vaccine in Mali have shown protective efficacies of up to 48% even though further trials in multiple geographical areas are required (Sissoko et al., 2017).

Frequent exposures to malaria parasites in the blood stream is known to elicit broad antibody repertoires and immuno-regulatory cellular states that provide a state of naturally acquired immunity (NAI) in preceding parasite exposures (Doolan et al., 2009). Chemically attenuated blood stage vaccines as well as those targeting specific subunits such as the placental *var* gene antigen VAR2CSA have been developed and trialled not just to mimic NAI, but to also possibly prevent the outcomes of severe malaria disease (Raja et al., 2017, Pehrson et al., 2017). However, most of these approaches have failed to produce significant efficacy in trials. This is partly due to the complex life cycle of the parasite (Figure 1.2), polymorphic strain specific antigens which do not cover substantive antigenic variation as well as highly developed immune evasion mechanisms in the parasites (Draper et al., 2018). Use of NAI pooled antibodies from African adults have been used to demonstrate that passive immunisation can be used to prevent severe disease in children by lowering parasitaemia through a targeted immunological inhibition of blood stages of the parasites (Cohen et al., 1961). However, these approaches have again not been actively pursued possibly due to underlying problems listed above as well ethical and safety issues regarding potential viral contaminations. Recent pursuits in development of subunit blood stage vaccines have also benefitted from the identification of the merozoite invasion ligand PfRH5 and its interaction with the basigin receptor on RBCs (section 1.3.2.1). Experimental vaccination of *Aotus* monkeys with PfRH5

induces antibodies that can block development of several lab as well as clinical *P. falciparum* isolates and more importantly prevents infection in ensuing parasite challenges (Douglas et al., 2015). As further structural and functional characterisation of PfRH5 based vaccines continues, clinical evaluation of their efficacy in humans will hopefully provide a further scope of their potential.

Transmission blocking vaccines (TBV) are malaria vaccine strategies that target sexual transmissible forms of the parasite. This is specifically important for recent accelerated efforts towards malaria eradication as these vaccines would crucially interrupt the parasite life cycle without necessarily delivering any clinical benefit. Several TBV vaccines have been trialled of which the leading candidates are those based on the ookinete surface protein P25 as well as the gamete antigens P45/P48 and P230 (Acquah et al., 2019). Preclinical evaluation of antibodies produced upon vaccination of mice with these antigens yielded strong transmission inhibitory phenotypes in standard membrane feeding assays using lab adapted *P. falciparum* strains (Kapulu et al., 2015). Hampered by the inability to produce clinically safe immunogens with most of these TBV candidates, efforts to develop P25 or P48/P45 based TBVs that are both safe and immunogenic are currently ongoing, reviewed by (Draper et al., 2018).

Nevertheless, despite the slow pace, malaria vaccine development efforts are rapidly improving as evidenced by the recent pilot introduction of the RTS, S. However, significant challenges are still in place. For instance, despite the complicated life cycle of malaria parasites that involves multiple morphological stage transitions, stage transcending immunity is not known to occur. As efforts to develop a vaccine that covers all life cycle stages continue in what would ideally be a “perfect vaccine”, a combination of different vaccines in “multi-stage” vaccine strategies would alternately provide a quick way of assessing additive or synergistic vaccine combinations that can be progressed. Indeed, recent preclinical evaluation that has demonstrated synergy between TBVs and pre-erythrocytic vaccines in the rodent malaria *P. berghei* nicely illustrates this potential (Sherrard-Smith et al., 2018) and could be further exploited as more vaccines and vaccine candidates are developed.

1.5 Antimalarial drugs and resistance

Antimalarial drugs are significant components of malaria control and prevention programs. They play a crucial role in preventing disease through chemoprophylaxis, intermittent prevention during pregnancy, preventing progression of severe disease and can as well be used in transmission blocking. Several classes of antimalarial drugs are currently in use for malaria treatment. These include quinolones, antifolates, naphthoquinones, artemisinin's, macrolides and tetracyclines which are classified based on relatedness of chemical scaffolds or mode of action (Table 1.1, Figure 1.7). The use of antimalarial drugs in malaria control was revolutionised in the 1930s when chloroquine (CQ), a 4-aminoquinolone, was discovered and formed the basis of malaria treatment for over four decades from the early 1950s to the 1990s. However, this apparent success which almost drove malaria to eradication (Hay et al., 2004), was quickly offset by emergence of resistance which rendered CQ to an almost unusable state in the early 1990s. Emergence of drug resistance in malaria parasites has thus far been a historical trend to almost all clinically available drugs (Table 1.1). This appears to be an evolutionary adaptation through a positive selection strategy that allows for propagation and maintenance of parasite lineages that carry genetic or phenotypic traits which minimises their elimination from the host upon drug treatment. Ideally, the mode of resistance (MOR) to most antimalarial drugs is frequently related to the mode of action (MOA) as mutations or alterations in the drug target routinely leads to either reduced uptake of the drug, increased efflux or changes in the target that reduces drug binding affinity or results in its overexpression (Fairlamb et al., 2016). However, these associations can also be obscure as in some cases, the MOA of certain antimalarial drugs have remained unknown or debatable despite well characterised resistance mechanisms.

In a simple linear evolutionary model, emergence of resistance is relatively straightforward when drugs are used as monotherapies. Under lab conditions, spontaneous mutations from drug sensitive to resistant alleles can emerge at the rate of 10^{-9} per nucleotide site per mitotic division (Paget-McNicol and Saul, 2001). This means in a complex human host environment where parasite biomass can reach as high as 10^{12} , at least 10^3 parasites will carry resistant conferring alleles and will be preferentially selected for upon further drug treatment or subsequent successful transmission. However, due to the complex parasite life

cycle (and or genetic differences between strains), differences in pharmacological profiles of individual drugs as well as recent combinational therapy approaches, these evolutions can be far from linear. For example, exposure of parasites with different pre-existing drug resistance conferring mutations to classes of drugs with different MOA can result in significant variations in the frequency of acquisition of resistance alleles (Rathod et al., 1997). Using two different parasite clones, one which was sensitive to all traditional antimalarial agents (D6) and the other which was resistant (W2), it was demonstrated that acquisition of drug resistance mutations to novel drugs with different MOA was more frequent in the W2 clones (up to 1000 fold) relative to the D6 clones (Rathod et al., 1997). Such phenotypes, also called “accelerated resistance to multiple drugs” (ARMD) could indeed have significant implications in the emergence of drug resistant malaria as it would mean resistance emerging from very few geographically localised strains; and/or easy propagation of such mutations in parasite backgrounds that may be already carrying appropriate compensatory or synergistic mutations. Indeed, genetic analysis of parasites resistant to CQ and some antifolates has demonstrated that resistance to these drugs emerged and spread from very few independent strains despite the worldwide usage of the drugs at the time (Roper et al., 2003). The ARMD phenotypes have also attracted more attention recently as resistance to artemisinins has emerged and is seemingly dependent on permissive underlying genetic architectures (Zhu et al., 2018, Miotto et al., 2015).

Nevertheless, in what is typical of an evolutionary arms race, drug resistance of malaria parasites has always preceded the introduction of almost all known antimalarial drugs. Even though the probability of developing resistance can be lowered by using combination therapies or high barrier compounds, this race which at times could be for the swift and strong, is also a question of time and chance as inevitably drug resistance in malaria parasites appear to always emerge. So far, drug resistance in malaria parasites has been reported for almost all clinically available forms of the drugs, Table 1.1 (Haldar et al., 2018).

1.5.1 Quinolines

Quinoline antimalarials include drugs such as CQ, quinine, primaquine and mefloquine which are and have been at the centre stage of malaria treatment

for over seven decades. These drugs can be further subdivided into 4-aminoquinolines (CQ, amodiaquine, piperazine), aryl aminoalcohols (quinine, lumefantrine and mefloquine) or 8-aminoquinolines (primaquine) based on the position of the amino group and or additional side chains (Figure 1.7).

Quinine is the first reported chemical compound used to treat malaria with discovery dates going back as far as the early 1600s (Achan et al., 2011). It is derived from the bark of the Cinchona (quina-quina) tree from which it was first isolated as an active chemical in 1820 by Pierre Joseph Pelletier and Joseph Caventou. Over 400 years down the line, quinine remains an important drug for treatment of uncomplicated and severe malaria (WHO, 2019). Despite its long history, the MOA of quinine is not understood even though it is thought to act by inhibiting haem polymerisation as is seemingly the case for most quinolines. Low level resistance to quinine by malaria parasites was first reported in 1910 (Peters, 1982), even though this has remained at relatively low grade up to date (Achan et al., 2011). This low-level resistance appears to be mediated by polymorphisms in standard drug resistance genes such as the P-glycoprotein multi drug resistance transporter (PfMDR1) and the CQ resistance transporter (PfCRT). However, the mechanistic details of which are still unknown (Ferdig et al., 2004). Nevertheless, poor tolerability of this drug limits its use for treatment of severe malaria even though it is clinically available for treatment of uncomplicated malaria in combination with other agents (WHO, 2019).

After quinine, the 4-aminoquinoline drug CQ became the backbone of malaria treatment from the early 1950s up until resistance emerged but is still used in some parts of the world to a limited extent (Table 1.1). CQ remains one of the most efficacious, safe and affordable antimalarial drug to have ever been produced (Ecker et al., 2012). However, CQ resistance emerged only a decade after the inception of its use which led to its subsequent withdrawal from recommendation for primary treatment of *P. falciparum* infections. Malaria parasites, upon invading red blood cells, ingests large amounts of host haemoglobin into a localised parasite structure, the digestive vacuole (DV) also called the food vacuole. Within the DV, the parasite proteolytically cleaves haemoglobin which is aided by aspartic (Plasmepsin I and II) and cysteine proteases (falcipains) to release amino acids for the parasite protein synthesis

(Goldberg, 2005). This catabolic process releases large amounts of Fe^{2+} haem which is rapidly oxidized to Fe^{3+} haem (ferriprotoporphyrin IX or FPIX). Fe^{3+} haem is an insoluble moiety that is highly toxic to the parasite as it can rapidly disrupt the parasite membranes. Malaria parasites, therefore, biomineralise Fe^{3+} haem moieties to β -haematin forming chemically inert brown pigments of haemozoin which are characteristic signatures of developing trophozoite and schizont stages as well as the non-toxic storage form of waste (Bannister and Mitchell, 2003). Microscopically, haemozoin has been historically defined as the classical “malaria pigment”(Roepe, 2009).

CQ is a weak base which rapidly and freely diffuses across membranes in its neutral form. Upon crossing the DV, the acidic environment of the DV results in its protonation which makes it impermeable thereby accumulating in the DV up to 1000-fold. Protonated CQ is presumed to bind Fe^{3+} haem which prevents haem detoxification pathway poisoning the parasite with its own waste machinery (Roepe, 2009). CQ resistance is known to have originated in six different regions in South East Asia, South America and Western Pacific regions in the 1950-1960s before spreading to Africa in the late 1970s (Figure 1.8). Mutations in the *P. falciparum* CQ transporter, PfCRT, have been widely accepted as markers of CQ resistance (Ecker et al., 2012). PfCRT natural role is thought to be the transportation of peptides produced by the proteolytic digestion of haemoglobin across parasite membranes. Mutations in PfCRT, specifically the K76T mutation, have been shown to mediate efflux of protonated CQ from the DV reducing the drugs accessibility to its Fe^{3+} haem target (Ecker et al., 2012). However, in malaria endemic countries, K76T mutations have sometimes been carried without conferring CQ resistance. Some patients still respond to CQ despite the parasites having the mutation landscape (Valderramos et al., 2010). PfCRT therefore, appears to be a primary marker of resistance, but may require secondary determinants such as mutations in the PfMDR1 and other unidentified factors (Ecker et al., 2012). The current clinical status, proposed MOA and MOR for other quinoline antimalarial drugs are summarised in Table 1.1.

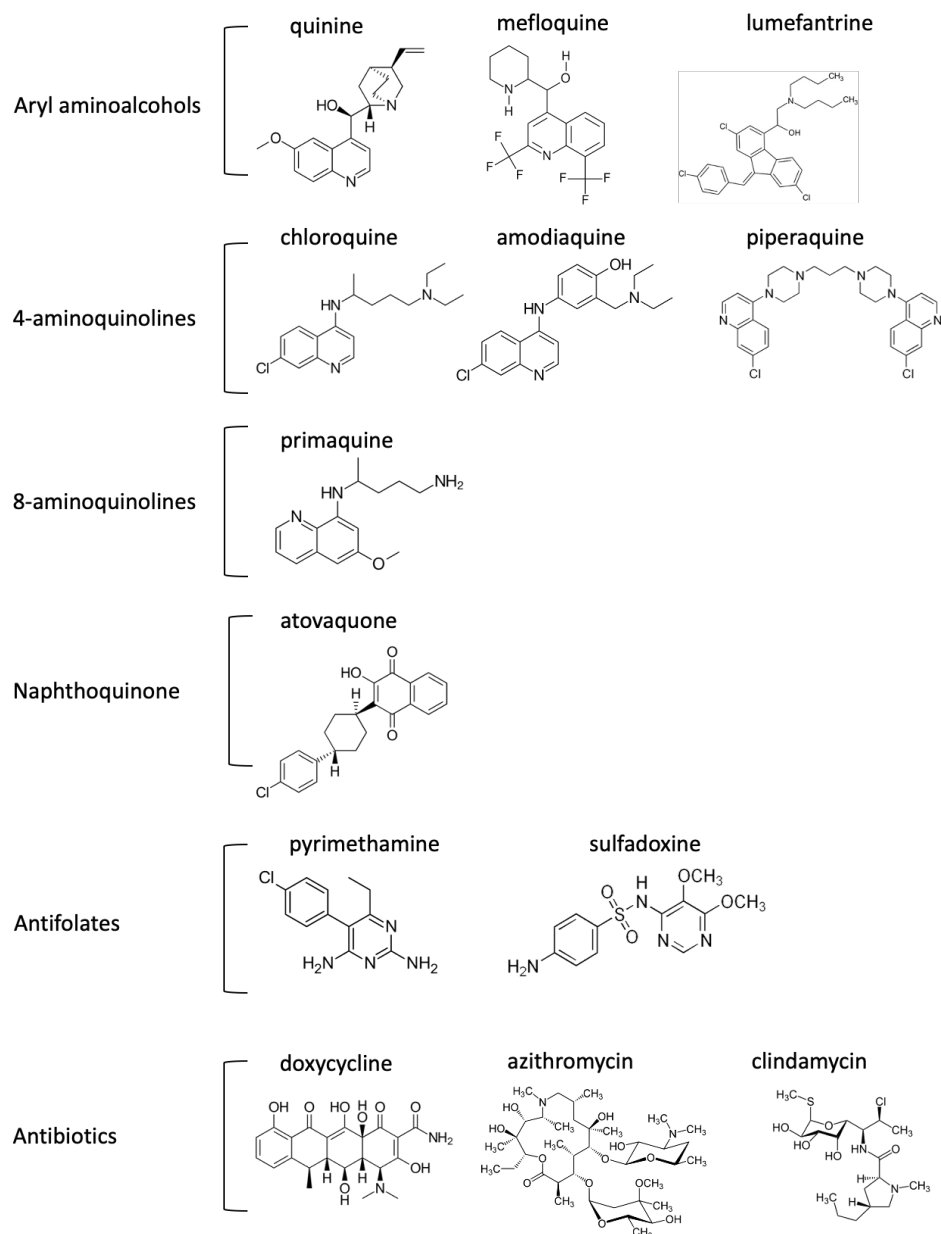


Figure 1.7: Chemical structure of common antimalarials in clinical usage.

The structures are for antimalarial drugs as summarised in Table 1.1

Drug Class	Class Examples	Current Clinical Usage	Proposed Mode of Action	Resistance Determinants
4-aminoquinolines	Chloroquine (CQ)	Treatment of <i>P. falciparum</i> and <i>P. vivax</i> malaria, uncomplicated cases ^a	Haem intoxication, accumulates in the digestive vacuole and inhibits parasite haem detoxification ^b .	PfCRT, PfMDR1 mutations, mediate efflux from digestive vacuole ^b .
	Amodiaquine (AQ)	Partner drug for ARTs and CQ for <i>P. falciparum</i> and <i>P. vivax</i> malaria, both severe and uncomplicated cases ^a .	Haem intoxication, accumulates in the digestive vacuole and inhibits parasite haem detoxification ^c .	Point mutations and copy number variations of PfMDR1 ^c
	Piperaquine (PPQ)	Uncomplicated <i>P. falciparum</i> malaria in combination with DHA ^a .	Unknown	Amplification of <i>plasmepsins</i> 2 and 3 ^d .
Aryl aminoalcohols	Quinine (Q)	Severe malaria ^a	Unknown, proposed to inhibit parasite haem detoxification ^c .	Point mutations and copy number variations of PfMDR1 ^c .
	Mefloquine	Severe and uncomplicated <i>P. falciparum</i> malaria, <i>P. vivax</i> malaria ^a .	Inhibits parasites 80S ribosome ^p , proposed to inhibit parasite haem detoxification ^c	Copy number variations of PfMDR1 ^c .
	Lumefantrine	Combination with AM ^a	Largely unknown	Point mutations and copy number variations of PfMDR1 ^f .

8-aminoquinolines	Primaquine (PQ)	Uncomplicated <i>P. falciparum</i> malaria in combination with CQ, SP or ARTs ^a , first choice drug for <i>P. vivax</i> malaria in combination with CQ ^a .	Unknown	Unknown
Endoperoxides	Artemisinin (ARTs)	Uncomplicated and severe forms of <i>P. falciparum</i> malaria in combination with other antimalarial agents ^a .	Unknown, disputed; promiscuous targeting of parasite components ^{e,f} .	Mutations and polymorphisms in the Kelch13 propeller domains ^g .
	Dihydroartemisinin (DHA)	Uncomplicated and severe forms of <i>P. falciparum</i> malaria in combination with other antimalarial agents ^a .		
	Artesunate (AS)	Uncomplicated and severe forms of <i>P. falciparum</i> malaria in combination with other antimalarial agents ^a .		
	Artemether (AM)	Uncomplicated and severe forms of <i>P. falciparum</i> malaria in combination with		

		other antimalarial agents ^a .		
Antifolates	Sulfadoxine-pyrimethamine	Uncomplicated <i>P. falciparum</i> malaria in combination with AS or PQ, first choice for intermittent prevention in pregnancy ^a .	Inhibits folate metabolism by acting on two enzymes; dihydroforate reductase (dhfr) and dihydropteroate sythetase (dhpts) ^h .	Mutations in dhfr and dhpts ^h .
	Proguanil (PG)	Chemoprophylaxis, uncomplicated <i>P. falciparum</i> malaria in combination with ATQ	Inhibits dhfr ⁱ	Mutations in dhfr ^j
Antibiotics	Tetracycline/Doxycyclines	Chemoprophylaxis, uncomplicated <i>P. falciparum</i> malaria, severe malaria in combination with Q ^a .	Inhibits protein synthesis in the parasite's apicoplast ^k .	Clinical resistance not reported - aside rare chemoprophylactic failures ^l .
	Macrolides (Clindamycin)	Uncomplicated and severe malaria in combination with Q ^a	Inhibits protein synthesis in the parasite's apicoplast ^m .	Not known
Naphthoquinone	Atovaquone (ATQ)	Chemoprophylaxis in combination with PG ^a .	Inhibits cytochrome bc-1 complex ⁿ .	Point mutations in the mitochondrial bc-1 ^o .

Table 1.1: Classes of selected antimalarial drugs in clinical use.

(WHO, 2019)^a, (Ecker et al., 2012)^{b c}, (Witkowski et al., 2017)^d, (O'Neill et al., 2010)^e, (Tilley et al., 2016)^f, (Ariey et al., 2014, Mbengue et al., 2015)^g, (Plowe et al., 1997)^h, (Srivastava and Vaidya, 1999)ⁱ, (Parzy et al., 1997)^j, (Dahl et al., 2006)^k, (Gaillard et al., 2015)^l, (Sidhu et al., 2007)^m, (Fry and Pudney, 1992)ⁿ, (Srivastava et al., 1997)^o, (Wong et al., 2017)

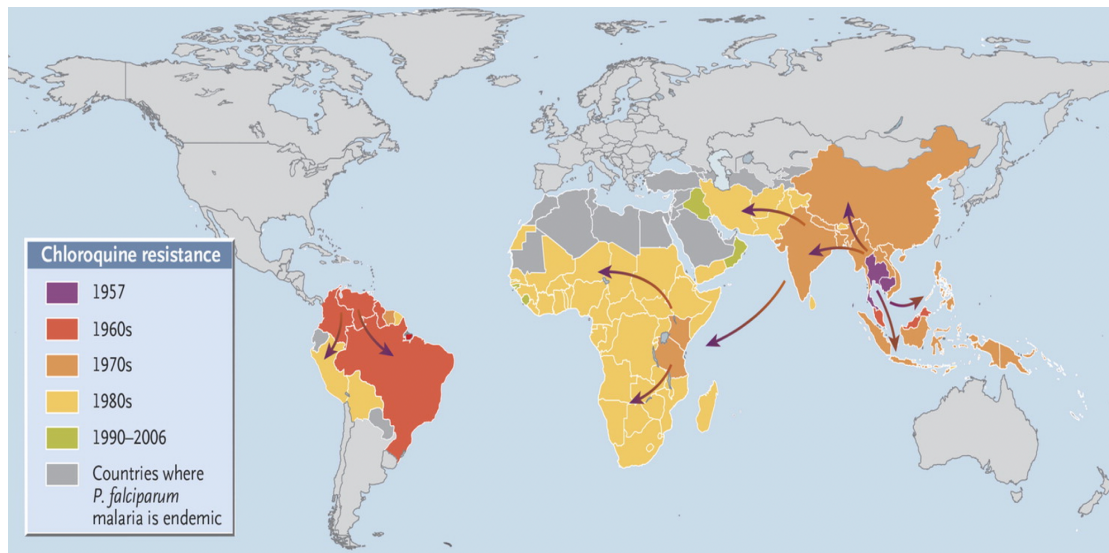


Figure 1.8: Emergence and spread of CQ resistance.

Figure reproduced with permission from (Packard, 2014), copyright Massachusetts Medical Society.

1.5.2 Atovaquone

Atovaquone is a hydroxynaphthoquinone that is known to specifically target the cytochrome bc1 complex, a crucial component of the electron transport chain in the parasite mitochondrion (Fry and Pudney, 1992). Activity of atovaquone is associated with a rapid onset of inhibition of the electron transport chain followed by an instant collapse of the parasite mitochondrial membrane potential (Srivastava et al., 1997). Resistance to atovaquone is however readily achieved through acquisition of point mutations in the cytochrome bc1 complex which abrogates drug binding efficiency (Srivastava et al., 1997). Uniquely, these atovaquone resistant parasites seemingly fail to transmit in mosquito vectors (Goodman et al., 2016). This is because the cytochrome bc1 complex, which is not entirely essential during the IDC, is critically required for the mosquito stages of the parasite and acquisition of mutations in the same impairs the parasites vector competency. Moreover, the cytochrome bc1 gene is encoded by the maternally inherited mitochondrial genome which acts as double hit to transmission as even in the case of outcrossing with the wild type parasites, resistance alleles cannot be successfully propagated (Goodman et al., 2016). Still, emergence of resistance to atovaquone was usually rapid when the drug was introduced for clinical use as a single agent which has necessitated its use in combination with other agents, more notably proguanil (Vaidya and

Mather, 2000). As of 2018, atovaquone (in combination with proguanil) is barely indicated for treatment of any form of malaria, aside prophylaxis for travellers (WHO, 2019).

1.5.3 Antibiotics: tetracyclines and macrolides

Tetracyclines are broad spectrum antibiotics that were discovered in the 1940s and are widely used in the treatment of bacterial infections. They inhibit protein synthesis by binding to 30S and 16S ribosomal subunits. Although not consensually agreed, it has been now recognised that the MOA of tetracycline in malaria parasites is associated with inhibition of protein synthesis in the parasite apicoplast (Dahl et al., 2006). Tetracyclines specifically disrupt expression of apicoplast specific genes which sequentially blocks downstream protein synthesis leading to parasite death (Dahl et al., 2006). Meanwhile, macrolides are macrocyclic lactone ring carrying antibiotics that inhibit protein synthesis by binding to the 50S subunit of bacterial ribosome and are widely used for treatment of bacterial infections. In malaria parasites, two macrolides; azithromycin and clindamycin display potent activity in malaria parasites and also target the apicoplast as their MOA (Sidhu et al., 2007). However, as is the case with almost all agents that target the apicoplast, both tetracyclines and macrolides display a delayed death effect which is characterised by parasites surviving a life cycle upon drug treatment without a functional apicoplast with death ensuing in the next cycle as daughter cells lack the organelle (Dahl and Rosenthal, 2007). These antibiotics are therefore not recommended for treatment of acute clinical malaria where rapid parasite reduction is required. Nevertheless, as of 2018, tetracycline and clindamycin are mostly used as prophylaxis agents even though they are still recommended by the WHO for the treatment of severe malaria in combination with quinine in the Philippines (WHO, 2019). Thus far, malaria parasites resistant to either tetracyclines or macrolides have not been convincingly described (Gaillard et al., 2015).

1.5.4 Antifolates

As CQ resistance spread across the world in the 1970s, a combination of two antifolate drugs sulfadoxine and pyrimethamine (SP) became suitable alternatives. The first nationwide switch from CQ to SP was made in Malawi in 1993 following which several countries adopted the same (Sibley et al., 2001).

However, SP resistance is readily achieved as it emerged in the 1970s almost immediately after introduction in the Asia Pacific and subsequently spread to all malaria endemic regions, reviewed by (Cui et al., 2015). These drugs act by inhibiting two key enzymes of the folate biosynthesis pathway; dihydrofolate reductase (*dhfr*) and dihydropteroate synthetase (*dhps*) (Plowe et al., 1997). Their activity blocks downstream synthesis of tetrahydrofolate which is a critical cofactor in the synthesis of nucleotides and amino acids (Sibley et al., 2001). This is specifically important in malaria parasites as *Plasmodium* spp. cannot salvage one class of nucleotides (pyrimidines) and require de novo synthesis which makes these drugs particularly potent (Cassera et al., 2011, Plowe et al., 1997). The MOR is attributed to point mutations in *dhfr* and *dhps* genes that renders resultant mutant enzymes less sensitive to the drugs (Plowe et al., 1997). As of 2018, SP is no longer recommended for first line treatment of *P. falciparum* malaria infections, but is still used in some countries (in combination with other agents) and remains the principle drug for intermittent prevention of malaria in pregnancy (WHO, 2019).

1.5.5 Artemisinins

Artemisinins (ARTs) or qinghaosu (as locally called in Chinese) are sesquiterpene lactones derived from a Chinese herb *Artemisia annua*. The discovery of ARTs can be traced back to project 523, a secret Chinese government military project that was launched on 23rd of May in 1967 aimed at finding antimalarial medications to a disease that had caused more deaths than the actual battle during the Vietnam war (White et al., 2015). Directed by Dr Youyou Tu, the project led to the discovery of ARTs in 1970 and was publicly announced to the world as a potential antimalarial agent in 1979, reviewed by (Tu, 2011). Despite early concerns on their safety and efficacy in monotherapies, superior ART efficacy in combination therapies (ACTs) and subsequent address of safety profiles in extended clinical trials as well as the continued spread of SP and CQ resistance led to the WHO recommendation of ACTs for treatment of uncomplicated malaria in all endemic regions of the world in 2006 (White et al., 2015). ARTs are highly effective antimalarial drugs and have indeed been partly credited with the recent declines in global malaria burdens (WHO, 2019, Cui et al., 2015). They are currently recommended by the WHO for first line treatment of malaria and are known to possess activity in both sexual and asexual blood

stages (Delves et al., 2012, WHO, 2019). A pharmacodynamic hallmark of ARTs and their derivatives is that they are highly active and fast acting against blood stages of malaria parasites, achieving up to 10,000 fold parasite reductions in the first life cycle upon drug exposure (White, 2008). This makes them specifically suited for treatment of severe disease. However, a significant disadvantage of ARTs is their short half-life *in vivo* (basically 1-2 hours) which necessitates their use in combination with longer half-life drugs to prevent recrudescence which is frequently common when they are used as single agents. Furthermore, parent ARTs have a poor bioavailability *in vivo*, and have been replaced by derivatives; dihydroartemisinin (DHA), artesunate and artemether (Figure 1.9) which display an improved pharmacokinetic profile. Structurally, ARTs are trioxane lactones with a characteristic endoperoxide bridge that forms a core and defining part of their structure (Figure 1.9). The endoperoxide bridge is central to the activity of ARTs and their derivatives in malaria parasites as it has been shown that, deoxyartemisinin, which lacks this bond displays no antimalarial activity (Wang et al., 2010).

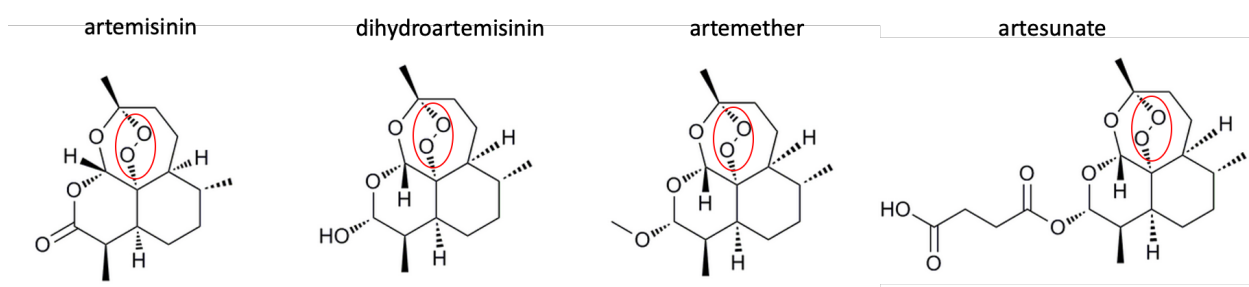


Figure 1.9: Structure of artemisinin and its derivatives dihydroartemisinin, artemether and artesunate.

Dihydroartemisinin is the active *in vivo* metabolite of all artemisinins while artesunate and artemether have improved bioavailability. Central to the structural activity of artemisinins is the highlighted endoperoxide bond.

1.5.5.1 ARTs MOA: a glass half full?

ARTs appear to have a unique MOA that is characteristically distinct from other antimalarial agents. Though the exact mode of parasite killing remains debatable, iron/haem mediated activation of the endoperoxide bridge is central to the core activity of ARTs. Activation of the endoperoxide bond produces carbon centred radicals that alkylate/react with downstream parasite proteins/other targets leading to parasite death.

Inside the DV, malaria parasites ingest and digest large amounts of host haemoglobin as a source of amino acids for protein synthesis. This process produces Fe^{2+} haem iron which is rapidly sequestered into chemically inert haemozoin crystals (Goldberg, 2005). It is believed that some Fe^{2+} haem iron pool remains available to catalyse a reductive activation of the ARTs endoperoxide bridge that generates carbon radicals which mediate parasite killing (Meunier and Robert, 2010). In line with this hypothesis, ARTs display a rapid and efficient activity in trophozoite malaria stages which are associated with massive haemoglobin catabolism. In contrast, ARTs display reduced activity in mid-rings, pre-erythrocytic and gametocyte stages which is consistent with reduced or no haemoglobin degradation in these stages, reviewed by (Tilley et al., 2016). ARTs are however, also, active in very early ring stage parasites in what has been described as a short “hypersensitive stage” (Xie et al., 2016) which would suggest alternative sources of iron for ART activation or an entirely independent MOA. Some of the proposed alternative sources of iron for ART activation include biosynthetic haem produced by the parasite, free non-haem bound iron pools or the inherent parasite mediated redox catabolism of haem (Tilley et al., 2016). However, the haem-iron hypothesis remains compelling for now, as has been demonstrated that haemoglobinase inhibitors can strongly antagonise ART action more so than standard iron chelators (Tilley et al., 2016, Klonis et al., 2011). It remains a formal possibility though, that other factors other than iron haem may play a role in ART activation which might explain the early ring stage hypersensitivity.

Once activated, ARTs are thought to target several parasite biological components, although the exact molecular targets remain under debate (O'Neill et al., 2010, Tilley et al., 2016). Among the key molecules thought to be targeted by ARTs is haem itself. Haem-ART adducts have been detected when ART is incubated with haem suggesting an interference with haematin formation as a possible mechanism of ART action (Meshnick et al., 1991). This remains disputed though, as even though these adducts have been detected *in vivo*, no clear evidence links them to ART action since their possible origin from *ex-vivo* interactions between the parasite and the drugs is yet to be ruled out (O'Neill et al., 2010). Another proposed mechanism is a generalised covalent modification/alkylation of parasite proteins. Over 120 proteins have been

identified to be covalently modified by ARTs in *P. falciparum*, suggesting a more complex and generalised protein damage that precedes parasite death (Wang et al., 2015a, Ismail et al., 2016). This has been further supported by a detection of polyubiquitination in parasites treated with ARTs suggesting a more pronounced and generalised protein damage (Dogovski et al., 2015, Bridgford et al., 2018). Early work on ARTs MOA identified a *P. falciparum* calcium ATPase, PfATP6 as a possible and sole target of these drugs (Eckstein-Ludwig et al., 2003). PfATP6 was expressed in frog's eggs (*Xenopus oocytes*) and it was found that ARTs significantly inhibited the purified enzyme while other antimalarials such as CQ and even deoxyartemisinin did not (Eckstein-Ludwig et al., 2003). In the same study, it was also demonstrated that PfATP6 inhibition by ARTs and another closely related endoperoxide thapsigargin can be abolished in the presence of an iron chelator further suggestive that ART activity requires iron activation. Even though several studies have contradicted this hypothesis, reviewed by (O'Neill et al., 2010), PfATP6 was among the many proteins identified to be targets of ARTs (Ismail et al., 2016, Wang et al., 2015a) illustrating that this protein could be one among many targets that are inhibited by ARTs. Furthermore, ARTs are thought to inhibit energy production in the parasites by targeting the parasite mitochondria (Wang et al., 2010) as well as cause parasite membrane damage by inducing accumulation of neutral lipid bodies (Hartwig et al., 2009). ARTs have also been shown to inhibit a *P. falciparum* phosphatidylinositol-3-kinase (PfPI3K) (Mbengue et al., 2015). PfPI3K is thought to play a role in parasite haemoglobin endocytosis and its inhibition by ARTs blocks delivery of haemoglobin to the parasite DV which in turn blocks parasite growth (Vaid et al., 2010). Nevertheless, despite the enormous research efforts to characterise ARTs MOA, the direct and indirect effects of these drugs on the malaria parasite are yet to be fully unravelled (O'Neill et al., 2010, Tilley et al., 2016).

1.5.5.2 Malaria parasite resistance to ARTs: a multifaceted trait

Compared to other antimalarial drugs, ART resistance has emerged at a relatively slow rate. This is particularly due to their short half-life *in vivo* which reduces parasite exposure time minimising the selective pressure that would underpin emergence of resistance. Further to that, ARTs are administered as ACTs which further reduces the probability of acquiring resistance conferring

genetic traits. Nevertheless, resistance to ART has emerged and was first reported in 2009, mostly as a reduction in parasite clearance rate following ART monotherapy in Cambodia (Dondorp et al., 2009). As of 2018, ART resistance is almost endemic in the greater Mekong region of Southeast Asia (SEA) (WHO, 2019). Meanwhile, ART resistance which is at the moment, defined by a delayed parasite clearance upon ART or ACT treatment, is still classified as “partial resistance” mostly because it is restricted to ring stage parasites and most patients with parasites harbouring the phenotype effectively clear the infection when an effective partner drug is used or treatment duration is extended (WHO, 2018a). Furthermore, whether ART resistance or partial resistance qualifies to be called as such remains a subject of continuing debate. For instance, the *in vivo* delayed clearance phenotype which is observed in patients does not correlate with decreased susceptibility to DHA in standard *in vitro* growth inhibition assays where parasites are exposed to the drug during the entire life cycle over 1-2 generations (Dondorp et al., 2009, Amaratunga et al., 2012, Phyo et al., 2012). A ring-stage survival assay (RSA) where early ring stage parasites (0-3 hours old) are exposed to DHA for a short period of time (4-6 hours) at a relevant pharmacological concentration provides a better correlate for the *in vivo* delayed parasite clearance phenotype, and has been the principle *in vitro* assay for determining resistance of malaria parasites to ARTs (Witkowski et al., 2013).

Primary determinant of ART resistance

In 2014, non-synonymous single nucleotide polymorphisms (SNPs) in the kelch13 propeller domain of malaria parasites were identified as molecular markers of ART resistance after *in vitro* selection for resistance for 5 years in the Tanzanian F32 isolate (Witkowski et al., 2010, Arie et al., 2014). After identification of the M476I Kelch13 substitution in these resistance lines, subsequent mutations (C580Y, R539T, I543T, Y493H) were identified in clinical isolates that presented with delayed clearance rate phenotype (Arie et al., 2014). Genetically engineered reversal of Kelch13 mutations has been used to confirm their role in mediating ART resistance in the *in vitro* RSA (Straimer et al., 2015, Ghorbal et al., 2014). However, additional genetic factors may play an additional role as has been shown that the level of ART resistance in clinical isolates harbouring

Kelch13 mutations is higher than in genetically engineered parasites (Straimer et al., 2015).

P. falciparum Kelch13 is a 726 amino acid long protein that displays sequence homology to a class of BTB/POZ/Kelch family of proteins that are believed to act as substrate adaptors for Cullin-3 E3 ligases which mediate polyubiquitination of proteins and their degradation by the ubiquitin proteasome system (UPS) (Genschik et al., 2013). By acting as adaptors to these ligases, these proteins regulate several crucial cellular processes such as cell cycle progression, gene expression, cellular trafficking and endocytic processes (Dhanoa et al., 2013). In *Drosophila* and many other organisms, the BTB/POZ/Kelch proteins are structurally made up of the BTB/POZ domain (Broad complex_Tramtrack_Bric-a-brac/Pox virus_Zinc finger) which is thought to act as an adaptor to the Cullin-3 E3 ligases and the C-terminal propeller domain made up of a six propeller bladed structure that specifically binds substrates for ubiquitination (Figure 1.10) (Adams et al., 2000). *P. falciparum* Kelch13 ART resistance mutations localise to the C-terminal of this protein, lie exclusively in the propeller domain and have been proposed to reduce substrate protein binding (Mbengue et al., 2015). However, whether *P. falciparum* Kelch13 plays the role of substrate adaptor for these ligases is still unknown (Xie et al., 2020). Early functional studies on the function and consequences of Kelch13 mutations in malaria parasites revealed that PfPI3K can bind wild type Kelch13 more efficiently than mutant Kelch13. Reduced targeting of PfPI3K to the UPS in Kelch13 mutants was shown to increase PfPI3K levels which in turn increases the levels of its downstream product, phosphatidylinositol-3- phosphate (PI3P), which was found to mediate ART resistance phenotypes even in absence of Kelch13 mutations (Mbengue et al., 2015). Further to that, transcriptomic surveys of clinical ART resistant isolates have shown that ART resistance is associated with an upregulation of genes that are involved in the ER unfolded protein response, a cell stress response defence mechanism (Mok et al., 2015). Overall, these processes appear to protect the parasites from ART induced proteotoxicity by upregulation of the stress response mechanisms which allows for a quick recovery from the drug induced assault or a post-stress recovery system which may allow for accumulation of substrates such as PI3P that promote survival (Xie et al., 2020). Indeed, when exposed to DHA, both Kelch13 and wild type parasites experience

a significant level of protein damage in the first three hours. However, six hours later, mutant parasites display a rapid recovery to normal protein homeostasis consistent with relatively less stress or better recovery systems (Yang et al., 2019). Using an ER stress response marker, eIF2 α phosphorylation (eIF2 α -P), eIF2 α -P levels are less elevated in Kelch13 mutants as compared to wild type upon short exposure to DHA which further illustrates reduced stress (Zhang et al., 2017). This suggests that one consequence Kelch13 mutations may be to promote parasite survival by improving a rapid and efficient recovery system from the ART-induced proteopathy.

More recently, functional studies of *P. falciparum* Kelch13 have revealed its cellular localisation to cytosomes, “cell mouths”, together with other endocytic markers such as the endocytosis protein Eps15, ubiquitin carboxyl-terminal hydrolase 1 (UBP-1) and the adaptor complex AP-2 μ (Birnbaum et al., 2020). This cytosomal Kelch13 endocytic machinery appears to mediate haemoglobin endocytosis into the parasite. Kelch13 mutations lead to partial loss of protein function which impairs haemoglobin endocytic uptake thereby lessening ART activation and promoting parasite survival (Birnbaum et al., 2020, Yang et al., 2019). Even though co-localisation studies by Birnbaum et al. do not identify stress response proteins or proteins involved in the Cullin-3 E3 ligase mediated ubiquitination, parallel immunoprecipitation studies have identified several other proteins which interact with Kelch13 in malaria parasites some of which include vesicular transport proteins Rab GTPases, mitochondrial proteins and proteins involved in the ER unfolded protein cell stress response (Gnädig et al., 2020, Siddiqui et al., 2020). Kelch13 mediated resistance to ARTs therefore appears to be a multifaced process which may involve upregulated stress response mechanisms which mitigate the damage caused by ARTs or altered haemoglobin uptake which lessens ART activation. How these processes intricately interact (independently or dependently) to yield resistance phenotypes is still unknown. For example, Kelch13 mutant parasites display a prolonged ring stage during the blood developmental stages (Mok et al., 2015). Even though this could be one of the stress adaptation mechanism, how this phenotype links to Kelch13 mutations is still uncharacterised (Xie et al., 2020). Moreover, a characteristic signature of Kelch13 mutant parasites is their ability to enter a state of growth quiescence upon ART treatment, also called the

“sleeping beauty” phenotype. This allows the parasites to survive drug exposure during the growth stasis as ARTs would presumably target active cellular processes (Witkowski et al., 2010). Nonetheless, some Kelch13 mutations appear not to associate with these phenotypes (Breglio et al., 2018).

Aside from these known primary determinants, there are other secondary determinants which have been proposed to play a role in Kelch13 mediated ART resistance. Mutations in PfCRT, PfMDR1, ribosomal proteins and several other proteins have been proposed to provide a genetic architecture upon which Kelch13 mediated ART resistance is more likely to occur (Miotto et al., 2015, Zhu et al., 2018). Kelch13 mediated resistance to ARTs is therefore not just unconventional, but also seemingly complex which is further compounded by a lack of detailed mechanism of ART-mediated parasite killing. The current definition of ART resistance as “partial resistance” which is confirmed or suspected when patients carry parasites with certain Kelch13 gene mutations, display a parasite clearance half-life of >5.5 hours or are microscopically smear positive on day 3 after initiation of treatment; which is in itself still not fully predictable of ACT treatment failure (Ferreira et al., 2013, Krishna and Kremsner, 2013, Hastings et al., 2016, WHO, 2019, WHO, 2018a) further complicates the conventional definition of ART resistance. This is also confounded by a lack of association between Kelch13 mutations and ACT treatment failure in some regions (Kheang et al., 2017), the role of host immunity in modulating ART delayed clearance phenotypes (Ataide et al., 2017) and the lack of appropriate *in vivo* models to clearly confirm causality of Kelch13 mutations in ART resistance despite compelling *in vitro* RSA profiles. Using an *in vivo* *Aotus* monkey model, a recent genetic cross of the Kelch13 C580Y ART-resistant line (most prevalent mutation in SEA) with an *Aotus* infecting *P. falciparum* strain has revealed that parasites carrying the C580Y mutation can display increased survival in *in vitro* RSAs with no accompanying *in vivo* ART resistance phenotypes which further complicates the definition and or causality of these mutations to ART resistance (Sa et al., 2018).

Secondary non-Kelch13 determinants of ART resistance

Polymorphisms in several other proteins have been implicated in ART resistance phenotypes, mostly in the *in vitro* RSA. Mutations in the cysteine protease gene (Falcipain 2a) are some of the genetic polymorphisms which were selected for in series of incremental exposure to DHA *in vitro* (Rocamora et al., 2018, Arie et al., 2014). Falcipains are involved in haemoglobin degradation, mutations of which could impact haemoglobin uptake hence force lessening ART activation (Goldberg, 2005). Falcipain 2a is also expressed in early ring stages of malaria parasites which would correspond with its potential role in initiating the haemoglobin catabolism pathway (Xie et al., 2016). Crucially, Falcipain 2a polymorphisms have been reported in SEA and they associate with ART resistance phenotypes (Siddiqui et al., 2018).

Recently, long term evolution of *P. falciparum* isolates from Senegal identified mutations in the F-actin binding protein, coronin, that mediate reduced susceptibility to DHA *in vitro* (Demas et al., 2018). Pfcoronin belongs to the WD40-propeller domain containing protein family which share the β -propeller motif with *P. falciparum* Kelch13. Pfcoronin seemingly interacts with the *Plasmodium* ESP15 containing domain protein which plays a role in endocytosis and vesicular trafficking (Thakur et al., 2015). In a similar manner as Kelch13, Pfcoronin would be involved in endocytic uptake of host factors such as haemoglobin which would be impacted on with the acquisition of the mutations. Nevertheless, Pfcoronin mutations that associate with ART resistance phenotypes have not yet been observed in field isolates (Velavan et al., 2019).

Further mutations in an adaptor protein AP-2 μ have been implicated in *in vitro* resistance to DHA (Henriques et al., 2015) as well as *in vivo* susceptibility to ARTs in rodent malaria parasite *P. chabaudi* (Henriques et al., 2013).

Experimental introduction of one of the AP-2 μ mutation I592T leads to increased survival of mutant parasites in the RSAs (Henrici et al., 2019a). AP-2 μ colocalises with malaria parasite's Kelch13 to the cytostome and appears to be involved in haemoglobin uptake and endocytosis (Henriques et al., 2013, Birnbaum et al., 2020). Limited directional selection in clinical *P. falciparum* isolates from Kenya has been observed at the AP-2 μ locus (Henriques et al., 2014).

Polymorphisms in a ubiquitin hydrolase, UBP-1 (HAUSP or USP7 close homologue), were also previously identified to modulate susceptibility to ART and CQ in the rodent infectious malaria parasite, *Plasmodium chabaudi*, after sequential experimental evolution and selection with a series of antimalarial drugs (Hunt et al., 2007). UBP-1, just like Kelch13 are all predicted components of the parasite UPS. More importantly, they both co-localise to the parasite cytosomes and their partial inactivation and or experimental engineered mutations lead to decreased susceptibility to ARTs in the *in vitro* RSA (Birnbaum et al., 2020). Even though UBP-1 has been shown to facilitate haemoglobin endocytosis (Birnbaum et al., 2020), its role in UPS mediated cell stress response mechanisms is yet to be ruled out. Ubiquitin hydrolases or deubiquitinating enzymes (DUBs) are proteases that cleave ubiquitin residues from conjugated substrate proteins in the UPS pathway. UPS targeting of proteins is initiated by ubiquitin (Ub) tagging of substrates which marks them either for specific cellular signal transduction processes like DNA repair and cell cycle progression or subsequent degradation at the 20s proteasomal unit (Lecker et al., 2006). Ub tagging is mediated by three sequential enzymes: E1, an activating enzyme; E2, a conjugating enzyme and Cullin-3 E3, a Ub ligase for substrate specificity (Figure 1.10). The activity of these enzymes results in polyubiquitination of substrate proteins, which signals for their degradation at the 20s complex depending on the number of Ub residues. DUBs reverse the activity of these downstream UPS enzymes by removing Ub from the conjugated substrates which results in diverse protein fates and cellular outcomes among which include; regulation of protein half-life, cell growth, differentiation, transcription; rescue of mis-tagged proteins as well as oncogenic and neuronal disease signalling (Hanpude et al., 2015). Over 100 DUBs have been identified in humans and they classify into five major families: Ub C- terminal hydrolases (UCHs), Ub specific proteases (USPs), ovarian tumour proteases (OTUs), Josephins and JAMM/MPN/MOV34 (Hanpude et al., 2015). Owing to their role in multiple biological pathways and disease states signalling, DUBs are rapidly emerging as drug targets, mostly, in oncology (Harrigan et al., 2017). In malaria parasites, up to 30 DUBs have been predicted across five *Plasmodium* species (*P. falciparum*, *P. vivax*, *P. berghei*, *P. chabaudi*, *P. yoelii*); although their functions remain to be fully explored (Ponder and Bogyo, 2007, Ponts et al., 2011). Nevertheless, *Plasmodium* DUBs seem to have intrinsic protease activity, are significantly

divergent and their human orthologues are known to be important regulators of cellular pathway which makes them suitable and potential drug targets (Aminake et al., 2012). More importantly, the fact that mutations in a DUB (UBP-1) can mediate susceptibility to ARTs also offers the opportunity to target *Plasmodium* DUBs not just antimalarial drug targets, but also as a means to offset ART resistance. Indeed reports of UBP-1 mutations associating with ART treatment failure in Africa and SEA (Henriques et al., 2014, Adams et al., 2018, Cerqueira et al., 2017, Borrmann et al., 2013) as well the recently reported strong positive selection at the UBP-1 loci in SEA (Ye et al., 2019) are indicative of the requirement for such pre-emptive interventions.

ART resistance is thus a complex trait which though primarily conferred by mutations in *P. falciparum* Kelch13, can also be mediated by several other independent mechanisms. Understanding of these mechanisms, such as the upregulation of the stress response and or protein trafficking/endocytic pathways, could therefore provide avenues to contain and rescue the emergent resistant to this important class of drugs. This could be through identification of suitable partner drugs or structural improvement of the already existing endoperoxides for increased *in vivo* half-life or high barrier to resistance characteristics. Some of these approaches are, indeed, already being pursued as targeting the cell stress response by inhibiting components of the UPS can enhance and synergize the activity of ARTs in both ART sensitive and resistant *P. falciparum* isolates (Dogovski et al., 2015). Figure 1.10 summarises the current outlook to ART MOA, MOR and possible intervention points.

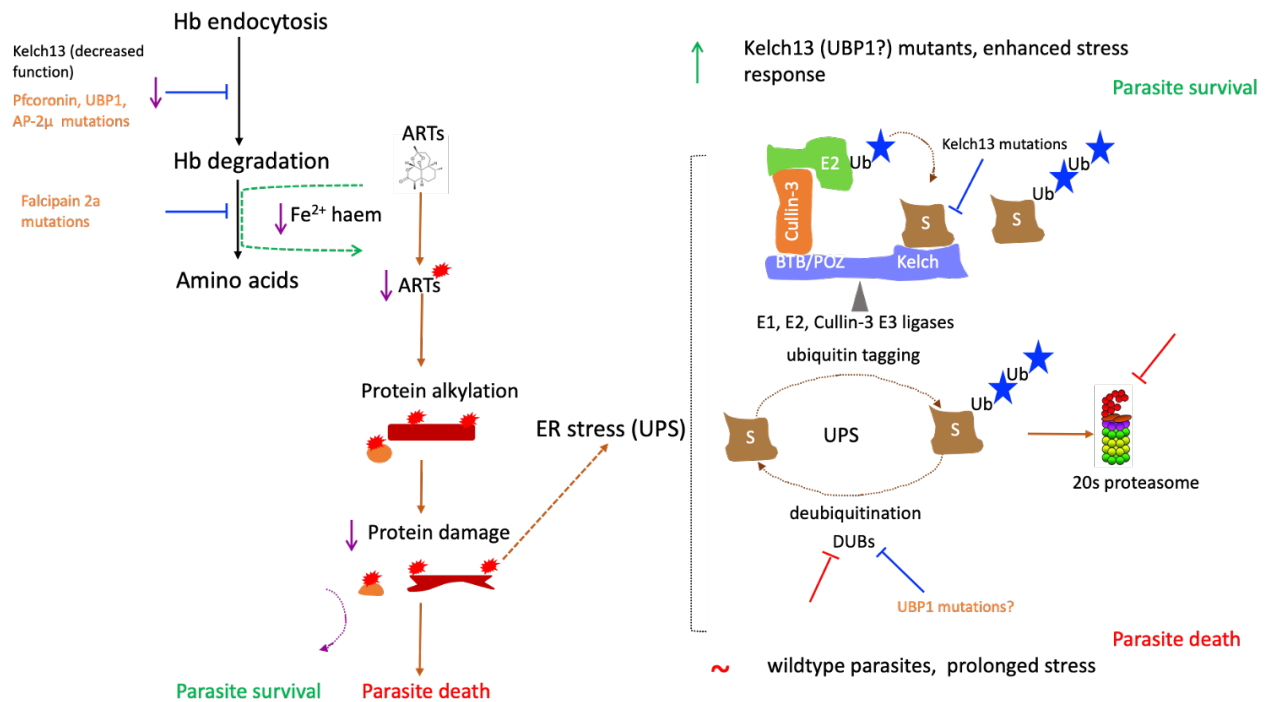


Figure 1.10: Artemisinin action, resistance and possible intervention points.

Endocytosis of haem precedes its degradation in the DV which releases Fe²⁺ haem iron and amino acids for parasite protein synthesis. Fe²⁺ haem catalyses reductive scission of the ARTs endoperoxide bond to produce radical ART adducts which in turn alkylate multiple parasite proteins. This leads to protein damage which when not sufficiently repaired results in parasite death. ART resistance is primarily conferred by *Kelch13* mutations which impair haemoglobin (Hb) uptake and in a cascade reduces Fe²⁺ haem available to activate ARTs as indicated by purple arrows. Reduced amount of activated ARTs leads to less protein damage hence force promoting parasite survival. This would be seemingly true for *Pfcoronin*, *UBP-1*, *AP-2μ* and *Falcipain 2a* mutations which are predicted or known to inhibit haemoglobin endocytosis or degradation as illustrated. An alternative mechanism of ART resistance which could be dependent or independent of haemoglobin uptake and degradation is through an enhanced cell stress response through the UPS. Ubiquitin (Ub) tagging of protein substrates (S) for UPS mediated proteasomal degradation which is facilitated by Cullin-3 ligases can be aided by *Kelch13* as a substrate adaptor. *Kelch13* mutations lead to less binding of substrates (*PfPI3K*) which make them accumulate and facilitate ART resistance phenotypes. Alternatively, the enhanced cell stress response could be facilitated by *UBP-1* mutations (by unknown mechanisms) which are known components of the UPS. In these mutant parasites, the parasites rapidly employ the cell stress response (upward green arrow) to clear damaged proteins and mitigate the ART induced protein damage which in turn promotes survival. Targeting the proteasome (red inhibition arrow) or potentially DUBs blocks the parasite stress response and offsets ART resistance phenotypes.

1.5.5.3 ART derived antimalarials

Due to the poor bioavailability of ARTs, their derivatives have been explored as alternatives for malaria treatment. DHA, artesunate and artemether were the first-generation ART derived antimalarials (Figure 1.9) that display an improved bioavailability and solubility profile. However, their inherent disadvantage remains their short half-life *in vivo*. ART derivatives with an improved bioavailability profile have therefore long been explored for development. Artemisone is among what are called “second generation ARTs” that display an improved bioavailability profile. Artemisone (Figure 1.11) is a synthetic 10-alkylaminoartemisinin that is derived from DHA in a one-step synthesis process (Haynes et al., 2006). In contrast to ARTs, artemisone has a significantly improved bioavailability and displays an enhanced activity in human plasma as compared to artesunate (Haynes et al., 2006). Artemisone has also been shown to be 10 times more potent than artesunate against *P. falciparum in vitro*, and > four times more potent in the *P. berghei in vivo* model (Vivas et al., 2007). First phase clinical trials of artemisone showed promising results for treatment of uncomplicated malaria (Nagelschmitz et al., 2008). However, no further development has currently been reported (Wells et al., 2015).

Another second-generation class of ART derived antimalarials is of the ozonide class. These are synthetic peroxide antimalarials that maintain an endoperoxide bridge for their activity but display a stable metabolic profile/half-life *in vivo* making them attractive ART substitutes (Charman et al., 2011, Maerki et al., 2006). OZ277 (Figure 1.11) was among the first ozonides to be developed and displays rapid activity against asexual blood stages of malaria parasites (Maerki et al., 2006). Despite displaying a slightly short half-life *in vivo* (yet 2-3 fold higher than DHA), OZ277 was the first ozonide to be licensed for malaria treatment and is available in India (as a combination with piperazine) and in seven African countries (Wells et al., 2015). OZ439 (Figure 1.11) is another current lead ozonide that is in advanced trials for malaria treatment. OZ439 has a long half-life compared to OZ277, is metabolically stable, rapidly clears asexual and sexual blood stages, displays a single dose efficacy in *P. berghei in vivo* model with reported activity in Kelch13 ART resistant parasites (Wells et al., 2015, Charman et al., 2011). Results of phase 2a trials in humans have shown that OZ349 is well tolerated, has a good long-half life and rapidly clears

parasitaemia in both *P. falciparum* and *P. vivax* infections (Phyo et al., 2016b). Phase 2/3 trials for OZ439 safety, efficacy and tolerability in combination with other antimalarial agents are currently ongoing.

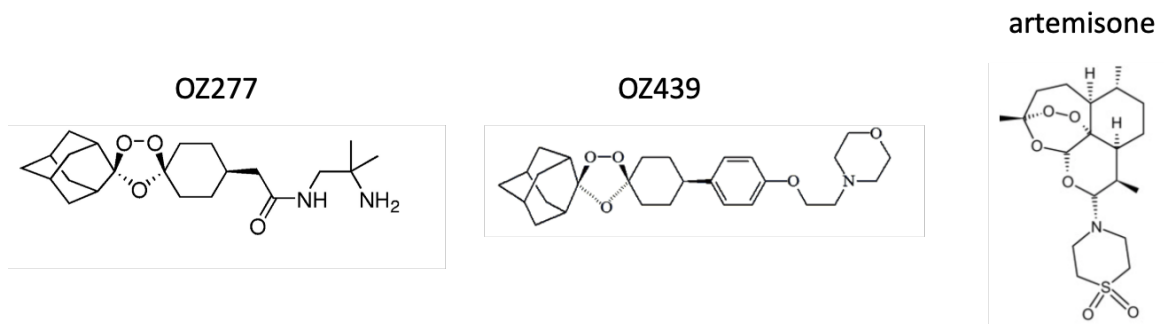


Figure 1.11: Structure of some of the second-generation ART-based antimalarials.

1.5.6 Antimalarial drugs in the pipeline

With the emergence of resistance to antimalarial drugs in current clinical use, efforts are ongoing to develop new and improved drugs. There are several drug candidates which are currently in the pipeline, underlying the enormous efforts drug development programs are investing in the field, reviewed by (Wells et al., 2015). As explained in the above chapter, some of the lead compounds are ART derived or close relatives underscoring the importance of structure-based function studies to derive improved drugs out of the existing antimalarial arsenal. There are, however, several others promising candidates in the pipeline.

KAE609 formerly NITD609, is a synthetic antimalarial compound of the spiroindolone class that has been developed by the Novartis Institute for Tropical Diseases (NITD) and is one of the lead antimalarial candidates currently in the pipeline (Wells et al., 2015). KAE609 is believed to act by inhibiting the *Plasmodium* Na⁺ ATPase pump, PfATP4 that plays an important role in maintaining cellular ion homeostasis (Rottmann et al., 2010). KAE609 is more potent than ARTs, has a long half-life *in vivo* and displays a single dose efficacy in the *P. berghei in vivo* model (Rottmann et al., 2010). Phase 2 trials have shown that KAE906 displays a rapid clearance of parasites in *P. falciparum* and *P. vivax* infections with an acceptable safety profile (White et al., 2014). KAE609 is currently undergoing further trials in preparation for registration and approval (Cully, 2014). However, unlike ARTs which appear to be high barrier compounds, selection for resistance to KAE609 was readily achieved in laboratory isolates

within 3-4 months (~5 years for ARTs). Even though this does not imply that field resistance would rapidly emerge when these compounds are introduced, their use in combination therapy will hopefully be among the implementation strategies when they are rolled out.

Another candidate of interest is MMV390048 which inhibits PfPI4K, a kinase that regulates the parasite's intracellular signalling and trafficking (Ghidelli-Disse et al., 2014, McNamara et al., 2013). PfPI4K is presumed to be important in all stages of malaria parasites, with MMV390048 having a potential for multistage activity. MMV390048 has successfully gone through phase 1 clinical trials in Africa with additional trials currently ongoing (Wells et al., 2015). DDD107498 has recently been identified as an antimalarial drug candidate with potential for multi-stage activity (Baragaña et al., 2015). DDD107498 has been shown to be more potent than ARTs, displays a multistage activity, has a single dose cure efficacy and displays a good pharmacokinetic profile. DDD107498 targets the parasites elongation factor 2 (eIF2 α) responsible for translocation of mRNA and subsequent protein synthesis (Baragaña et al., 2015). Evaluation of DDD107498 is currently ongoing in phase 1 trials. KAF156, another lead antimalarial compound developed by the NITD, has successfully passed through phase 2 trials with good safety and efficacy profiles (White et al., 2016). Phase 2b combination studies for this drug candidate began in Africa in August 2017 and are ongoing. KAF156 is believed to target the cyclin amine resistance protein, PfCARL, the exact function of which remains unknown (Kuhlen et al., 2014). Meanwhile, KAF156 resistance can also be modulated by mutations in multidrug resistance genes UDP-galactose and acetyl-CoA transporters (Lim et al., 2016). More recently, it has been demonstrated that this class of compounds inhibit ER associated protein trafficking pathways (LaMonte et al., 2020). Nevertheless, for both KAF156 and DDD107498, *in vitro* resistance can be selected for (within 4 months) further illustrating the threat of resistance should these compounds be clinically deployed in isolation.

1.6 Approaches to characterising antimalarial drugs MOA

1.6.1 Forward genetic approaches

MOA elucidation in malaria parasites mainly involve forward genetics approaches which require *in vitro* selection for resistance to the drugs followed by whole genome sequencing, transcriptome and or proteome analysis (Flannery et al., 2013). These approaches have (at least partially) identified the MOA of known antimalarial drugs such as CQ and pyrimethamine (Lukens et al., 2014, Ganesan et al., 2008). They have also pointed to potential molecular targets of novel compounds targeting PfPI3K (McNamara et al., 2013), protein and pyrimidine biosynthesis pathways (Lukens et al., 2014, Baragaña et al., 2015). However, these approaches have their own limitations in characterising the MOA of drugs as they do not reveal full molecular and biochemical networks involved in drug resistance cascades (Creek and Barrett, 2014). Moreover, these screens cannot be used to identify the MOA or molecular targets of drugs and drug candidates when drug resistance cannot be selected (high barrier compounds), drug resistance is phenotypic (no genetic architecture e.g. persistence) or when resistance is conferred by genetic mutations in multi-drug resistance transporters which provide little or no clue as to the intracellular target of the compounds.

1.6.2 Metabolomics

Ever since 1986 when Dr. Thomas Roderick first coined the word genomics, the omics field has exploded, providing an in depth understanding of biological systems from genomes, transcriptomes, proteomes, metabolomes all the way to the phenotype (“phenome”). Compared to other omics fields like genomics, metabolomics is rather a new field that provides a comprehensive biological aspect of cells by detecting and quantifying small molecule metabolites, typically less than 1.5 kDa (Wishart et al., 2007). Metabolomics has been a culmination of years of biochemistry applications where biomarkers like plasma cholesterol levels have been linked to atherosclerosis, plasma glucose to diabetes and many more others; reviewed by (German et al., 2005). Metabolomics is now being widely applied for the system level analysis of metabolites in biological systems providing application platforms in drug discovery, drug MOA studies, precision medicine, biomarker discovery and toxicological screens (Wishart, 2016). An inherent advantage of metabolomics is

that, metabolites, being closer to the phenotype provide a bridge between other omics technologies and the observed biological phenotypes as well as a closer and direct view of intracellular dynamics.

1.6.2.1 Metabolomic approaches

Metabolomics approaches are broadly categorised into two branches; untargeted or targeted based on the hypotheses driving the data acquisition paradigm.

Untargeted metabolomics are hypothesis generating experiments where a global analysis of metabolites is conducted to provide a system wide screen of perturbations that may arise due to predefined set of experimental or natural conditions. On the other hand, targeted metabolomics are hypothesis driven where quantification of metabolites is restricted to a biochemical pathway of a particular interest (Patti et al., 2012). Untargeted analyses offer a classic unbiased system of investigating biological differences in identical or experimental conditions that may arise due to natural or experimentally induced perturbations. Coupled to other omics like genomics, transcriptomics, proteomics or standard molecular biological approaches like reverse genetics, untargeted metabolomics analyses provide a powerful scope of knowledge outputs that would otherwise remain unaddressed when employing upstream omics approaches. With targeted approaches, analyses are limited to known biochemical pathways by specifically quantifying metabolites in respect to predefined experimental conditions (Patti et al., 2012). This approach is particularly attractive in respect to answering very specific questions like drug metabolism/xenobiotics, perturbations due to enzyme specific alterations as well as specific biomarker responses in induced or un-induced conditions (Patti et al., 2012). Targeted metabolomics being “targeted” offer a unique challenge on the core definition of omics which are generally considered as being global, system-wide analyses. However, both targeted and untargeted metabolomics approaches are being widely applied with a huge wealth of knowledge outputs in biomarker discovery, pathogenesis of cancers, infectious diseases and many others (Creek and Barrett, 2014, Griffiths et al., 2010, Patti et al., 2012, Wishart, 2016).

1.6.2.2 Metabolomic platforms

The human metabolome consists of over 2000 metabolites (Wishart et al., 2007) with over millions existing in the biosphere. Their diversity, ranging from structural to physicochemical, provide an enormous challenge to effectively quantify their abundance with a single analysing system (Kell, 2004). A basic metabolomics platform therefore relies on efficient sample or metabolite extraction, metabolite separation, detection and consequent identification. The importance of efficient sampling techniques, good biological replicates and sample handling for metabolomics studies cannot, therefore, be over-emphasized (Wishart, 2016).

The basic metabolomics workflow starts with sample preparation and extraction of metabolites. To maximise metabolome coverage, most metabolite extraction protocols employ a mixture of chloroform, methanol and water in the extraction solvent to comprehensively cover polar and non-polar metabolites (Mushtaq et al., 2014). Once extracted, metabolites are separated and detected using a diverse set of technology platforms. The commonly used detection platforms are mass spectrometry (MS) based or nuclear magnetic resonance (NMR) (de Raad et al., 2016, Markley et al., 2017). NMR has proven to be powerful for structural characterisation of unknown compounds, doesn't need elaborate sample preparation as in MS, has good reproducibility as well as excellent *in vivo* performance (Markley et al., 2017). Indeed, NMR spectroscopy has been widely used to identify key metabolites associated with infections or disorders across a wide spectrum of plants, animals and human conditions; reviewed by (Pontes et al., 2017). Nevertheless, an inherent disadvantage of NMRs platforms is their low sensitivity which significantly lessens their appeal as compared to modern, ultrasensitive powerful MS (de Raad et al., 2016, Markley et al., 2017). The most commonly used MS platforms are GC-MS and LC-MS (de Raad et al., 2016). GC-MS platforms consists of MS coupled to a gas chromatography (GC). Extracted metabolites are passed through a GC column which allows initial separation of the metabolites based on migration through a column and later mass detection in the MS. Since the mobile phase in GC is a gas, samples are made volatile and polar which makes it less optimal for detecting non-polar metabolites. LC-MS on the other hand use liquid chromatography (LC) as a separation technique providing a good coverage of both polar and non-polar metabolites, with good

sensitivity and reproducibility as well as easier sample preparation (de Raad et al., 2016, Lei et al., 2011). Another MS platform is capillary electrophoresis (CE) based (CE-MS) which allows separation of ion metabolites and subsequent detection by MS. Despite being cheap and requiring less sample volume, CE-MS is no longer used widely due to its poor reproducibility (de Raad et al., 2016). For elaborate and comprehensive metabolome coverage, most metabolomics platforms are used together in dual sample analysis (for example a GC-MS and LC-MS) to provide complementary metabolite analyses.

1.6.2.3 Metabolomic data analysis

As is the case with other omics technologies, metabolomics data sets are complex requiring extensive pre-and post-acquisition data processing to get meaningful outputs. In classic MS screens, majority of MS peaks are due to background noise providing an analytical challenge to separate significant result outputs from mere noise. In standard LC-MS screens, for example, over 80% of detected mass peaks are due to noise background (Jankevics et al., 2012). Computational platforms that allow accurate distinction of mass peaks with efficient noise filtering are therefore required for meaningful interpretation of metabolomics data sets. There are currently several bioinformatic packages such as IDEOM and mZMatch that allow simultaneous MS peak detection, quantification and noise filtering, providing fast and efficient ways of handling metabolomic data sets (Creek et al., 2012, Scheltema et al., 2011). The development of automated metabolomics data analysis pipelines like PiMP by the University of Glasgow Polyomics has provided additional efficiency to handling of these data sets (Gloaguen et al., 2017). Another hurdle in handling of metabolomics data is accurate identification of metabolites and the challenge of mapping metabolites to their corresponding biochemical pathway. Thanks to the expanding online biochemical pathway databases like KEGG, and ongoing efforts to link these to metabolite databases, the full scope of metabolomics in biological systems is beginning to emerge (Okuda et al., 2008, Wishart et al., 2007).

1.6.5. Metabolomics and antimalarial drugs MOA

Development of antimalarial drugs is largely dependent on phenotypic screens where thousands of compounds are screened to determine their anti-

proliferative effects in *Plasmodium* species. These methods have indeed contributed to the arsenal of antimalarial drugs in current clinical use or in the pipeline. However, a disadvantage of phenotypic screens is lack of detailed mechanics underlying the parasite killing properties of the drugs (Guiguemde et al., 2012). Indeed, as is the case with most antiprotozoal drugs, the MOA of most antimalarial drugs are currently uncertain, disputed or completely unknown (Creek and Barrett, 2014, Muller and Hyde, 2010). This provides a bottleneck challenge, especially in the context of predicting drug resistance, resistance mechanisms, rational medicinal chemistry-based improvement of current drugs as well as identification of suitable partner drugs which could be ideal in combination.

Metabolomics has proven potential in drug discovery as well as characterising MOA of drugs already in use (Wishart, 2016, Creek and Barrett, 2014). Metabolomics platforms can detect metabolic perturbations induced by drug treatment which has allowed their usage in characterising the MOA of antiprotozoal compounds as well as several antibiotics (Creek and Barrett, 2014, Kwon et al., 2008, Vincent et al., 2016). In malaria parasites, targeted metabolomics screens have been used to characterise the action of polyamine inhibitors in *P. falciparum* (van Brummelen et al., 2009), validated the activity of new quinolone drugs targeting the parasite electron transport chain (Biagini et al., 2012) as well as metabolic specific phenotypes associated with antimalarial drugs in use such as DHA (Cobbold et al., 2016). Metabolomic screens of the malaria box compounds have also revealed established as well novel targets of potential malarial drug candidates (Creek et al., 2016, Allman et al., 2016). High-resolution metabolomics combined with peptidomics and biochemical analyses have also revealed that a fast acting lead drug candidate being developed by the Medicine's for Malaria Venture (JPC-3210, MMV 892646) as well as the second generation ART derived ozonide's possibly act by inhibiting haemoglobin catabolism and protein translation (Birrell et al., 2019, Giannangelo et al., 2020). This has illustrated the utility of metabolomics screens in ascertaining the MOA of antimalarial drugs under circumstances where other omics or forward genetic screens would be less informative.

1.7 Genome editing strategies for validating genetic determinants of antimalarial drug resistance

Forward genetic screens and metabolomics approaches described above can easily identify genetic polymorphisms, SNPs or biochemical pathways that are unique in either resistant parasites or over-represented upon drug exposure. In such situations, candidate markers that confer drug action and resistance traits are consistently observed across several independent resistant clones or multiple biological repeats. Nevertheless, these lead candidates are always flanked by several other potential genetic and biochemical changes that would contribute to the observed phenotypes. It is imperative therefore, that these candidate markers are artificially introduced in naïve parasites to independently confirm causality. Reverse genetics approaches which are deployed in such situations are indeed incorporated in almost all current antimalarial drug discovery programs and in similar approaches used to understand and characterise antimalarial drug resistance determinants (Flannery et al., 2013).

Since the successful adaptation of transfection technologies in *P. falciparum* and *P. berghei* between 1995-1996 (van Dijk et al., 1995, Wu et al., 1996), genetic manipulation of these parasites has provided a wealth of knowledge into the malaria parasite biology. However, up until recently, transfection of *P. falciparum* has mainly been restricted to episomal maintenance of plasmids or single cross over integration of transgenes. Due to low transformation efficiency, episomal transfection in *P. falciparum* requires maintenance of the introduced DNA as replicating concatemerized episomes for an extended period of time (O'Donnell et al., 2001). This is particularly disadvantageous as these episomes are unevenly segregated during mitosis and are easily lost in the absence of drug pressure. Even though chromosomal integration under such situations could be achieved, this can be slow and laborious with up to 6 months of selection required to obtain stable transformants (Crabb et al., 2004). Nevertheless, with recent improved technologies, single crossover methods are at the forefront of site-specific gene editing approaches for a reversed characterisation of drug resistance candidate mutations and polymorphisms in *P. falciparum*.

1.7.1 The Bxb1 integrase system

A site-specific integration system was first successfully adapted in *P. falciparum* by the David Fidock lab in 2006 (Nkrumah et al., 2006). This system shortens the length of episomal maintenance by using the mycobacterial phage Bxb1 integrase encoded in the plasmid which catalyses an artificial recombination between *attP* (co-engineered in the transfected plasmid) and *attB* (pre-inserted in the *P. falciparum* specific genomic loci) sites (Figure 1.12). By including a coding region of the gene of interest in the transfected plasmid, this allows for stable introduction of specific alleles of interest as transgenes in the parasite for subsequent phenotype analysis such as drug resistance traits. However, since cells still express the wild type endogenous locus, characterisation of the phenotypes can still be problematic.

1.7.2 Zinc finger nucleases

Despite the availability of the integrase system described above, site specific genome editing in *P. falciparum* was still less tractable until the development and adaptation of zinc finger nucleases (ZFNs) in 2012 (Straimer et al., 2012). ZFNs are customisable sequence specific endonucleases that can induce double stranded breaks at any genomic site of choice. These engineered ZFNs are made of up two domains: a zinc finger DNA binding domain and a catalytic nuclease or cleavage domain (Figure 1.12). Specifically, the nuclease domain is typically a split FokI endonuclease which functions as an obligate heterodimer. Three to six individual zinc finger proteins that recognise triple DNA sequences on either side of the DNA strand of the genomic region of interest are fused to each half of the split FokI which allows the endonuclease to dimerise and induce a double stranded break when the fingers recognise and bind the target region. Since malaria parasites rely on the classic homologous recombination for DNA damage repair as the canonical non-homologous end joining pathway is absent (Kirkman et al., 2014), this can be specifically exploited by supplying donor DNA repair templates carrying polymorphisms of interest to achieve highly precise genome editing up to single base level. This approach has indeed been successfully deployed to validate the role of PfCRT and Kelch13 mutations in modulating *in vitro* resistance phenotypes to CQ and ART respectively (Straimer et al., 2015, Straimer et al., 2012).

1.7.3 CRISPR-Cas9

Two years after the report of ZFNs in *P. falciparum*, two independent groups reported the first adaptation of CRISPR-Cas9 genome editing in malaria parasites in 2014 (Ghorbal et al., 2014, Wagner et al., 2014). Cas9 (CRISPR associated protein 9) is a bacterial derived endonuclease that uses CRISPR (clustered regularly interspaced short palindromic repeats) sequences as a guide to cleave foreign DNA sequences as part of the prokaryotic immune system (Ratner et al., 2016). Cas9 forms a complex with ~20 bp short guide RNA (sgRNA) which is homologous to a particular region of the genome and induces a double stranded break immediately upstream of the protospacer adjacent motif (PAM) which is typically NGG for Cas9 and can be different for different Cas nucleases (Figure 1.12) (Ratner et al., 2016). The 20 bp sgRNA and PAM motif are particularly important for specific targeting of Cas9 to a genomic locus of interest. Even though some mismatches in the 20 bp sgRNA can be tolerated, targets lacking the PAM motif are poorly or not recognised at all by the CRISPR-Cas9 complex (Hsu et al., 2013). Just like ZFNs, these customisable double stranded breaks can be exploited by supplying donor repair templates with modifications of interest to achieve highly precise editing. Unlike ZFNs which require initial identification of specific modules and screening for their activity, CRISPR-Cas9 is rapidly scalable by easy sgRNA designs and identification of PAM sites which is readily achieved with the availability of numerous online tools.

Efficient CRISPR-Cas9 editing require precise transcription at the start site of sgRNA which corresponds to the Cas9 binding homology region in the target genome. This is achieved by driving the expression of sgRNA from an RNA polymerase III promoter. In *P. falciparum*, this has been achieved by using an endogenous U6 promoter or a T7 phage promoter (Wagner et al., 2014, Ghorbal et al., 2014). A similar approach using the endogenous U6 promoter has been successfully employed for rapid and iterative CRISPR-Cas9 genome manipulation in zoonotic and rodent malaria parasites, *P. knowlesi* and *P. yoelii* (Mohring et al., 2019, Zhang et al., 2014). Despite some limitations like low editing efficiency with some sgRNAs and paucity of PAM NGG motifs for some genes due to the A-T rich genome of malaria parasites, CRISPR-Cas9 systems are becoming employed widely to the study of *Plasmodium* biology with specific applications in rapid gene knockouts, mutagenesis, tagging and gene expression analyses,

reviewed by (Lee et al., 2019). Crucially the CRISPR-Cas9 system is now the principle reverse genetic approach to validating antimalarial drug resistance polymorphisms identified by most forward genetic screens (Ghorbal et al., 2014, Demas et al., 2018, Lim et al., 2016).

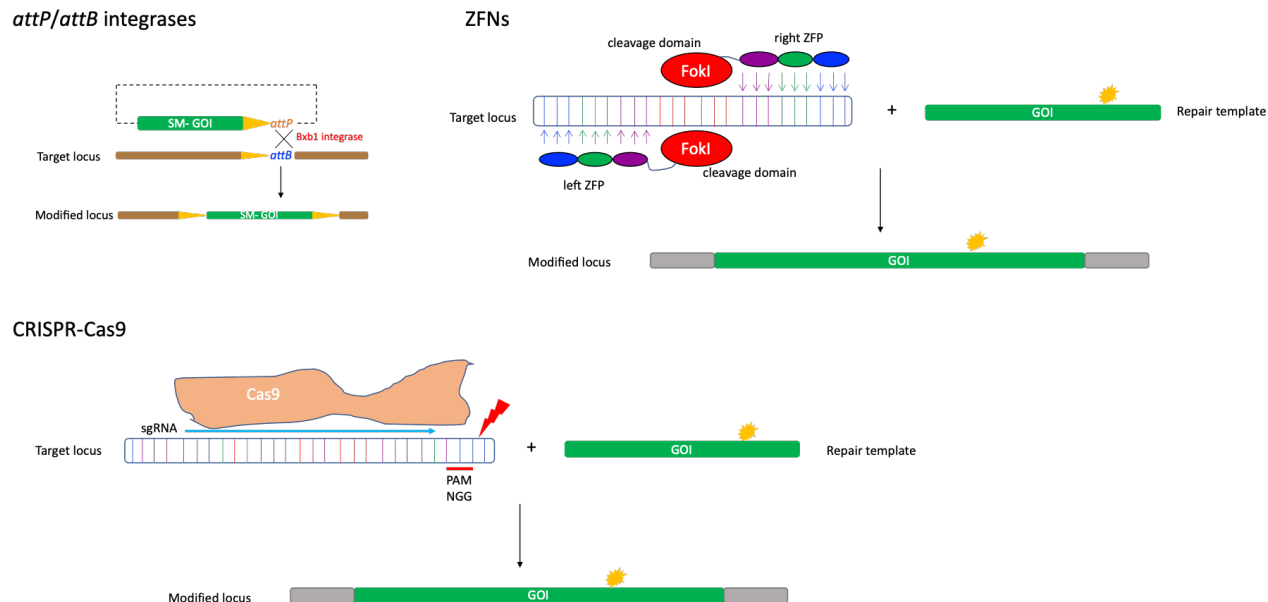


Figure 1.12: Schematic overview of genome editing strategies in malaria parasites.

The *attP/attB* integrase system relies on a Bxb1 mediated recombination between an *attP* plasmid encoded site with an *attB* site pre-engineered into the parasite specific locus. This can be through a one plasmid system which carries the *attP* sequence, gene of interest (GOI) and a drug selectable marker (SM) or a two-plasmid system where the Bxb1 can be expressed on a separate plasmid from the one carrying the SM-GOI. The recombination introduces the GOI (that can be modified to carry specific genetic polymorphisms) as a transgene into the parasite. ZFNs rely on a pair of zinc finger proteins which when bound to their recognition sequences allow dimerization and activation of the FokI cleavage domain to induce double stranded breaks. By supplying donor repair templates carrying mutations or polymorphism of interest (indicated by yellow star), these modifications are introduced into the parasite genome by homologous repair mechanisms. This is also similar for CRISPR-Cas9 mediated genome editing as Cas9 binds to a 20bp sgRNA and induces a double stranded break upstream of the NGG PAM motif (red lightning bolt) that can be repaired by supplying donor templates carrying modifications of interest.

1.8 Animal models of malaria and antimalarial drug resistance

Throughout the history of malaria research, animal models (non-human primates and rodents) have been at the forefront of understanding malaria parasite biology. The use of these models to study human malaria are mainly based on the genetic and phenotypic similarities between the spp. which can be inferred to mimic actual disease conditions.

1.8.1 Rodent models and antimalarial drug resistance

Rodent models have been particularly attractive due to availability of malaria parasite species that readily infect rats and mice. Four species of rodent malaria parasites (*P. berghei*, *P. yoelii*, *P. chabaudi*, *P. vinckei*) that were isolated in Central African thicket rats have been extensively used for *in vivo* malaria research applications (De Niz and Heussler, 2018). The four rodent malaria parasites share a highly conserved chromosomal gene synteny (Janse et al., 1994a) with however subtle differences in morphology, duration of life cycle and host cell preferences. *P. chabaudi* and *P. vinckei* preferentially invade mature RBCs just like the human *P. falciparum* and *P. malariae* while *P. berghei* and *P. yoelii* invade reticulocytes which is similar to human infecting *P. vivax* and *P. ovale*. Table 1.2 compares and summarizes features of rodent malaria parasites as they relate to disease pathology, duration and synchronicity of life cycle, host cell tropism and common use.

The utility of rodent malaria parasites in understanding the genetic basis of drug resistance has been exploited (Carlton et al., 2001). Even though differences exist between *P. falciparum* and rodent malarias, these parasites still share a conserved gene synteny which has indeed been used either to confirm some of drug resistance mutations observed in *P. falciparum* in the rodent malaria *P. berghei* or using some of the candidate resistance mutation alleles as selection markers for transfection experiments across the spp. (Carlton et al., 1998b, van Dijk et al., 1995, Carlton et al., 2001). Another advantage of rodent malaria parasites is the ease of which drug resistance can be selected. In *P. falciparum* forward genetic screens, selection for drug resistance can be a long and tedious process which can take from a few weeks to years. For example, *in vitro* selection for resistance to ARTs took almost 4-5 years to obtain stable resistant parasites (Demas et al., 2018, Witkowski et al., 2010). On the contrary, drug

resistant rodent malaria parasites *P. berghei* and *P. chabaudi* can be readily selected within a short period of time. Resistance to GNF179, a related compound to KAF156 was selected for just after 2 single *in vivo* dose treatments in *P. berghei* (Lim et al., 2016). In *P. chabaudi*, resistance to pyrimethamine was obtained within 2 weeks after a single dose treatment (Carter and Walliker, 1975). From these pyrimethamine resistant *P. chabaudi* lines, additional lines resistant to ascending doses of CQ, mefloquine, ART and artesunate have been easily derived (Rosario, 1976, Padua, 1981, Carlton et al., 1998a, Afonso et al., 2006, Cravo et al., 2003). Unlike in *P. falciparum*, drug resistance in rodent malarias can also be easily tested for phenotype stability in the absence of drug pressure through blood passage, freeze thaw cycles and the mosquito infectivity/transmission filter (Rosario, 1976, Afonso et al., 2006).

After obtaining drug resistant parasites, genetic markers responsible for these phenotypes have been historically characterised by carrying out genetic crosses between sensitive parasites and resistant clones. This typically involves transmission of sensitive and resistant parasites in a mixture into a mosquito then into a new host which allows for selection of recombinant progenies from which chromosomal linkage analysis can be used to map candidate genes to the observed phenotypes. Even though this is also possible in *P. falciparum* (which may require non-human primates or adapted mouse models), rodent malaria parasites are uniquely suited for such endeavours due to the ease of handling rodents and the ability to complete the entire *in vivo* life cycle under lab conditions (Carlton et al., 2001). In the meantime, the advent of recent genome sequencing technologies means candidate drug resistant mutations in these rodent models can be quickly identified and characterised (Hunt et al., 2007, Hunt et al., 2010, Borges et al., 2011, Kinga Modrzynska et al., 2012). The role of rodent malaria parasites in understanding the MOA and MOR for principle antimalarial drugs that are and have been in clinical usage is described in detail in the following sections.

1.8.1.1 Sulfadoxine and pyrimethamine

Resistance to antifolates is perhaps one of the well-studied and characterised resistance mechanisms in malaria parasites. SP resistance emerged immediately after this drug combination was rolled out for clinical use, faster than CQ, the

mechanistic detail of which is well characterised (Plowe et al., 1997).

Meanwhile, pyrimethamine resistance has historically been selected for in all the four rodent malaria parasites. The earliest report was perhaps in 1952 where a *P. berghei* strain with up to 20-fold resistance to pyrimethamine as compared to the wild type was obtained after two rounds of passages and treatment with single curative doses (Rollo, 1952). Several other *P. berghei* parasites resistant to pyrimethamine have also been easily obtained and reported (Diggens, 1970, van Dijk et al., 1994). Similar pyrimethamine drug resistance phenotypes have also been reported in *P. chabaudi* (Walliker et al., 1975), *P. yoelii* (Walliker et al., 1973) and *P. vinckei* (Yoeli et al., 1969).

However, the mechanism of pyrimethamine resistance in these lines was not convincingly known until mutations in the *dhfr* gene, specifically the S108N substitution, was identified in *P. falciparum* after a genetic cross of pyrimethamine resistant field isolates with laboratory sensitive lines (Peterson et al., 1988, Cowman et al., 1988). In these crosses, resistant parasites consistently inherited a fragment within the *dhfr* gene which differed from sensitive parasites by either the S108N substitutions or other candidate mutations such as N51I or C59R. Crucially, equivalent mutations in the *dhfr* such as the S106N were later identified in the *P. chabaudi* pyrimethamine resistant line (AS-Pyr) (Cheng and Saul, 1994). A similar mutation (S110N) is also responsible for the *dhfr* mediated pyrimethamine resistance phenotype in *P. berghei* (van Dijk et al., 1994). More importantly, mutant *dhfr* coupled to thymidylate synthase (*dhfr/ts*) carrying pyrimethamine resistance mutations is currently the widely used drug selection marker for transfection experiments in both *P. berghei* and *P. falciparum* (van Dijk et al., 1995, Wu et al., 1996) as well as *P. knowlesi* (Mohring et al., 2019, van der Wel et al., 1997).

Even though mutations in the *dhps* gene are predicted determinants of resistance to sulfadoxine (Plowe et al., 1997), this has remained circumstantial due to a lack of *in vitro* assays that can reliably distinguish sulfadoxine resistant from sensitive parasites (Wang et al., 1997). Sulfadoxine is a sulphonamide that acts as a substrate analogue of p-aminobenzoic acid (PABA) to competitively inhibit the *dhps* enzyme which in turn affects downstream folate synthesis for the parasite. Due to the variations in the levels of PABA in most culture medias,

phenotyping of resistance levels to sulfadoxine have been particularly difficult (Wang et al., 1997, Watkins et al., 1985). Nevertheless, transfection and allelic exchange experiments have been used to validate some of *dhps* enzyme mutations such as the A437G substitution in modulating *in vitro* susceptibility to this drug (Triglia et al., 1998). Due to these complexities, the genetics of dual resistance to SP drug combinations has been difficult to unravel. Parasites exhibiting SP drug resistance can carry mutations in the *dhfr* and *dhps* genes even though *dhfr* gene mutations alone are known to mediate resistance phenotypes to both drugs while *dhps* polymorphisms can sometimes less clearly correlate with SP resistance (Plowe et al., 1997).

Rodent malaria parasites can, therefore, in these situations offer a unique opportunity for studying resistant phenotypes emanating from such drug combinations as levels of interfering parameters such as PABA can be controlled, physiologically or through artificial diet supplementation. Parasites resistant to sulfadoxine have been selected for in both *P. berghei* and *P. chabaudi*, both of which appear to need less PABA as they develop an increased capacity to synthesize this metabolite *de novo* (Singh et al., 1954, Carlton et al., 2001). However, the genetic determinants in these resistant lines have remained uncharacterised. Crucially, *P. berghei* parasites resistant to SP drug combinations have been successfully obtained using a continuous low dose selection strategy even though the resistant phenotypes were unstable and the genetic determinants have not been identified (Merkli and Richle, 1983b). Perhaps one of the best characterised SP resistant rodent malaria parasite line is the AS (50S/P) line. This line was obtained by further selection of the AS-Pyr line with a single four-day high dose exposure with the SP drug combination to obtain parasite progenies that were strongly resistant to the drug combination. However, quantitative trait loci and genetic analysis of the AS (50S/P) line revealed that *dhfr* mutations were still the major determinant of the SP drug resistance phenotype as no additional *dhps* mutations were identified (Hayton et al., 2002).

Strain characteristics	<i>P. berghei</i>	<i>P. chabaudi</i>	<i>P. vinckei</i>	<i>P. yoelii</i>
Commonly used strains	NK65, ANKA, K173	AS	ATCC 30091	17X, YM
Use	Important model for genetic studies due to the ease of genetic manipulation. Can induce severe malaria and has been used as a model of cerebral malaria. Primary model for <i>in vivo</i> drug efficacy evaluation	Results in chronic infection. Widely used model for drug resistance studies and antigenic variation. This model has also been used to study sequestration even though host tissue sequestration patterns significantly differ from <i>P. falciparum</i>	Used in studying host immune responses to parasites.	The two strains 17X and YM significantly differ in disease pathology which is particularly suited to studying differences in human disease pathology and immunity. Also widely used in RBC parasite ligand interaction studies
Duration of lifecycle (hours)	22-24	24	24	18
Host cell tropism	Reticulocytes	Mature RBCs	Mature RBCs	Reticulocytes
Synchronicity of blood stage life cycle	No	Yes	Yes	No
Virulence ligands	Unknown	<i>Plasmodium</i> interspersed Repeat proteins (PIR)	unknown	YIR proteins
Tissue sequestration	Multi-organ, mostly in the lungs, spleen and adipose tissue	Yes, mostly in the liver	Yes (specific organs not characterised)	Yes (specific organs not characterised)
Natural cyclic hosts	<i>Grammomys surdaster</i>	<i>Grammomys surdaster</i>	<i>Grammomys surdaster</i>	<i>Grammomys surdaster</i>

Table 1.2: Comparison of life cycle and utility features of rodent malaria parasites.

1.8.1.2 ART resistance

Resistance to ARTs was first selected for in the rodent malaria parasites *P. berghei* and *P. yoelii* in the late 1990s (Peters and Robinson, 1999b). This involved the application of the 2% relapse technique where parasites are inoculated into mice and treated with a high subcutaneous dose of the drug 3-hours post infection. Upon recrudescence, parasites are passaged into a new host and retreated with similar drug doses. Levels of resistance are quantified by graphing the changes in time required to reach 2% parasitaemia in the treatment group which can be graded as a progressive reduction in the time required to reach 2% parasitaemia over the course of the passages when resistance is successfully obtained.

Using these approaches, resistance to ARTs was obtained in both *P. berghei* and *P. yoelii* which was, however, unstable as resistant parasites of both species easily lost the phenotype when the drug was withdrawn. Biochemical characterisation of one of the ART resistant *P. yoelii* strain which displayed up to four fold resistance compared to the sensitive lines revealed a reduced accumulation of the radiolabelled drug in the resistant parasites and even now the exact MOR are still unknown (Walker et al., 2000). Another selection for ART resistance in *P. berghei* was attempted using the ART derivative artemether in the early 2000s (Xiao et al., 2004). Infected mice were treated with high doses of artemether, passaged into a new host upon recrudescence and retreated every passage for 50 passages. Even though up to 8-fold resistance was achieved in these lines, the phenotype was unstable as drug sensitivity was retained after a few rounds of infections without drug pressure. The most studied rodent malaria parasites which displayed stable ART resistance phenotypes were obtained in *P. chabaudi* and were first reported in 2006 (Afonso et al., 2006). These lines were selected from *P. chabaudi* clones which had and were already previously selected for resistance to pyrimethamine and CQ. The original *P. chabaudi* AS isolate was exposed to four consecutive doses of pyrimethamine at 50 mg/kg from which a pyrimethamine resistant line (AS-Pyr) was obtained and cloned (Walliker et al., 1975). The AS-Pyr line was then selected for resistance to CQ from which a line resistant to six consecutive doses of CQ at 3 mg/kg (AS-3CQ) was obtained (Rosario, 1976). Selection of the AS-3CQ line with a stepwise CQ dose increment yielded a *P. chabaudi* line that was resistant to up six

consecutive daily doses of CQ at 15 mg/kg (AS-15CQ) (Padua, 1981). From the AS-15CQ line, several lines with differing drug resistance phenotypes were subsequently obtained. Exposure of the AS-15CQ line to a gradual ascending dose of mefloquine (7-30 mg/kg) resulted in the parasite line that was initially resistant to up to four consecutive doses of mefloquine at 30 mg/kg but eventually lost some degree of resistance by only surviving four consecutive doses of the drug at 15 mg/kg hence force was designated AS-15MF (Cravo et al., 2003). The AS-15CQ line was also subjected to a further CQ selection until a line resistant to up to 30 mg/kg of CQ (AS-30CQ) was obtained (Padua, 1981, Carlton et al., 1998a). Selection of AS-30CQ with gradually increasing doses of ART (up to 300 mg/kg) yielded an ART resistant line (AS-ART) that survived three to five consecutive doses (up to 300 mg/kg) of the drug (Afonso et al., 2006, Henriques et al., 2013). From the AS-15CQ, another selection with incremental doses of artesunate also yielded an independent line (AS-ATN) that was resistant to artesunate surviving up to 60 mg/kg of the drug (Afonso et al., 2006). Interestingly, both the AS-30CQ and AS-ART appear to have shared a cross resistance to ART phenotype (Henriques et al., 2013).

Three independent genetic crosses of the AS-ART line with a parallel *P. chabaudi* sensitive line and follow-up linkage group selection analysis identified a selection valley on chromosome 2 on the resistant parasites that strongly associated with the ART resistance phenotype. Within this locus, two mutations in a deubiquitinating enzyme, UBP-1 appear to have arose or fixated independently in the AS-ATN (V2697F), AS-30CQ and AS-ART line (V2728F) (Hunt et al., 2007). Meanwhile, whole genome sequencing further revealed that the V2728F mutation was not just common in the AS-30CQ and AS-ART lines, but also in the AS-15MF line (Hunt et al., 2010). Prior analysis of the AS-Pyr already identified the S106N *dhfr* gene mutation that was chiefly responsible for the pyrimethamine resistance phenotype (Cheng and Saul, 1994). Further genetic analysis of these lines also revealed several other polymorphisms which may have arisen as a consequence of the drug selection cascade from the original AS line. These included a mutation (A173E) in the amino acid transporter (*aat*) that seemingly was responsible for the CQ resistance phenotype in the AS-30CQ line and another mutation (T719N) in a predicted unknown transporter (PCHAS_0313700) which appears to have led to the emergence of the CQ

resistance phenotype in the AS-15CQ line (Kinga Modrzynska et al., 2012). Nevertheless, it appears that the two UBP-1 mutations may have arose independently in the AS-15CQ uncloned line which resulted in their specific fixation when a drug pressure of mefloquine, artesunate or a higher dose of CQ was applied (Henriques et al., 2013). Further analysis of the ART cross resistance phenotype between the AS-30CQ and AS-ART also revealed that selection of the former line with ART led to successful acquisition of an additional mutation (I568T) in the AP-2 μ gene which was responsible for the higher level of ART resistance in the AS-ART as compared to the AS-30CQ (Henriques et al., 2013). However, despite the observation of some of these mutations (UBP-1 and AP-2 μ) in clinical isolates that have presented with potential ART resistance phenotypes (Henriques et al., 2013, Henriques et al., 2014), their role in mediating resistance to these drugs is yet to be fully explored which is in part due to the complexity of the selection procedure with multiple drugs as well as absence of appropriate reverse genetics approaches. Figure 1.13 summarises the selection procedures and candidate gene mutations responsible for the phenotypes in these *P. chabaudi* lines.

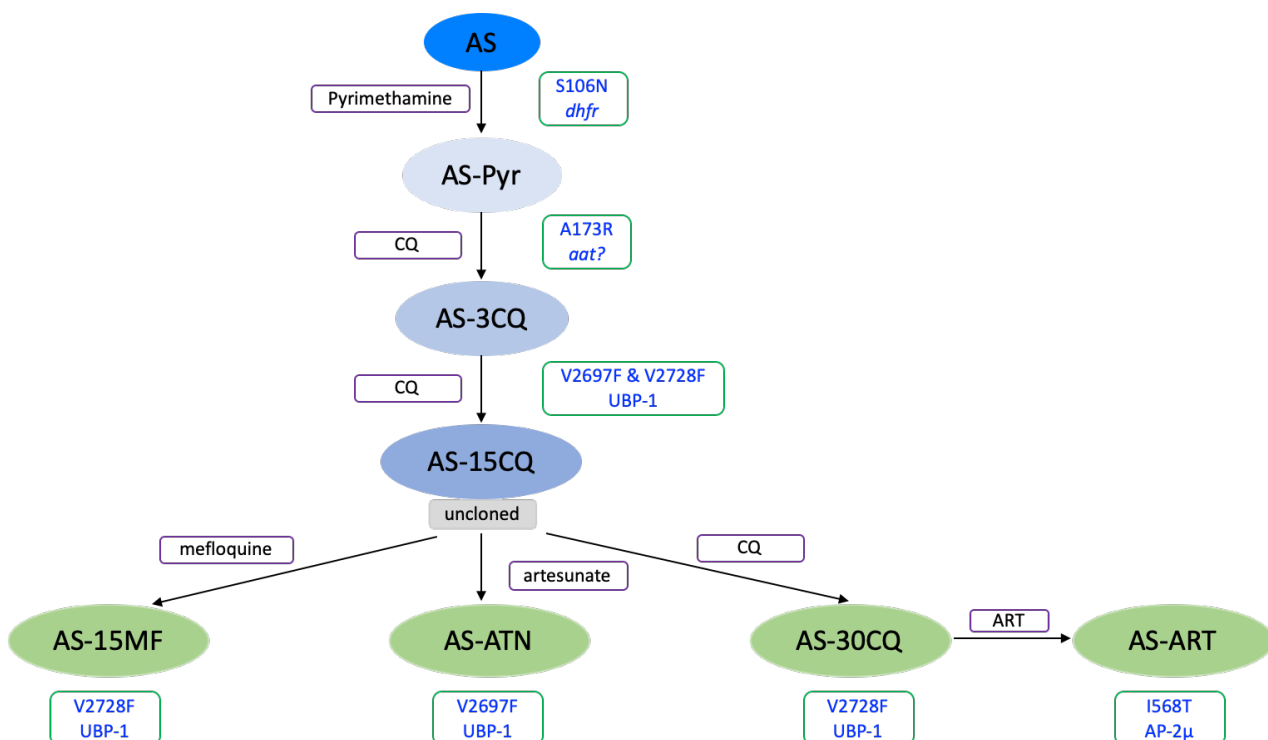


Figure 1.13: selection strategies used to obtain *P. chabaudi* ART resistant lines and the causal genetic determinants.

The original AS line was subjected to four daily doses of pyrimethamine to obtain the AS-Pyr resistant line that carry the S106N mutation in the *dhfr* gene. Further selection of this

line with CQ resulted in the AS-3CQ resistant line that was able to tolerate up to six consecutive doses of CQ at 3 mg/kg. Whole genome sequencing identified the A173R mutation in an amino acid transporter (*aat*) to be responsible for this phenotype. Further selection of this line with incremental doses of CQ resulted in the AS-15CQ line which carried two UBP-1 mutations, V2697F and V2728F. From this line, incremental dose selection with mefloquine, artesunate and further high doses of CQ yielded the AS-15MF, AS-ATN and AS-30CQ which appear to have fixated the UBP-1 mutations differently as indicated. Selection of the AS-30CQ line with ART resulted in the AS-ART line which carries an additional mutation in the AP-2 μ gene.

1.8.1.3 Atovaquone

Resistance to atovaquone (a chemical analogue of coenzyme Q) is readily achieved with the acquisition of mutations in the cytochrome bc1 complex both under laboratory conditions and in clinical field settings (Vaidya and Mather, 2000, Srivastava et al., 1997). This appears to be a similar case in rodent malaria parasites, as resistant to atovaquone has been selected for in *P. berghei*, *P. yoelii* and *P. chabaudi* (Srivastava et al., 1999, Afonso et al., 2010, Syafruddin et al., 1999). The *P. chabaudi* atovaquone resistant line was selected from the AS-3CQ line after stepwise dose escalation while resistant parasites in *P. berghei* and *P. yoelii* were selected from naïve parasite backgrounds. In all the three parasite species, genetic analysis revealed that the resistance phenotypes were due to mutations in the cytochrome bc1 complex even though independent reverse genetics have not been carried out to further validate their involvement. Reverse genetics approaches could also be particularly difficult in these situations as the cytochrome bc1 complex is encoded by the mitochondrial genome.

1.8.1.4 Mefloquine

Until recently, the mechanism of action of and resistance to mefloquine has remained relatively elusive. An aryl aminoalcohol, mefloquine was initially believed to act by inhibiting the haem polymerisation pathway within the parasite DV while increased copy numbers of PfMDR1 have been implicated as a mechanism of resistance (Ecker et al., 2012, Price et al., 2004). However, a more recent study has demonstrated that this drug can also act as a protein synthesis inhibitor in malaria parasites, specifically targeting the 80s ribosomal

translational unit (Wong et al., 2017). Nevertheless, rodent malaria parasites resistant to mefloquine have been selected and characterised. The most studied line is perhaps the AS-15MF which emerged from the AS drug selection panel of lines as described in section 1.8.1.2. This line was selected from a pre-existing CQ resistant line (AS-15CQ) using an incremental dose of mefloquine until stable resistance at 15 mg/kg was obtained. Linkage and genetic cross analysis of this line further revealed that increased expression of the PcMDR1 through copy duplication was indeed a constant feature of all resistant progenies which inherited the resistant phenotypes (Cravo et al., 2003). However, further genetic analysis of the AS-15MF line also implicated the UBP-1 V2728F mutation (Hunt et al., 2010). Mefloquine resistant *P. yoelii* parasites have also been selected for, even though the genetic determinants have not been characterised (Merkli and Richle, 1983a). In *P. berghei*, cloning and sequencing of the PbMDR1 gene from a line which was selected for and attained stable resistance to mefloquine also revealed 2-3 fold amplification of this gene in resistant parasites as compared to the sensitive wild type (Gervais et al., 1999). In these circumstances, even though the 50s ribosome might be the direct target of mefloquine, it can be relatively difficult to fully pinpoint the MOA as UBP-1 and MDR1 which are implicated in the MOR could be involved with transport of the drug.

1.8.1.5 CQ

Since resistance to CQ emerged in the 1970s, the MOR remained poorly characterised until the early 2000s (Ecker et al., 2012). This is because it proved specifically difficult to select for CQ resistance under laboratory conditions from naïve parasite strains. Identification of PfCRT as the principle determinant of CQ resistance involved detailed genomic, biochemical and allele exchange experiments to identify a 13-exon gene within a 36 kb chromosomal fragment that was strongly associated with the CQ resistance phenotype after a genetic cross of CQ resistance and sensitive parasites (Fidock et al., 2000, Wellems et al., 1990).

Rodent malaria parasites have, however, provided an additional spectre into understanding CQ resistance as even though it has proved to be difficult to generate parasites with stable resistant phenotypes, a number of lines have

been reported. The most widely studied rodent models of CQ resistance are perhaps of the *P. chabaudi* AS lineage as described in section 1.8.1.2. The AS-3CQ was the first *P. chabaudi* line with a stable CQ resistance phenotype (Rosario, 1976). In this line, initial biochemical analysis revealed reduced accumulation of CQ in the resistant parasites as compared to their sensitive counterparts (Ohsawa et al., 1991). Quantitative genome sequence analysis of the AS-3CQ line also identified a single mutation in an amino acid transporter *aat* (Figure 1.13) that could be a possible determinant of this drug resistance phenotype (Kinga Modrzynska et al., 2012). However, reverse genetics approaches have not been carried out to further validate its contribution. In the meanwhile, further selection of the AS-3CQ line generated higher degree CQ resistance lines (AS-15CQ and AS-30CQ), both of which carried UBP-1 mutations (V2697F and V2728F) as genetic determinants (Figure 1.13). A *P. vinckei* line resistant to CQ was also selected and reported in 1969 even though the genetic determinants have remained uncharacterised (Powers et al., 1969). In both of these *P. chabaudi* and *P. vinckei* lines, CQ resistance was selected from lines that were already resistant to pyrimethamine as attempts to select from naïve parasites was always unsuccessful. This is indeed in agreement with ARMD phenotypes where acquisition of certain drug resistance mutations is easily achieved in parasite backgrounds with pre-existing favourable architectures (Rathod et al., 1997).

P. berghei strains resistant to CQ have also been selected and reported which, however, has in most cases resulted in relatively unstable phenotypes. In some of the early work, exposure of *P. berghei* parasites to CQ supplied in animal diet for four months resulted in highly resistant strains that easily tolerated above maximum effective doses of the drug under standard treatment conditions (Hawking, 1966). These CQ resistant parasites also displayed a cross resistance phenotype to other drugs such as sulfadiazine and pyrimethamine. However, the phenotype was easily lost and could not be resuscitated when the drug pressure was removed. Around the same time, other unstable CQ resistant *P. berghei* RC strains that displayed up to 60 fold resistance as compared to the wild type were also reported (Peters, 1965). However, these lines were seemingly mislabelled as *P. berghei* (Peters et al., 1978) as they were basically *P. yoelii* which is naturally highly resistant to CQ (Warhurst and Killick-Kendrick, 1967). The only

P. berghei parasites with stable CQ resistant phenotypes were reported in 1998. These lines were selected from the NK65 line with an incremental dose of CQ ranging from 1, 3, 6, 10 through to 30 mg/kg. From each of these doses, stable phenotypes were obtained at various levels of the drug selection (CQR3, CQR6, CQR10 and CQR30) which, crucially, displayed high level resistance in both the *P. berghei* *in vitro* short term assay as well as *in vivo* (Platel et al., 1998). Nevertheless, the genetic determinants of the CQ resistance phenotypes in these lines have not been characterised.

1.8.2 Non-human primates, humanized mouse models and antimalarial drug resistance

Apart from rodent models described above, non-human primates have also provided an invaluable resource for malaria drug and vaccine efficacy testing before actual clinical use in humans. Primates of the *Aotus* genus are susceptible to some *P. falciparum* and *P. vivax* strains providing good *in vivo* models of human disease (Galinski and Barnwell, 2012). Another advantage of using non-human primates for antimalarial drug discovery programs is the ease of dose standardisation with humans as they can share comparable body mass, especially with young children. These models (the *Aotus* for example) have indeed been used to evaluate the *in vivo* efficacy of the second generation endoperoxide antimalarial artemisone in combination with either mefloquine or amodiaquine (Obaldia et al., 2009). More recently, the *Aotus* model has also been used to evaluate the *in vivo* ART resistance profile of the most prevalent Kelch13 mutation in SEA, C580Y (Sa et al., 2018). Non-human primates (rhesus-monkeys in particular) are specifically important for the study of *P. vivax* biology, as they are readily infected by *P. cynomolgi*, which is the most genetically related parasite to *P. vivax* and share important life cycle features like the presence of hypnozoites (Joyner et al., 2016). The *P. cynomolgi*/rhesus monkey model remains at the centre stage of evaluating the efficacy of most antimalarial drugs against *P. vivax* and most importantly drugs with potential activity in difficult to eliminate liver stage hypnozoites, reviewed by (Zeeman and Kocken, 2017). Nevertheless, as ethics-based campaigns to end the use of non-human primates in biomedical research intensify, suitable alternatives for the broader malaria world will need to be identified.

Some of these alternatives could include humanized mouse models, which can recapitulate *in vivo* infections with human infecting *P. falciparum*. Humanized mouse models have improved over the last ten years providing invaluable tools for evaluating malaria parasite biology (Minkah et al., 2018). Human liver chimeric mice, have for instance, been used to evaluate antibody mediated inhibition of pre-erythrocytic development stages of *P. falciparum* (Sack et al., 2014). However, the current generation of humanised mouse models are still incapable of fully reproducing a complete replica of *P. falciparum* life cycle (Minkah et al., 2018) and their use in characterising antimalarial drug resistance phenotypes *in vivo* is still in infancy.

1.8.3 Precise genome editing: a new era to revive rodent models of malaria for genetic validation of candidate drug resistance markers *in vivo*?

Rodent malaria parasites (*P. berghei* and *P. yoelii*) are easily amenable to genetic manipulation as they demonstrate high transfection efficiency as compared to *P. falciparum* (Janse et al., 2006a, Jongco et al., 2006). Moreover, rodent malaria parasites allow for the entire parasite life cycle to be reproduced under laboratory conditions, something which is technically and ethically not always feasible in human malaria. Reverse genetics approaches by introducing *P. falciparum* drug resistance alleles in these rodent parasites through allelic exchanges could thus be suitable alternatives as it would not just provide an opportunity to assess potential drug resistance phenotypes under *in vivo* conditions, but also delineate the fitness and transmission capacity of parasites carrying such polymorphisms. These approaches have indeed been tested as PfCRT mutant forms responsible for CQ resistance have been introduced in *P. berghei* (Ecker et al., 2011). Even though these PfCRT alleles did not result in equivalent CQ resistance phenotypes as observed in *P. falciparum*, it was demonstrated that under CQ pressure, *P. berghei* parasites carrying PfCRT mutant forms achieved better and efficient transmission.

An inherent disadvantage of such approaches is that it involves introduction of a transgene into parasites that maintain normal gene expression of the internal loci irrespective of how conserved the alleles are between the spp. In such situations, it is relatively difficult to quantify drug resistance phenotypes especially if the markers under study occur in proteins or enzymes that are less

amenable to gene dosage or if the background expression is sufficient to overshadow any resulting phenotype from the introduced alleles. Nevertheless, with the development of recent highly precise genome editing technologies such as CRISPR-Cas9, instead of introducing *P. falciparum* antimalarial drug resistant candidate alleles in rodent malaria parasites as transgenes, orthologous polymorphisms can be introduced with high precision to characterise phenotypes based on gene function conservation.

1.9 Aims and objectives

1.9.1 Using genome editing to test orthologous ART resistance mutations in *P. berghei*

With the continued development and adaptation of precise genome editing technologies such as CRISPR-Cas9 in malaria parasites, these approaches have been explored for use in introducing and validating several orthologous *P. falciparum* and *P. chabaudi* ART resistance mutations in the *in vivo* murine model of malaria, *P. berghei*. In light of the continued debate on the causal role of Kelch13 mutations in ART resistance especially under *in vivo* conditions, reported discrepancies between *in vitro* ART resistance profiles from actual *in vivo* conditions in the *Aotus* model and a lack of clear validation for other determinants such as UBP-1, equivalent mutations have been introduced in *P. berghei* using CRISPR-Cas9. Mutant parasites have been phenotyped to validate their role in ART resistance phenotypes both *in vitro* and *in vivo*.

1.9.2 Profiling the activity of ubiquitin hydrolase inhibitors as candidate antimalarial agents with potential to overcome ART resistance

With the supposed role of DUBs (ubiquitin hydrolases) in mediating ART and or CQ resistance, small molecule inhibitors targeting mammalian DUBs were profiled for *in vitro* and *in vivo* activities in both *P. falciparum* and *P. berghei*. Their potential in synergising ART action alone or in complex multi-drug combinations targeting different enzymatic pathways was also assessed.

1.9.3 Metabolomics profiling of NITD drug candidates to characterise their MOA

Using metabolomics screening platforms, this work also characterised the MOA of some lead antimalarial drug candidates that are emerging from the NITD drug discovery programs. As ART resistance emerges, some of the potential lead replacement antimalarial drug candidates which are either in development phase or in advanced clinical trials have been developed by the NITD. However, the MOA for most of these leads are either unknown, uncharacterised or still debated. By employing LC-MS untargeted metabolomics, the biochemical features elicited by some of these leads has been profiled.

2 Materials and methods

2.1 *P. berghei* general methods

2.1.1 Maintenance of *P. berghei* parasites in rodents

All mice infections with *P. berghei* parasites were carried out in female Theiler's Original (TO) mice (Envigo) weighing between 25-30 g. Parasite infections were established either by intraperitoneal injection (IP) of 200-400 µl of cryopreserved parasite stocks or intravenous injections (IVs) of purified schizonts or diluted parasites (obtained by cardiac puncture or tail drop) in phosphate-buffered saline (PBS). Cryopreserved parasites (~500 µl) were thawed at room temperature and the suspension was injected immediately by IP. Since *P. berghei* parasites preferentially invades reticulocytes (Cromer et al., 2006), pre-treatment of mice by IP injection with 100 µl of phenylhydrazine-HCl (Phz) at 12.5 mg/ml in physiological saline was done two days before the infections to induce reticulocytosis for some experiments. All animal work was performed in compliance with the UK home office licensing (Project reference: P6CA91811) and ethical approval from the University of Glasgow Animal Welfare and Ethical Review Body.

2.1.2 *P. berghei* lines

P. berghei parasite lines used in this work are derived from the ANKA strain, clone 15Cy1A from the Leiden Malaria research group also known as "HP". The 820 line that express green fluorescent protein (GFP) and red fluorescent protein (RFP) in male and female gametocytes respectively as previously described by (Ponzi et al., 2009) was used. The 507 line which express GFP constitutively under the control of the constitutive *P. berghei* Ef-1α promoter (Janse et al., 2006a) was used for some experiments. Two other HP ANKA-derived parasite lines, 1804cl1 and G159, were also used. The 1804cl1 (Burda et al., 2015) and G159 (Katie Hughes, unpublished) lines express mCherry and GFP respectively, under the control of the strong constitutive *Pb*hsp70 promoter (PBANKA_0711900).

2.1.3 Monitoring parasitaemia in infected mice

Parasitaemia in infected mice was monitored by examining methanol fixed thin blood smears stained in Giemsa (Sigma) or by flow cytometry analysis of infected blood. A small drop (~2.5 µl) of blood from the tail vein of infected mice was

used to make thin blood smears which were air dried, fixed in methanol for 5-15 seconds and stained in 12% Giemsa (Sigma) for 10-15 minutes. Slides were air dried and examined microscopically on a standard light microscope (100X objective, oil immersion). Estimated parasitaemia was quantified by counting the total number of parasites in at least 10 microscopy fields against the absolute number of RBCs. In some cases, percentage parasitaemia was estimated by flow cytometry analysis of blood stained with Hoescht 33342 (Invitrogen) or based on the expression of pre-engineered fluorescent reporters.

2.1.4 *In vitro* short-term culture of *P. berghei*

Blood from infected mice was collected by cardiac puncture under terminal anaesthetic conditions with the anaesthetic, isoflurane. Blood collection needles and syringes were pre-loaded with 10-50 µl heparin (200 U/ml, Sigma) to prevent blood clotting. *P. berghei* parasites in the infected blood (~1 ml) were cultured and maintained for one developmental cycle using schizont culture media (~150 ml in TC 150CM corning culture flasks) containing RPMI1640 with 5 mM hypoxanthine, 25mM Hepes, 10 mM sodium bicarbonate, 20% foetal calf serum, 100 U/ml Penicillin and 100 µg/ml streptomycin. Culture flasks were gassed for 30 seconds with a special gas mix of 5% CO₂, 5% O₂, 90% N₂ and incubated for up to 22-24 hours at 37⁰ C with gentle shaking (50 rpm), conditions that allow for development of ring stage parasites to mature schizonts. Schizont maturation was monitored by microscopic examination of thin blood smears as described in section 2.1.3.

2.1.5 Isolation of mature schizonts

Schizonts were enriched from the cultures by Nycodenz density flotation as previously described (Janse et al., 2006a, Philip et al., 2013). Cultured parasites were pelleted by spinning at 1700 rpm for 8 minutes, supernatant removed and resuspended in 35 ml volumes in 50 ml Falcon tubes. 10 ml of 55% Nycodenz/PBS (% v/v) solution pre-warmed at 37 °C was then carefully laid at the bottom of the Falcon tube to create a visible layer of separation from the cells. This was then spun at 1700 rpm for 20 minutes with zero deceleration to generate a brown layer interphase of schizonts. Schizonts were pulled out using a sterile Pasteur pipette and pooled in a 15 ml falcon tube. These were further spun

down to obtain cell pellets of schizonts which were resuspended in 300-1000 μ l volumes depending on yield and downstream application.

2.1.6 Parasite transfection and positive selection of transformants

Transfection of *P. berghei* parasites with episomal plasmid DNA was carried out as previously described (Janse et al., 2006a, Philip et al., 2013). In brief, ~10 μ g of plasmid DNA was mixed with Nycodenz purified *P. berghei* schizonts and electroporated using the Amaxa Nucleofector Device II program U-o33. Parasites were then immediately IV injected into the tail vein of naïve mice. Positive selection of transfected parasites was commenced 24 hours later by inclusion of pyrimethamine (0.7 mg/ml, Sigma) in drinking water as all vectors carried the *dhfr* marker which confers resistance to pyrimethamine. Drug selection was maintained for 6-12 days or until transformant parasites were obtained.

2.1.7 Parasite cryopreservation

At a parasitaemia of between 1-5%, infected blood was collected by cardiac puncture under terminal anaesthesia. Preparation of stabilate cryotubes for long term parasite preservation was carried out by mixing in a 1:1 ratio infected blood and freeze mix. The latter solution contained 30% glycerol/PBS (% v/v) solution with Heparin 10 U/ml. The suspensions were transferred to labelled cryotubes, allowed to incubate at room temperature for 5 minutes and stored at -80 °C overnight. Long term storage was carried out by deep freezing in liquid nitrogen.

2.1.8 Cloning by limiting dilution

A donor mouse pre-treated with Phz two days before infection was inoculated with a thawed suspension of cryopreserved stabilates of the parasite line to be cloned. On day 2 post infection, at a parasitaemia of approximately ~0.5% (singly infected), actual parasitaemia in the donor mouse was accurately counted within 1-2 hours before cloning. A tail drop from the donor mouse (~5 μ l) was collected into 1 ml of 1x PBS. 10 μ l of this suspension was used to determine RBC counts using a haemocytometer. After obtaining the cell count, calculations and cell dilutions were carried out to ascertain how many RBCs are required to be injected in order to obtain 0.4 parasites per mouse. A final dilution of 0.4 parasites per 100 μ l was therefore made and injected IV into 10 naïve mice

which achieves an approximate infection rate of 40%. The levels of parasitaemia in the 10 mice was monitored in Giemsa-stained blood films a week after the injection of parasites. Blood from the infected clonal lines was collected by cardiac puncture and used either for cryopreservation or DNA extraction and downstream genotype analysis.

2.1.9 Genomic DNA extraction

Infected blood (~100 µl) was resuspended in 50 ml of ice cold 1x erythrocyte lysis buffer (Thermo), incubated on ice for 10 minutes and spun at 2000 rpm for 10 minutes to obtain parasite pellets. Parasite genomic DNA was extracted from these pellets using the Qiagen DNeasy Blood and Tissue kit according to manufacturers' instructions. DNA was eluted in 50 µl volume of deionised water. Concentration and purity of the extracted DNA was analysed on a Nanodrop spectrophotometer.

2.2 Generation of *P. berghei* mutant parasites by CRISPR-Cas9

2.2.1 Sequence alignment and 3D structural homology modelling

Amino acid sequences were retrieved from PlasmoDB or the standard NCBI protein databases. Amino acid alignments were carried out using the online tool Clustal Omega (Sievers et al., 2011). Basic phylogenetic analysis was carried out using CLC work bench 7.0 (Qiagen). For structural alignment and 3D homology modelling, protein structures for specific amino acid residues were constructed in SWISS-MODEL (Waterhouse et al., 2018) using built in PDB templates and visualized using pyMol 2.3.

2.2.2 Primary vectors

CRISPR-Cas9 vector constructs for *P. berghei* precise genome editing were generated by standard cloning techniques. The Cas9 expressing plasmid ABR099 was used for targeted nucleotide replacement. ABR099 (kindly provided by Dr. Brett Roberts, Figure 2.1) contains the Cas9 endonuclease driven by the *P. berghei* Ef-1α promoter, a Cas9 binding scaffold (scRNA) and a site for cloning the sgRNA both driven by the *P. yoelii* U6 promoter, an *hdhfr* cassette (for pyrimethamine drug resistance selection) and a linker site for insertion of homologous repair templates. sgRNAs targeting the UBP-1 or Kelch13 locus were designed using the web based eukaryotic pathogen CRISPR guide RNA/DNA design

tool (<http://grna.ctegd.uga.edu/>) (Peng and Tarleton, 2015) by directly inputting the sequence of interest. Primary vectors containing the sgRNAs were generated by annealing complementary oligonucleotide pairs (Appendix Table 8.1, 8.2) encoding the guide sequence and cloning them in the dual *Esp3I* sites upstream of the Cas9 binding domain (Figure 2.1). sgRNA pairs were annealed by mixing 15 µl of each primer (100 µM) with 20 µl of deionised water. These were incubated at 72°C for 5 minutes on a heat block. The heat block was then switched off and allowed to cool to room temperature. To assemble the primary vector carrying the sgRNA, the ABR099 plasmid was digested with *Esp3I* (New England Biolabs) according to manufacturer's instructions. The digested plasmid was run on a 0.8% agarose gel (w/v) in a 3x purple loading dye (New England Biolabs) and 1 Kb plus DNA ladder (Thermo). The plasmid backbone was gel extracted and purified using the QIAquick gel extraction kit (Qiagen) according to manufacturer's instructions.

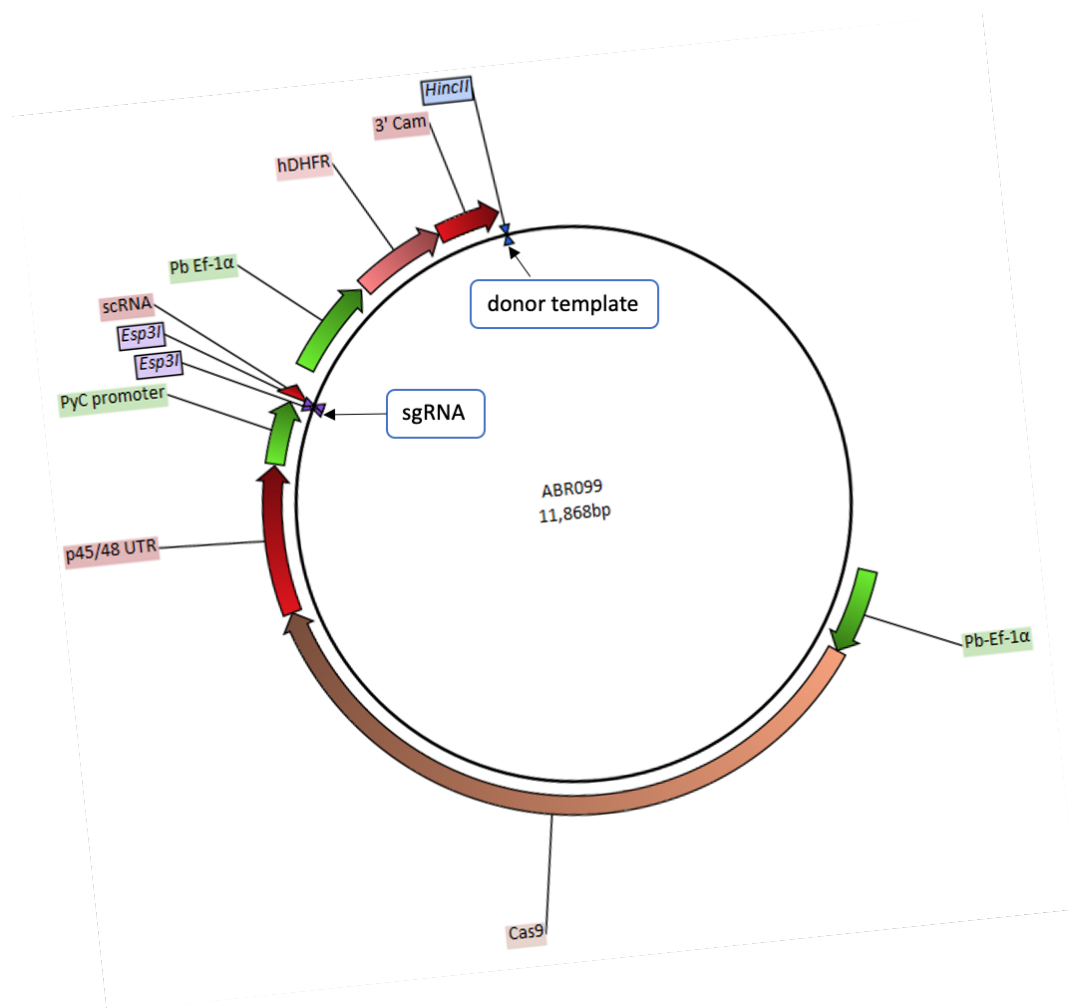


Figure 2.1: Schematic of the ABR099 Cas9 plasmid.

The plasmid contains the gene encoding Cas9 endonuclease and the *hdhfr* gene (for pyrimethamine drug selection) both under the control of separate *P. berghei* EF-1α

promoter units and the sgRNA expression cassettes under the control of *P. yoelii* U6 promoter. A 20bp sgRNA designed to contain *Esp3I* digestion overhangs is cloned into the vector after restriction digestion with *Esp3I*. Donor templates containing mutations of interest are cloned into the secondary vectors carrying appropriate sgRNAs at the *HincII* linker site.

A ligation reaction of the vector backbone and annealed sgRNAs was set up at a molar ratio of 1:10 using the Rapid DNA ligation kit (Roche) according to manufacturer's instructions. Ligated plasmids were transformed into competent *E. coli* cells (DH5 α) by mixing 5 μ l of the ligation with 45 μ l of competent cells and incubated for 30 minutes. In some cases, XL10-Gold[®] Ultracompetent cells (Agilent) were used for transformation as per manufacturer's instructions. The cells were then heat shocked at 42 $^{\circ}$ C for 30 seconds, allowed to recover on ice for 2 minutes following which 250 μ l of pre-warmed SOC media (Thermo) was added and incubated further at 37 $^{\circ}$ C in shaking conditions for 30-45 minutes. Transformed bacteria was then plated on LB (10 g/l tryptone, 5 g/l yeast extract, 5 g/l NaCl) agar plates (1.5 % (w/v) containing ampicillin (100 μ g/ml) and incubated at 37 $^{\circ}$ C overnight. After overnight incubation, individual colonies were isolated and re-incubated in 10 ml of LB liquid broth (100 μ g/ml ampicillin) overnight at 37 $^{\circ}$ C. Plasmid DNA was prepared from the overnight cultures using the QIAprep miniprep kit (Qiagen) according to manufacturer's instructions. For long term storage of the plasmids, 1 ml of the culture was mixed with 100% glycerol in a 1:1 ratio and stored at -80 $^{\circ}$ C. To verify plasmid integrity and correct cloning of the sgRNAs, the plasmid was digested with appropriate restriction enzymes and analyzed by gel electrophoresis. Further confirmation of the sgRNA was confirmed by Sanger DNA sequencing (MWG eurofins).

2.2.3 Site directed mutagenesis (SDM) and generation of secondary vectors

To generate the final vectors for gene editing, donor DNA was amplified by high fidelity KAPA hifi PCR kit (Roche) using a master-mix and reaction conditions as detailed in Table 2.1, 2.2. PCR primers used for amplification of the donor fragments were designed to incorporate the *HincII* restriction site at the 5' end. All primers were designed in CLC work bench 7.0 (Qiagen) and ordered from Sigma Aldrich. Donor PCR fragments were purified using the QIAquick PCR purification kit (Qiagen) according to manufacturer's instructions. Two

approaches to SDM were employed to insert mutations of interest in the donor fragments.

Component	50µl reaction	Final concentration
Deionised water	30 µl	N/A
5X KAPA HIFI buffer	10 µl	1x
10mM dNTP	1.5 µl	0.3 mM
10µM forward primer	1.5 µl	0.3 µM
10µM reverse primer	1.5 µl	0.3 µM
Template DNA	5 µl	50-150 ng
KAPA HIFI polymerase (1U/µl)	0.5 µl	0.5 U

Table 2.1: PCR master mix components.

PCR step	Temperature (°C)	Time	30 cycles
Initial denaturation	95	3 min	
Denaturation	95	30 sec	
Annealing	Primer T _m °C	30 sec	
Extension	68	1 min/kb	
Final extension	68	10 min	
Hold	10	For ever	

Table 2.2: PCR cycling conditions

In the first approach, purified PCR fragments were A-tailed (additional of an A nucleotide overhang) using the standard Taq DNA polymerase and cloned into the TOPO 2.1 vector using the TOPO TA cloning kit (Invitrogen) according to manufacturer's instructions. Primer sets (Appendix Table 8.1) complementary to the TOPO 2.1 cloned PCR fragments were designed to contain specific nucleotide substitutions that carried 1) silent mutations mutating the sgRNA and PAM sites to prevent Cas9 binding the donor templates and the edited loci in the mutant parasites as well as introducing restriction sites for restriction fragment length polymorphism (RFLP) analysis 2) the mutations of interest (Appendix Table 8.2). A site directed mutagenesis of the cloned PCR products in the TOPO 2.1 vector was then carried out using a QuikChange® multi-site directed mutagenesis kit (Agilent technologies) using primer mixes that achieved desired mutation

combinations. Resulting mutant fragments in the TOPO 2.1 vector were then digested out by *HincII* (New England Biolabs), gel purified and cloned into the linker site of the primary vectors carrying appropriate sgRNAs (section 2.2.2) to generate final vectors ready for transfection (Appendix Table 8.2). These final plasmids were also stored in glycerol stocks at -80°C as described in section 2.2.2.

In the second approach, SDM was carried out using overlapping PCR as previously described (Heckman and Pease, 2007). Internal complementary primers carrying silent mutations (for mutating the sgRNA and PAM) and mutations of interest were used to amplify two overlapping PCR products from parasite DNA upon linkage to *HincII* introducing outer primers. Resulting PCR fragments were gel extracted and purified following which ~50 ng of each of the PCR fragment was used as template in a second round of PCR using the two outer primers to generate donor fragments with mutations of interest (Figure 2.2). The resulting fragments were subsequently cloned into the sgRNA carrying vectors (section 2.2.2) at the linker site using the *HincII* restriction site. All plasmids and cloned in donor templates carrying mutations of interest were further verified by Sanger DNA sequencing prior to further use.

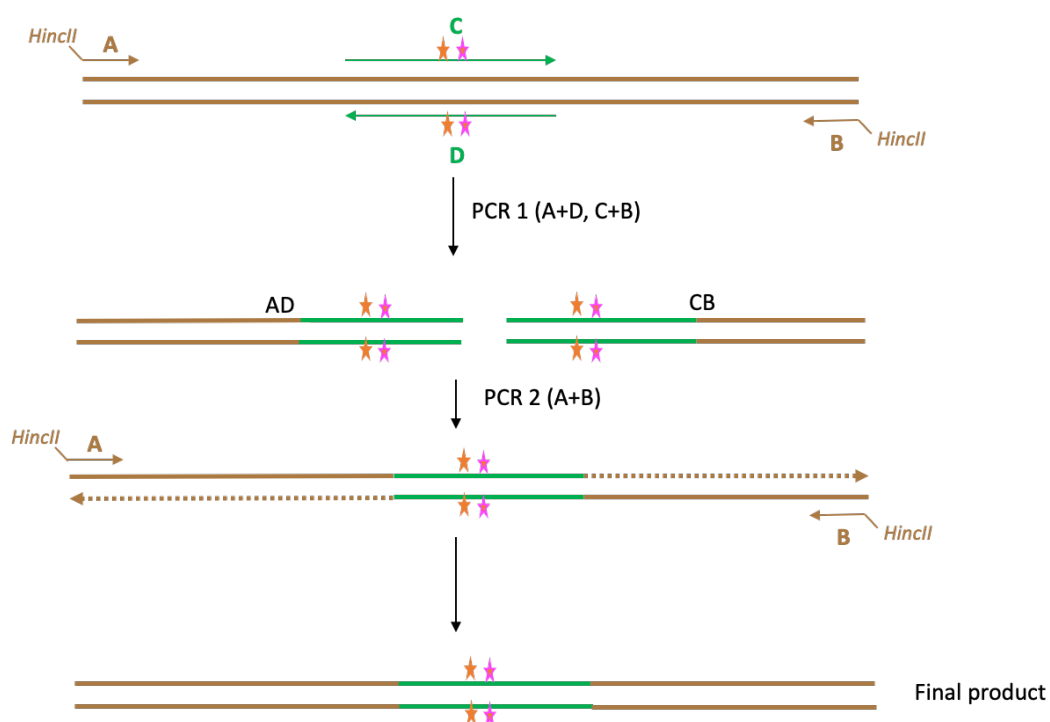


Figure 2.2: Overview of site directed mutagenesis by overlapping PCR.

Two internal complementary primers (C, D in green) carrying mutations of interest (orange and magenta star symbols) were linked to outer primers (A, B) to generate two PCR

fragments (AD, CB) that contain an overlapping sequence (green). These fragments were gel purified and used as templates in PCR 2 using primer sets A and B. Due to the complementary sequence in the AD CB PCR products, these fragments anneal in the first few cycles of PCR and are extended by the polymerase (indicated by arrows) to form a complete template that is amplified in subsequent cycles.

2.2.4 Preparation of plasmid DNA for transfection

~10 µg of plasmid DNA in 10 µl deionised water was used for episomal transfection as described in section 2.1.6. Glycerol stocks of bacterial colonies carrying plasmids of interest were inoculated in 10 ml LB liquid broth (100 µg/ml ampicillin) and incubated at 37 °C overnight. Plasmid DNA was extracted as described in 2.2.2. In case of low plasmid yields, large cultures (midi-preps) were prepared by inoculating 200 ml of LB liquid broth and plasmid DNA was extracted using the QIAprep midiprep kit (Qiagen) according to manufacturer's instructions.

2.2.5 Genotyping of mutant parasites

Blood from parasite infected mice was collected by cardiac puncture under terminal anaesthesia and lysed by resuspension in 1x erythrocyte-lysis buffer (Thermo). Parasite genomic DNA was extracted as described in section 2.1.9. Genotype analysis of the transfected or cloned parasite lines was analysed, initially by a dual PCR-RFLP. PCR was carried out with procedures as specified in Tables 2.1 and 2.2 using primers that bind exterior of the donor DNA templates supplied in the transfection plasmids. Amplified PCR fragments were PCR purified followed by restriction digests with the artificially introduced restriction enzymes to verify successful editing of the target locus (Figure 2.3). Transfection efficiencies were estimated by relative densitometric quantification of individual RFLP fragments by ImageJ2 (Rueden et al., 2017). Further confirmation of the mutations was carried out by Sanger DNA sequencing (MWG eurofins).

2.2.6 Asexual growth competitions of mutant and wild type parasites

Clonal mutant lines in the 820 background were mixed with the 1804cl1 line (~5 x 10⁵ of each line) at a 1:1 mixture and injected IV in mice on a day 0. Parasitaemia in the competition mixtures was quantified by flow cytometry

quantification of mCherry positive parasites for the 1804cl1 proportional percentage and by subtracting the total parasitaemia (Hoechst positive) from the mCherry positive proportion for the 820 control and or mutant lines. Differentiation of the mCherry positive population from the RFP in the 820 line was carried out by applying flow gating strategies (Appendix Figure 8.1). For mutant lines in the 1804cl1 background, competition mixtures were set up as above, besides using the G159 GFP line as a comparative control. Parasitaemias and fractions of mutant versus wild type parasites in these competition mixtures were determined by flow cytometry-based quantification of mCherry or GFP positive parasite populations. In both cases, fractional representation of mutant or wild type lines in the competitions was monitored up to day 9. On day 4 or 5, when parasitaemia was ~5%, mice were bled, and blood diluted in 1x PBS. $\sim 10^6$ parasites from each mouse were passaged into a new naïve host.

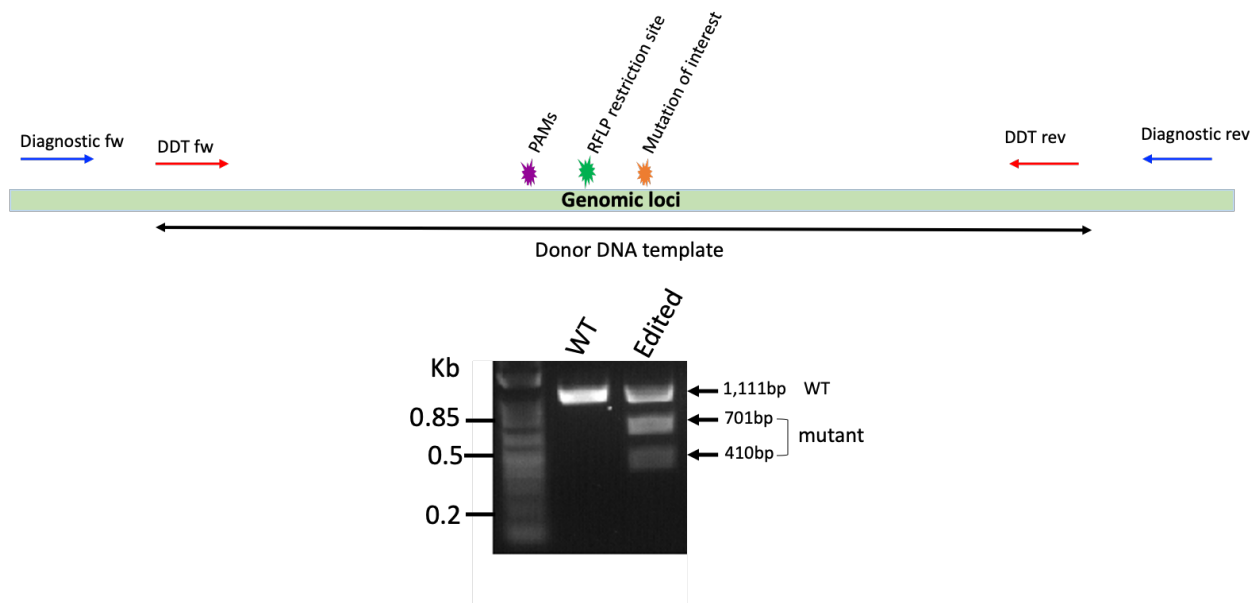


Figure 2.3: Schematic of donor templates supplied in Cas9 plasmids and example RFLP analysis.

Donor DNA templates (DDT) were PCR amplified from the loci of interest by forward and reverse primers as indicated by red arrows. These fragments were modified by site directed mutagenesis to introduce silent mutations that in-activate the PAM site (PAMs), silent mutations to introduce restriction sites for restriction fragment length polymorphism (RFLP) and the mutation of interest as indicated by coloured star symbols. The donor templates were cloned in Cas9 plasmids carrying appropriate sgRNAs and transfected in parasites. To analyse the genotypes of mutant parasites, PCR was used to amplify fragments from genomic DNA of the mutant parasites using exterior diagnostic primers (blue arrows). These PCR fragments were digested by the introduced restriction site as shown in an RFLP analysis in the gel picture. In the displayed gel, diagnostic primers

amplify a 1,111 bp PCR product. In successfully edited parasites, mutants are represented by two RFLP fragments (701, 410bp; *Bst*UI digestion) and some residual wild type (1, 1111 bp) which may or may not be present depending on the editing efficiency. In the wild type, only one fragment (1,111 bp) is observed.

2.3 *P. falciparum* culture and maintenance

Three *P. falciparum* lines, the CQ and ART sensitive 3D7 line, the 3D7 luciferase reporter line (Judith Straimer, unpublished) and the ART resistant Cambodian Kelch13 C580Y mutant line (a kind gift from David Fidock), were used in this work. All lines were cultured and maintained at 1-5% parasitaemia in fresh group O-positive RBCs re-suspended to a 5% haematocrit in custom reconstituted RPMI 1640 complete media (Thermo Scientific) containing 0.23% sodium bicarbonate, 0.4% D-glucose, 0.005% hypoxanthine 0.6% HEPES, 0.5% Albumax II, 0.03% L-glutamine and 25mg/L gentamicin. Culture flasks were gassed with a mixture of 1% O₂, 5% CO₂, and 94% N₂ and incubated at 37°C. Prior to the start of the experiments, asynchronous stock cultures containing mainly ring stages were synchronised with 5% sorbitol as previously described (Lambros and Vanderberg, 1979). In brief, cultures were pelleted by centrifugation at 1,600 rpm for 3 minutes and resuspended in a 10x volume of 5% sorbitol (Sigma), followed by incubation at 37 °C for 10 min. Following incubation, the infected RBCs cells were pelleted again as above and washed in 40 pellet volumes of complete media before placing the infected RBCs back in fresh media and subsequent incubation at 37°C. Human blood was obtained and used within the ethical remit of the Scottish National Blood Transfusion Service for the work carried out at the University of Glasgow.

2.4 Drug susceptibility assays

2.4.1 Drugs and inhibitors

DHA (Selleckchem) was prepared at 1 mM stock concentration in 100% DMSO and diluted to working concentration in complete (*P. falciparum*) or schizont media (*P. berghei*). ART (Sigma) and Epoxomicin (Sigma) were dissolved in 100% DMSO to stock concentrations of 100 µM and 90 µM respectively and diluted in complete culture media or schizont culture media to their respective working concentrations. CQ diphosphate (Sigma) was dissolved to a stock concentration of 10 mM in 1x PBS and diluted to working concentration in complete or schizont culture media. Seven different classes of DUB inhibitors screened in this work

(Appendix Table 8.6) were all obtained from Focus Biomolecules except for 1,10 phenanthroline which was obtained from BPS biosciences. Stocks of DUB inhibitors were prepared at 10 mM in 100% DMSO and diluted in complete or schizont media to working concentrations. All DUB inhibitors were supplied at a purity grade of >97% (Appendix Table 8.6) and further analysed for chemical integrity on a High-Performance Liquid Chromatography (HPLC) platform (Appendix Table 8.7, Appendix Figure 8.16) as detailed below (section 2.4.2). Testing concentrations ranged from 2000-0.01 nM for epoxomicin, DHA, ART and CQ and 100-0.002 μ M for DUB inhibitors. The *Plasmodium* selective proteasome inhibitor EY5-125 also known as compound 28 (Yoo et al., 2018) was used to further test synergy of proteasome inhibitors with DHA in some mutant and wild type parasites. For *in vivo* drug treatment, AS (Sigma) was dissolved in 5 % sodium bicarbonate prepared in 0.9 % NaCl. CQ diphosphate (Sigma) was dissolved in 1x PBS. ART and b-AP15 were prepared in a 1:1 mixture of DMSO and Tween® 80 (Sigma) and diluted 10-fold in sterile distilled water immediately before administration. All drugs were prepared fresh before *in vivo* administration and drug delivery was carried out by IP injection.

2.4.2 HPLC analysis of DUB inhibitors

HPLC solvents were purchased from standard suppliers and used without additional purification. DUB inhibitors were analysed on a Shimadzu reverse-phase HPLC (RP-HPLC) system equipped with Shimadzu LC-20AT pumps, a SIL-20A auto sampler and a SPD-20A UV-vis detector (monitoring at 254 nm) using a Phenomenex, Aeris, 5 μ m, peptide XB-C18, 150 x 4.6 mm column at a flow rate of 1 mL/min. RP-HPLC gradients were run using a solvent system consisting of solution A (H₂O + 0.1% trifluoroacetic acid) and B (acetonitrile + 0.1% trifluoroacetic acid). Further gradient analyses were run from 0% to 100% using solution B over 20 minutes. Analytical RP-HPLC data was reported as column retention time in minutes. Percentage purity was quantified by percentage peak area in relation to main peak.

2.4.3 *P. berghei* short term *in vitro* asexual growth inhibition assays

Drug assays to determine *in vitro* growth inhibition of *P. berghei* by various compounds during the IDC were performed in standard short-term cultures as previously described (Franke-Fayard et al., 2008, Janse et al., 1994b). Briefly, 1

ml of infected blood with a non-synchronous parasitaemia of 3-5% was collected from an infected mouse and cultured for 22-24 hours in 150 ml of schizont culture media. Schizonts were enriched from the cultures by Nycodenz density flotation as described in section 2.1.5 followed by immediate IV injection into a tail vein of a naive mouse. Upon IV injection of schizonts, they immediately rupture with resulting merozoites invading new RBCs within minutes to obtain synchronous *in vivo* infection containing >90% rings and a parasitaemia of 0.5-1.5%. Blood was collected from the infected mice 1-2 hours post injection and mixed with serially diluted drugs in schizont culture media in 96 well plates at a final haematocrit of 0.5% in a 200 µl well volume. Plates were gassed and incubated overnight at 37 °C. Schizont maturation was used as a surrogate marker of growth inhibition. This was quantified based on Hoechst-33258 (Invitrogen) fluorescence intensity or mCherry expression on a BD FACS-Celesta or a BD LSR Fortessa (BD Biosciences, USA) flow cytometer. To determine growth inhibitions and calculate IC₅₀, quantified schizonts in no drug controls were set to correspond to 100% with subsequent growth percentages in presence of drugs calculated accordingly. Dose response curves were plotted in Graph-pad Prism 8.

2.4.4 Adapted *P. berghei* ring stage survival assay

The *P. falciparum* RSA was adapted for *P. berghei* to further assess the *in vitro* ART resistance phenotypes of some mutant parasites based on a previously published protocol (Witkowski et al., 2013). Blood from infected mice (~1.5-hour old ring stage parasites obtained as described in 2.4.3) was adjusted to 0.5% haematocrit and exposed to 700 nM DHA or 0.1% DMSO in 96-well plates or 10 ml culture flasks. The plates and flasks were incubated with the drug under standard culture conditions for 3 hours, following which the drug was washed off at least three times. Parasites were then returned to standard culture conditions in new plates and flasks with fresh schizont media for *in vitro* maturation. After 24 hours of incubation, parasite survival was assessed by flow cytometry analysis of Hoechst-33258 stained infected cells and by mCherry expression. DHA treated samples were compared to DMSO treated controls processed in parallel. Percent survival was calculated using the formula below:

$$\% \text{ survival} = (\% \text{ viability (DHA-treated)}) / (\% \text{ viability (mock DMSO-treated)})$$

To improve the robustness of the viability readouts beyond the 24-hour flow cytometry counts, an *in vivo* expansion of the 3-hour DHA or DMSO exposed parasites was used for selected mutants and the wild type control. After 24 hours of recovery, 2 ml of DHA or DMSO treated parasites were pelleted and resuspended in a 1 ml volume, from which 200 µl was injected IV into mice. *In vivo* parasitaemia was quantified on day 4 post injection, from which % survival based on *in vivo* parasitaemia (absolute counts of mCherry positive parasites) was calculated using the slightly modified formula below:

$$\% \text{ survival} = (\text{parasitaemia (DHA treated)}) / (\text{parasitaemia (mock DMSO-treated)})$$

2.4.5 *P. falciparum* SYBR Green I® assay for parasite growth inhibition

Parasitaemia in the stock cultures was determined and drug assays were performed when the parasitaemia was between 1.5-5% with >90% rings as described in section 2.3. The stock culture was diluted to a haematocrit of 4% and 0.3% parasitaemia in complete media following which 50 µl was mixed with 50 µl of serial diluted drugs/inhibitors in complete media pre-dispensed in black 96 well optical culture plates (Thermo scientific) for a final haematocrit of 2%. Plates were gassed and incubated at 37 °C for 72 hours followed by freezing at -20 °C for at least 24 hours. The plate setup also included no drug controls as well as uninfected red cells at 2% haematocrit. After 72 hours of incubation and at least overnight freezing at -20 °C, plates were thawed at room temperature for ~4 hours. This was followed by addition of 100 µl to each well of 1X SYBR Green I® (Invitrogen) lysis buffer containing 20 mM Tris, 5 mM EDTA, 0.008% saponin and 0.08% Triton X-100. Plate contents were mixed thoroughly by shaking at 700 rpm for 5 minutes and incubated for 1 hour at room temperature in the dark. After incubation, plates were read to quantify SYBR Green I® fluorescence intensity in each well by a PHERAstar® FSX microplate reader (BMG Labtech) with excitation and emission wavelengths of 485 and 520 nm respectively. To determine growth inhibition, background fluorescence intensity from uninfected RBCs was subtracted first. Fluorescence intensity of no drug controls was then set to correspond to 100 % and subsequent intensity in presence of drug/inhibitor was calculated accordingly. Dose response curves and IC₅₀ concentrations were plotted in Graph-pad Prism 8.

2.4.6 *P. falciparum* viability assays

The 3D7 or Kelch13 C580Y lines were synchronised with 5% sorbitol over three life cycles followed by Nycodenz enrichment of later schizonts. Enriched schizonts were incubated with fresh RBCs in a shaking incubator for 3 hours followed by another round of sorbitol treatment to eliminate residual late stage parasites. Resultant ring cultures were diluted to around ~1% parasitaemia and incubated with predefined drug combinations for set time periods. Drugs were washed off 3 times after the set incubation times. Parasite viability was assessed 66 hours later in the second cycle by flow cytometry analysis of parasite cultures stained with Syber Green I and MitoTracker Deep Red dyes (Invitrogen). Flow cytometry analysis was carried on a MACSQuant® Analyzer 10.

2.4.7 *In vitro* drug combinations

P. berghei or *P. falciparum* parasites to be tested in drug combinations were maintained and cultivated as described in sections 2.4.3 and 2.4.5. To determine drug interactions of ARTs in combination with DUB or proteasome inhibitors, serial dilutions of DHA or ART were mixed with fixed ratios of the inhibitors or their fractional combinations at their respective IC_{50} or half IC_{50} . The drug combinations were incubated with parasites from which parasite growth was quantified and dose response curves were plotted, for DHA or ART alone or in combination with the fixed doses of the DUB or proteasome inhibitors. IC_{50} values were obtained and the fold change or IC_{50} shifts were plotted in Graph-pad Prism. For drug interactions in fixed ratios, a modified fixed ratio interaction assay was employed as previously described (Fivelman et al., 2004). Drug combinations were prepared in six distinct molar concentration combination ratios; 5:0, 4:1, 3:2, 2:3 1:4, 0:5 and dispensed in top wells of 96-well plates. This was followed by a 2 or 3-fold serial dilution with precisely pre-calculated estimates that made sure that the IC_{50} of individual drugs falls to the middle of the plate. The drug combinations were then incubated with parasites from which parasite growth and dose response curves were calculated for each drug alone or in combination. For some drug combinations in *P. berghei*, these interactions were assessed using a modified RSA as described in section 2.4.4. ~1.5-hour old post invasion rings were exposed to combination drug ratios as above for 3 hours in 96-well plates following which the drugs were washed off at least 3-times. Percent viability was quantified 24 hours later by flow cytometry

analysis of Hoechst-33258-stained infected cells and mCherry expression. 3-hour exposure dose-response curves were then plotted for each drug alone or in combination. In both cases, fractional inhibitory concentrations (FIC₅₀) were obtained and summed to obtain the Σ FIC₅₀ using the formula below:

$$\Sigma\text{FIC}_{50} = (\text{IC}_{50} \text{ of drug A in combination} / \text{IC}_{50} \text{ of drug A alone}) + (\text{IC}_{50} \text{ of drug B in combination} / \text{IC}_{50} \text{ of drug B alone}).$$

An Σ FIC₅₀ of >4 was used to denote antagonism, Σ FIC₅₀ ≤0.5 synergism and Σ FIC₅₀ = 0.5-4 additivity (Odds, 2003). FIC₅₀ for the drug combinations were plotted to obtain isobolograms for the drug combination ratios.

2.4.8 *In vivo* drug assays: Peter's 4-day suppressive test and recrudescence

To evaluate *in vivo* activity of compounds against *P. berghei*, the Peters' four day suppressive test was employed as previously described (Vega-Rodríguez et al., 2015). A donor mouse was initially infected with *P. berghei* parasites from which blood was obtained when the parasitaemia was between 2-5%. Donor blood was diluted in 1x PBS following which ~10⁵ parasites were inoculated by IP into groups of mice (3-4 mice per group). 1-hour post infection, mice groups received drug doses by IP injection for four consecutive days. Parasitaemia was monitored daily by flow cytometry analysis of infected cells stained with Hoechst-33258 and microscopic analysis of methanol fixed Giemsa stained smears. To quantify drug resistance phenotypes based on recrudescence, infections were initiated by IP as above, inoculating ~10⁶ parasites instead. ~3 hours post inoculation, mice were dosed with either ART or CQ for 3 consecutive days. Parasitaemia was monitored up to day 18 or until recrudescence was observed.

2.4.9 *In vivo* drug assays: Rane's curative test and parasite clearance

To evaluate the potential synergy of some DUB inhibitors (b-AP15) and ART *in vivo*, a modified Rane's curative test in established infections was used (Boampong et al., 2013). Blood was obtained from a donor mouse at a parasitaemia of 2-3% and diluted in 1x PBS. Mice were inoculated with ~10⁵ parasites by IP on day 0 allowing the parasitaemia to rise to ~2-2.5%, typically on day 4. Following the establishment of infection, mice were divided into groups

and received ART or b-AP15 drug doses alone or in combination for three consecutive days. Parasitaemia was monitored daily by flow cytometry analysis of infected cells stained with Hoechst-33258 and microscopic analysis of methanol fixed Giemsa stained smears. The Rane's curative test was further modified to ascertain clearance kinetics of mutant and wild type parasites upon AS treatment. Briefly, the parasitaemia in mice infected with mutant or wild type parasites as above was allowed to rise to ~10%, typically on day 5. On day 5, at time zero, 2 μ l of blood was collected and diluted 200-fold in 1x PBS. Thin blood smears were also collected at this time. Mice were then dosed with AS at 64 mg/kg at 0, 24 and 48 hours. Blood sampling (every 3 hours in the first 24 hours and at least twice thereafter) was performed for flow cytometry analysis and thin blood smears. Parasite density at each time point was determined by absolute cell counts and mCherry expression (for lines in the 1804cl1 background) in 0.1 μ l of whole blood diluted in 1x PBS analysed on a MACSQuant® Analyzer 10. Thin blood smears of parasite morphologies were analysed by microscopy. Significant viability counts in microscopy smears were based on microscopic confirmation of at least four viable parasites in a minimum of 10 fields. Clearance kinetics of normalised parasite densities vs. time were plotted in GraphPad prism.

2.4.10 General statistical methods

All statistical methods (graphs, means and standard deviations) were carried out in at least three biological repeats in GraphPad prism unless otherwise stated. Error bars in graphs are standard deviations. Significant differences between variables were calculated using student's paired t-test for two group comparisons or the one-way ANOVA alongside the Dunnet's multiple comparison test for more than two groups. Significance is indicated with asterisks; * $p < 0.05$, ** $p < 0.01$, *** $p < 0.001$, **** $p < 0.0001$.

2.5 Untargeted metabolomics using LC-MS for MOA studies

2.5.1 *P. falciparum* luciferase kill rate assay

Standard metabolomics screens to characterise MOA of compounds in malaria parasites rely on adequate exposure of parasites to the drugs for a good metabolic signal while avoiding over-exposure which can lead to death related

metabolic signatures (Allman et al., 2016, Cobbold et al., 2016, Creek et al., 2016). This is, however, difficult to quantify especially for fast acting compounds which could potentially elicit metabolic signatures very early on in the parasite killing cascade. A biochemical assay that monitors luciferase expression was therefore used to determine the killing kinetics for the compounds under study. A 3D7 reporter line that expresses NanoLuc and luciferase (3D7 luc; Judith Straimer, unpublished) under the control of a constitutive calmodulin promoter was used. Synchronised trophozoites (~30 hours old) at 2% haematocrit and 2% parasitaemia were incubated with the compounds at 10x IC₅₀ for 0.5, 1, 1.5, 2, 2.5, 3, 3.5, 4, 5, 6 hours. Luciferase expression was quantified on a CLARIOstar microplate reader (BMG Labtech). Briefly, 100 µl of the reconstituted Dual-Luciferase® Reporter reagent (Promega) was mixed with 100 µl parasite culture and incubated at room temperature in the dark for 15 minutes. Luciferase signal was quantified immediately after the incubation. Parasite viability was also monitored by microscopy analysis of methanol fixed Giemsa stained smears.

2.5.2 Magnetic purification of trophozoites

Drug induced metabolomics screens are mostly performed on 24-30 hour old trophozoites as they yield better metabolic signatures as well as less variability (Allman et al., 2016). To enrich for ~24-30 hour old trophozoites of the *P. falciparum* 3D7 line, a magnetic separation was employed as previously described (Kim et al., 2010). Custom magnet stands were 3D printed based on previously reported designs (Kim et al., 2010) and used to assemble a magnetic apparatus which was used to enrich for mature trophozoites in conjunction with cell separation LD columns (Miltenyi Biotech). Briefly, synchronized cultures at 5-7% parasitaemia (~24-30 hours old) were re-suspended to 8% haematocrit following which 5 ml was loaded into the LD columns on the magnetic stands and allowed to flow through. Uninfected RBCs and early stage parasites were washed off by loading the LD column with 5 ml of clean complete media which allows for removal of all unbound RBCs. Bound parasites were then eluted in 5 ml of fresh complete media after removal of the LD columns from the magnetic stands. Eluted parasites were pooled into a single 50 ml Falcon tube from which cell counts (haemocytometer counting) were performed and adjusted to a concentration of $\sim 1 \times 10^8$ cells/ml. Purified parasites, containing >90% purified

trophozoites were allowed to recover for ~1 hour at 37 °C at ~0.5% haematocrit before the start of experiments. Further quality and purity of the enriched trophozoites was assessed by microscopy analysis of methanol fixed Giemsa stained smears.

2.5.3 Metabolite sample preparation

Magnetically purified trophozoites as described above were exposed to compounds (Table 6.1) at 10 x IC₅₀. Atovaquone was used as a positive control while DMSO (0.1%) was used in untreated controls. 1 ml of purified trophozoites (1 x 10⁸ cells) was mixed with 4 ml of complete media containing the drugs at 10x IC₅₀ in 6-well plates for 2.5 hours initially. The concentration used and the time of exposure was based on time kill kinetics of these compounds based on the luciferase assay in section 2.5.1 as well as previously validated drug concentration and corresponding time points which are known to achieve a better metabolic signals (Allman et al., 2016). To resolve the metabolic profiles of fast acting compounds at earlier time points, a similar approach as above was used for selected compounds albeit with a dynamic drug exposure for 0.5, 1 and 2 hours. Incubations at all time points were performed in triplicate over 2 biological repeats. After drug incubation, 4 ml of media was aspirated from the 6-well plates and cells were resuspended in 1 ml volume and centrifuged to pellet the cells. Metabolism was immediately quenched by aspirating the supernatant and resuspending the cells in ice cold 1x PBS. All experiments were performed on ice onwards.

2.5.4 Metabolite extraction

A mixture of water, methanol and chloroform (1:3:1) was used for metabolite extraction to allow for complimentary coverage of both polar and non-polar metabolites as previously described (Srivastava et al., 2015). The chilled suspension of cells was centrifuged at 8,500 g for 30 seconds at 4 °C. After removing the supernatant, the cells were further washed by re-suspending in fresh 500 µl of ice cold 1x PBS and the supernatant was removed again. Cell pellets were then re-suspended in 200 µl of ice-cold chloroform/methanol/water in a 1:3:1 ratio. After vigorously shaking for 1 hour in the cold room or chilled shaker at 4 °C, the samples were sonicated for 2 minutes in ice-cold water and centrifuged at 15, 300 g for 5 minutes at 4 °C. ~180 µl of the supernatant was

transferred to 2 ml clean screw capped tubes for LC-MS analysis. Pooled sample controls were also prepared during this time for quality control during the LC-MS processing. An extraction solvent blank was also included as part of the internal controls. Samples were kept at -80 °C until processed.

2.5.5 LC-MS Metabolomics analysis

Untargeted LC-MS sample processing was carried out at the University of Glasgow Polyomics on a hydrophilic interaction liquid chromatography (pHILIC) on a Dionex UltiMate 3000 RSLC system (Thermo Fisher Scientific) using a ZIC-pHILIC column (150 mm × 4.6 mm, 5 µm column) coupled to a Thermo Orbitrap Q-Exactive mass spectrometer (Thermo Fisher Scientific). 10 µl of the sample maintained on a 5 °C auto-sampler was injected on a column that was maintained at 30 °C. Samples were eluted on a linear gradient, starting with 20% A and 80% B for 15 min, followed by a 2 min wash with 95% A and 5% B, and 8 min re-equilibration with 20% A and 80% B, where solvent A is 20 mM ammonium carbonate in water while solvent B is acetonitrile. The LC-MS method was based on previously published protocols (Creek et al., 2011). Mass spectrometry was operated in polarity switching mode at a resolution of 70 000, 10⁶ cts AGC target, spray voltages + 3.8 and – 3.8 kV, capillary temperature of 320 °C, heater temperature of 150 °C, sheath gas flow rate of 40 a.u., auxiliary gas flow rate of 5 a.u., sweep gas flow rate of 5 a.u., and a full scan mass window of 70–1050 m/z. m/z 83.0604, 149.0233 and 445.1200 were used as lock masses in the positive mode while m/z 89.0244 was used as a lock mass in the negative mode.

2.5.6 Mass spectrometry fragmentation

Samples were also subjected to a fragmentation mass spectrometry analysis (LC-MS/MS) to allow for additional structural information on detected mass features. Fragmentation of the samples was carried out in either the positive or negative ionisation modes or both using duty cycles (1 full scan event and 1 top 5 or top 10 fragmentation event) as previously described (van der Hooft et al., 2016).

2.5.7 Data acquisition

Control runs consisting of blank runs and standardised internal controls were run in accordance with standard procedures at the Glasgow Polyomics to monitor the performance of the mass spectrometer in terms of chromatography and mass

intensities. A mixture of standards containing 150 reference compounds available from Glasgow Polyomics were also run to assess the quality of the mass spectrometer and to aid in metabolite annotation and identification (Creek et al., 2011). Pooled samples containing fractional representation of samples were run prior to and across the batch every 6th sample to monitor the stability and quality of the LC-MS run, whereas the actual samples were run in a randomised manner to minimise batch effects. Thermo Xcalibur Tune software was used for instrument control and data acquisition. After acquisition, all raw files were converted into mzXML format, separating positive and negative ionization mode spectra into two different mzXML files using the command line version of MSconvert (ProteoWizard).

2.5.8 Data processing, analysis and metabolite identification

Data files in mzXML format were processed using an excel interface, IDEOM (Creek et al., 2012), which is based on XCMS and mzmatch R tools that allow raw peak extraction, noise filtering, gap filling and peak annotations (Smith et al., 2006, Scheltema et al., 2011). mzXML files were also processed using PiMP, a web based Glasgow Polyomics metabolomics data processing pipeline (Gloaguen et al., 2017). PiMP is also based on XCMS and mzmatch R tools (Smith et al., 2006, Scheltema et al., 2011) but allows for easy and multiple sample comparisons across experimental conditions. Volcano plots and principal component analysis were visualised and plotted both in IDEOM, PiMP and Metaboanalyst 3 (Xia et al., 2015). Metabolite changes across different conditions and time points were plotted as fold changes or log₂ fold changes. Identification of metabolites was based on fragmentation spectra, retention time and mass compared to authentic standards as previously outlined by the metabolomics standards initiative (MSI) (Sumner et al., 2007). Metabolites that matched an authentic standard with or without fragmentation spectra were classified as identified (MSI level 1). Metabolites which did not match to any authentic standards but had spectral similarities with spectral libraries <https://www.genome.jp/kegg/pathway.html>, were classified as putatively annotated and analysed further based on fragmentation spectra if available.

3 UBP-1 mutations mediate reduced *in vivo* susceptibility to ARTs and CQ in *P. berghei*

3.1 Chapter aim

The aim of this chapter was to examine the role of *P. chabaudi* UBP-1 mutations described in section 1.8.1.2 in modulating resistance to ARTs in an independent rodent model of malaria *P. berghei*.

3.2 Introduction

The emergence of ART (and even ACT) resistance in SEA is seriously threatening recent gains achieved in malaria control (Hamilton et al., 2019, Dondorp et al., 2009). ART resistance is primarily conferred by specific mutations in the *P. falciparum* Kelch13 gene, and such mutations are currently endemic in most parts of SEA (Mbengue et al., 2015, Ashley et al., 2014, WHO, 2018c).

Phenotypically, these mutations are associated with delayed parasite clearance rates *in vivo* and reduced susceptibility of ring stage parasites *in vitro* in RSAs (Dondorp et al., 2009, Witkowski et al., 2013). Interestingly, the prevalence of Kelch13 mutations remains low outside SEA (Menard et al., 2016) where the few observed Kelch13 polymorphisms in Sub-Saharan Africa do not associate with treatment failure and/or delayed parasite clearance rates (Sutherland et al., 2017). Moreover, polymorphisms in other genes such as multidrug resistance protein 2, ferredoxin, coronin, AP-2 μ , Falcipains and many others (section 1.5.5.2) also associate with ART resistance phenotypes. Deconvoluting the geographic complexities of ART resistance, the direct causal role of genetic determinants and molecular mechanism involved would thus provide an avenue to contain or rescue the emergent ART resistance through efficient surveillance and/or suitable combinational therapies.

UBP-1 mutations which were identified as determinants of ART resistance in *P. chabaudi* (Hunt et al., 2007) are some of the candidate ART resistance mutations which despite being observed in cases of ART clinical failure in the field (Henriques et al., 2014, Henriques et al., 2013, Adams et al., 2018, Borrmann et al., 2013, Cerqueira et al., 2017), have remained uncharacterised due to the absence of reverse genetics approaches to validate their involvement. Moreover, the reported drug resistant phenotypes that emerged in these *P. chabaudi* mutant lines were due to selection with a series of drugs in multiple cascades

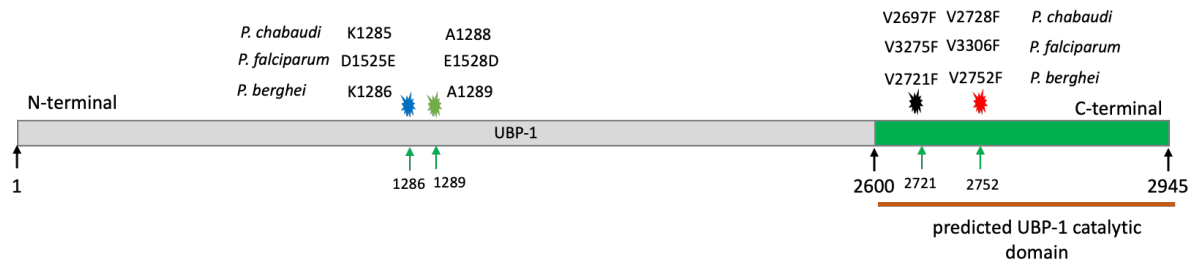
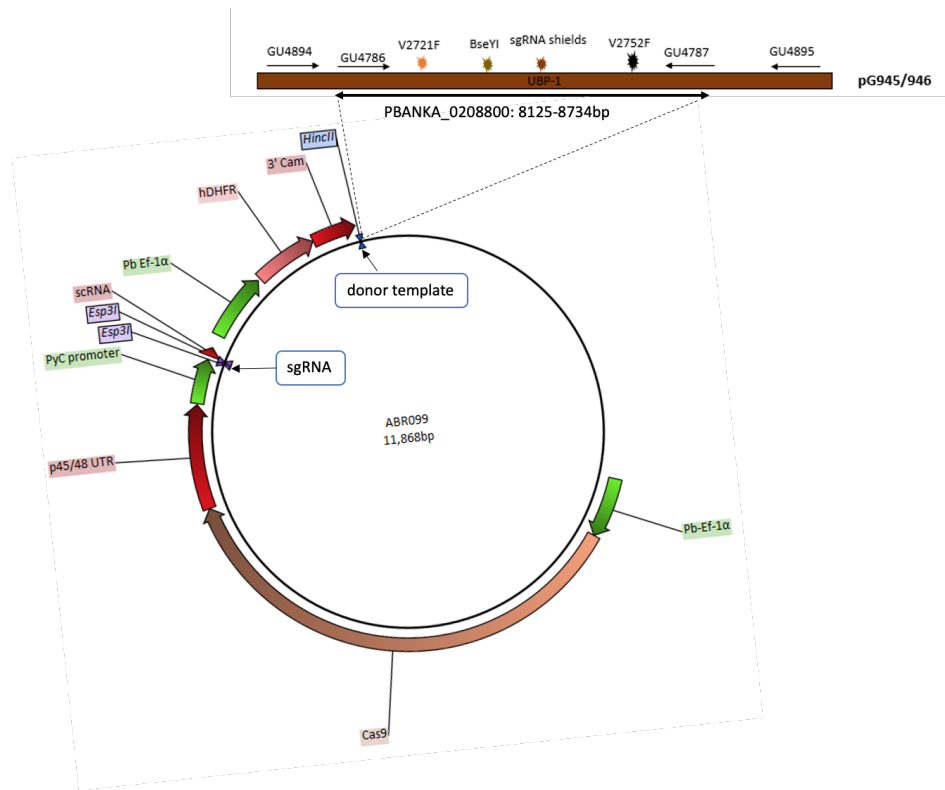
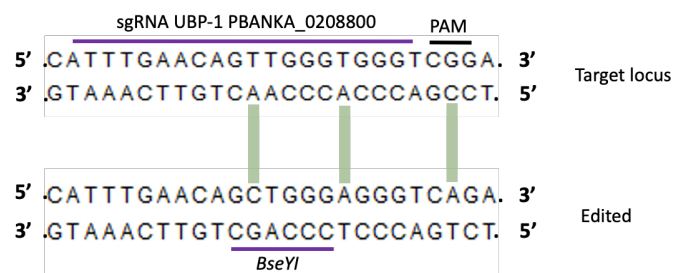
(Section 1.8.1.2). Due to these complexities, it has been specifically difficult to confidently associate these *P. chabaudi* UBP-1 mutations with actual ART resistance phenotypes in the absence of appropriate reverse genetics approaches.

To explore and validate the role of these UBP-1 mutations in mediating ART and possibly CQ resistance, CRISPR-Cas9 genome editing system was employed to engineer orthologous *P. chabaudi* candidate mutations (V2697F and V2728F) in *P. berghei* (V2721F and V2752F). Upon introduction of these mutations, further phenotype analysis was carried out to assess their direct involvement in conferring ART and CQ resistance both under *in vitro* and *in vivo* conditions. The relative fitness of these mutant parasites was also assessed and compared to the wild type non-mutant parasites.

3.3 Results

3.3.1 CRISPR-Cas9 introduction of UBP-1 mutations in *P. berghei*

To experimentally demonstrate that UBP-1 mutations confer selective advantage upon ART pressure, *P. chabaudi* UBP-1 candidate mutation (V2697F and V2728F) equivalents (Figure 3.1a, Appendix Figure 8.2) were introduced in the *P. berghei* 820 line using the CRISPR-Cas9 plasmid system as described in section 2.2. Two plasmids were initially designed to either introduce the single mutation, V2752F (V2728F *P. chabaudi* equivalent) or both mutations, V2721F (V2697F *P. chabaudi* equivalent) and V2752F in an attempt to generate a double mutant (Figure 3.1b). Silent mutations to mutate the Cas9 cleavage site and introduce a restriction site (*Bse*YI) were also introduced to prevent re-targeting of mutated loci by Cas9 for the former and diagnosis by RFLP for the latter (Figure 3.1b, 3.1c, Appendix Table 8.2). Transfections of these plasmids (pG945, pG946, Appendix Table 8.2) into the 820 line yielded ~0.48% mutants for the V2752F mutant line (G1807, pG945) and ~23.00% mutants for the V2721F and V2752F double mutant line (G1808, pG946) as confirmed by RFLP analysis (*Bse*YI digestion) of the edited UBP-1 loci (Figure 3.1d, Appendix Table 8.3).

a**b****c**

d

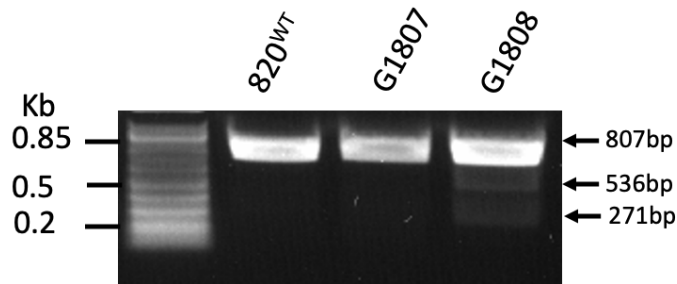


Figure 3.1: Introduction of UBP-1 mutations in *P. berghei*.

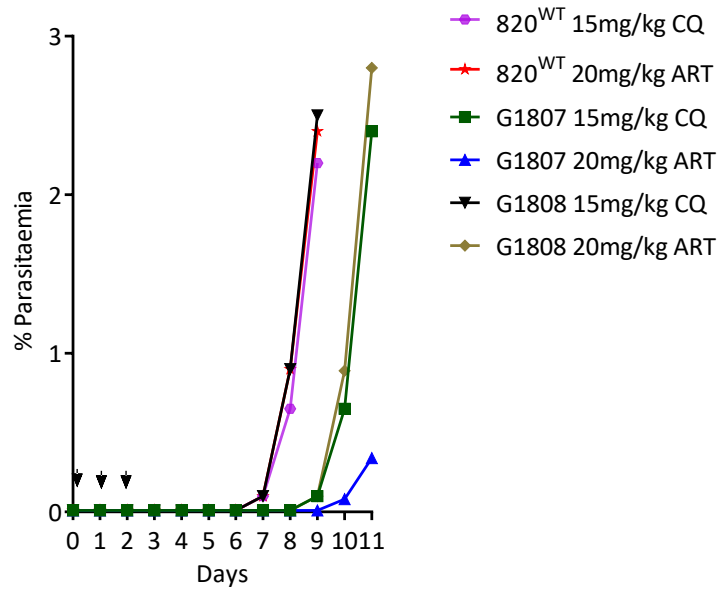
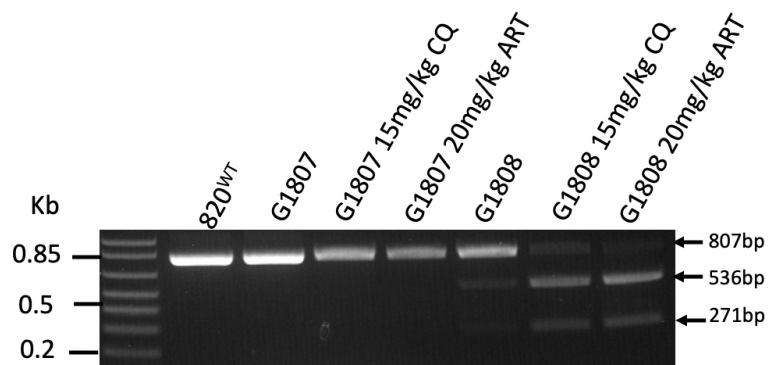
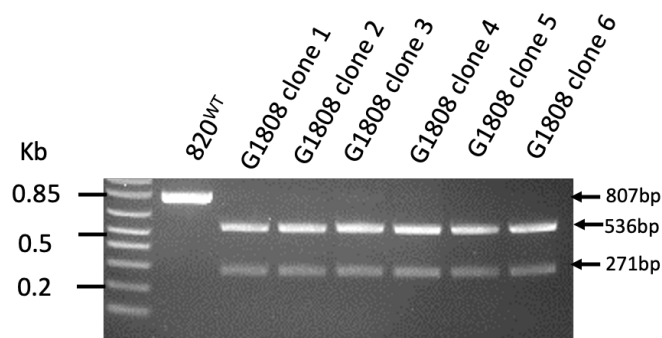
a. Schematic of *P. berghei* UBP-1 showing the predicted catalytic domain and localisation of the engineered mutations and their *P. falciparum* and *P. chabaudi* equivalents. Positions of *P. falciparum* UBP-1 D1525E and E1528D mutations which have been reported in the field but are not conserved in *P. berghei* and *P. chabaudi* are indicated. **b.** Plasmid constructs for the UBP-1 targeted gene editing to introduce the V2721F and V2752F mutation. The plasmid contains Cas9 and *hdhfr* (for pyrimethamine drug selection) under the control of the Pb EF-1 α promoter and the sgRNA expression cassettes under the control of PyU6 promoter. A 20 bp sgRNA was designed and cloned into the sgRNA section of the vector illustrated in B. The donor UBP-1 sequence (610 bp) is identical to the wild type albeit with the desired mutations of interest as indicated by coloured star symbols: V2752F (pG945), V2721F V2752F (pG946) and silent mutations that mutate the Cas9 binding site as well as introduce the restriction site *Bse*YI for RFLP analysis. **c.** Illustrated 20 bp sgRNA. **d.** RFLP analysis of mutant parasites. Successful editing in the transfected parasites was observed on day 12 after transfection and pyrimethamine drug selection. RFLP (*Bse*YI digestion) analysis of the transformed lines PCR products (primers GU4894 + GU4895, 807 bp) revealed ~0.5% and ~23% efficiency for the G1807 and G1808 lines respectively as indicated by 2 distinct bands (536 bp, 271 bp) as compared to 807 bp bands in the parent 820 line.

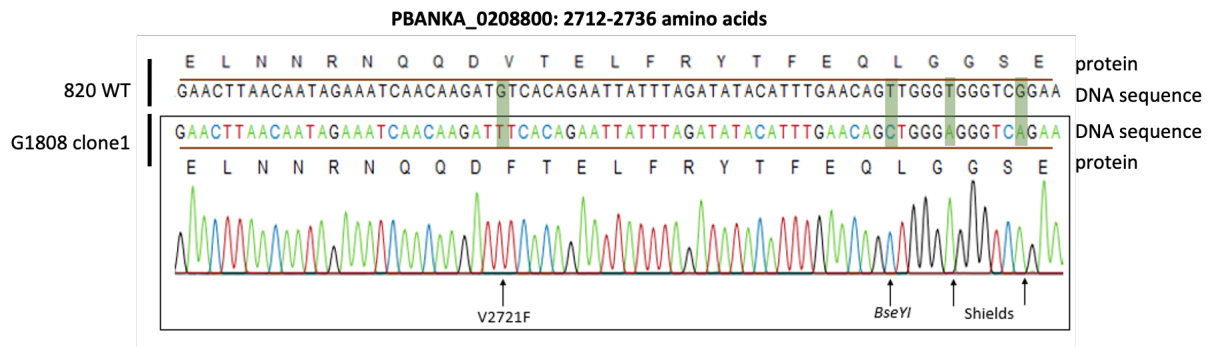
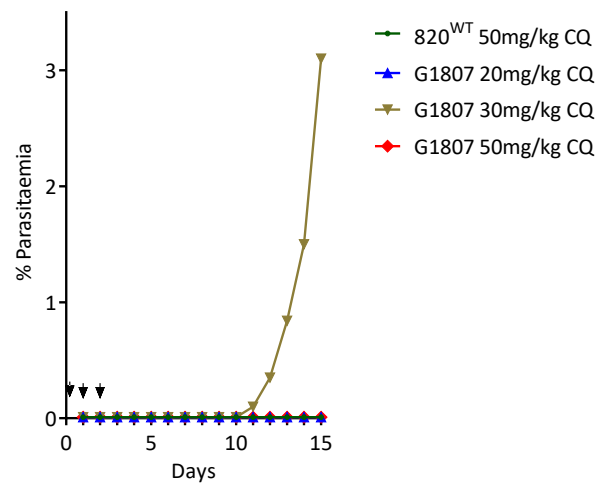
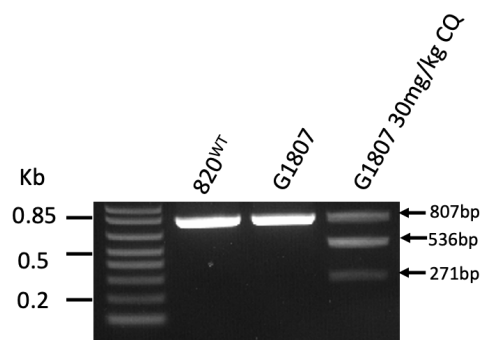
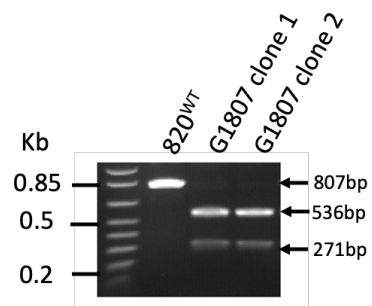
3.3.2 Engineered mutations in UBP-1 confer *in vivo* selective advantage to ART and CQ pressure in *P. berghei*

Since the editing efficiency in these UBP-1 mutant lines was too low to clone out the mutant population by limiting dilution, a pre-emptive drug selection with CQ and ART was attempted for the G1807 and G1808 lines to examine if selective enrichment of the mutant population could be achieved with these drugs.

Indeed, after infecting mice with the G1808 line and treating for three consecutive days with ART at 20 mg/kg, the recrudescence parasite population on Day 9 was enriched to ~90% mutant as confirmed by RFLP analysis (Figure 3.2a,

3.2b, Appendix Figure 8.3, Appendix Table 8.3). Meanwhile, CQ at 15 mg/kg also enriched the G1808 line to ~80%, relatively less compared to ART (Figure 3.2a, 3.2b, Appendix Table 8.3). On the contrary, a very low-level mutant enrichment of the G1807 line (0.5% to 2.6%) was observed with CQ at 15 mg/kg while ART did not produce any enrichment in the same line (0.5%). Interestingly, cloning of the G1808 ART enriched lines yielded six clones which were all single mutants positive for the V2721F mutation despite coming from a plasmid with donor templates that carried both the V2721F and V2752F mutations (Figure 3.2c, Figure 3.2d). This suggests that the single V2721F mutation carrying parasites were predominant in the G1808 line (despite resulting from transfection with a plasmid carrying both mutations) and were selectively enriched by ART. These data also suggested that introducing both mutations into the same parasite could either be lethal or results in very unfit parasites that are easily cleared by the host during early growth following transformation. Indeed, bulk DNA sequence analysis of the G1808 uncloned line revealed the absence of traces for both mutations as only the V2721F with silent mutations were present (Appendix Figure 8.4). Sequence analysis of the G1808 line isolated after CQ challenge at 15 mg/kg also confirmed specific enrichment for the V2721F mutation (Appendix Figure 8.3) suggesting that despite being principally enriched by ART, the V2721F mutation also modulates some low-level protection to CQ. Meanwhile, when the G1807 line (V2752F single mutation) was challenged with CQ at higher doses (20, 30, 50 mg/kg), a recrudescence population was observed on Day 10 with CQ 30 mg/kg (Figure 3.2e). The CQ 30 mg/kg recrudescence parasites were enriched to ~61 % for the mutant population (Figure 3.2f, Appendix Figure 8.5, Appendix Table 8.3) and were subsequently cloned (Figure 3.2g). Sanger sequencing of G1808 ART enriched and G1807 CQ enriched clones confirmed the presence of the single V2721F and V2752F mutations respectively, as well as the Cas9 cleavage silencing mutations and the silent mutations introducing the *Bse*YI diagnostic restriction site (Figure 3.2d, 3.2h).

a**b****c**

d**e****f****g**

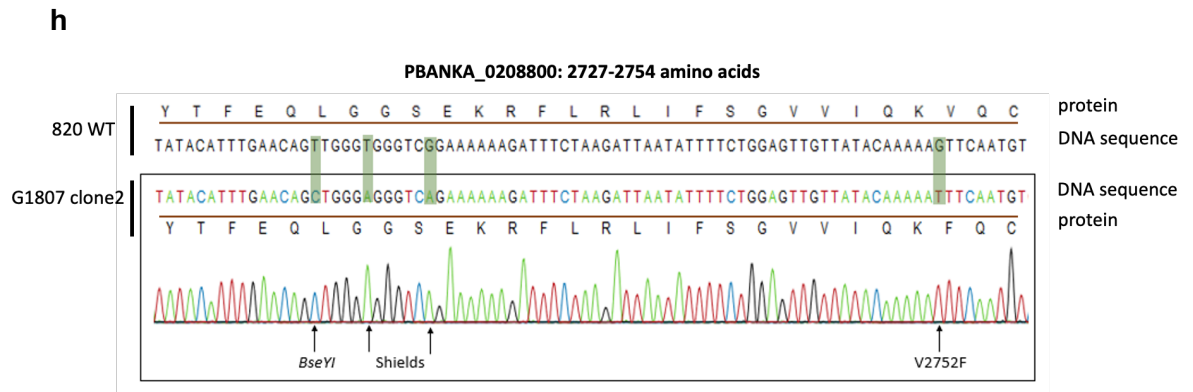


Figure 3.2: Enrichment of UBP-1 mutant lines by drug challenges and cloning of mutant lines.

a. pre-emptive challenge of the G1807 and G1808 lines with ART and CQ at 20 mg/kg and 15 mg/kg respectively. Mice were infected with $\sim 2 \times 10^7$ parasites by IP on day 0. Treatment was started ~ 3 hours post infection by IP for three consecutive days. Parasitaemia was monitored by microscopy analysis until recrudescence was observed. **b.** RFLP analysis of recrudescence parasites. **c.** RFLP analysis of the cloned G1808 ART 20 mg/kg recrudescence parasites. **d.** DNA sequencing confirming successful nucleotide editing in the G1808 clone1 line. The top sequence represents the 820^{WT} unedited sequence with positions for sgRNA, PAM and V2721F mutations indicated. The bottom sequence illustrates the nucleotide replacements at the V2721F mutation loci and silent mutations to prevent Cas9 retargeting as well as introduce the *BseYI* restriction site for RFLP analysis in the G1808^{V2721F} lines. **e.** Pre-emptive challenge of the G1807 line with higher doses of CQ. Mice were infected and treated with CQ as in Figure 3.2a. **f.** RFLP analysis (*BseYI* digestion) of the G1807 recrudescence population after challenge with 30 mg/kg CQ. **g.** RFLP analysis of the cloned G1807 CQ 30 mg/kg recrudescence parasites. **h.** DNA sequencing confirming successful nucleotide editing in the G1807 clone2 line indicating mutation sites.

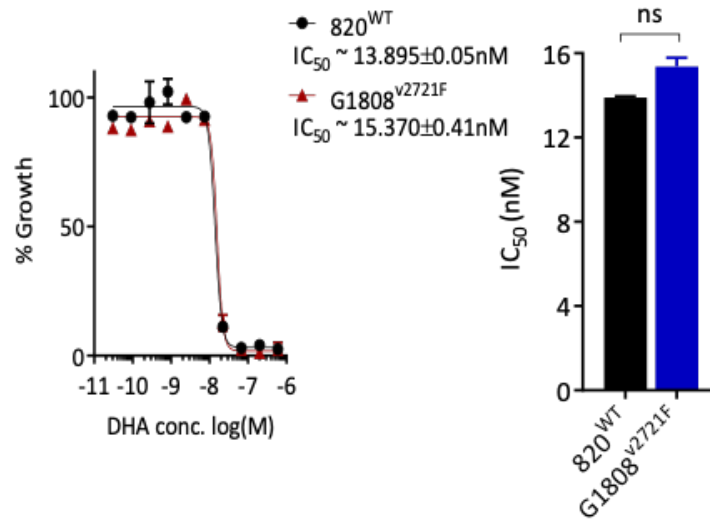
3.3.3 The V2721F mutation confers observable reduced *in vivo* susceptibility to ARTs while the V2752F mutation confers resistance to CQ and low-level protection to ARTs in *P. berghei*

After cloning the UBP-1 mutant parasites (Figure 3.2), a quantification of the drug response profiles of the cloned lines (first clone in each of the lines) was carried out to assess their *in vitro* and *in vivo* phenotypic responses to DHA, ART and CQ. In short term *P. berghei* *in vitro* drug assays, both the G1808^{V2721F} and G1807^{V2752F} parasites showed no difference in sensitivity to DHA compared to the parental 820 line (Figure 3.3a, 3.3b). The lack of decreased drug sensitivity of

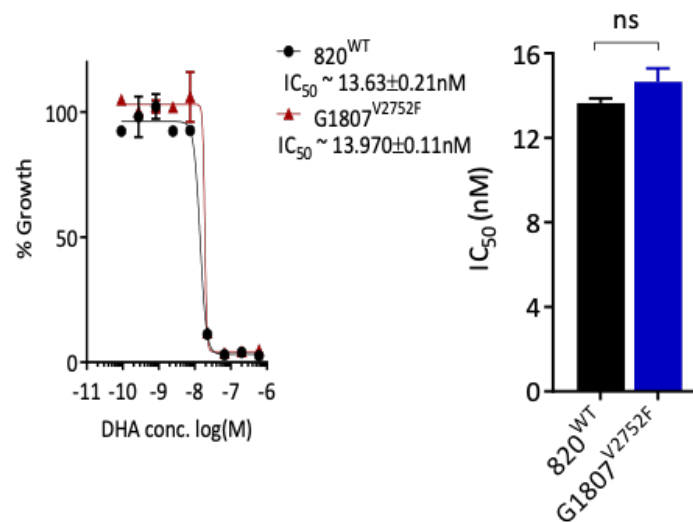
both lines is consistent with the failure of the standard 72-hour drug assays to differentiate similar Kelch13 ART resistant parasites from sensitive lines in *P. falciparum* (Witkowski et al., 2013, Dondorp et al., 2009). Meanwhile, a 1.8-fold increase in IC_{50} was observed for the G1807^{V2752F} line when challenged with CQ (Figure 3.3c) and not the G1808^{V2721F} (Figure 3.3d). However, rodent malaria parasites offer the advantage of experimental drug resistance assessment *in vivo*. Therefore, the *in vivo* drug responses of the mutant lines to parental ART, which with controlled parasite inocula has been shown to effectively suppress wild type parasites for up to 18 days following 100 mg/kg dosing for three consecutive days (Hunt et al., 2010) was profiled. This is unlike with the ART derivative, and clinically relevant AS, which permits recrudescence in wild type rodent malaria parasites at doses as high as 300 mg/kg within 14 days (Walker and Sullivan, 2017). This approach when applied to G1808^{V2721F} demonstrated that this mutation does indeed confer enhanced *in vivo* tolerance to ARTs compared to the parental 820 line. G1808^{V2721F} parasites survived three consecutive doses of 75 mg/kg ART with the recrudescence population appearing on day 9 after last dosing while 820 wild type parasites were effectively suppressed up to day 17 of follow-up (Figure 3.3e). Both the G1808^{V2721F} and 820 lines survived 45 mg/kg dose of ART with the former having a slightly faster recrudescence rate on day 7 while the latter recrudescence a day later (Figure 3.3e). Even though ART at 45 mg/kg did not significantly separate wild type from mutant parasites, this could be due to the fitness cost that the V2721F mutation carries (Figure 3.4) which would explain their recrudescence at almost the same time as the wild type as they would require a slightly longer time to achieve quantifiable parasitaemias. Both lines remained sensitive to 125 mg/kg ART dose with no recrudescence observed up to day 17 (Figure 3.3e). In contrast, the G1807^{V2752F} line was relatively resistant to CQ *in vivo* (Figure 3.3f), surviving three consecutive doses at 25 mg/kg, with recrudescence parasites observed on day 4 after the last dose as compared to the parental 820 line and the G1808^{V2721F} lines which were susceptible and effectively suppressed up to day 17. Interestingly, the G1807^{V2752F} line also displayed low level reduced susceptibility to ART at 75 mg/kg dose, with parasites coming up on day 12, later than the G1808^{V2721F} line (Figure 3.3f). These data confirmed that the V2721F mutation confers protection from ART drug challenge while the V2752F mutation mediates resistance primarily to CQ and to some extent, a low-level

protection to ARTs. The recrudescence of the wild type 820 and G1808^{V2721F} at 45 mg/kg ART is also in agreement with previous findings that *P. berghei* is less sensitive to ARTs, especially in the spleen and bone marrow which could be the source of recrudescence infection at relatively lower doses (Lee et al., 2018).

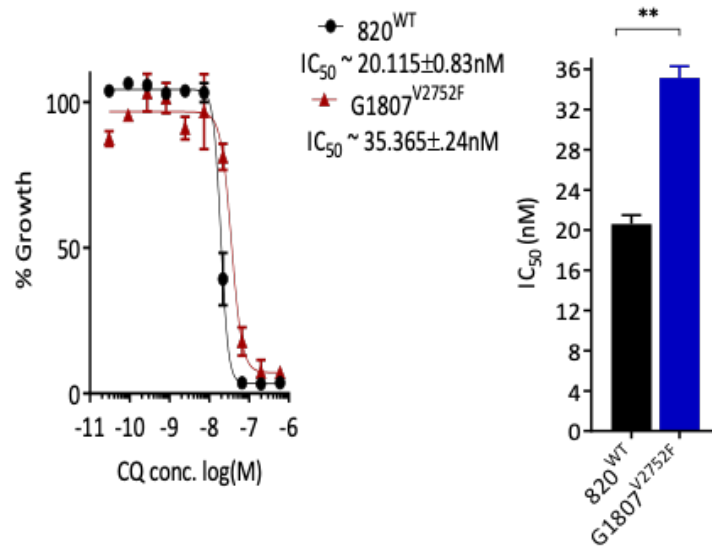
a



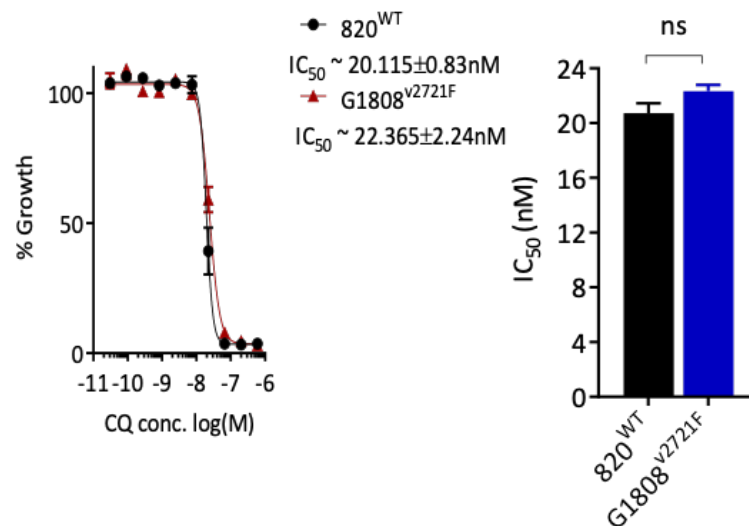
b



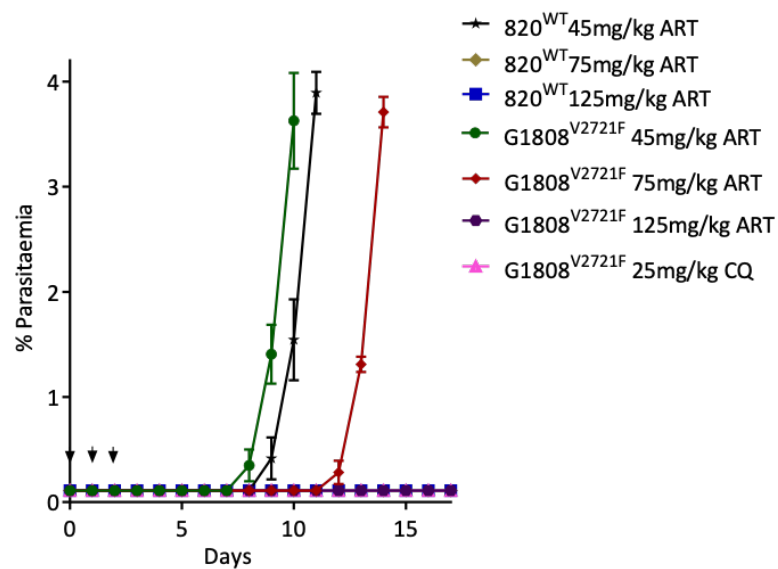
c



d



e



f

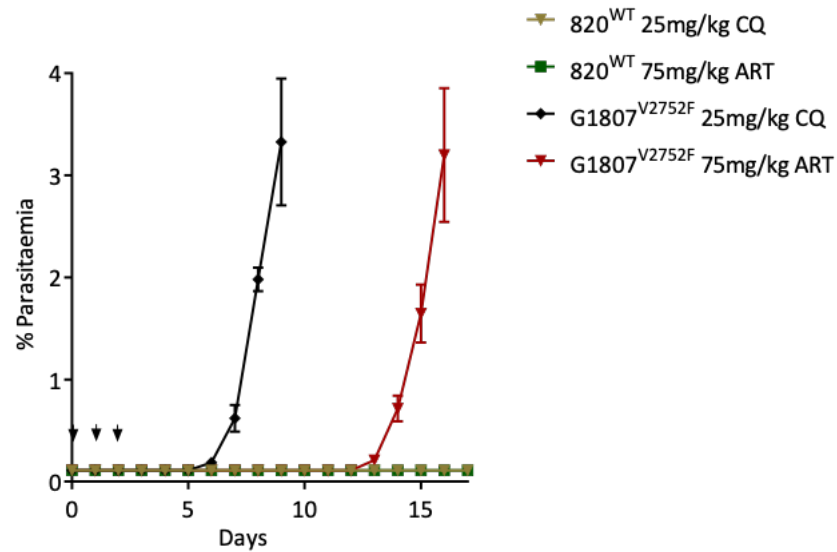


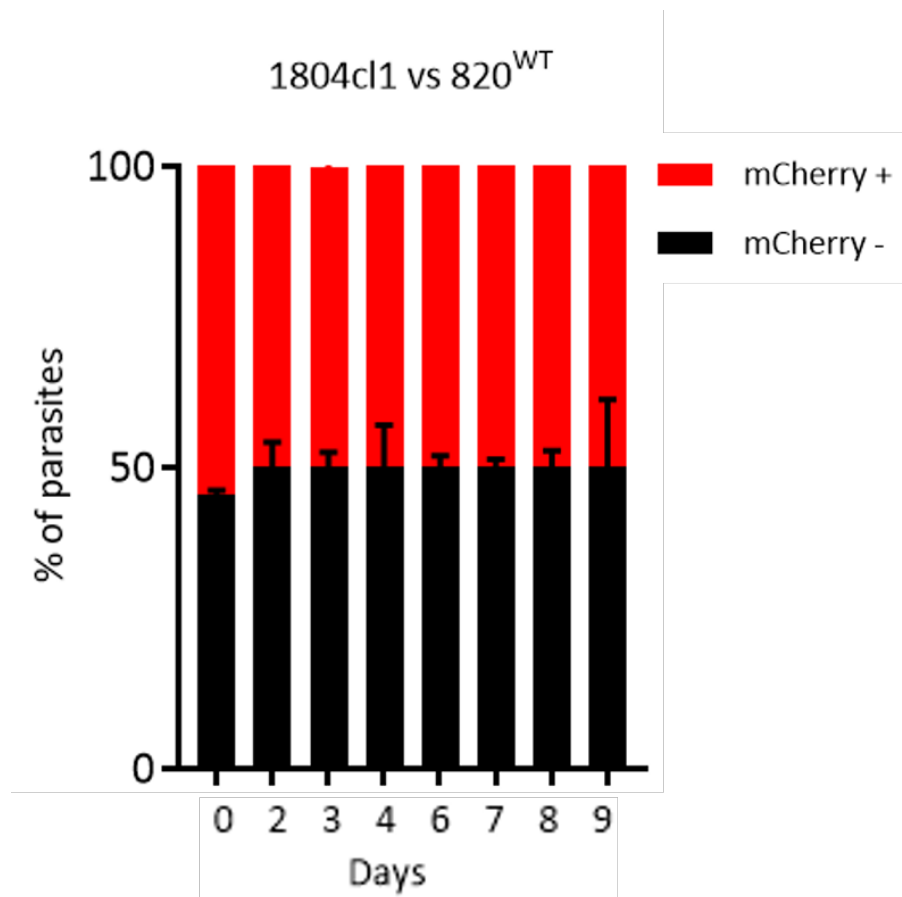
Figure 3.3: ART and CQ *in vitro* and *in vivo* resistance profiles of the G1807^{V2752F} and G1808^{V2721F} lines.

a, b. DHA dose response curves and IC₅₀ comparisons of the G1808^{V2721F} (**a**) and G1807^{V2752F} (**b**) lines relative to the wild type 820 line. **c, d.** CQ dose response curves and IC₅₀ comparisons of the G1807^{V2752F} (**c**) and G1808^{V2721F} (**d**) lines relative to the wild type 820 line. Significant differences between mean IC₅₀ or IC₅₀ shifts were calculated using the paired t-test. Error bars are standard deviations from three biological repeats. Significance is indicated with asterisks; **p < 0.01, ns; not significant. **e, f.** Modified Peters' 4-day suppressive test to monitor resistance to ART and CQ *in vivo* in the G1808^{V2721F} (**e**) and the G1807^{V2752F} (**f**) mutant lines. Groups of 3 mice were infected with 1 x 10⁶ parasites on day 0. Treatment started ~1.5 hours later with indicated drug doses every 24 hours for three consecutive days (treatment days shown by arrows). Parasitaemia was monitored by microscopy analysis of Giemsa stained blood smears up to day 18. Error bars are standard deviations of parasitaemia from 3 mice.

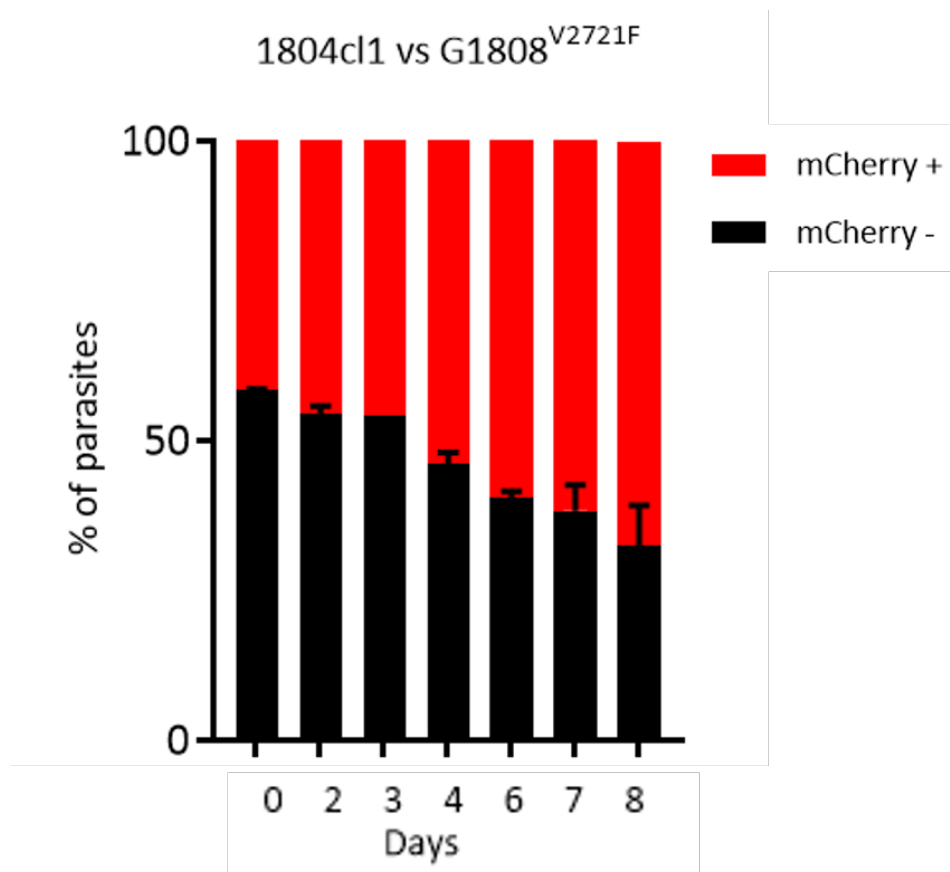
3.3.4 Growth of parasites carrying UBP-1 V2752F and V2721F mutations is impaired

The spread of drug resistance as is the case in most microbial pathogens is partly limited by detrimental fitness costs that accompany acquisition of such mutations in respective drug transporters, enzymes or essential cellular components. The G1807 and G1808 lines carrying UBP-1 V2721F and V2752F mutations respectively were each grown in competition with a parental line expressing mCherry *in vivo* and shown to be characteristically slow growing (Figure 3.4a-c).

a



b



c

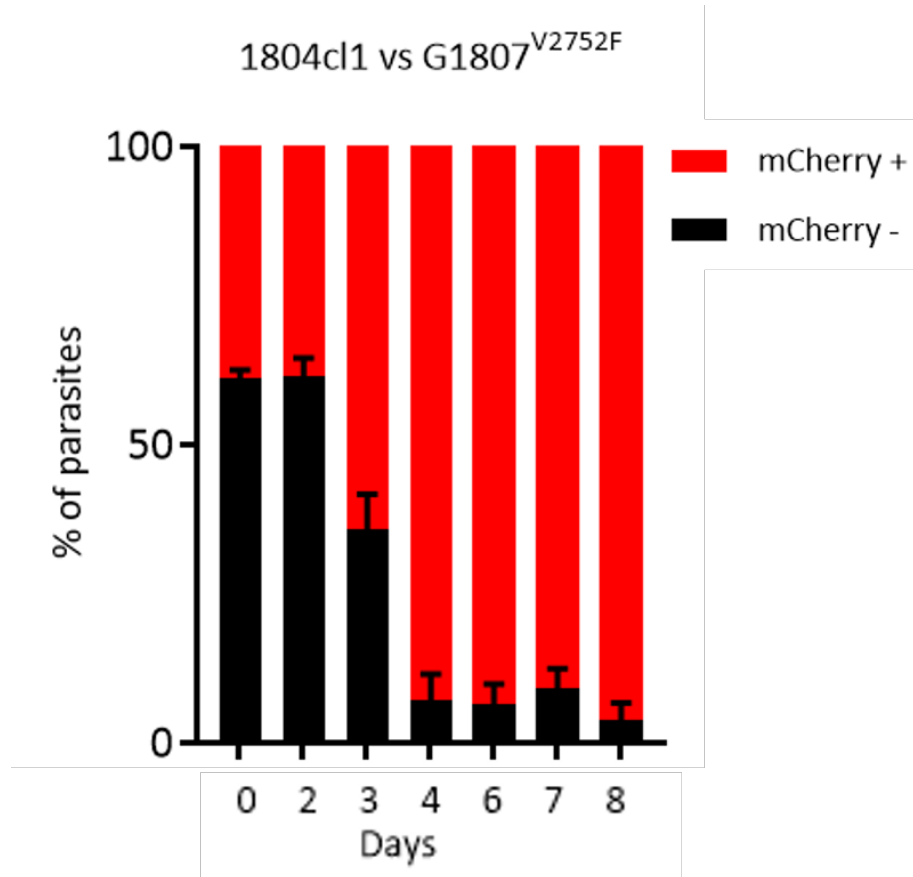


Figure 3.4: Growth kinetics of the 820, G1808^{V2721F} and G1808^{V2752F} relative to the 1804cl1 line.

a, b, c. The 1804cl1 line constitutively expresses mCherry under the control of the *hsp70* promoter. The 820, G1808^{V2721F} and G1808^{V2752F} were mixed with the 1804cl1 at a 1:1 ratio and injected at a parasitaemia of 0.01% by IV on Day 0. Daily percentages of representative parasitaemia of the 820 or mutant lines in the competition mixture were quantified by subtracting the total parasitaemia based on positivity for Hoescht DNA stain from the fraction of the population that is mCherry positive (1804cl1) as determined by flow cytometry. On day 4, when parasitaemia was ~5%, blood from each mouse was passaged into new naïve host and parasitaemia was monitored until day 9. Percentage population changes of the mutant and wild type lines relative to the 1804cl1 in the 820 (**a**), G1808^{V2721F} (**b**) and G1807^{V2752F} (**c**). Error bars are standard deviations from three biological repeats.

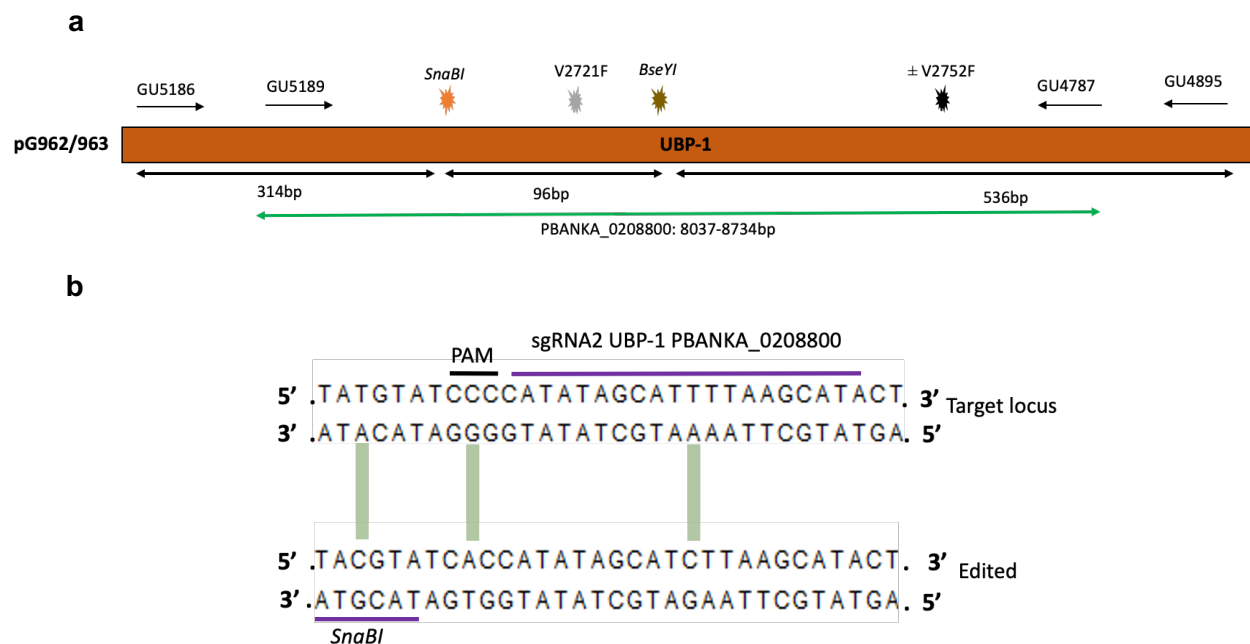
Comparatively, the G1807^{V2752F} mutation was severely impaired relative to the G1808^{V2721F} being completely outcompeted by day 8 (Figure 3.4b, 3.4c). These data and the earlier failure to generate the double mutant (Figure 3.1, 3.2) demonstrated that UBP-1 is an important (possibly essential) protein for parasite

growth and that acquisition of resistance through mutation of UBP-1 confers mutation specific fitness costs.

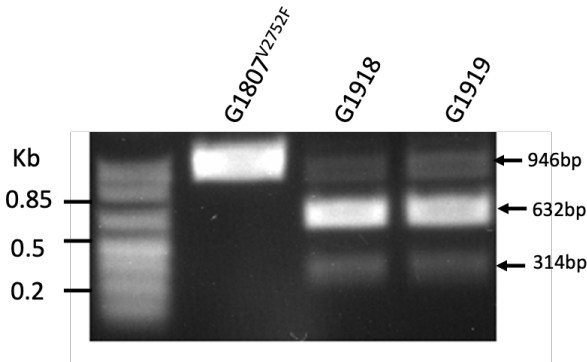
3.3.5 Reversal of the V2752F mutation restores CQ sensitivity in the G1807^{V2752F} line while introduction of the V2721F in the same line appears to be lethal

Drug pressure can select, in the long or short term, for mutations in sensitive parasite populations that would affect responses to the same drug. To further confirm that the phenotypes observed in the mutant lines were due to the V2721F or V2752F mutations and not possible secondary mutations which may have been acquired during the pre-emptive drug pressure, an attempt was made to reverse the V2752F mutation in the G1807^{V2752F} line by swapping it to the V2721F genotype. This would allow for a determination of whether wild type CQ phenotypes can be restored in the G1807^{V2752F} line while at the same time assess if the ART susceptibility profiles of the G1808^{V2721F} mutants could be reproduced in an independent line. Using a CRISPR-Cas9 editing strategy similar to the one outlined in Figures 3.1, a sgRNA targeting a region ~50 bp upstream of the V2721F mutation was designed and cloned in the Cas9 expressing vectors (Figure 3.5a, 3.5b). 698 bp of donor DNA (GU5189 + GU4787) containing the V2721F (for targeted mutation swap) or both the V2721F and V2752F mutations (for a forced introduction of the V2721F in the G1807^{V2752F} background) was used to generate the vectors pG963 and pG962 respectively (Figure 3.2a, Appendix Table 8.2). Silent mutations mutating the PAM site as well as introducing a second restriction site, *SnaBI*, for RFLP analysis were also included. Transfection of the G1807^{V2752F} line with pG963 and pG962 vectors successfully edited the UBP-1 loci generating the G1918 and G1919 lines respectively with ~88 % and ~79 % efficiency as confirmed by *SnaBI* RFLP analysis (Figure 3.5c, Appendix Table 8.3). Cloning and sequencing of the G1918 line revealed successful targeted mutation swap, introducing the V2721F mutation and re-editing of the 2752F to 2752V wild type genotype (Figure 3.5d, 3.5e). Phenotype analysis of the G1918 clone1 line revealed a restored *in vitro* susceptibility to CQ similar to the 820 wild type and a similar *in vitro* DHA sensitivity (Figure 3.5f, 3.5g). Under *in vivo* conditions, the G1918cl1 line displayed a similar ART susceptibility profile at 75 mg/kg as the G1808^{V2721F} line while CQ sensitivity was completely restored (Figure 3.5h). This provided further experimental evidence, that the drug

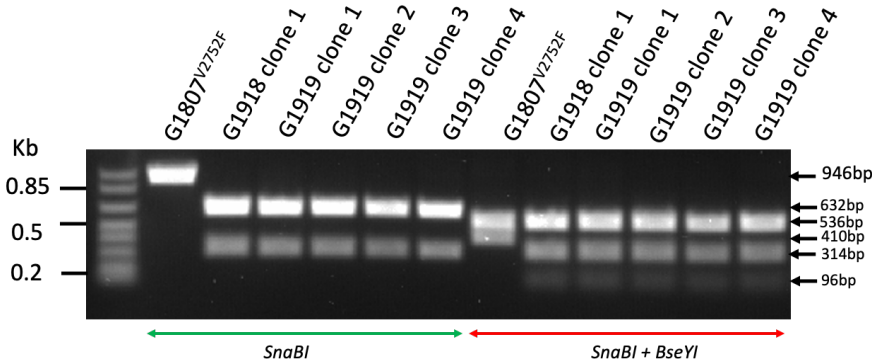
susceptibility profiles observed were due to the V2721F or V2752F amino acid substitutions and not the introduced silent mutations or secondary mutations that may have been acquired during the pre-emptive drug exposure. Interestingly, cloning and sequencing of the G1919 line (Figure 3.5d, 3.5j) revealed successful introduction of the silent mutations (PAM mutating and *SnaBI*) while the V2721F mutation was absent in all four clonal lines, yet retained the parental V2752F mutation. This suggested that introduction of the V2721F in the V2752F background is lethal or refractory in the parasite and further supported initial failed attempts to generate a double mutant line (Figure 3.1,3.2). Detailed sequence analysis of the transfected parasite populations before cloning revealed the presence of only one mutation trace in the G1919 line (despite the donor DNA containing both mutations) further confirming that the double mutant parasites do not survive or are severely growth-impaired and quickly overgrown by the single mutation parasites (Figure 3.5i).



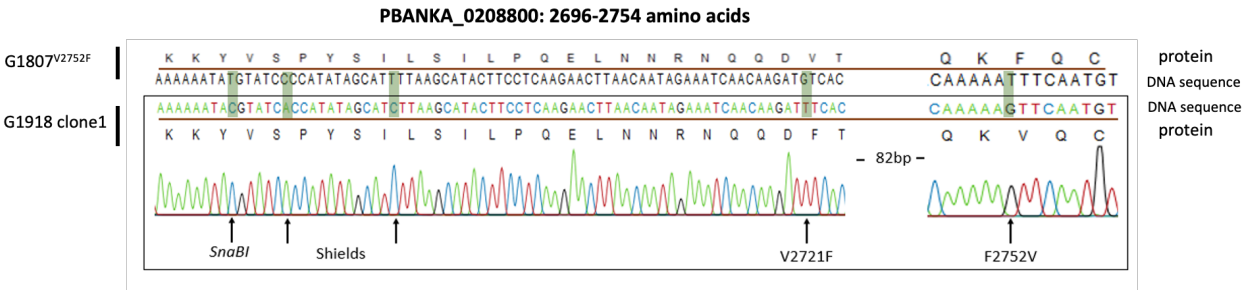
c



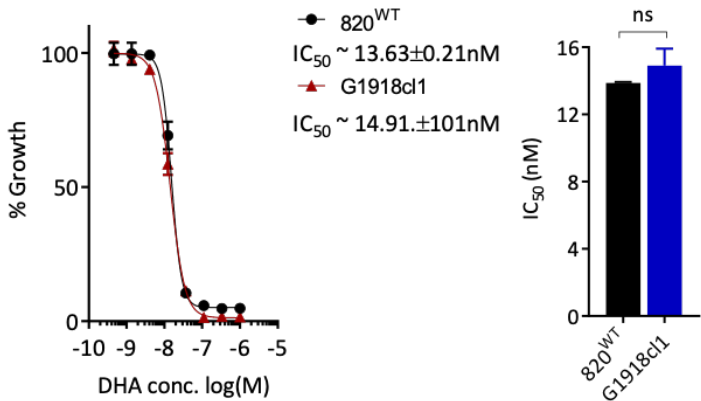
d



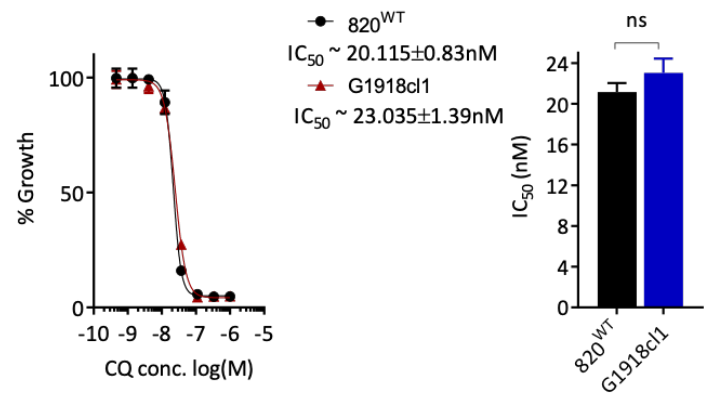
e



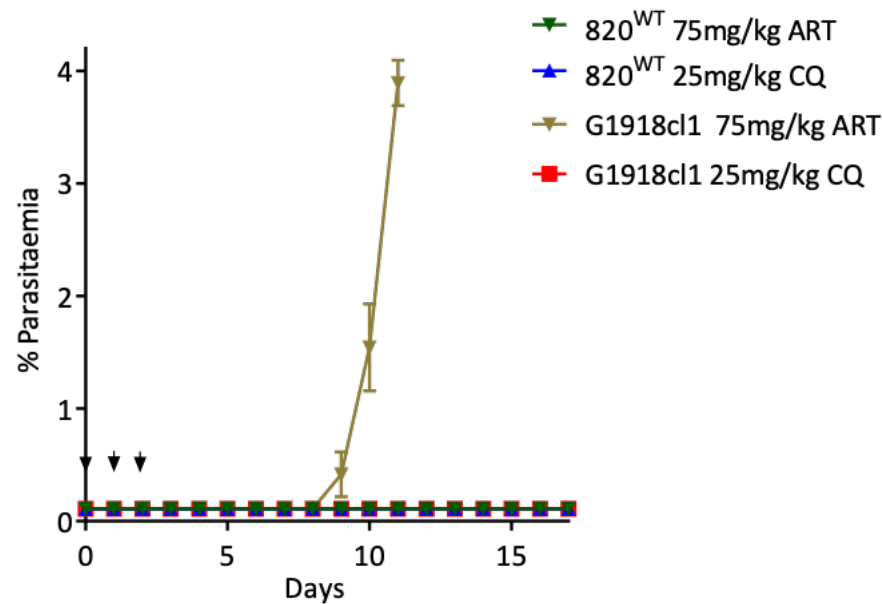
f



g



h



i



PBANKA_0208800: 2696-2754 amino acids

G1807^{V2752F}

protein
DNA sequence

G1919 clone1

DNA sequence
protein

-- 82bp --

*Sna*BI Shields V2721V F2752F

a. Schematic of the UBP-1 donor DNA in the pG962 and pG963 vectors. **b.** A 20bp sgRNA used to target the UBP-1 region upstream of the V2721F mutation in the Cas9 expressing vectors with introduced silent mutation sites indicated. **c.** RFLP (*SnaBI* digestion) analysis of PCR products (GU5186 + GU4895, 946bp) of the G1918 and G1919 lines relative to the mutants showing successful editing by 2 distinct RFLP bands for the mutants (632bp, 314bp) and residual traces of the parental wild type genotype. **d.** RFLP analysis of the cloned G1918 and G1919 lines. First six lanes to the left are RFLP analyses of G1918 and G1919 cloned lines PCR products (GU5186 + GU4895, 946bp) digested by *SnaBI* showing 2 bands (632bp, 314bp) as compared to 1 band for the parental G1807^{V2752F}. Six lanes to the right are the same clones digested by both *SnaBI* and *BseYI* showing parental G1807^{V2752F} with 2 RFLP bands (536bp, 410bp) as a result of digestion with *BseYI* only as the *SnaBI* restriction site is absent and 3 RFLP bands (536bp, 314bp, 96bp) in the G1918, G1919 clones as a result of digestion of the PCR product by both *BseYI* and *SnaBI*. **e.** Sequencing of G1918 clone1 showing successful swapping of the V2752F in the parent G1807^{V2752F} line to the V2721F mutation. **f, g.** *In vitro* DHA and CQ dose response curves and IC₅₀ comparisons of the G1918cl1 revertant line relative to the wild type showing reversion of the CQ phenotype and similar sensitivity to DHA. Significant differences between mean IC₅₀s or IC₅₀ shifts were calculated using the paired t-test. Error bars are standard deviations from three biological repeats. Significance is indicated with asterisks; ns, not significant. **h.** *In vivo* tolerance to ARTs at 75 mg/kg in the G1918cl1 line and complete restoration of CQ sensitivity. **i, j.** Sequence analysis of the G1919 uncloned (**i**) and G1919 (**j**) clone1 line showing absence of double mutant populations.

3.4 Discussion

Ubiquitin hydrolases or DUBs are essential elements of the eukaryotic UPS which is primarily involved in maintaining cellular protein homeostasis and responding to stress. Despite the proposed involvement of *Plasmodium* DUBs in modulating

susceptibility to multiple drugs, lack of conclusive experimental evidence has thus far limited studies into their detailed involvement in MOA and or resistance phenotypes such as those observed with ARTs. In this chapter, using a CRISPR-Cas9 mediated reverse genetics approach; experimental evidence is provided on the direct involvement of a DUB (UBP-1) in modulating parasite responses to ART and CQ, more importantly under *in vivo* conditions. As the debate into the mechanism of action and resistance to ARTs continues, a consensus understanding is converging that ART resistance is more complex as several factors, genetic determinants and possibly mechanisms of action appear to be involved. In *P. falciparum*, ART resistance is confined to early ring stage parasites which has been translated in laboratory conditions to increased survival in RSAs (Witkowski et al., 2013). Mutations in kelch13, PfCoronin as well as transient (hypo-hyperthermic) temperatures have all been shown to enhance ring stage parasite survival in the RSAs (Straimer et al., 2015, Demas et al., 2018, Henrici et al., 2019b). More recently, characterisation of Kelch13 interacting factors has revealed that disruption of proteins that co-localise with Kelch13 such as the parasites endocytosis protein ESP15, UBP-1 and others of unknown function, modulate susceptibility to ARTs (Birnbaum et al., 2020). As demonstrated in this study, ART and more so, CQ reduced susceptibility can be mediated by mutations in UBP-1 underscoring a potential mechanism of cross-resistance and some commonality in MOA between CQ and ART especially relating to haemoglobin digestion and trafficking in malaria parasites (Birnbaum et al., 2020, Yang et al., 2019, Klonis et al., 2011).

3.4.1 UBP-1 mutations carry ART and CQ cross-resistance traits in *P. berghei*

The UBP-1 V2728F mutation was previously designated as a principle determinant of ART reduced susceptibility despite its common fixation with mefloquine and higher doses of CQ (Hunt et al., 2010). Contrary to this argument, ART did not enrich for this mutation (V2752F) in this work enriching for the V2721F mutation instead which was fixed with AS in *P. chabaudi*. However, enrichment of the V2752F mutation with a higher dose of CQ was achieved showing that this mutation does indeed modulate parasite responses to CQ while the V2721F mutation is chiefly responsible for the ART reduced susceptibility phenotype in the *P. berghei* model *in vivo*. Interestingly, drug challenge of these mutant lines *in vivo* revealed that both mutations give low-

level cross-protection to both ARTs and CQ. This confirms that both of these UBP-1 mutations modulate some form of protection to both ARTs and CQ drug challenges albeit to some differing degrees which is, therefore, in strong agreement with previous observations in *P. chabaudi* (Hunt et al., 2010). This also demonstrates a plurality of pathways to resistance involving the same target. At a time when this work was ongoing, the exact equivalent UBP-1 mutations in *P. falciparum*, V3275F and V3306F were successfully engineered (Henrici et al., 2019a). In *P. falciparum* UBP-1, the V3275F mutation (V2721F *P. berghei* equivalent) shows enhanced survival to DHA in RSAs but remains sensitive to CQ. However, unlike in *P. berghei*, the V3306F (V2752F *P. berghei* equivalent) showed no enhanced survival to DHA in RSAs or resistance to CQ (Henrici et al., 2019a). Whilst not entirely in agreement with the data reported here, this could be due to limitations in the ability of *in vitro* assays to fully predict actual drug responses *in vivo* which data in this work highlights and has been a concern with Kelch13 mutations recently (Sa et al., 2018). These observations may also somewhat be confounded by species specific differences in drug responses, pharmacodynamics, MOA and resistance that, in part, remain to be fully investigated. For example, previous and original linkage studies in *P. chabaudi* identified additional mutations in an amino acid transporter, *aat*, as being strongly associated with CQ resistance phenotypes in tandem with UBP-1 mutations (Hunt et al., 2010). Even though this could partly explain the observed *in vitro* sensitivity of *P. falciparum* V3275F mutants to CQ, data in this work suggests that UBP-1 mutations are sufficient to mediate quantifiable protective phenotypes to both ARTs and CQ as the reversal of the V2752F mutation performed in this study, for example, completely restores CQ sensitivity. This has provided, therefore, additional independent evidence on the direct causative role of UBP-1 mutations in modulating parasite responses not just to ARTs, but CQ as well. The study also illustrates the potential of the *P. berghei* rodent model in proving causality to antimalarial drug resistance phenotypes under *in vivo* conditions especially in light of recent reported discrepancies between some *in vitro* RSA resistance profiles of *P. falciparum* Kelch13 mutants and actual *in vivo* phenotypes using the *Autos* monkey model (Sa et al., 2018).

3.4.2 Fitness costs could possibly explain lack of expansion of UBP-1 mutations in *P. falciparum*

Interestingly, the V2721F and V2752F mutation carrying parasites are significantly slow growing and are easily outcompeted in the presence of non-mutants. Natural *P. falciparum* UBP-1 mutations have been reportedly associated with ART treatment failure in Kenya (Henriques et al., 2014, Borrmann et al., 2013), SEA (Cerqueira et al., 2017) and more recently in Ghana (Adams et al., 2018) (Appendix Figure 8.6). However, unlike their rodent counterparts which associate with ART reduced susceptibility, the natural reported E1528D and D1525E mutations occur towards the less conserved N-terminus of the protein and outwith the conserved, bioinformatically predicted UBP-1 catalytic domain (Hunt et al., 2007) (Figure 3.1a). This would suggest that acquisition of the mutations at the well conserved C-terminal in *P. falciparum* has a potential growth defect as has been observed with *P. berghei* in this work. However, as these upstream mutation residues are not conserved between *P. falciparum* and *P. berghei* UBP-1, these hypotheses could not be tested in this model. In fact, *P. falciparum* UBP-1 is highly polymorphic with over 480 reported SNPs <https://plasmodb.org> all of which are in the N-terminal region. *P. falciparum* UBP-1 has also been recently shown to be undergoing a strong positive selection in SEA (Ye et al., 2019). UBP-1 mutations could, therefore, be an independent avenue to which ART or multidrug resistance phenotypes could emerge in endemic regions like has been seen in Africa (Ghana and Kenya), without actually requiring a permissive genetic background as seems to be the current landscape with Kelch13 mutations. However, there are constraints upon the evolution of drug resistance and UBP-1. Whilst these data confirm that a single protein that does not transport drugs can mediate resistance to two quite distinct drug entities, it was not possible to generate a *P. berghei* line that simultaneously contained the two UBP-1 drug resistance mutations examined in this work illustrating the balance between fitness cost and resistance.

3.4.3 UBP-1 mutations could be impairing haemoglobin endocytosis in malaria parasites

In yeasts, UBP-1 localises to the endoplasmic reticulum playing roles in protein transport specifically internalisation of substrates across membranes (Schmitz et

al., 2005). Mutations in UBP-1 could, therefore, modulate endocytosis of important essential host derived products such as haemoglobin to the DV in a similar manner thereby reducing exposure of the parasite to activated drug for both ARTs and CQ. Interestingly, mutations in the AP-2 μ adaptor complex that is involved in clathrin mediated endocytosis have also been implicated in ART resistance in rodent malaria parasites (Henriques et al., 2013). One of the AP-2 μ adaptor complex mutation (I592T) has been recently engineered in *P. falciparum* and has been shown to enhance ring stage parasite survival in RSAs (Henrici et al., 2019a). This further suggests that inhibition of the endocytic trafficking system is a possible generic mechanism for the parasites to survive lethal doses of drugs that require transport and activation in the DV. This would further explain the multidrug resistance phenotype observed with the UBP-1 mutations in *P. chabaudi* and *P. berghei* in this work. Acquisition of the V2728F mutation in *P. chabaudi* was structurally predicted to reduce deubiquitination (Hunt et al., 2007). In such a situation, the cellular increase in ubiquitinated proteins would be anticipated to positively feedback to the cellular machinery to rapidly degrade protein substrates at the 20s proteasome promoting a non-specific and rapid protein turnover or impaired substrate trafficking. This would result in generally slow growing parasites with reduced expression of, for example, multi-drug resistance transporters as well as reduced endocytosis of host-derived products like haemoglobin, which would in turn modulate parasite responses to these drugs. More recently, functional studies have revealed that *P. falciparum* Kelch13 localises to the parasite cytostomes and plays a role in haemoglobin trafficking (Birnbaum et al., 2020, Yang et al., 2019). Consequently, Kelch13 mutations have been shown to lead to a partial loss of the Kelch13 protein function which leads to decreased haemoglobin trafficking to the parasite DV and less DHA activation, which in turn mediates parasite survival (Yang et al., 2019, Birnbaum et al., 2020). Strikingly, protein pulldowns at the parasite cytostomal foci where kelch13 localises have identified UBP-1 as a key interacting partner in the Kelch13 mediated endocytic machinery that is involved in haemoglobin trafficking. By analysing haemoglobin endocytosis in ring and trophozoite stages, it has been shown that partial inactivation of UBP-1 impairs haemoglobin endocytosis in both rings and trophozoites as opposed to inactivation of Kelch13 which impairs haemoglobin uptake in ring stages of the parasites only (Birnbaum et al., 2020). This is indeed in agreement with the

observed *P. berghei* phenotypes in this work on the consequences of UBP-1 mutations which in a similar manner could impair trafficking of haemoglobin leading to less activation of ARTs and CQ. Moreover, the potential role of UBP-1 in trafficking haemoglobin in both rings and trophozoites would possibly explain the ART and CQ potential cross-resistance phenotype, which has been observed with UBP-1 mutations in this work; unlike with Kelch13 mutations which thus far are known to mediate resistance to ARTs only and in early ring stages. The experimental validation on the involvement of UBP-1 mutations in mediating potential cross-resistance to ART and CQ in malaria parasites, therefore, provides an additional understanding of drug resistance in malaria parasites, specifically for compounds that require access and/or activation in the DV. Furthermore, the *P. berghei* model provides a useful sensitive and robust system in which to investigate the interplay and impact of simultaneous mutations of both Kelch13 and UBP-1 *in vivo* as well as assess whether Kelch13 mutations would modulate responses to CQ under *in vivo* conditions.

3.4.4 Conclusion

In conclusion, the work presented here provides further experimental evidence for the involvement of conserved mutations in a polymorphic ubiquitin hydrolase protein that serves as a nexus for resistance to two very diverse classes of drugs. The findings also underscore the potential difficulties that *in vitro* assays may have in appropriately assigning mutant parasites with appropriate phenotypes in absence of conclusive *in vivo* measurements. *P. berghei* should therefore, be a suitable and adaptable *in vivo* model for the rapid evaluation and/or genetic engineering of mutations associated with human-infectious *Plasmodium* drug resistance observed in the field for concurrent assigning of drug resistance phenotypes under both *in vitro* and *in vivo* conditions.

4 *In vitro* and *in vivo* phenotypes of orthologous ART resistance Kelch13 mutations in *P. berghei*

4.1 Chapter aim

In light of the absence of appropriate *in vivo* models to infer causality of *P. falciparum* Kelch13 mutations in ART resistance, the aim of this chapter was to introduce a selected orthologous *P. falciparum* Kelch13 mutations in *P. berghei*. This would allow for quantification and assessment of associated ART resistance phenotypes under *in vivo* conditions which is still debated and has recently been disputed in *P. falciparum*.

4.2 Introduction

ART resistance which is primarily mediated by Kelch13 mutations is further complicated by high frequencies of recrudescence in ART monotherapies. The use of ARTs in ACTs is therefore an appropriate remedy and indeed originated from early clinical trials (before ART resistance emerged) that showed that despite achieving faster parasite clearance, ART monotherapies resulted in recrudescence rates of up to 40% (Li et al., 1984). ACTs deliver a pharmacological cure by taking advantage of ARTs to rapidly clear the parasite biomass in the early days of treatment, while relying on the partner drug to eliminate residual parasites (WHO, 2018a). So far, ACTs remain highly effective in Sub-Saharan Africa, a region that harbours the highest disease burden, with efficacy rates of >98% (WHO, 2019). Nevertheless, ACTs have been threatened by the emergence and spread of resistance to ARTs in SEA, and resistance has the potential to spread to other malaria-endemic regions as has been a historical trend with prior antimalarial drugs (Dondorp et al., 2009, WHO, 2019, Ashley et al., 2014). Moreover, the recent aggressive expansion of a parasite lineage carrying the genetic determinants of both ART resistance (Kelch13 mutations) and resistance to the ACT partner drug piperaquine has been reported across SEA, further threatening the efficacy of such combinations (Hamilton et al., 2019, van der Pluijm et al., 2019).

Decreased susceptibility to ARTs is now widespread throughout SEA and manifests as reduced *in vivo* parasite clearance upon treatment with ACTs (WHO, 2019, Ashley et al., 2014). *P. falciparum* ART clearance phenotypes are based on the WWARN parasite clearance estimator (PCE) (Flegg et al., 2011),

which quantifies relative resistance by estimating parasitaemia lag phases and clearance half-lives upon treatment with AS or ACTs. This involves *in vivo* quantification of viable parasitaemia (in patients) upon treatment with AS (2-4 mg/kg/day) or ACTs at specified time intervals, and subsequent graphing of parasite densities as a function of time (Flegg et al., 2011). The PCE has been used to generate massive baseline data that classifies ART resistance as parasites with clearance half-lives >5.5 hours and ART-sensitive parasites as those with clearance half-lives <3 hours (Group et al., 2015). However, interpretation of clearance half-lives can still be confounded by differences in initial parasite biomass, efficacy of partner drug and host immunity (Ataide et al., 2017, Group et al., 2015). Typically, ART resistance which is still classified as “partial resistance” is characterised by delayed *in vivo* parasite clearance and increased *in vitro* RSA survival which all strongly associate with genetic polymorphisms in the *P. falciparum* Kelch13 propeller domain (Section 1.5.5.2). Despite strong compelling reverse genetic approaches which have been successfully used to show that *P. falciparum* Kelch13 mutations such as M476I, R539T, I543T, Y493H and C580Y do indeed modulate increased *in vitro* DHA survival in RSAs (Straimer et al., 2015, Ghorbal et al., 2014), this remains obscure and controversial due to the many confounding factors to the definition of ART resistance especially under *in vivo* conditions (Section 1.5.5.2). This has even been made more complex with recent observations that the *P. falciparum* C580Y mutation does not replicate *in vivo* ART resistance phenotypes despite strong *in vitro* DHA RSA survival rates in the *Aotus* monkey *in vivo* model (Sa et al., 2018).

Moreover, malaria drug resistance mutations are known to often associate with significant fitness costs (as demonstrated in Chapter 3) that can limit the prevalence and eventual propagation of resistance-conferring alleles in natural infections. For example, PfCRT mutations that modulate resistance to CQ massively expanded when CQ was in use in the 1970s but eventually were outcompeted and replaced with parasites carrying wild type alleles once the drug was withdrawn from use (Gabryszewski et al., 2016, Laufer et al., 2010). Similarly, *P. falciparum* Kelch13 mutations have been shown to carry *in vitro* fitness costs, however, the degree to which a given mutation is detrimental for growth seems to be dependent on the parasite genetic background (Straimer et

al., 2017). Relative to other Kelch13 mutations, *P. falciparum* R539T and I543T mutant parasites that are associated with the highest RSA survival rates (Straimer et al., 2015, Mbengue et al., 2015) and most significant delays in parasite clearance (Takala-Harrison et al., 2015) also carry the most pronounced fitness costs (Straimer et al., 2017). Intriguingly, the most prevalent SEA mutation, C580Y, is fitness neutral *in vitro* when experimentally introduced into recent Cambodian clinical isolates whereas when it is introduced into ART naïve parasites isolated before ARTs were widely clinically employed, it displays a significant growth defect (Straimer et al., 2017, Nair et al., 2018). Crucially, these Kelch13 mediated ART resistance phenotypes are associated with increased ER stress responses which can be targeted by selective inhibition of the downstream proteasomes to overcome resistance (Dogovski et al., 2015, Mok et al., 2015).

This chapter describes the *in vitro* and *in vivo* phenotypes of orthologous *P. falciparum* Kelch13 mutations in the rodent malaria parasite *P. berghei*. Using a CRISPR-Cas9 genetic editing system, these mutations have been engineered in wild type *P. berghei* parasites and here in, a profile of their *in vitro* phenotypes in standard growth inhibition assays and adapted RSAs as well as their *in vivo* phenotypes upon treatment with AS and ART is provided. Fitness of these *P. berghei* Kelch13 mutant parasites relative to their isogenic wild type counterparts has also been assessed as well as their sensitivity to combinations of DHA and proteasome inhibitors.

4.3 Results

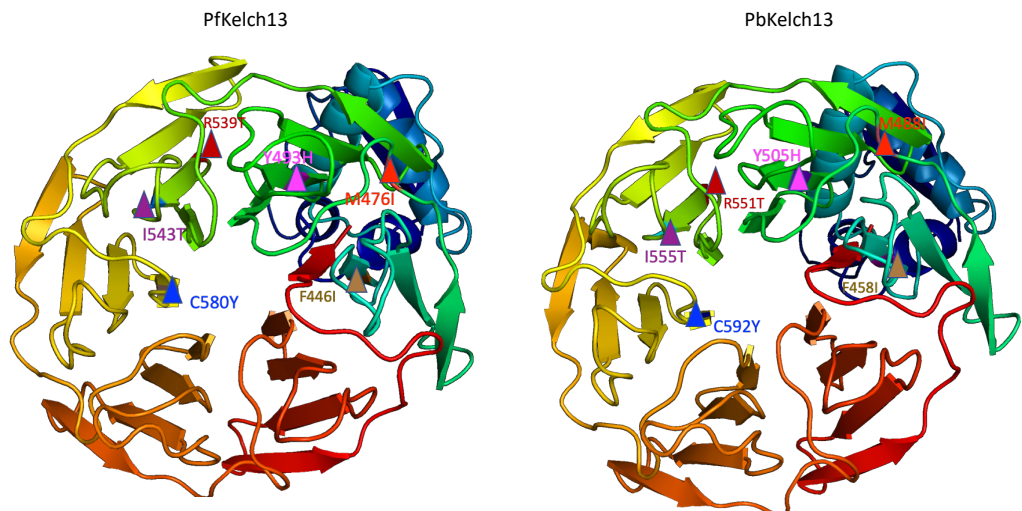
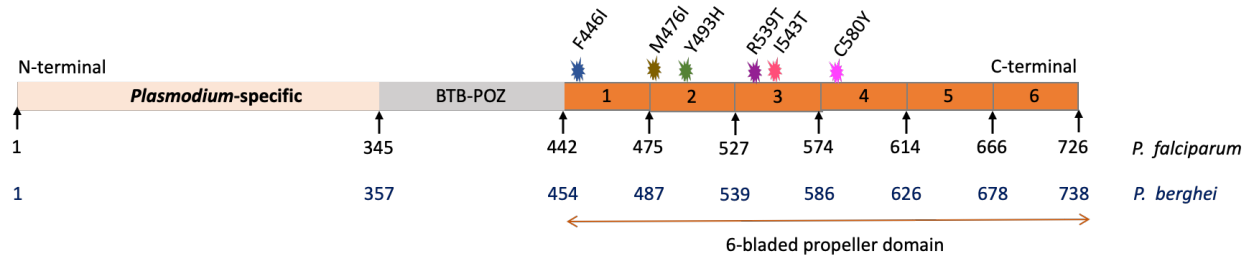
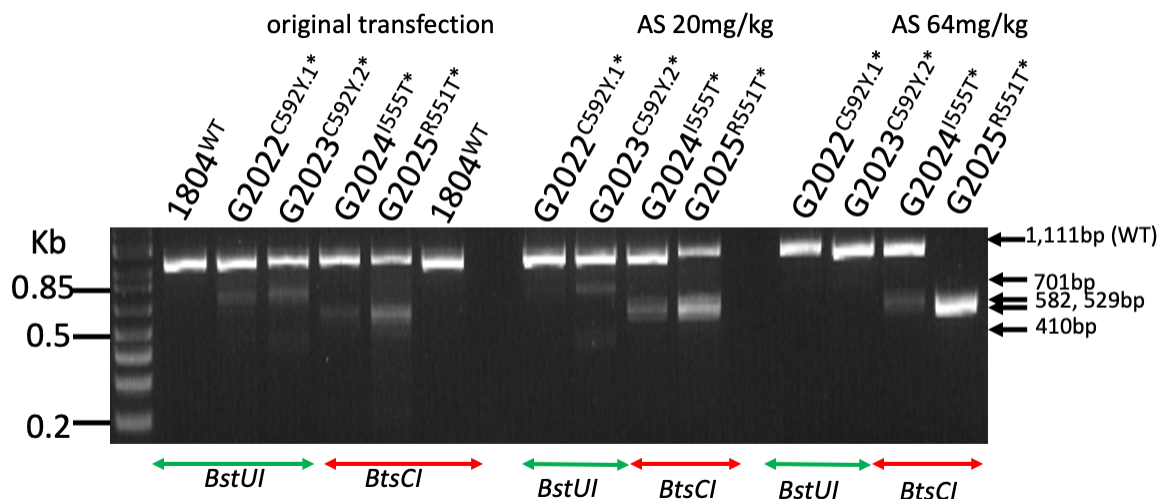
4.3.1 CRISPR-Cas9 mediated introduction of *P. berghei* orthologous Kelch13 mutations and *in vivo* mutant enrichment by AS

In order to generate *P. berghei* mutant parasites carrying orthologous *P. falciparum* Kelch13 mutations, an attempt was made to introduce *P. berghei* equivalents of five *P. falciparum* Kelch13 mutations (M476I, Y493H, R539T, I543T and C580Y) that, by reverse genetics, have been previously shown to confer enhanced *in vitro* DHA RSA survival (Straimer et al., 2015), as well as the F446I mutation that is predominant in Southern China along the Myanmar border (Ashley et al., 2014). These mutations are all validated determinants of reduced

P. falciparum susceptibility to ARTs (WHO, 2018a). Structural homology modelling and sequence alignment revealed that *P. berghei* (PBANKA_1356700) and *P. falciparum* (PF3D7_1343700) Kelch13 are highly conserved (~84% sequence identity overall, Appendix Figure 8.7) especially at the C-terminal propeller domain where resistance-conferring mutations localise (Figure 4.1a). *P. berghei* Kelch13 carries 12 extra amino acids (726 amino acids for *P. falciparum*, 738 for *P. berghei*, Figure 4.1b); however, modelling suggests these do not appear to change the overall propeller structure of Kelch13 or the amino acid identity at the orthologous positions of the mutations examined in this work (Figure 4.1a, Appendix Figure 8.7). Using a CRISPR-Cas9 system as in section 3.3 (Appendix Figure 8.8), Cas9 plasmids carrying appropriate sgRNAs were designed to target the *P. berghei* Kelch13 locus with corresponding homology repair templates which carried the mutations of interest as well as silent mutations for PAMs and restriction sites for RFLP analysis (Appendix Table 8.1, 8.2). Episomal transfection of the plasmids pG1004 (C592Y), pG1005 (I555T) and pG1006 (R551T) into the *P. berghei* 1804cl1 line yielded transformant parasites (G2022^{C592Y.1*}, G2023^{C592Y.2*}, G2024^{I555T*} and G2025^{R551T*}) with ~13.37%, ~18.53%, ~7.74% and ~29.99% efficiencies respectively by RFLP analysis (Figure 4.1c, Appendix Table 8.3). Intriguingly, bulk DNA sequencing of these transformed parasites revealed that only the G2025^{R551T*} line carried sequence traces for the R551T amino acid substitution and accompanying silent mutations (Appendix Figure 8.9c) while the rest had traces only of the silent mutations (Appendix Figure 8.9a, 8.9b). These data suggested that the C592Y and I555T mutations either result in extremely slow growing parasites or are entirely lethal in *P. berghei*. Attempts to clone the G2025^{R551T*} line by limiting dilution were unsuccessful, possibly, due to the low mutant population (29.99%).

In earlier efforts to introduce UBP-1 mutations in *P. berghei* (Chapter 3), it was demonstrated that a pre-emptive drug pressure to which the engineered mutation is anticipated to confer protective advantage can selectively enrich for the mutant in a mixed, transfected parasite population even when the mutant population is <1% in the mixture. Using this approach, a larger inoculum (~2 x 10⁷) of the G2022^{C592Y.1*}, G2023^{C592Y.2*}, G2024^{I555T*} and G2025^{R551T*} lines was subjected to AS at 20 or 64 mg/kg to see if any enrichment in the recrudescence parasite populations could be achieved (Figure 4.1d). Indeed, AS at both 20 and

64 mg/kg specifically enriched the R551T mutant population in the G2025^{R551T*} line from 29.99% in the initial transfection to ~49.71% at AS 20 mg/kg and ~99.78% at 64 mg/kg (Figure 4.1c, 4.1e, Appendix Table 8.3). In contrast, apart from a minor enrichment that was observed for the G2024^{I555T*} line, no useful enrichment in both the G2022^{C592Y.1*} and G2023^{C592Y.2*} lines was observed by RFLP at either concentration of AS (Figure 4.1c, Appendix Table 8.3). Furthermore, no I555T or C592Y amino acid substitution traces could be seen after population-level DNA sequencing of these lines. These data further supported the relative non-viability of *P. berghei* parasites bearing Kelch13 C592Y and I555T mutations. In agreement with the above observations, further attempts to introduce the C592Y mutation using a different sgRNA and or different codons for the tyrosine residue in the donor template (TAT or TAC) were also unsuccessful. A >90% editing efficiency was, however, observed when introducing only silent mutations that maintained the C592C wild type genotype in the donor template (Appendix Figure 8.9e, 8.9f, Appendix Table 8.3). This, plus other failed attempts to generate the I555T mutant further implies that these two Kelch13 mutations are not viable in *P. berghei*. Meanwhile, transfection of the 1804cl1 line with pG983 (F458I), pG984 (Y505H) and pG1008 (M488I) (Appendix Table 8.2) successfully introduced these mutations in *P. berghei* Kelch13 yielding the G1957^{F458I*}, G1979^{Y505H*} and G1989^{M488I*} lines with >93% efficiencies as confirmed by RFLP analysis (Figure 4.1f, Appendix Table 8.3) as well as population level DNA sequencing (Appendix Figure 8.9g, 8.9h, 8.9i). These three lines (G1957^{F458I*}, G1979^{Y505H*}, G1989^{M488I*}) and the G2025^{R551T*} AS 64 mg/kg challenged line were all cloned by limiting dilution and mutations further confirmed by RFLP analysis (Appendix Figure 8.9d) and sequencing. The V2721F UBP-1 mutant line, which mediates reduced susceptibility to ARTs in *P. berghei* (Chapter 3) was also generated in the 1804cl1 background and cloned (Appendix Table 8.3).

a**b****c**

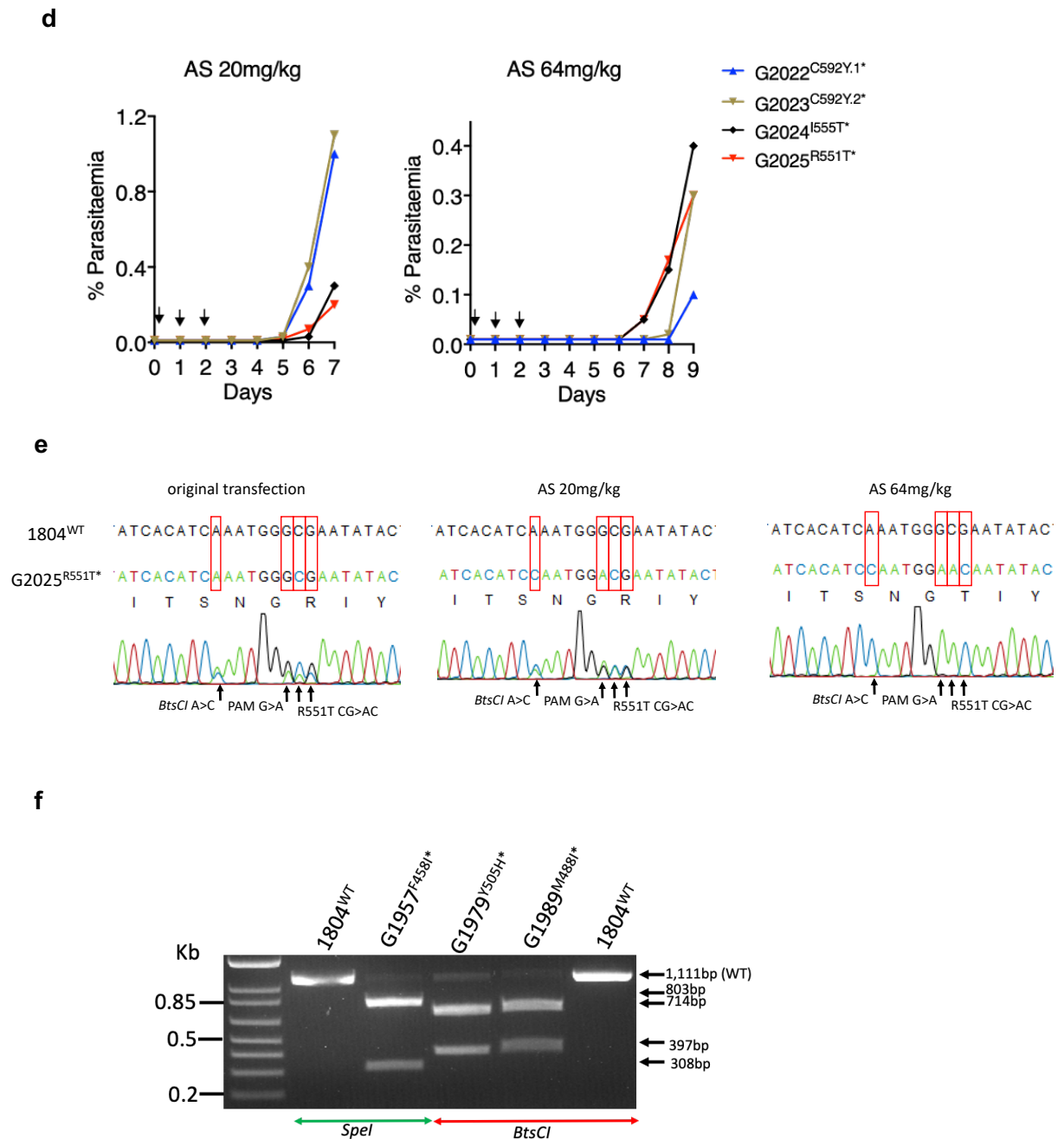


Figure 4.1: Introduction of orthologous Kelch13 nucleotide substitutions in *P. berghei*.

a. 3D homology model of *P. falciparum* (PF3D7_1343700) and *P. berghei* (PBANKA_1356700) Kelch13 for amino acids residues 350-726 and 362-738, respectively. *P. falciparum* Kelch13 mutation sites (F446I, M476I, Y493H, R539T, I543T and C580Y) are indicated in the structure on the left and *P. berghei* orthologous mutation sites are modelled on the right. Models were created in SwissModel using PDB template 4zgc.1.A. Structures were visualized and annotated using pyMol 2.3. **b.** Kelch13 schematic for the *P. falciparum* Kelch13 showing amino acid positions and the protein domains. Positions of Kelch13 mutations that have been investigated in this study are indicated. Equivalent amino acid positions for *P. berghei* are indicated in parallel at the

bottom (in blue). **c.** RFLP analysis of transfected parasite populations before and after challenge with AS at 20 or 64 mg/kg for the G2022 (C592Y.1), G2023 (C592Y.2), G2024 (I555T) and G2025 (R551T) lines. RFLP analysis was carried out using the restriction enzymes shown on the bottom of the gel on PCR fragments amplified from genomic DNA of transfected parasites using primers binding exterior to the donor DNA (Appendix Table 8.1, 8.3). * on the transfectant parasite lines indicates that the line is uncloned. **d.** Parasitaemia growth curves monitoring recrudescence of the G2022, G2023, G2024 and G2025 lines upon AS challenge. Mice were infected with $\sim 2 \times 10^7$ parasites by IP injection on day 0. Treatment with AS was commenced ~ 3 hours post infection by IP and was continued for three consecutive days as indicated by arrows. Parasitaemia was monitored microscopically until recrudescence was observed. Mice were bled when the parasitaemia was less than 1.5% to minimize competition from wild type parasites in case mutants carried growth defects. **e.** Sanger sequencing of bulk DNA from the G2025 R551T line showing selective enrichment of this mutation upon AS treatment at 20 or 64 mg/kg. Enrichment of this mutation was also observed in the RFLP analysis shown in **c.** **f.** RFLP analysis of parasite bulk populations for the G1957 (F458I), G1979 (Y505H), G1989 (M488I) transfected lines. RFLP analysis was carried out using the restriction enzymes shown on the bottom of the gel as described above.

4.3.2 *P. berghei* Kelch13 mutants display reduced susceptibility to DHA in a standard 24-hour *in vitro* assay

Unlike *P. falciparum*, *P. berghei* can only be maintained in one blood stage cycle *in vitro* which restricts drug susceptibility assays to one developmental 24-hour cycle, with readouts based on flow cytometry quantification of schizont maturation (Franke-Fayard et al., 2008, Janse et al., 1994b). Using this approach, DHA dose-responses of the *P. berghei* Kelch13 mutants were characterised and compared to wild type parasites or to UBP-1 mutant parasites with ART reduced susceptibility (Chapter 3). Interestingly, in contrast with the equivalent *P. falciparum* Kelch13 mutants, *P. berghei* M488I, R551T and Y505H Kelch13 mutant parasites display reduced susceptibility to DHA in standard growth inhibition assays with 3.3, 1.4 and 1.2-fold IC_{50} increases, respectively, as compared to isogenic Kelch13 wild type parasites (Figure 4.2). The *P. berghei* F458I Kelch13 mutant displayed equal sensitivity to DHA as the wild type, as did the UBP-1 V2721F mutant (Figure 4.2) which is in agreement with similar observations in Chapter 3. These data suggest that despite being limited to a single cycle 24-hour exposure, the *P. berghei* standard assay can distinguish even

modestly ART-resistant parasites from sensitive ones, unlike equivalent assays in *P. falciparum*.

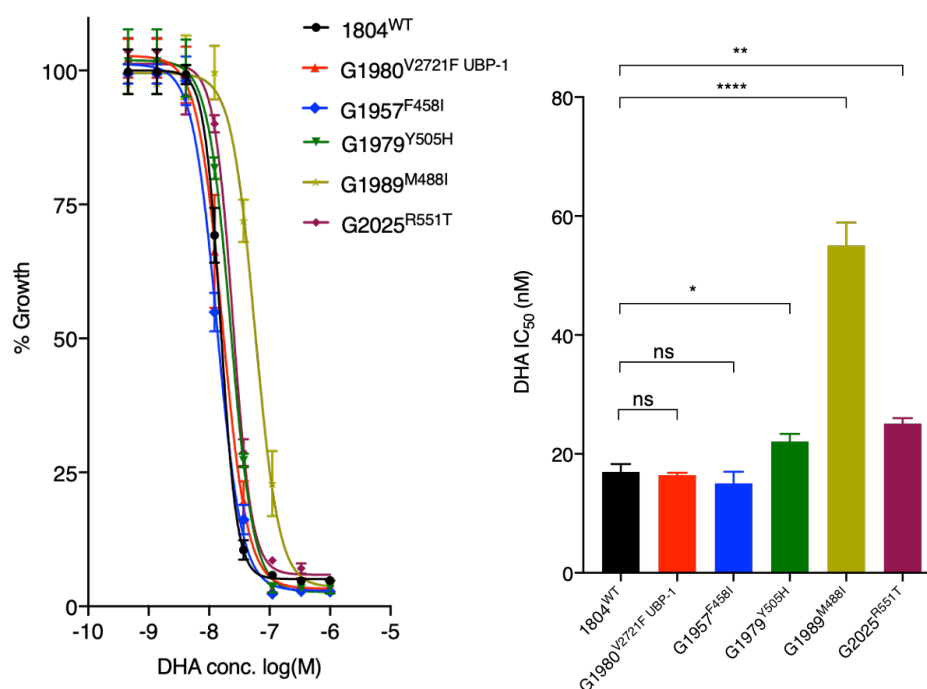


Figure 4.2: DHA dose response curves and IC₅₀ values for *P. berghei* Kelch13 mutant lines as compared to wild type 1804^{WT} and the UBP-1 G1980^{V2721F} mutant line.

Error bars show standard deviation calculated from three biological repeats. Statistical significance was calculated using one-way ANOVA alongside the Dunnett's multiple comparison test. Significance is indicated with asterisks; ns not significant * $p < 0.05$, ** $p < 0.01$, **** $p < 0.0001$.

4.3.3 *P. berghei* Kelch13 mutants display increased survival in an adapted RSA

To assess DHA susceptibility of early ring stage parasites of the *P. berghei* Kelch13 mutants, the *P. falciparum* RSA (Witkowski et al., 2013) was adapted for *P. berghei* and used to profile survival rates of the mutants after short term exposure to DHA pulses. The *P. falciparum* RSA relies on exposure of early ring-stage parasites (0-3 hours post invasion) to DHA at a pharmacologically relevant concentration (700 nM) for 4-6 hours, followed by assessment of viability in the 2nd life cycle which allows drug-exposed parasites to re-invade fresh RBCs. With this approach, current RSA parameters define *in vitro* ART resistance as survival of $\geq 1\%$ and ART sensitivity as $< 1\%$ survival (Witkowski et al., 2013). Using a

similar approach, ~1.5-hour old post invasion *P. berghei* Kelch13 mutant ring-stage parasites were exposed to DHA at 700 nM for 3 hours (to accommodate for the shorter life cycle in *P. berghei*). Viability was assessed 24 hours later by flow cytometry-based quantification of schizont maturation and mCherry expression. Interestingly, a significant fraction of the *P. berghei* wild type parasites survive exposure to DHA at 700 nM, with percentage survival rates of ~20.9% (Figure 4.3a). This is in agreement with previous observations that *P. berghei* is less susceptible to ARTs as compared to *P. falciparum* (Lee et al., 2018). Both the UBP-1 mutant and F458I or Y505H Kelch13 mutant parasites had the same survival rates as the wild type line, while the M488I and R551T mutants exhibited significantly higher survival rates (32.3% or 39.0% respectively) (Figure 4.3a). This is consistent with previous reports that in *P. falciparum*, the R539T mutation together with the I543T mutation are associated with the highest rates of RSA survival (Straimer et al., 2015). However, there were clear inconsistencies between drug susceptibility of the mutants in the standard assay (Figure 4.2) and the adapted RSA (Figure 4.3a). This may be due to the inability to maintain *P. berghei* in long-term culture and extend the analysis beyond the 24-hour read out. Therefore, a modified *in vivo* RSA was developed where parasites (wild type, UBP-1 V2721F, M488I and R551T mutants) were injected back into mice 24 hours after DMSO or DHA exposure as in the adapted RSA described above. Viability was then assessed by quantifying *in vivo* parasitaemia on Day 4. Remarkably, percentage survival in the R551T mutant parasites significantly increased from ~39.0% (24-hours readout) to ~62.5%, while M488I mutant parasites survival increased from ~32.3% (24-hours readout) to ~38.0% (Figure 4.3b). In contrast, the percentage survival of the wild type and UBP-1 mutant (which has a minor growth defect) did not significantly change in the extended assay, demonstrating that the *P. berghei in vitro* RSA and standard growth inhibition assays with 24-hour readouts may be less robust in quantifying resistance phenotypes, especially if mutant parasites are less fit.

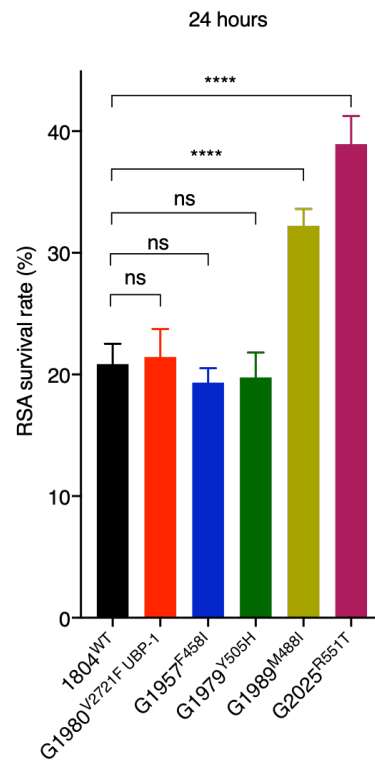
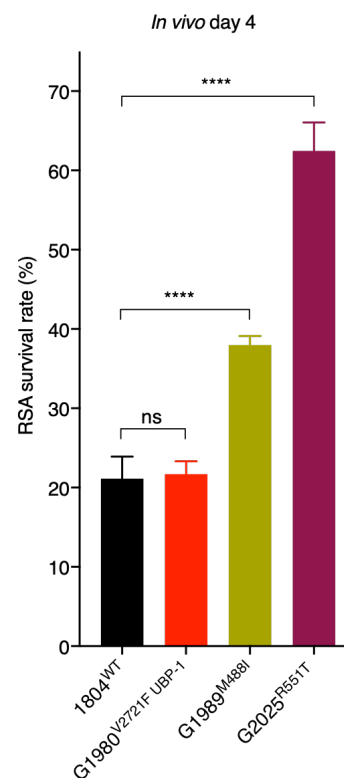
a**b**

Figure 4.3: RSA survival of *P. berghei* Kelch13 mutants.

a. Results show the percentage of synchronized early ring-stage parasites (1.5 hours post invasion) that survived a 3-hour exposure to 700 nM of DHA relative to DMSO-treated parasites. Survival was quantified 24 hours post treatment by flow cytometry analysis

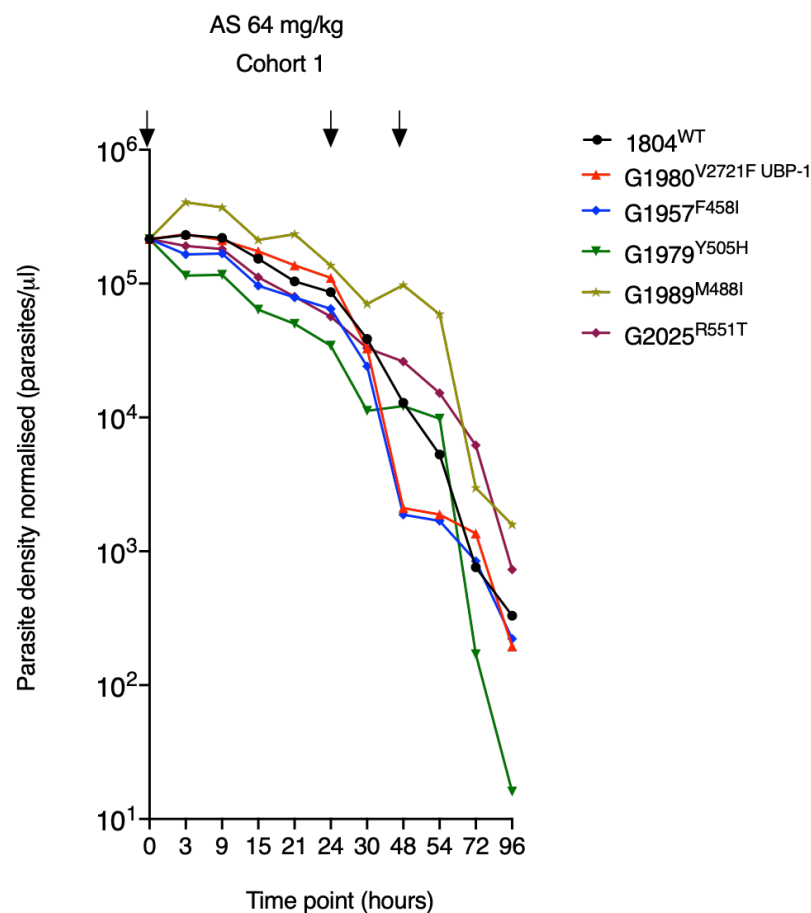
based on Hoescht 33258 DNA staining and mCherry expression. **b.** *In vivo* RSA survival for two Kelch13 mutant lines (G1989^{M488I} and G2025^{R551T}) as compared to the wild type (1804^{WT}) and UBP-1 mutant (G1980^{V2721F}) controls. After *in vitro* exposure to DHA or DMSO as described above, parasites were IV injected back into mice as described in methods. Parasitaemia was quantified by flow cytometry analysis of mCherry expression on Day 4 post IV, from which % survivals were calculated. Error bars show standard deviation calculated from three biological repeats. Statistical significance was calculated using one-way ANOVA alongside the Dunnet's multiple comparison test. Significance is indicated with asterisks; ns not significant, ****p < 0.0001.

4.3.4 *P. berghei* Kelch13 mutants mimic the delayed parasite clearance phenotype *in vivo* upon AS treatment

In order to determine the clearance kinetics of the *P. berghei* Kelch13 mutants upon AS treatment, *in vivo* parasite clearance rates in mice with established infections were investigated. Parasite clearance rates are important measures of drug efficacy (White, 2011), particularly in the case of ARTs, which show accelerated clearance of ring-stage parasites (White, 2008) and manifest delayed clearance phenotypes as a mode of resistance (Dondorp et al., 2009). To monitor equivalent clearance of *P. berghei* Kelch13 mutants, mice were infected with a fixed inoculum of Kelch13 and UBP-1 mutant parasites (~10⁵) in four cohorts and allowed the parasitaemia to rise to ~10%. This was followed by dosing with AS at 64 mg/kg, which is slightly higher than the equivalent of the maximal human clinical dose of 4 mg/kg (mouse equivalent = 49.2 mg/kg) to accommodate for the reduced ART susceptibility observed in *P. berghei* parasites. Parasitaemia was quantified by flow cytometry (mCherry positivity) and microscopic analysis every 3 hours for the first 24 hours and at least once after the second and third doses at 24 and 48 hours respectively. Plotting of parasite density in *P. berghei* Kelch13 and UBP-1 mutant parasites against time revealed that in the first 24-hours of sampling, parasite clearance kinetics do not sufficiently discriminate Kelch13 or UBP-1 mutant parasites from wild type. However, as the majority of dying parasites were cleared by the host and mice received further doses, extended analysis revealed that *P. berghei* M488I and R551T mutant parasites consistently and significantly persisted compared to the wild type, F458I, Y505H and UBP-1 mutant parasites (Figure 4.4a, Appendix Figure 8.10a-c).

Starting AS treatment at a high initial parasitaemia (~10%) also ensured a good proportion of parasites would be within the early ring-stage window and therefore, would be expected to preferentially survive the first AS dose. Surviving rings could be easily distinguished as viable trophozoites at 18, 21 and 24 hours by microscopic examination of blood smears, which enabled comparisons of the drug responses between parasite lines. Therefore, a concurrent collection and analysis of thin blood smears was carried out at all time points examined for flow analysis (Figure 4.4a, Appendix Figure 8.10a-c). These analyses demonstrated that enhanced survival of the first AS dose was evident for all four *P. berghei* Kelch13 mutant parasites as well as the UBP-1 mutant compared to wild type (Figure 4.4b, Appendix Figure 8.10d). Microscopy provided a more sensitive discrimination than the flow estimation of clearance kinetics, which was unable to distinguish mutant from wild type parasites in the first 24 hours.

a



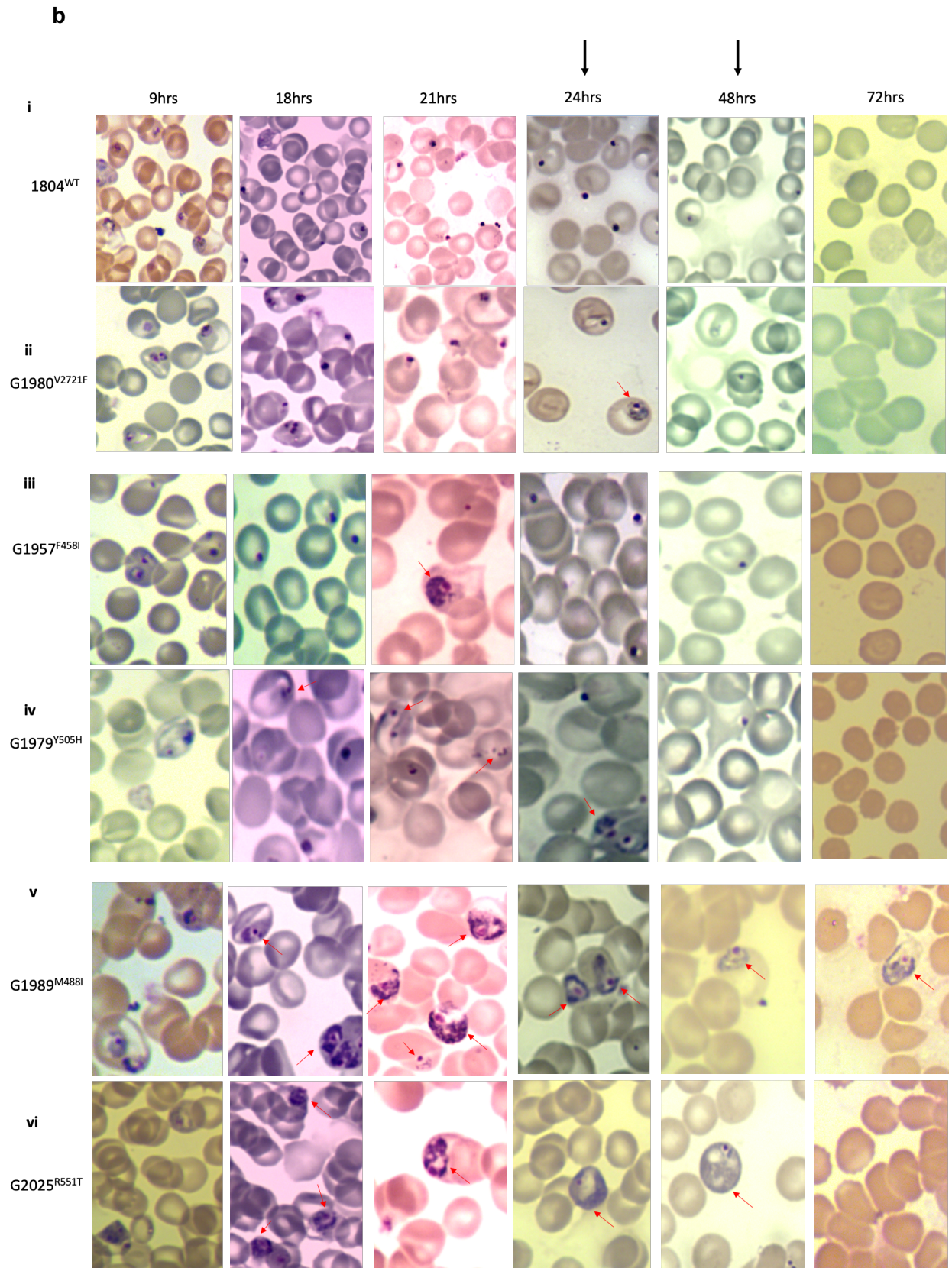


Figure 4.4: *In vivo* clearance kinetics and microscopy analysis of *P. berghei* Kelch13 mutants upon AS treatment.

a. Parasite clearance curves in mice infected with Kelch13 mutant lines following treatment with AS. Six mice (in four cohorts) were infected with $\sim 10^5$ parasites of each of the four Kelch13 mutants, the UBP-1 mutant and wild type control on day 0. On day 5, at

a parasitaemia of ~10%, mice were dosed with AS at 64 mg/kg. Day 5 was the designated 0 hours for the dosing regimen. Parasite density per μ l of blood was quantified based on absolute counts of mCherry positive parasites at staggered time points for each of the two cohorts, with 5 time points in the first 24 hours (corresponding to at least 3-hour interval coverage between the two cohorts) and at least once daily thereafter. Mice were dosed three times at 0, 24 and 48 hours as indicated by arrows. Concurrent thin blood smears were prepared at each time point for microscopic analysis. **b. i-vi.** Microscopic analysis of Giemsa-stained thin blood smears showing preferential survival of UBP-1 (ii) and Kelch13 mutant parasites; G1957^{F458I} (iii), G1979^{Y505H} (iv), G1989^{M488I} (v) and G2025^{R551T} (vi) as compared to wild type parasites (i) upon treatment with AS for cohorts 1 and 2. Smears were taken at time points corresponding to those shown in the clearance plots in Figure 4.4a, Appendix Figure 8.10a-c. 2nd and 3rd dose treatment days are indicated by black arrows. Red arrows indicate viable parasites. Viability was deemed significant if at least 4 viable parasites were observed in minimum of 10 microscopic fields.

False positives could be due to continual retention of mCherry positivity by dying parasites, as for instance, a significant proportion of wild type parasites remained mCherry positive and were counted as viable by flow cytometry (Figure 4.4a, Appendix Figure 8.10a-c) while microscopically, they were pyknotic forms (Figure 4b i, Appendix Figure 8.10d i). Remarkably, the M488I and R551T mutants remained smear positive after two consecutive AS doses (Figure 4.4b v, 4.4b vi, Appendix Figure 8.10d v, 8.10d vi) while the wild type, F458I, Y505H or UBP-1 mutant parasites were cleared (microscopically smear negative) after 48 hours (Figure 4.4b i, ii-iv, Appendix Figure 8.10d i, ii-iv). These data suggest that the M488I and R551T mutants meet the classical definition of ART resistance as defined by the WHO, which is based on day 3 (second generation) microscopy positivity if the duration of the *P. berghei* life cycle and dosing intervals are accounted for (WHO, 2018a). One of the four mice in the M488I treatment group remained smear positive after three consecutive AS doses (Figure 4.4b v). These data clearly show that *P. berghei* Kelch13 mutants modulate *in vivo* susceptibility to ARTs resulting in a persister/delayed clearance phenotype under controlled conditions of initial parasite biomass and host immune status (naïve mice of same age, gender, breed and genetic background were used).

4.3.5 *P. berghei* Kelch13 mutants achieve faster recrudescence than wild type parasites at higher ART doses

Another *in vivo* marker of reduced ART susceptibility in *P. falciparum* is the rate of recrudescence upon AS treatment, which acts as a possible indicator of AS treatment failure. However, at pharmacologically safe doses in humans, ART treatment leads to >40% recrudescence rates (Li et al., 1984), making it difficult to use this approach to separate clinically ART-sensitive from ART-resistant parasites. This can also be further confounded by differences in the starting parasite inoculum, drug dosing strategies as well as the relative fitness of mutant parasites. *P. berghei* Kelch13 mutants, therefore, provide the opportunity to test for recrudescence rates using controlled parasite inocula as well as AS or ART dose ascendency, which could potentially provide separation between mutant and wild type parasites. Such experiments are practically and ethically not feasible in human malaria. Groups of 3-4 mice were thus infected with ~10⁶ parasites of the four Kelch13 mutants, the UBP-1 V2721F mutant and wild type parasites. Mice were then dosed with ART at 80mg/kg starting from three hours post infection for three consecutive days. This ART dose sufficiently suppresses the wild type for up to 18 days of follow-up (Section 3.3.3). At this dose, all UBP-1 mutant infections recrudescenced 11 days after the last ART dose while no recrudescence (0%) was observed for the wild type, which is in agreement with previous observations (Section 3.3.3) (Figure 4.5, Appendix Table 8.4). R551T mutant parasite infections achieved even faster recrudescence, 50% on day 4 after the last dosing and 100% a day later, indicating a higher level of *in vivo* resistance for this Kelch13 mutation than for the comparative UBP-1. M488I mutant parasites had a similar recrudescence profile beginning on day 6. The Y505H and F458I mutant lines both achieved recrudescence at approximately the same time as the UBP-1 mutant; however, the latter achieved only 50% recrudescence across the 18-days follow-up period (Figure 4.5, Appendix Table 8.4). These data further confirm that *P. berghei* Kelch13 mutants modulate *in vivo* susceptibility to ARTs and crucially, that recrudescence rates strongly correlate with *in vitro* DHA RSA profiles (Figure 4.3) as well as *in vivo* clearance kinetics in established infections (Figure 4.4, Appendix Figure 8.10).

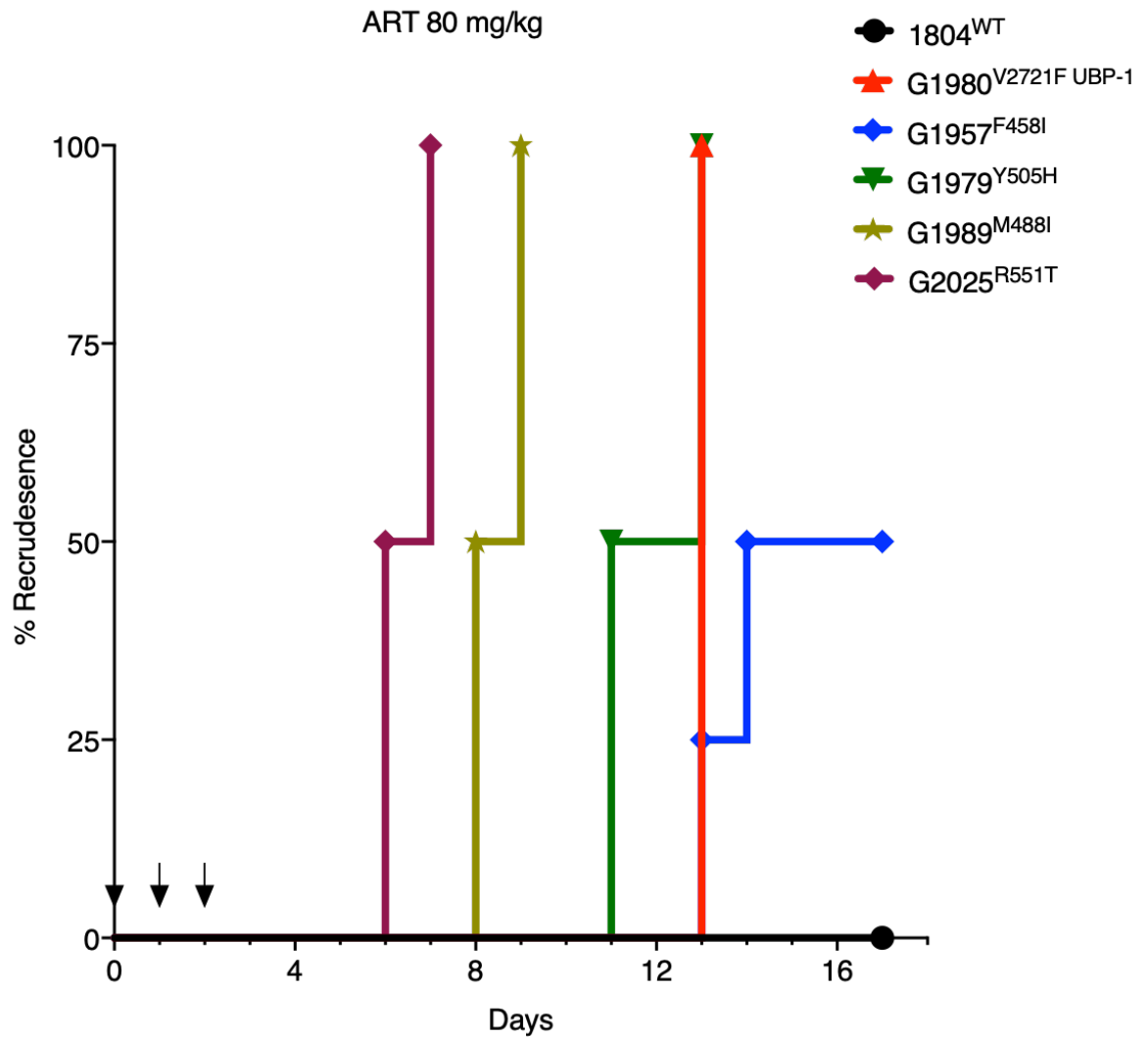


Figure 4.5: *In vivo* recrudescence rates of *P. berghei* Kelch13 mutants upon treatment with ART.

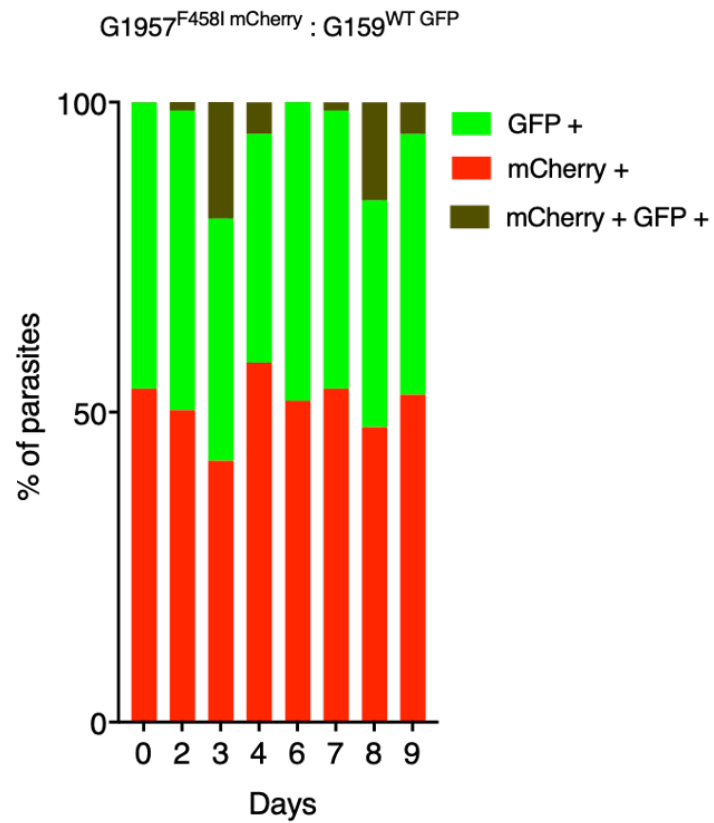
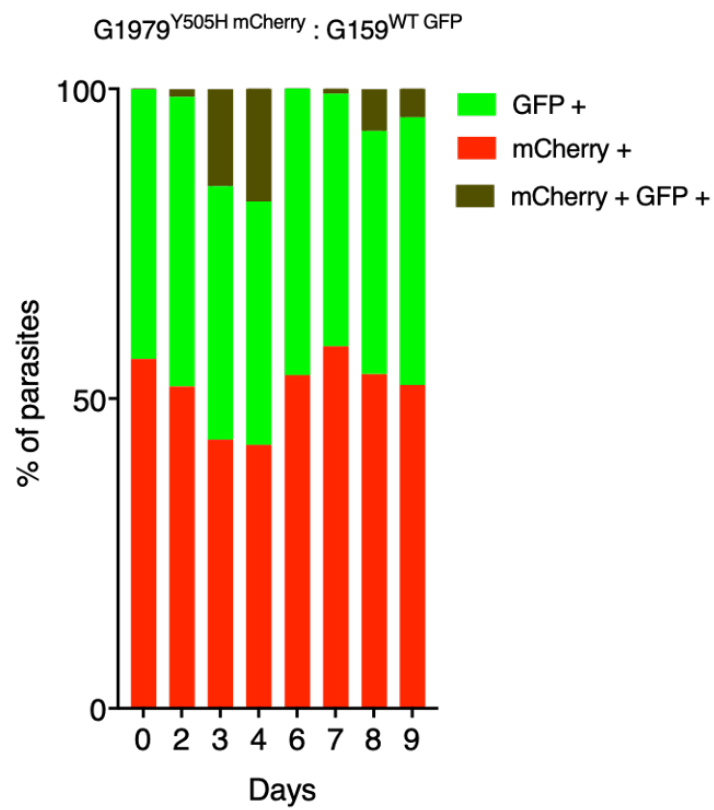
Kaplan–Meier plots of recrudescence in wild type and UBP-1 mutant controls as compared to Kelch13 mutants. A modified Peters’ 4-day suppressive test was used to monitor susceptibility of the Kelch13 mutants to 80 mg/kg ART, a dose that effectively suppresses wild type parasites for up to 18 days. Groups of three (UBP-1 mutant, 1804^{WT}) or four mice (Kelch13 mutants) were infected with $\sim 1 \times 10^6$ parasites on day 0. ART treatment was initiated ~ 3 hours later and continued every 24 hours for three consecutive days (treatment days shown by arrows). Parasitaemia was monitored by microscopic analysis of Giemsa-stained blood smears up to day 18 (Appendix Table 8.4). Recrudescence rates were plotted as the proportion of mice in the treatment groups that became smear positive on every individual day for the 18 days of follow-up.

4.3.6 *P. berghei* Kelch13 mutants are associated with an *in vivo* fitness cost but are preferentially selected for in the presence of AS or CQ

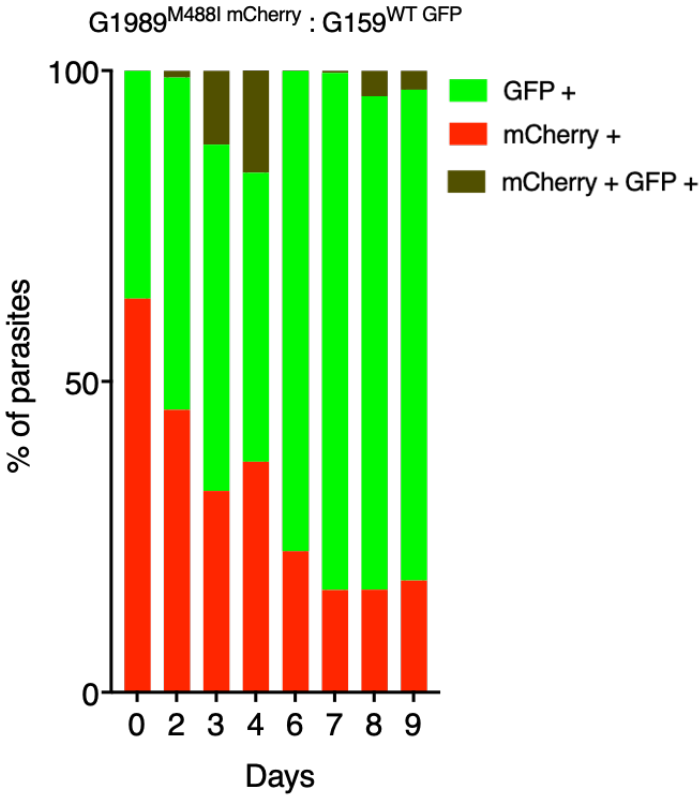
To assess the fitness of the *P. berghei* Kelch13 mutants, direct head-to-head competitions with wild type parasites under *in vivo* growth conditions were performed. *P. berghei* Kelch13 or UBP-1 mutant lines or the parental 1804^{WT} (mCherry positive) line were mixed at a 1:1 ratio with the G159^{WT} (GFP-positive) line and injected into mice, after which changes in the proportion of GFP- or mCherry-positive parasites in the competition mixture were quantified by flow cytometry over 9 days. These assays revealed that the F458I and Y505H mutant parasites were fitness neutral relative to the G159^{WT} line while the M488I and R551T mutants carried significant fitness costs (Figure 4.6a-d). Both the M488I and R551T mutations were associated with high levels of reduced susceptibility to DHA *in vitro* (Figure 4.3), delayed clearance kinetics (Figure 4.4a, Appendix Figure 8.10a-c), and faster recrudescence following ART treatment *in vivo* (Figure 4.5, Appendix Table 8.4). Comparatively, the R551T mutant parasites had a more severe growth defect than the M488I mutants and were completely outcompeted by the GFP-positive wild-type line by day 7 (Figure 4.6c, 4.6d). This is consistent with previous observations of high *in vitro* fitness costs for the equivalent *P. falciparum* R539T mutation (Straimer et al., 2017). In comparisons to the G159^{WT} line, the parental wild type line (1804^{WT}) was fitness neutral while the UBP-1 V2721F mutant carried a minor growth defect as previously observed (Section 3.3.4) (Appendix Figure 8.11a, 8.11b). To examine the potential for preferential survival of *P. berghei* Kelch13 mutants in competition mixtures with the wild type (as described above) upon AS treatment, an examination of the proportions of GFP versus mCherry-positive parasites was carried out following drug treatment at the time of recrudescence. Mutant parasites were mixed at 1:1 ratio with the G159^{WT} line, injected into mice and treated with AS at 50 mg/kg beginning 3 hours after infection for three consecutive days. Monitoring of recrudescence up to day 9 revealed that, upon AS treatment, the M488I and R551T mixtures recrudescenced slightly faster than the wild type mixture and were highly enriched for the mutant population (>90%) at the time of recrudescence (Figure 4.6f, 4.6g). The F458I and Y505H mutant mixtures recrudescenced slightly later (Figure 4.6e), as did the UBP-1 V2721F mutant (Appendix Figure 8.11d) and were all significantly enriched for the mutants. In contrast, the proportions of GFP-positive versus mCherry-positive parasites in the parent 1804^{WT} and G159^{WT}

competition mixture after AS treatment did not change at the time of recrudescence (Appendix Figure 8.11c). These data show that mutant *P. berghei* Kelch13 parasites are preferentially selected for upon AS treatment, despite some carrying growth defects that rendered them at a complete competitive disadvantage in the absence of drug.

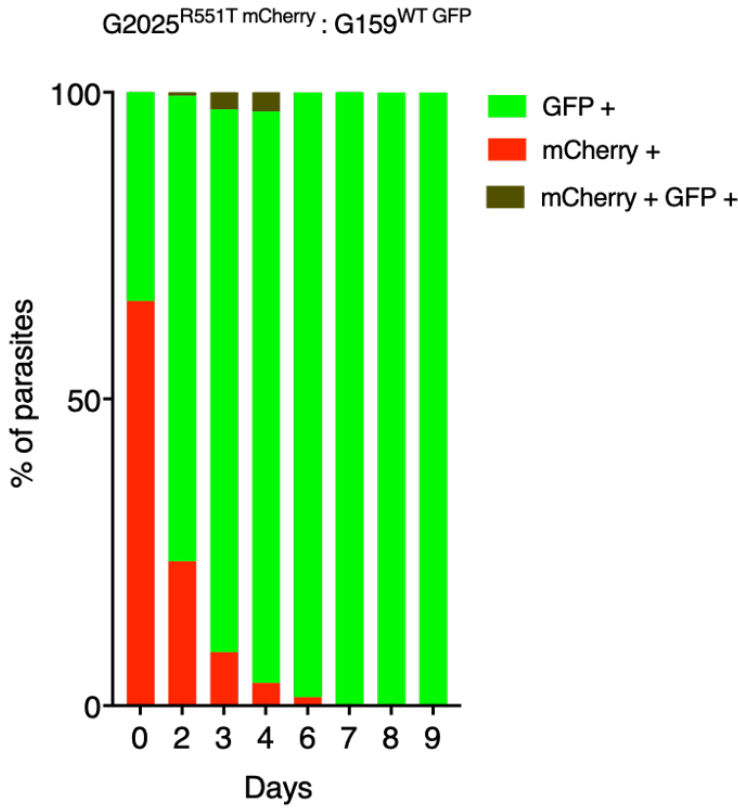
Recently, it has been shown that *P. falciparum* Kelch13 localises to the parasite cytostomes and plays a role in parasite haemoglobin endocytosis and trafficking DV (Birnbaum et al., 2020, Yang et al., 2019). Kelch13 mutations lead to a partial loss of function to this protein which impairs haemoglobin endocytic uptake henceforth lessening ART activation which culminates into a parasite resistance phenotype (Yang et al., 2019). Inactivation of Kelch13 interacting components such as Eps15, UBP-1 and AP-2 μ which are involved in the Kelch13 endocytic pathway also impact haemoglobin uptake and, more importantly, mimic ART resistance phenotypes (Birnbaum et al., 2020). In the meanwhile, mutations in AP-2 μ or UBP-1 do not just modulate susceptibility to ARTs, but to other drugs such as CQ which may need endocytic uptake into the DV or require sufficient haemoglobin endocytosis (exposure to haem moieties) to exert their activity (Hunt et al., 2007, Henrici et al., 2019a, Birnbaum et al., 2020). *P. berghei* Kelch13 mutant parasites with strong ART resistance phenotypes might, therefore, be able to modulate susceptibility to CQ (to some degree) through a similar dysregulation of the endocytic pathway. Using the *in vivo* competition assay under drug pressure as with AS above, the parental 1804^{WT} line, the UBP-1 V2721F line and the Kelch13 R551T mutant line were mixed at 1:1 ratio with the G159^{WT} line and treated with CQ at 15 mg/kg. At the time of recrudescence, the proportion of 1804^{WT} parasites (mCherry-positive) did not significantly change as compared to the proportion of GFP-positive G159^{WT} parasites (Appendix Figure 8.11c). In comparison, the UBP-1 V2721F mutant was enriched to ~70% (Appendix Figure 8.11d), which mirrors previous observations that this mutation can indeed be selectively enriched by CQ (section 3.3.2). Interestingly, upon CQ treatment, the combination of R551T mutant parasites and the G159^{WT} line achieved recrudescence at almost the same rate as under AS pressure, with mutant parasites enriched to ~72% (Figure 4.6g). These data suggest that Kelch13 mutations can contribute to low level protection to CQ (Birnbaum et al., 2020, Yang et al., 2019).

a**b**

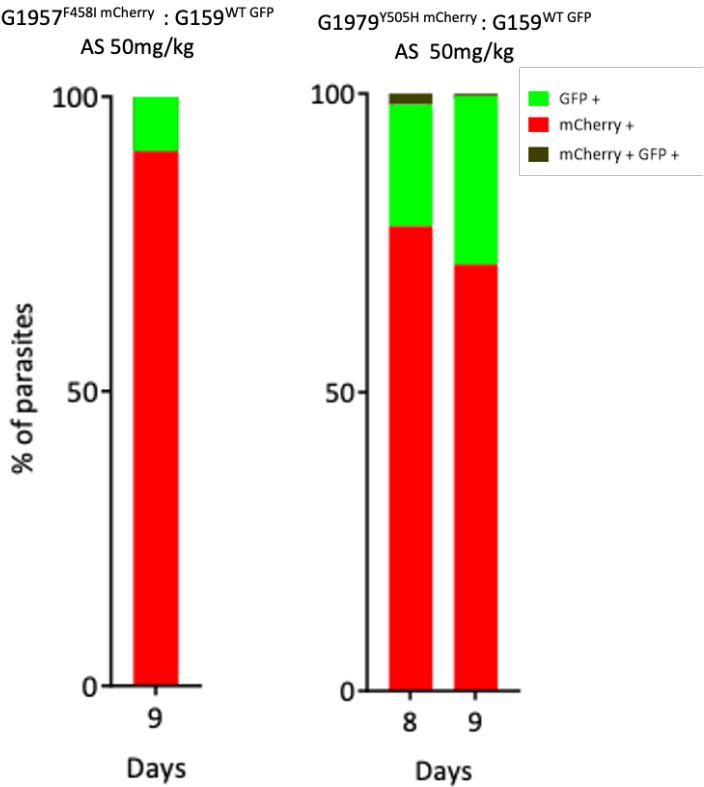
c



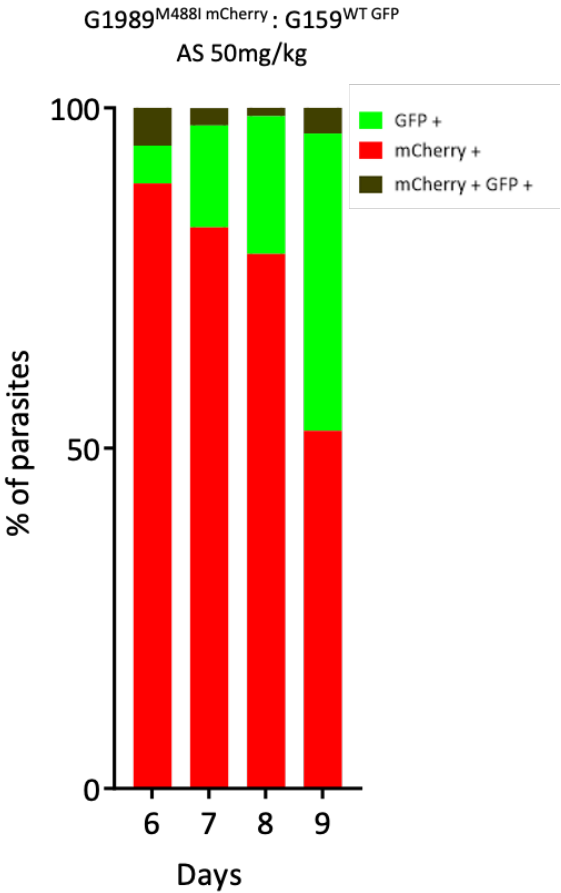
d



e



f



g

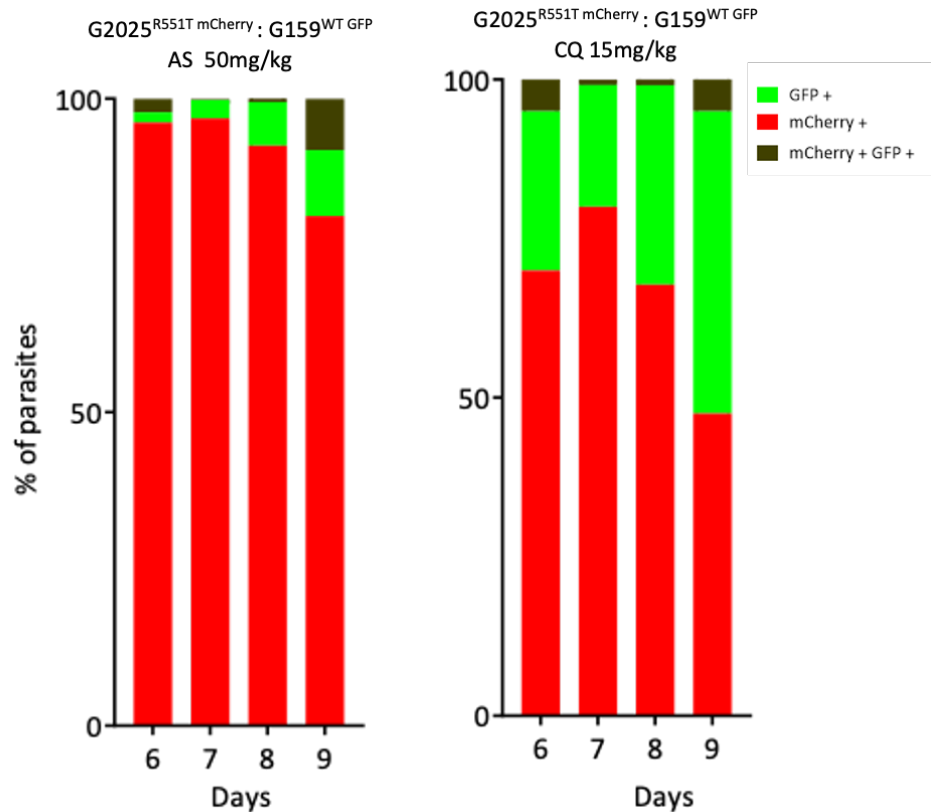


Figure 4.6: Relative fitness of *P. berghei* Kelch13 mutants in presence or absence of AS or CQ.

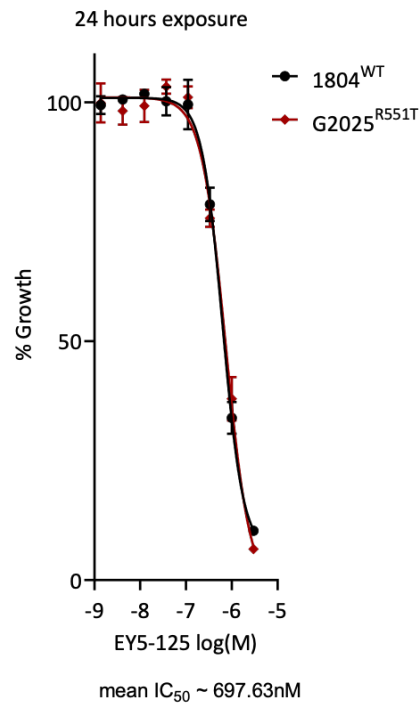
Growth competition assays with Kelch13 mutant lines that constitutively express mCherry as compared to the wild type G159^{WT} line that constitutively expresses GFP in the presence or absence of drug pressure. The G159^{WT} line was mixed with a given mutant line at 1:1 ratio in three groups of mice on Day 0. The first group was left untreated, the second group received a dose of AS at 50 mg/kg starting from 3 hours after IP injection, for three consecutive dose while the third group consisting of the 1804^{WT}, G1980^{V2721F} and one Kelch13 mutant (G2025^{R551T}) received CQ at 15 mg/kg at similar dosing times as AS. Percentages of mCherry or GFP positive parasites were determined by flow cytometry as described in methods. **a-d.** Percentage population changes as measured by flow cytometry of the G1957^{F458I} (a), G1979^{Y505H} (b), G1989^{M488I} (c) and G2025^{R551T} (d) mutant lines relative to the G159^{WT} wild type line. **e-g.** Proportion representation of the G159^{WT} line in mixture with G1957^{F458I} and, G1979^{Y505H} (e), G1989^{M488I} (f) and G2025^{R551T} (g) lines on the days of recrudescence upon treatment with AS or CQ as indicated.

4.3.7 A *Plasmodium*-selective proteasome inhibitor is potent against *P. berghei* wild type and Kelch13 mutant parasites and synergizes DHA action

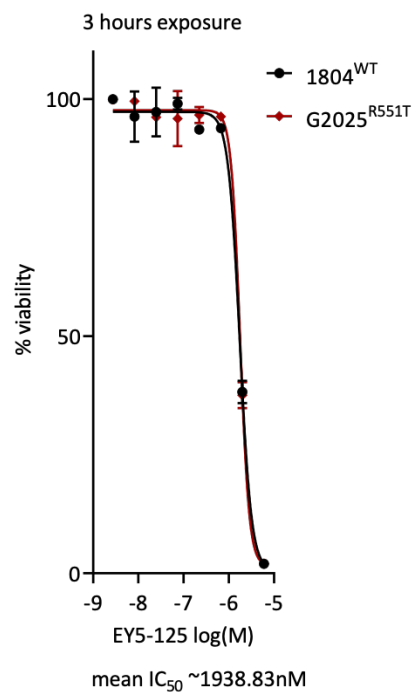
An enhanced cell stress response characterised by upregulation of genes in the unfolded protein response (UPR) is a typical signature of ART resistant parasites (Mok et al., 2015). Resistant parasites (Kelch13 mutants) also display enhanced activity of the UPS, a conserved eukaryotic pathway that acts downstream of the UPR by degrading unfolded proteins (Bridgford et al., 2018, Dogovski et al., 2015). UPS inhibitors are available for cancer treatment and have been shown to synergize DHA activity in wild type and Kelch13 mutant *P. falciparum* both *in vitro* and *in vivo* marking them as promising agents for overcoming ART resistance (Dogovski et al., 2015, Li et al., 2016). The *Plasmodium* selective proteasome inhibitor, EY5-125 is a potent antimalarial (standard IC_{50} = 19 nM) and also acts in synergy with ART against both ART resistant and sensitive *P. falciparum* strains *in vitro* (Yoo et al., 2018). Therefore, the efficacy of EY5-125 against *P. berghei* wild type and Kelch13 mutant parasites was tested as well as its potential ability to synergize DHA action. *P. berghei* wild type and the most ART-resistant Kelch13 mutant (R551T) were equally sensitive to EY5-125 (Figure 4.7a, 4.7b) which is consistent with previous reports for this class of compounds against wild type and Kelch13 mutant *P. falciparum* lines (Stokes et al., 2019, Yoo et al., 2018). Compared to *P. falciparum* (standard IC_{50} ~19 nM and 1hr IC_{50} ~648 nM), EY5-125 is much less potent in *P. berghei* in both standard *in vitro* growth inhibition (IC_{50} = ~700 nM) and 3-hour assays (IC_{50} = ~1900 nM) respectively (Figure 4.7a, 4.7b). These differences could be due to species-specific differences in drug sensitivity as has been observed with ARTs, Figure 4.3, (Lee et al., 2018) and many other drugs (Fidock et al., 2004). However, combinations of DHA and EY5-125 in fixed ratio isobologram analyses revealed a strong synergistic interaction against the *P. berghei* parent wild type and Kelch13 M488I and R551T mutant lines (Figure 4.7c-e). The *in vivo* RSA (Figure 4.3b) was also employed to examine whether a combination of DHA at 700 nM and EY5-125 at the equivalent 3-hour IC_{50} (1.94 μ M) or 2x IC_{50} (3.88 μ M) could impact the parasite survival rates. Indeed, at both 3-hour IC_{50} or 2x IC_{50} concentrations, EY5-125 strongly synergized DHA (700nM) as evidenced by significant abrogation of survival for both the wild type and R551T mutant lines (Figure 4.7e). These data demonstrated that proteasome inhibitors synergize

DHA action in *P. berghei* Kelch13 mutants equally as well as wild type parasites both *in vitro* and *in vivo* and have the potential to be used to overcome ART resistance.

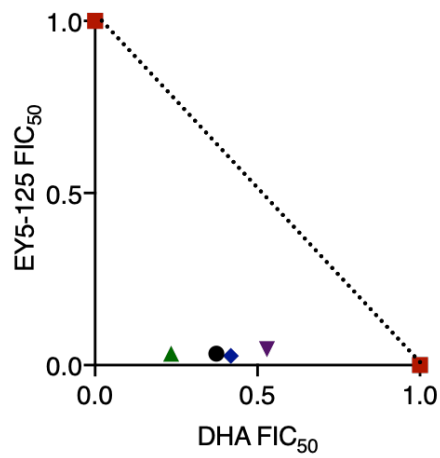
a



b

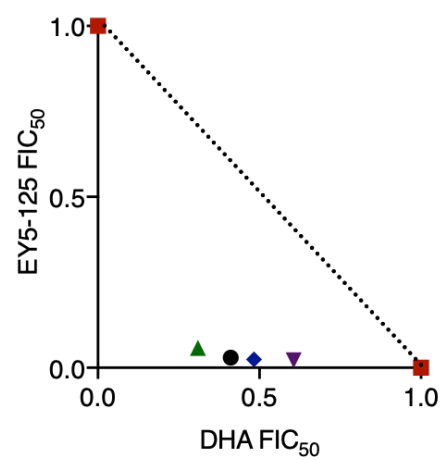


c

1804^{WT}

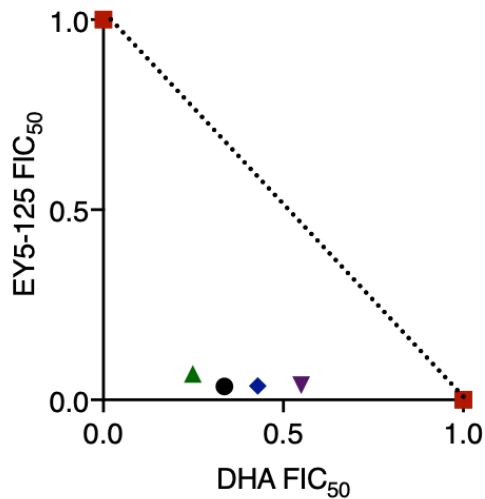
Drug Combination Ratio	Σ FIC ₅₀
DHA 100%	1
DHA 80% : EY5-125 20%	0.562944
DHA 60% : EY5-125 40%	0.451393
DHA 40% : EY5-125 60%	0.400207
DHA 20% : EY5-125 80%	0.280418
EY5-125 100%	1

d

G1989^{M488I}

Drug Combination Ratio	Σ FIC ₅₀
DHA 100%	1
DHA 80% : EY5-125 20%	0.664209
DHA 60% : EY5-125 40%	0.512835
DHA 40% : EY5-125 60%	0.435438
DHA 20% : EY5-125 80%	0.33111
EY5-125 100%	1

e

G2025^{R551T}

Drug Combination Ratio	Σ FIC ₅₀
DHA 100%	1
DHA 80% : EY5-125 20%	0.618069
DHA 60% : EY5-125 40%	0.464512
DHA 40% : EY5-125 60%	0.373582
DHA 20% : EY5-125 80%	0.286664
EY5-125 100%	1

f

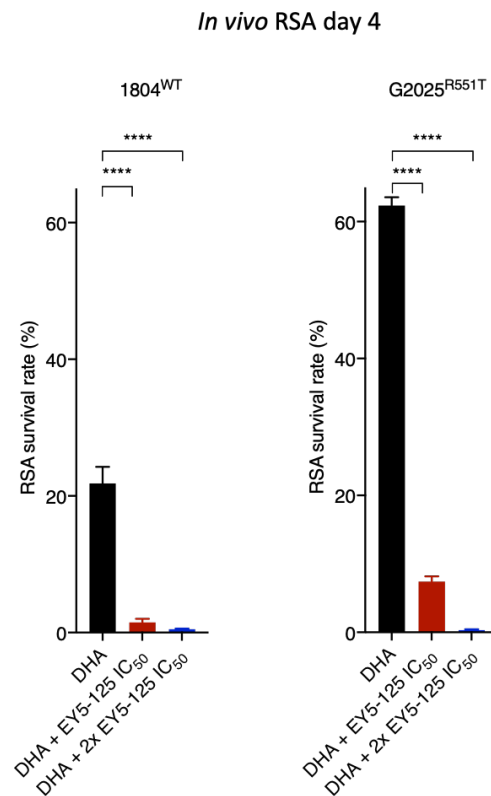


Figure 4.7: Activity and DHA synergy of proteasome inhibitor in *P. berghei* Kelch13 mutants.

a, b. Dose response curves and mean IC₅₀ values for the *Plasmodium*-selective proteasome inhibitor EY5-125 for the wild type 1804^{WT} and Kelch13 mutant G2025^{R551T} lines in standard 24-hour assays (**a**) or 3-hour exposure assays conducted on early ring-stage parasites (**b**). Mean IC₅₀ is a calculated average for the 2 lines independently screened in 3 biological repeats. **c-e.** Isobologram plots and Σ FIC₅₀ values representing the interaction between DHA and EY5-125 in the wild type 1804^{WT}, G1989^{M488I} and G2025^{R551T} lines. FIC₅₀ plots and Σ FIC₅₀ values are mean values for each drug ratio calculated from three biological repeats. **f.** Synergy of EY5-125 proteasome inhibitor with DHA in the *in vivo* RSA. After exposure to DMSO or DHA at 700 nM alone or in combination with EY5-125 at 3-hour IC₅₀ or 2x IC₅₀, parasites were injected back into mice 24 hours later. Parasitaemia in mice infected with drug or DMSO-treated parasites was determined by flow analysis of mCherry expression on Day 4 post IV injection and used to calculate percent survivals relative to DMSO-treated parasites. Error bars are standard deviations from three biological repeats. Statistical significance was calculated using one-way ANOVA alongside the Dunnett's multiple comparison test. Significance is indicated with asterisks; ****p < 0.0001.

4.4 Discussion

In this study, CRISPR-Cas9 genome editing was successfully employed to introduce four of the six targeted orthologous *P. falciparum* Kelch13 (F446I, M476I, Y493H, R539T) mutations in the Kelch13 gene of the rodent model of malaria *P. berghei*. Meanwhile, introduction of two mutations (C580Y and I543T) could not be achieved. As questions and debates continue on the role of Kelch13 in mediating susceptibility to ARTs, particularly *in vivo*, phenotyping of these *P. berghei* Kelch13 (F458I, M488I, Y505H and R551T) mutants has provided experimental evidence for the ability of Kelch13 to confer *in vivo* resistance to ARTs and in a naïve genome background. These mutants displayed reduced *in vitro* susceptibility to DHA, and more importantly phenocopied *P. falciparum* delayed clearance phenotypes. Moreover, these Kelch13 mutants achieved faster recrudescence upon ART treatment under *in vivo* growth conditions. As in *P. falciparum*, certain *P. berghei* Kelch13 mutations carry significant growth defects, which further highlights the structural and functional conservation of this protein across the two *Plasmodium* species while at the same time illustrating the fitness trade-offs that acquisition of such mutations exerts on malaria parasite physiology.

4.4.1 Acquisition of certain Kelch13 mutations may require permissive genetic backgrounds

ART resistance, principally associated with mutations in Kelch13, is now almost endemic in SEA with risks of spreading threatening the utility of ACTs that are at the forefront of malaria control programs (WHO, 2019). The *P. falciparum* C580Y Kelch13 mutation is the most prevalent (>50% prevalence) and has reached fixation in most parts of SEA (Menard et al., 2016, Miotto et al., 2015). Why the *P. falciparum* C580Y mutation is so successful as compared to other Kelch13 mutations remains unclear. For instance, this mutation does not associate with high RSA survival rates as compared to *P. falciparum* R539T or I543T mutations nor are treatment failure rates and parasite clearance rates more significant in C580Y-harboursing parasites as compared to other Kelch13 mutants (Anderson et al., 2017, Phyo et al., 2016a, Straimer et al., 2015). Do fitness constraints, founder genetic landscapes or species-specific differences between *P. berghei* and *P. falciparum* Kelch13 explain failed attempts to introduce the C592Y or I555T mutations in *P. berghei*? The structural homology model of the Kelch13

propeller domain presented here demonstrates that this Kelch13 region is highly conserved between *P. berghei* and *P. falciparum*, with identical amino acids at the sites of mutations associated with ART resistance. Failed attempts to introduce the *P. berghei* C592Y or I555T mutations could therefore be more related to growth disadvantages or other deleterious effects. For example, in *P. falciparum*, the equivalent I543T and R539T mutations carry the most pronounced fitness costs (Straimer et al., 2017) which would partly explain failure to introduce the I555T mutation in *P. berghei*. Moreover, *P. berghei* Kelch13 mutations were introduced into ART naïve PBANKA parasites with no history of ART exposure. These parasites might therefore be more sensitive to fitness impacts conferred by the I555T or C592Y substitutions, as it was previously demonstrated for the latter that introduction of the equivalent *P. falciparum* C580Y in parasites isolated before ART was clinically introduced carried significant growth defects as opposed to when it was introduced in more recent Cambodian isolates where it was fitness neutral (Straimer et al., 2017). Moreover, a less successful Kelch13 allele, *P. falciparum* R561H that associates with significant delays in parasite clearance and peaked in prevalence in 2012 but has since declined (Anderson et al., 2017); easily outcompetes the *P. falciparum* C580Y mutation in head to head competitions (Nair et al., 2018). These data suggest that acquisition and propagation of certain *P. falciparum* Kelch13 alleles, mostly the C580Y substitution, require appropriate founder architectures to compensate for the deleterious phenotypes. In these situations, Kelch13 mutations (*P. falciparum* C580Y for example), would arise in a necessary compensatory background that mitigates the deleterious growth effects leading to an initial soft sweep. In case of ACTs, these compensatory backgrounds may also serve as general templates upon which partner drug resistance mutations might arise as seems to be the case with the recent aggressive expansion of parasite co-lineages carrying the *P. falciparum* C580Y mutation and piperaquine resistance determinants (Hamilton et al., 2019, van der Pluijm et al., 2019).

4.4.2 Some *P. berghei* Kelch13 mutations carry a pronounced fitness cost

Introduction of the *P. falciparum* R539T equivalent in *P. berghei* (R551T) was achieved despite low editing efficiency in the initial transfection. Selection with AS applied *in vivo* was, however, used to enrich for this mutation yielding almost clonal levels of the *P. berghei* R551T mutants. Similar to the *P. falciparum* R539T mutants, clonal *P. berghei* R551T mutant parasites carried the strongest DHA resistance phenotypes *in vitro* as well as the clearest AS or ART resistance profiles *in vivo*. The *P. falciparum* R539T and I543T mutations occur at relatively low frequencies in SEA with the prevalence of both mutations ranging between 0.3-3.5% (Takala-Harrison et al., 2015, Menard et al., 2016, Malaria, 2016). This could be due to the pronounced fitness cost of these mutations (Straimer et al., 2017) limiting their expansion which was also observed with the *P. berghei* R551T mutant parasites. The combination of a naive genomic background and species-specific differences can also be invoked to explain some phenotypic differences (growth rate and level of ART resistance) seen between mutant lines of *P. falciparum* and *P. berghei* Kelch13 as observed in this study. For example, *P. falciparum* Y493H mutants clearly associate with increased RSA survival (Ariey et al., 2014, Straimer et al., 2015) and delayed parasite clearance phenotypes (Amaratunga et al., 2014, Takala-Harrison et al., 2015, Ariey et al., 2014) unlike the *P. berghei* counterpart (Y505H) which display low level resistance to ARTs *in vitro* (in the standard assay but not in the adapted RSA) and *in vivo*. This could indeed be due additional underlying genetic factors in *P. falciparum* isolates providing an additive effect to the observed phenotypes which would be absent in naive *P. berghei*. Nevertheless, the other tested *P. berghei* Kelch13 mutations do, however, appear to directly reflect the impact of the equivalent mutations in *P. falciparum*. Both *P. berghei* F458I (this work) and *P. falciparum* F446I Kelch13 mutants are fitness neutral (Siddiqui et al., 2020), offer no advantage in their RSA tests (Siddiqui et al., 2020, Wang et al., 2018) yet appear to offer ART protective phenotypes *in vivo* (Wang et al., 2015d, Huang et al., 2015, Tun et al., 2016). Furthermore, *P. berghei* M488I Kelch13 mutants display a significant growth defect phenotype which has not yet been characterised in the *P. falciparum* equivalent (M476I) and might explain its relative scarcity in SEA (Tun et al., 2015, Nyunt et al., 2014).

4.4.3 Proteasome inhibition off-sets ART resistance in *P. berghei* Kelch13 mutants

Enhanced proteostasis is a characteristic signature of *P. falciparum* Kelch13 ART resistant parasites which is typified by upregulation of genes in the UPR as well as enhanced activity of the UPS (Mok et al., 2015, Dogovski et al., 2015, Bridgford et al., 2018). Inhibition of the UPS by 20s proteasome inhibitors synergizes DHA action both *in vitro* and *in vivo*, which has offered a potential avenue to overcome ART resistance (Dogovski et al., 2015). Despite UPS inhibitors (which are clinically available for treatment of certain cancers) displaying activity in malaria parasites and synergising DHA action, their translation into animal studies has been limited by host toxicity (Li et al., 2012, Gantt et al., 1998). Recent structure-based design of *Plasmodium* selective proteasome inhibitors has provided classes of compounds with a wider therapeutic window and improved host toxicity profiles (Li et al., 2016, Yoo et al., 2018). These inhibitors not only display activity in diverse genetic backgrounds of *P. falciparum* including those harbouring Kelch13 mutations but also synergize DHA action (Stokes et al., 2019). Even though the *P. berghei* proteasome structures have not been solved, functional and life cycle conservation between this parasite and *P. falciparum* is pronounced. Therefore, using EY5-125, an inhibitor selective for the *P. falciparum* proteasome (Yoo et al., 2018), similar activity and synergy with DHA in *P. berghei* wild type and Kelch13 ART resistant mutants is demonstrated. More importantly, these activities are demonstrated *in vivo*, which significantly strengthens the potential of these compounds in overcoming ART resistance.

4.4.4 Conclusion

In conclusion, this work provides experimental evidence that Kelch13 mutations modulate *in vitro* and *in vivo* susceptibility to ARTs in the *P. berghei* rodent model of malaria. The cause and effect link between *P. falciparum* Kelch3 mutations with reduced ART susceptibility is strong (Straimer et al., 2015, Arie et al., 2014). However, the reason for ART clinical failure has remained obscure because, in some cases, delayed parasite clearance phenotypes have been reported in parasites carrying wild type Kelch13 alleles (Kheang et al., 2017, Mukherjee et al., 2017). This confusion is further compounded by a lack of correlation between Kelch13 mutations and parasite clearance half-lives or the

frequencies of recrudescence in certain cases of ART monotherapies (Kheang et al., 2017). As demonstrated in this study, some of these observations may be attributable to fitness defects in mutant parasites which confound the interpretation of recrudescence rates. These fitness differences might be especially relevant at the relatively low ART doses used in humans, which are already known to permit higher rates of recrudescence (Li et al., 1984). Although a recent genetic cross of the *P. falciparum* Kelch13 C580Y mutant parasites with *Aotus* infecting strains demonstrated a lack of association of this mutation with *in vivo* ART resistance (recrudescence and clearance half-lives) (Sa et al., 2018), this could be due to 1) the AS doses used being insufficiently high to clearly separate the lineages; 2) the small sample sizes used; and 3) the inherent limitation of using heterogenous *Aotus* monkeys from varying history of parasite exposure and spleen status (spleen intact or splenectomised). Nevertheless, the *in vitro* and *in vivo* phenotypes for the *P. falciparum* F446I, M476I, Y493H and R539T Kelch13 mutation equivalents in *P. berghei*, presented here, support their direct involvement in mediating resistance to ARTs. These data also provide a robust immune-replete rodent host model to test for synergistic antimalarial combinations that can restore ART efficacy and overcome ART resistance. Continued tracking of the emergence and spread of Kelch13 mutations should thus help in mitigating the spread of ART resistance as well as the preservation of this important class of antimalarial drugs through the identification of suitable partners.

5 Small molecule inhibitors of mammalian deubiquitinating enzyme display activity in malaria parasites and show evidence of potentiating ART action

5.1 Chapter aim

As resistance to front line antimalarial drugs, ARTs, emerges, there is urgent need to develop replacement antimalarial drugs or rescue the emergent resistance by identifying suitable partner drugs. The latter approach is being actively pursued through targeted inhibition of the downstream component of the UPS, the 20s proteasome, in classical MOA and MOR informed strategies. As demonstrated in Chapter 3, ART resistance (reduced susceptibility) can also be mediated by mutations in upstream UPS components, DUBs, offering another potential arm of the UPS which can be targeted to overcome ART resistance. Work in this chapter, was therefore aimed at screening DUB inhibitors for *in vitro* and *in vivo* activity in malaria parasites. Their potential to synergize and potentiate ART action was also assessed.

5.2 Introduction

Despite recent significant gains achieved in malaria control, the disease remains the most important parasitic disease in tropical and Sub-Tropical regions of the world with high rates of morbidity and mortality (WHO, 2019). The recently reported global stalls in malaria control over the past 3-4 years are making the situation even more worrisome (WHO, 2018c, WHO, 2019). Even though *P. falciparum* causes the majority of infections in Sub-Saharan Africa where the disease is a big problem, human malaria caused by other *Plasmodium* spp. such as *P. vivax*, *P. ovale*, *P. malaria* and the zoonotic *P. knowlesi* also remains a significant public health problem causing significant morbidity and economic impact in already poverty stricken communities (WHO, 2019).

A significant arm of current malaria control programs rely on ARTs, to which the emergence of resistance (described in detail in section 1.5.5.2) is a ticking time bomb. ART resistance in malaria parasites primarily correlates with point mutations in the Kelch13 protein which is a predicted adaptor protein of the Cullin E3 ligases of the UPS (section 1.5.5.2). Meanwhile ART resistant parasites (Kelch13 mutants) are associated with an upregulation of genes involved in the

UPR stress response pathways (Mok et al., 2015). Functional studies have, indeed, revealed that Kelch13 co-localises with multiple UPR components, proteins specific to the ER and mitochondria as well as intracellular vesicular trafficking Rab GTPases (Siddiqui et al., 2020, Nina F. Gnädig, 2020). Central to the activity of the UPR is the UPS, a downstream pathway that plays a role in maintaining protein homeostasis. Under ART pressure, activity of the UPS is more upregulated in Kelch13 mutant parasites compared to wild type while UPS inhibitors have been shown to synergize ART action suggesting that this pathway could be selectively targeted to overcome ART resistance (Dogovski et al., 2015, Li et al., 2016). Mutations in upstream components of the UPS (ubiquitin hydrolases or DUBs) also modulate susceptibility to ARTs, Chapter 3, (Hunt et al., 2007, Henrici et al., 2019a). Chemotherapeutic targeting of the UPS has been successfully pursued in cancers (Soave et al., 2017) and is increasingly becoming attractive in malaria parasites (Ng et al., 2017) even more so as potential combinatorial partners to ARTs to overcome resistance (Dogovski et al., 2015, Li et al., 2016).

Here, the activity of DUB inhibitors in both rodent and human malaria parasites is provided. DUBs are proteases that act upstream of the 20s proteasome by removing ubiquitin residues from conjugated substrate proteins (section 1.5.5.2). Using generic mammalian DUB inhibitors that have been used as exploratory research tools as well as in clinical trials, it is, here, demonstrated that DUB inhibitors do possess *in vitro* and *in vivo* inhibitory activities against malaria parasites across two diverged *Plasmodium* species. Different classes of DUB inhibitors can also be combined to provide greater killing efficacy as well as enhance the potency of ARTs both *in vitro* and *in vivo*. These data demonstrate that DUB inhibition can be exploited to overcome ART resistance with similar potency as first generation proteasome inhibitors. Furthermore, inhibition of both the UPS and DUBs can be combined simultaneously to further improve the potency of ARTs and negate ART resistance. These findings have the potential to be applied to the treatment of all human malaria.

5.3 Results

5.3.1 *In vitro* activity of DUB inhibitors in malaria parasites

To assay for *in vitro* activity of DUB inhibitors in malaria parasites, short term *P. berghei* culture assays and *P. falciparum* Sybergreen I[®] culture assays were employed. The *P. berghei* 820 and *P. falciparum* 3D7 lines were initially screened to determine susceptibility to inhibitors and antimalarials with known activity in malaria parasites; ART, DHA, CQ and epoxomicin (20s proteasome inhibitor). The IC₅₀ obtained for epoxomicin, DHA, ART and CQ in both the 820 and 3D7 lines (Table 5.1) were all in agreement with previously published IC₅₀ values in both *Plasmodium* species (Franke-Fayard et al., 2008, Janse et al., 1994b, Kreidenweiss et al., 2008, Bhattacharya et al., 2008). Next, seven DUB inhibitors (Table 5.1, Appendix Table 8.6) were screened in both the 820 and 3D7 line to characterise their inhibitory activity during the intraerythrocytic stages of malaria parasites. The selected compounds are DUB inhibitors being currently pursued as promising anticancer agents (Table 5.1, Appendix Table 8.6) that also offered a broad coverage targeting of the five classes of DUBs. As shown in Table 5.1, activity was observed for six of the seven DUBs tested in the 820 and 3D7 lines. The activity of USP acting DUB inhibitors; b-AP15, P5091 and NSC632839 corresponds with the reported *in vitro* IC₅₀s of the compounds screened in cancer cell lines (Chauhan et al., 2012, D'Arcy et al., 2011, Nicholson et al., 2008). b-AP15 IC₅₀ also compared to previously reported IC₅₀s of 1.54 ± 0.7 µM and 1.10 ± 0.4 µM in *P. falciparum* CQ sensitive (3D7) and resistant (Dd2) lines respectively (Wang et al., 2015b). Growth inhibition was also observed for broad spectrum DUB inhibitors; PR-619 and 1,10 phenanthroline, as well as a partially selective DUB inhibitor, WP1130 (Table 5.1). These data suggested that DUBs are potentially essential enzymes in *Plasmodium*, and they could be pursued as potential antimalarial drug targets. Indeed, a manual curation of up to 17 of the predicted DUBs in malaria parasites (Ponts et al., 2011, Ponder and Bogyo, 2007) shows that a majority of these (~70%, 12 of 17) are essential in either *P. falciparum* and *P. berghei* or both (Appendix Table 8.5) based on previous functional studies for selected DUBs (Artavanis-Tsakonas et al., 2006, Artavanis-Tsakonas et al., 2010) or recent genome wide gene knockout screens (Zhang et al., 2018, Bushell et al., 2017). Strikingly, no growth inhibition was observed for TCID (IC₅₀ >100 µM), a UCH-L3 inhibitor, in both the 820 and 3D7 lines (Table 5.1, Appendix Figure 8.12a, 8.12b). Among the well

characterised DUBs in malaria parasites is *P. falciparum* UCH-L3 (PfUCH-L3, PF3D7_1460400) which was identified by activity based chemical profiling and has been shown to retain core deubiquitinating activity (Frickel et al., 2007). Structural and functional characterisation of PfUCH-L3 also demonstrated that this enzyme is essential for parasite survival (Appendix Table 8.5) (Artavanis-Tsakonas et al., 2010). Meanwhile, in this screen, TCID, a highly selective mammalian UCH-L3 inhibitor with an IC_{50} of 0.6 μ M in mammalian cancer cell lines (Liu et al., 2003) displayed no activity in both the 820 and 3D7 lines (Table 5.1, Appendix Figure 8.12a, 8.12b). To possibly address this (unexpected) lack of activity, a phylogenetic analysis of *Plasmodium*, human and mouse UCH-L3 based on predicted protein sequences was performed to infer their similarities which might possibly explain the observed lack of anti-plasmodial activity of TCID. A distinct evolutionary divergence of this enzyme was observed between human, mouse and the most similar *Plasmodium* homologues (PBANKA_1324100/PF3D7_1460400) which whilst annotated as UCH-L3 shares only 33% predicted protein sequence identity with the human UCH-L3 (Appendix Figure 8.12c, 8.12d). Structurally, human UCH-L3 and PfUCH-L3 have similar modes of Ub recognition and binding. However, the PfUCH-L3 Ub binding groove is structurally different from the human UCH-L3 at atomic bonding level and possesses non-conserved amino acid residues (Artavanis-Tsakonas et al., 2010). This lack of complete identity across active sites would perhaps further explain the observed inactivity of TCID in both *P. falciparum* and *P. berghei*.

Inhibitor	Predicted UPS target	IC ₅₀	
		<i>P. berghei</i> 820	<i>P. falciparum</i> 3D7
Artemisinin	-	17.23±0.4 nM	6.50±0.4 nM
Dihydroartemisinin	-	13.89±0.1 nM	6.23±0.34 nM
Chloroquine	-	20.4±0.3 nM	16.23±0.5 nM
Epoxomicin	20s proteasome	14.20±3.0 nM	11.12±0.23 nM
PR-619	broad spectrum DUB inhibitor ^a	3.30±2.0 µM	2.41±0.5 µM
P5091	USP7 and USP47 DUBs ^b	8.38±2.10 µM	Not done
TCID	UCH-L3 and UCH-L1 DUBs ^c	>100 µM	>100 µM
WP1130	UCH-L1, USP9X, USP14, UCH37 DUBs ^d	1.19±1.0 µM	2.92±0.1 µM
b-AP15	USP14 and UCH-L5 DUBs ^e	1.06±0.9 µM	1.55±0.1 µM
NSC-632839	USP2, USP7, SENP2 DUBs ^f	27.97±0.8 µM	Not done
1,10 phenanthroline	Metalloproteases and JAMM isopeptidases ^g	0.63±0.3 µM	Not done

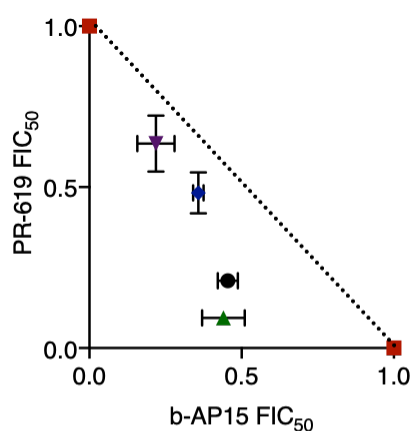
Table 5.1: *In vitro* activity of DUB inhibitors in rodent and human malaria parasites.

IC₅₀ values and error bars are means and standard deviations from at least 3 independent repeats. (Altun et al., 2011)^a, (Chauhan et al., 2012)^b, (Liu et al., 2003)^c, (Kapuria et al., 2010)^d (D'Arcy et al., 2011)^e, (Nicholson et al., 2008)^f, (Cooper et al., 2009)^g.

5.3.2 Different classes of DUB inhibitors can be combined to provide more effective blocking of malaria parasite growth *in vitro*

To explore interactions between DUB inhibitors, and their potential synergy, b-AP15, a highly selective USP14 inhibitor (D'Arcy et al., 2011) and the relatively most potent inhibitor of parasite growth in both *P. falciparum* and *P. berghei*, was tested in fixed ratios with broad-spectrum DUB inhibitors; PR-619 and WP1130. Combinations at fixed ratios of 5:0, 4:1, 3:2, 1:4 and 0:5 were serially diluted and incubated with parasite cultures of the 3D7 line from which parasite growth and IC₅₀s were obtained. FIC₅₀s and Σ FIC₅₀s were calculated and isobologram interactions were plotted. A combination of b-AP15 and PR-619 is mostly additive with a mean Σ FIC₅₀ of 0.753 ± 0.23 , (Figure 5.1a). Meanwhile, b-AP15 and WP1130 seemingly trends towards synergy with a mean Σ FIC₅₀ of 0.653 ± 0.23 , (Figure 5.1b) even though the interaction remains overall additive. These data suggested that DUB inhibitors, as potential antimalarial drug candidates, can be used in combination to block parasite growth presumably by simultaneously targeting several different DUB enzymatic targets.

a



Drug Combination Ratio	Σ FIC ₅₀
b-AP15 100%	1
b-AP15 80% : PR-619 20%	0.623
b-AP15 60% : PR-619 40%	0.712
b-AP15 40% : PR-619 60%	0.731
b-AP15 20% : PR-619 80%	0.896
PR-619 100%	1

b

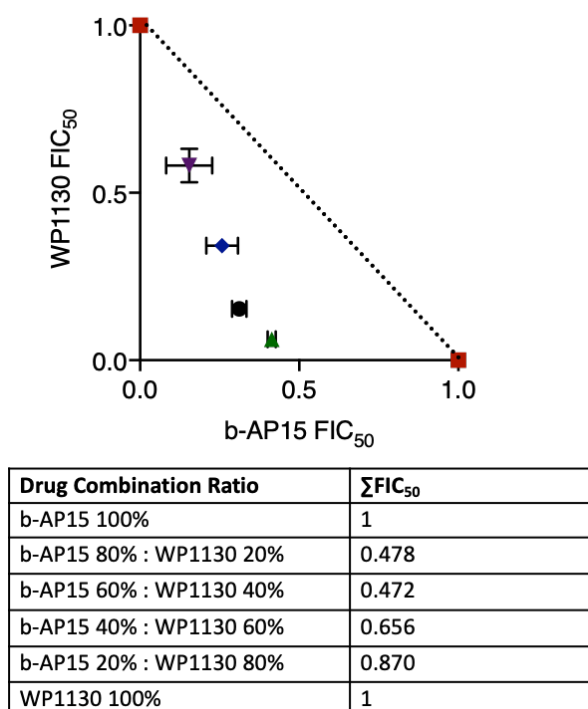


Figure 5.1: *In vitro* interaction of different classes of DUB inhibitors in malaria parasites.

Isobologram interaction plots and ΣFIC_{50} values of interactions between DUB inhibitors in the *P. falciparum* 3D7 line. **a.** Interaction between b-AP15 and WP1130 and their raw ΣFIC_{50} values. **b.** Interaction between b-AP15 and PR-619 and their raw ΣFIC_{50} values. ΣFIC_{50} values, plotted FIC_{50} s and error bars are means and standard deviations from three biological repeats.

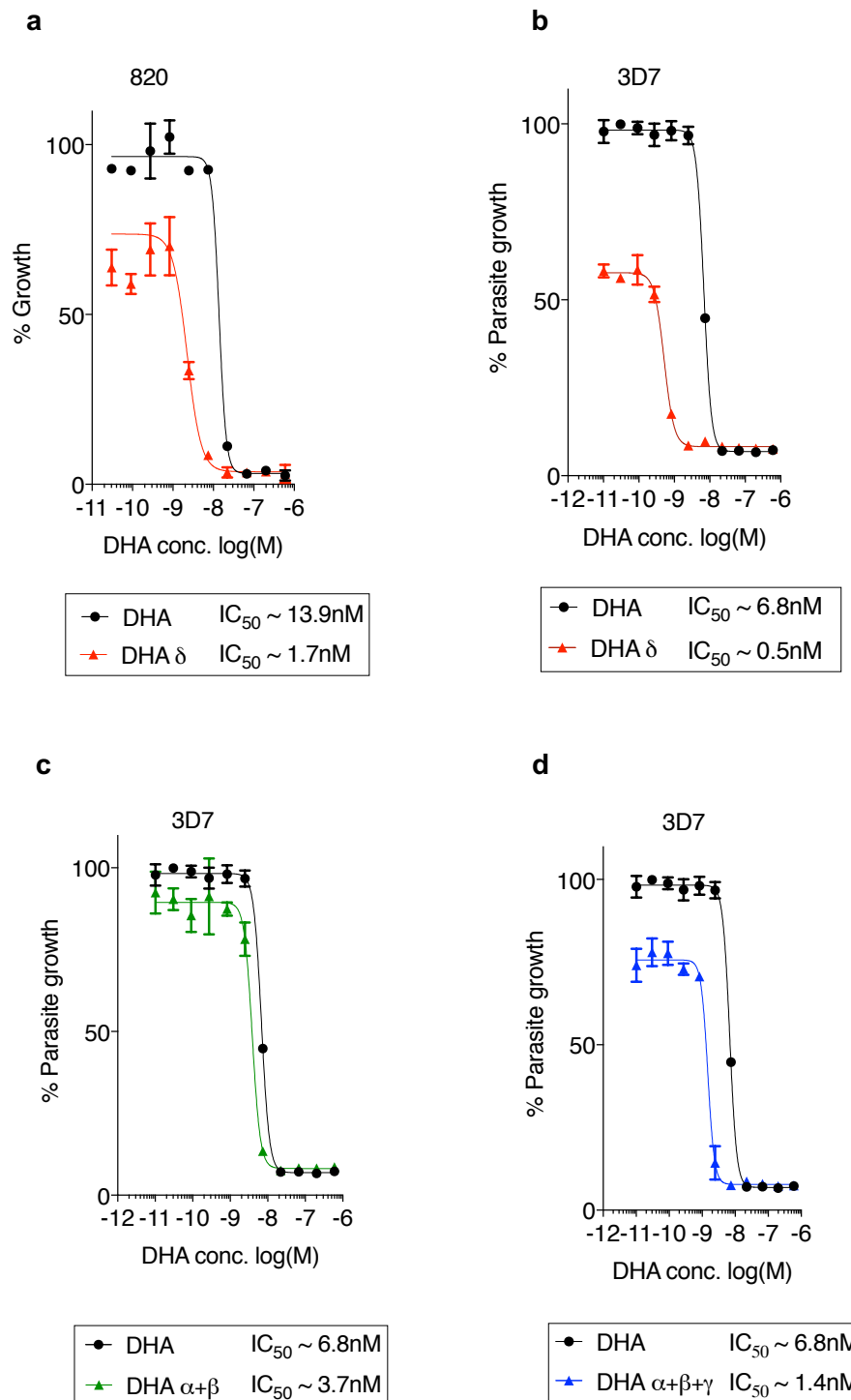
5.3.3 DUB inhibitors alone or in combination can potentiate DHA action in malaria parasites *in vitro*

In order to test the hypothesis that DUB inhibitors might have a similar effect of potentiating ART activity as 20s proteasome inhibitors, the effects of DUB inhibitors on the dose response profiles of DHA *in vitro* on wild type *P. berghei* and *P. falciparum* growth as well as their potential to synergize DHA action in fixed ratio interaction assays was investigated. The most potent DUB inhibitor b-AP15 at equivalent IC_{50} concentration improved DHA action with up to ~8-fold IC_{50} shift in wild type *P. berghei* growth inhibition (Figure 5.2a) and up to 15-fold enhancement in the wild type *P. falciparum* growth inhibition (Figure 5.2b). The differences in potentiation between *P. berghei* and *P. falciparum* could be due to the inherent reduced susceptibility of *P. berghei* to ARTs (Lee et al., 2018). The enhancement of DHA action by b-AP15 was also almost similar to previously

reported profiles with epoxomicin, a 20s proteasome inhibitor (Dogovski et al., 2015). In the meanwhile, it was demonstrated that experimental introduction of mutations in a DUB, UBP-1, mediates reduced susceptibility to ARTs in *P. berghei* (Chapter 3). UBP-1 has a close human orthologue, HAUSP/USP7, which is itself inhibited by P5091, a drug which in this *Plasmodium* screen was poorly potent with a relatively high micromolar IC₅₀ (Table 5.1). Nevertheless, b-AP15 (a USP-14 inhibitor) potentiated DHA action to the same extent as in wild type ART-sensitive *P. berghei* (9-11-fold) in two UBP-1 mutant lines that have reduced susceptibility to ART (V2721F) or both ART and CQ (V2752F) (Appendix Figure 8.13a, 8.13b). Therefore, ART (and potentially CQ) reduced susceptibility could be offset by a combinatorial drug administration approach involving DUB inhibitors through a targeted disruption of protein homeostasis most likely at the level of the UPS.

In an attempt to maximise DUB inhibitor combinations, which offered improved inhibition of parasite growth (Figure 5.1) as a strategy for simultaneously targeting several DUBs in the presence of DHA, the effect of combining b-AP15, PR-619 and WP1130 on the dose response profile of DHA was tested. WP1130 and PR-619 at IC₅₀ concentration mildly potentiated DHA action with 1.8- and 1.4-fold improvements respectively (Appendix Figure 8.14a, 8.14b). Meanwhile, a combination of b-AP15 and WP1130 at half IC₅₀ mildly potentiated DHA action (~2-fold, Figure 5.2c), while all three inhibitors (b-AP15, WP1130 and PR-619) at half IC₅₀ improved DHA action up to 5-fold in the ART sensitive *P. falciparum* (Figure 5.2d) and *P. berghei* (Figure 5.2e) as well as the ART resistant *P. falciparum* Kelch13 C580Y mutant lines (Figure 5.2f). Further isobologram interaction assays for DUB inhibitor ratio combinations were also carried out in an attempt to achieve improved *in vitro* killing (Table 5.1, Figure 5.1) in combination with DHA. Both b-AP15 and WP1130 were essentially additive when combined with DHA in isobologram interactions with $\Sigma\text{FIC}_{50}\text{s}$ of 0.967 and 1.013 respectively (Appendix Figure 8.14c, 8.14d). However, when b-AP15 and WP1130 were mixed at a 3:2 molar concentration ratio as a cocktail and combined with DHA, a slight improvement in efficacy was observed with an ΣFIC_{50} of ~0.868 (Figure 5.2g) compared with 0.972 at 1:4 b-AP15 WP1130 molar concentration ratios (Figure 5.2h) or 0.941 at 2:3 b-AP15 WP1130 molar concentration ratio (Figure 5.2i). These data would suggest that optimized ratios of (improved) DUB

inhibitor combinations or other proteasome inhibitors might yet achieve synergy with DHA, which would be a prerequisite to simultaneously targeting multiple DUBs or parallel enzymes in the UPS in future antimalarial combination therapies.



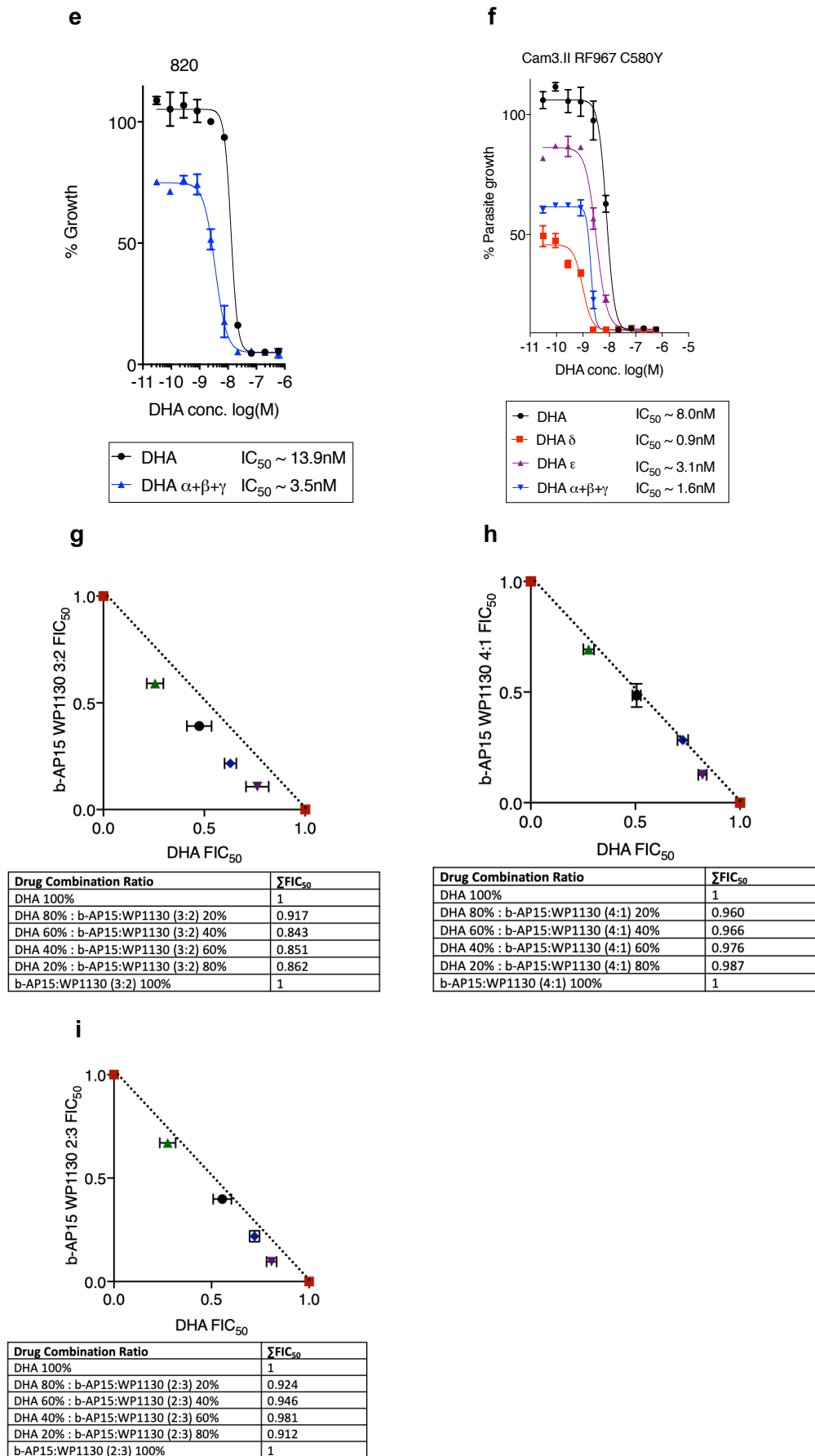


Figure 5.2: *In vitro* potentiation of DHA by DUB inhibitors.

a, b. Dose response profiles and IC_{50} values of DHA in the presence of b-AP15 at IC_{50} equivalent concentration (DHA δ) in the *P. berghei* 820 line (**a**) and 3D7 line (**b**). **c.** Dose

response profiles and IC_{50} values of DHA in the presence of WP1130 and PR-619 at their respective half IC_{50} s (DHA $\alpha+\beta$) in the 3D7 line. **d, e.** Dose response profiles and IC_{50} values of DHA in combination with b-AP15, WP1130 and PR-619 at half IC_{50} (DHA $\alpha+\beta+\gamma$) in the 3D7 (**d**) and 820 line (**e**). **f.** Dose response profiles and IC_{50} values of DHA combined with b-AP15 and WP1130 at IC_{50} (DHA δ , DHA ϵ) or b-AP15, WP1130 and PR-619 at half IC_{50} (DHA $\alpha+\beta+\gamma$) in ART resistant Kelch13 C580Y mutant line. Dose response curves were plotted in Graph pad prism 7. Error bars are standard deviations from 3 independent biological repeats. **g-i.** Isobologram plots of DHA in combination with b-AP15 and WP1130 at 3:2 (**g**), 1:4 (**h**) and 2:3 (**i**) ratios and their raw ΣFIC_{50} values. ΣFIC_{50} values, plotted FIC_{50} s and error bars are means and standard deviations from three biological repeats.

5.3.4 A combination of DUB and 20s proteasome inhibitor can synergize with DHA

An alternative approach to alleviating antimalarial resistance is combination therapies that target multiple points within known resistance mediating pathways and/or novel antimalarial drug pathways to prevent the emergence of or overcome resistance. Therefore, a combination of an upstream DUB inhibitor (b-AP15) and a 20s proteasome inhibitor (epoxomicin) with DHA in fixed ratio isobologram interactions was explored. Firstly, epoxomicin in combination with DHA as well as b-AP15 was tested in fixed ratios against *P. falciparum*. Epoxomicin improved DHA action mildly with an ΣFIC_{50} of 0.881 (Figure 5.3a) which corresponds with previously reported profiles (Dogovski et al., 2015). Interestingly, b-AP15 and epoxomicin as a combination alone were not an improved regimen with an ΣFIC_{50} of 1.162 (Figure 5.3b). This failure may result from a suppression mechanism where targeting the USP14 DUB upstream by b-AP15 (Figure 5.3d) would potentially counteract the activity of downstream 20s proteasome inhibitor and vice versa (Yeh et al., 2009). However, a 1:1 molar ratio of b-AP15 and epoxomicin when combined with DHA, an improved interaction with DHA (ΣFIC_{50} of 0.614) was achieved (Figure 5.3c) than by either of the drugs alone (Figure 5.3a, Appendix Figure 8.14c). This illustrates that targeting the UPS at several points with the optimized inhibitor concentrations can significantly improve DHA efficacy.

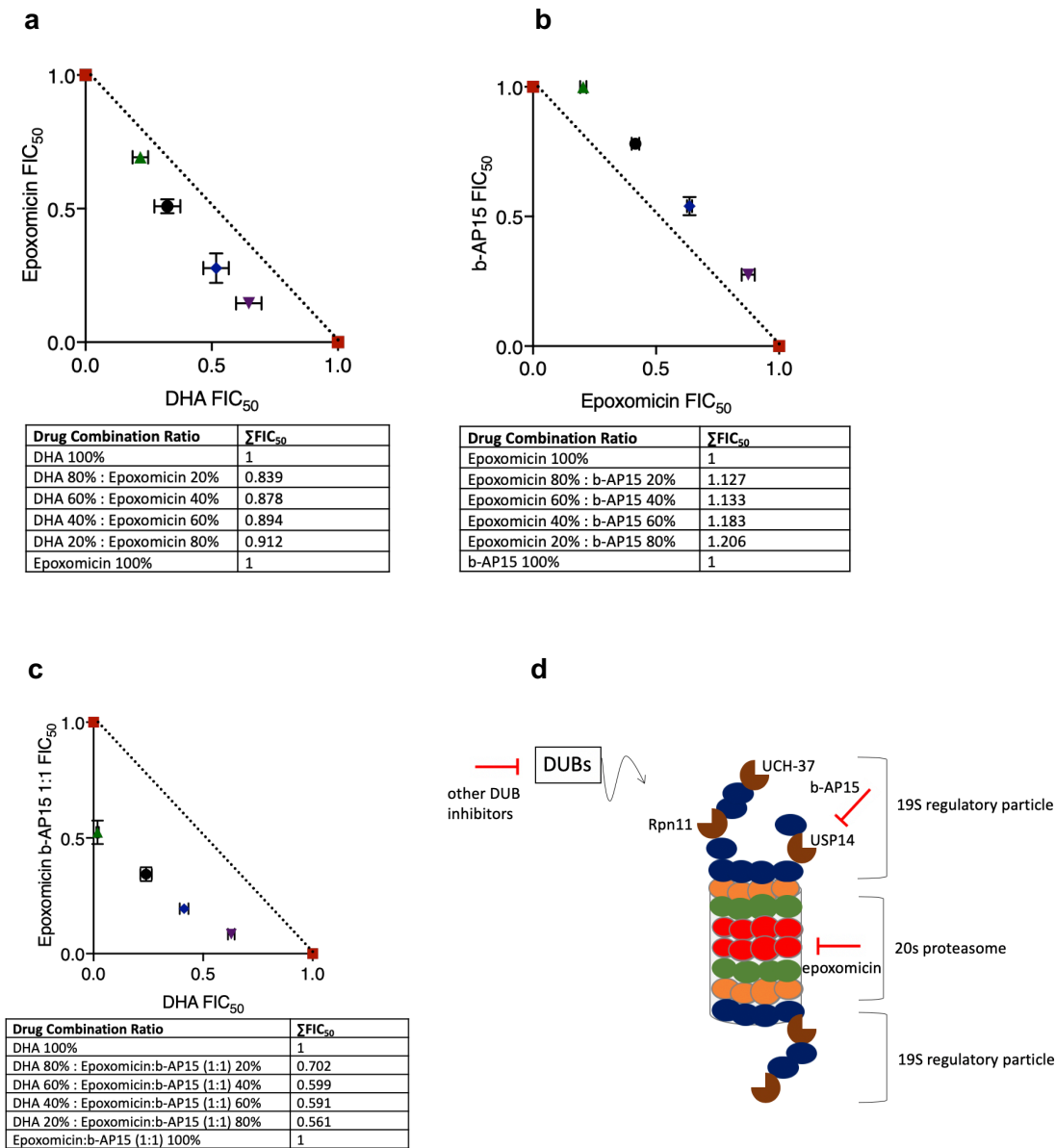


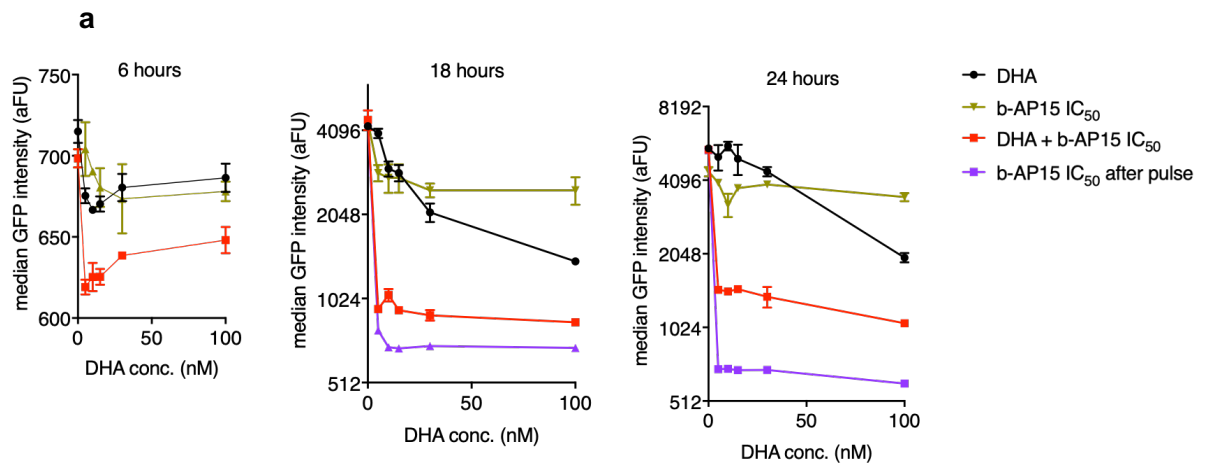
Figure 5.3: A combination of DUB and 20s proteasome inhibitor improves synergy with DHA.

a-c. Isobologram interaction between epoxomicin and DHA (**a**), b-AP15 and epoxomicin (**b**) and a mixture of b-AP15 and epoxomicin at 1:1 molar concentration ratio in combination with DHA (**c**). ΣFIC_{50} values, plotted FIC_{50} s and error bars are means and standard deviations from three biological repeats. **d.** Illustrated figure of the UPS indicating positional scope of USP14 and 20s units of the UPS and the inhibitor targets.

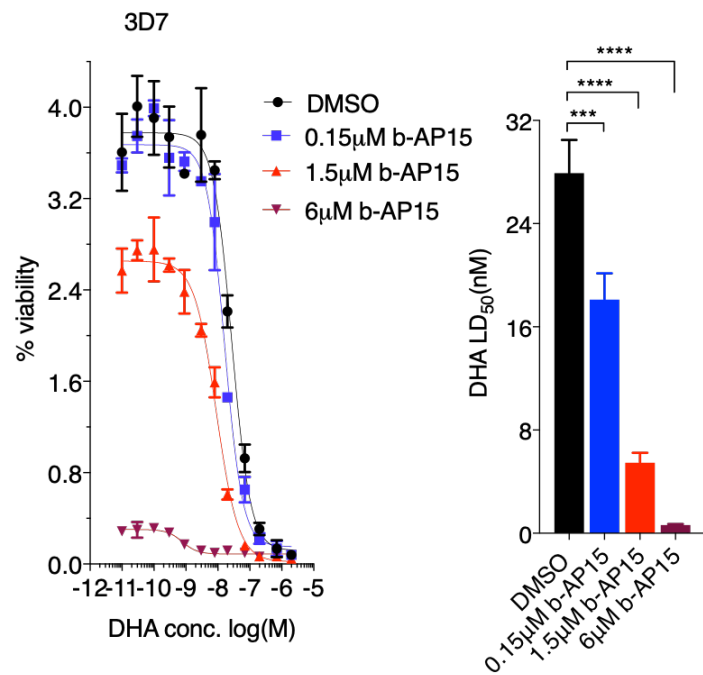
5.3.5 Pre-incubation of malaria parasites with UPS inhibitors efficiently mediates DHA potentiation

A further way to combat drug resistance in malaria, which is being explored with antibiotics (Tyers and Wright, 2019) and has been the case with cancer neo-adjuvant therapies, would be to pre-expose parasites to lethal or sub-lethal

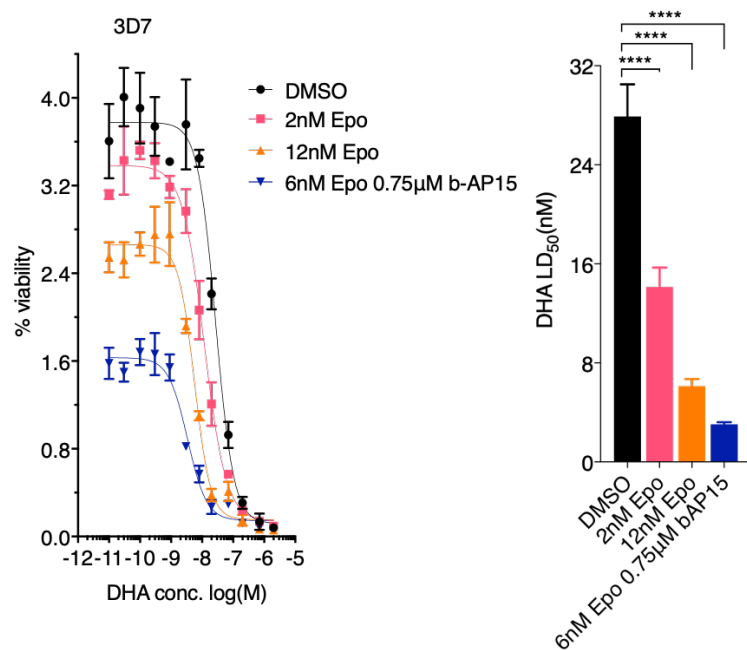
doses of inhibitors that target the resistance pathways before the main treatment course. A targeted inhibition of the resistance conferring pathways might then in turn improve the activity of any downstream main treatment drug. Therefore, the effect of pre-exposing malaria parasites to DUB or 20s proteasome inhibitors on the short time exposure dose response profiles to DHA in both *P. berghei* and *P. falciparum* was investigated. The *P. berghei* 507 line, which expresses GFP constitutively, was used to monitor GFP intensity across the life cycle after exposure to serial concentrations of DHA for 3 hours, administration of which followed prior exposure of the parasites (~1.5-hour old rings) for 3 hours to IC₅₀ concentrations of b-AP15. Quantification of the GFP fluorescent signal expressed from a constitutive promoter in *P. berghei* would permit investigation of the global dynamics of protein homeostasis, recycling, unfolding and or damage which occurs in the parasites upon exposure to DHA and or UPS inhibitors. Monitoring of GFP intensity at 6, 18 and 24 hours revealed that b-AP15 pre-exposure enhances the potency of DHA as indicated by significant abrogation of GFP intensity at all the time points (Figure 5.4a). Additional administration of b-AP15 after DHA incubation further abrogates GFP intensity illustrating that b-AP15 compromises UPS activity in tandem with DHA, which would make them suitable partner drugs. In the *P. falciparum* 3D7 line, pre-incubation of ~0-3 hour old rings with b-AP15 at IC₅₀ or half IC₅₀ for 3 hours followed by DHA treatment for 4 hours markedly impacts parasite viability (5 and 1.6 fold respectively) compared to DMSO exposed parasites, while pre-exposing the parasites to b-AP15 at 4x IC₅₀ is almost entirely lethal to the parasites (Figure 5.4b). Meanwhile, pre-exposure of the 3D7 or an ART resistant Kelch13 C580Y line to epoxomicin at IC₅₀ or 0.2x IC₅₀ followed by DHA also significantly impacted parasite viability (~4.6 and ~1.4 fold respectively) as compared to DMSO (Figure 5.4c, 5.4d). Remarkably, in both the 3D7 and ART resistant Kelch13 C580Y lines, a combination of b-AP15 and epoxomicin at half IC₅₀ achieves better potency with DHA (18 and 33-fold respectively) compared to either of the drugs alone at IC₅₀ (Figure 5.4b-d) further illustrating that targeting multiple UPS components (Figure 5.3c) could be a flexible approach to overcoming ART resistance.



b



c



d

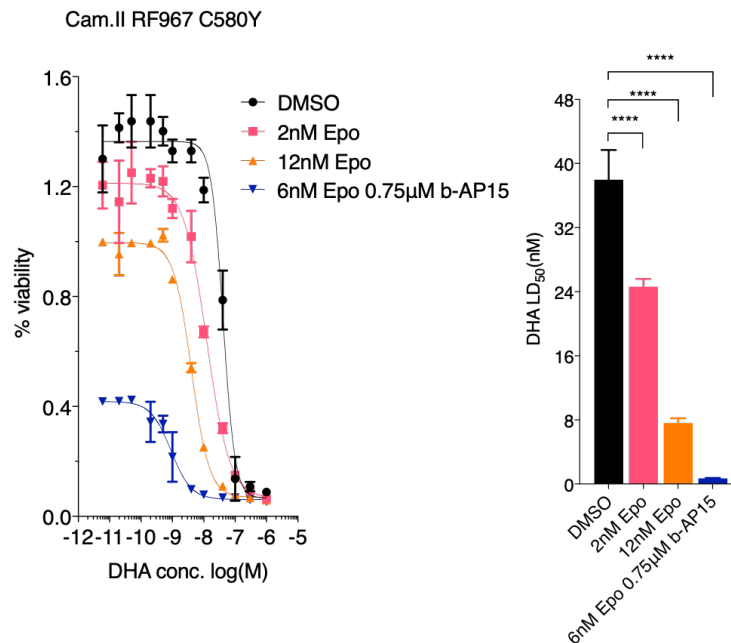


Figure 5.4: Pre-exposure of malaria parasites to UPS inhibitors alone or in combination enhances DHA action.

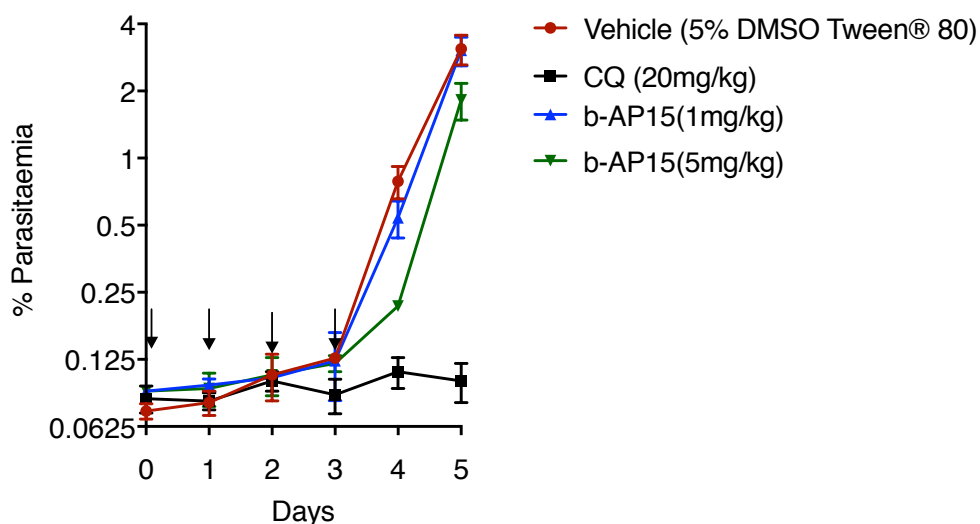
a. pre-treatment of the *P. berghei* 507 line (~1.5 hours old rings) with b-AP15 at IC₅₀ (1.5 μM) for 3 hours followed by a wash and then DHA for another 3 hours. Median GFP intensity was quantified by flow cytometry at 6 hours, 18 hours and 24 hours. b-AP15 at IC₅₀ was re-added after DHA wash off in one experimental condition (magenta plot) while b-AP15 alone was used as an additional control. Results are representative of three independent experiments. **b.** DHA dose response viability plots and lethal dose (LD₅₀) comparisons at 66 hours after pre-exposure of 0-3 hours old rings of the 3D7 line to DMSO (0.1%) or b-AP15 at half IC₅₀ (0.75 μM), IC₅₀ (1.5 μM) or 4x IC₅₀ (6 μM) followed by DHA for 4 hours. **c, d.** DHA dose response viability plots and LD₅₀ comparisons at 66 hours after pre-exposure of 0-3 hours old rings of the 3D7 line (**c**) and ART resistant Kelch13 C580Y line (**d**) to DMSO (0.1%) or epoxomicin at 0.2x IC₅₀ (2 nM), IC₅₀ (12 nM) or a combination of b-AP15 and epoxomicin at half IC₅₀ followed by DHA for 4 hours. Data from three independent experimental repeats. Significant differences between the conditions were calculated using one-way ANOVA alongside the Dunnett's multiple comparison test. Significance is indicated with asterisks; ****p < 0.0001.

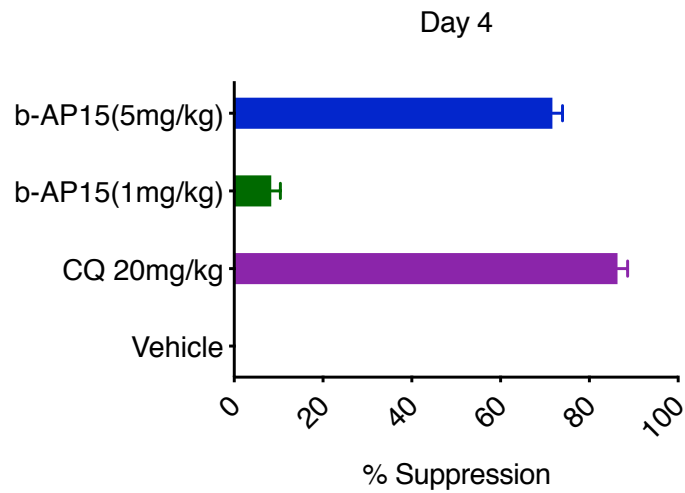
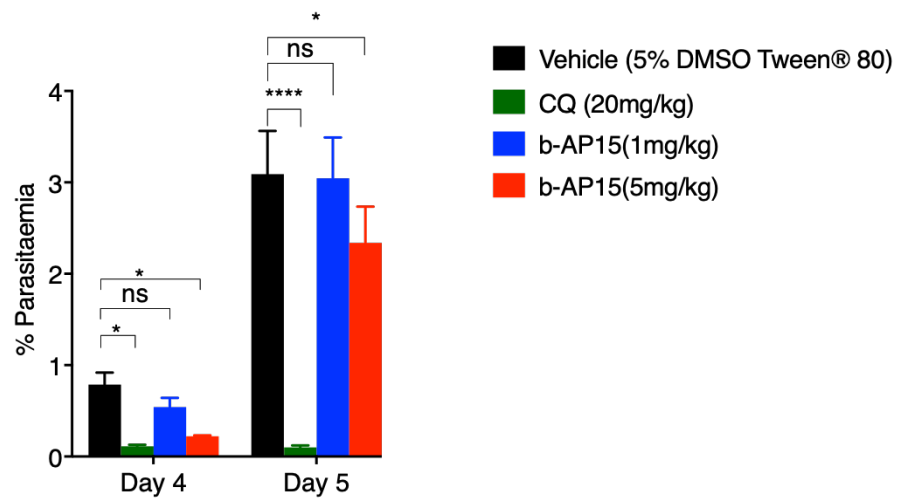
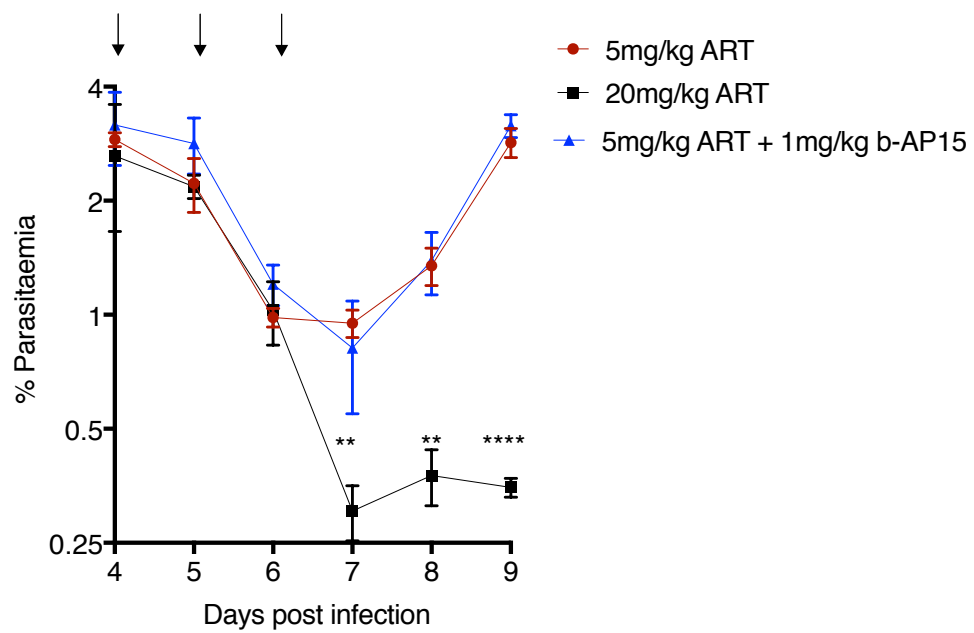
5.3.6 b-AP15 fails to block parasite growth but potentiates ART action *in vivo*

Following on to the *in vitro* experiments that demonstrated activity of DUB inhibitors in malaria parasites in above sections, the ability of b-AP15 (the most potent lead) to block parasite growth *in vivo* and its potential to enhance ART action was investigated. An analogue of b-AP15, VLX1570 entered clinical trials

for the treatment of multiple myeloma (Wang et al., 2016), despite being later terminated due to dose ascending toxicities (NCT02372240). b-AP15 showed strong antiproliferative effects in human cancer cell lines and displayed significant antitumor activity at 5 mg/kg in *in vivo* mouse models without any side effects (D'Arcy et al., 2011). However, in a Peters' 4 day suppressive test, b-AP15 failed to clear *P. berghei* parasites *in vivo* at both 1 mg/kg and 5 mg/kg with only minor reductions in parasite burdens on day 4 and 5 post treatment at the latter dose which corresponds to ~70% parasite suppression on day 4 (Figure 5.5a-c). Contrary to the previous reported safety profiles of b-AP15 (D'Arcy et al., 2011), mice (Theiler's Original) treated with 5 mg/kg b-AP15 started to develop toxicity signs as demonstrated by significant weight loss on day 4 and 5 post-treatment. Further treatments at 5 mg/kg or higher doses were thus not pursued. To investigate the ability of b-AP15 to potentiate ART action *in vivo*, b-AP15 was administered at 1 mg/kg (a safe dose that did not have any effect on parasite growth alone, Figure 5.5a) in combination with ART at 5 mg/kg and 10 mg/kg in established mice infections at a parasitaemia of 2-2.5% for three consecutive days. A combination of ART (5 mg/kg) and b-AP15 (1 mg/kg) did not have any significant parasite reduction as compared to ART (5 mg/kg) alone, while ART at 20mg/kg cleared the parasites after three consecutive doses as anticipated (Figure 5.5d). However, a combination of ART (10 mg/kg) and b-AP15 (1 mg/kg) significantly abrogated parasite burden as compared to ART (10 mg/kg) alone to the same extent as ART at 20 mg/kg (Figure 5.5e). These data further showed that b-AP15 can enhance ART action *in vivo*, to a similar extent as observed *in vitro*.

a



b**c****d**

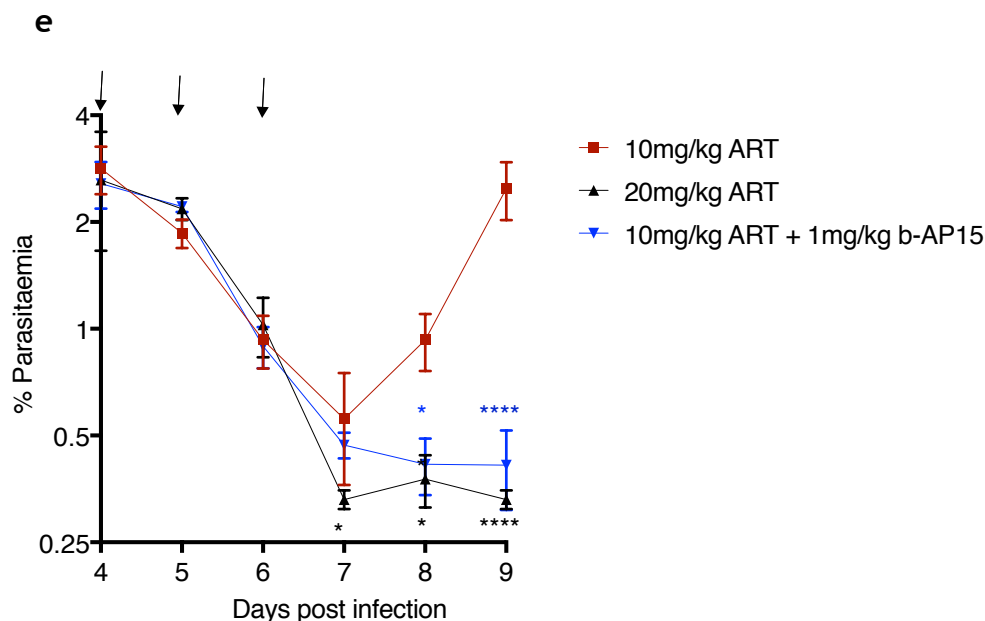


Figure 5.5: *In vivo* activity of b-AP15 alone and or in combination with ART.

a. Mice (4 groups of 3 mice each) were infected with $\sim 10^5$ parasites on day 1 and treated with indicated drug doses ~ 1 -hour post infection for four consecutive days (indicated by arrows). Parasitaemia was monitored daily by flow cytometry and analysis of Giemsa stained smears. **b, c.** Percentage suppressions on day 4 (**b**) and bar plots of parasitaemia's on day 4 and day 5 (**c**). **d, e.** Combination of ART and b-AP15 in established mouse infections. ART at 5 mg/kg (**d**) or 10 mg/kg (**e**) combined with b-AP15 (1 mg/kg) administered in established mice infections at a parasitaemia of 2-2.5% for three consecutive days (indicated by arrows). Parasitaemia was monitored daily. ART at 20 mg/kg was used as a curative control. Significant differences were calculated using one-way ANOVA alongside the Dunnet's multiple comparison test. Significance is indicated with asterisks; * $p < 0.05$, ** $p < 0.01$, *** $p < 0.001$, **** $p < 0.0001$.

5.4 Discussion

With the increasing incidence of resistance to (even combinations of) antimalarial drugs by *P. falciparum* and the lack of rapidly amenable drug discovery programs for related *Plasmodium* spp. such as *P. vivax*, pipelines to develop new antimalarial drugs to treat the disease as well as improve the activity of current antimalarials and tackle resistance are urgently needed. Work in this chapter reports the *in vitro* and *in vivo* activity of a class of compounds targeting the parasite upstream UPS components, DUBs, in *P. falciparum* and *P. berghei*. Antimalarial drugs are typically discovered for their activity against *P. falciparum* *in vitro*. Lead compounds from *P. falciparum* *in vitro* screens are evaluated for *in vivo* efficacy using rodent malaria parasites which have been for

a long time, crucial components of these drug discovery programs (Fidock et al., 2004). *P. berghei* is the most commonly used rodent model (in what is called the Peters' four-day suppressive test) and the development of methods that allow assessment of both *in vitro* drug sensitivity and *in vivo* efficacy in this model, (Janse and Waters, 1995) as is demonstrated in this work, permits easy comparisons with *P. falciparum in vitro* efficacy data. Moreover, this provides crucial *in vitro* bridging information on whether potential drug efficacy discrepancies between *P. falciparum in vitro* and *P. berghei in vivo* are due to pharmacokinetics of the drug or intrinsic differences in drug sensitivity between the *Plasmodium* spp. As a species of *Plasmodium* that is well diverged from both *P. falciparum* and other human-infectious *Plasmodium*, *P. berghei* drug efficacy assessment also offers a useful comparative for other non *P. falciparum* human causing *Plasmodium* spp. as chemical entities that display *P. falciparum* inhibitory activity *in vitro* and *P. berghei* inhibitory activity *in vitro* and *in vivo* are also likely to be active against other (human infectious) *Plasmodium* species.

5.4.1 DUB inhibitors inhibit malaria parasites IDC proliferation

Herein, activity is reported for six DUB inhibitors covering most of the DUB enzyme families and include b-AP15, P5091 and NSC632839 which specifically target USPs that all displayed antimalarial activity against both rodent and human malaria parasites *in vitro*. USPs are the largest family of DUBs comprising of up to 56 individual enzymes in humans (Davis and Simeonov, 2015). However, since less is known of USPs in malaria parasites, with their current assignments largely based on *in silico* predictions (Ponder and Bogyo, 2007, Ponts et al., 2011), the precise targets of these drugs remain largely obscure. Human USP14 has been demonstrated to be the target of b-AP15 (D'Arcy et al., 2011) and its *P. falciparum* orthologue PfUSP14 (PF3D7_0527200) has been recently characterised and shown to bind the parasite 20s proteasome (Wang et al., 2015b). Moreover, purified PfUSP14 cleaves di-ubiquitin bonds in intact polyubiquitin chains illustrating functional identity of this *Plasmodium* DUB with its human counterpart (Wang et al., 2015b). This provides evidence that PfUSP14 may be specifically essential in parasite proliferation during the asexual blood cycle which was supported by a whole genome piggyBac saturation mutagenesis screen in which PfUSP14 was shown to be refractory to deletion (Zhang et al.,

2018), Appendix Table 8.5). Data in this work also support these observations in both *P. falciparum* and *P. berghei* despite the *P. berghei* counterpart (PBANKA_1242000) appearing to be dispensable in a recombinase mediated genetic screen (Bushell et al., 2017). The differences in essentiality could be due to functional differences between the two *Plasmodium* spp. USP14s as they seem to share only ~62% sequence identity (Appendix Figure 8.15). The activity of b-AP15 in both *P. falciparum* and *P. berghei* however, at almost equivalent potencies, could thus be suggestive of possible suitable compensatory effects from other DUBs upon deletion in *P. berghei* which is not sufficiently compensated for when an inhibitor is used. b-AP15 may also target other DUB (or possess off target) activities in *Plasmodium* as the inhibition of purified PfUSP14 by b-AP15 is less potent than its overall parasite killing potency (Wang et al., 2015b). Nevertheless, the observed structural difference between human USP14 and PfUSP14 at the core catalytic domain, it's possible essentiality during the IDC and the activity of b-AP15 in both *P. falciparum* and *P. berghei* *in vitro* suggests that PfUSP14 can be selectively targeted throughout the *Plasmodium* genus (Wang et al., 2015b). Furthermore, the observed activity of other USP inhibitors, P5091 and NSC632839 in this study suggests that their targets are essential (Appendix Table 8.5) during the asexual proliferation stages of malaria parasites and can serve as useful chemical leads for more potent antimalarial drugs discovery. More importantly, b-AP15 possesses antiparasitic activity *in vivo* achieving up to 70% parasite suppression of *P. berghei* at the highest concentrations that have been tested in cancer models (D'Arcy et al., 2011). Malaria parasites have been shown to rapidly replenish proteasomes in the presence of sub-lethal doses of proteasome inhibitors (Li et al., 2012) which would possibly explain the observed inability of b-AP15 to completely block parasite growth at this concentration as compared to control antimalarial drugs. Whilst promising, some host toxicity profiles of b-AP15 at 5 mg/kg were noted as mice significantly lost weight after 4 consecutive doses despite reported safety records at similar doses in cancerous mouse models (D'Arcy et al., 2011). This effect could be due to the combination of a chemical inhibitor and parasite challenge making the mice more susceptible to toxic effects of b-AP15, a phenomenon which has been previously reported with carfilzomib, a 20s proteasome inhibitor (Li et al., 2012). Meanwhile, the *in vitro* activity of broad-spectrum DUB inhibitors, PR-619 and WP1130 as well as a zinc chelating

metalloprotease inhibitor (1, phenanthroline) further alludes to the promise of DUBs as drug targets in malaria parasites.

5.4.2 *Plasmodium* UCH-L3 could be an even more attractive drug target

A further striking finding was the inactivity of TCID (a UCH-L3 inhibitor) in both rodent and human malaria parasites. PfUCH-L3 has been well characterised in malaria parasites and has been shown to retain core deubiquitinating activity (Frickel et al., 2007). Moreover, disruption of PfUCH-L3 by experimentally replacing the native enzyme with a catalytically dead form was shown to be lethal to the parasite (Artavanis-Tsakonas et al., 2010). The inactivity of TCID in both rodent and human malaria parasites reported here is therefore suggestive of striking differences between mammalian and *Plasmodium* UCH-L3s. Sequence analysis demonstrated that PfUCH-L3 shares ~33% sequence identity with human UCH-L3 consistent with previous structural and molecular docking comparisons of PfUCH-L3 and human UCH-L3 which also revealed significant differences between the enzymes especially at the ubiquitin binding groove (Artavanis-Tsakonas et al., 2010). This makes PfUCH-L3 an even more attractive drug target for ultra-selectivity as it is also known to possess denedylating activities which are absent in mammalian UCH-L3s (Frickel et al., 2007).

5.4.3 DUBs can be targeted to overcome ART resistance

Targeting the *Plasmodium* UPS is an emerging interventional point, not just as a potential drug target, but now also to curb emerging ART resistance. 20s proteasome inhibitors have been shown to enhance ART action in both ART sensitive and resistant lines (Li et al., 2016, Dogovski et al., 2015). Data in this work also show that upstream targeting of the UPS by some but by no means all DUB inhibitors can potentiate and enhance ART action in certain cases to a similar extent as 20s proteasome inhibitors. ARTs act by targeting several (possibly random) parasite proteins upon activation (Ismail et al., 2016, Wang et al., 2015a) which necessitates, among other things, an upregulated UPS mediated stress response which rapidly recycles and clears damaged proteins henceforth promoting survival in ART resistant parasites (Tilley et al., 2016, Bridgford et al., 2018, Dogovski et al., 2015). As with 20s proteasome inhibitors, (Li et al., 2016, Dogovski et al., 2015) inhibition of parasite UPS by targeting single or multiple DUBs simultaneously potentiates ART or DHA action. Inhibition

of parasite UPS by b-AP15, for example, would prevent the normal protein homeostasis flux through the UPS, boosting the activity of pleiotropic ARTs by blocking the parasite stress and recovery system. Indeed, despite DHA being only additive in isobole analyses with b-AP15, sublethal concentrations of b-AP15 can boost DHA activity up to 15-fold. This boost is further enhanced when 2-3 DUB inhibitors at sub-lethal concentrations are combined as they improve DHA activity more than either inhibitors alone. This suggests that carefully titrated use of current DUB inhibitors in isolation, or simultaneously in mixtures may be a means to overcome ART resistance and the rodent model deployed here could be useful tool to optimise such drug combinations. Indeed, recent findings have shown that accumulation of polyubiquitinated proteins in malaria parasites either by DUB or 20s proteasome inhibition is critical in activating the stress responses and contributes to DHA lethality in malaria parasites (Bridgford et al., 2018). The observed increase in ART efficacy when combined with DUB inhibitors which is of a similar level to that achieved by inhibition of the proteasome by epoxomicin *in vitro* and Carfilzomib *in vivo* (Dogovski et al., 2015) further alludes to the potential of DUB inhibitors for achieving similar attributes in malaria parasites.

Whilst useful as independent potential antimalarial agents, DUB inhibitors show potential for partnership and this study demonstrated that different classes of DUBs can be targeted simultaneously to achieve better parasite killing while potentially minimising the resistance emergence window. More importantly, low and safe doses of b-AP15 with no effect on parasite growth alone significantly potentiated sub-curative dose of ART to almost curative levels *in vivo* providing a proof of concept that DUB inhibitors can enhance the activity of ARTs both *in vitro* and *in vivo* making them potential adjunct drugs to enhance ART action and tackle resistance. Similarly, other potential radical ways of overcoming resistance in malaria parasites would be combining drugs with different MOAs in complex combinations or using multiple (different) first line combinational therapies at once to raise the probability barrier of developing resistance by simultaneously targeting several pathways (Boni et al., 2016). Data in this work exemplify these concepts, as for example when b-AP15 and epoxomicin are combined in a fixed ratio isobole analysis, there appears to be no interaction or possibly even an antagonistic effect. This observation would be symptomatic of

an antagonistic suppression mechanism where the activity of two inhibitors in the same pathway upstream or downstream negatively feeds back to the activity of the other leading to counteractive effects. However, when b-AP15 and epoxomicin are mixed in equal concentration ratios and combined with DHA, their overall activity achieves a better efficacy with DHA than either of the inhibitors alone. The optimal simultaneous exposure of the parasite UPS to DUBs and 20s proteasome inhibitors could thus act as an additional opportunity to overcome resistance to ARTs if the parasites would acquire resistance mutations to either of the UPS inhibitors. This has indeed been recently illustrated where combined inhibition of the parasite $\beta 2$ and $\beta 5$ subunits of the parasites 20s proteasome was shown to strongly synergize DHA activity (Kirkman et al., 2018).

5.4.4 Conclusion

In conclusion, work in this chapter confirm DUBs as potential druggable candidates in malaria parasites. Drug discovery programs take a long time, with for example a minimum of five years required to take a lead compound to a clinical candidate in malaria (Lotharius et al., 2014, Wells et al., 2015). The emergent resistance to ACTs, a paucity in the number of antimalarial drugs in the developmental pipeline and a lack of scalable pipelines for drug discovery in other human malaria parasites such as *P. vivax* and *P. ovale* (Wells et al., 2015), all necessitates both radical as well as alternative approaches to identify new drugs and drug targets. As DUBs are already being actively explored as anticancer agents with candidate inhibitors already entering clinical trials (Harrigan et al., 2017), antimalarial drug discovery programs could take advantage to structurally improve or re-purpose such entities not just as potential drug targets in malaria, but also as combinational partners to ARTs to overcome the spectre of resistance.

6 A metabolic profile of fast acting antimalarial drugs and drug candidates

6.1 Chapter aim

Development of replacement antimalarial drugs is urgently needed for rapid deployment in case ARTs or even ACTs completely fail. Some of these lead antimalarial drug candidates are being developed by the NITD and are, indeed, in advanced clinical trials (section 1.5.6). Even though selection for resistance and forward genetic screens have been used to identify the potential MOA and MOR for some of these leads, a full mechanistic overview on how they exert their antimalarial activity is still unknown, disputed or uncharacterised. This chapter was, therefore, aimed at using LC-MS untargeted metabolomics to decipher the MOA of some of these lead compounds. By characterising the MOA and or biochemical features that arise when parasites are exposed to these compounds, the MOR can be identified or anticipated for with appropriate interventions put in place even before the drugs are clinically deployed.

6.2 Introduction

ARTs in ACTs, are and have been the backbone of malaria control strategies for the last decade (Hemingway et al., 2016b, WHO, 2018c, WHO, 2019). However, despite high ACT efficacy rates in Sub-Saharan Africa, resistance to ARTs (and now to some ACTs) which has emerged in SEA (Hamilton et al., 2019, van der Pluijm et al., 2019, Ashley et al., 2014, Dondorp et al., 2009) is seriously threatening the utility of this class of compounds which have significantly contributed to recent reductions in malaria cases (WHO, 2019). Pipelines to identify new drugs to combat the emerging resistance or for effective combination therapies are thus urgently needed.

Over the past ten years, thousands of chemical entities that block malaria parasite growth have been reported from pharmaceutical companies and public funded product development partnerships (Guiguemde et al., 2010, Van Voorhis et al., 2016, Gamo et al., 2010). These libraries are serving as appropriate starting points for antimalarial drug discovery which could serve as potential replacements and/or suitable combination partners with current drugs to combat and overcome resistance. However, as is the case with a majority of antimalarial drugs (antiprotozoal drugs at large), the MOA of these leads is unknown (Muller and Hyde, 2010, Creek and Barrett, 2014). Characterising the

MOA of lead drug candidates, or drugs which are already in clinical use, though not critically essential during drug development, is important as it provides a platform to understand or predict resistance mechanisms as well as identify suitable combination drug partners using MOA informed strategies. MOA characterisation also helps in identifying the actual drug targets which can be exploited in structure-based design of better drugs or improvement of the existing drugs. MOA elucidation in malaria parasites has primarily involved forward genetics approaches, which involve *in vitro* selection for resistance followed by whole genome sequencing, transcriptome and or proteome analysis (Section 1.6). However, due to numerous limitations of these approaches (Section 1.6.1), a complimentary approach that utilises several independent platforms is required.

Metabolomics platforms have recently provided an alternative approach to elucidating the MOA of both known drugs and lead drug candidates in bacterial pathogens (Vincent et al., 2016, Zampieri et al., 2018) and malaria parasites (Allman et al., 2016, Cobbold et al., 2016, Creek et al., 2016) as many antimicrobial agents target metabolic enzymes and pathways. This has been made possible because metabolomics platforms can detect perturbations induced by drug treatment under controlled *in vitro* exposure conditions (Creek and Barrett, 2014, Vincent et al., 2016, Kwon et al., 2008). In malaria parasites, these approaches have been successfully adapted for characterisation of the MOA of several known and candidate antimalarial drugs (Section 1.6.5).

In this work, an untargeted metabolomics approach was used to screen novel fast acting drug candidates of the ITD class that are emerging from the NITD drug discovery pipelines. The metabolic profile of ITDs, which display an even faster parasite killing rate as compared to DHA, was compared to other drug candidates from the NITDs pipeline; spiroindolones which are known to target the *P. falciparum* Na⁺ H⁺ ATPase (PfATP4) (Rottmann et al., 2010) and KAF156 whose MOA is still unknown (LaMonte et al., 2016, Lim et al., 2016) even though more recent evidence suggests inhibition of the parasite's protein trafficking as the possible MOA (LaMonte et al., 2020). Using a fixed time point exposure as well as a dynamic time course over the early 2 hours of drug exposure, a metabolic profile of fast acting antimalarial drugs and drug candidates is

provided, which despite some differences appear to be fundamentally similar. Validating these metabolic profiles using atovaquone which has a well characterised metabolic fingerprint (Allman et al., 2016, Cobbold et al., 2016), it is here demonstrated that fast acting compounds display a common metabolic profile, which may highlight a commonality in the MOA or a common parasite response to rapidly induced death.

6.3 Results and discussion

6.3.1 ITDs display a fast killing rate relative to DHA and Spiroindolones

Parasite killing rates allow for identification of fast acting compounds which are required for malaria control as they allow for rapid clearance of parasitaemia in patients which in turn minimises parasite drug exposure time and narrows the window for the parasites to develop resistance. *In vitro* assays to predict the parasite killing rates of antimalarial compounds are based on parasite reduction ratios (PRR), quantified over 28 days by fresh exposure of defined parasite inoculum every 24 hours in series of limiting dilutions (Sanz et al., 2012). Even though the PRR method allows for determination of parasite clearance times as well as drug lag phases (the time required for compounds to achieve maximum killing effect), the extent to which parasite metabolic and biochemical fingerprints change, especially for potential pleiotropic fast acting compounds, cannot accurately be predicted. The killing kinetics of ITDs, KAE609a, DHA, KAF156a and atovaquone (Table 6.1) were thus determined by biochemically monitoring luciferase expression using a *P. falciparum* 3D7 luc line which constitutively express a dual NanoLuc and luciferase reporter. Synchronised trophozoites at 2% parasitaemia and 2% haematocrit were cultured with the compounds at 10x IC₅₀ (Table 6.1) or DMSO (0.1%) after which the relative luminescence signal (RLU) was monitored over the course of 6 hours. DHA (1µM), which is a known fast acting compound, depleted the luciferase signal after 2.5 hours of incubation (Figure 6.1a). Spiroindolone analogue (KAE609a) also depleted the signal at 2.5 hours but at a faster rate than DHA (Figure 6.1a). This is in agreement with previous observations that spiroindolones exert a faster MOA and parasite clearance than ARTs in patients (White et al., 2014). Meanwhile, both ITD1a and ITD2a at 10x IC₅₀ displayed an even faster killing rate, depleting the luciferase signal after 2 hours of drug incubation. On the

contrary, KAF156a and atovaquone which are known to act slowly did not have any effect on the luciferase signal over the course of 6 hours, displaying an almost identical response to the DMSO control (Figure 6.1a). Microscopic analysis of parasite morphologies during the time points did not show any significant differences relative to the DMSO control (Figure 6.1b). Based on these data, the 2.5 hour time point was chosen for initial metabolomics drug incubation as it was the time which corresponded with maximal biochemical signal disruption (based on luciferase expression) for the fast acting compounds (Figure 6.1a) and was also previously shown to yield good metabolic signals even for slow acting compounds such as atovaquone (Allman et al., 2016).

Abbreviation	Name	IC ₅₀ (nM)
ATQ	Atovaquone	1.05±0.03
ITD1a	ITD1a	31.25±0.83
ITD2a	ITD2a	24.15±2.06
KAE609a	KAE609 analog	0.72±0.04
KAE609ia	KAE609 inactive analog	143.55±7.75
KAF156a	KAF156 analog	27.14±0.61
ITD1ia	Inactive analog of ITD1a	>1000
ITD2ia	Inactive analog of ITD2a	>1000
DHA	Dihydroartemisinin	6.23±0.34

Table 6.1: *In vitro* growth inhibition of the *P. falciparum* 3D7 line for the compounds used in the metabolomics screen.

IC₅₀ values are means and standard deviations from three biological repeats.

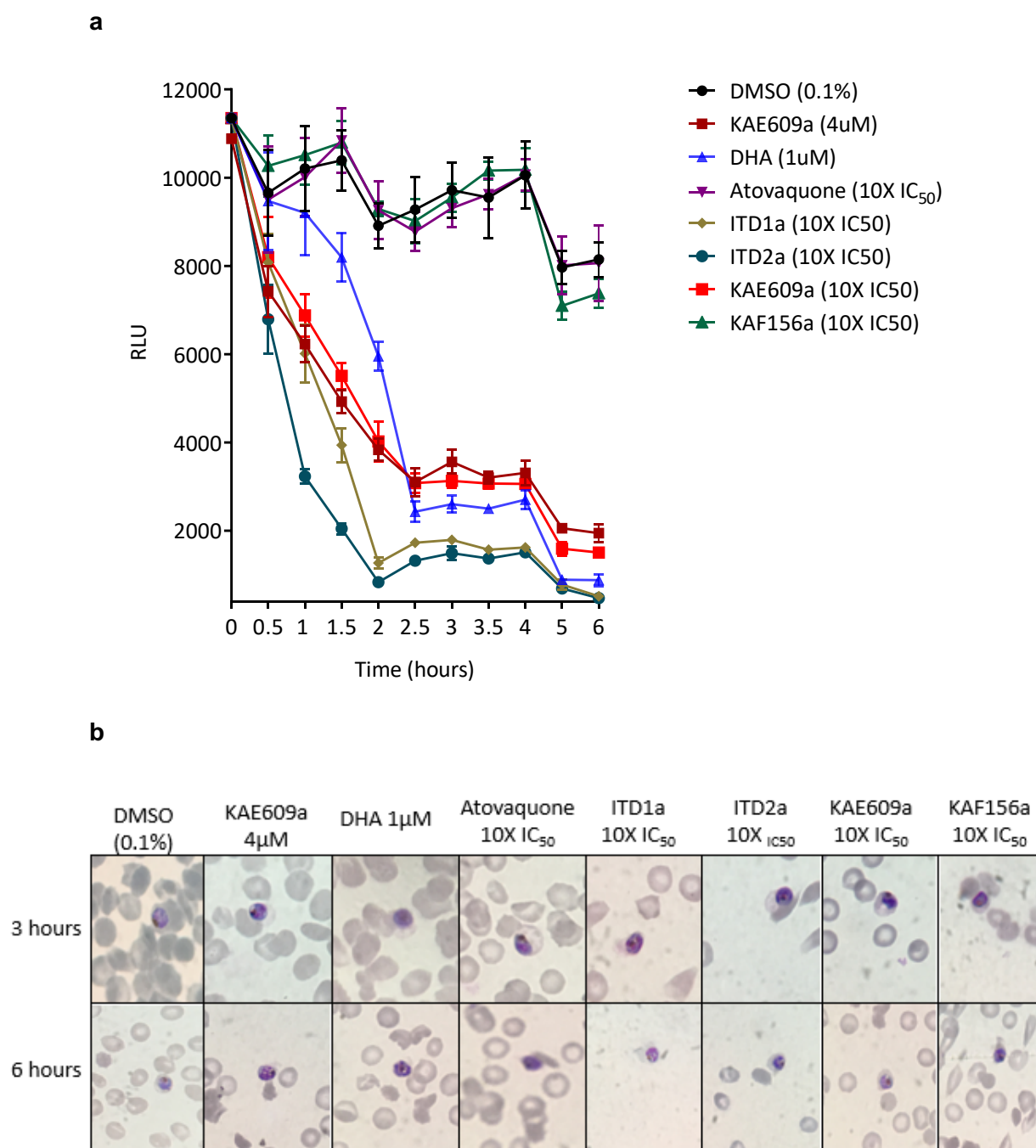


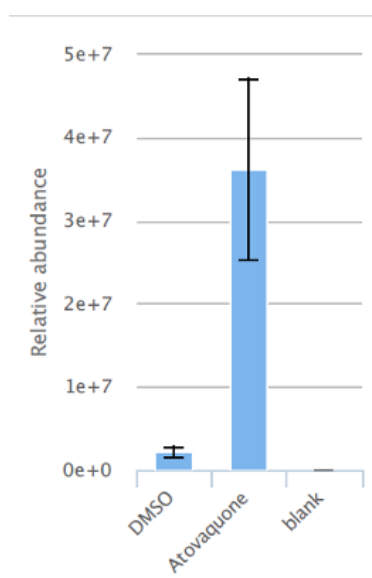
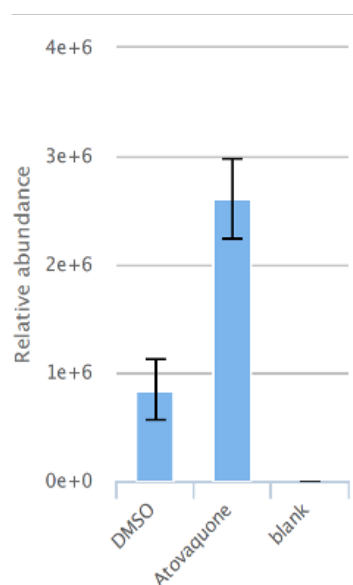
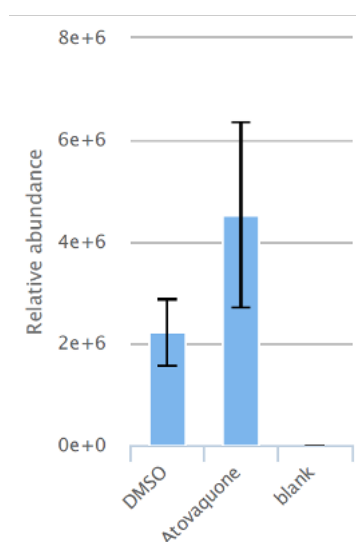
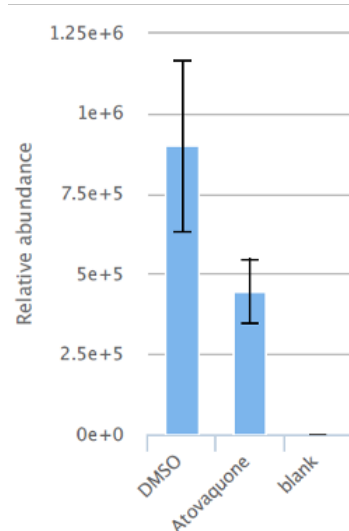
Figure 6.1: Killing kinetics of KAE609a, DHA, Atovaquone, ITD1a, ITD2a and KAF156a in the 3D7 luc line.

~30-hour old trophozoites at 2% haematocrit and 2% parasitaemia were incubated with the compounds at the indicated concentrations for the indicated times. Luciferase expression was quantified at each time point. **a.** plot of relative luminescence unit (RLU) over the 6-hour incubation periods for the compounds. Incubations were carried out in quadruplicate over 2 independent biological repeats. **b.** Microscopy analysis of Giemsa stained smears at the 3- and 6-hour incubation periods for all the compounds.

6.3.2 Atovaquone disrupts pyrimidine biosynthesis pathway in malaria parasites

Atovaquone targets the mitochondrial electron transport chain bc1 complex that plays a crucial role in oxidative phosphorylation in most organisms (Srivastava et al., 1999). However, malaria parasites do not require oxidative phosphorylation and have maintained an active mitochondrial electron transport chain for the sole purpose of recycling ubiquinone, which acts as an electron acceptor for dihydroorotate dehydrogenase (DHODH), a critical enzyme in the pyrimidine biosynthesis pathway (Painter et al., 2007). Treatment of malaria parasites with atovaquone, therefore, leads to a rapid accumulation of pyrimidine intermediates upstream of DHODH with a corresponding drop in downstream metabolites (Cobbold et al., 2016, Allman et al., 2016). Indeed when purified trophozoites were incubated with atovaquone at 10x IC₅₀ for 2.5 hours, a rapid accumulation of N-carbamoyl L-aspartate and dihydroorotate was observed while the level of downstream pyrimidine metabolites; uridine diphosphate (UDP) and uridine triphosphate (UTP) declined (Figure 6.2a, 6.2b) which is in agreement with previously reported profiles (Allman et al., 2016, Cobbold et al., 2016). A steady maintenance of orotate pools was also observed (Figure 6.2a iii) despite DHODH inhibition with atovaquone, as previously observed (Cobbold et al., 2016), the mechanisms of which are basically unknown. Atovaquone treatment also disrupted the citric acid cycle (TCA) leading to a decrease in cellular levels of citrate (Figure 6.2c). The electron transport chain and TCA cycles are sequentially linked as the TCA plays a role in maintaining a steady supply of ubiquinone which is a critical component of the electron transport chain and is a required co-factor for DHODH activity in the pyrimidine biosynthesis pathway. Enzymes of the TCA cycle, specifically succinate dehydrogenase (SDH) and malate dehydrogenase (MDH) reduce ubiquinol to ubiquinone which in turn acts as an electron acceptor for DHODH. Treatment of malaria parasites with atovaquone, therefore, blocks the bc-1 complex of the electron transport chain, preventing the recycling of ubiquinol to ubiquinone which in effect inactivates all ubiquinone requiring enzymes such as SDH, MDH and DHODH. Indeed, isotope glucose labelling studies have shown a significant decrease in flux through the TCA cycle upon atovaquone treatment (Ke et al., 2015). Moreover, previous atovaquone metabolomics profiles also revealed disruption in the TCA cycle as an accumulation of fumarate was observed, consistent with interference of SDH

or MDH, as a consequence of bc-1 complex inhibition (Cobbold et al., 2016). Even though an accumulation of fumarate in this metabolomics screen was not observed (Figure 6.2c), this could be due to relatively shorter drug exposure time. A steady decrease in the TCA cycle metabolites which was comprehensively profiled upon stable isotope labelling (Cobbold et al., 2016) is, however, mirrored by the observed decrease in levels of citrate in this work. Taken together, these results validated the metabolomics approach for MOA elucidation of selected NITD drug candidates (Table 6.1).

a**i****carbamoyl aspartate****ii****dihydroorotate****iii****orotate****iv****UTP**

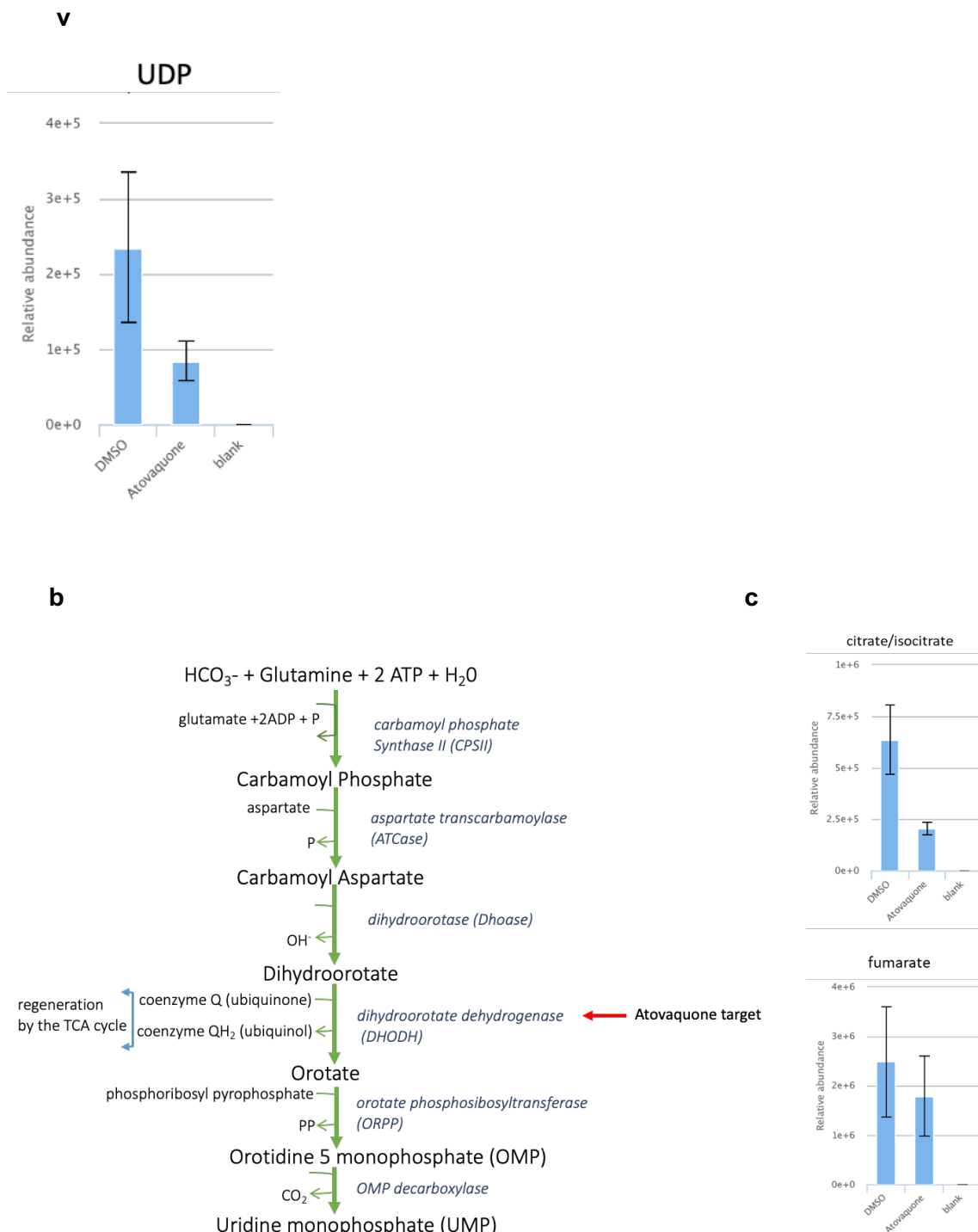


Figure 6.2: Metabolomics profile of atovaquone.

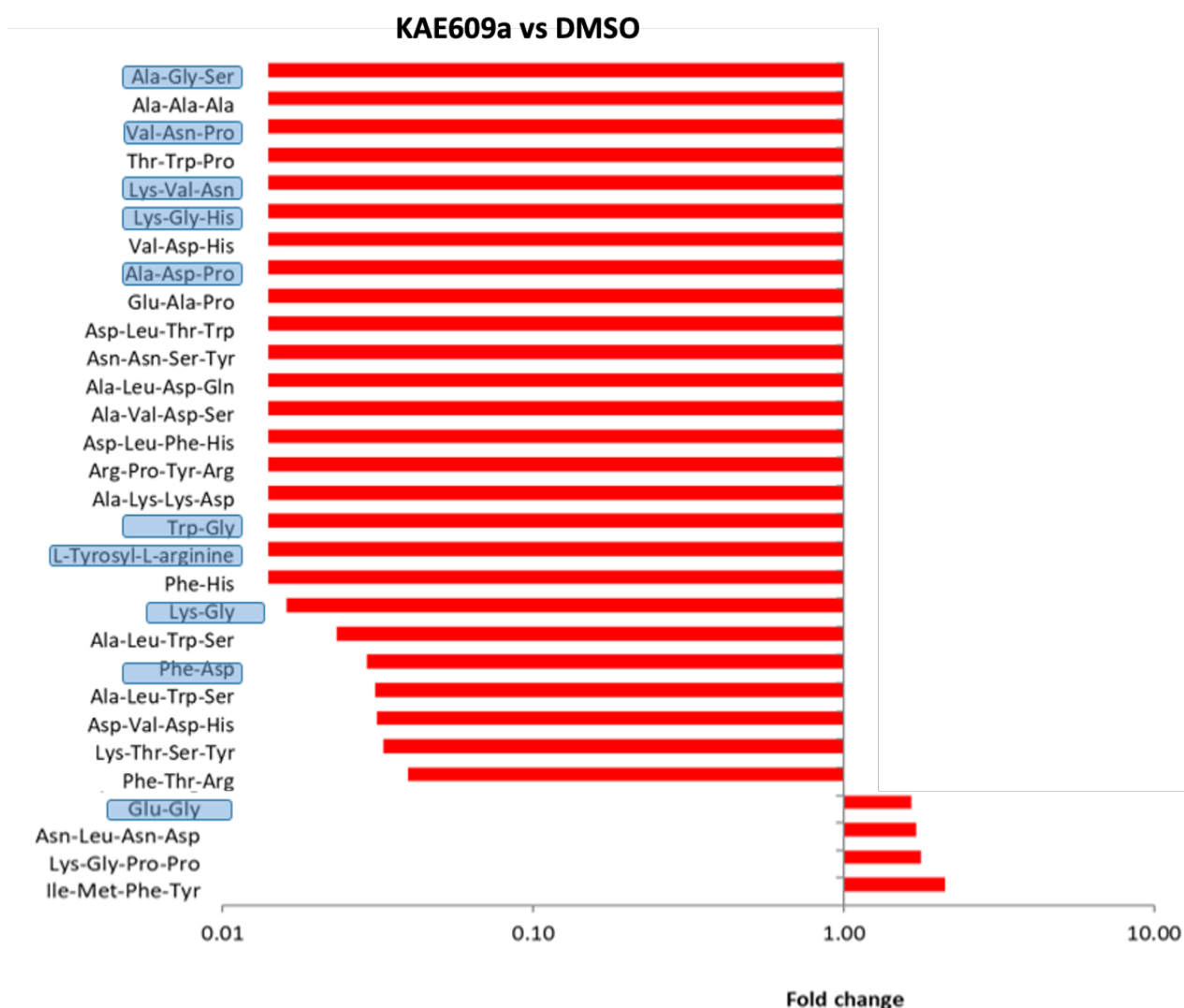
~1 x 10⁸ purified trophozoites were exposed to either DMSO or atovaquone at 10x IC₅₀ for 2.5 hours. Untargeted metabolomics on an LC-MS platform was carried out on extracted metabolites. **a.** Relative abundance of the indicated pyrimidine metabolites in DMSO vs atovaquone treatments. **b.** Schematic of the pyrimidine pathway indicating atovaquone target point. **c.** Relative abundance of citrate and fumarate, metabolites of the TCA cycle, in DMSO vs atovaquone treatments. Relative abundance measurements are comparisons of total ion counts of the metabolites in the treatment conditions. Treatments were carried out in triplicates over 2 independent biological repeats. mzXML mass spectrometry files and graphs were processed and plotted in PiMP.

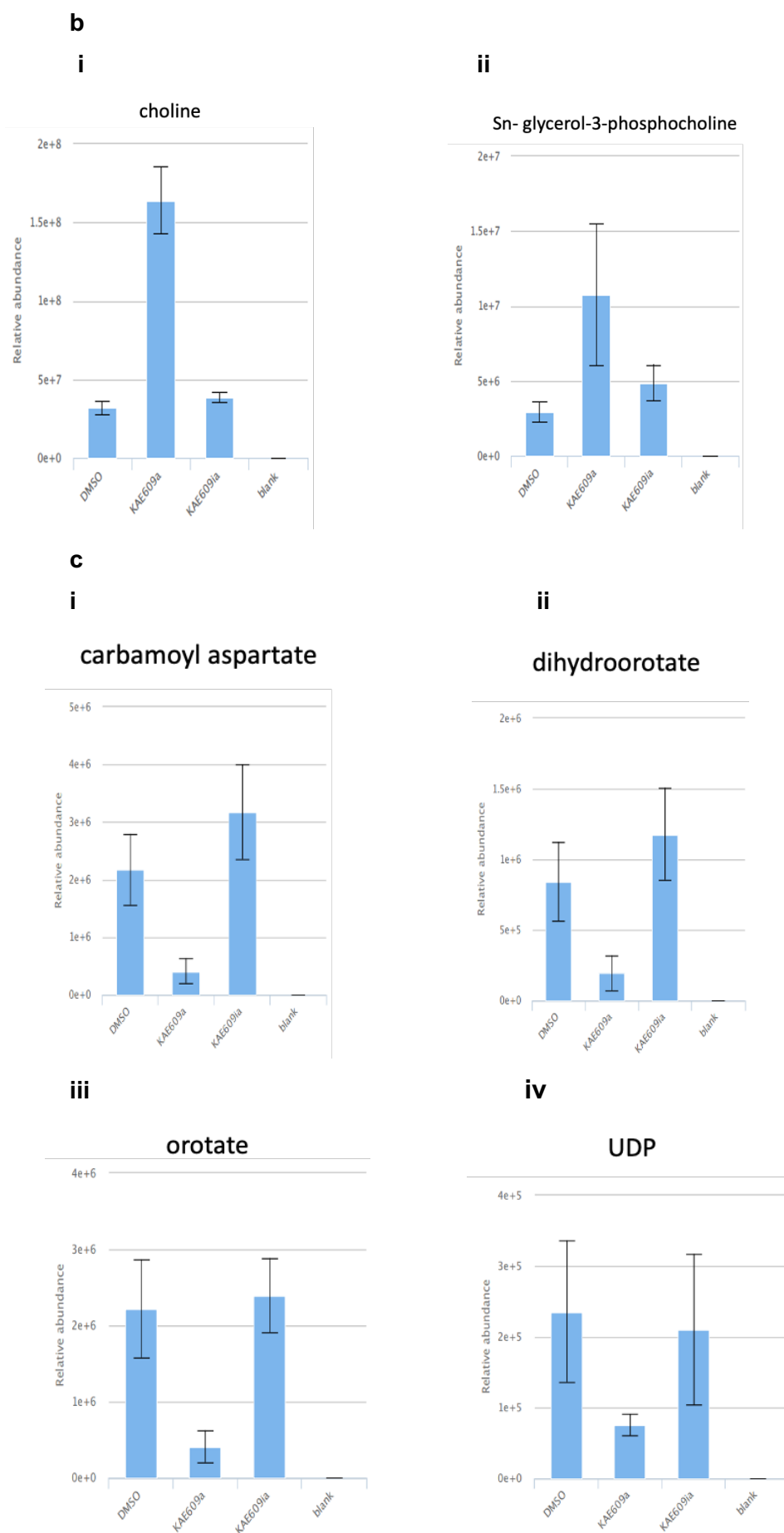
6.3.3 KAE609a elicits a pleiotropic metabolic response in malaria parasites

KAE609a, a spiroindolone analog of KAE609, is one of the fast-acting compounds developed by NITD and has shown promising results in clinical trials (White et al., 2014). Using forward genetic screens after *in vitro* selection for resistance, spiroindolone KAE609 has been proposed to target PfATP4, a Na⁺ H⁺ ATPase, even though the exact events preceding parasite death remain mostly unknown (Rottmann et al., 2010). Meanwhile, treating malaria parasites with KAE609 was shown to elicit a rapid influx of sodium, parasite membrane rigidity and consequent alteration of parasite morphology (Das et al., 2016). In this metabolomic profiling, incubation of malaria parasites with KAE609a for 2.5 hours at 10x IC₅₀ led to a massive loss of peptides, many of them potentially haemoglobin derived (Figure 6.3a). Moreover, KAE609a incubation resulted in accumulation of cholines and phosphocholine derivatives (Figure 6.3b), disrupted pyrimidine biosynthesis pathway (but with a different signature to atovaquone, Figure 6.3c, 6.3d) and it also caused a loss in purine metabolites (Figure 6.3e). This is in contrast to the inactive analogues which yielded profiles similar to the DMSO control. These observations are also similar to the previous metabolomic profiles for KAE609 which reported a loss of haemoglobin derived peptides, amino acid derivatives and central carbon metabolites (Allman et al., 2016). This illustrates a potential pleiotropic metabolic response which could arise as a result of rapid disruption of cellular homeostasis upon PfATP4 inhibition and sodium influx. Nevertheless, despite the evidence that KAE609 targets PfATP4, questions remain on whether PfATP4 is a direct target of this compound or a multidrug resistance gene. This is because mutations in PfATP4 do not just confer resistance to KAE609, but to a diverse array of chemically unrelated compounds which possess antimalarial activity (Spillman and Kirk, 2015, Lehane et al., 2014, Jimenez-Diaz et al., 2014). Thus, if a wide array of chemotypes converge on PfATP4, there remains a possibility that the exact killing events of this class of compounds could be unrelated to PfATP4 inhibition. As observed in this study, this could indeed be in part due to primary or secondary pleiotropic events such as a shutdown in haemoglobin catabolism and inhibition of pyrimidine pathways. Interestingly, the pyrimidine metabolic fingerprint of KAE609a which though different from atovaquone (Figure 6.3d) is similar to the previously reported pyrimidine metabolomic profile of DHA albeit at differing time points (Cobbold et al., 2016). This would suggest that both DHA and

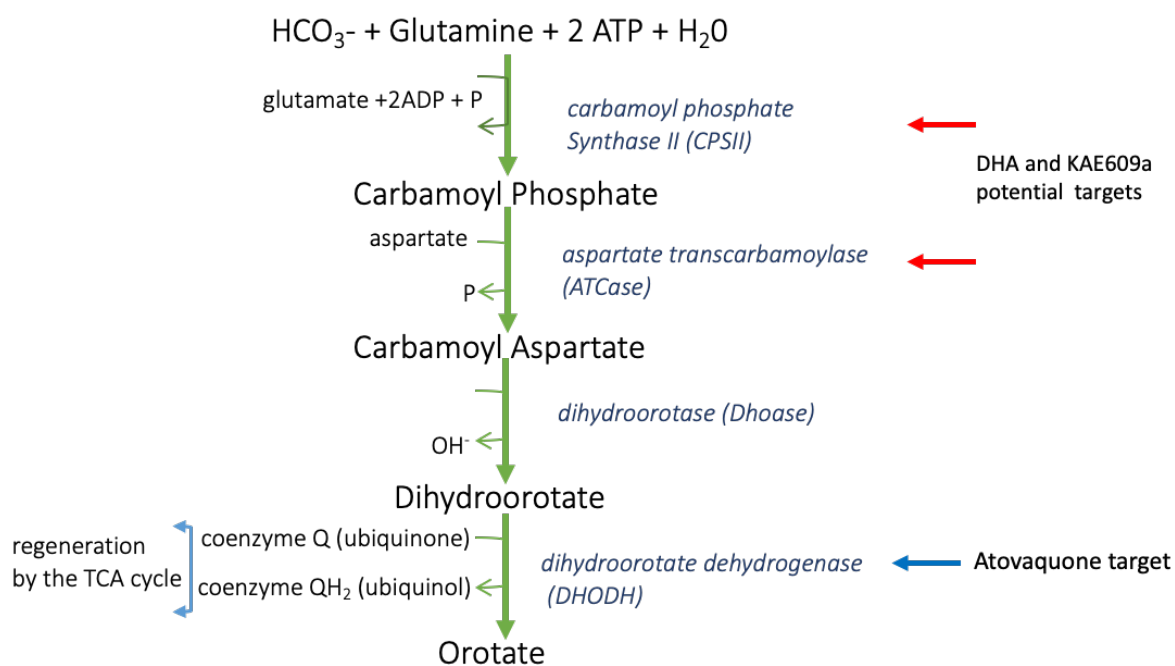
spiroindolones directly or indirectly perturb the early enzymes of the pyrimidine biosynthesis pathway (ATCase, CPSII) leading to a shutdown in the synthesis of downstream metabolites. In a different metabolomics profiling of malaria box compounds, metabolic fingerprints of DHA were shown to cluster together with KAE609 and some other PfATP4 inhibitors; SJ733 and MMV006427 (Creek et al., 2016). Even though the metabolomics profiles observed in this study (KAE609a) and previously for both DHA and KAE609 could be unspecific pleiotropic events of fast acting compounds, this remains to be fully explored as some of the known PfATP4 inhibitors (MMV011567, MMV665805) (Lehane et al., 2014) which rapidly disrupt parasite ion homeostasis, just like KAE609 elicit no metabolomic signatures at all (Creek et al., 2016). The actual events leading to parasite death in KAE609a could thus potentially involve promiscuous targeting, just like with DHA, shutting down the parasite's multiple biochemical and molecular pathways.

a





d



Cobbold et al. 2016

Metabolite	Atovaquone (2.5 hours)	KAE609a (2.5 hours)	DHA (up to 6 hours)
L-glutamine	~	~	~
Carbamoyl phosphate	~	-	~
Carbamoyl aspartate	↑	↓	↓
Dihydroorotate	↑	↓	↓
Orotate	↓	↓	↓
Orotidine	↓	-	~
UMP, UDP, UTP	↓	↓	↓

- ↑ significant increase
- ↓ significant decrease
- ↓ decrease trend
- ~ unchanged
- not reported

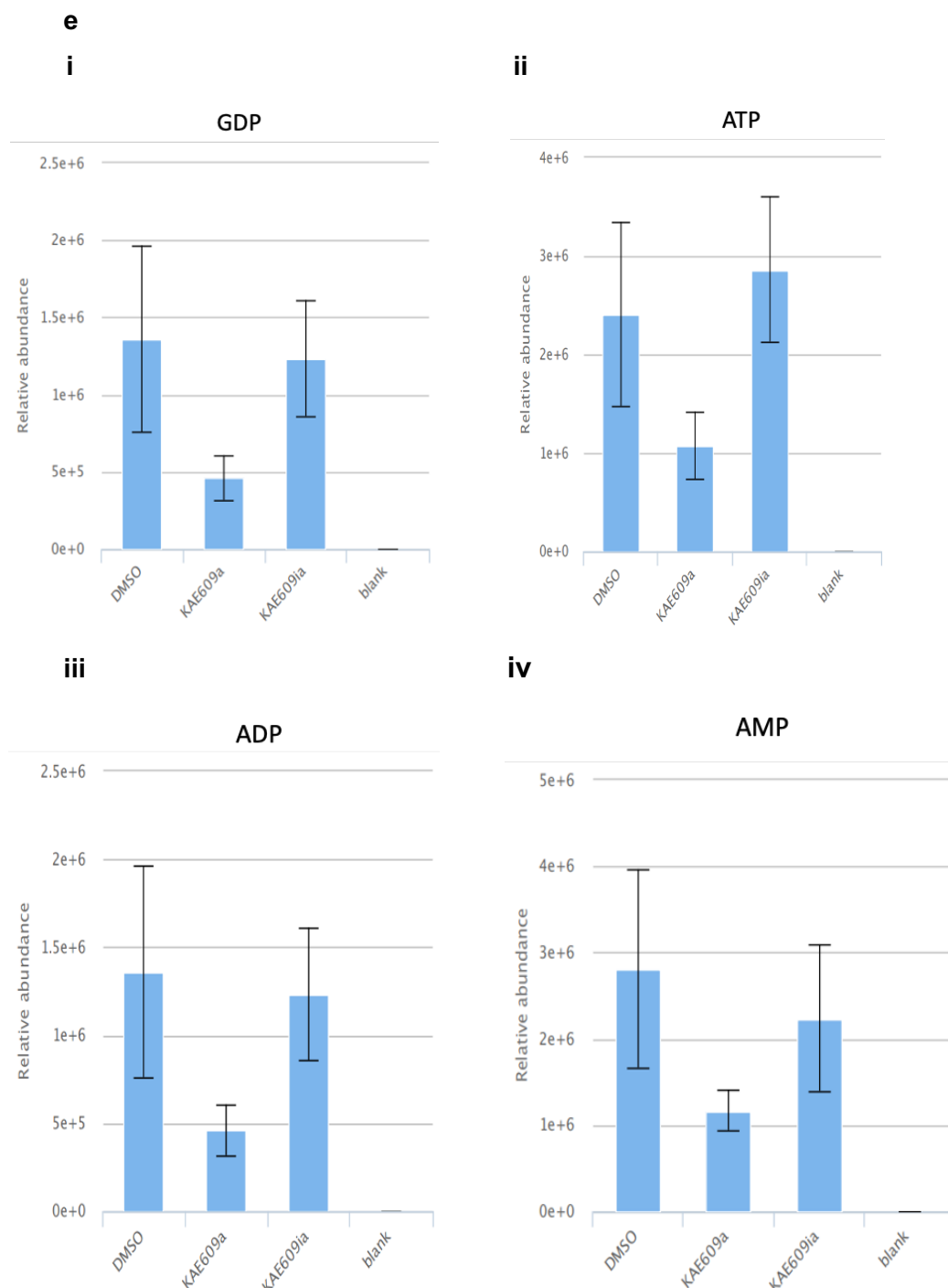


Figure 6.3: Pleiotropic metabolic response of malaria parasites after exposure to KAE609a for 2.5 hours.

a. Global untargeted metabolomic response of selected peptides in KAE609a treated trophozoites as compared to DMSO. Peptides with haemoglobin matching sequences as well as those which are potentially haemoglobin derived (Allman et al., 2016, Creek et al., 2016, Cobbold et al., 2016) are highlighted. **b.** Relative abundance of choline and choline derivatives in the KAE609a treated parasites as compared to DMSO and in-active analogues. **c.** Relative abundance of the indicated pyrimidine biosynthesis pathway metabolites in the KAE609a treated parasites as compared to DMSO and in-active analogue. **d.** Schematic of the pyrimidine biosynthesis pathway showing atovaquone

(Figure 6.2) and KAE609a /DHA potential action points. Potential target points for DHA are based on previously reported profiles (Cobbold et al., 2016) while target points for KAE609a are based on the observed profiles in this work. The table is a direct comparison of atovaquone and KAE609a pyrimidine biosynthesis pathway metabolites. **e.** Relative abundance of purine derived metabolites; guanosine diphosphate (GDP), adenosine triphosphate (ATP), adenosine diphosphate (ADP) and adenosine monophosphate (AMP) in the KAE609a treated parasites as compared to DMSO and inactive analogue. Fold changes (relative to DMSO control) and relative abundance comparisons are means from 2 biological repeats collected in triplicate at each time of drug incubation.

6.3.4 ITD series elicit minimal metabolic responses that suggest inhibition of haemoglobin catabolism as a possible MOA

ITD1a and ITD2a are analogues of another novel class of compounds in the development pipeline at the NITD. They are very fast acting, faster than spiroindolones (KAE609a) and DHA (Figure 6.1a). Attempts to generate parasites lines highly resistant to these compounds by *in vitro* selection have so far been unsuccessful making attempts to characterise their MOA particularly difficult. In this metabolomics screen, ITD1a and ITD2a induced very similar metabolic profiles, almost entirely restricted to peptides, and mainly consist of loss and or gain of peptides (Figure 6.4a, Figure 6.4b). Some of the peptides which significantly decreased in the ITD treatment include Trp-Gly, Phe-Gly, Leu-Ala, Lys-Gly-His, Pro-Glu-Glu which can be mapped to the α and β sequences of haemoglobin, the perturbation of which was also reported previously in metabolic profiling of DHA, a known inhibitor of haemoglobin uptake and catabolism (Cobbold et al., 2016, Creek et al., 2016). This would suggest that ITDs, in a similar manner, could be potentially targeting haemoglobin breakdown as their MOA. However, the ITD peptide response with some identical peptides appear to be similar to the ones observed with KAE609a as well as DHA. Even though DHA is known to target haemoglobin catabolism, KAE609a on the other hand is believed to target PfATP4, a $\text{Na}^+ \text{H}^+$ ATPase (Rottmann et al., 2010), which seemingly has no role in haemoglobin breakdown. The ITD peptide response could thus be a secondary consequence of a target specific inhibition which these metabolomics screen could not reveal. Moreover, it is difficult to tell the true source of di/tripeptides with short sequences which metabolomics

screening platforms like the LC-MS platform used in this work reveal and quantify. For example, the Met-Ala, Trp-Pro, Leu-Met peptide combinations which are significantly perturbed in the ITDs metabolic profile (Figure 6.4a, 6.4b), are not present in haemoglobin sequences. This could point towards a more general inhibition of protein degradation systems or a signal of dying parasites which would be characteristically unrelated to the MOA. Moreover, several compounds with unrelated MOA have been shown to perturb haemoglobin catabolism (Murithi et al., 2019, Allman et al., 2016). Assigning the MOA of compounds based on haemoglobin peptide profiles is, therefore, specifically difficult. Nevertheless, the uniqueness of the ITD peptide response which does not correspond with disruption to other pathways such as pyrimidine or purine responses as is the case with KAE609a or DHA suggests that these compounds could be specifically targeting enzymes involved in haemoglobin catabolism. More interestingly, another fast acting compound which has been developed by the MMV, JPC-3210, elicits a similar metabolic profile like ITDs which is mostly restricted to peptides and has been proposed to target haemoglobin catabolism as its MOA after follow-up biochemical and peptidomic analyses (Birrell et al., 2019). Meanwhile, JPC-3210 also appears to interfere with protein translation (Birrell et al., 2019), suggesting that besides interfering with haemoglobin catabolism, ITDs could also, in a similar way, affect other parasite's metabolic and biochemical pathway such as protein translation as their mode of activity.

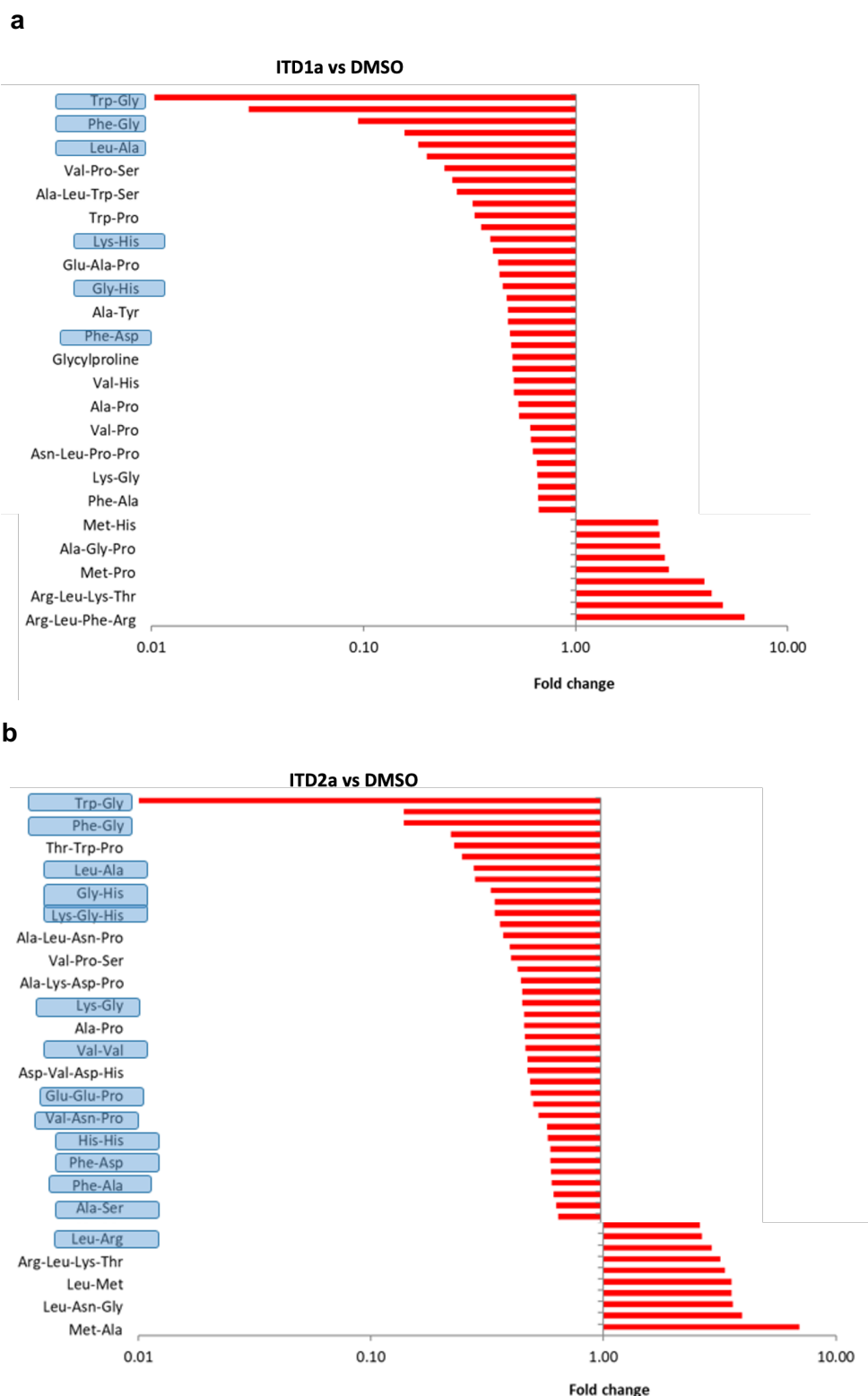


Figure 6.4: Peptide metabolic responses of the ITD series compounds in malaria parasites.

a, b. Global response of selected peptides upon treatment with ITD1a (**a**) or ITD2a (**b**). Peptides with haemoglobin matching sequences as well as those which most likely derive from the same (Cobbold et al., 2016, Creek et al., 2016) are highlighted. Fold changes relative to the DMSO control are means from 2 biological repeats collected in triplicate at each time of drug incubation.

6.3.5 KAF156a elicits a minimal non-specific metabolic response

KAF156 belongs to the imidazolopiperazines class of compounds that have been developed by the NITD and have shown potential as antimalarial agents for use in malaria treatment, prophylaxis and transmission blocking (Kuhlen et al., 2014, White et al., 2016). The exact MOA of KAF156 is currently unknown but mutations in the *P. falciparum* cyclic amine resistance locus (PfCARL) as well as UDP-galactose and Acetyl-CoA transporters have all been shown to confer resistance to KAF156 and its close analogues (Lim et al., 2016, LaMonte et al., 2016). In this metabolomics screen, KAF156a did not induce any significant metabolic effect after incubating parasites with the compound for 2.5 hours. Some low-level increase in purine metabolites (Figure 6.5a) was observed along with a low-level accumulation of central carbon metabolism metabolites (malate, succinate and oxoglutarate) (Figure 6.5b). This is in agreement with previous reported metabolomics profiles of KAF156 as no significant changes in the parasites metabolome was observed after the same period of drug incubation (Allman et al., 2016). It is therefore difficult to predict the MOA of KAF156a based on these profiles. Nevertheless, it is important to note that KAF156a is relatively slow acting (Figure 6.1a) which would potentially suggest that the 2.5 hours of drug incubation is relatively short to elicit a significant biochemical response. A longer incubation period (which was not pursued) would perhaps reveal unique signatures specific to this compound MOA. This seems unlikely though, as atovaquone (with a similar biochemical killing rate) seemed to induce a significant metabolic signal over the same duration of drug exposure (2.5 hours). Recently, *in vitro* selection for resistance and forward genetic screens have pointed towards inhibition of protein trafficking as a possible MOA of KAF156 and other imidazolopiperazines (LaMonte et al., 2020).

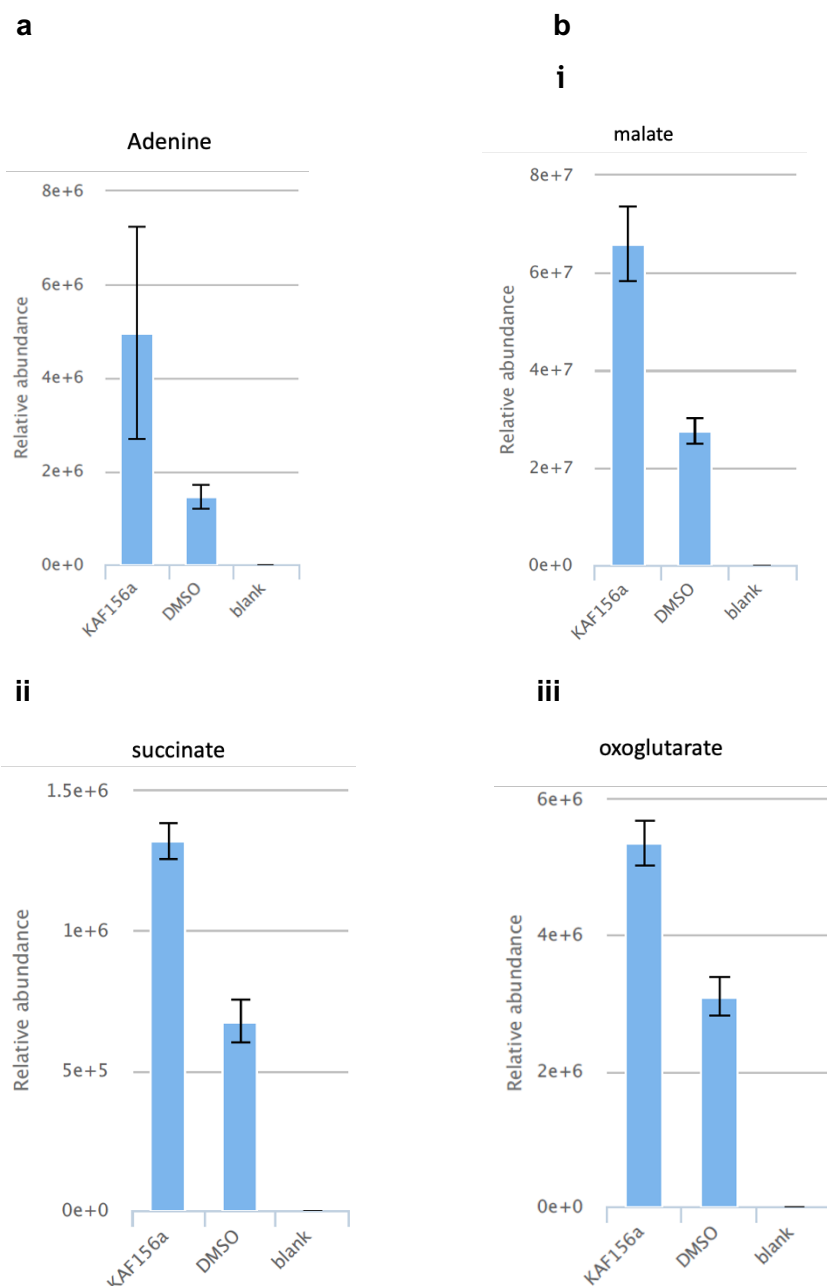


Figure 6.5: KAF156a metabolomic response for selected metabolites.

a, b Relative abundance of adenine (**a**) and a selected central carbon metabolism intermediates (**b**) in KAF156a treated parasites as compared to DMSO. Relative abundance comparisons of total ion counts are means from 2 biological repeats collected in triplicate at each time of drug incubation.

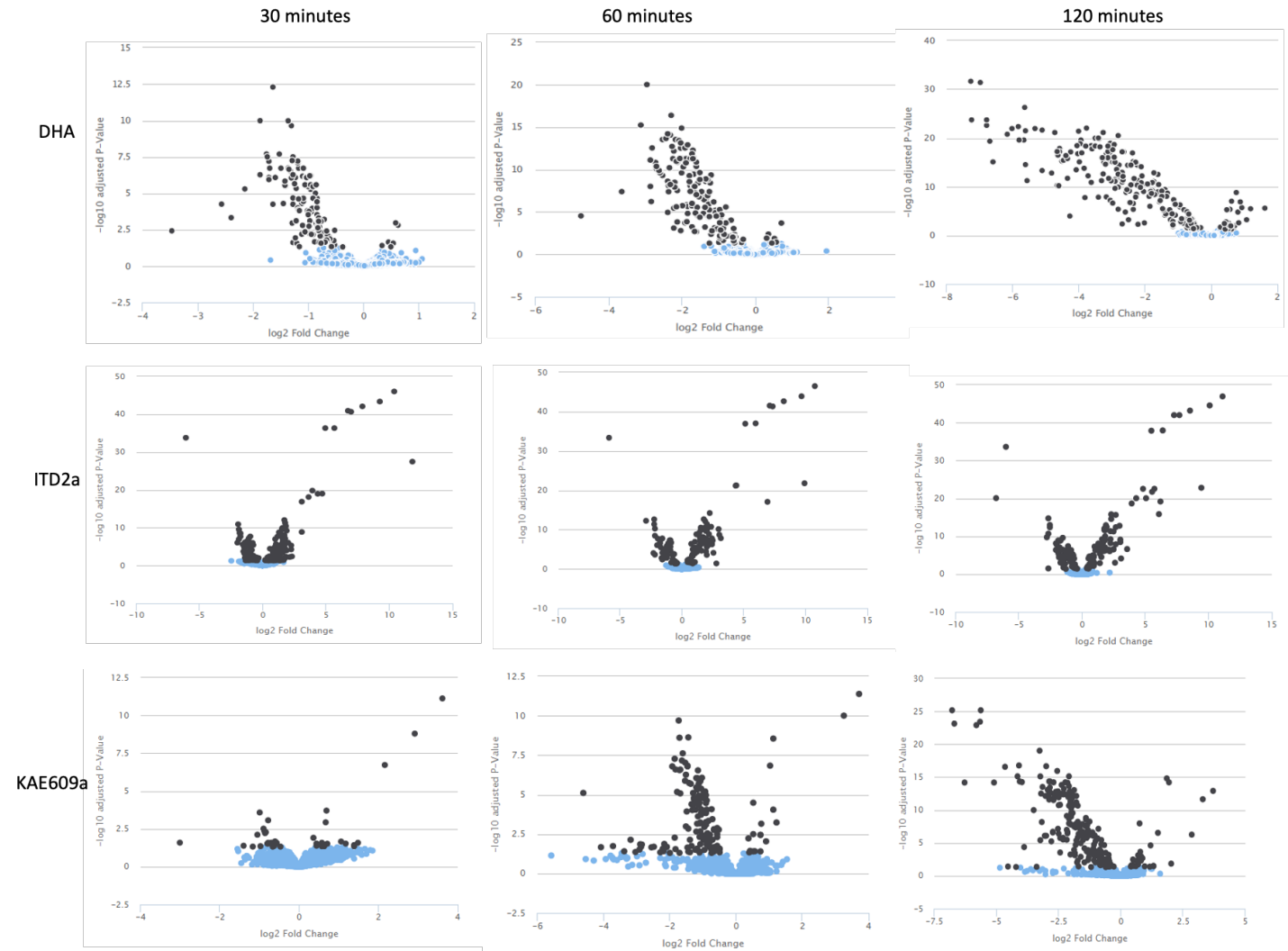
6.3.6 Metabolomics time point resolution of fast acting compounds; DHA, ITD2a and KAE609a during early points of drug incubation

Fast acting compounds appear to exert a malaria parasite killing event in seconds or minutes with resulting metabolic profiles over time reminiscent of parasite dying cascades that are perhaps unrelated to the exact MOA of the

compounds. For example, the spiroindolone, KAE609 was shown to lead to a rapid influx of sodium which disrupts the parasite ion homeostasis within seconds of drug exposure (Das et al., 2016, Spillman et al., 2013). DHA is also known to simultaneously target several (possibly random) parasite proteins in a promiscuous targeting cascade leading to parasite death as a result of a disruption in several biological pathways (Wang et al., 2015a, Ismail et al., 2016). In such events, metabolic and biochemical perturbation in essential pathways that are directly or indirectly involved in the MOA of the compounds would be quantifiable within minutes of drug exposure. To this end, the dynamic parasite's metaprints upon exposure to these fast-acting compounds at 10x IC₅₀ for 30 minutes, 1 hour and 2 hours was resolved. Enriched trophozoites as described above were incubated with the drugs for the stated time period following which untargeted metabolomics LC-MS was carried out on the extracted metabolites at each time point.

6.3.6.1 Global metabolomic responses to DHA, ITD2a and KAE609a are unique and respond to duration of drug exposure

In all the three compounds, significant changes to the global parasite metabolome were observed after 30 minutes of drug exposure. However, this change was time dependent. Of the ~3000 mass features which were detected by LC-MS, 4.3%, 1.6% and 4.6% significantly changed at 30 minutes which increased to 5.6%, 5.8% and 5.2% at 1 hour and 7.8%, 8.1% and 7.9% at 2 hours for DHA, KAE609a and ITD2a respectively. Meanwhile, careful analysis of the volcano plots (Figure 6.6) revealed that despite the compounds eliciting a similar change in the number of features that are perturbed at each time point, DHA elicited a stronger downregulated response after 30 minutes of drug exposure which became relatively similar to KAE609a after 1 and 2 hours. On the contrary, ITD2a global metabolomic response seemed to be different from both DHA and KAE609a at all the time points displaying less intensity and equal distribution in upregulated and downregulated mass features (Figure 6.6). This would suggest that, despite displaying a similar fast killing rate, these compounds exert their killing cascade in a slightly different mode which would reflect differences in their MOA.



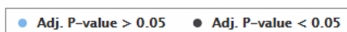


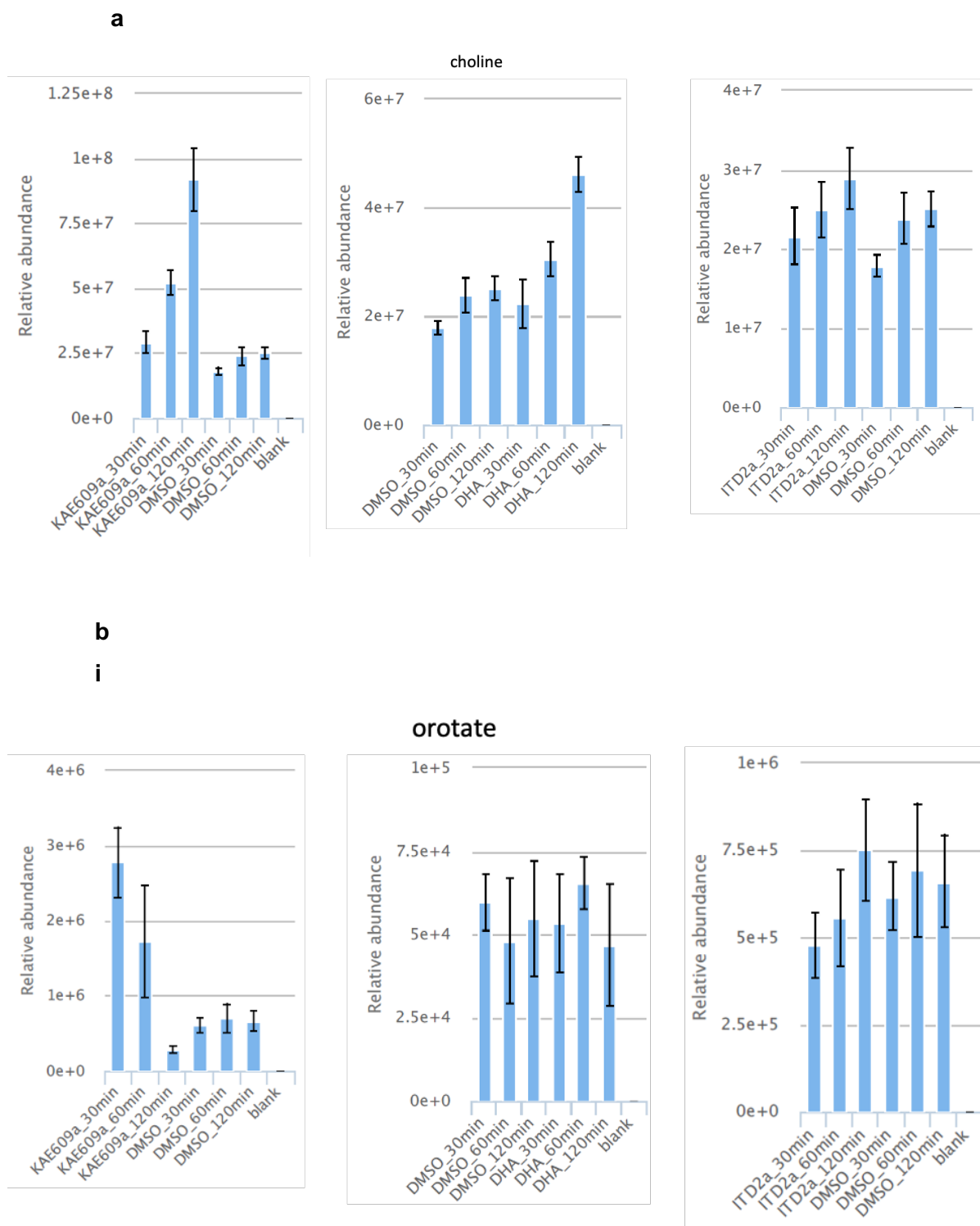
Figure 6.6: Global volcano plots of all detected mass features in DHA, ITD2a and KAE609a treatments according to their fold change relative to DMSO treatments.

Significant features are represented as black dots while non-significant features are in light blue. n=2 with three technical replicates at each biological repeat.

6.3.6.2 KAE609a perturbation of choline, pyrimidine and purine metabolites at 2.5 hours is reflected in time dependent changes at earlier time points

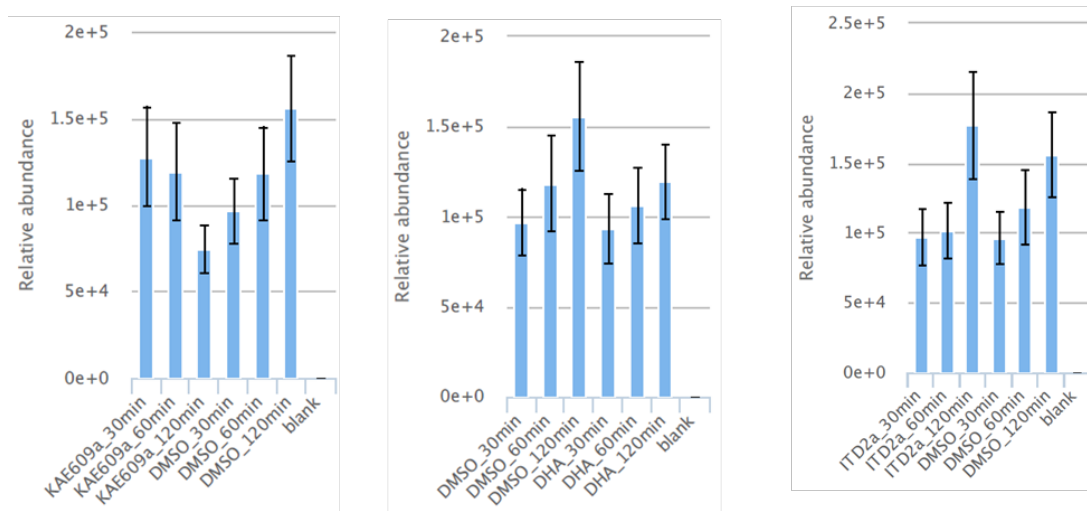
KAE609a significantly perturbs metabolites in the pyrimidine, purine and choline biosynthesis pathway after 2.5 hours of drug incubation (Figure 6.3). The dynamic profiles of these metabolites at the earlier time points was therefore analysed to see if the changes observed reflect a gradual and dynamic response or a mere one-off metabolic shock response. Indeed, in complete agreement with these observations (Figure 6.3), KAE609a induces a gradual accumulation of cholines (Figure 6.7a) which is not significantly observable after 30 minutes, but gradually increases at 1- and 2-hour time points. Interestingly, DHA elicits a similar choline profile as KAE609a which would suggest that this response is perhaps a consequence of a global alteration to the parasite metabolism as a result of simultaneous targeting of multiple targets by DHA or rapid disruption of ion homeostasis by KAE609a. On the contrary, ITD2a does not alter choline homeostasis with choline metabolites comparable to DMSO control (Figure 6.7a). These data would further suggest that the metabolic consequences of DHA and KAE609a exposure in malaria parasites overlap while ITD2a acts via a different MOA which does not elicit a global repression of other biochemical pathways. A similar trend is observed for pyrimidine and purine derived metabolites that gradually decrease over 2 hours of KAE609a drug incubation (Figure 6.7b, 6.7c). Uniquely, orotate pools sharply accumulate in KAE609a treated parasites after 30 minutes of drug incubation and rapidly decline thereafter to significantly lower levels after 2 hours. This could be a result of preferential inhibition of the orotate phosphoribosyltransferase (ORPP) enzyme in the pyrimidine pathway during the parasites initial ion insult, which would lead to accumulation of orotate that rapidly declines as other enzymes upstream of the pathway respond to the inhibition. ITD2a and DHA do not induce any significant alteration in

either purines or metabolites of the pyrimidine biosynthesis during the 2 hour time period which, although is in contrast to the previously reported pyrimidine profiles for the latter (Cobbold et al., 2016), may be due to the short duration of exposure time in this study



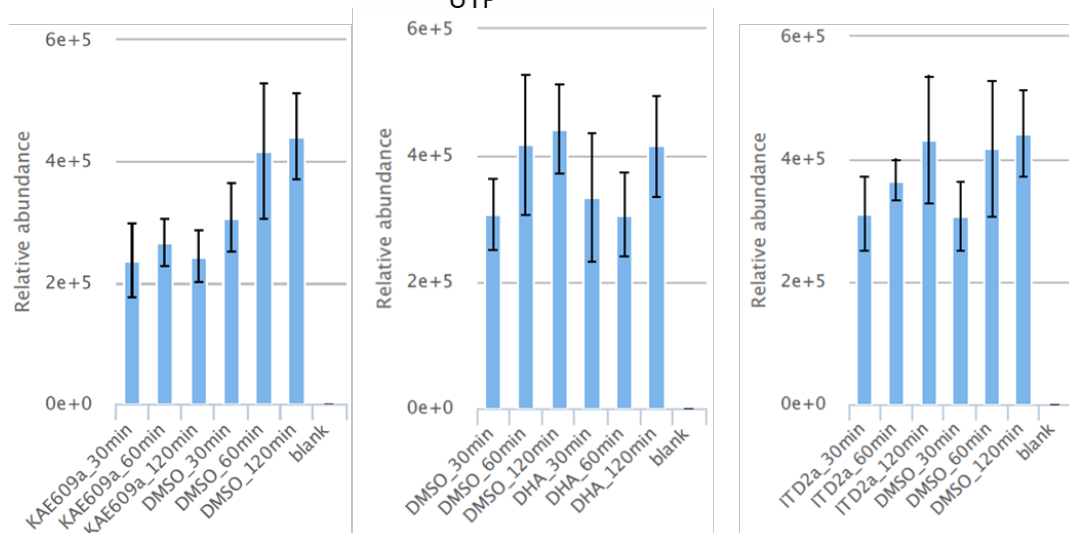
ii

dihydroorotate



iii

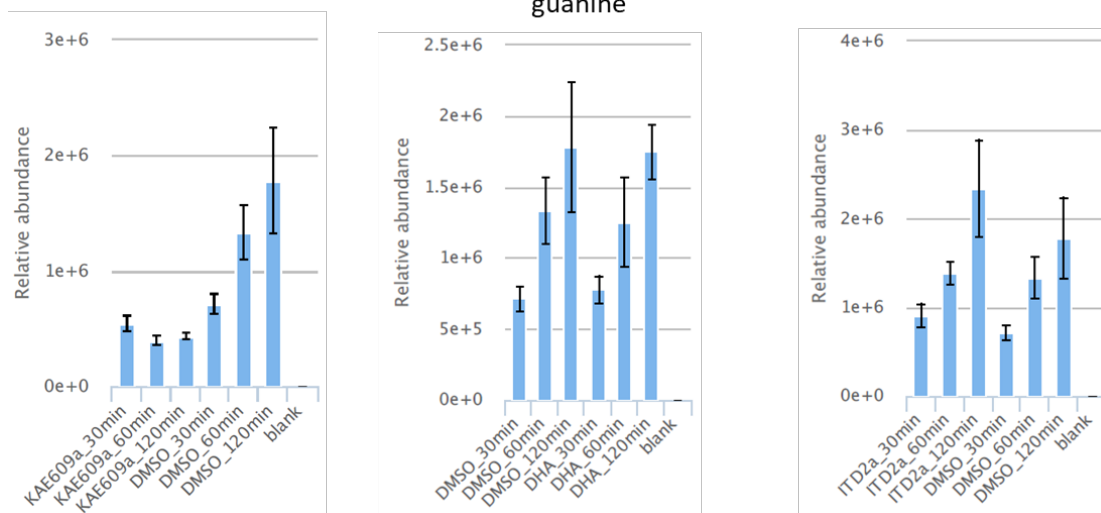
UTP



c

i

guanine



ii

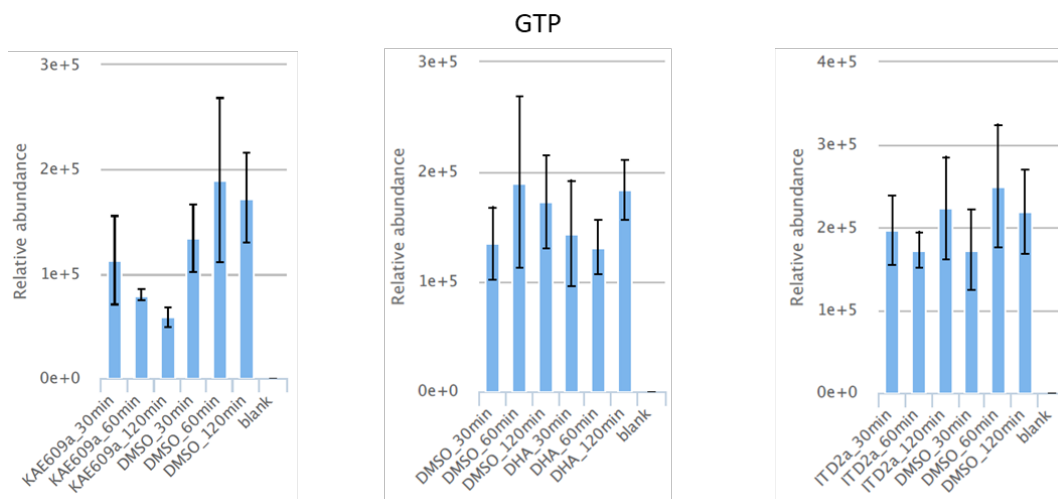


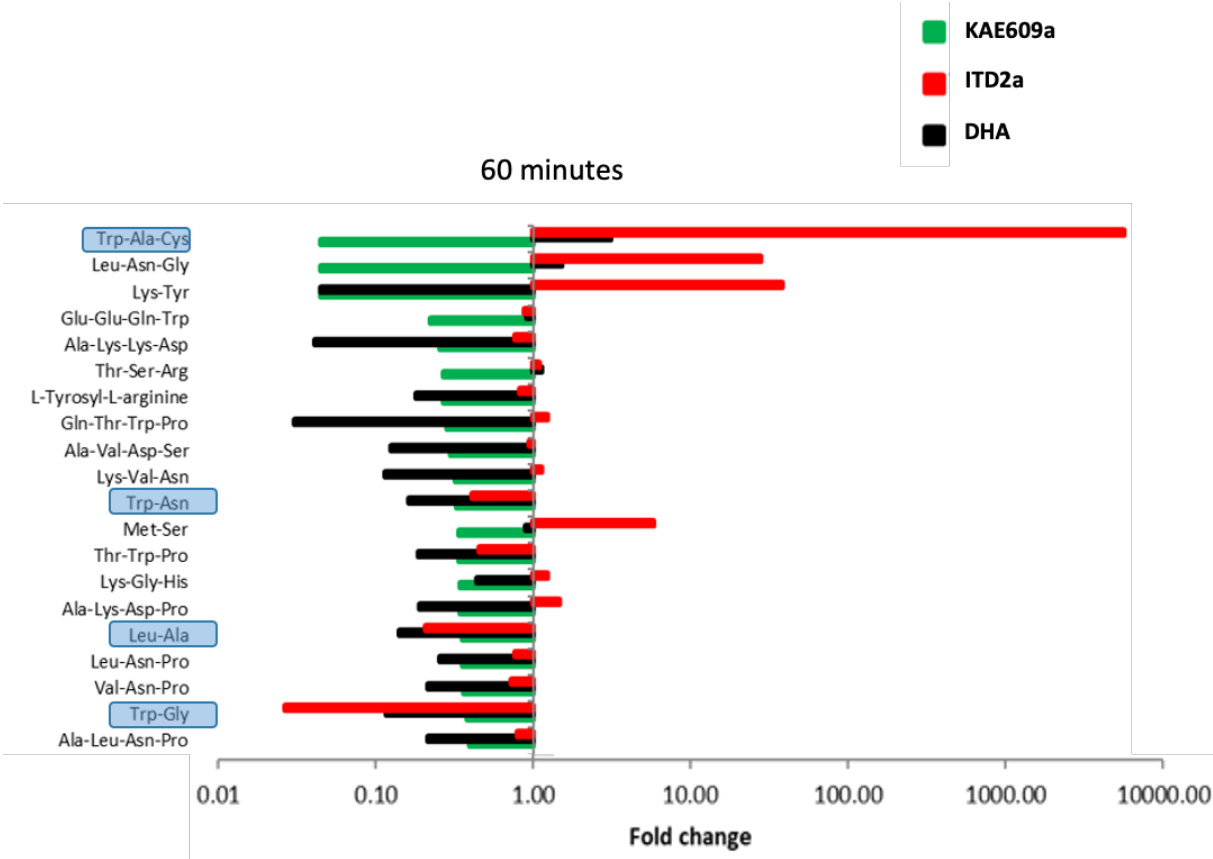
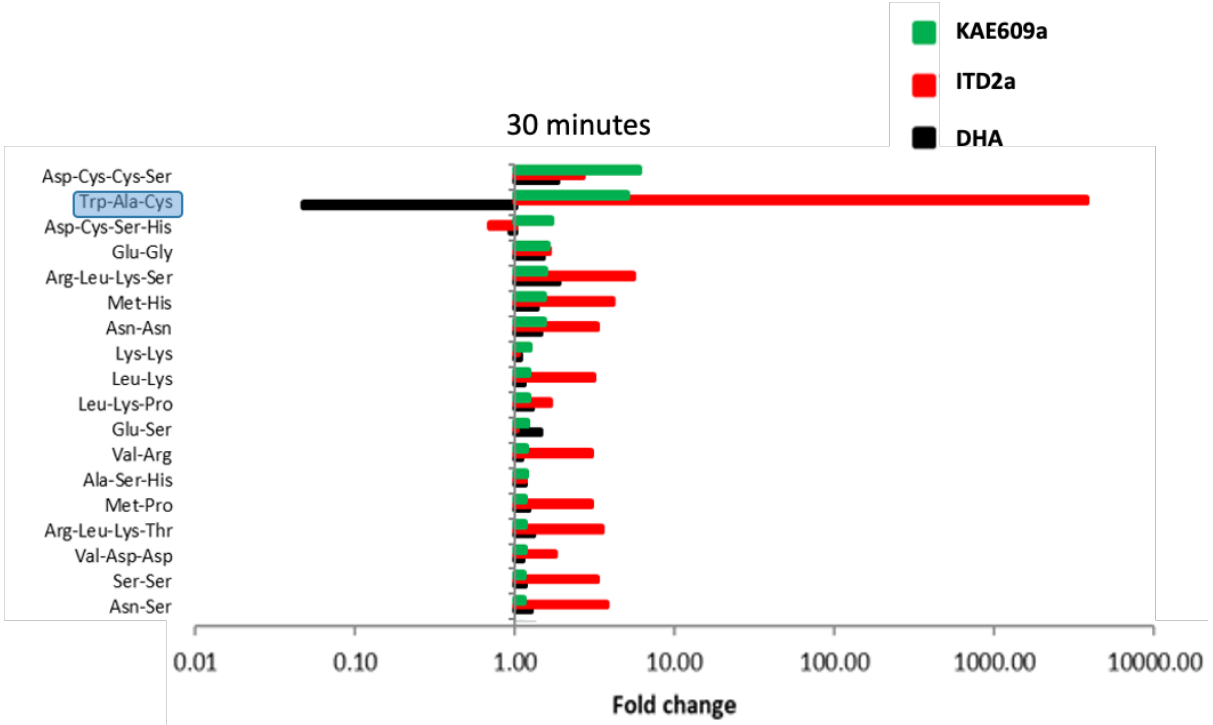
Figure 6.7: Time course comparisons of choline, pyrimidine and purine metabolites in DHA, KAE609a and ITD2a parasite treatments.

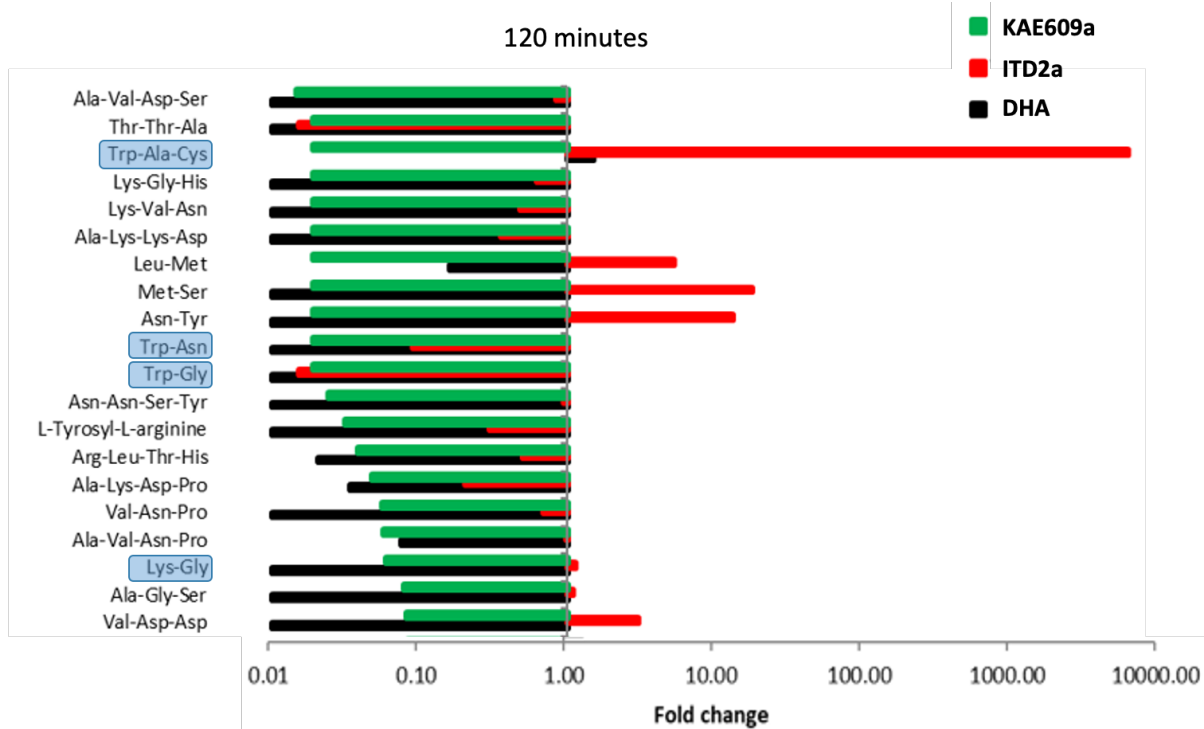
a-c. Relative abundance of choline (a), selected indicated pyrimidine (b) and purine (c) metabolites. Comparisons of total ion counts are means from 2 biological repeats collected in triplicate at each time of drug incubation.

6.3.6.3 Time dependent changes in peptide response for KAE609, DHA and ITD2a

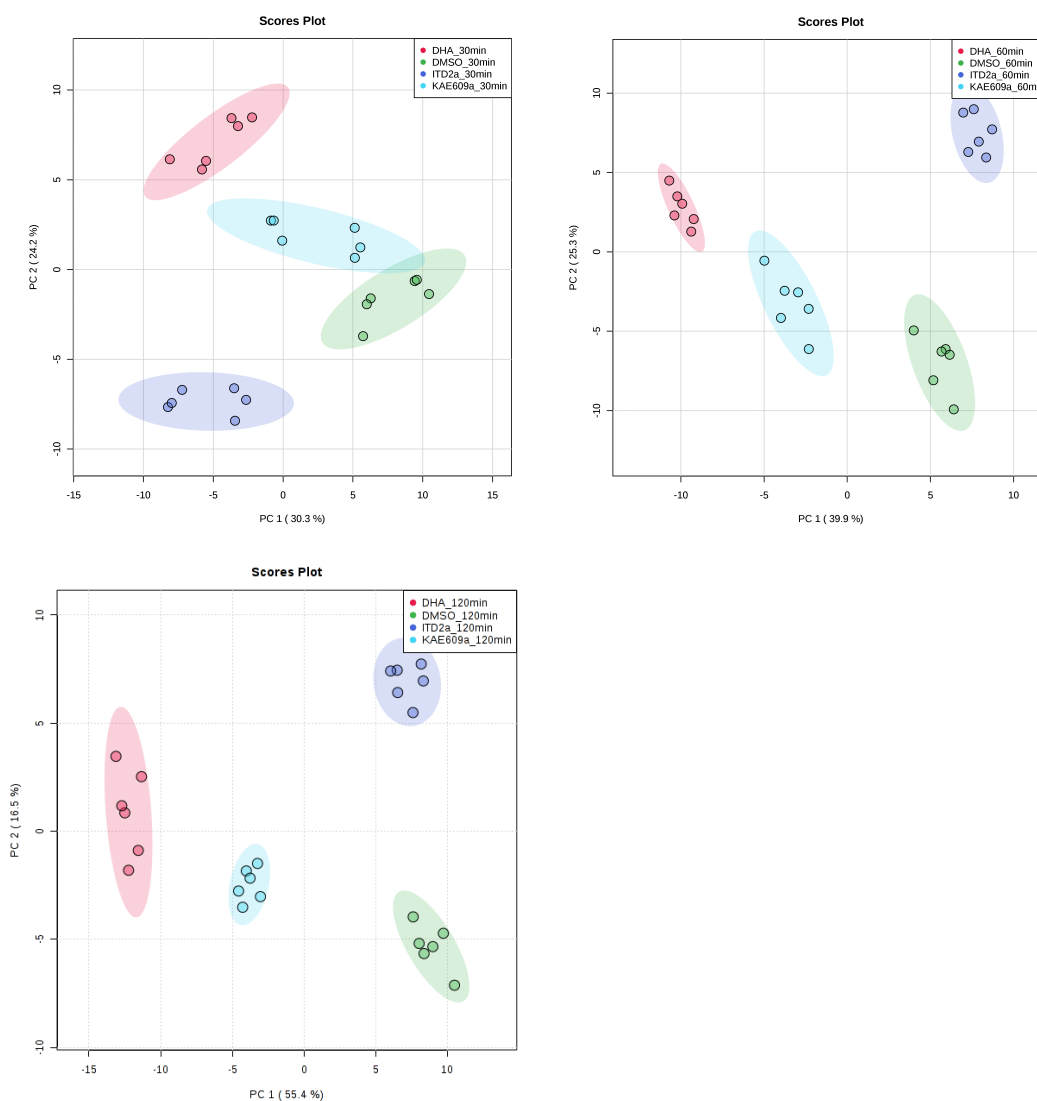
Next, the metabolomics peptide response in KAE609a, DHA and ITD2a treated parasites was profiled over the 0.5, 1 and 2 hours of drug incubation. Clustering of the global peptide response in the three drug treatments revealed that this response is minimal at 30 minutes of drug incubation and becomes more pronounced at 1-and 2-hours respectively (Figure 6.8a). Moreover, even though the global responses appear similar across the three compounds, ITD2a elicits a unique peptide response as compared to DHA and KAE609a which would suggest a unique targeting of parasite haemoglobin catabolism by this class of compound that does not directly or indirectly impact other biochemical pathways. Indeed, supervised clustering of the global peptidomes in these treatments by principal component analysis (PCA) revealed that at both time points, DHA and KAE609a peptide response clustered closer together as compared to ITD2a or DMSO in the first and second principle components (Figure 6.8b). Furthermore, some of the potentially haemoglobin derived peptides such Trp-Gly show a time-dependent decline (Figure 6.8c) in both compounds further suggestive of a global decline in parasite haemoglobin catabolism as a consequence of drug treatment.

a





b



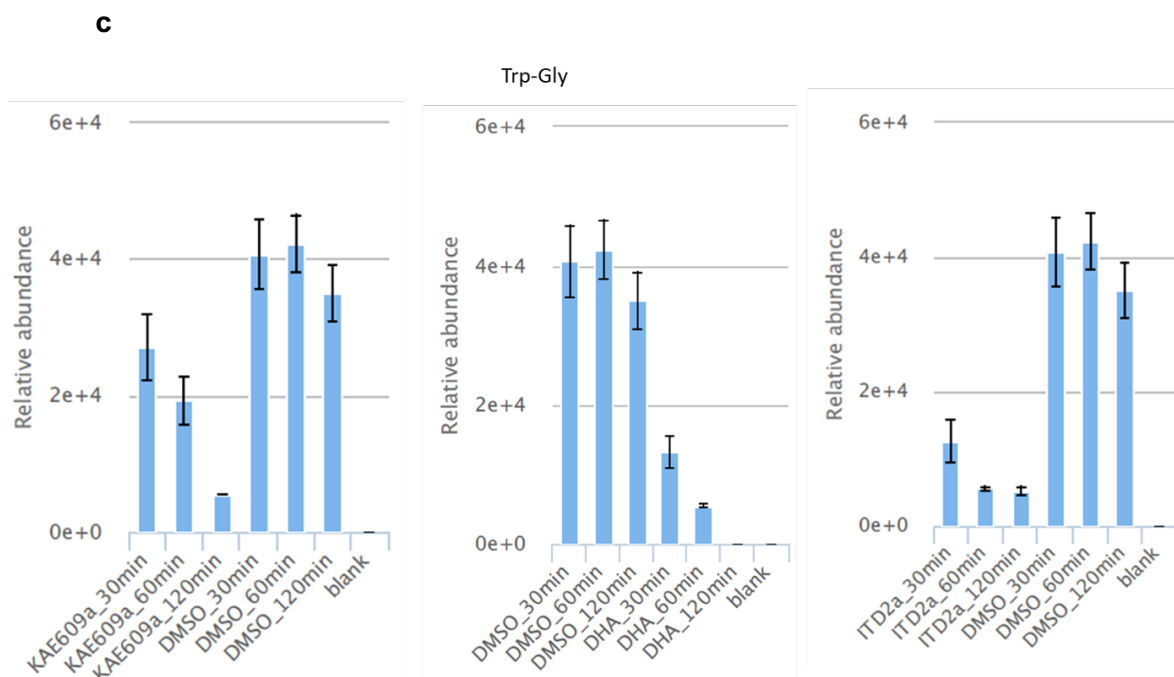


Figure 6.8: Time point resolution of global peptide responses in KAE609a, DHA and ITD2a treated parasites.

a. Global responses of top 20 significantly changed peptides upon treatment with DHA, KAE609a and ITD2a for 30 minutes, 1 and 2 hours. Peptides with haemoglobin matching sequences as well as those which are likely to be haemoglobin derived (Cobbold et al., 2016, Creek et al., 2016) are highlighted. **b.** PCA plots of the peptidomes of the three compounds after treatment for 30 minutes, 1 and 2 hours. **c.** Relative abundance of a potential haemoglobin derived peptide Trp-Gly in DMSO vs the three compounds at the three time points. Fold changes and relative abundance comparisons are means from 2 biological repeats collected in triplicate at each time of drug incubation. PCA plots were carried out on log transformed data in Metaboanalysit 3 (Xia et al., 2015). 95% confidence intervals for each treatment group in the PCAs are highlighted with the indicated colors.

6.4 Conclusions

In conclusion, this study reports the metabolomic profile of a novel class of fast acting compounds belonging to the ITD class which suggests haemoglobin catabolism as their possible MOA or an essential event that precedes their parasite killing mechanism. By direct comparison with DHA and spiroindolones, it is demonstrated that fast acting compounds elicit a unique, but broadly similar, metabolomics profile which could form a useful biochemical metaprint to identify fast acting compounds.

7 Summary and future work

7.1 Drug resistance in rodent malaria parasites in the CRISPR-Cas9 era

As discussed in section 1.8.1, rodent malaria parasites have played significant roles in deciphering the MOR, and sometimes the MOA for several antimalarial drugs. Of the four rodent malaria parasites (*P. berghei*, *P. yoelii*, *P. chabaudi*, *P. vinckei*), the choice of which model to use is always dependent on the primary question of interest as these species can display significant differences in their host cell tropisms or synchronicity of infection (Table 1.2). *P. chabaudi* and *P. vinckei* infections, for example, result in highly synchronous parasitaemia with a specific tropism for mature RBCs just like the human infecting *P. falciparum*. This is basically the opposite case for *P. berghei* and *P. yoelii* which are largely asynchronous and preferentially invade reticulocytes. In these situations, *P. chabaudi* and *P. vinckei* are ideal models to test and or characterise the *in vivo* stage specificity of antimalarial drugs. Moreover, rodent malaria parasite display variations in sensitivity to different classes of antimalarial drugs. *P. berghei* is relatively resistant to ARTs and iron chelating drugs as compared to *P. chabaudi* or *P. vinckei* (Peters and Robinson, 1999a). *P. yoelii* is also inherently more resistant to CQ (Warhurst and Killick-Kendrick, 1967) making it less suitable for evaluation of antimalarial drugs belonging to the aminoquinoline class. Further to that, rodent malaria parasites (*P. berghei* and *P. yoelii*), just like the human infecting *P. vivax*, can escape or survive extended drug assaults due to the rich metabolic niche of reticulocytes that provide appropriate compensatory mechanisms and or nutrient reserves (Srivastava et al., 2015). In view of these variables, the choice of which rodent malaria parasite to use should, indeed, be tailored to specific hypotheses and on a case to case basis.

Nevertheless, *P. berghei* is the mostly used rodent malaria parasite for initial *in vivo* efficacy evaluation of antimalarial drugs in drug discovery programs (Peters and Robinson, 1999a, Fidock et al., 2004). An added advantage of *P. berghei* and to some extent *P. yoelii*, is the availability of high efficiency transfection technologies for these parasites which allow for easy genetic manipulation (Janse et al., 2006b, Jongco et al., 2006). Through allelic exchange experiments, *P. falciparum* drug resistant or MOA alleles can be introduced in *P. berghei* to assess associating phenotypes under *in vivo* conditions. These approaches have indeed been pursued as mutant PfCRT forms have been

introduced in *P. berghei* to characterise equivalent drug resistant phenotypes as well as transmission capacity of such alleles (Ecker et al., 2011). As demonstrated in this work for UBP-1 and Kelch13 (Chapters 3 and 4), development and successful adaptation of highly precise genome editing by CRISPR-Cas9 means gene and allele orthology between *P. falciparum*, *P. berghei* or other *Plasmodium* spp. can be investigated at a single nucleotide base and amino acid level. This is particularly important in antimalarial drug resistance studies as this will allow for simultaneous interrogation of *P. falciparum in vitro* phenotypes of drug resistance genetic determinants with *in vivo* phenotypes.

Between *P. berghei*, *P. falciparum* and *P. chabaudi*, UBP-1 is syntenic but poorly conserved overall. *P. berghei* and *P. falciparum* UBP-1 share 41.4% sequence identity while *P. chabaudi* and *P. falciparum* share 40.2% identity. As expected, given their phylogenetic proximity, *P. berghei* and *P. chabaudi* UBP-1 are relatively conserved with ~70% sequence identity. Even though these observations illustrate a potential evolutionary divergence, the C-terminal of this protein which forms the catalytic component of the enzyme (Figure 3.1a) is highly conserved, and more importantly the amino acid residues that were associated with the modulation of ART resistance in *P. chabaudi* (section 1.8.1.2) are conserved across the three *Plasmodium* species (Appendix Figure 8.2). In contrast, *Plasmodium* Kelch13 is much more conserved between *P. berghei* and *P. falciparum* than UBP-1 sharing over 80% sequence identity (Appendix Figure 8.7). All crucial *P. falciparum* ART resistance Kelch13 mutation sites are conserved between the two spp. both in terms of localisation and predicted structures. Using CRISPR-Cas9 editing to introduce orthologous mutations in *P. berghei*, work in Chapters 3 and 4 does indeed demonstrate a functional conservation of these proteins in modulating resistance to ARTs and CQ. Subtle to major differences can exist in the overall amino acid sequence identity of a protein, but the ability to precisely alter single amino acids at conserved loci as demonstrated in this work provides a unique opportunity to test *P. falciparum* candidate drug resistance mutations in a *P. berghei* model for concurrent *in vivo* evaluation of equivalent phenotypes. Moreover, such *P. berghei* mutant parasites offer an opportunity to evaluate the fitness impacts as well as evolution of drug resistant mutations in the context of single or multiple infections under *in vivo* conditions, something which is not possible *in vitro* with

human infecting *P. falciparum*. The versatility of *P. berghei* to various and or multiple levels of genetic manipulation also provides a unique opportunity to assess the impact of several different mutations in a single parasite line, evolutionary events that are observed in complex natural infections (Miotto et al., 2015, Zhu et al., 2018, Hamilton et al., 2019, van der Pluijm et al., 2019). Indeed, preliminary work which is not part of this thesis has demonstrated some degree of mutual exclusion to simultaneous acquisition of certain drug resistance mutations in malaria parasites as several ART resistance Kelch13 mutations could not be introduced in parasites carrying UBP-1 ART resistance alleles in *P. berghei* (Simwela, unpublished).

Acquisition of certain if not all drug resistance mutations in malaria parasites can require “ARMD” like backgrounds to compensate for potential deleterious consequences such polymorphisms can render to parasites on their own (Rathod et al., 1997). These phenomena have been observed in multiple situations, as for instance, CQ resistance in *P. chabaudi* could only be selected from parasites that were resistant to pyrimethamine as selection for resistance to the same from naive parasites was always unsuccessful (section 1.8.1.5). This is, seemingly, more evident with *P. falciparum* ART resistant Kelch13 mutations which require a necessary architectural landscape to either compensate for the fitness impact of these mutations or synergize for stronger ART resistance phenotypes (Zhu et al., 2018, Miotto et al., 2015). As evidenced in Chapter 4, introduction of some Kelch13 mutations, more importantly the C580Y and I543T mutation equivalents, could not be achieved in naive PBANKA parasites with no history of pre-exposure to or resistance to either ARTs or other antimalarial drugs. Polymorphisms in ferredoxin, apicoplast ribosomal protein S10, PfMDR2 and PfCRT are some of the possible markers of a genetic landscape upon which Kelch13 mutations are more likely to arise (Miotto et al., 2015). Even though it is likely to be far from simple, naive *P. berghei* parasites with powerful CRISPR-Cas9 genome editing strategies as demonstrated in Chapters 3 and 4 could serve as important tools to investigate such relationships. This could involve engineering some of these candidate compensatory polymorphisms in wild type *P. berghei* parasites and assessing whether introduction of refractory mutations such as the C592Y or I555T could be achieved in such situations.

7.2 Targeting the upstream components of the UPS to overcome ART resistance

One of the key aims of ART MOA or MOR studies in malaria parasites is to identify drugs that target the drug action or resistance pathways directly or indirectly so that they can be used in combination with ARTs to overcome resistance. A key feature of ART resistance Kelch13 mutant parasites is that they display an enhanced cellular stress response through the upregulation of genes in the UPR and an over-active UPS (Dogovski et al., 2015, Mok et al., 2015). Inhibition of the UPS by targeting the 20s proteasome can indeed synergize ART activity to the extent that the resistance phenotypes can be offset. Central to the UPS activity are DUBs which recycle Ub pools by cleaving off Ub residues from substrate proteins before they enter the 20s proteasome complex for degradation. The activity of DUBs on determining the cellular fate of proteins result in numerous outcomes (Lecker et al., 2006), which as demonstrated in Chapter 3 can among other things result in drug resistance phenotypes upon acquisition of mutations in malaria parasites. As further demonstrated in Chapter 5, DUB inhibition could be a source of novel antimalarial drugs, and more importantly drugs which can be used in combination with ARTs to impair the parasite UPS while boosting the activity of ARTs. A multipronged attack on the parasite UPS by simultaneously targeting several components of this pathway could also serve as the parasite's Achilles heel through which the emergent resistance to ARTs can be overcome.

The UPS is a highly conserved eukaryotic pathway which makes it specifically challenging to identify inhibitors that would specifically target *Plasmodium* DUBs or the 20s proteasome as evidenced by *in vivo* toxicities of b-AP15 in this work and 20s proteasome inhibitors previously (Li et al., 2012). However, recent characterisation of the *Plasmodium* DUB, USP14, which identified unique conserved *Plasmodium* residues (Wang et al., 2015b) offers hope that selective inhibition can be achieved. More importantly, structure-based design of *Plasmodium* selective 20s proteasome inhibitors that display minimal to no host cell toxicities (Li et al., 2016, Yoo et al., 2018) offers even more hope of selectively targeting the UPS not just as antimalarial drug target, but also as a direct countermeasure to curb ART resistance. Recent solving of the *P. falciparum* 20s proteasome complex (Xie et al., 2019) has also provided unique

opportunities for more precise structure-based design of *Plasmodium* selective proteasome inhibitors that would achieve superior potency and ultra-selectivity.

7.3 Capturing the metabolomic fingerprint of fast acting antimalarial drugs and drug candidates: any cues to the MOA?

Application of metabolomics platforms to characterising antimalarial drugs MOA and antiprotozoal drugs at large has been clearly demonstrated, reviewed by (Creek and Barrett, 2014). Untargeted metabolomics in particular, offer a unique opportunity to decipher the biochemical responses that drug treatment induces in pathogens of interest without prior knowledge of the compounds MOA. These approaches have been used to classify hundreds of antimalarial compounds based on the biochemical metaprints with probable cues to their MOA (Allman et al., 2016). As demonstrated in part of this work (Chapter 6), the MOA of novel antimalarial drugs belonging to the ITD class was predicted by application of untargeted metabolomics despite failure to select for resistance and henceforth unable to apply forward genetics approaches for MOA elucidation. ITDs were shown to elicit a unique peptide perturbation which points to inhibition of haemoglobin catabolism as a possible MOA. However, this response, was to some extent, shared with other fast acting antimalarial drugs, notably; DHA which is known to interfere with haemoglobin catabolism as well as spiroindolones which, thus far, are not known to interfere with any form of haemoglobin biosynthesis pathways in malaria parasites.

These observations illustrate the limitations of these untargeted metabolomics approaches in providing clear distinction of the compounds MOA especially if the responses observed are due to non-specific stress related metabolic features or other secondary responses. This is specifically relevant for fast compounds like the ones examined in this work, which would either exert a parasite killing event rapidly or result in pleiotropic responses which could be unrelated to the MOA. Nevertheless, these metabolomics approaches provide crucial hypothesis generating questions which can be followed up by other systems biology approaches or functional studies to fully characterise the MOA of the compounds of interest.

7.4 Future work

7.4.1 Cellular localisation of UBP-1 and Kelch13 in *P. berghei*

P. falciparum Kelch13 tagged at the N-terminal localises to a discrete single punctum in ring stage parasites that spreads out into multiple puncta as the parasite progresses through the life cycle. These structures, called “cytostomes”, occur near to the parasites cytoplasmic periphery and tend to segregate into individual merozoites in developing and maturing schizonts (Birnbaum et al., 2020, Yang et al., 2019). Cytostomes are believed to play a role in facilitating invaginations of the parasites PM and PVM which delivers the hosts cytoplasmic components, most importantly, haemoglobin into the parasites DV (Bakar et al., 2010). More intriguingly, *P. falciparum* Kelch13 appears to act as an endocytic organiser of several proteins among which include UBP-1 and Eps15 which facilitate haemoglobin uptake and endocytosis in malaria parasites (Birnbaum et al., 2020). Parasites co-expressing fluorescent tagged Kelch13 with UBP-1, Eps15 or AP-2 μ also revealed a distinct overlap and co-localisation of these proteins into a distinct endocytic machinery that is devoid of clathrin in what is seemingly a clathrin independent endocytic pathway (Birnbaum et al., 2020). Are *P. berghei* Kelch13 or UBP-1 similarly conserved in their cellular localisation and co-expression?

Some of the future studies that would stem from this work would be to characterise the cellular localisation of the *P. berghei* Kelch13 and UBP-1 by fluorescent microscopy of fluorescently tagged parasites (N or C-terminally). Co-localisation of these proteins would be investigated by co-expressing them with different fluorescent markers in the same lines or other cell compartment markers especially in light of further observations that *P. falciparum* Kelch13 does not just localise to the cytostomes, but to other cellular structures such as the mitochondria, ER and several vesicular transport compartments (Gnädig et al., 2020, Siddiqui et al., 2020). Further investigations would also include co-immunoprecipitation of both *P. berghei* Kelch13 and UBP-1 to characterise the interacting partners. Overall, these outcomes would further help in establishing *P. berghei* as an even better model to understanding ARTs MOA and MOR.

7.4.2 Transmission competency and competitive release of drug resistance mutations in *P. berghei*

Drug resistance mutations in malaria parasites are often associated with fitness defects which can limit their spread in natural populations where a competitive suppression from wild type parasites would easily offer an evolutionary barrier. As demonstrated in Chapters 3 and 4, *P. berghei* parasites carrying Kelch13 or UBP-1 mutations do indeed suffer from significant growth defects. Would these fitness constraints limit the transmission of parasites carrying such mutations? As further demonstrated in Chapters 3 and 4, the effects of some of these mutations on malaria parasite growth are very significant to the extent that in the absence of drug, they are completely outcompeted within few days. However, this can be reversed when drug pressure is applied which would suggest that continued drug use can serve as an important driver through which certain drug resistance alleles (especially those with more pronounced fitness costs) can be maintained in natural circulation. This would be specifically important as in a previous study, it was demonstrated that *P. falciparum* Kelch13 ART resistance mutations offer no barrier to transmission to a wide variety of mosquito vectors (St Laurent et al., 2015).

With the availability of *P. berghei* lines that express fluorescent reporters in male and female gametocytes, further studies would involve introducing these mutations in such lines and assessing the specific physiological impacts of the mutations in these transmission stages. The transmission capacity of both UBP-1 and Kelch13 mutants in Chapters 3 and 4 could also be assessed in the absence and or presence of drug (AS) which would hopefully mirror the actual environmental conditions in the natural field settings. Moreover, in a large multi-site clinical study, patients carrying parasites with Kelch13 mutations seemingly carried more gametocytes both before and after drug treatment (Ashley et al., 2014). Whether these were biologically linked to Kelch13 mutations is unknown. *P. berghei* Kelch13 mutations in gametocyte fluorescent reporter lines could help in further unravelling such relationships. Crucially, most of the above scenarios assume that at one time point, a patient is infected with either a sensitive parasite or utmost a sensitive and resistant parasite. However, this can be far from simple. In complex natural environments, especially in areas of high malaria transmission, there is always a

high chance that a patient would be infected with parasites carrying more than one drug resistance mutation (Juliano et al., 2010). In such situations, if a patient is infected with wild type and say, more than one Kelch13 mutant parasites, the within host competition would favour wild type parasites as well as Kelch13 mutant parasites that are fitness neutral in what is called a competitive suppression (de Roode et al., 2004). In face of drug treatment, this competitive suppression could be alleviated resulting in a competitive release of mutant parasites which would accelerate the spread of drug resistance (Pollitt et al., 2014). *P. berghei* Kelch13 and UBP-1 mutant parasites generated in this work offer a unique opportunity to assess such relationships. The ability to use PCR-RFLP to discriminate the mutant lines and quantify mutant alleles would mean a mixture of wild type and up to four different mutant parasites can be mixed in a single host infection which would allow for assessment of the within host competition of different drug resistant alleles. These could also be carried out in the presence of drug to examine the extent to which, for instance, drug resistance alleles that are associated with minimal drug resistance phenotypes would behave when mixed with mutant parasites carrying alleles with significant fitness defects as well as strong drug resistance phenotypes. By further manipulating such parasites to introduce gametocyte specific fluorescent reporters, these relationships can be further analysed to examine the transmission dynamics and interplay in such complex situations.

7.4.3 Phenotypic heterogeneity of drug resistance mutants in *P. berghei*

Current *in vitro* assays for ART resistance rely on the RSA which defines ART resistance as ring stage survival of $\geq 1\%$ and ART sensitivity as survival of $< 1\%$ (Witkowski et al., 2013). This assay is technically challenging and can be subject to high levels of intra-lab variations even between the same parasite isolates (Ariey et al., 2014, Straimer et al., 2015). As demonstrated in Chapter 4, the adapted RSA in *P. berghei* results in significant survival in M488I and R551T mutant parasites as compared to the wild type. Nevertheless, in both *P. falciparum* and *P. berghei* Kelch13 mutant parasites, ART resistance (as measured by % survival) does not result in absolute or 100% survival rates. Basically, in isogenic parasite populations that differ only by a single SNP, why does ART survival occur only in a fraction of the parasites (~13% survival when *P. falciparum* C580Y is introduced in PfNF54 vs $< 1\%$ in parent wild type or ~38%

survival for M488I mutants in *P. berghei* vs ~21% in parent wild type) while the majority of the population remains sensitive? Despite the observations that Kelch13 mutant parasites are associated with an upregulation of genes involved in the stress response pathways (Mok et al., 2015) which could possibly explain such observations, population level transcriptomics cannot precisely deconvolute such phenotypic differences. Further work with these *P. berghei* Kelch13, and possibly UBP-1 mutant parasites would be to capture these levels of phenotypic heterogeneities by using single cell transcriptomics on mutant parasites exposed or not exposed to drug under *in vivo* conditions.

8 Appendix

8.1 Appendix figures for chapter 2

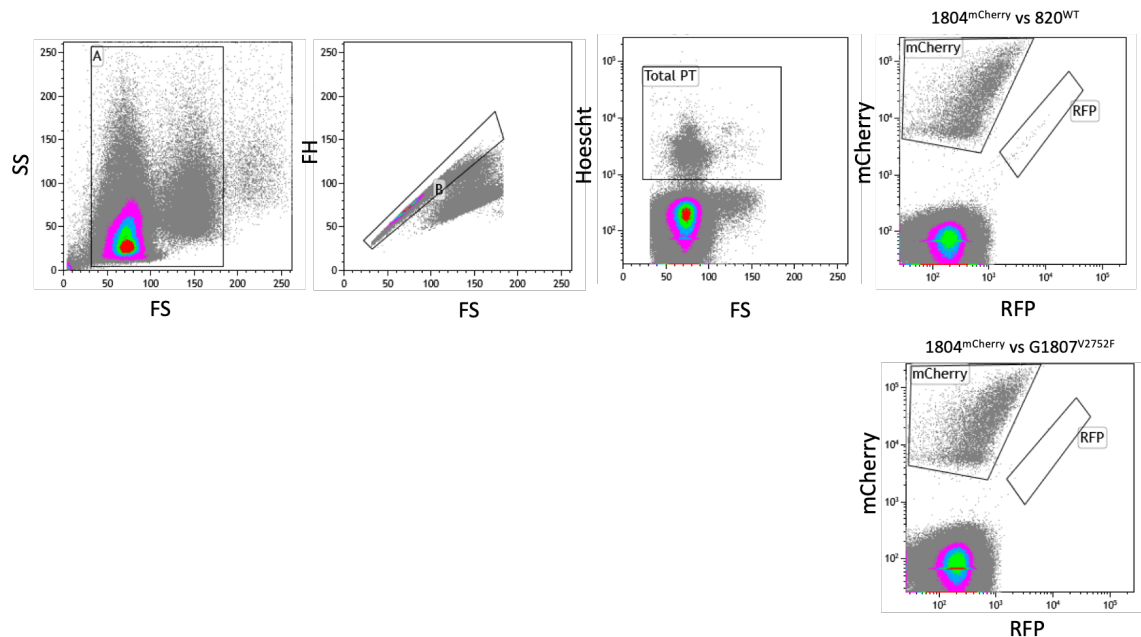


Figure 8.1: Flow cytometry gating strategy for growth competition experiments.

Representative flow cytometry gating strategies for growth competitions of wild type and mutant UBP-1 lines on Day 3. Acquired events were plotted on a forward (FS) and side (SS) scatter. Gate A was drawn to exclude debris. Events from gate A were plotted on a FS vs FH where gate B was drawn to exclude cell clumps and potential doublets. Events from gate B were then plotted on Hoescht vs FS and Total PT gate was drawn to quantify total parasitaemia. Events from gate B were also plotted on mCherry vs RFP where the mCherry positive population was distinguished from RFP positive female gametocytes by applying compensation spill-over filters that allow discrimination of the two colours as illustrated in the plots. Parasitaemia of mutant parasites was quantified by subtracting the mCherry positive population from the total parasitaemia as quantified by Hoescht staining of parasite DNA.

	V3275F, V2697F	
PF3D7_0104300	NSELDYFL EEIKSFFKNMLTTDKSYISADRVLNMLPVELNNRNQQQMTVEVFRYIFDKLGG	3288
PCHAS_0207200	NLLSKRFLYLKILFKLMTTNNKKYVSPDNILGILPQLNLRNQQTTELFRTYFEQLGG	2710
PBANKA_0208800	NLLSKRFLYLKILFKLMSTTNKKYVSPYSILSLPQLNLRNQQTTELFRTYFEQLGG	2734
	* . * *: * * * * * : * : * *	
	V3306F, V2728F	V2721F
PF3D7_0104300	SEKEFLRLIFSGVVIQMQCQCLFISKKEEIIHDLSPVPPISTNEKL SIQRFFDTFIQK	3348
PCHAS_0207200	SEKKFLRLIFSGVVIQMQCQCF FISKKEEIIHDL SFHPAKSSKKQS IQKFDDTYIQK	2770
PBANKA_0208800	SEKRFLRLIFSGVVIQMQCQCF FISKKEEIIHDL SFHPAKSTKKESI QKFDDTYIQK	2794
	** * : * * * * * : * * * * * * * : * : * * * : * * * :	
	V2752F	
PF3D7_0104300	EKIYGNNKYKCSRCNKRRNALKWNEIISPCHLILILNRYNW SFSSENEKKKIKTHVKINS	3408
PCHAS_0207200	EKIYGNNKYKCSCKNKR RNAL KWNEIISPCHLILILNRYNW SFSSENEKKKIKTHVKINK	2830
PBANKA_0208800	EKIYGNNKYKCSCKNKR RNAL KWNEIISPCHLILILNRYNW SFTSNEKKKIKTHVKINK	2854
	***** : * * : ***** : ***** :	
PF3D7_0104300	KIVVNNFDYKLYGAIIHGGISASSGHYYFIGKKSERQNKKSSWYQMND SVTKANSKMI	3468
PCHAS_0207200	KIVVNNFDYRL YGGI IHSGV SAS SGHY YFIG KKS EKGDS NKNEWYQMD DSAITKVSSKSI	2890
PBANKA_0208800	KIVVNNFDYKLYGGI IHSGV SAS SGHY YFIG KKS EKCDNS KNEWYQMD DSVITKVSSKSI	2914
	***** : * * * * * : * * * * * : * : * * * * * : * * * * *	
PF3D7_0104300	NKISKDLSNDHTPYVLFYRCKQAPISPDLYF	3499
PCHAS_0207200	NRISKDP SNDH TPYVLFYRCKQAPDSPSLYF	2921
PBANKA_0208800	NRISKDLSNDHTPYVLFYRCKQAPVPSLYF	2945
	* . *	

Figure 8.2: Sequence alignment of *P. falciparum*, *P. chabaudi* and *P. berghei* UBP-1 at the conserved C-terminal. Mutation sites are indicated for *P. falciparum* and *P. chabaudi* on top and *P. berghei* on the bottom. Conserved sites are indicated by the * symbol.

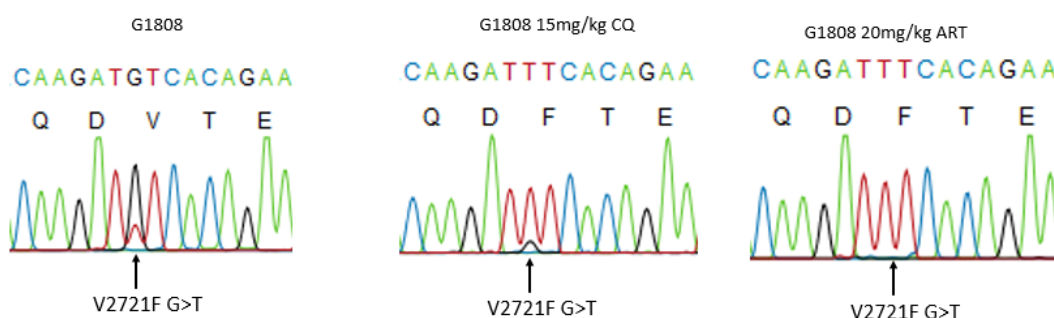


Figure 8.3: Enrichment of the G1808 line with CQ and ART. DNA sequencing and trace analysis of CQ and ART challenged G1808 lines (Figure 3.2a) showing enrichment of the V2721F mutation by both drugs.

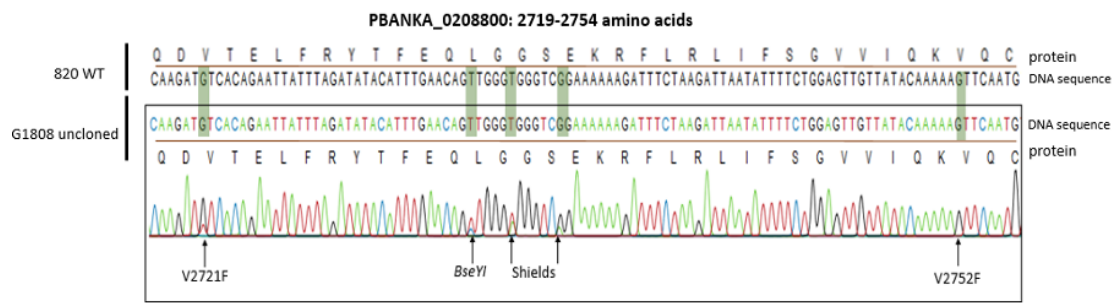


Figure 8.4: DNA sequence analysis of the G1808 uncloned line compared to the parent wild type showing the presence of traces for the V2721F mutation and absence of double mutants.

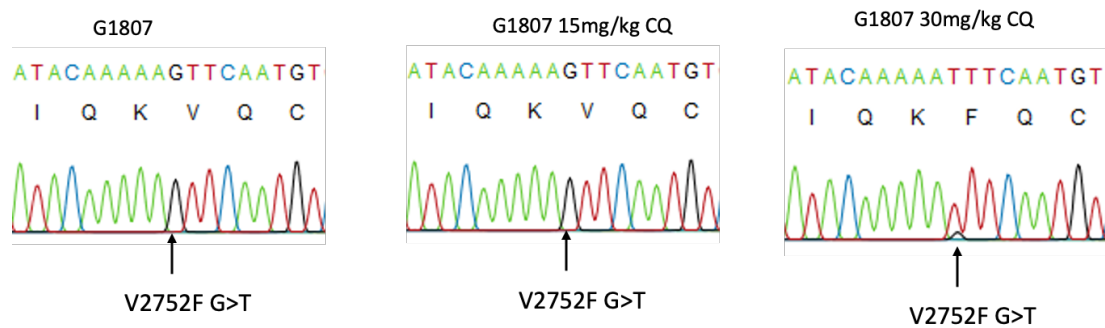


Figure 8.5: Enrichment of the G1807 line with CQ. DNA sequence and trace analysis of the G1807 recrudescence parasites in Figures 3.2a, 3.2e showing enrichment with CQ at 30 mg/kg.

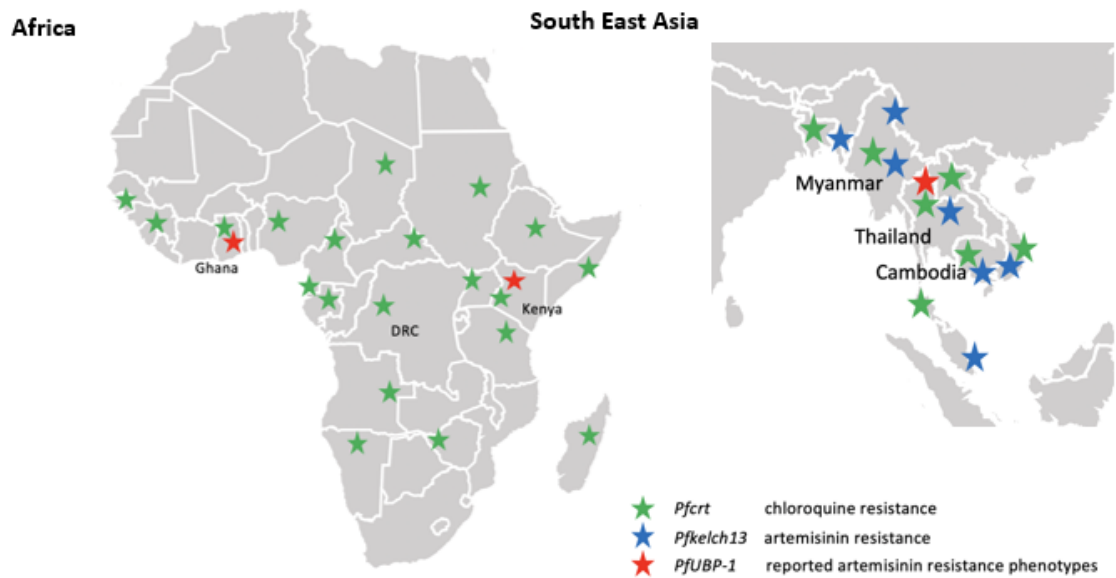


Figure 8.6: Distribution of ART and CQ resistance mutations in Africa and South East Asia. CQ resistance is believed to have originated in SEA and some parts of South America and eventually spread to Africa (Ecker et al., 2012). Current distribution of Kelch13 mutations in SEA (Mbengue et al., 2015, Ashley et al., 2014, Menard et al., 2016) and reported UBP-1 polymorphisms (Cerqueira et al., 2017, Adams et al., 2018, Henriques et al., 2014, Borrmann et al., 2013) .

8.3 Appendix figures for chapter 4

PF3D7_1343700.1	MEGEKVKTKANSISNFSMTYDRESGGNSNSDDKSGSSSEENDSNFNMNLTSDKNEKTENN	60
PBANKA_1356700.1	--MEDDKIKSNSISNFSVTYERESGNSNSSEERDMSSDENESLYMNLTGDKNEKIEDN--	57
	* *	
PF3D7_1343700.1	FLLNNSSYGNVKDSLLESIDMSVLDNSFDSKKDFLPSNLSRTFNMSKDNIGNKYLKLL	120
PBANKA_1356700.1	-----SSFVNIKDSLLESIDLSDNSFDSKNDFLPNNFSGKLNNTKDNINNLYLNKYL	112
	* *	
PF3D7_1343700.1	NKKKDTITNENNN---INHN---NNNNLTANNI-----TNNLINNNMNSPSIMN	164
PBANKA_1356700.1	NKNDSAFMAMNKDNNSIDLNSLVSNNNLGNNIIVSNDGGNKNMHVIGNNNINGSTGAP	172
	* *	
PF3D7_1343700.1	TNKKENFLDA---ANLINDDSGLNNLKFFSTVNNVNDTYEKKIIETELSDASDFENMVG	220
PBANKA_1356700.1	TNKKEIFMDSGASSINMNEEDNSTMHNIRIYKNTNNINDTYEKKIIETELSDSSDFENMVG	232
	* *	
PF3D7_1343700.1	DLRITFINWLKKTQMNFIREDKLFKDKKELEMERVRLYKELENKKNIEEQKLHDERKKL	280
PBANKA_1356700.1	DLRITFINWLKKTQMNFIREDKLFKDKKELEMERIRLYKEIENKKAIEEQKLQDERKKL	292
	* *	
PF3D7_1343700.1	DIDISNGYKQIKKEKEEHKRRFDEERLRLQEIQIKIKLVLYLEKEKYQYKFNENDKKK	340
PBANKA_1356700.1	DIDISNGYKQIKKEKEEHKRRFDEERLRLQEIQIKIKLVLYLEKEKYQYKFNENDKKK	352
	* *	
PF3D7_1343700.1	IVDANIATETMIDINVGAIFETSRLTLTQQKDSFIEKLLSGRHHVTRDKQGRIFLDRDS	400
PBANKA_1356700.1	IVDANIATETMIDINVGGALFETSRLTLTQQKDSFIEKLLSGRYHITRDKQGRIFLDRDS	412
	* *	
	F446I	
PF3D7_1343700.1	ELFRIIILNFLRNPLTIPIPKDLSESEALLKEAEFYGIKFLPFPPLVFCIGGFDGVEYLN	460
PBANKA_1356700.1	ELFRIIILNFLRNPLTIPIPKDLSESEALLKEAEFYGIKFLPFPPLVFCIGGFDGVEYLN	472
	* *	
	M476I Y493H	
PF3D7_1343700.1	ELLDISQQCWRMCTPMSTKKAYFGSAVLNLFVFGGNNYDYKALFETEVYDRLRD	520
PBANKA_1356700.1	ELLDISQQCWRMCTPMSTKKAYFGSAVLNLFVFGGNNYDYKALFETEVYDRLRD	532
	* *	
	R539T I543T C580Y	
PF3D7_1343700.1	SSNLNIPRRNCGVTSNGRIYCIIGYDGSSIIPNVEAYDHRMKAWVEAPLNTPRSSAM	580
PBANKA_1356700.1	SSNLNIPRRNCGITSNGRIYCIIGYDGSSIIPNVEAYDHRMKAWIEVAPLNTPRSSAM	592
	* *	
PF3D7_1343700.1	VAFDNKIYVIGGTNGERLNSIEVYEEKMKWEQFPYALLEARSSGAIFYNLQIYVVG	640
PBANKA_1356700.1	VAFDNKIYVVGANGERLNSIEVYDEKMKWENFPYALLEARSSGAIFYNLQIYVVG	652
	* *	
PF3D7_1343700.1	DNEHNILDSVEQYQPFNKRQFLNGVPEKKMNFGAATLSDSYIITGGENGVDLNSCH	700
PBANKA_1356700.1	DNEHNILESVEQYQPFNKRQFLNGIPEKKMNFGATLSDSYIITGGENGVDLNSCH	712
	* *	
PF3D7_1343700.1	PDTNEWQLGPSLLVPRFGHSLVLIANI	726
PBANKA_1356700.1	PDTNEWQIGPPLLVPFRGHSLVLIANI	738
	* *	

Figure 8.7: Protein alignment of *P. falciparum* and *P. berghei* Kelch13 showing conservation at the mutation sites. Alignments were carried out using Clustal Omega protein alignment tool. Conserved sites are indicated by *

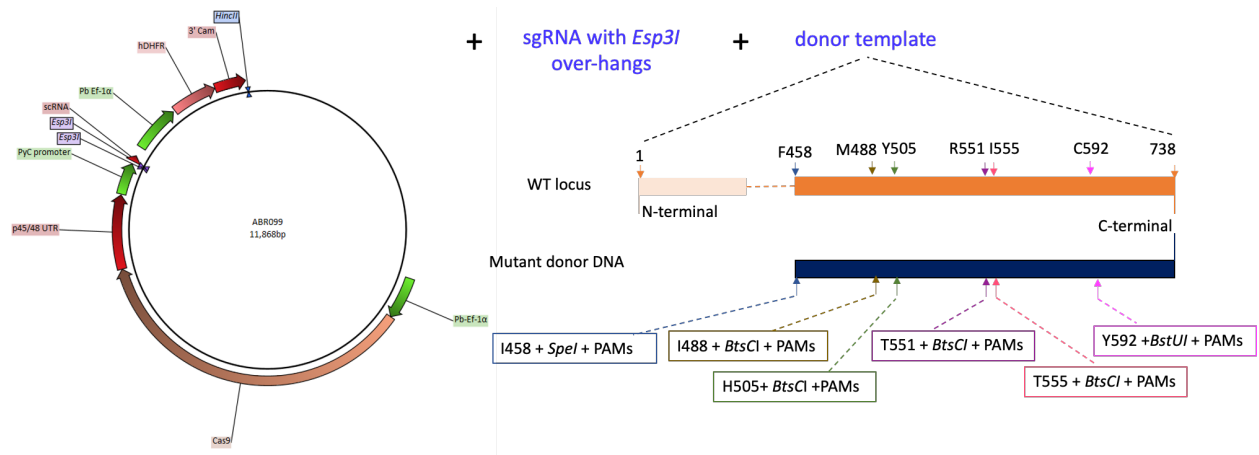
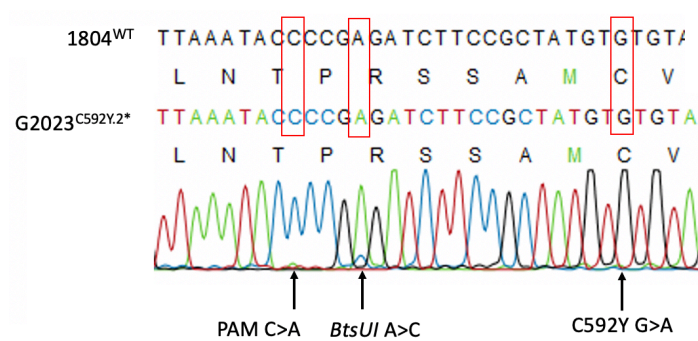
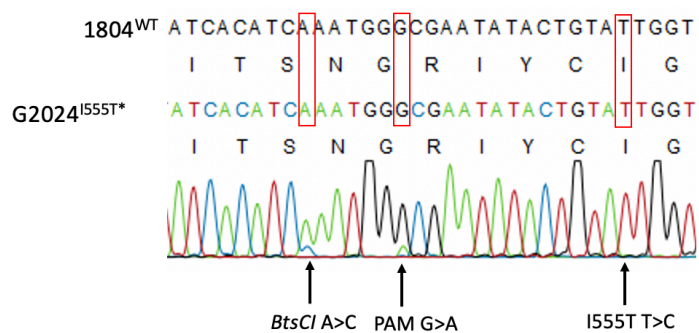


Figure 8.8: Schematic of the CRISPR-Cas9 strategy used to introduce Kelch13 mutations in *P. berghei*. 20bp sgRNA targeting regions within 0-30 bp of the mutation site (Appendix Table 8.1, 8.2) were designed to contain *Esp3I* digestion overhangs and cloned into the illustrated Cas9 plasmid, ABR099, as previously described in section 3.3.1. Donor templates were generated by overlapping extension PCR as described in methods and subsequently cloned into the ABR099 plasmids carrying the appropriate sgRNA (Appendix Table 8.1, 8.2) at the *HincII* linker site. The donor templates carried the mutation of interest as well as silent mutations to introduce a restriction site for RFLP analysis and to inactivate the PAM site recognition sequence (as illustrated in the schematic). Details of plasmids, sgRNA and lines generated are shown in Appendix Tables 8.1, 8.2, 8.3.

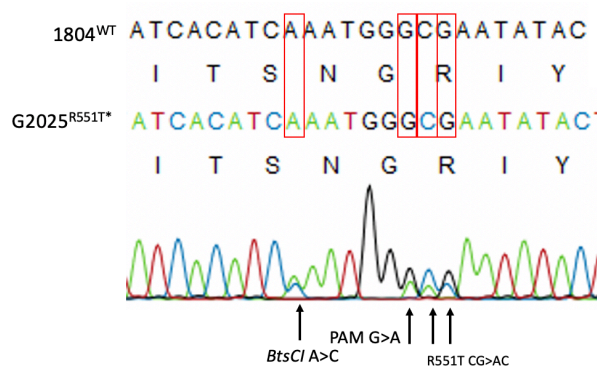
a



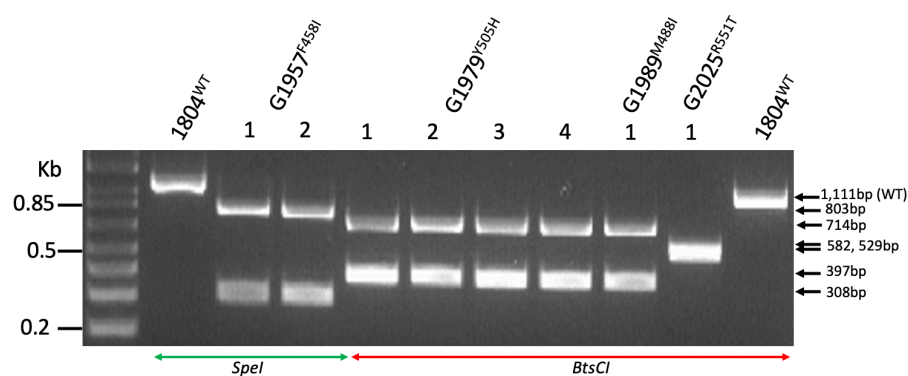
b



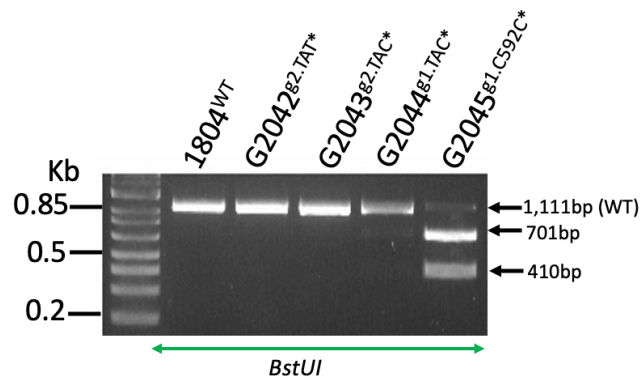
C



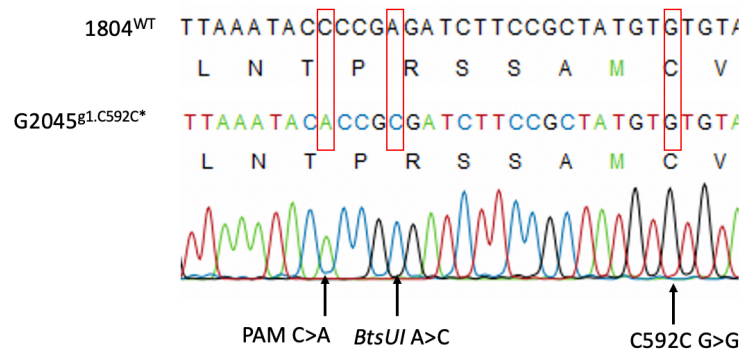
d



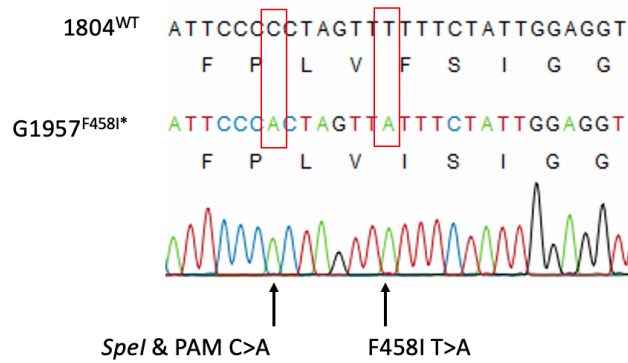
e



f



g



h



i

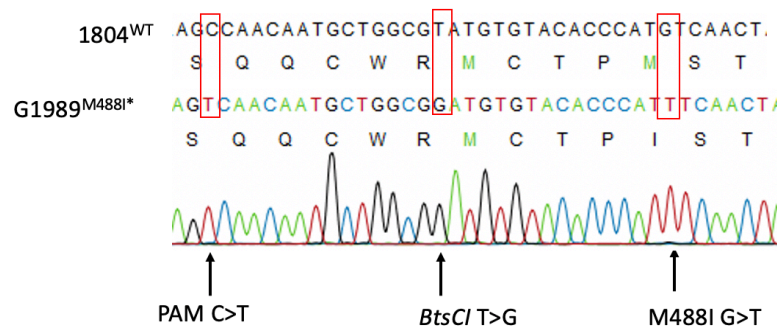
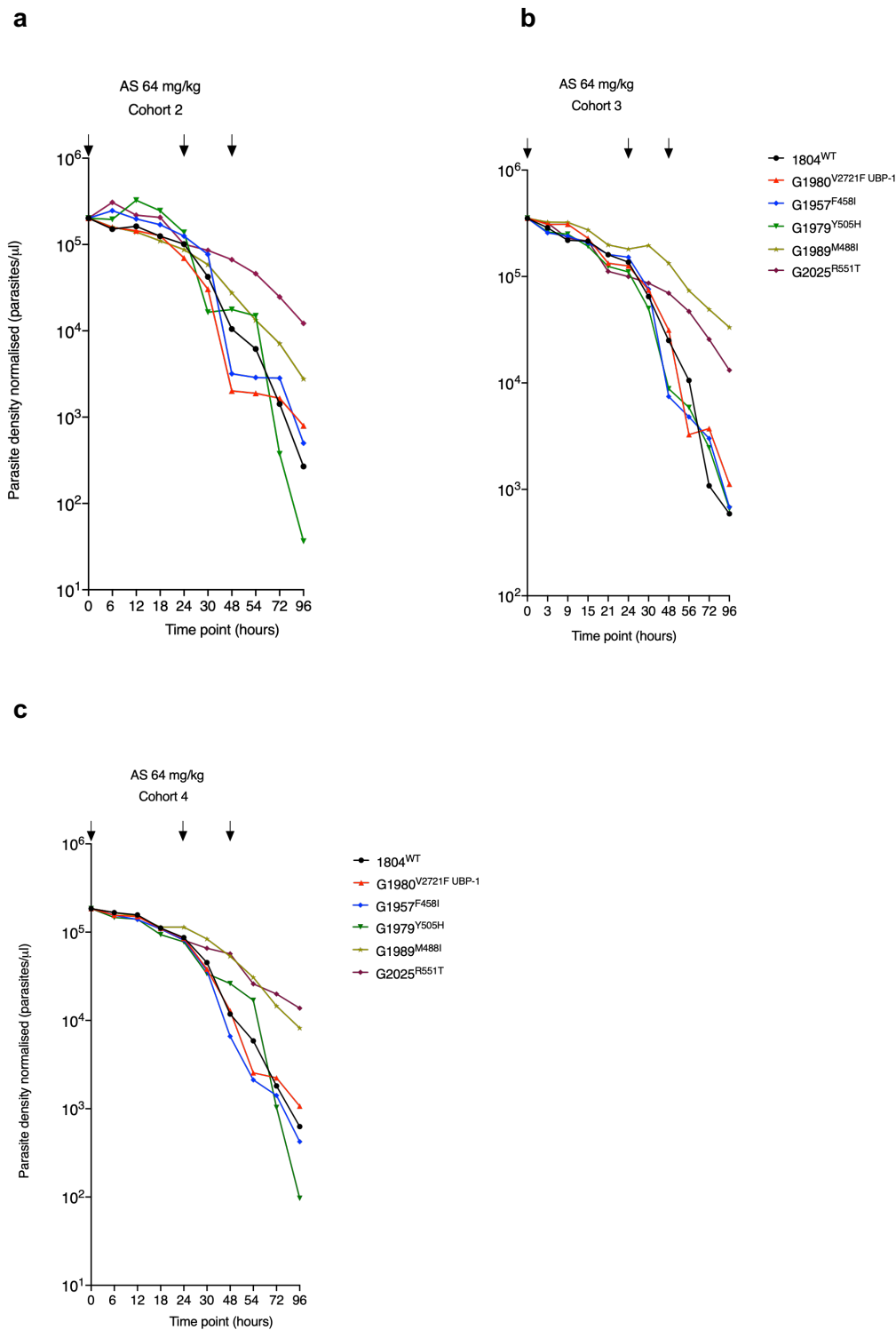


Figure 8.9: DNA sequence and RFLP analysis of *P. berghei* Kelch13 mutant lines a, b. DNA sequencing showing the absence of the C592Y and I555T nucleotide substitutions and the presence of minor traces of the silent mutations in the G2023 (a) and G2024 (b) transfected lines. **c.** Sequencing analysis of the G2025 line showing the presence of traces for both the silent mutations and the R551T substitution in the original transfection. * on the transfectant parasite lines indicates that the line is uncloned. **d.** RFLP analysis with indicated restriction enzymes for the cloned parasite lines; G1957 (F458I), G1979 (Y505H), G1989 (M488I) and G2025 (R551T, AS 64 mg/kg). **e.** RFLP analysis of the G2042 (C592Y, sgRNA 2, TAT codon), G2043 (C592Y, sgRNA 2, TAC codon) and G2044 (C592Y, sgRNA 1, TAC codon) transfected lines (Appendix Table 8.2, 8.3), showing further unsuccessful attempt to introduce the C592Y in *P. berghei*. RFLP analysis of the G2045 control line (C592C, sgRNA 1, silent mutations control) where editing was readily achieved is shown for comparison. **f.** Sequencing analysis of the G2045 line showing successful editing with high efficiency to introduce silent mutations without the C592Y substitution. **g-i.** DNA sequence analysis showing high efficiency editing to introduce silent mutations and mutations of interest in the G1957 (F458I; **g**), G1979 (Y505H; **h**) and G1989 (M488I; **i**) lines.



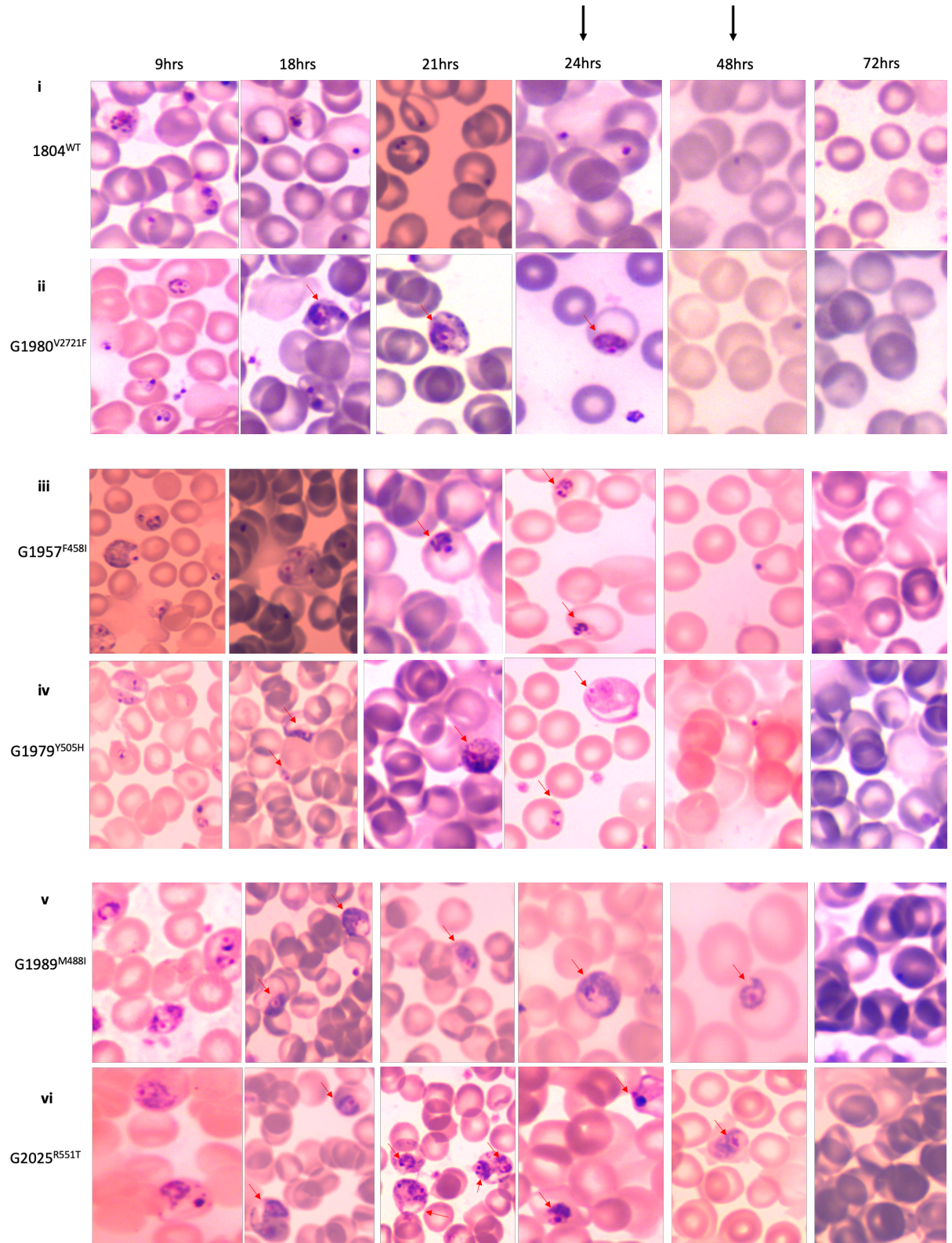
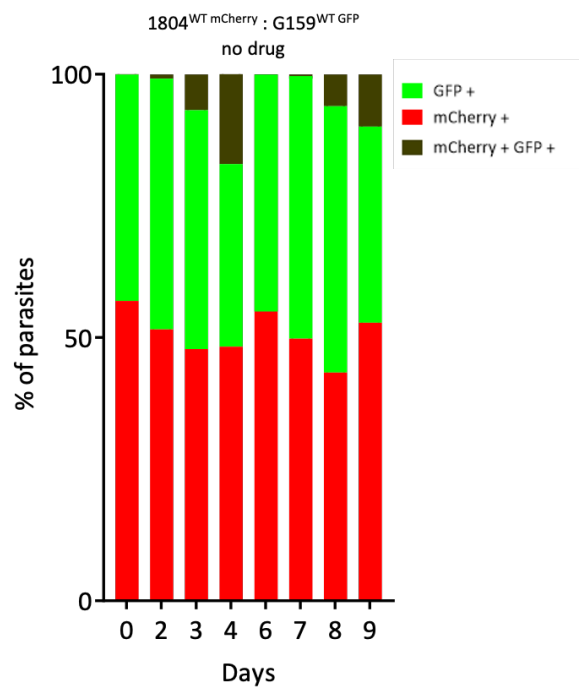
d

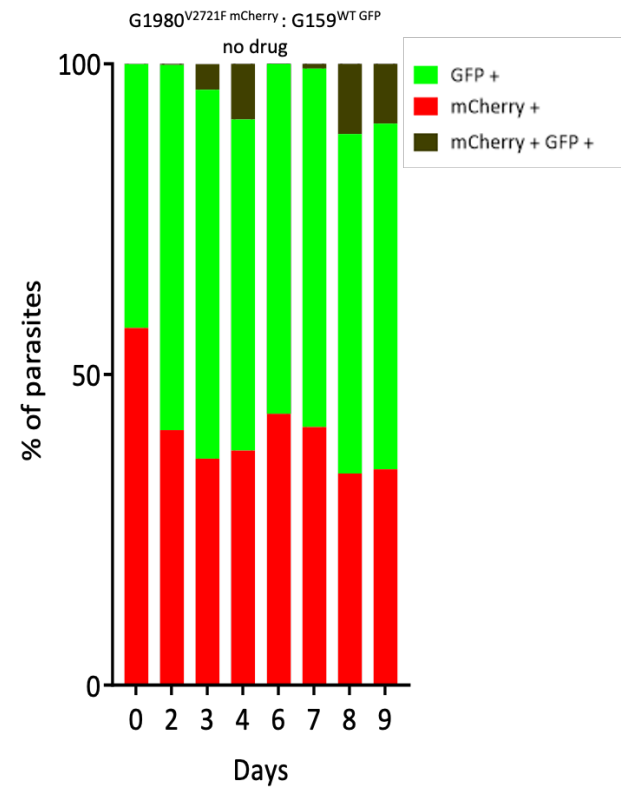
Figure 8.10: Clearance kinetics and microscopy analysis of *P. berghei* Kelch13 mutants upon AS treatment. a, b, c. Parasite clearance curves in mice with established parasitemia's of Kelch13 mutant lines following treatment with AS at 64 mg/kg for cohorts 2, 3 and 4 as described in Figure 4.4a. d. Microscopic analysis of Giemsa-stained thin blood smears showing preferential survival of UB1-1 (ii) and Kelch13 mutant parasites;

G1957^{F458I} (iii), G1979^{Y505H} (iv) , G1989^{M488I} (v) and G2025^{R551T} (v) as compared to wild type parasites (i) upon treatment with AS for cohorts 3 and 4. Smears were collected and analyzed as described in Figure 4.4b.

a



b



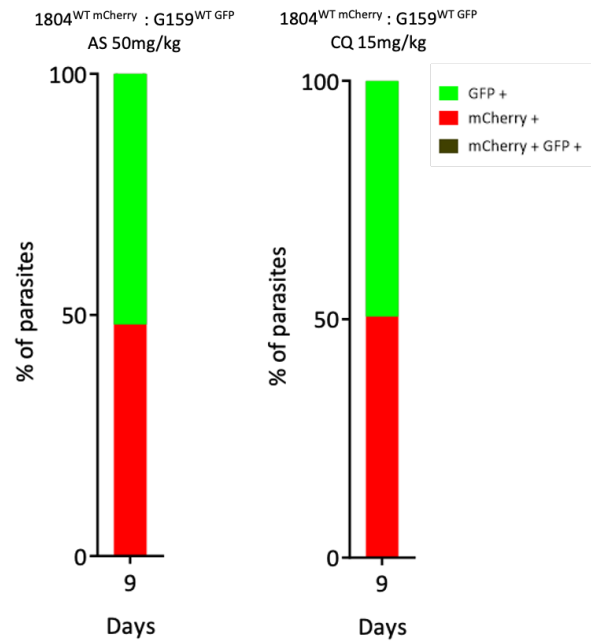
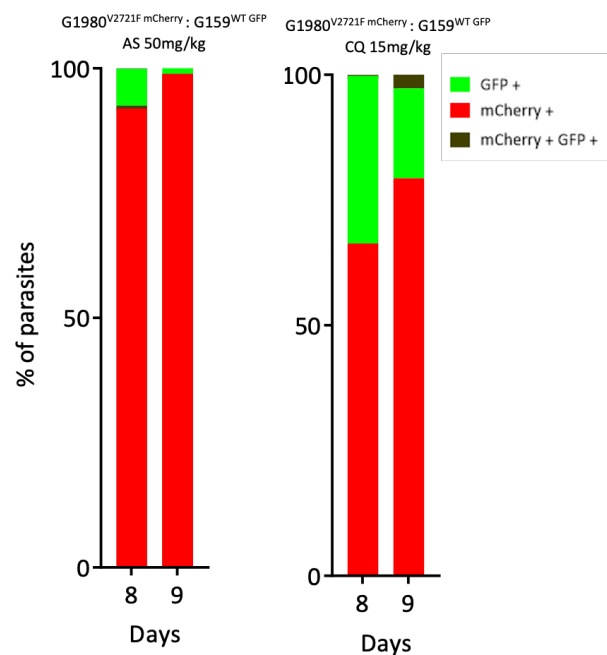
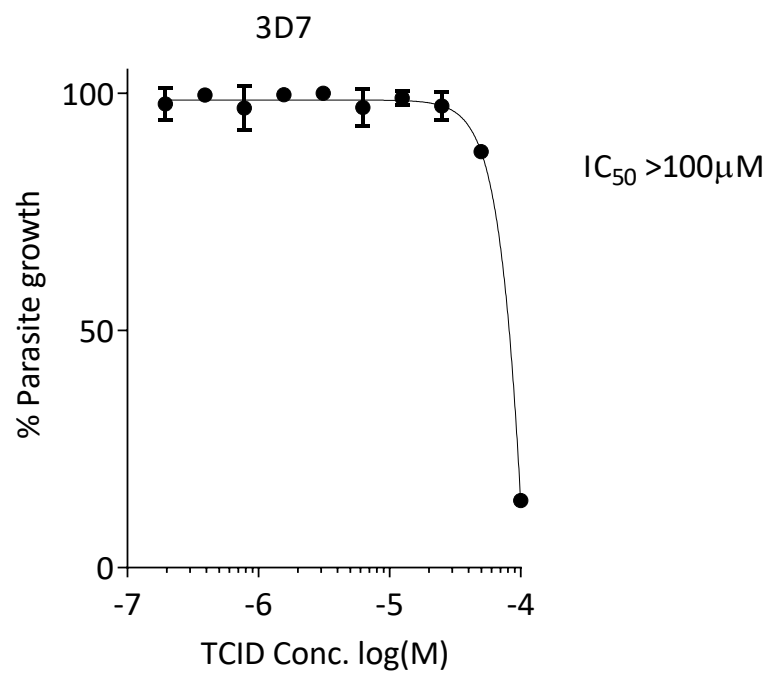
c**d**

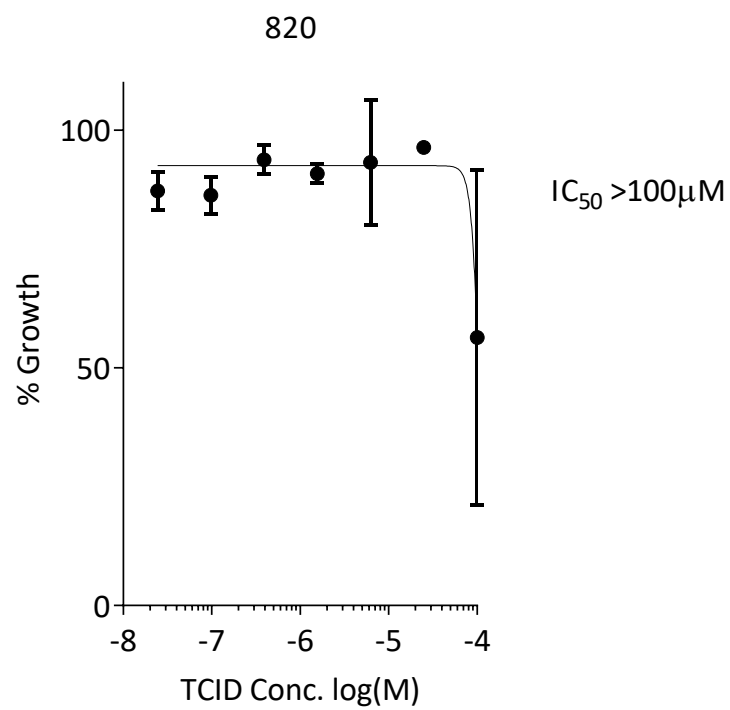
Figure 8.11: Growth competition of the parent 1804^{WT} and UBP-1 V2721F mutant line as compared to the G159^{WT} in the presence or absence of AS or CQ drug pressure. Parasites were mixed at a 1:1 ratio, injected into mice and left treated or untreated with AS at 50 mg/kg or CQ at 15 mg/kg. **a.** Percentage population changes of the 1804^{WT} and wild type G159^{WT} in the absence of drug. **b.** Proportion representation of the G159^{WT} line in mixture with G1980^{V2721F} in the absence of drug. **c, d.** Proportion representation of the 1804^{WT} (**c**) or G1980^{V2721F} (**d**) as compared to the G159^{WT} line upon AS or CQ treatment on the days of recrudescence.

8.4 Appendix figures for chapter 5

a



b



c

```

sp|P15374.1|UCHL3_HUMAN      -MEGQRWLPLEANPEVTNQFLKQLGLHPNWQFVDVYGMDFELLSMVPRPVCVALLFPIT      59
PBANKA_1324100.1             MTKKKKWIPIESNPDSLYLYSCKLGQ-QKLSFVDIYGFNKDLLDMIPQPVHAIIFLYPIK      59
PF3D7_1460400.1             MAKNDIWTPLESNPDSLYLYSCKLGQ-SKLKFPVDIYGFNNDLDMIPQPVQAVIFLYPVN      59
PVP01_1246400.1             MLRNNVWVPIESNPALYLYSCKLGQ-TKLAFQDIYGFDAELLDMPQPVHAIILLYPLK      59
PKNH_1221300.1              MLRNNIWPVIESNPESLYLYSCKLGQ-TKLIFQDIYGFDAELLDMPQPVHAIILLYPLK      59
                               . . * *:***: : **: : * *:***: **:***:***:***:***:***:***:***:
                               . . * *:***: : **: : * *:***: **:***:***:***:***:***:***:***:

sp|P15374.1|UCHL3_HUMAN      EKYEVFRTEEEKIKSQGDVTSSVYFMKQTISNACGTIGLIHAIANNKDKMHFESGSTL      119
PBANKA_1324100.1             DDIDNSIGSSH----INTNGDINIWFIKQTVSNSCGTIALLHLFANLRNTFPLDKDSVL      115
PF3D7_1460400.1             DNIVSENNTND---KHNLEKFNPNVFIKQYIPNSCGTIALLHLYGNLRNKFELDKDSVL      116
PVP01_1246400.1             EGMVTPNAATD---GSAEQNIDNIWFIKQVVPNSCGTVALFHLVGNLRNKFELDKDSLL      115
PKNH_1221300.1              EGMINPNDEAN---GSTEQNVENIWFIKQIVPNSCGTVALFHLVGNLRNKFELDKDSLL      115
                               : . . . : . : * *:***: : * *:***:***:***:***:***:***:***:

sp|P15374.1|UCHL3_HUMAN      KKFLEESVSMSPPEARARYLENYDAIRVTHETSAHEGQTEAPSIDEKVDLHFIALVHVDGH      179
PBANKA_1324100.1             DTFFTKVDNLKPEGRALEFENNDIEQLHHEF--SGNELNLGESIDVDTHFIVFLEINGM      173
PF3D7_1460400.1             DDFFNKVNEMSAEKRGQELKNNKSIENLHHEF--CGQVENDDILDVDTHFIVFVQIEGK      174
PVP01_1246400.1             ANFFDKVKDMSPEKRGQEFVKNKSIENLHHEF--SGKSSGTGDDIDVDTHFIVFLEIDGR      173
PKNH_1221300.1              ANFFDRVKDMTPKRGKFEVKNKSIENLHHEF--SGKASGTGDDIDVDTHFIVFVEIDGK      173
                               * : . . : * * . : : . * * . * : . . * * * * * : * : *

sp|P15374.1|UCHL3_HUMAN      LYELDGRKFPPINHGSETLLEDAI-EVCKKFMERDPDELRFNAIALSAA----- 230
PBANKA_1324100.1             LIELDGRKNHPIIHGQTTSNNFVYDAGKLIQDNFISKYQDCHSFSIAIIVPNNAV--- 228
PF3D7_1460400.1             IIELDGRKDHPVHCFVTNGDNFLYDTGKIIQDKFIEKCKDDLRFSAIAVVPNDNFII 232
PVP01_1246400.1             LVELDGRKDHPIVHCPTTPASFYDTGSGVIQKFFIEKCEDDNRFSAIAVVSDDVV--- 228
PKNH_1221300.1              LVELDGRKDNPIVHCTTTPATFKYDTGNIKKKFFIEKCGQDNRFSAIAVVSDDVV--- 228
                               : ***** * * * . : : * : : . : * : * : * : * : * : * : *

```

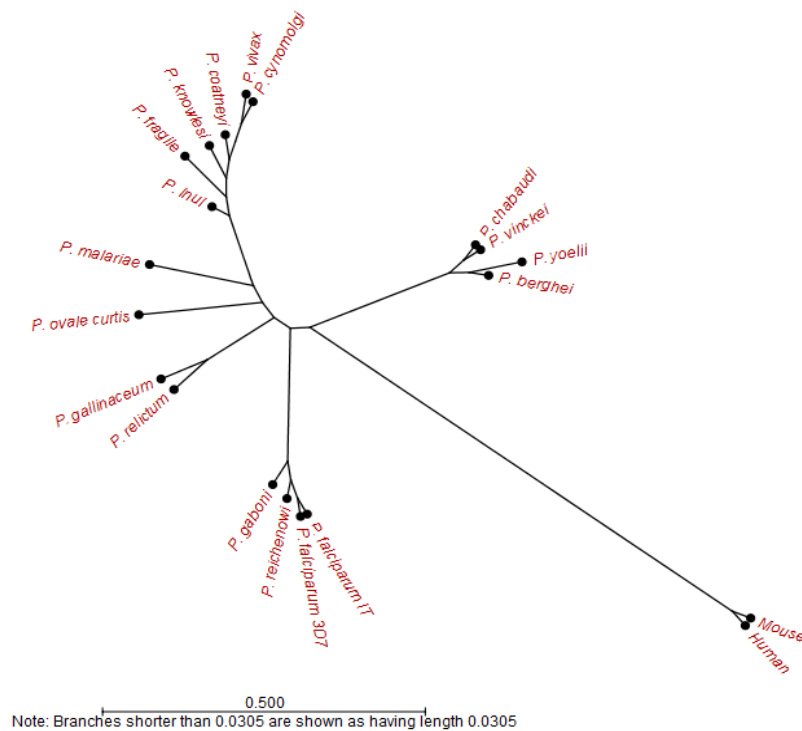
d

Figure 8.12: UCH-L3 inhibitor displays no activity in malaria parasites. a, b. Selected growth inhibition plots of TCID in 3D7 (**a**) and 820 line (**b**). **c.** Amino acid sequence alignment of indicated *Plasmodium* spp. UCH-L3 against human UCH-L3. Conserved residues across human and *Plasmodium* UCH-L3s are indicated by asterisks. **d.** Phylogenetic tree of human, mouse and *Plasmodium* UCH-L3 predicted protein sequences showing their evolutionary divergence.

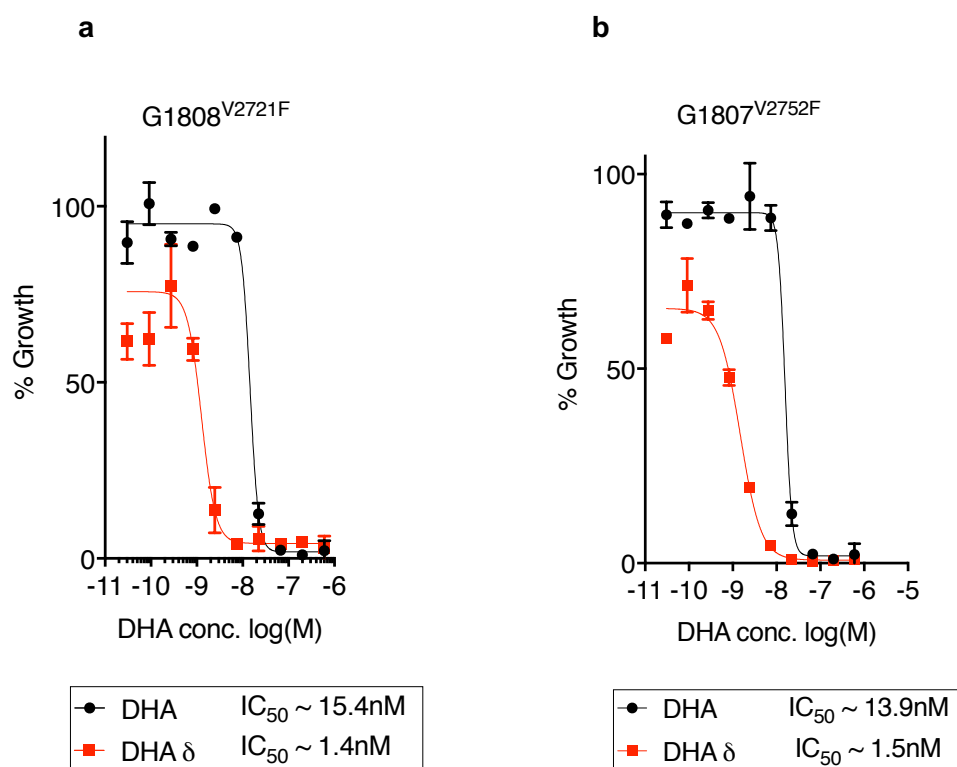


Figure 8.13: b-AP15 potentiates DHA action in UB-P-1 G1808^{V2721F} and G1807^{V2752F} mutant lines. **a, b.** Dose response curves and IC_{50} values of DHA alone or combined with b-AP15 at IC_{50} (DHA δ) in the UB-P-1 G1808^{V2721F} (**a**) and G1807^{V2752F} (**b**) UB-P-1 mutant lines.

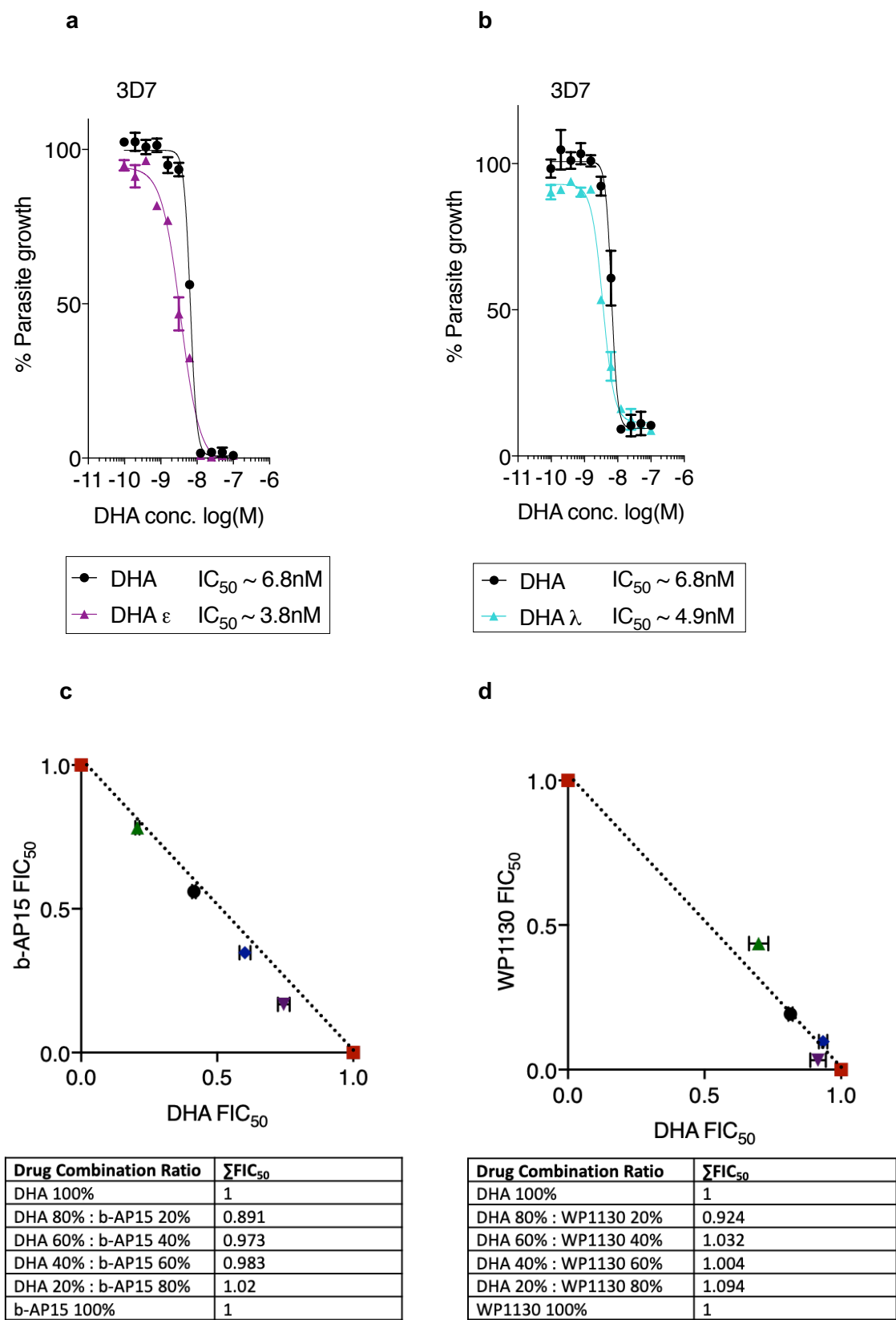
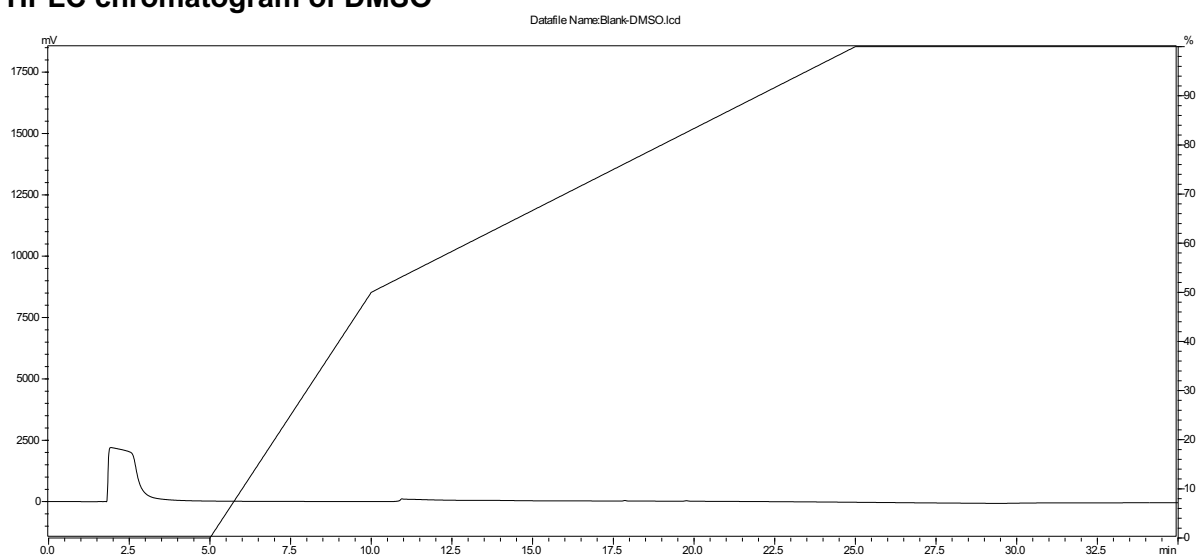
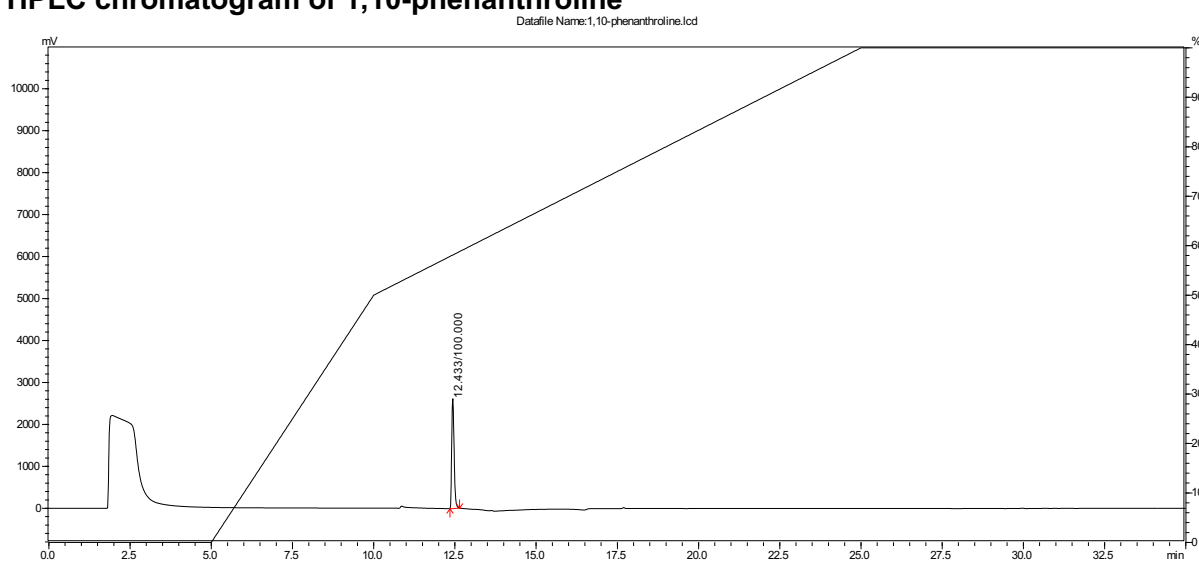
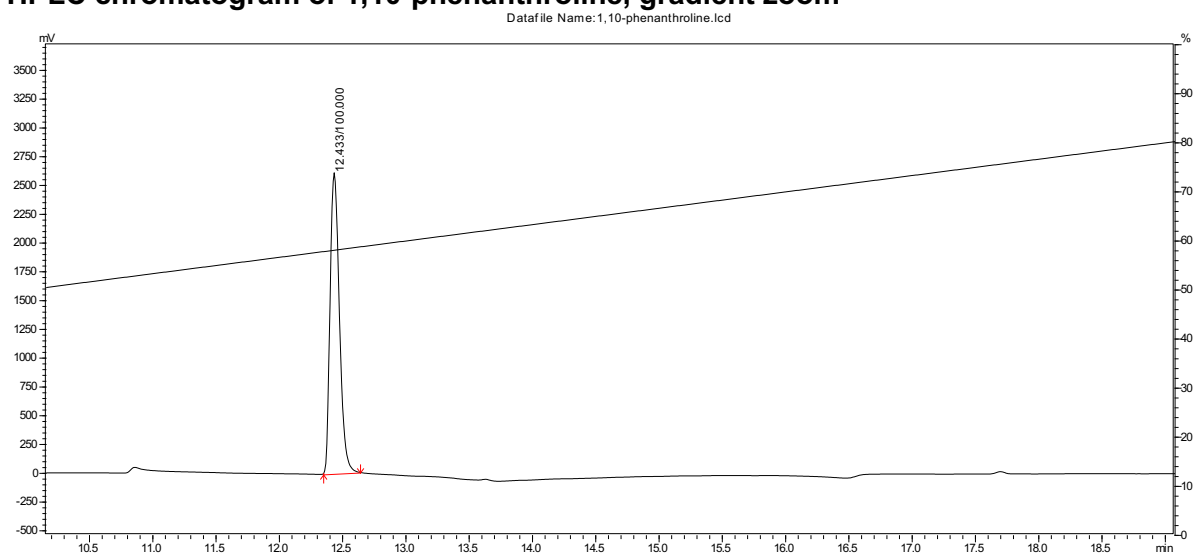
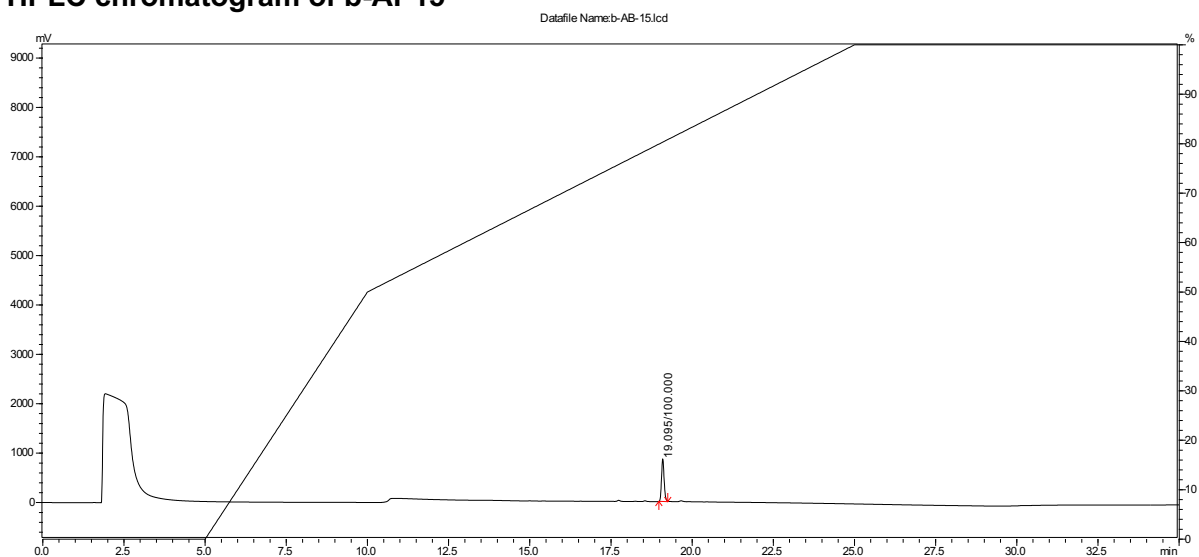


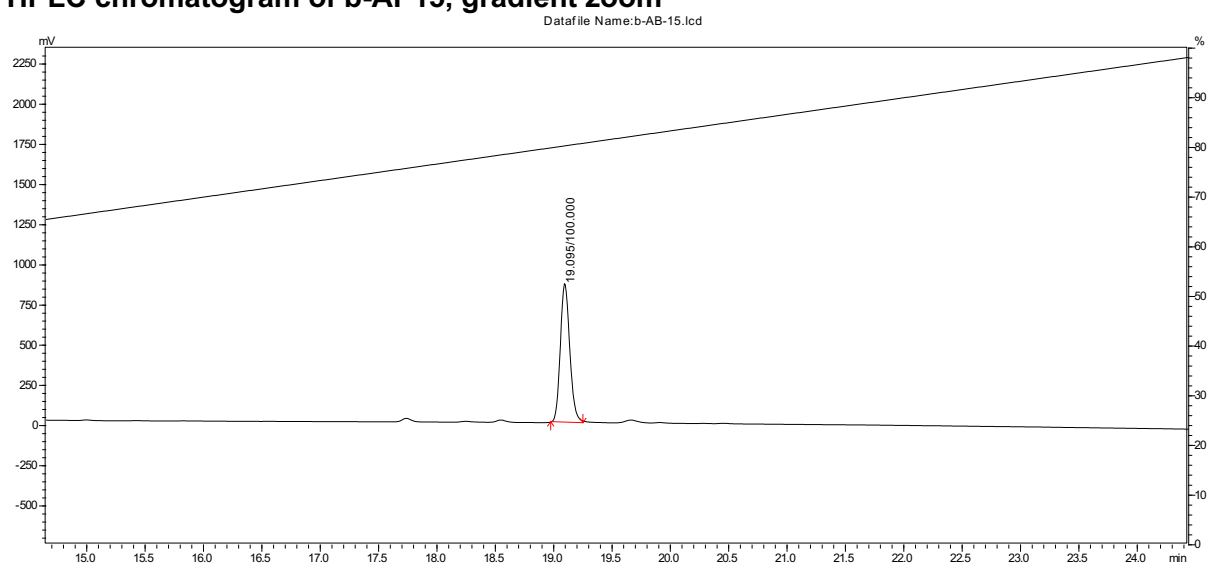
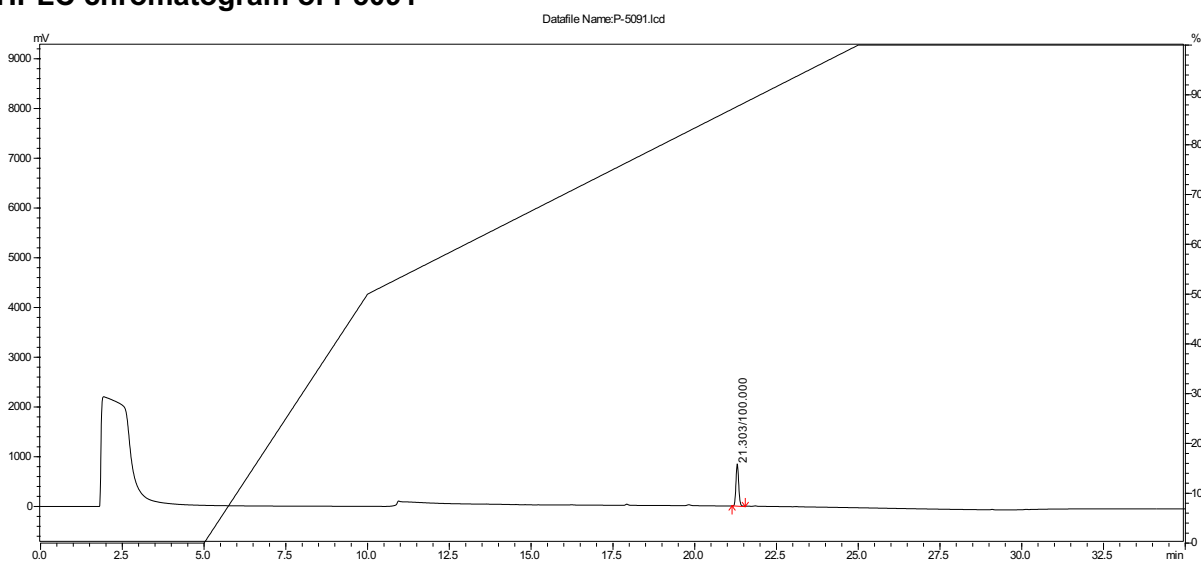
Figure 8.14: Interaction of DHA and WP1130, PR-619 and b-AP15. **a, b.** Dose response curves and IC_{50} values of DHA alone or combined with WP1130 (DHA ϵ) (**a**) or PR-619 (DHA λ) (**b**) at IC_{50} concentration in the *P. falciparum* 3D7 line. **c, d.** Isobologram plots of DHA in combination with b-AP15 (**c**) and WP1130 (**d**) and their raw ΣFIC_{50} values. ΣFIC_{50} values, plotted FIC_{50} s and error bars are means and standard deviations from three biological repeats.

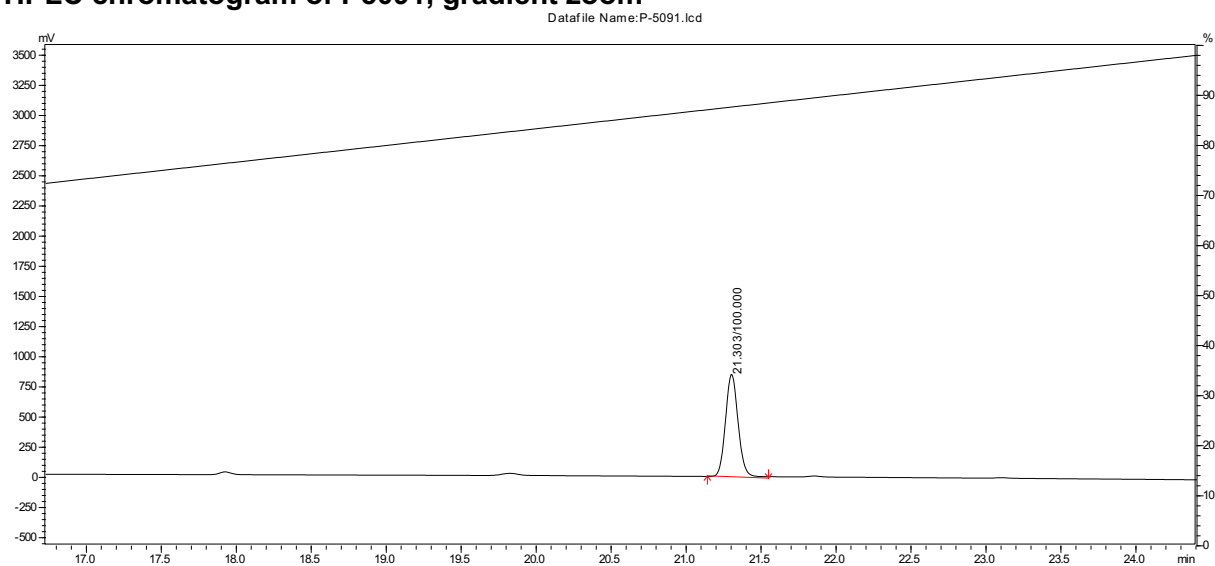
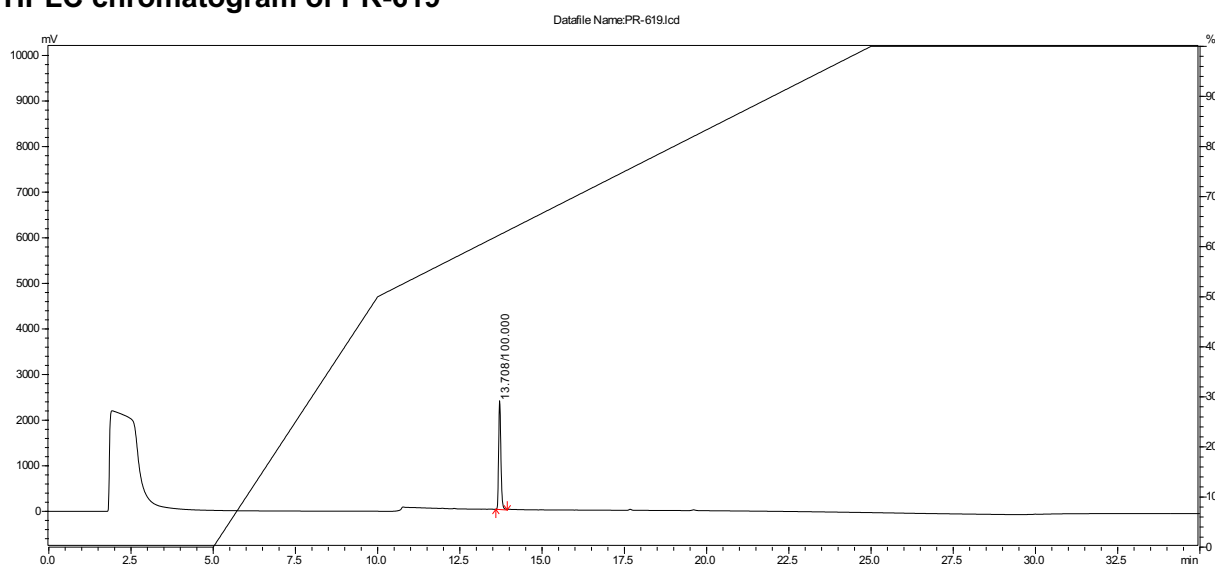
PF3D7_0527200.1	MTLVNITVKWKNQVFNNIELDVSEPLILLKTQLWQLTNVPEKQKLMYKGLLKDDVDLSL	60
PBANKA_1242000.1	MTIVKVTVKWKTNINYDLELNINEPIALFKEQLWKITSVPPEKQKLMYKGLIKNDNLHT	60
	:	
PF3D7_0527200.1	LNLIKENDKIMLVGSAESLVEKPKDIIFEEEDLTNEEKQKIHTKENIIFEEQGIIVNLGNTCY	120
PBANKA_1242000.1	LNLIKNDKIMLVGSSELLAEKPKDITFFEDLSKEDKEKLNEDKNIIFEEQGIIVNLGNTCY	120
	:	
PF3D7_0527200.1	FNAVLQFLTSTFDDLGNFLRSYKSKESKLIKTNKDILFDSFIEFAHSFEKSSEPYVPVTLL	180
PBANKA_1242000.1	FNAVLQFLTSTFNDLGEFLSNIKKIQNFGRSNKDILFDCYIHFSQTFGKSSKPYVPLELL	180
	:	
PF3D7_0527200.1	KSFRDVYPKFKSVNLRKTQYAQQDAEECMNAILTCLNEQTDNKIIDKLFQIISNMKFV	240
PBANKA_1242000.1	KAFRDVFPKFKTINIRKTQYAQQDAEECMNAILTSLNDHTESKIIDKLFQIIGKIKCV	240
	*:**	
PF3D7_0527200.1	ETVEQHEQEKKEKDEKKDEKKDEKKDEKKDEKKDEKKDEKKDEKKDEKKDEKKDEKKDEKK	300
PBANKA_1242000.1	EQNSQDDEPNKQKESQK---NENSQ-----	262
	* . : : : * : . : . : *	
PF3D7_0527200.1	NNNSVQONDHNNKDISHNNIFETTQEFNNKLICYMGTPTPNVNLHEGIRLSLHEKIRKN	360
PBANKA_1242000.1	---KPESDKNNPSQNEENDHFELTQEFKHNKLICYMGTQNTPNVNLHEGIRLSLIEKIKKK	319
	. : : : : * . : . : : * * * * : *	
PF3D7_0527200.1	RNED-NKECIYEKKSEINSLPPYLIVHFLRFESKKIVESNNSGVSVVTAICRKVSFPDT	419
PBANKA_1242000.1	KNDNDKEDTLYEKKSEIDS LPPYLIIHFLRFESKRIVDTSN-TVSVVTAICRKVSFPPEI	378
	: * : : : : : : : *	
PF3D7_0527200.1	FDMYDFCSEKIKEELKIARDIIMKRKDKETSLSPQKENIQNIQNNINNQYNQNNNSNDNP	479
PBANKA_1242000.1	FDIYDFCSDRIKADLKISRNIIMNRKDIKTPIVQENKNEDD-----	419
	*:**	
PF3D7_0527200.1	KHVQEH-NQINKEELIELPTGEYELISVITHKGRNEESGHYIAWKMKKFFSSNSNIDQ	538
PBANKA_1242000.1	KMLETLTNQDDKNKEFVEIPNGEYELISVITHKGRNEESGHYIAWKMRNRVNKNSEYDA	479
	* : : * : : : : : * : *	
PF3D7_0527200.1	NESSNKKTKNANDSLWLKMDDDKVSTHKFSSIDFYGGCSDYNIAVLLLYKRNISCTPDE	598
PBANKA_1242000.1	NGPRTKKNKSNNPTWFKMDDDKVSLHNFSSLDLFGGCSDYNTAVLLLYKRTISCTKDE	539
	* . * . * . * : * : *	
PF3D7_0527200.1	MNMDIKE 605	
PBANKA_1242000.1	LNKYSV- 545	
	: *	

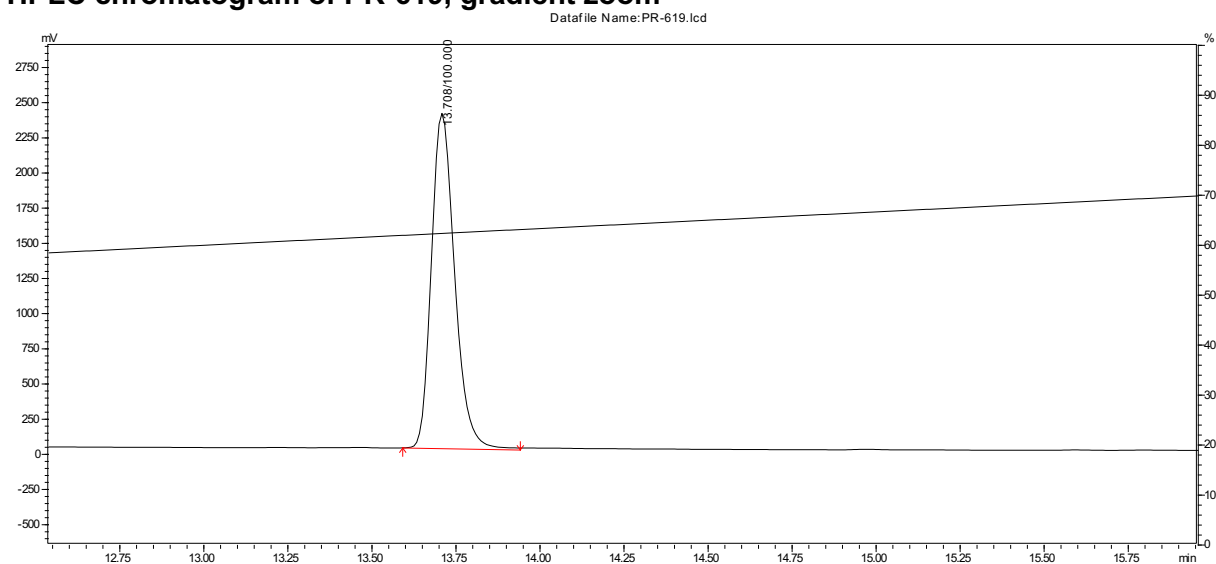
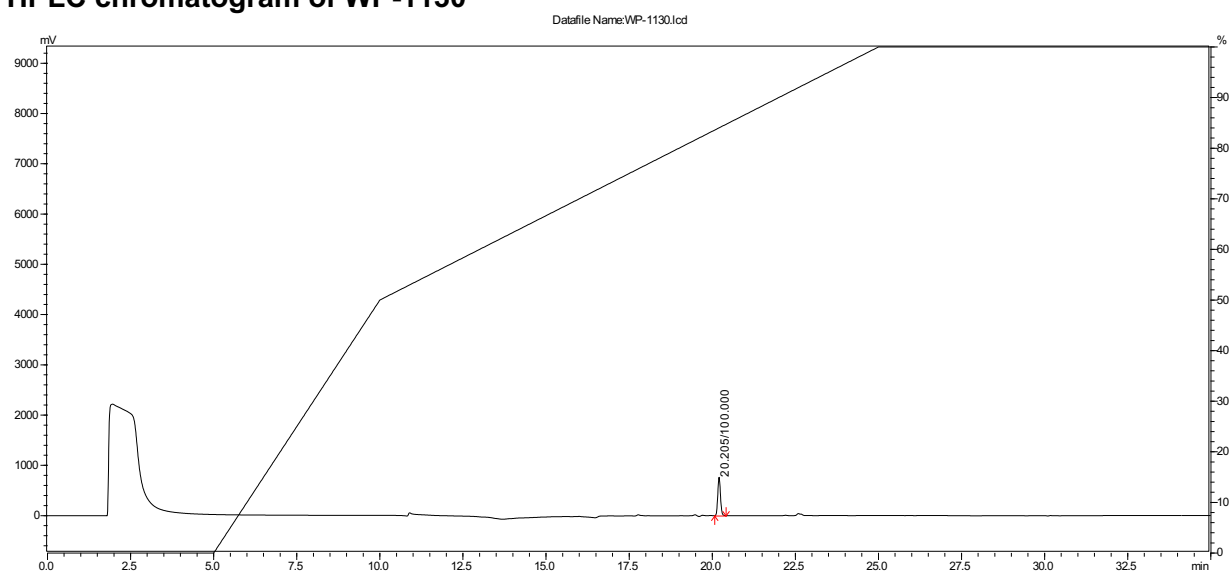
Figure 8.15: Amino acid sequence alignment of indicated *P. berghei* and *P. falciparum* USP14. Conserved residues are indicated by asterisks.

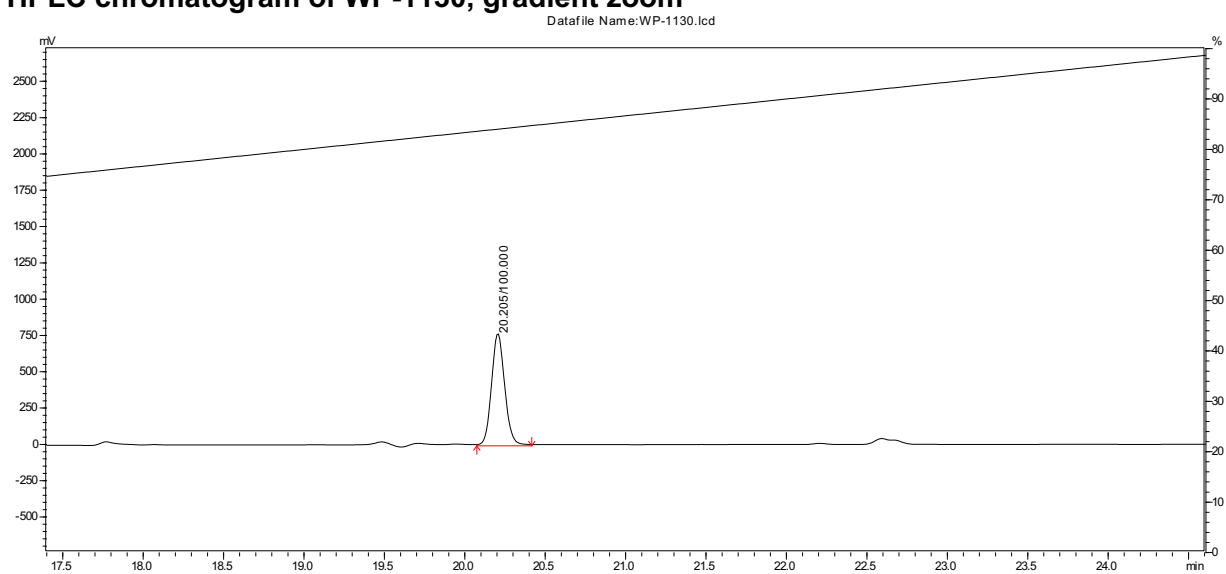
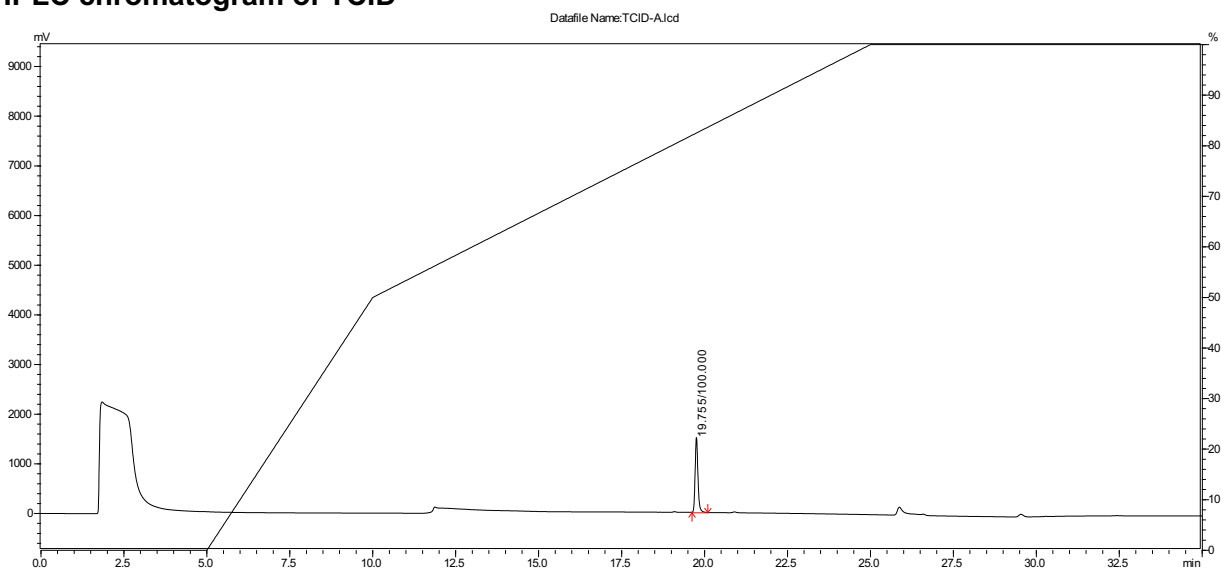
HPLC chromatogram of DMSO**HPLC chromatogram of 1,10-phenanthroline**

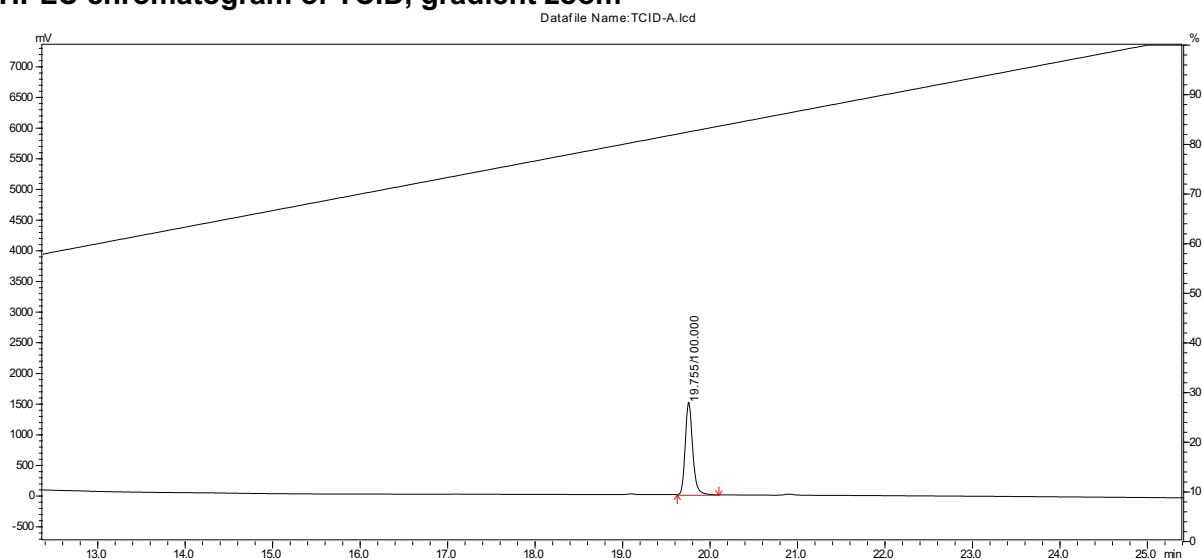
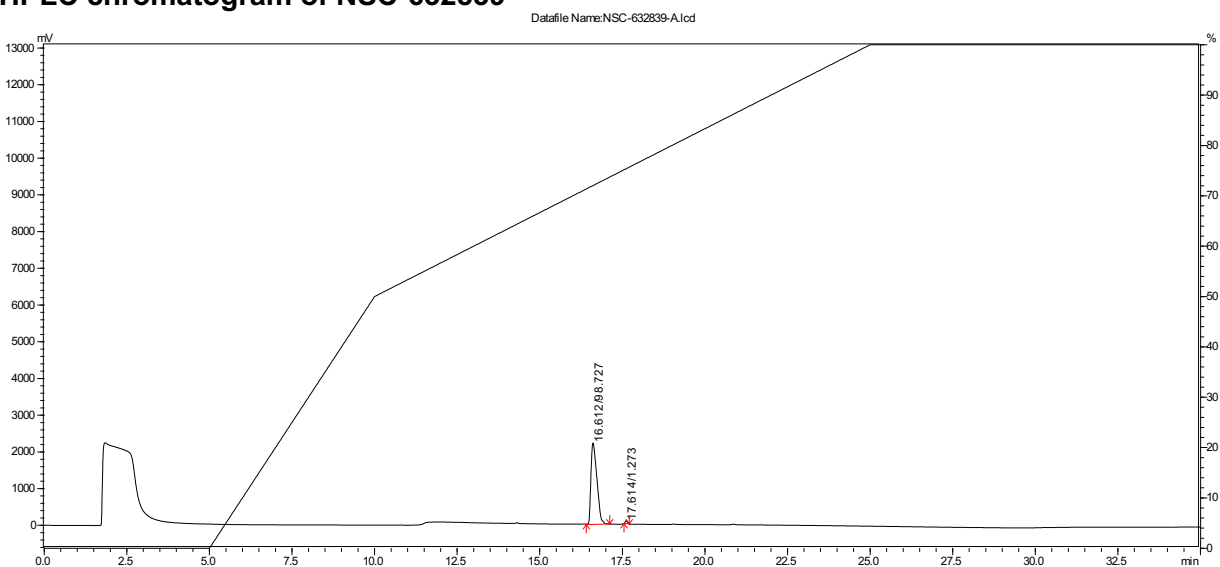
HPLC chromatogram of 1,10-phenanthroline, gradient zoom**HPLC chromatogram of b-AP15**

HPLC chromatogram of b-AP15, gradient zoom**HPLC chromatogram of P5091**

HPLC chromatogram of P5091, gradient zoom**HPLC chromatogram of PR-619**

HPLC chromatogram of PR-619, gradient zoom**HPLC chromatogram of WP-1130**

HPLC chromatogram of WP-1130, gradient zoom**HPLC chromatogram of TCID**

HPLC chromatogram of TCID, gradient zoom**HPLC chromatogram of NSC-632839**

HPLC chromatogram of NSC-632839, gradient zoom

Datafile Name: NSC-632839-A.lcd

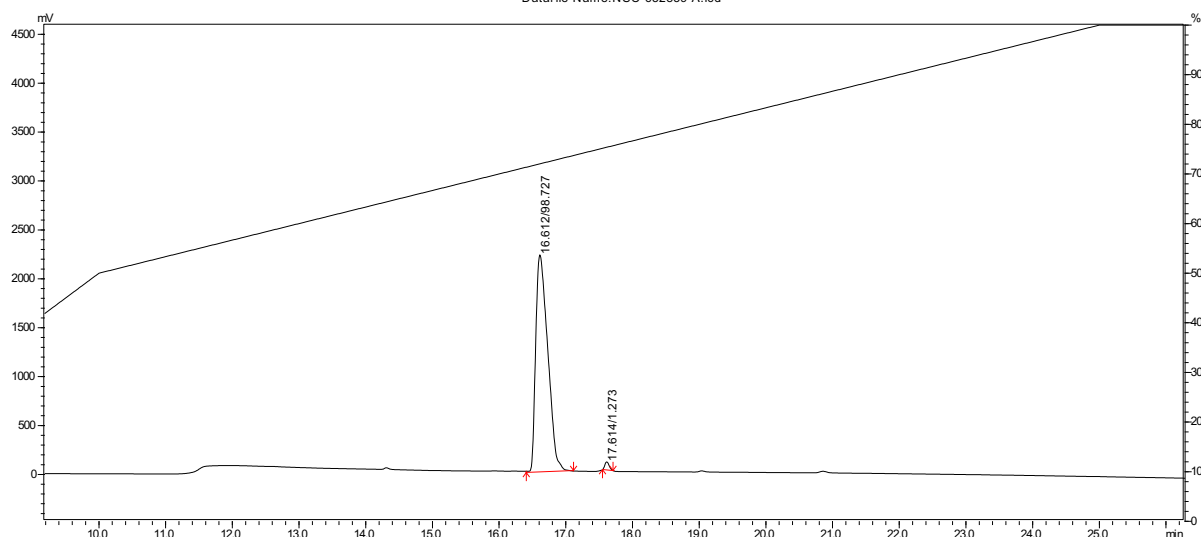


Figure 8.16: HPLC chromatograms of the drug solvent (DMSO) and indicated DUB inhibitors. HPLC runs were carried out as described in section 2.4.2.

8.5 Appendix tables

Appendix table 8.1: List of primers used for Chapters 3 and 4

Primer ID	Gene target	Sequence (5'-3')	Description
GU4783	UBP-1 (PBANKA_0208800)	TACATTTGAACAGCTGGGAGGGTCAGAAAAAAGATTTTC	Shield Mutations and <i>Bse</i> YI introducing mutagenesis primer
GU4784	UBP-1 (PBANKA_0208800)	TTCTGGAGTTGTTATACAAAAATTTCAATGTCAAAAATG	V2752F Mutagenesis primer
GU4785	UBP-1 (PBANKA_0208800)	TAACAATAGAAATCAACAAGATTTTCACAGAATTATTTAG	V2721F Mutagenesis primer
GU4786	UBP-1 (PBANKA_0208800)	cgttaacGATAGCTACACAAACCTTCTTTC	Mutagenesis donor DNA forward primer
GU4787	UBP-1 (PBANKA_0208800)	cgttaacCTCATTTGAGGTAAATGACCAG	Mutagenesis donor DNA reverse primer
GU4788	UBP-1 (PBANKA_0208800)	tattGATTTGAACAGTTGGGTGGGT	sgRNA forward UBP-1 mutagenesis
GU4789	UBP-1 (PBANKA_0208800)	aaacACCCACCCAACTGTTCAAATC	sgRNA reverse UBP-1 mutagenesis
GU4894	UBP-1 (PBANKA_0208800)	CCAAAGTTCCTCTAACATAATATCTATC	UBP-1 mutagenesis diagnostic primer forward
GU4895	UBP-1 (PBANKA_0208800)	CTGATGATGCTGATACACCAC	UBP-1 mutagenesis diagnostic primer reverse
GU5186	UBP-1 (PBANKA_0208800)	CCCCTGTTGGTTTAATAAATTTAG	UBP-1 mutagenesis diagnostic primer forward (upstream)
GU5189	UBP-1 (PBANKA_0208800)	cgttaacCCAAAGTTCCTCTAACATAATATCTATC	GU4894 plus <i>Hinc</i> II introducing sequence at 5' end
GU5190	UBP-1 (PBANKA_0208800)	GAATAAAAAATACGTATCACCATATAGCATCTTAAGCATAC	V2752F to V2721F swapping internal primer carrying V2721F mutation, <i>Sna</i> BI and PAMs sites
GU5191	UBP-1 (PBANKA_0208800)	GTATGCTTAAGATGCTATATGGTGATACGTATTTTTTATTC	Reverse complement of GU5190
GU5206	UBP-1 (PBANKA_0208800)	tattGTATGCTTAAAATGCTATAT	V2752F to V2721F swapping: sgRNA forward
GU5207	UBP-1 (PBANKA_0208800)	aaacATATAGCATTTTAAGCATAC	V2752F to V2721F swapping: sgRNA reverse
GU5274	Kelch13 (PBANKA_1356700)	tattATTGTGGTATCACATCAAAT	R551T I555T sgRNA forward primer
GU5275	Kelch13 (PBANKA_1356700)	aaacATTTGATGTGATACCACAAT	R551T I555T sgRNA reverse complement
GU5276	Kelch13 (PBANKA_1356700)	GTGGTATCACATCCAATGGAACAATATAC	forward primer introducing R551T, <i>Bts</i> CI for RFLP and PAMs

GU5277	Kelch13 (PBANKA_1356700)	GTATATTGTTCCATTGGATGTGATACCAC	Reverse complement of GU5276
GU5278	Kelch13 (PBANKA_1356700)	cgttaacGAAATCCACTAACCATACCTATAACC	Kelch13 mutagenesis donor DNA (R551T, I555T, C592Y) PCR forward
GU5279	Kelch13 (PBANKA_1356700)	cgttaacCCCTGAACTTCTAGCTTC	Kelch13 mutagenesis donor DNA (R551T, I555T, C592Y) PCR reverse
GU5280	Kelch13 (PBANKA_1356700)	GTGGTATCACATCCAATGGACGAATATACTGTACTGGTGGT	forward primer introducing I555T, <i>BtsCI</i> for RFLP and PAMs
GU5281	Kelch13 (PBANKA_1356700)	ACCACCAGTACAGTATATTCGTCCATTGGATGTGATACCAC	Reverse complement of GU5280
GU5282	Kelch13 (PBANKA_1356700)	tattACACATAGCGGAAGATCTCG	C592Y 1st sgRNA forward
GU5283	Kelch13 (PBANKA_1356700)	aaacCGAGATCTTCCGCTATGTGT	C592Y 1st sgRNA reverse
GU5284	Kelch13 (PBANKA_1356700)	GTTAAATACACCGCGATCTTCCGCTATGTATGTAGC	forward primer introducing C592Y, <i>BstUI</i> for RFLP and PAMs
GU5285	Kelch13 (PBANKA_1356700)	GCTACATACATAGCGGAAGATCGCGGTGTATTTAAC	Reverse complement of GU5284
GU5286	Kelch13 (PBANKA_1356700)	cgttaacAACATCACCATTTTTCACCTCCTG	Reverse primer for donor DNA, C592Y mutation
GU5287	Kelch13 (PBANKA_1356700)	tattGTACACATACGCCAGCATTTGT	M488I Y505H sgRNA forward primer
GU5288	Kelch13 (PBANKA_1356700)	aaacACAATGCTGGCGTATGTGTAC	M488I Y505H sgRNA reverse complement
GU5289	Kelch13 (PBANKA_1356700)	TATAAGTCAACAATGCTGGCGGATGTGTACACCCATTTCAAC	forward primer introducing M488I, <i>BtsCI</i> for RFLP and PAMs
GU5290	Kelch13 (PBANKA_1356700)	GTTGAAATGGGTGTACACATCCGCCAGCATTTGTTGACTTATA	Reverse complement of GU5290
GU5291	Kelch13 (PBANKA_1356700)	cgttaacTGTAGGAGGAGCTCTTTTTGAAAC	Forward primer for donor DNA (F458I, M488I, Y505H)
GU5292	Kelch13 (PBANKA_1356700)	CTTTTTTACATGTATTTCGGTGG	forward primer introducing Y505H
GU5293	Kelch13 (PBANKA_1356700)	CCACCGAATACATGTAAAAAG	Reverse complement of GU5293
GU5294	Kelch13 (PBANKA_1356700)	TATAAGTCAACAATGCTGGCGGATGTGTACACCCATGTCAAC	Y505H mutagenesis 2nd forward primer introducing <i>BtsCI</i> for RFLP and PAMs
GU5295	Kelch13 (PBANKA_1356700)	GTTGACATGGGTGTACACATCCGCCAGCATTTGTTGACTTATA	Reverse complement of GU5294
GU5296	Kelch13 (PBANKA_1356700)	tattAACCTCCAATAGAAAAAACT	F458I sgRNA forward
GU5297	Kelch13 (PBANKA_1356700)	aaacAGTTTTTTTCTATTGGAGGTT	F458I sgRNA reverse
GU5298	Kelch13 (PBANKA_1356700)	CCATTCCCCTAGTTATTTCTATTGGAGGTTTT	forward primer introducing F458I PAMs and <i>SpeI</i> for RFLP
GU5299	Kelch13 (PBANKA_1356700)	AAAACCTCCAATAGAAATAACTAGTGGGAATGG	Reverse complement of GU5298

GU5300	Kelch13 (PBANKA_1356700)	TTGTAGATGCTAATATAGCAACTG	Kelch13 mutagenesis forward diagnostic primer
GU5301	Kelch13 (PBANKA_1356700)	GGTGGACCAATTTGCCATTC	Kelch 13 mutagenesis reverse diagnostic primer
GU5458	Kelch13 (PBANKA_1356700)	tattATCAAAAGCTACACACATAG	C592Y 2nd sgRNA forward
GU5459	Kelch13 (PBANKA_1356700)	aaacCTATGTGTGTAGCTTTTGAT	C592Y 2nd sgRNA reverse
GU5460	Kelch13 (PBANKA_1356700)	TACCCCGCGATCTTCAGCTATGTATGTAGCTTTTG	forward primer introducing C592Y Y TAT codon, <i>Bst</i> UI for RFLP and PAMs
GU5461	Kelch13 (PBANKA_1356700)	CAAAAGCTACATACATAGCTGAAGATCGCGGGGTA	Reverse compliment of GU5460
GU5462	Kelch13 (PBANKA_1356700)	TACCCCGCGATCTTCAGCTATGTACGTAGCTTTTG	forward primer introducing C592Y Y codon TAC, <i>Bst</i> UI for RFLP and PAMs
GU5463	Kelch13 (PBANKA_1356700)	CAAAAGCTACGTACATAGCTGAAGATCGCGGGGTA	reverse complement of GU5262
GU5464	Kelch13 (PBANKA_1356700)	GTAAATACACCGCGATCTTCCGCTATGTACGTAGCT	forward primer introducing C592Y Y codon TAC for 1st sgRNA, <i>Bst</i> UI for RFLP and PAMs
GU5465	Kelch13 (PBANKA_1356700)	AGCTACGTACATAGCGGAAGATCGCGGTGTATTTAAC	reverse complement of GU5464
GU5466	Kelch13 (PBANKA_1356700)	GTAAATACACCGCGATCTTCCGCTATGTGTGTAGCT	forward primer, 1st sgRNA C592C control; only silent mutations <i>Bst</i> UI and PAMs
GU5467	Kelch13 (PBANKA_1356700)	AGCTACACACATAGCGGAAGATCGCGGTGTATTTAAC	reverse complement of GU5466

Appendix table 8.2: List of plasmids generated, sgRNA pairs and details of supplied donor templates

Plasmid ID	Primary plasmid ID (sgRNA primer pair cloned into ABR099)	Donor template DNA (PCR primers) and nucleotide substitutions
pG945	pG944 (GU4788+GU4789)	GU4786 + GU4787 (516 bp), V2752F, <i>Bse</i> YI, PAMs
pG946	pG944 (GU4788+GU4789)	GU4786 + GU4787 (516 bp), V2721F, V2752F, <i>Bse</i> YI, PAMs
pG962	pG960 (GU5206 + GU5207)	GU5189 + GU4787 (698 bp), V2721F, V2752F, <i>Sna</i> BI, PAMs
pG963	pG960 (GU5206 + GU5207)	GU5189 + GU4787 (698 bp), V2721F, <i>Sna</i> BI, PAMs
pG983	pG975 (GU5296 + GU5297)	GU5291 + GU5279 (811 bp), F458I, <i>Spe</i> I/PAMs
pG984	pG976 (GU5287 + GU5288)	GU5291 + GU5279 (811 bp), Y505H, <i>Bts</i> CI, PAMs
pG1004	pG1001 (GU5282 + GU5283)	GU5278 + GU5286 (845 bp), C592Y, <i>Bst</i> UI, PAMs
pG1005	pG1002 (GU5274 + GU5275)	GU5278 + GU5279 (644 bp), I555T, <i>Bts</i> CI, PAMs
pG1006	pG1002 (GU5274 + GU5275)	GU5278 + GU5279 (644 bp), R551T, <i>Bts</i> CI, PAMs
pG1008	pG976 (GU5287 + GU5288)	GU5291 + GU5279 (811 bp), M488I, <i>Bts</i> CI, PAMs
pG1010	pG1009 (GU5458 + GU5459)	GU5278 + GU5286 (845 bp), C592Y_Y TAT codon, <i>Bst</i> UI, PAMs
pG1011	pG1009 (GU5458 + GU5459)	GU5278 + GU5286 (845 bp), C592Y_Y TAC codon, <i>Bst</i> UI, PAMs
pG1012	pG1001 (GU5282 + GU5283)	GU5278 + GU5286 (845 bp), C592Y_Y TAC codon, <i>Bst</i> UI, PAMs
pG1013	pG1001 (GU5282 + GU5283)	GU5278 + GU5286 (845 bp), C592C sgRNA control, <i>Bst</i> UI, PAMs

Appendix table 8.3: Plasmids, generated lines, transfection efficiencies and outcome line genotypes for Chapters 3 & 4.

analysis of the bulk transfected parasites was carried out on PCR fragments amplified using diagnostic PCR primers exterior of the donor template; GU5300 + GU5301 (1,111 bp) for Kelch13 and GU4894 + GU4895 (807 bp), GU5186 + GU4895 (946 bp) for UBP-1.

Plasmid ID	Target gene	Parent line	Outcome line ID	RFLP expected fragment sizes	~ RFLP efficiency	Outcome line genotype
pG945	UBP-1	820	G1807	<i>Bse</i> YI RFLP 536, 271 bp	99.52% wild type, 0.48% mutant	V2752F positive? <i>Bse</i> YI & PAMs positive?
pG946	UBP-1	820	G1808	<i>Bse</i> YI RFLP 536, 271 bp	77.268% wild type, 22.732% mutant	V2721F positive, V2752F negative, <i>Bse</i> YI & PAMs positive
pG962	UBP-1	G1807 ^{V2752F}	G1919	<i>Sna</i> BI RFLP 632, 314 bp	20.828% wild type 79.172% mutant	V2721F negative, <i>Sna</i> BI & PAMs positive
pG963	UBP-1	G1807 ^{V2752F}	G1918	<i>Sna</i> BI RFLP 632, 314 bp	11.671% wild type, 88.329% mutant	V2721F positive, <i>Sna</i> BI & PAMs positive
pG963	UBP-1	1804cl1	G1980	<i>Sna</i> BI RFLP 632, 314 bp	34.503% wild type, 65.497% mutant	V2721F positive, <i>Sna</i> BI & PAMs positive
pG983	Kelch13	1804cl1	G1957	<i>Spe</i> I RFLP 803, 308 bp	1.676% wild type, 98.324% mutant	F458I, <i>Spe</i> I/PAMs positive
pG984	Kelch13	1804cl1	G1979	<i>Bts</i> CI RFLP 714, 397 bp	6.05% wild type, 93.950% mutant	Y505H, <i>Bts</i> CI, PAMs positive
pG1004	Kelch13	1804cl1	G2022	<i>Bst</i> UI RFLP 701, 410 bp	86.625% wild type, 13.374% mutant	C592Y negative, <i>Bst</i> UI & PAMs positive
pG1004	Kelch13	1804cl1	G2023	<i>Bst</i> UI RFLP 701, 410 bp	81.467% wild type, 18.534% mutant	C592Y negative, <i>Bst</i> UI & PAMs positive
pG1005	Kelch13	1804cl1	G2024	<i>Bts</i> CI RFLP 582, 529 bp	92.261% wild type, 7.739% mutant	I555T negative, <i>Bts</i> CI & PAMs positive
pG1006	Kelch13	1804cl1	G2025	<i>Bts</i> CI RFLP 582, 529 bp	70.006% wild type, 29.994% mutant	R551T positive, <i>Bts</i> CI & PAMs positive

pG1008	Kelch13	1804cl1	G1989	<i>BtsCI</i> RFLP 714, 397 bp	2.087% wild type, 97.913% mutant	M488I, <i>BtsCI</i> , PAMs positive
pG1010	Kelch13	1804cl1	G2042	<i>BstUI</i> RFLP 701, 410 bp	99.861% wild type, 0.138% mutant	C592Y negative, <i>BstUI</i> & PAMs positive
pG1011	Kelch13	1804cl1	G2043	<i>BstUI</i> RFLP 701, 410 bp	97.381% wild type, 2.619% mutant	C592Y negative, <i>BstUI</i> & PAMs positive
pG1012	Kelch13	1804cl1	G2044	<i>BstUI</i> RFLP 701, 410 bp	91.883% wild type, 8.117% mutant	C592Y negative, <i>BstUI</i> & PAMs positive
pG1013	Kelch13	1804cl1	G2045	<i>BstUI</i> RFLP 701, 410 bp	5.539% wild type, 94.461% mutant	C592C positive, <i>BstUI</i> & PAMs positive
			G1807 CQ 15mg/kg	<i>BseYI</i> RFLP 536, 271 bp	97.375% wild type, 2.625% mutant	V2752F positive? <i>BseYI</i> & PAMs positive?
			G1807 CQ 30mg/kg	<i>BseYI</i> RFLP 536, 271 bp	38.927% wild type, 61.073% mutant	V2752F positive, <i>BseYI</i> & PAMs positive
			G1807 ART 20mg/kg	<i>BseYI</i> RFLP 536, 271 bp	99.539% wild type, 0.461% mutant	V2752F positive? <i>BseYI</i> & PAMs positive?
			G1808 CQ 15mg/kg	<i>BseYI</i> RFLP 536, 271 bp	19.791% wild type, 80.209% mutant	V2721F positive, V2752F negative, <i>BseYI</i> & PAMs positive
			G1808 ART 20mg/kg	<i>BseYI</i> RFLP 536, 271 bp	9.545% wild type, 90.455% mutant	V2721F positive, V2752F negative, <i>BseYI</i> & PAMs positive
			G2022 AS 20mg/kg	<i>BstUI</i> RFLP 701, 410 bp	96.13% wild type, 3.87% mutant	C592Y negative <i>BstUI</i> & PAMs positive
			G2022 AS 64mg/kg	<i>BstUI</i> RFLP 701, 410 bp	97.299% wild type, 2.701% mutant	C592Y negative <i>BstUI</i> & PAMs positive
			G2023 AS 20mg/kg	<i>BstUI</i> RFLP 701, 410 bp	87.814% wild type, 12.186% mutant	C592Y negative, <i>BstUI</i> & PAMs positive
			G2023 AS 64mg/kg	<i>BstUI</i> RFLP 701, 410 bp	97.139% wild type, 2.861% mutant	C592Y negative, <i>BstUI</i> & PAMs positive

	G2024 AS 20mg/kg	<i>BtsCI</i> RFLP 582, 529 bp	81.484% wild type, 18.516% mutant	I555T negative, <i>BtsCI</i> & PAMs positive
	G2024 AS 64mg/kg	<i>BtsCI</i> RFLP 582, 529 bp	88.154% wild type, 11.846% mutant	I555T negative, <i>BtsCI</i> & PAMs positive
	G2025 AS20mg/kg	<i>BtsCI</i> RFLP 582, 529 bp	50.295% wild type, 49.705% mutant	R551T positive, <i>BtsCI</i> & PAMs positive
	G2025 AS 64mg/kg	<i>BtsCI</i> RFLP 582, 529 bp	0.219% wild type, 99.781% mutant	R551T positive, <i>BtsCI</i> & PAMs positive

Appendix table 8.4: Recrudescence of *P. berghei* Kelch13 and UBP-1 mutants as compared to wild type. Groups of 3 or 4 mice (M0-M3) were infected with $\sim 10^6$ parasites on Day 0 and treated from 3 hours with ART at 80 mg/kg as indicated by arrows. A recrudescence event was recorded as – for negative smears or + with associated parasitaemia.

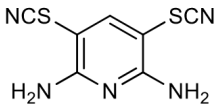
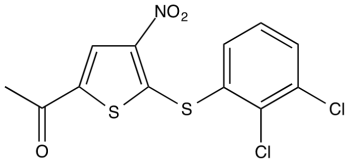
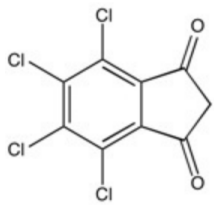
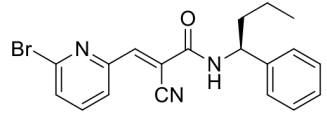
		1804 ^{WT}			G1980 ^{V2721F UBP-1}			G1957 ^{F458I}				G1979 ^{V505H}				G1989 ^{M488I}				G2025 ^{R551T}			
	Days	M0	M1	M2	M0	M1	M2	M0	M1	M2	M3	M0	M1	M3	M4	M0	M1	M2	M3	M0	M1	M2	M3
→	0	-	-	-	-	-	-	-	-	-	-	-	-	-	-	-	-	-	-	-	-	-	-
→	1	-	-	-	-	-	-	-	-	-	-	-	-	-	-	-	-	-	-	-	-	-	-
→	2	-	-	-	-	-	-	-	-	-	-	-	-	-	-	-	-	-	-	-	-	-	-
	3	-	-	-	-	-	-	-	-	-	-	-	-	-	-	-	-	-	-	-	-	-	-
	4	-	-	-	-	-	-	-	-	-	-	-	-	-	-	-	-	-	-	-	-	-	-
	5	-	-	-	-	-	-	-	-	-	-	-	-	-	-	-	-	-	-	-	-	-	-
	6	-	-	-	-	-	-	-	-	-	-	-	-	-	-	-	-	-	-	+(0.14)	-	-	+(0.21)
	7	-	-	-	-	-	-	-	-	-	-	-	-	-	-	-	-	-	-	+(0.31)	+(0.25)	+(0.35)	+(0.67)
	8	-	-	-	-	-	-	-	-	-	-	-	-	-	-	+(0.25)	-	+(0.11)	-	+(0.99)	+(0.77)	+(0.78)	+(1.48)
	9	-	-	-	-	-	-	-	-	-	-	-	-	-	-	+(0.8)	+(0.15)	+(0.99)	+(0.35)	+(1.88)	+(1.55)	+(1.63)	+(2.33)
	10	-	-	-	-	-	-	-	-	-	-	-	-	-	-	+(2.23)	+(0.65)	+(2.5)	+(1.12)	+(2.89)	+(3.23)	+(2.53)	+(3.93)
	11	-	-	-	-	-	-	-	-	-	-	+(0.2)	-	-	+(0.11)	+(4.23)	+(2.23)	+(4.5)	+(3.23)		+(4.23)	+(3.43)	
	12	-	-	-	-	-	-	-	-	-	-	+(1.56)	-	-	+(1.23)		+(4.28)		+(5.99)				
	13	-	-	-	+(0.15)	+(0.21)	+(0.21)	-	-	-	+(0.14)	+(4.53)	+(0.35)	+(0.18)	+(3.87)								
	14	-	-	-	+(1.0)	+(1.3)	+(1.3)	-	+(0.34)	-	+(1.6)		+(1.8)	+(1.23)									
	15	-	-	-	+(3.5)	+(3.9)	+(3.9)	-	+(1.7)	-	+(4.17)		+(5.23)	+(4.56)									
	16	-	-	-				-	+(3.97)	-													
	17	-	-	-				-		-													

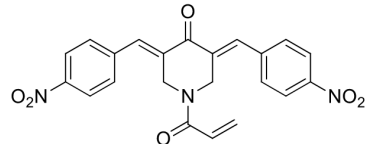
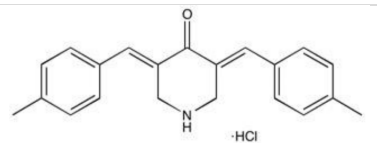
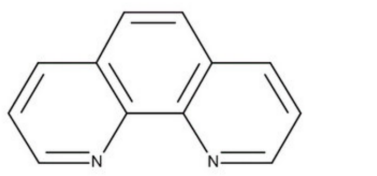
Appendix table 8.5: A manually created list of 17 DUBs in malaria parasites, their predicted function and essentiality. The list was created based on previous *in silico* predictions (Ponder and Bogyo, 2007, Ponts et al., 2011) and a selected functional studies (Artavanis-Tsakonas et al., 2006, Artavanis-Tsakonas et al., 2010) as well as recent genome wide knockout screens (Bushell et al., 2017, Zhang et al., 2018).

<i>P. falciparum</i> / <i>P. berghei</i> gene ID	Close human orthologue	Essential? (<i>P. falciparum</i> / <i>P. berghei</i>)	Predicted function in malaria parasites
PF3D7_1460400/PBANKA_1324100	UCH-L3	Yes/not characterised	deNeddylase/DUB activity
PF3D7_1117100/PBANKA_0930900	UCH54	Yes/dispensable	deNeddylase/DUB activity
PF3D7_0726500/PBANKA_0210600	UCH-L1	Yes/Yes	Not known
PF3D7_0104300/PBANKA_0208800	HAUSP/USP7 (UBP-1)	Yes/not characterised	Implicated in drug resistance
PF3D7_0413900/PBANKA_0715900	USP13	Yes/not characterised	Not known
PF3D7_0527200/PBANKA_1242000	USP14	Yes/dispensable	DUB activity
PF3D7_0516700/PBANKA_1231500	USP2	not characterised/dispensable	Not known
PF3D7_0904600/PBANKA_0416800	USP14?	dispensable/dispensable	Not known
PF3D7_1317000/PBANKA_1415500	USP39	Yes/not characterised	Not known
PF3D7_1414700/PBANKA_1028000	UCH36?	dispensable/not characterised	Not known
PF3D7_1226800/PBANKA_1441600	Ataxin 3	Yes/dispensable	Not known
PF3D7_0403500/PBANKA_1001100	USP?	Yes/Yes	Not known
PF3D7_1111900/PBANKA_0935700	Josephin domain	Yes/not characterised	Not known

PF3D7_0923100/PBANKA_0824000	OTU domain	dispensable/dispensable	Not known
PF3D7_1031400/PBANKA_0515350	OTU like	not characterised/dispensable	Not known
PF3D7_1141700/PBANKA_0907300	OTU domain	Yes/not characterised	Not known
PF3D7_0920300/PBANKA_0821200	OTU domain	Yes/not characterised	Not known

Appendix table 8.6: A list of DUB inhibitors used in the study, their targets, chemical structure, supplier and primary references.

Inhibitor, Mw	UPS target	Supplier	Purity grade	Chemical structure
PR-619, 223.28	broad spectrum DUB inhibitor ^a	Focus biomolecules (CAS #: 2645-32-1)	98% by TLC NMR	
P5091, 348.23	USP7 and USP47 DUBs ^b	Focus biomolecules (CAS #: 882257-11-6)	98% by TLC NMR	
TCID, 283.93	UCH-L3 and UCH-L1 DUBs ^c	Focus biomolecules (CAS #: 30675-13-9)	97% by TLC NMR	
WP1130	UCH-L1, USP9X, USP14, UCH37 DUBs ^d	Focus biomolecules (CAS #: 856243-80-6)	98% by TLC NMR	

b-AP15, 419.4	USP14 and UCH-L5 DUBs ^e	Focus biomolecules (CAS #: 1009817-63-3)	>98% by HPLC	
NSC-632839, 339.86	USP2, USP7, SENP2 DUBs ^f	Focus biomolecules (CAS #: 157654-67-6)	>98% by HPLC NMR	
1,10 phenanthroline, 198.2	Metalloproteases and JAMM isopeptidases ^g	BPS biosciences (CAS #: 5144-89-8)	≥99% by HPLC	

(Altun et al., 2011)^a, (Chauhan et al., 2012)^b, (Liu et al., 2003)^c, (Kapuria et al., 2010)^d (D'Arcy et al., 2011)^e, (Nicholson et al., 2008)^f, (Cooper et al., 2009)

Appendix table 8.7: HPLC chemical purity and retention times of DUB inhibitors used in chapter 5

DUB inhibitor	HPLC Purity (%)	Retention time (minutes)
1,10-phenanthroline	>99	12.433
b-AP15	>99	19.095
P5091	>99	21.303
PR-619	>99	13.708
WP1130	>99	20.205
TCID	>99	19.755
NSC-632839	99	16.612

9 References

- Achan, J., Talisuna, A. O., Erhart, A., Yeka, A., Tibenderana, J. K., Baliraine, F. N., Rosenthal, P. J. & D'Alessandro, U. 2011. Quinine, an old anti-malarial drug in a modern world: role in the treatment of malaria. *Malaria journal*, **10**, 144-144.
- Acquah, F. K., Adjah, J., Williamson, K. C. & Amoah, L. E. 2019. Transmission-blocking vaccines: old friends and new prospects. *Infection and immunity*, **87**, e00775-18.
- Adams, J., Kelso, R. & Cooley, L. 2000. The kelch repeat superfamily of proteins: propellers of cell function. *Trends in cell biology*, **10**, 17-24.
- Adams, T., Ennusun, N. A. A., Quashie, N. B., Futagbi, G., Matrevi, S., Hagan, O. C. K., Abuaku, B., Koram, K. A. & Duah, N. O. 2018. Prevalence of *Plasmodium falciparum* delayed clearance associated polymorphisms in adaptor protein complex 2 mu subunit (pfap2mu) and ubiquitin specific protease 1 (pfUBP-1) genes in Ghanaian isolates. *Parasites and vectors*, **11**, 175-175.
- Adisa, A., Rug, M., Klonis, N., Foley, M., Cowman, A. F. & Tilley, L. 2003. The signal sequence of exported protein-1 directs the green fluorescent protein to the parasitophorous vacuole of transfected malaria parasites. *Journal of biological chemistry*, **278**, 6532-42.
- Afonso, A., Hunt, P., Cheesman, S., Alves, A. C., Cunha, C. V., do Rosário, V. & Cravo, P. 2006. Malaria parasites can develop stable resistance to artemisinin but lack mutations in candidate genes atp6 (encoding the sarcoplasmic and endoplasmic reticulum Ca²⁺ ATPase), tctp, mdr1, and cg10. *Antimicrobial agents and chemotherapy*, **50**, 480-489.
- Afonso, A., Neto, Z., Castro, H., Lopes, D., Alves, A. C., Tomás, A. M. & Rosário, V. D. 2010. *Plasmodium chabaudi chabaudi* malaria parasites can develop stable resistance to atovaquone with a mutation in the cytochrome b gene. *Malaria journal*, **9**, 135-135.
- Allman, E. L., Painter, H. J., Samra, J., Carrasquilla, M. & Llinas, M. 2016. Metabolomic profiling of the malaria box reveals antimalarial target pathways. *Antimicrobial agents and chemotherapy*, **60**, 6635-6649.
- Altun, M., Kramer, H. B., Willems, L. I., McDermott, J. L., Leach, C. A., Goldenberg, S. J., Kumar, K. G., Konietzny, R., Fischer, R., Kogan, E., Mackeen, M. M., McGouran, J., Khoronenkova, S. V., Parsons, J. L., Dianov, G. L., Nicholson, B. & Kessler, B. M. 2011. Activity-based chemical proteomics accelerates inhibitor development for deubiquitylating enzymes. *Chemical biology*, **18**, 1401-12.
- Aly, A. S. I. & Matuschewski, K. 2005. A malarial cysteine protease is necessary for *Plasmodium* sporozoite egress from oocysts. *The Journal of experimental medicine*, **202**, 225-230.

- Aly, A. S. I., Vaughan, A. M. & Kappe, S. H. I. 2009. Malaria parasite development in the mosquito and infection of the mammalian host. *Annual review of microbiology*, **63**, 195-221.
- Amaratunga, C., Sreng, S., Suon, S., Phelps, E. S., Stepniewska, K., Lim, P., Zhou, C., Mao, S., Anderson, J. M., Lindegardh, N., Jiang, H., Song, J., Su, X.-z., White, N. J., Dondorp, A. M., Anderson, T. J. C., Fay, M. P., Mu, J., Duong, S. & Fairhurst, R. M. 2012. Artemisinin-resistant *Plasmodium falciparum* in Pursat province, western Cambodia: a parasite clearance rate study. *The lancet infectious diseases*, **12**, 851-858.
- Amaratunga, C., Witkowski, B., Dek, D., Try, V., Khim, N., Miotto, O., Ménard, D. & Fairhurst, R. M. 2014. *Plasmodium falciparum* founder populations in western Cambodia have reduced artemisinin sensitivity *in vitro*. *Antimicrobial agents and chemotherapy*, **58**, 4935-4937.
- Aminake, M. N., Arndt, H. D. & Pradel, G. 2012. The proteasome of malaria parasites: a multi-stage drug target for chemotherapeutic intervention? *International journal for parasitology: drugs and drug resistance*, **2**, 1-10.
- Anderson, T. J., Nair, S., McDew-White, M., Cheeseman, I. H., Nkhoma, S., Bilgic, F., McGready, R., Ashley, E., Pyae Phyo, A., White, N. J. & Nosten, F. 2017. Population parameters underlying an ongoing soft sweep in Southeast Asian malaria parasites. *Molecular biology and evolution*, **34**, 131-144.
- Arastu-Kapur, S., Ponder, E. L., Fonović, U. P., Yeoh, S., Yuan, F., Fonović, M., Grainger, M., Phillips, C. I., Powers, J. C. & Bogyo, M. 2008. Identification of proteases that regulate erythrocyte rupture by the malaria parasite *Plasmodium falciparum*. *Nature chemical biology*, **4**, 203-13.
- Ariey, F., Witkowski, B., Amaratunga, C., Beghain, J., Langlois, A. C., Khim, N., Kim, S., Duru, V., Bouchier, C., Ma, L., Lim, P., Leang, R., Duong, S., Sreng, S., Suon, S., Chuor, C. M., Bout, D. M., Menard, S., Rogers, W. O., Genton, B., Fandeur, T., Miotto, O., Ringwald, P., Le Bras, J., Berry, A., Barale, J. C., Fairhurst, R. M., Benoit-Vical, F., Mercereau-Puijalon, O. & Menard, D. 2014. A molecular marker of artemisinin-resistant *Plasmodium falciparum* malaria. *Nature*, **505**, 50-5.
- Artavanis-Tsakonas, K., Misaghi, S., Comeaux, C. A., Catic, A., Spooner, E., Duraisingh, M. T. & Ploegh, H. L. 2006. Identification by functional proteomics of a deubiquitinating/deNeddylating enzyme in *Plasmodium falciparum*. *Molecular microbiology*, **61**, 1187-95.
- Artavanis-Tsakonas, K., Weihofen, W. A., Antos, J. M., Coleman, B. I., Comeaux, C. A., Duraisingh, M. T., Gaudet, R. & Ploegh, H. L. 2010. Characterization and structural studies of the *Plasmodium falciparum* ubiquitin and Nedd8 hydrolase UCHL3. *Journal of biological chemistry*, **285**, 6857-6866.
- Ashley, E. A., Dhorda, M., Fairhurst, R. M., Amaratunga, C., Lim, P., Suon, S., Sreng, S., Anderson, J. M., Mao, S., Sam, B., Sopha, C., Chuor, C. M., Nguon, C., Sovannaroeth, S., Pukrittayakamee, S., Jittamala, P., Chotivanich, K., Chutasmit, K., Suchatsoonthorn, C., Runchaoen, R., Hien, T. T., Thuy-Nhien, N. T., Thanh, N. V., Phu, N. H., Htut, Y., Han, K.-T., Aye, K. H., Mokuolu, O. A., Olaosebikan, R. R., Folaranmi, O. O., Mayxay, M., Khantavong, M., Hongvanthong, B.,

- Newton, P. N., Onyamboko, M. A., Fanello, C. I., Tshefu, A. K., Mishra, N., Valecha, N., Phyo, A. P., Nosten, F., Yi, P., Tripura, R., Borrmann, S., Bashraheil, M., Peshu, J., Faiz, M. A., Ghose, A., Hossain, M. A., Samad, R., Rahman, M. R., Hasan, M. M., Islam, A., Miotto, O., Amato, R., MacInnis, B., Stalker, J., Kwiatkowski, D. P., Bozdech, Z., Jeeyapant, A., Cheah, P. Y., Sakulthaew, T., Chalk, J., Intharabut, B., Silamut, K., Lee, S. J., Vihokhern, B., Kunasol, C., Imwong, M., Tarning, J., Taylor, W. J., Yeung, S., Woodrow, C. J., Flegg, J. A., Das, D., Smith, J., Venkatesan, M., Plowe, C. V., Stepniewska, K., Guerin, P. J., Dondorp, A. M., Day, N. P., White, N. J. & Tracking Resistance to Artemisinin, C. 2014. Spread of artemisinin resistance in *Plasmodium falciparum* malaria. The New England journal of medicine, **371**, 411-423.
- Ataide, R., Ashley, E. A., Powell, R., Chan, J. A., Malloy, M. J., O'Flaherty, K., Takashima, E., Langer, C., Tsuboi, T., Dondorp, A. M., Day, N. P., Dhorda, M., Fairhurst, R. M., Lim, P., Amaratunga, C., Pukrittayakamee, S., Hien, T. T., Htut, Y., Mayxay, M., Faiz, M. A., Beeson, J. G., Nosten, F., Simpson, J. A., White, N. J. & Fowkes, F. J. 2017. Host immunity to *Plasmodium falciparum* and the assessment of emerging artemisinin resistance in a multinational cohort. Proceedings of the national academy of sciences of the USA, **114**, 3515-3520.
- Bakar, N. A., Klonis, N., Hanssen, E., Chan, C. & Tilley, L. 2010. Digestive-vacuole genesis and endocytic processes in the early intraerythrocytic stages of *Plasmodium falciparum*. Journal of cell science, **123**, 441.
- Bancells, C., Llorà-Batlle, O., Poran, A., Nötzel, C., Rovira-Graells, N., Elemento, O., Kafsack, B. F. C. & Cortés, A. 2019. Revisiting the initial steps of sexual development in the malaria parasite *Plasmodium falciparum*. Nature microbiology, **4**, 144-154.
- Bannister, L. & Mitchell, G. 2003. The ins, outs and roundabouts of malaria. Trends in parasitology, **19**, 209-213.
- Bannister, L. H., Hopkins, J. M., Fowler, R. E., Krishna, S. & Mitchell, G. H. 2000. A Brief illustrated guide to the ultrastructure of *Plasmodium falciparum* asexual blood stages. Parasitology today, **16**, 427-433.
- Baragaña, B., Hallyburton, I., Lee, M. C. S., Norcross, N. R., Grimaldi, R., Otto, T. D., Proto, W. R., Blagborough, A. M., Meister, S., Wirjanata, G., Ruecker, A., Upton, L. M., Abraham, T. S., Almeida, M. J., Pradhan, A., Porzelle, A., Luksch, T., Martínez, M. S., Luksch, T., Bolscher, J. M., Woodland, A., Norval, S., Zuccotto, F., Thomas, J., Simeons, F., Stojanovski, L., Osuna-Cabello, M., Brock, P. M., Churcher, T. S., Sala, K. A., Zakutansky, S. E., Jiménez-Díaz, M. B., Sanz, L. M., Riley, J., Basak, R., Campbell, M., Avery, V. M., Sauerwein, R. W., Dechering, K. J., Noviyanti, R., Campo, B., Frearson, J. A., Angulo-Barturen, I., Ferrer-Bazaga, S., Gamo, F. J., Wyatt, P. G., Leroy, D., Siegl, P., Delves, M. J., Kyle, D. E., Wittlin, S., Marfurt, J., Price, R. N., Sinden, R. E., Winzeler, E. A., Charman, S. A., Bebrevska, L., Gray, D. W., Campbell, S., Fairlamb, A. H., Willis, P. A., Rayner, J. C., Fidock, D. A., Read, K. D. & Gilbert, I. H. 2015. A novel multiple-stage antimalarial agent that inhibits protein synthesis. Nature, **522**, 315-320.
- Bargieri, D. Y., Andenmatten, N., Lagal, V., Thiberge, S., Whitelaw, J. A., Tardieux, I., Meissner, M. & Ménard, R. 2013. Apical membrane antigen 1

mediates apicomplexan parasite attachment but is dispensable for host cell invasion. *Nature communications*, **4**, 2552-2552.

Baton, L. A. & Ranford-Cartwright, L. C. 2005. Spreading the seeds of million-murdering death: metamorphoses of malaria in the mosquito. *Trends in parasitology*, **21**, 573-580.

Bayoh, M. N., Walker, E. D., Kosgei, J., Ombok, M., Olang, G. B., Githeko, A. K., Killeen, G. F., Otieno, P., Desai, M., Lobo, N. F., Vulule, J. M., Hamel, M. J., Kariuki, S. & Gimnig, J. E. 2014. Persistently high estimates of late night, indoor exposure to malaria vectors despite high coverage of insecticide treated nets. *Parasites and vectors*, **7**, 380-380.

Bennink, S., Kiesow, M. J. & Pradel, G. 2016. The development of malaria parasites in the mosquito midgut. *Cellular microbiology*, **18**, 905-918.

Bhatt, S., Weiss, D. J., Cameron, E., Bisanzio, D., Mappin, B., Dalrymple, U., Battle, K., Moyes, C. L., Henry, A., Eckhoff, P. A., Wenger, E. A., Briët, O., Penny, M. A., Smith, T. A., Bennett, A., Yukich, J., Eisele, T. P., Griffin, J. T., Fergus, C. A., Lynch, M., Lindgren, F., Cohen, J. M., Murray, C. L. J., Smith, D. L., Hay, S. I., Cibulskis, R. E. & Gething, P. W. 2015. The effect of malaria control on *Plasmodium falciparum* in Africa between 2000 and 2015. *Nature*, **526**, 207-211.

Bhattacharjee, S., Stahelin, R. V., Speicher, K. D., Speicher, D. W. & Haldar, K. 2012. Endoplasmic reticulum PI(3)P lipid binding targets malaria proteins to the host cell. *Cell*, **148**, 201-12.

Bhattacharya, A., Mishra, L. C. & Bhasin, V. K. 2008. *In vitro* activity of artemisinin in combination with clotrimazole or heat-treated amphotericin B against *Plasmodium falciparum*. *The American journal of tropical medicine and hygiene*, **78**, 721-8.

Biagini, G. A., Fisher, N., Shone, A. E., Mubarak, M. A., Srivastava, A., Hill, A., Antoine, T., Warman, A. J., Davies, J., Pidathala, C., Amewu, R. K., Leung, S. C., Sharma, R., Gibbons, P., Hong, D. W., Pacorel, B., Lawrenson, A. S., Charoensutthivarakul, S., Taylor, L., Berger, O., Mbekeani, A., Stocks, P. A., Nixon, G. L., Chadwick, J., Hemingway, J., Delves, M. J., Sinden, R. E., Zeeman, A. M., Kocken, C. H., Berry, N. G., O'Neill, P. M. & Ward, S. A. 2012. Generation of quinolone antimalarials targeting the *Plasmodium falciparum* mitochondrial respiratory chain for the treatment and prophylaxis of malaria. *Proceedings of the national academy of sciences of the USA*, **109**, 8298-303.

Billker, O., Dechamps, S., Tewari, R., Wenig, G., Franke-Fayard, B. & Brinkmann, V. 2004. Calcium and a calcium-dependent protein kinase regulate gamete formation and mosquito transmission in a malaria parasite. *Cell*, **117**, 503-14.

Billker, O., Lindo, V., Panico, M., Etienne, A. E., Paxton, T., Dell, A., Rogers, M., Sinden, R. E. & Morris, H. R. 1998. Identification of xanthurenic acid as the putative inducer of malaria development in the mosquito. *Nature*, **392**, 289-292.

Birnbaum, J., Scharf, S., Schmidt, S., Jonscher, E., Hoeijmakers, W. A. M., Flemming, S., Toenhake, C. G., Schmitt, M., Sabitzki, R., Bergmann, B.,

- Fröhlke, U., Mesén-Ramírez, P., Blancke Soares, A., Herrmann, H., Bártfai, R. & Spielmann, T. 2020. A Kelch13-defined endocytosis pathway mediates artemisinin resistance in malaria parasites. *Science*, **367**, 51.
- Birrell, G. W., Challis, M. P., De Paoli, A., Anderson, D., Devine, S. M., Heffernan, G. D., Jacobus, D. P., Edstein, M. D., Siddiqui, G. & Creek, D. J. 2019. Multi-omic characterisation of the mode of action of a potent new antimalarial compound, JPC-3210, against *Plasmodium falciparum*. *Molecular cell proteomics*, **19**, 308-325
- Blackman, M. J. 2008. Malarial proteases and host cell egress: an 'emerging' cascade. *Cell microbiology*, **10**, 1925-34.
- Boampong, J. N., Ameyaw, E. O., Aboagye, B., Asare, K., Kyei, S., Donfack, J. H. & Woode, E. 2013. The Curative and prophylactic effects of Xylopic acid on *Plasmodium berghei* Infection in mice. *Journal of parasitology research*, **2013**, 356107.
- Boddey, J. A. & Cowman, A. F. 2013. *Plasmodium* nesting: remaking the erythrocyte from the inside out. *Annual reviews microbiology*, **67**, 243-69.
- Boddey, J. A., Hodder, A. N., Günther, S., Gilson, P. R., Patsiouras, H., Kapp, E. A., Pearce, J. A., de Koning-Ward, T. F., Simpson, R. J., Crabb, B. S. & Cowman, A. F. 2010. An aspartyl protease directs malaria effector proteins to the host cell. *Nature*, **463**, 627-631.
- Boddey, J. A., O'Neill, M. T., Lopaticki, S., Carvalho, T. G., Hodder, A. N., Nebl, T., Wawra, S., van West, P., Ebrahimzadeh, Z., Richard, D., Flemming, S., Spielmann, T., Przyborski, J., Babon, J. J. & Cowman, A. F. 2016. Export of malaria proteins requires co-translational processing of the PEXEL motif independent of phosphatidylinositol-3-phosphate binding. *Nature communications*, **7**, 10470.
- Boni, M. F., White, N. J. & Baird, J. K. 2016. The Community as the patient in malaria-endemic areas: preempting drug resistance with multiple first-line therapies. *PLoS medicine*, **13**, e1001984-e1001984.
- Borges, S., Cravo, P., Creasey, A., Fawcett, R., Modrzynska, K., Rodrigues, L., Martinelli, A. & Hunt, P. 2011. Genomewide scan reveals amplification of *mdr1* as a common denominator of resistance to mefloquine, lumefantrine, and artemisinin in *Plasmodium chabaudi* malaria parasites. *Antimicrobial agents and chemotherapy*, **55**, 4858-4865.
- Borrmann, S., Straimer, J., Mwai, L., Abdi, A., Rippert, A., Okombo, J., Muriithi, S., Sasi, P., Kortok, M. M., Lowe, B., Campino, S., Assefa, S., Auburn, S., Manske, M., Maslen, G., Peshu, N., Kwiatkowski, D. P., Marsh, K., Nzila, A. & Clark, T. G. 2013. Genome-wide screen identifies new candidate genes associated with artemisinin susceptibility in *Plasmodium falciparum* in Kenya. *Scientific reports*, **3**, 3318-3318.
- Brancucci, N. M. B., Bertschi, N. L., Zhu, L., Niederwieser, I., Chin, W. H., Wampfler, R., Freymond, C., Rottmann, M., Felger, I., Bozdech, Z. & Voss, T. S. 2014. Heterochromatin protein 1 secures survival and transmission of malaria parasites. *Cell host and microbe*, **16**, 165-176.

- Brancucci, N. M. B., De Niz, M., Straub, T. J., Ravel, D., Sollelis, L., Birren, B. W., Voss, T. S., Neafsey, D. E. & Marti, M. 2018. Probing *Plasmodium falciparum* sexual commitment at the single-cell level. Wellcome open research, **3**, 70-70.
- Brancucci, N. M. B., Gerdt, J. P., Wang, C., De Niz, M., Philip, N., Adapa, S. R., Zhang, M., Hitz, E., Niederwieser, I., Boltryk, S. D., Laffitte, M.-C., Clark, M. A., Grüning, C., Ravel, D., Blancke Soares, A., Demas, A., Bopp, S., Rubio-Ruiz, B., Conejo-Garcia, A., Wirth, D. F., Gendaszewska-Darmach, E., Duraisingh, M. T., Adams, J. H., Voss, T. S., Waters, A. P., Jiang, R. H. Y., Clardy, J. & Marti, M. 2017. Lysophosphatidylcholine regulates sexual stage differentiation in the human malaria parasite *Plasmodium falciparum*. Cell, **171**, 1532-1544.e15.
- Brancucci, N. M. B., Goldowitz, I., Buchholz, K., Werling, K. & Marti, M. 2015. An assay to probe *Plasmodium falciparum* growth, transmission stage formation and early gametocyte development. Nature protocols, **10**, 1131-1142.
- Breglio, K. F., Rahman, R. S., Sa, J. M., Hott, A., Roberts, D. J. & Wellems, T. E. 2018. Kelch mutations in *Plasmodium falciparum* protein K13 do not modulate dormancy after artemisinin exposure and sorbitol selection *in vitro*. Antimicrobial agents and chemotherapy, **62**.
- Bridgford, J. L., Xie, S. C., Cobbold, S. A., Pasaje, C. F. A., Herrmann, S., Yang, T., Gillett, D. L., Dick, L. R., Ralph, S. A., Dogovski, C., Spillman, N. J. & Tilley, L. 2018. Artemisinin kills malaria parasites by damaging proteins and inhibiting the proteasome. Nature communications, **9**, 3801.
- Brown, A. W. 1986. Insecticide resistance in mosquitoes: a pragmatic review. Journal of the American mosquito control association, **2**, 123-40.
- Bruce, M. C., Alano, P., Duthie, S. & Carter, R. 1990. Commitment of the malaria parasite *Plasmodium falciparum* to sexual and asexual development. Parasitology, **100 Pt 2**, 191-200.
- Buckling, A., Ranford-Cartwright, L. C., Miles, A. & Read, A. F. 1999. Chloroquine increases *Plasmodium falciparum* gametocytogenesis *in vitro*. Parasitology, **118 (Pt 4)**, 339-46.
- Burda, P.-C., Roelli, M. A., Schaffner, M., Khan, S. M., Janse, C. J. & Heussler, V. T. 2015. A *Plasmodium* phospholipase is involved in disruption of the liver stage parasitophorous vacuole membrane. PLoS pathogens, **11**, e1004760-e1004760.
- Burda, P. C., Caldelari, R. & Heussler, V. T. 2017. Manipulation of the host cell membrane during *Plasmodium* liver stage egress. mBio, **8**, e00139-17
- Bushell, E., Gomes, A. R., Sanderson, T., Anar, B., Girling, G., Herd, C., Metcalf, T., Modrzynska, K., Schwach, F., Martin, R. E., Mather, M. W., McFadden, G. I., Parts, L., Rutledge, G. G., Vaidya, A. B., Wengelnik, K., Rayner, J. C. & Billker, O. 2017. Functional profiling of a *Plasmodium* genome reveals an abundance of essential genes. Cell, **170**, 260-272.e8.
- Canning, E. U. & Sinden, R. E. 1973. The organization of the ookinete and observations on nuclear division in oocysts of *Plasmodium berghei*. Parasitology, **67**, 29-40.

- Carlton, J., Mackinnon, M. & Walliker, D. 1998a. A chloroquine resistance locus in the rodent malaria parasite *Plasmodium chabaudi*. *Molecular and biochemical parasitology*, **93**, 57-72.
- Carlton, J. M. R., Hayton, K., Cravo, P. V. L. & Walliker, D. 2001. Of mice and malaria mutants: unravelling the genetics of drug resistance using rodent malaria models. *Trends in parasitology*, **17**, 236-242.
- Carlton, J. M. R., Vinkenoog, R., Waters, A. P. & Walliker, D. 1998b. Gene synteny in species of *Plasmodium*. *Molecular and biochemical parasitology*, **93**, 285-294.
- Carter, R. & Walliker, D. 1975. New observations on the malaria parasites of rodents of the Central African Republic - *Plasmodium vinckei petteri* subsp. nov. and *Plasmodium chabaudi* Landau, 1965. *Annals of tropical medicine and parasitology*, **69**, 187-96.
- Cassera, M. B., Zhang, Y., Hazleton, K. Z. & Schramm, V. L. 2011. Purine and pyrimidine pathways as targets in *Plasmodium falciparum*. *Current topics in medicinal chemistry*, **11**, 2103-2115.
- Cerqueira, G. C., Cheeseman, I. H., Schaffner, S. F., Nair, S., McDew-White, M., Phyto, A. P., Ashley, E. A., Melnikov, A., Rogov, P., Birren, B. W., Nosten, F., Anderson, T. J. C. & Neafsey, D. E. 2017. Longitudinal genomic surveillance of *Plasmodium falciparum* malaria parasites reveals complex genomic architecture of emerging artemisinin resistance. *Genome biology*, **18**, 78-78.
- Charman, S. A., Arbe-Barnes, S., Bathurst, I. C., Brun, R., Campbell, M., Charman, W. N., Chiu, F. C. K., Chollet, J., Craft, J. C., Creek, D. J., Dong, Y., Matile, H., Maurer, M., Morizzi, J., Nguyen, T., Papastogiannidis, P., Scheurer, C., Shackelford, D. M., Sriraghavan, K., Stingelin, L., Tang, Y., Urwyler, H., Wang, X., White, K. L., Wittlin, S., Zhou, L. & Vennerstrom, J. L. 2011. Synthetic ozonide drug candidate OZ439 offers new hope for a single-dose cure of uncomplicated malaria. *Proceedings of the national academy of sciences of the USA*, **108**, 4400-4405.
- Chauhan, D., Tian, Z., Nicholson, B., Kumar, K. G., Zhou, B., Carrasco, R., McDermott, J. L., Leach, C. A., Fulciniti, M., Kodrasov, M. P., Weinstock, J., Kingsbury, W. D., Hideshima, T., Shah, P. K., Minvielle, S., Altun, M., Kessler, B. M., Orlowski, R., Richardson, P., Munshi, N. & Anderson, K. C. 2012. A small molecule inhibitor of ubiquitin-specific protease-7 induces apoptosis in multiple myeloma cells and overcomes bortezomib resistance. *Cancer cell*, **22**, 345-58.
- Cheng, Q. & Saul, A. 1994. The dihydrofolate reductase domain of rodent malarias: point mutations and pyrimethamine resistance. *Molecular and biochemical parasitology*, **65**, 361-363.
- Cobbold, S. A., Chua, H. H., Nijagal, B., Creek, D. J., Ralph, S. A. & McConville, M. J. 2016. Metabolic dysregulation induced in *Plasmodium falciparum* by dihydroartemisinin and other front-line antimalarial drugs. *The journal of infectious diseases*, **213**, 276-86.
- Cohen, S., Mc, G. I. & Carrington, S. 1961. Gamma-globulin and acquired immunity to human malaria. *Nature*, **192**, 733-7.

- Coleman, B. I., Skillman, K. M., Jiang, R. H. Y., Childs, L. M., Altenhofen, L. M., Ganter, M., Leung, Y., Goldowitz, I., Kafsack, B. F. C., Marti, M., Llinás, M., Buckee, C. O. & Duraisingh, M. T. 2014. A *Plasmodium falciparum* histone deacetylase regulates antigenic variation and gametocyte conversion. *Cell host and microbe*, **16**, 177-186.
- Collins, C. R., Hackett, F., Atid, J., Tan, M. S. Y. & Blackman, M. J. 2017. The *Plasmodium falciparum* pseudoprotease SERA5 regulates the kinetics and efficiency of malaria parasite egress from host erythrocytes. *PLoS pathogens*, **13**, e1006453-e1006453.
- Collins, C. R., Hackett, F., Strath, M., Penzo, M., Withers-Martinez, C., Baker, D. A. & Blackman, M. J. 2013. Malaria parasite cGMP-dependent protein kinase regulates blood stage merozoite secretory organelle discharge and egress. *PLoS pathogens*, **9**, e1003344-e1003344.
- Collins, C. R., Withers-Martinez, C., Hackett, F. & Blackman, M. J. 2009. An inhibitory antibody blocks interactions between components of the malarial invasion machinery. *PLoS pathogens*, **5**, e1000273.
- Cooper, E. M., Cutcliffe, C., Kristiansen, T. Z., Pandey, A., Pickart, C. M. & Cohen, R. E. 2009. K63-specific deubiquitination by two JAMM/MPN+ complexes: BRISC-associated Brcc36 and proteasomal Poh1. *The EMBO journal*, **28**, 621-31.
- Cowman, A. F., Berry, D. & Baum, J. 2012. The cellular and molecular basis for malaria parasite invasion of the human red blood cell. *The Journal of cell biology*, **198**, 961-971.
- Cowman, A. F., Morry, M. J., Biggs, B. A., Cross, G. A. & Foote, S. J. 1988. Amino acid changes linked to pyrimethamine resistance in the dihydrofolate reductase-thymidylate synthase gene of *Plasmodium falciparum*. *Proceedings of the national academy of sciences of the USA*, **85**, 9109-9113.
- Cowman, A. F., Tonkin, C. J., Tham, W.-H. & Duraisingh, M. T. 2017. The molecular basis of erythrocyte invasion by malaria parasites. *Cell host and microbe*, **22**, 232-245.
- Crabb, B. S., de Koning-Ward, T. F. & Gilson, P. R. 2010. Protein export in *Plasmodium* parasites: from the endoplasmic reticulum to the vacuolar export machine. *International journal for parasitology*, **40**, 509-513.
- Crabb, B. S., Rug, M., Gilberger, T. W., Thompson, J. K., Triglia, T., Maier, A. G. & Cowman, A. F. 2004. Transfection of the human malaria parasite *Plasmodium falciparum*. *Methods in molecular biology*, **270**, 263-76.
- Cravo, P. V. L., Carlton, J. M. R., Hunt, P., Bioni, L., Padua, R. A. & Walliker, D. 2003. Genetics of mefloquine resistance in the rodent malaria parasite *Plasmodium chabaudi*. *Antimicrobial agents and chemotherapy*, **47**, 709-718.
- Creek, D. J. & Barrett, M. P. 2014. Determination of antiprotozoal drug mechanisms by metabolomics approaches. *Parasitology*, **141**, 83-92.
- Creek, D. J., Chua, H. H., Cobbold, S. A., Nijagal, B., MacRae, J. I., Dickerman, B. K., Gilson, P. R., Ralph, S. A. & McConville, M. J. 2016. Metabolomics-based

screening of the malaria box reveals both novel and established mechanisms of action. *Antimicrobial agents and chemotherapy*, **60**, 6650-6663.

Creek, D. J., Jankevics, A., Breitling, R., Watson, D. G., Barrett, M. P. & Burgess, K. E. 2011. Toward global metabolomics analysis with hydrophilic interaction liquid chromatography-mass spectrometry: improved metabolite identification by retention time prediction. *Analytical chemistry*, **83**, 8703-10.

Creek, D. J., Jankevics, A., Burgess, K. E., Breitling, R. & Barrett, M. P. 2012. IDEOM: an Excel interface for analysis of LC-MS-based metabolomics data. *Bioinformatics*, **28**, 1048-9.

Cromer, D., Evans, K. J., Schofield, L. & Davenport, M. P. 2006. Preferential invasion of reticulocytes during late-stage *Plasmodium berghei* infection accounts for reduced circulating reticulocyte levels. *International journal for parasitology*, **36**, 1389-1397.

Crosnier, C., Bustamante, L. Y., Bartholdson, S. J., Bei, A. K., Theron, M., Uchikawa, M., Mboup, S., Ndir, O., Kwiatkowski, D. P., Duraisingh, M. T., Rayner, J. C. & Wright, G. J. 2011. Basigin is a receptor essential for erythrocyte invasion by *Plasmodium falciparum*. *Nature*, **480**, 534-7.

Cui, L., Mharakurwa, S., Ndiaye, D., Rathod, P. K. & Rosenthal, P. J. 2015. Antimalarial drug resistance: literature review and activities and findings of the ICEMR network. *The American journal of tropical medicine and hygiene*, **93**, 57-68.

Cully, M. 2014. Trial watch: next-generation antimalarial from phenotypic screen shows clinical promise. *Nature reviews drug discovery*, **13**, 717-717.

Currà, C., Gessmann, R., Pace, T., Picci, L., Peruzzi, G., Varamogianni-Mamatsi, V., Spanos, L., Garcia, C. R. S., Spaccapelo, R., Ponzi, M. & Siden-Kiamos, I. 2016. Release of *Plasmodium* sporozoites requires proteins with histone-fold dimerization domains. *Nature communications*, **7**, 13846.

D'Arcy, P., Brnjic, S., Olofsson, M. H., Fryknas, M., Lindsten, K., De Cesare, M., Perego, P., Sadeghi, B., Hassan, M., Larsson, R. & Linder, S. 2011. Inhibition of proteasome deubiquitinating activity as a new cancer therapy. *Nature medicine*, **17**, 1636-40.

Dahl, E. L. & Rosenthal, P. J. 2007. Multiple antibiotics exert delayed effects against the *Plasmodium falciparum* apicoplast. *Antimicrobial agents and chemotherapy*, **51**, 3485-3490.

Dahl, E. L., Shock, J. L., Shenai, B. R., Gut, J., DeRisi, J. L. & Rosenthal, P. J. 2006. Tetracyclines specifically target the apicoplast of the malaria parasite *Plasmodium falciparum*. *Antimicrobial agents and chemotherapy*, **50**, 3124-3131.

Das, S., Bhatanagar, S., Morrissey, J. M., Daly, T. M., Burns, J. M., Jr., Coppens, I. & Vaidya, A. B. 2016. Na⁺ influx induced by new antimalarials causes rapid alterations in the cholesterol content and morphology of *Plasmodium falciparum*. *PLoS pathogens*, **12**, e1005647-e1005647.

- Das, S., Hertrich, N., Perrin, A. J., Withers-Martinez, C., Collins, C. R., Jones, M. L., Watermeyer, J. M., Fobes, E. T., Martin, S. R., Saibil, H. R., Wright, G. J., Treeck, M., Epp, C. & Blackman, M. J. 2015. Processing of *Plasmodium falciparum* merozoite surface protein MSP1 activates a spectrin-binding function enabling parasite egress from RBCs. *Cell host and microbe*, **18**, 433-44.
- Davis, M. I. & Simeonov, A. 2015. Ubiquitin-specific proteases as druggable targets. *Drug target review*, **2**, 60-64.
- de Koning-Ward, T. F., Gilson, P. R., Boddey, J. A., Rug, M., Smith, B. J., Papenfuss, A. T., Sanders, P. R., Lundie, R. J., Maier, A. G., Cowman, A. F. & Crabb, B. S. 2009. A newly discovered protein export machine in malaria parasites. *Nature*, **459**, 945-949.
- De Niz, M. & Heussler, V. T. 2018. Rodent malaria models: insights into human disease and parasite biology. *Current opinion in microbiology*, **46**, 93-101.
- de Raad, M., Fischer, C. R. & Northen, T. R. 2016. High-throughput platforms for metabolomics. *Current opinion in chemical biology*, **30**, 7-13.
- de Roode, J. C., Culleton, R., Bell, A. S. & Read, A. F. 2004. Competitive release of drug resistance following drug treatment of mixed *Plasmodium chabaudi* infections. *Malaria journal*, **3**, 33-33.
- Delves, M., Plouffe, D., Scheurer, C., Meister, S., Wittlin, S., Winzeler, E. A., Sinden, R. E. & Leroy, D. 2012. The activities of current antimalarial drugs on the life cycle stages of *Plasmodium*: A comparative study with human and rodent parasites. *PLoS medicine*, **9**, e1001169.
- Demas, A. R., Sharma, A. I., Wong, W., Early, A. M., Redmond, S., Bopp, S., Neafsey, D. E., Volkman, S. K., Hartl, D. L. & Wirth, D. F. 2018. Mutations in *Plasmodium falciparum* actin-binding protein coronin confer reduced artemisinin susceptibility. *Proceedings of the national academy of sciences of the USA*, **115**, 12799-12804.
- Dhanao, B. S., Cogliati, T., Satish, A. G., Bruford, E. A. & Friedman, J. S. 2013. Update on the Kelch-like (KLHL) gene family. *Human genomics*, **7**, 13-13.
- Diggens, S. M. 1970. Single step production of pyrimethamine-resistant *P. berghei*. *Transactions of the royal society of tropical medicine and hygiene*, **64**, 9.
- Dogovski, C., Xie, S. C., Burgio, G., Bridgford, J., Mok, S., McCaw, J. M., Chotivanich, K., Kenny, S., Gnädig, N., Straimer, J., Bozdech, Z., Fidock, D. A., Simpson, J. A., Dondorp, A. M., Foote, S., Klonis, N. & Tilley, L. 2015. Targeting the cell stress response of *Plasmodium falciparum* to overcome artemisinin resistance. *PLoS biology*, **13**, e1002132.
- Dondorp, A. M., Nosten, F., Yi, P., Das, D., Phyo, A. P., Tarning, J., Lwin, K. M., Ariey, F., Hanpithakpong, W., Lee, S. J., Ringwald, P., Silamut, K., Imwong, M., Chotivanich, K., Lim, P., Herdman, T., An, S. S., Yeung, S., Singhasivanon, P., Day, N. P., Lindegardh, N., Socheat, D. & White, N. J. 2009. Artemisinin resistance in *Plasmodium falciparum* malaria. *The New England Journal of medicine*, **361**, 455-67.

- Donnelly, M. J., Corbel, V., Weetman, D., Wilding, C. S., Williamson, M. S. & Black, W. C. t. 2009. Does kdr genotype predict insecticide-resistance phenotype in mosquitoes? *Trends in parasitology*, **25**, 213-9.
- Doolan, D. L., Dobaño, C. & Baird, J. K. 2009. Acquired immunity to malaria. *Clinical microbiology reviews*, **22**, 13-36.
- Douglas, A. D., Baldeviano, G. C., Lucas, C. M., Lugo-Roman, L. A., Crosnier, C., Bartholdson, S. J., Diouf, A., Miura, K., Lambert, L. E., Ventocilla, J. A., Leiva, K. P., Milne, K. H., Illingworth, J. J., Spencer, A. J., Hjerrild, K. A., Alanine, D. G., Turner, A. V., Moorhead, J. T., Edgel, K. A., Wu, Y., Long, C. A., Wright, G. J., Lescano, A. G. & Draper, S. J. 2015. A PfRH5-based vaccine is efficacious against heterologous strain blood-stage *Plasmodium falciparum* infection in *Aotus* monkeys. *Cell host and microbe*, **17**, 130-9.
- Draper, S. J., Sack, B. K., King, C. R., Nielsen, C. M., Rayner, J. C., Higgins, M. K., Long, C. A. & Seder, R. A. 2018. Malaria Vaccines: recent advances and new horizons. *Cell host and microbe*, **24**, 43-56.
- Ecker, A., Lakshmanan, V., Sinnis, P., Coppens, I. & Fidock, D. A. 2011. Evidence that mutant PfCRT facilitates the transmission to mosquitoes of chloroquine-treated *Plasmodium* gametocytes. *The journal of infectious diseases*, **203**, 228-236.
- Ecker, A., Lehane, A. M., Clain, J. & Fidock, D. A. 2012. PfCRT and its role in antimalarial drug resistance. *Trends in parasitology*, **28**, 504-514.
- Eckstein-Ludwig, U., Webb, R. J., Van Goethem, I. D., East, J. M., Lee, A. G., Kimura, M., O'Neill, P. M., Bray, P. G., Ward, S. A. & Krishna, S. 2003. Artemisinins target the SERCA of *Plasmodium falciparum*. *Nature*, **424**, 957-61.
- Eksi, S., Morahan, B. J., Haile, Y., Furuya, T., Jiang, H., Ali, O., Xu, H., Kiattibutr, K., Suri, A., Czesny, B., Adeyemo, A., Myers, T. G., Sattabongkot, J., Su, X.-z. & Williamson, K. C. 2012. *Plasmodium falciparum* gametocyte development 1 (Pfgdv1) and gametocytogenesis early gene identification and commitment to sexual development. *PLoS pathogens*, **8**, e1002964-e1002964.
- Elissa, N., Mouchet, J., Riviere, F., Meunier, J. Y. & Yao, K. 1993. Resistance of *Anopheles gambiae* s.s. to pyrethroids in Cote d'Ivoire. *Annales de la Societe belge de medecine tropicale*, **73**, 291-4.
- Elsworth, B., Matthews, K., Nie, C. Q., Kalanon, M., Charnaud, S. C., Sanders, P. R., Chisholm, S. A., Counihan, N. A., Shaw, P. J., Pino, P., Chan, J.-A., Azevedo, M. F., Rogerson, S. J., Beeson, J. G., Crabb, B. S., Gilson, P. R. & de Koning-Ward, T. F. 2014. PTEX is an essential nexus for protein export in malaria parasites. *Nature*, **511**, 587-591.
- Fairlamb, A. H., Gow, N. A. R., Matthews, K. R. & Waters, A. P. 2016. Drug resistance in eukaryotic microorganisms. *Nature microbiology*, **1**, 16092-16092.
- Feachem, R. G. A., Chen, I., Akbari, O., Bertozzi-Villa, A., Bhatt, S., Binka, F., Boni, M. F., Buckee, C., Dieleman, J., Dondorp, A., Eapen, A., Sekhri Feachem, N., Filler, S., Gething, P., Gosling, R., Haakenstad, A., Harvard, K., Hatefi, A., Jamison, D., Jones, K. E., Karema, C., Kamwi, R. N., Lal, A., Larson, E., Lees,

- M., Lobo, N. F., Micah, A. E., Moonen, B., Newby, G., Ning, X., Pate, M., Quinones, M., Roh, M., Rolfe, B., Shanks, D., Singh, B., Staley, K., Tulloch, J., Wegbreit, J., Woo, H. J. & Mpanju-Shumbusho, W. 2019. Malaria eradication within a generation: ambitious, achievable, and necessary. *Lancet*, **394**, 1056-1112.
- Ferdig, M. T., Cooper, R. A., Mu, J., Deng, B., Joy, D. A., Su, X. Z. & Wellems, T. E. 2004. Dissecting the loci of low-level quinine resistance in malaria parasites. *Molecular microbiology*, **52**, 985-97.
- Ferreira, P. E., Culleton, R., Gil, J. P. & Meshnick, S. R. 2013. Artemisinin resistance in *Plasmodium falciparum*: what is it really? *Trends in parasitology*, **29**, 318-20.
- Fidock, D. A., Nomura, T., Talley, A. K., Cooper, R. A., Dzekunov, S. M., Ferdig, M. T., Ursos, L. M., Sidhu, A. B., Naudé, B., Deitsch, K. W., Su, X. Z., Wootton, J. C., Roepe, P. D. & Wellems, T. E. 2000. Mutations in the *P. falciparum* digestive vacuole transmembrane protein PfCRT and evidence for their role in chloroquine resistance. *Molecular cell*, **6**, 861-871.
- Fidock, D. A., Rosenthal, P. J., Croft, S. L., Brun, R. & Nwaka, S. 2004. Antimalarial drug discovery: efficacy models for compound screening. *Nature reviews drug discovery*, **3**, 509-520.
- Filarsky, M., Fraschka, S. A., Niederwieser, I., Brancucci, N. M. B., Carrington, E., Carrió, E., Moes, S., Jenoe, P., Bártfai, R. & Voss, T. S. 2018. GDV1 induces sexual commitment of malaria parasites by antagonizing HP1-dependent gene silencing. *Science (New York, N.Y.)*, **359**, 1259-1263.
- Fivelman, Q. L., Adagu, I. S. & Warhurst, D. C. 2004. Modified fixed-ratio isobologram method for studying *in vitro* interactions between atovaquone and proguanil or dihydroartemisinin against drug-resistant strains of *Plasmodium falciparum*. *Antimicrob agents and chemotherapy*, **48**, 4097-102.
- Flannery, E. L., Fidock, D. A. & Winzeler, E. A. 2013. Using genetic methods to define the targets of compounds with antimalarial activity. *Journal of medicinal chemistry*, **56**, 7761-7771.
- Flegg, J. A., Guerin, P. J., White, N. J. & Stepniewska, K. 2011. Standardizing the measurement of parasite clearance in *falciparum* malaria: the parasite clearance estimator. *Malaria journal*, **10**, 339.
- Franke-Fayard, B., Djokovic, D., Dooren, M. W., Ramesar, J., Waters, A. P., Falade, M. O., Kranendonk, M., Martinelli, A., Cravo, P. & Janse, C. J. 2008. Simple and sensitive antimalarial drug screening *in vitro* and *in vivo* using transgenic luciferase expressing *Plasmodium berghei* parasites. *International journal for parasitology*, **38**, 1651-62.
- Fraschka, S. A., Filarsky, M., Hoo, R., Niederwieser, I., Yam, X. Y., Brancucci, N. M. B., Mohring, F., Mushunje, A. T., Huang, X., Christensen, P. R., Nosten, F., Bozdech, Z., Russell, B., Moon, R. W., Marti, M., Preiser, P. R., Bártfai, R. & Voss, T. S. 2018. Comparative heterochromatin profiling reveals conserved and unique epigenome signatures linked to adaptation and development of malaria parasites. *Cell host and microbe*, **23**, 407-420.e8.

- Frénal, K., Polonais, V., Marq, J. B., Stratmann, R., Limenitakis, J. & Soldati-Favre, D. 2010. Functional dissection of the apicomplexan glideosome molecular architecture. *Cell host and microbe*, **8**, 343-57.
- Frickel, E. M., Quesada, V., Muething, L., Gubbels, M. J., Spooner, E., Ploegh, H. & Artavanis-Tsakonas, K. 2007. Apicomplexan UCHL3 retains dual specificity for ubiquitin and Nedd8 throughout evolution. *Cell microbiology*, **9**, 1601-10.
- Fry, M. & Pudney, M. 1992. Site of action of the antimalarial hydroxynaphthoquinone, 2-[trans-4-(4'-chlorophenyl) cyclohexyl]-3-hydroxy-1,4-naphthoquinone (566C80). *Biochemical pharmacology*, **43**, 1545-53.
- Gabryszewski, S. J., Modchang, C., Musset, L., Chookajorn, T. & Fidock, D. A. 2016. Combinatorial genetic modeling of pfCRT-mediated drug resistance evolution in *Plasmodium falciparum*. *Molecular biology and evolution*, **33**, 1554-1570.
- Gaillard, T., Madamet, M. & Pradines, B. 2015. Tetracyclines in malaria. *Malaria journal*, **14**, 445-445.
- Galinski, M. R. & Barnwell, J. W. 2012. Chapter 5 - Nonhuman primate models for human malaria research. In: Abee, C. R., Mansfield, K., Tardif, S. & Morris, T. (eds.) *Nonhuman primates in biomedical research (Second Edition)*. Boston: Academic Press.
- Gamo, F.-J., Sanz, L. M., Vidal, J., de Cozar, C., Alvarez, E., Lavandera, J.-L., Vanderwall, D. E., Green, D. V. S., Kumar, V., Hasan, S., Brown, J. R., Peishoff, C. E., Cardon, L. R. & Garcia-Bustos, J. F. 2010. Thousands of chemical starting points for antimalarial lead identification. *Nature*, **465**, 305-310.
- Ganesan, K., Ponmee, N., Jiang, L., Fowble, J. W., White, J., Kamchonwongpaisan, S., Yuthavong, Y., Wilairat, P. & Rathod, P. K. 2008. A genetically hard-wired metabolic transcriptome in *Plasmodium falciparum* fails to mount protective responses to lethal antifolates. *PLoS pathogens*, **4**, e1000214-e1000214.
- Gantt, S. M., Myung, J. M., Briones, M. R., Li, W. D., Corey, E. J., Omura, S., Nussenzweig, V. & Sinnis, P. 1998. Proteasome inhibitors block development of *Plasmodium* spp. *Antimicrobial agents and chemotherapy*, **42**, 2731-8.
- Garcia, G. E., Wirtz, R. A., Barr, J. R., Woolfitt, A. & Rosenberg, R. 1998. Xanthurenic acid induces gametogenesis in *Plasmodium*, the malaria parasite. *Journal of biological chemistry*, **273**, 12003-5.
- Garg, S., Agarwal, S., Kumar, S., Yazdani, S. S., Chitnis, C. E. & Singh, S. 2013. Calcium-dependent permeabilization of erythrocytes by a perforin-like protein during egress of malaria parasites. *Nature communications*, **4**, 1736.
- Genschik, P., Sumara, I. & Lechner, E. 2013. The emerging family of CULLIN3-RING ubiquitin ligases (CRL3s): cellular functions and disease implications. *The EMBO journal*, **32**, 2307-2320.

- German, J. B., Hammock, B. D. & Watkins, S. M. 2005. Metabolomics: building on a century of biochemistry to guide human health. *Metabolomics : official journal of the metabolomic society*, **1**, 3-9.
- Gervais, G. W., Trujillo, K., Robinson, B. L., Peters, W. & Serrano, A. E. 1999. *Plasmodium berghei*: Identification of anmdr-like gene associated with drug resistance. *Experimental parasitology*, **91**, 86-92.
- Ghidelli-Disse, S., Lafuente-Monasterio, M. J., Waterson, D., Witty, M., Younis, Y., Paquet, T., Street, L. J., Chibale, K., Gamo-Benito, F. J., Bantscheff, M. & Drewes, G. 2014. Identification of *Plasmodium* PI4 kinase as target of MMV390048 by chemoproteomics. *Malaria Journal*, **13**, P38-P38.
- Ghorbal, M., Gorman, M., Macpherson, C. R., Martins, R. M., Scherf, A. & Lopez-Rubio, J.-J. 2014. Genome editing in the human malaria parasite *Plasmodium falciparum* using the CRISPR-Cas9 system. *Nature biotechnology*, **32**, 819-821.
- Giannangelo, C., Siddiqui, G., De Paoli, A., Anderson, B. M., Edgington-Mitchell, L. E., Charman, S. A. & Creek, D. J. 2020. System-wide biochemical analysis reveals ozonide antimalarials initially act by disrupting *Plasmodium falciparum* haemoglobin digestion. *PloS pathogens*, **16**, e1008485.
- Gilson, P. R., Chisholm, S. A., Crabb, B. S. & de Koning-Ward, T. F. 2017. Host cell remodelling in malaria parasites: a new pool of potential drug targets. *International journal for parasitology*, **47**, 119-127.
- Gilson, P. R. & Crabb, B. S. 2009. Morphology and kinetics of the three distinct phases of red blood cell invasion by *Plasmodium falciparum* merozoites. *International journal for parasitology*, **39**, 91-96.
- Gloaguen, Y., Morton, F., Daly, R., Gurden, R., Rogers, S., Wandy, J., Wilson, D., Barrett, M. & Burgess, K. 2017. PiMP my metabolome: an integrated, web-based tool for LC-MS metabolomics data. *Bioinformatics*, **33**, 4007-4009.
- Gnädig, N. F., Stokes, B. H., Edwards, R. L., Kalantarov, G. F., Heimsch, K. C., Kuderjavy, M., Crane, A., Lee, M. C. S., Straimer, J., Becker, K., Trakht, I. N., Odom John, A. R., Mok, S. & Fidock, D. A. 2020. Insights into the intracellular localization, protein associations and artemisinin resistance properties of *Plasmodium falciparum* K13. *PloS pathogens*, **16**, e1008482.
- Goldberg, D. E. 2005. Hemoglobin degradation. *Current topics in microbiology and immunology*, **295**, 275-91.
- Goodman, C. D., Siregar, J. E., Mollard, V., Vega-Rodríguez, J., Syafruddin, D., Matsuoka, H., Matsuzaki, M., Toyama, T., Sturm, A., Cozijnsen, A., Jacobs-Lorena, M., Kita, K., Marzuki, S. & McFadden, G. I. 2016. Parasites resistant to the antimalarial atovaquone fail to transmit by mosquitoes. *Science (New York, N.Y.)*, **352**, 349-353.
- Graewe, S., Rankin, K. E., Lehmann, C., Deschermeier, C., Hecht, L., Froehlke, U., Stanway, R. R. & Heussler, V. 2011. Hostile takeover by *Plasmodium*: reorganization of parasite and host cell membranes during liver stage egress. *PLoS pathogens*, **7**, e1002224-e1002224.

- Green, J. L., Wall, R. J., Vahokoski, J., Yusuf, N. A., Ridzuan, M. A. M., Stanway, R. R., Stock, J., Knuepfer, E., Brady, D., Martin, S. R., Howell, S. A., Pires, I. P., Moon, R. W., Molloy, J. E., Kursula, I., Tewari, R. & Holder, A. A. 2017. Compositional and expression analyses of the glideosome during the *Plasmodium* life cycle reveal an additional myosin light chain required for maximum motility. *The journal of biological chemistry*, **292**, 17857-17875.
- Griffiths, W. J., Koal, T., Wang, Y., Kohl, M., Enot, D. P. & Deigner, H. P. 2010. Targeted metabolomics for biomarker discovery. *Angewandte Chemie (International ed. in English)*, **49**, 5426-45.
- Group, W. P. C. S., Abdulla, S., Ashley, E. A., Bassat, Q., Bethell, D., Björkman, A., Borrmann, S., D'Alessandro, U., Dahal, P., Day, N. P., Diakite, M., Djimde, A. A., Dondorp, A. M., Duong, S., Edstein, M. D., Fairhurst, R. M., Faiz, M. A., Falade, C., Flegg, J. A., Fogg, C., Gonzalez, R., Greenwood, B., Guérin, P. J., Guthmann, J.-P., Hamed, K., Hien, T. T., Htut, Y., Juma, E., Lim, P., Mårtensson, A., Mayxay, M., Mokuolu, O. A., Moreira, C., Newton, P., Noedl, H., Nosten, F., Ogutu, B. R., Onyamboko, M. A., Owusu-Agyei, S., Phyto, A. P., Premji, Z., Price, R. N., Pukrittayakamee, S., Ramharther, M., Sagara, I., Se, Y., Suon, S., Stepniewska, K., Ward, S. A., White, N. J. & Winstanley, P. A. 2015. Baseline data of parasite clearance in patients with *falciparum* malaria treated with an artemisinin derivative: an individual patient data meta-analysis. *Malaria journal*, **14**, 359-359.
- Gruring, C., Heiber, A., Kruse, F., Flemming, S., Franci, G., Colombo, S. F., Fasana, E., Schoeler, H., Borgese, N., Stunnenberg, H. G., Przyborski, J. M., Gilberger, T. W. & Spielmann, T. 2012. Uncovering common principles in protein export of malaria parasites. *Cell host and microbe*, **12**, 717-29.
- Gryseels, C., Durnez, L., Gerrets, R., Uk, S., Suon, S., Set, S., Phoeuk, P., Sluydts, V., Heng, S., Sochantha, T., Coosemans, M. & Peeters Grietens, K. 2015. Re-imagining malaria: heterogeneity of human and mosquito behaviour in relation to residual malaria transmission in Cambodia. *Malaria journal*, **14**, 165-165.
- Guiguemde, W. A., Shelat, A. A., Bouck, D., Duffy, S., Crowther, G. J., Davis, P. H., Smithson, D. C., Connelly, M., Clark, J., Zhu, F., Jiménez-Díaz, M. B., Martinez, M. S., Wilson, E. B., Tripathi, A. K., Gut, J., Sharlow, E. R., Bathurst, I., El Mazouni, F., Fowble, J. W., Forquer, I., McGinley, P. L., Castro, S., Angulo-Barturen, I., Ferrer, S., Rosenthal, P. J., Derisi, J. L., Sullivan, D. J., Lazo, J. S., Roos, D. S., Riscoe, M. K., Phillips, M. A., Rathod, P. K., Van Voorhis, W. C., Avery, V. M. & Guy, R. K. 2010. Chemical genetics of *Plasmodium falciparum*. *Nature*, **465**, 311-315.
- Guiguemde, W. A., Shelat, A. A., Garcia-Bustos, J. F., Diagana, T. T., Gamo, F.-J. & Guy, R. K. 2012. Global phenotypic screening for antimalarials. *Chemistry and biology*, **19**, 116-129.
- Haldar, K., Bhattacharjee, S. & Safeukui, I. 2018. Drug resistance in *Plasmodium*. *Nature reviews microbiology*, **16**, 156-170.
- Hamilton, W. L., Amato, R., van der Pluijm, R. W., Jacob, C. G., Quang, H. H., Thuy-Nhien, N. T., Hien, T. T., Hongvanthong, B., Chindavongsa, K., Mayxay, M., Huy, R., Leang, R., Huch, C., Dysoley, L., Amaratunga, C., Suon, S., Fairhurst,

- R. M., Tripura, R., Peto, T. J., Sovann, Y., Jittamala, P., Hanboonkunupakarn, B., Pukrittayakamee, S., Chau, N. H., Imwong, M., Dhorda, M., Vongprommek, R., Chan, X. H. S., Maude, R. J., Pearson, R. D., Nguyen, T., Rockett, K., Drury, E., Goncalves, S., White, N. J., Day, N. P., Kwiatkowski, D. P., Dondorp, A. M. & Miotto, O. 2019. Evolution and expansion of multidrug-resistant malaria in Southeast Asia: a genomic epidemiology study. *The lancet infectious diseases*, **19**, 943-951.
- Hanpude, P., Bhattacharya, S., Dey, A. K. & Maiti, T. K. 2015. Deubiquitinating enzymes in cellular signaling and disease regulation. *IUBMB life*, **67**, 544-555.
- Harbut, M. B., Patel, B. A., Yeung, B. K., McNamara, C. W., Bright, A. T., Ballard, J., Supek, F., Golde, T. E., Winzeler, E. A., Diagana, T. T. & Greenbaum, D. C. 2012. Targeting the ERAD pathway via inhibition of signal peptide peptidase for antiparasitic therapeutic design. *Proceedings of the national academy of sciences of the USA*, **109**, 21486-91.
- Harrigan, J. A., Jacq, X., Martin, N. M. & Jackson, S. P. 2017. Deubiquitylating enzymes and drug discovery: emerging opportunities. *Nature reviews drug discovery*, **17**, 57.
- Hartwig, C. L., Rosenthal, A. S., D'Angelo, J., Griffin, C. E., Posner, G. H. & Cooper, R. A. 2009. Accumulation of artemisinin trioxane derivatives within neutral lipids of *Plasmodium falciparum* malaria parasites is endoperoxide-dependent. *Biochemical pharmacology*, **77**, 322-36.
- Hastings, I. M., Kay, K. & Hodel, E. M. 2016. The importance of scientific debate in the identification, containment, and control of artemisinin resistance. *Clinical infectious diseases*, **63**, 1527-1528.
- Hawking, F. 1966. Chloroquine resistance in *Plasmodium Berghei*. *The American journal of tropical medicine and hygiene*, **15**, 287-293.
- Hawking, F., Wilson, M. E. & Gammage, K. 1971. Evidence for cyclic development and short-lived maturity in the gametocytes of *Plasmodium falciparum*. *Transactions of the royal society of tropical medicine and hygiene*, **65**, 549-59.
- Hay, S. I., Guerra, C. A., Tatem, A. J., Noor, A. M. & Snow, R. W. 2004. The global distribution and population at risk of malaria: past, present, and future. *The Lancet infectious diseases*, **4**, 327-336.
- Haynes, R. K., Fugmann, B., Stetter, J., Rieckmann, K., Heilmann, H. D., Chan, H. W., Cheung, M. K., Lam, W. L., Wong, H. N., Croft, S. L., Vivas, L., Rattray, L., Stewart, L., Peters, W., Robinson, B. L., Edstein, M. D., Kotecka, B., Kyle, D. E., Beckermann, B., Gerisch, M., Radtke, M., Schmuck, G., Steinke, W., Wollborn, U., Schmeer, K. & Romer, A. 2006. Artemisone--a highly active antimalarial drug of the artemisinin class. *Angewandte Chemie (International ed. in English)*, **45**, 2082-8.
- Hayton, K., Ranford-Cartwright, L. C. & Walliker, D. 2002. Sulfadoxine-pyrimethamine resistance in the rodent malaria parasite *Plasmodium chabaudi*. *Antimicrobial agents and chemotherapy*, **46**, 2482-2489.

- Heckman, K. L. & Pease, L. R. 2007. Gene splicing and mutagenesis by PCR-driven overlap extension. *Nature protocols*, **2**, 924.
- Hemingway, J., Ranson, H., Magill, A., Kolaczinski, J., Fornadel, C., Gimnig, J., Coetzee, M., Simard, F., Roch, D. K., Hinzoumbe, C. K., Pickett, J., Schellenberg, D., Gething, P., Hoppé, M. & Hamon, N. 2016a. Averting a malaria disaster: will insecticide resistance derail malaria control? *Lancet* (London, England), **387**, 1785-1788.
- Hemingway, J., Shretta, R., Wells, T. N. C., Bell, D., Djimdé, A. A., Achee, N. & Qi, G. 2016b. Tools and strategies for malaria control and elimination: What do we need to achieve a grand convergence in malaria? *PLoS biology*, **14**, e1002380.
- Henrici, R. C., van Schalkwyk, D. A. & Sutherland, C. J. 2019a. Modification of pfap2mu and pfUBP-1 markedly reduces ring-stage susceptibility of *Plasmodium falciparum* to artemisinin *in vitro*. *Antimicrobial agents and chemotherapy*, **64**, e01542-19.
- Henrici, R. C., van Schalkwyk, D. A. & Sutherland, C. J. 2019b. Transient temperature fluctuations severely decrease *P. falciparum* susceptibility to artemisinin *in vitro*. *International journal for parasitology: drugs and drug resistance*, **9**, 23-26.
- Henriques, G., Hallett, R. L., Beshir, K. B., Gadalla, N. B., Johnson, R. E., Burrow, R., van Schalkwyk, D. A., Sawa, P., Omar, S. A., Clark, T. G., Bousema, T. & Sutherland, C. J. 2014. Directional selection at the pfmdr1, pfcr1, pfUBP-1, and pfap2mu loci of *Plasmodium falciparum* in Kenyan children treated with ACT. *The journal of infectious diseases*, **210**, 2001-8.
- Henriques, G., Martinelli, A., Rodrigues, L., Modrzynska, K., Fawcett, R., Houston, D. R., Borges, S. T., d'Alessandro, U., Tinto, H., Karema, C., Hunt, P. & Cravo, P. 2013. Artemisinin resistance in rodent malaria--mutation in the AP2 adaptor mu-chain suggests involvement of endocytosis and membrane protein trafficking. *Malaria journal*, **12**, 118.
- Henriques, G., van Schalkwyk, D. A., Burrow, R., Warhurst, D. C., Thompson, E., Baker, D. A., Fidock, D. A., Hallett, R., Flueck, C. & Sutherland, C. J. 2015. The mu subunit of *Plasmodium falciparum* clathrin-associated adaptor protein 2 modulates *in vitro* parasite response to artemisinin and quinine. *Antimicrobial agents and chemotherapy*, **59**, 2540-2547.
- Hiller, N. L., Bhattacharjee, S., van Ooij, C., Liolios, K., Harrison, T., Lopez-Estrano, C. & Haldar, K. 2004. A host-targeting signal in virulence proteins reveals a secretome in malarial infection. *Science*, **306**, 1934-7.
- Hirai, M., Arai, M., Mori, T., Miyagishima, S. Y., Kawai, S., Kita, K., Kuroiwa, T., Terenius, O. & Matsuoka, H. 2008. Male fertility of malaria parasites is determined by GCS1, a plant-type reproduction factor. *Current biology*, **18**, 607-13.
- Ho, C.-M., Beck, J. R., Lai, M., Cui, Y., Goldberg, D. E., Egea, P. F. & Zhou, Z. H. 2018. Malaria parasite translocon structure and mechanism of effector export. *Nature*, **561**, 70-75.

- Hoffman, S. L., Billingsley, P. F., James, E., Richman, A., Loyevsky, M., Li, T., Chakravarty, S., Gunasekera, A., Chattopadhyay, R., Li, M., Stafford, R., Ahumada, A., Epstein, J. E., Sedegah, M., Reyes, S., Richie, T. L., Lyke, K. E., Edelman, R., Laurens, M. B., Plowe, C. V. & Sim, B. K. 2010. Development of a metabolically active, non-replicating sporozoite vaccine to prevent *Plasmodium falciparum* malaria. *Human vaccines*, **6**, 97-106.
- Hsu, P. D., Scott, D. A., Weinstein, J. A., Ran, F. A., Konermann, S., Agarwala, V., Li, Y., Fine, E. J., Wu, X., Shalem, O., Cradick, T. J., Marraffini, L. A., Bao, G. & Zhang, F. 2013. DNA targeting specificity of RNA-guided Cas9 nucleases. *Nature biotechnology*, **31**, 827-832.
- Huang, F., Takala-Harrison, S., Jacob, C. G., Liu, H., Sun, X., Yang, H., Nyunt, M. M., Adams, M., Zhou, S., Xia, Z., Ringwald, P., Bustos, M. D., Tang, L. & Plowe, C. V. 2015. A Single mutation in K13 predominates in Southern China and is associated with delayed clearance of *Plasmodium falciparum* following artemisinin treatment. *The journal of infectious diseases*, **212**, 1629-35.
- Hunt, P., Afonso, A., Creasey, A., Culleton, R., Sidhu, A. B., Logan, J., Valderramos, S. G., McNae, I., Cheesman, S., do Rosario, V., Carter, R., Fidock, D. A. & Cravo, P. 2007. Gene encoding a deubiquitinating enzyme is mutated in artesunate- and chloroquine-resistant rodent malaria parasites. *Molecular microbiology*, **65**, 27-40.
- Hunt, P., Martinelli, A., Modrzynska, K., Borges, S., Creasey, A., Rodrigues, L., Beraldi, D., Loewe, L., Fawcett, R., Kumar, S., Thomson, M., Trivedi, U., Otto, T. D., Pain, A., Blaxter, M. & Cravo, P. 2010. Experimental evolution, genetic analysis and genome re-sequencing reveal the mutation conferring artemisinin resistance in an isogenic lineage of malaria parasites. *BMC genomics*, **11**, 499.
- Hviid, L. & Jensen, A. T. R. 2015. Chapter two - PfEMP1 - a parasite protein family of key importance in *Plasmodium falciparum* malaria immunity and pathogenesis. *In*: Rollinson, D. & Stothard, J. R. (eds.) *Advances in Parasitology*. Academic Press.
- Ishino, T., Chinzei, Y. & Yuda, M. 2005. Two proteins with 6-cys motifs are required for malarial parasites to commit to infection of the hepatocyte. *Molecular microbiology*, **58**, 1264-75.
- Ismail, H. M., Barton, V., Phanchana, M., Charoensutthivarakul, S., Wong, M. H., Hemingway, J., Biagini, G. A., O'Neill, P. M. & Ward, S. A. 2016. Artemisinin activity-based probes identify multiple molecular targets within the asexual stage of the malaria parasites *Plasmodium falciparum* 3D7. *Proceedings of the national academy of sciences of the USA*, **113**, 2080-5.
- Jankevics, A., Merlo, M. E., de Vries, M., Vonk, R. J., Takano, E. & Breitling, R. 2012. Separating the wheat from the chaff: a prioritisation pipeline for the analysis of metabolomics datasets. *Metabolomics*, **8**, 29-36.
- Janse, C. J., Carlton, J. M. R., Walliker, D. & Waters, A. P. 1994a. Conserved location of genes on polymorphic chromosomes of four species of malaria parasites. *Molecular and biochemical parasitology*, **68**, 285-296.

- Janse, C. J., Franke-Fayard, B., Mair, G. R., Ramesar, J., Thiel, C., Engelmann, S., Matuschewski, K., Gemert, G. J. v., Sauerwein, R. W. & Waters, A. P. 2006a. High efficiency transfection of *Plasmodium berghei* facilitates novel selection procedures. *Molecular and biochemical parasitology*, **145**, 60-70.
- Janse, C. J., Ramesar, J. & Waters, A. P. 2006b. High-efficiency transfection and drug selection of genetically transformed blood stages of the rodent malaria parasite *Plasmodium berghei*. *Nature protocols*, **1**, 346-356.
- Janse, C. J., van der Klooster, P. F., van der Kaay, H. J., van der Ploeg, M. & Overdulve, J. P. 1986. DNA synthesis in *Plasmodium berghei* during asexual and sexual development. *Molecular and biochemical parasitology*, **20**, 173-82.
- Janse, C. J. & Waters, A. P. 1995. *Plasmodium berghei*: the application of cultivation and purification techniques to molecular studies of malaria parasites. *Parasitology today*, **11**, 138-143.
- Janse, C. J., Waters, A. P., Kos, J. & Lugt, C. B. 1994b. Comparison of *in vivo* and *in vitro* antimalarial activity of artemisinin, dihydroartemisinin and sodium artesunate in the *Plasmodium berghei*-rodent model. *International journal for parasitology*, **24**, 589-94.
- Jennison, C., Lucantoni, L., O'Neill, M. T., McConville, R., Erickson, S. M., Cowman, A. F., Sleebs, B. E., Avery, V. M. & Boddey, J. A. 2019. Inhibition of Plasmeprin V activity blocks *Plasmodium falciparum* gametocytogenesis and transmission to mosquitoes. *Cell reports*, **29**, 3796-3806.e4.
- Jiang, Y., Wei, J., Cui, H., Liu, C., Zhi, Y., Jiang, Z., Li, Z., Li, S., Yang, Z., Wang, X., Qian, P., Zhang, C., Zhong, C., Su, X.-z. & Yuan, J. 2020. An intracellular membrane protein GEP1 regulates xanthurenic acid induced gametogenesis of malaria parasites. *Nature communications*, **11**, 1764.
- Jimenez-Diaz, M. B., Ebert, D., Salinas, Y., Pradhan, A., Lehane, A. M., Myrand-Lapierre, M. E., O'Loughlin, K. G., Shackleford, D. M., Justino de Almeida, M., Carrillo, A. K., Clark, J. A., Dennis, A. S., Diep, J., Deng, X., Duffy, S., Endsley, A. N., Fedewa, G., Guiguemde, W. A., Gomez, M. G., Holbrook, G., Horst, J., Kim, C. C., Liu, J., Lee, M. C., Matheny, A., Martinez, M. S., Miller, G., Rodriguez-Alejandre, A., Sanz, L., Sigal, M., Spillman, N. J., Stein, P. D., Wang, Z., Zhu, F., Waterson, D., Knapp, S., Shelat, A., Avery, V. M., Fidock, D. A., Gamo, F. J., Charman, S. A., Mirsalis, J. C., Ma, H., Ferrer, S., Kirk, K., Angulo-Barturen, I., Kyle, D. E., DeRisi, J. L., Floyd, D. M. & Guy, R. K. 2014. (+)-SJ733, a clinical candidate for malaria that acts through ATP4 to induce rapid host-mediated clearance of *Plasmodium*. *Proceedings of the national academy of sciences of the USA*, **111**, e5455-62.
- Jongco, A. M., Ting, L. M., Thathy, V., Mota, M. M. & Kim, K. 2006. Improved transfection and new selectable markers for the rodent malaria parasite *Plasmodium yoelii*. *Molecular and biochemical parasitology*, **146**, 242-50.
- Josling, G. A., Russell, T. J., Venezia, J., Orchard, L., van Biljon, R., Painter, H. J. & Llinás, M. 2020. Dissecting the role of PfAP2-G in malaria gametocytogenesis. *Nature communications*, **11**, 1503.

- Josling, G. A., Williamson, K. C. & Llinás, M. 2018. Regulation of sexual commitment and gametocytogenesis in malaria parasites. *Annual review of microbiology*, **72**, 501-519.
- Joyner, C., Moreno, A., Meyer, E. V. S., Cabrera-Mora, M., Kong, A., Ibegbu, C., Arafat, D., Jones, D., Nace, D. P., Voit, E. O., Pohl, J., Humphrey, J., DeBarry, J., Sullivan, J., Gutierrez, J. B., Kevin, K. J., Fonseca, L. L., Styczynski, M., Nural, M., Pruett, S. T., Lapp, S. A., Pakala, S., Lamb, T. J., Williams, T., Uppal, K., Tran, V., Yin, W., Yan, Y., Kissinger, J. C., Barnwell, J. W., Galinski, M. R. & The Ma, H. C. 2016. *Plasmodium cynomolgi* infections in rhesus macaques display clinical and parasitological features pertinent to modelling *vivax* malaria pathology and relapse infections. *Malaria journal*, **15**, 451.
- Juliano, J. J., Porter, K., Mwapasa, V., Sem, R., Rogers, W. O., Arie, F., Wongsrichanalai, C., Read, A. & Meshnick, S. R. 2010. Exposing malaria in-host diversity and estimating population diversity by capture-recapture using massively parallel pyrosequencing. *Proceedings of the national academy of sciences of the USA*, **107**, 20138-20143.
- Kafsack, B. F. C., Rovira-Graells, N., Clark, T. G., Bancells, C., Crowley, V. M., Campino, S. G., Williams, A. E., Drought, L. G., Kwiatkowski, D. P., Baker, D. A., Cortés, A. & Llinás, M. 2014. A transcriptional switch underlies commitment to sexual development in malaria parasites. *Nature*, **507**, 248-252.
- Kaneko, I., Iwanaga, S., Kato, T., Kobayashi, I. & Yuda, M. 2015. Genome-wide identification of the target genes of AP2-O, a *Plasmodium* AP2-family transcription factor. *PLoS pathogens*, **11**, e1004905-e1004905.
- Kapulu, M. C., Da, D. F., Miura, K., Li, Y., Blagborough, A. M., Churcher, T. S., Nikolaeva, D., Williams, A. R., Goodman, A. L., Sangare, I., Turner, A. V., Cottingham, M. G., Nicosia, A., Straschil, U., Tsuboi, T., Gilbert, S. C., Long, C. A., Sinden, R. E., Draper, S. J., Hill, A. V. S., Cohuet, A. & Biswas, S. 2015. Comparative assessment of transmission-blocking vaccine candidates against *Plasmodium falciparum*. *Scientific reports*, **5**, 11193-11193.
- Kapur, V., Peterson, L. F., Fang, D., Bornmann, W. G., Talpaz, M. & Donato, N. J. 2010. Deubiquitinase inhibition by small-molecule WP1130 triggers aggresome formation and tumor cell apoptosis. *Cancer research*, **70**, 9265-76.
- Kauth, C. W., Woehlbier, U., Kern, M., Mekonnen, Z., Lutz, R., Mücke, N., Langowski, J. & Bujard, H. 2006. Interactions between merozoite surface proteins 1, 6, and 7 of the malaria parasite *Plasmodium falciparum*. *The journal of biological chemistry*, **281**, 31517-27.
- Kawamoto, F., Alejo-Blanco, R., Fleck, S. L. & Sinden, R. E. 1991. *Plasmodium berghei*: ionic regulation and the induction of gametogenesis. *Experimental parasitology*, **72**, 33-42.
- Ke, H., Lewis, I. A., Morrissey, J. M., McLean, K. J., Ganesan, S. M., Painter, H. J., Mather, M. W., Jacobs-Lorena, M., Llinás, M. & Vaidya, A. B. 2015. Genetic investigation of tricarboxylic acid metabolism during the *Plasmodium falciparum* life cycle. *Cell reports*, **11**, 164-174.

- Kell, D. B. 2004. Metabolomics and systems biology: making sense of the soup. *Current opinion in microbiology*, **7**, 296-307.
- Kent, R. S., Modrzynska, K. K., Cameron, R., Philip, N., Billker, O. & Waters, A. P. 2018. Inducible developmental reprogramming redefines commitment to sexual development in the malaria parasite *Plasmodium berghei*. *Nature microbiology*, **3**, 1206-1213.
- Kheang, S. T., Sovannaroeth, S., Ek, S., Chy, S., Chhun, P., Mao, S., Nguon, S., Lek, D. S., Menard, D. & Kak, N. 2017. Prevalence of K13 mutation and Day-3 positive parasitaemia in artemisinin-resistant malaria endemic area of Cambodia: a cross-sectional study. *Malar journal*, **16**, 372.
- Kim, C. C., Wilson, E. B. & DeRisi, J. L. 2010. Improved methods for magnetic purification of malaria parasites and haemozoin. *Malar journal*, **9**, 17.
- Kinga Modrzynska, K., Creasey, A., Loewe, L., Cezard, T., Trindade Borges, S., Martinelli, A., Rodrigues, L., Cravo, P., Blaxter, M., Carter, R. & Hunt, P. 2012. Quantitative genome re-sequencing defines multiple mutations conferring chloroquine resistance in rodent malaria. *BMC genomics*, **13**, 106-106.
- Kirchner, S., Power, B. J. & Waters, A. P. 2016. Recent advances in malaria genomics and epigenomics. *Genome medicine*, **8**, 92-92.
- Kirkman, L. A., Lawrence, E. A. & Deitsch, K. W. 2014. Malaria parasites utilize both homologous recombination and alternative end joining pathways to maintain genome integrity. *Nucleic acids research*, **42**, 370-379.
- Kirkman, L. A., Zhan, W., Visone, J., Dziedziech, A., Singh, P. K., Fan, H., Tong, X., Bruzual, I., Hara, R., Kawasaki, M., Imaeda, T., Okamoto, R., Sato, K., Michino, M., Alvaro, E. F., Guiang, L. F., Sanz, L., Mota, D. J., Govindasamy, K., Wang, R., Ling, Y., Tumwebaze, P. K., Sukenick, G., Shi, L., Vendome, J., Bhanot, P., Rosenthal, P. J., Aso, K., Foley, M. A., Cooper, R. A., Kafack, B., Doggett, J. S., Nathan, C. F. & Lin, G. 2018. Antimalarial proteasome inhibitor reveals collateral sensitivity from intersubunit interactions and fitness cost of resistance. *Proceedings of the national academy of sciences of the USA*, **115**, e6863-E6870.
- Klonis, N., Crespo-Ortiz, M. P., Bottova, I., Abu-Bakar, N., Kenny, S., Rosenthal, P. J. & Tilley, L. 2011. Artemisinin activity against *Plasmodium falciparum* requires hemoglobin uptake and digestion. *Proceedings of the national academy of sciences of the USA*, **108**, 11405-10.
- Kreidenweiss, A., Kremsner, P. G. & Mordmüller, B. 2008. Comprehensive study of proteasome inhibitors against *Plasmodium falciparum* laboratory strains and field isolates from Gabon. *Malaria journal*, **7**, 187-187.
- Krishna, S. & Kremsner, P. G. 2013. Antidogmatic approaches to artemisinin resistance: reappraisal as treatment failure with artemisinin combination therapy. *Trends in parasitology*, **29**, 313-7.
- Krotoski, W. A., Collins, W. E., Bray, R. S., Garnham, P. C., Cogswell, F. B., Gwadz, R. W., Killick-Kendrick, R., Wolf, R., Sinden, R., Koontz, L. C. & Stanfill, P. S. 1982. Demonstration of hypnozoites in sporozoite-transmitted *Plasmodium*

vivax infection. The American journal of tropical medicine and hygiene, **31**, 1291-3.

Kuhen, K. L., Chatterjee, A. K., Rottmann, M., Gagaring, K., Borboa, R., Buenviaje, J., Chen, Z., Francek, C., Wu, T., Nagle, A., Barnes, S. W., Plouffe, D., Lee, M. C., Fidock, D. A., Graumans, W., van de Vegte-Bolmer, M., van Gemert, G. J., Wirjanata, G., Sebayang, B., Marfurt, J., Russell, B., Suwanarusk, R., Price, R. N., Nosten, F., Tungtaeng, A., Gettayacamin, M., Sattabongkot, J., Taylor, J., Walker, J. R., Tully, D., Patra, K. P., Flannery, E. L., Vinetz, J. M., Renia, L., Sauerwein, R. W., Winzeler, E. A., Glynn, R. J. & Diagana, T. T. 2014. KAF156 is an antimalarial clinical candidate with potential for use in prophylaxis, treatment, and prevention of disease transmission. Antimicrobial agents and chemotherapy, **58**, 5060-7.

Kwon, Y. K., Lu, W., Melamud, E., Khanam, N., Bogner, A. & Rabinowitz, J. D. 2008. A domino effect in antifolate drug action in *Escherichia coli*. Nature chemical biology, **4**, 602-8.

Lambros, C. & Vanderberg, J. P. 1979. Synchronization of *Plasmodium falciparum* erythrocytic stages in culture. The journal of parasitology, **65**, 418-20.

LaMonte, G., Lim, M. Y., Wree, M., Reimer, C., Nachon, M., Corey, V., Gedeck, P., Plouffe, D., Du, A., Figueroa, N., Yeung, B., Bifani, P. & Winzeler, E. A. 2016. Mutations in the *Plasmodium falciparum* cyclic amine resistance locus (PfCARL) confer multidrug resistance. mBio, **7**, e00696-16.

LaMonte, G. M., Rocamora, F., Marapana, D. S., Gnädig, N. F., Otilie, S., Luth, M. R., Worgall, T. S., Goldgof, G. M., Mohunlal, R., Santha Kumar, T. R., Thompson, J. K., Vigil, E., Yang, J., Hutson, D., Johnson, T., Huang, J., Williams, R. M., Zou, B. Y., Cheung, A. L., Kumar, P., Egan, T. J., Lee, M. C. S., Siegel, D., Cowman, A. F., Fidock, D. A. & Winzeler, E. A. 2020. Pan-active imidazolopiperazine antimalarials target the *Plasmodium falciparum* intracellular secretory pathway. Nature communications, **11**, 1780.

Laufer, M. K., Takala-Harrison, S., Dzinjalama, F. K., Stine, O. C., Taylor, T. E. & Plowe, C. V. 2010. Return of chloroquine-susceptible *falciparum* malaria in Malawi was a reexpansion of diverse susceptible parasites. The journal of infectious diseases, **202**, 801-808.

Lecker, S. H., Goldberg, A. L. & Mitch, W. E. 2006. Protein degradation by the ubiquitin-proteasome pathway in normal and disease states. Journal of the American society of nephrology, **17**, 1807-19.

Lee, M. C. S., Lindner, S. E., Lopez-Rubio, J.-J. & Llinás, M. 2019. Cutting back malaria: CRISPR/Cas9 genome editing of *Plasmodium*. Briefings in functional genomics, **18**, 281-289.

Lee, R. S., Waters, A. P. & Brewer, J. M. 2018. A cryptic cycle in haematopoietic niches promotes initiation of malaria transmission and evasion of chemotherapy. Nature communications, **9**, 1689.

- Lehane, A. M., Ridgway, M. C., Baker, E. & Kirk, K. 2014. Diverse chemotypes disrupt ion homeostasis in the malaria parasite. *Molecular microbiology*, **94**, 327-339.
- Lei, Z., Huhman, D. V. & Sumner, L. W. 2011. Mass spectrometry strategies in metabolomics. *The journal of biological chemistry*, **286**, 25435-25442.
- Leykauf, K., Treeck, M., Gilson, P. R., Nebl, T., Braulke, T., Cowman, A. F., Gilberger, T. W. & Crabb, B. S. 2010. Protein kinase A dependent phosphorylation of apical membrane antigen 1 plays an important role in erythrocyte invasion by the malaria parasite. *PLoS pathogens*, **6**, e1000941.
- Li, G. Q., Arnold, K., Guo, X. B., Jian, H. X. & Fu, L. C. 1984. Randomised comparative study of mefloquine, qinghaosu, and pyrimethamine-sulfadoxine in patients with falciparum malaria. *Lancet*, **2**, 1360-1.
- Li, H., O'Donoghue, A. J., van der Linden, W. A., Xie, S. C., Yoo, E., Foe, I. T., Tilley, L., Craik, C. S., da Fonseca, P. C. A. & Bogyo, M. 2016. Structure- and function-based design of *Plasmodium*-selective proteasome inhibitors. *Nature*, **530**, 233.
- Li, H., Ponder, E. L., Verdoes, M., Asbjornsdottir, K. H., Deu, E., Edgington, L. E., Lee, J. T., Kirk, C. J., Demo, S. D., Williamson, K. C. & Bogyo, M. 2012. Validation of the proteasome as a therapeutic target in *Plasmodium* using an epoxyketone inhibitor with parasite-specific toxicity. *Chemistry and biology*, **19**, 1535-1545.
- Lim, M. Y.-X., LaMonte, G., Lee, M. C. S., Reimer, C., Tan, B. H., Corey, V., Tjahjadi, B. F., Chua, A., Nachon, M., Wintjens, R., Gedeck, P., Malleret, B., Renia, L., Bonamy, G. M. C., Ho, P. C.-L., Yeung, B. K. S., Chow, E. D., Lim, L., Fidock, D. A., Diagana, T. T., Winzeler, E. A. & Bifani, P. 2016. UDP-galactose and acetyl-CoA transporters as *Plasmodium* multidrug resistance genes. *Nature microbiology*, **1**, 16166-16166.
- Liu, Y., Lashuel, H. A., Choi, S., Xing, X., Case, A., Ni, J., Yeh, L. A., Cuny, G. D., Stein, R. L. & Lansbury, P. T., Jr. 2003. Discovery of inhibitors that elucidate the role of UCH-L1 activity in the H1299 lung cancer cell line. *Chemical biology*, **10**, 837-46.
- Liu, Y., Tewari, R., Ning, J., Blagborough, A. M., Garbom, S., Pei, J., Grishin, N. V., Steele, R. E., Sinden, R. E., Snell, W. J. & Billker, O. 2008. The conserved plant sterility gene HAP2 functions after attachment of fusogenic membranes in *Chlamydomonas* and *Plasmodium* gametes. *Genes and development*, **22**, 1051-1068.
- Llorà-Batlle, O., Michel-Todó, L., Witmer, K., Toda, H., Fernández-Becerra, C., Baum, J. & Cortés, A. 2020. Conditional expression of PfAP2-G for controlled massive sexual conversion in *Plasmodium falciparum*. *Science advances*, **6**, eaaz5057.
- Lotharius, J., Gamo-Benito, F. J., Angulo-Barturen, I., Clark, J., Connelly, M., Ferrer-Bazaga, S., Parkinson, T., Viswanath, P., Bandodkar, B., Rautela, N., Bharath, S., Duffy, S., Avery, V. M., Möhrle, J. J., Guy, R. K. & Wells, T. 2014.

- Repositioning: the fast track to new anti-malarial medicines? *Malaria journal*, **13**, 143-143.
- Lukens, A. K., Ross, L. S., Heidebrecht, R., Javier Gamo, F., Lafuente-Monasterio, M. J., Booker, M. L., Hartl, D. L., Wiegand, R. C. & Wirth, D. F. 2014. Harnessing evolutionary fitness in *Plasmodium falciparum* for drug discovery and suppressing resistance. *Proceedings of the national academy of sciences of the USA*, **111**, 799-804.
- Lumjuan, N., McCarroll, L., Prapanthadara, L. A., Hemingway, J. & Ranson, H. 2005. Elevated activity of an Epsilon class glutathione transferase confers DDT resistance in the dengue vector, *Aedes aegypti*. *Insect biochemistry and molecular biology*, **35**, 861-71.
- Maerki, S., Brun, R., Charman, S. A., Dorn, A., Matile, H. & Wittlin, S. 2006. *In vitro* assessment of the pharmacodynamic properties and the partitioning of OZ277/RBx-11160 in cultures of *Plasmodium falciparum*. *Journal of antimicrobial chemotherapy*, **58**, 52-8.
- Maier, A. G., Rug, M., O'Neill, M. T., Brown, M., Chakravorty, S., Szestak, T., Chesson, J., Wu, Y., Hughes, K., Coppel, R. L., Newbold, C., Beeson, J. G., Craig, A., Crabb, B. S. & Cowman, A. F. 2008. Exported proteins required for virulence and rigidity of *Plasmodium falciparum*-infected human erythrocytes. *Cell*, **134**, 48-61.
- Mair, G. R., Braks, J. A. M., Garver, L. S., Wiegant, J. C. A. G., Hall, N., Dirks, R. W., Khan, S. M., Dimopoulos, G., Janse, C. J. & Waters, A. P. 2006. Regulation of sexual development of *Plasmodium* by translational repression. *Science (New York, N.Y.)*, **313**, 667-669.
- Mair, G. R., Lasonder, E., Garver, L. S., Franke-Fayard, B. M. D., Carret, C. K., Wiegant, J. C. A. G., Dirks, R. W., Dimopoulos, G., Janse, C. J. & Waters, A. P. 2010. Universal features of post-transcriptional gene regulation are critical for *Plasmodium* zygote development. *PLoS pathogens*, **6**, e1000767.
- Malaria, G. E. N. P. f. C. P. 2016. Genomic epidemiology of artemisinin resistant malaria. *eLife*, **5**, e08714.
- Markley, J. L., Brüschweiler, R., Edison, A. S., Eghbalnia, H. R., Powers, R., Raftery, D. & Wishart, D. S. 2017. The future of NMR-based metabolomics. *Current opinion in biotechnology*, **43**, 34-40.
- Marti, M., Good, R. T., Rug, M., Knuepfer, E. & Cowman, A. F. 2004. Targeting malaria virulence and remodeling proteins to the host erythrocyte. *Science*, **306**, 1930-3.
- Mbengue, A., Bhattacharjee, S., Pandharkar, T., Liu, H., Estiu, G., Stahelin, R. V., Rizk, S. S., Njimoh, D. L., Ryan, Y., Chotivanich, K., Nguon, C., Ghorbal, M., Lopez-Rubio, J. J., Pfrender, M., Emrich, S., Mohandas, N., Dondorp, A. M., Wiest, O. & Haldar, K. 2015. A molecular mechanism of artemisinin resistance in *Plasmodium falciparum* malaria. *Nature*, **520**, 683-7.
- McNamara, C. W., Lee, M. C., Lim, C. S., Lim, S. H., Roland, J., Simon, O., Yeung, B. K., Chatterjee, A. K., McCormack, S. L., Manary, M. J., Zeeman, A. -

- M., Dechering, K. J., Kumar, T. S., Henrich, P. P., Gagaring, K., Ibanez, M., Kato, N., Kuhen, K. L., Fischli, C., Nagle, A., Rottmann, M., Plouffe, D. M., Bursulaya, B., Meister, S., Rameh, L., Trappe, J., Haasen, D., Timmerman, M., Sauerwein, R. W., Suwanarusk, R., Russell, B., Renia, L., Nosten, F., Tully, D. C., Kocken, C. H., Glynn, R. J., Bodenreider, C., Fidock, D. A., Diagana, T. T. & Winzeler, E. A. 2013. Targeting *Plasmodium* PI(4)K to eliminate malaria. *Nature*, **504**, 248-253.
- McRobert, L., Taylor, C. J., Deng, W., Fivelman, Q. L., Cummings, R. M., Polley, S. D., Billker, O. & Baker, D. A. 2008. Gametogenesis in malaria parasites is mediated by the cGMP-dependent protein kinase. *PLoS biology*, **6**, e139-e139.
- Menard, D., Khim, N., Beghain, J., Adegnika, A. A., Shafiul-Alam, M., Amodu, O., Rahim-Awab, G., Barnadas, C., Berry, A., Boum, Y., Bustos, M. D., Cao, J., Chen, J. H., Collet, L., Cui, L., Thakur, G. D., Dieye, A., Djalle, D., Dorkenoo, M. A., Eboumbou-Moukoko, C. E., Espino, F. E., Fandeur, T., Ferreira-da-Cruz, M. F., Fola, A. A., Fuehrer, H. P., Hassan, A. M., Herrera, S., Hongvanthong, B., Houze, S., Ibrahim, M. L., Jahirul-Karim, M., Jiang, L., Kano, S., Ali-Khan, W., Khanthavong, M., Kremsner, P. G., Lacerda, M., Leang, R., Leelawong, M., Li, M., Lin, K., Mazarati, J. B., Menard, S., Morlais, I., Muhindo-Mavoko, H., Musset, L., Na-Bangchang, K., Nambozi, M., Niare, K., Noedl, H., Ouedraogo, J. B., Pillai, D. R., Pradines, B., Quang-Phuc, B., Ramharter, M., Randrianarivelojosa, M., Sattabongkot, J., Sheikh-Omar, A., Silue, K. D., Sirima, S. B., Sutherland, C., Syafruddin, D., Tahar, R., Tang, L. H., Toure, O. A., Tshibangu-wa-Tshibangu, P., Vigan-Womas, I., Warsame, M., Wini, L., Zakeri, S., Kim, S., Eam, R., Berne, L., Khean, C., Chy, S., Ken, M., Loch, K., Canier, L., Duru, V., Legrand, E., Barale, J. C., Stokes, B., Straimer, J., Witkowski, B., Fidock, D. A., Rogier, C., Ringwald, P., Ariey, F. & Mercereau-Puijalon, O. 2016. A Worldwide Map of *Plasmodium falciparum* K13-propeller polymorphisms. *The New England journal of medicine*, **374**, 2453-64.
- Ménard, R., Sultan, A. A., Cortes, C., Altszuler, R., van Dijk, M. R., Janse, C. J., Waters, A. P., Nussenzweig, R. S. & Nussenzweig, V. 1997. Circumsporozoite protein is required for development of malaria sporozoites in mosquitoes. *Nature*, **385**, 336-340.
- Menard, R., Tavares, J., Cockburn, I., Markus, M., Zavala, F. & Amino, R. 2013. Looking under the skin: the first steps in malarial infection and immunity. *Nature reviews microbiology*, **11**, 701-12.
- Merkli, B. & Richle, R. 1983a. Experimentally derived, stable mefloquine resistance in *Plasmodium yoelii nigeriensis*. *Transactions of the royal society of tropical medicine and hygiene*, **77**, 141-142.
- Merkli, B. & Richle, R. 1983b. *Plasmodium berghei*: diet and drug dosage regimens influencing selection of drug-resistant parasites in mice. *Experimental parasitology*, **55**, 372-6.
- Meshnick, S. R., Thomas, A., Ranz, A., Xu, C. M. & Pan, H. Z. 1991. Artemisinin (qinghaosu): the role of intracellular heme in its mechanism of antimalarial action. *Molecular and biochem parasitology*, **49**, 181-9.
- Meunier, B. & Robert, A. 2010. Heme as trigger and target for trioxane-containing antimalarial drugs. *Accounts of chemical research*, **43**, 1444-51.

- Minkah, N. K., Schafer, C. & Kappe, S. H. I. 2018. Humanized mouse models for the study of human malaria parasite biology, pathogenesis, and immunity. *Frontiers in immunology*, **9**, 807-807.
- Miotto, O., Amato, R., Ashley, E. A., MacInnis, B., Almagro-Garcia, J., Amaratunga, C., Lim, P., Mead, D., Oyola, S. O., Dhorda, M., Imwong, M., Woodrow, C., Manske, M., Stalker, J., Drury, E., Campino, S., Amenga-Etego, L., Thanh, T. N., Tran, H. T., Ringwald, P., Bethell, D., Nosten, F., Phyo, A. P., Pukrittayakamee, S., Chotivanich, K., Chuor, C. M., Nguon, C., Suon, S., Sreng, S., Newton, P. N., Mayxay, M., Khanthavong, M., Hongvanthong, B., Htut, Y., Han, K. T., Kyaw, M. P., Faiz, M. A., Fanello, C. I., Onyamboko, M., Mokuolu, O. A., Jacob, C. G., Takala-Harrison, S., Plowe, C. V., Day, N. P., Dondorp, A. M., Spencer, C. C., McVean, G., Fairhurst, R. M., White, N. J. & Kwiatkowski, D. P. 2015. Genetic architecture of artemisinin-resistant *Plasmodium falciparum*. *Nature genetics*, **47**, 226-34.
- Mohring, F., Hart, M. N., Rawlinson, T. A., Henrici, R., Charleston, J. A., Diez Benavente, E., Patel, A., Hall, J., Almond, N., Campino, S., Clark, T. G., Sutherland, C. J., Baker, D. A., Draper, S. J. & Moon, R. W. 2019. Rapid and iterative genome editing in the malaria parasite *Plasmodium knowlesi* provides new tools for *P. vivax* research. *eLife*, **8**, e45829.
- Mok, S., Ashley, E. A., Ferreira, P. E., Zhu, L., Lin, Z., Yeo, T., Chotivanich, K., Imwong, M., Pukrittayakamee, S., Dhorda, M., Nguon, C., Lim, P., Amaratunga, C., Suon, S., Hien, T. T., Htut, Y., Faiz, M. A., Onyamboko, M. A., Mayxay, M., Newton, P. N., Tripura, R., Woodrow, C. J., Miotto, O., Kwiatkowski, D. P., Nosten, F., Day, N. P., Preiser, P. R., White, N. J., Dondorp, A. M., Fairhurst, R. M. & Bozdech, Z. 2015. Drug resistance: population transcriptomics of human malaria parasites reveals the mechanism of artemisinin resistance. *Science*, **347**, 431-5.
- Mons, B. 1985. Induction of sexual differentiation in malaria. *Parasitology today*, **1**, 87-89.
- Moon, R. W., Taylor, C. J., Bex, C., Schepers, R., Goulding, D., Janse, C. J., Waters, A. P., Baker, D. A. & Billker, O. 2009. A cyclic GMP signalling module that regulates gliding motility in a malaria parasite. *PLoS pathogens*, **5**, e1000599-e1000599.
- Muhia, D. K., Swales, C. A., Deng, W., Kelly, J. M. & Baker, D. A. 2001. The gametocyte-activating factor xanthurenic acid stimulates an increase in membrane-associated guanylyl cyclase activity in the human malaria parasite *Plasmodium falciparum*. *Molecular microbiology*, **42**, 553-60.
- Mukherjee, A., Bopp, S., Magistrado, P., Wong, W., Daniels, R., Demas, A., Schaffner, S., Amaratunga, C., Lim, P., Dhorda, M., Miotto, O., Woodrow, C., Ashley, E. A., Dondorp, A. M., White, N. J., Wirth, D., Fairhurst, R. & Volkman, S. K. 2017. Artemisinin resistance without pfkelch13 mutations in *Plasmodium falciparum* isolates from Cambodia. *Malar journal*, **16**, 195.
- Muller, I. B. & Hyde, J. E. 2010. Antimalarial drugs: modes of action and mechanisms of parasite resistance. *Future microbiology*, **5**, 1857-73.

- Murithi, J. M., Owen, E. S., Istvan, E. S., Lee, M. C. S., Otilie, S., Chibale, K., Goldberg, D. E., Winzeler, E. A., Llinás, M., Fidock, D. A. & Vanaerschot, M. 2019. Combining stage specificity and metabolomic profiling to advance antimalarial drug discovery. *Cell chemical biology*, **27**, 158-173.e3.
- Mushtaq, M. Y., Choi, Y. H., Verpoorte, R. & Wilson, E. G. 2014. Extraction for metabolomics: access to the metabolome. *Phytochemical analysis*, **25**, 291-306.
- Nagelschmitz, J., Voith, B., Wensing, G., Roemer, A., Fugmann, B., Haynes, R. K., Kotecka, B. M., Rieckmann, K. H. & Edstein, M. D. 2008. First assessment in humans of the safety, tolerability, pharmacokinetics, and *ex vivo* pharmacodynamic antimalarial activity of the new artemisinin derivative artemisone. *Antimicrobial agents and chemotherapy*, **52**, 3085-3091.
- Nair, S., Li, X., Arya, G. A., McDew-White, M., Ferrari, M., Nosten, F. & Anderson, T. J. C. 2018. Fitness costs and the rapid spread of kelch13-C580Y substitutions conferring artemisinin resistance. *Antimicrobial agents and chemotherapy*, **62**, e00605-18.
- Nash, G. B., O'Brien, E., Gordon-Smith, E. C. & Dormandy, J. A. 1989. Abnormalities in the mechanical properties of red blood cells caused by *Plasmodium falciparum*. *Blood*, **74**, 855-61.
- Ng, C. L., Fidock, D. A. & Bogyo, M. 2017. Protein degradation systems as antimalarial therapeutic targets. *Trends in parasitology*, **33**, 731-743.
- Ngotho, P., Soares, A. B., Hentzschel, F., Achcar, F., Bertuccini, L. & Marti, M. 2019. Revisiting gametocyte biology in malaria parasites. *FEMS microbiology reviews*, **43**, 401-414.
- Nicholson, B., Leach, C. A., Goldenberg, S. J., Francis, D. M., Kodrasov, M. P., Tian, X., Shanks, J., Sterner, D. E., Bernal, A., Mattern, M. R., Wilkinson, K. D. & Butt, T. R. 2008. Characterization of ubiquitin and ubiquitin-like-protein isopeptidase activities. *Protein science*, **17**, 1035-43.
- Nilsson, S. K., Childs, L. M., Buckee, C. & Marti, M. 2015. Targeting human transmission biology for malaria elimination. *PLoS pathogens*, **11**, e1004871-e1004871.
- Nina F. Gnädig, B. H. S., Rachel L. Edwards, Gavreel F. Kalantarov, Kim Heimsch, Michal Kuderjavy, Audrey Crane, Marcus C.S. Lee, Judith Straimer1, Katja Becker, Ilya N. Trakht, Audrey R. Odom John, Sachel Mok, David A. Fidock 2020. Insights into the intracellular localization, protein associations and artemisinin resistance properties of *Plasmodium falciparum* K13. *PLoS pathogens*, **16**, e1008482.
- Nkrumah, L. J., Muhle, R. A., Moura, P. A., Ghosh, P., Hatfull, G. F., Jacobs, W. R., Jr. & Fidock, D. A. 2006. Efficient site-specific integration in *Plasmodium falciparum* chromosomes mediated by mycobacteriophage Bxb1 integrase. *Nature methods*, **3**, 615-621.
- Nussenzweig, R. S., Vanderberg, J., Most, H. & Orton, C. 1967. Protective immunity produced by the injection of x-irradiated sporozoites of *Plasmodium berghei*. *Nature*, **216**, 160-2.

- Nyunt, M. H., Hlaing, T., Oo, H. W., Tin-Oo, L.-L. K., Phway, H. P., Wang, B., Zaw, N. N., Han, S. S., Tun, T., San, K. K., Kyaw, M. P. & Han, E.-T. 2014. Molecular assessment of artemisinin resistance markers, polymorphisms in the K13 propeller, and a multidrug-resistance gene in the Eastern and Western Border Areas of Myanmar. *Clinical infectious diseases*, **60**, 1208-1215.
- O'Donnell, R. A., Preiser, P. R., Williamson, D. H., Moore, P. W., Cowman, A. F. & Crabb, B. S. 2001. An alteration in concatameric structure is associated with efficient segregation of plasmids in transfected *Plasmodium falciparum* parasites. *Nucleic acids research*, **29**, 716-724.
- O'Neill, P. M., Barton, V. E. & Ward, S. A. 2010. The molecular mechanism of action of artemisinin--the debate continues. *Molecules*, **15**, 1705-21.
- Obaldia, N., 3rd, Kotecka, B. M., Edstein, M. D., Haynes, R. K., Fugmann, B., Kyle, D. E. & Rieckmann, K. H. 2009. Evaluation of artemisone combinations in *Aotus* monkeys infected with *Plasmodium falciparum*. *Antimicrobial agents and chemotherapy*, **53**, 3592-3594.
- Odds, F. C. 2003. Synergy, antagonism, and what the checkerboard puts between them. *Journal of antimicrobial chemotherapy*, **52**, 1-1.
- Ohsawa, K., Tanabe, K., Kimata, I. & Miki, A. 1991. Ultrastructural changes associated with reversal of chloroquine resistance by verapamil in *Plasmodium chabaudi*. *Parasitology*, **103 Pt 2**, 185-9.
- Okuda, S., Yamada, T., Hamajima, M., Itoh, M., Katayama, T., Bork, P., Goto, S. & Kanehisa, M. 2008. KEGG atlas mapping for global analysis of metabolic pathways. *Nucleic acids research*, **36**, W423-W426.
- Olivieri, A., Bertuccini, L., Deligianni, E., Franke-Fayard, B., Currà, C., Siden-Kiamos, I., Hanssen, E., Grasso, F., Superti, F., Pace, T., Fratini, F., Janse, C. J. & Ponzi, M. 2015. Distinct properties of the egress-related osmiophilic bodies in male and female gametocytes of the rodent malaria parasite *Plasmodium berghei*. *Cell microbiology*, **17**, 355-68.
- Packard, R. M. 2014. The origins of antimalarial-drug resistance. *The New England journal of medicine*, **371**, 397-399.
- Padua, R. A. 1981. *Plasmodium chabaudi*: genetics of resistance to chloroquine. *Experimental parasitology*, **52**, 419-26.
- Paget-McNicol, S. & Saul, A. 2001. Mutation rates in the dihydrofolate reductase gene of *Plasmodium falciparum*. *Parasitology*, **122**, 497-505.
- Painter, H. J., Morrissey, J. M., Mather, M. W. & Vaidya, A. B. 2007. Specific role of mitochondrial electron transport in blood-stage *Plasmodium falciparum*. *Nature*, **446**, 88-91.
- Parzy, D., Doerig, C., Pradines, B., Rico, A., Fusai, T. & Doury, J. C. 1997. Proguanil resistance in *Plasmodium falciparum* African isolates: assessment by mutation-specific polymerase chain reaction and *in vitro* susceptibility testing. *The American journal of tropical medicine and hygiene*, **57**, 646-50.

- Patti, G. J., Yanes, O. & Siuzdak, G. 2012. Metabolomics: the apogee of the omics trilogy. *Nature reviews molecular cell biology*, **13**, 263.
- Pehrson, C., Salanti, A., Theander, T. G. & Nielsen, M. A. 2017. Pre-clinical and clinical development of the first placental malaria vaccine. *Expert review of vaccines*, **16**, 613-624.
- Peng, D. & Tarleton, R. 2015. EuPaGDT: a web tool tailored to design CRISPR guide RNAs for eukaryotic pathogens. *Microbial genomics*, **1**, e000033-e000033.
- Perrin, A. J., Collins, C. R., Russell, M. R. G., Collinson, L. M., Baker, D. A. & Blackman, M. J. 2018. The Actinomyosin motor drives malaria parasite red blood cell invasion but not egress. *mBio*, **9**, e00905-18.
- Peters, W. 1965. Drug resistance in *Plasmodium berghei* Vincke and Lips, 1948. I. chloroquine resistance. *Experimental parasitology*, **17**, 80-89.
- Peters, W. 1982. Antimalarial drug resistance: an increasing problem. *British medical bulletin*, **38**, 187-92.
- Peters, W., Chance, M. L., Lissner, R., Momen, H. & Warhurst, D. C. 1978. The chemotherapy of rodent malaria, XXX. The enigmas of the 'NS lines' of *P. berghei*. *Annals of tropical medicine and parasitology*, **72**, 23-36.
- Peters, W. & Robinson, B. L. 1999a. Chapter 92 - Malaria. In: Zak, O. & Sande, M. A. (eds.) *Handbook of Animal Models of Infection*. London: Academic Press.
- Peters, W. & Robinson, B. L. 1999b. The chemotherapy of rodent malaria. LVI. Studies on the development of resistance to natural and synthetic endoperoxides. *Annals of tropical medicine and parasitology*, **93**, 325-9.
- Peterson, D. S., Walliker, D. & Wellems, T. E. 1988. Evidence that a point mutation in dihydrofolate reductase-thymidylate synthase confers resistance to pyrimethamine in *falciparum* malaria. *Proceedings of the national academy of sciences of the USA*, **85**, 9114-9118.
- Philip, N., Orr, R. & Waters, A. P. 2013. Transfection of rodent malaria parasites. *Methods in molecular biology*, **923**, 99-125.
- Phyo, A. P., Ashley, E. A., Anderson, T. J. C., Bozdech, Z., Carrara, V. I., Sriprawat, K., Nair, S., White, M. M., Dziekan, J., Ling, C., Proux, S., Konghahong, K., Jeeyapant, A., Woodrow, C. J., Imwong, M., McGready, R., Lwin, K. M., Day, N. P. J., White, N. J. & Nosten, F. 2016a. Declining efficacy of artemisinin combination therapy against *P. falciparum* malaria on the Thai-Myanmar border (2003-2013): the role of parasite genetic factors. *Clinical infectious diseases*, **63**, 784-791.
- Phyo, A. P., Jittamala, P., Nosten, F. H., Pukrittayakamee, S., Imwong, M., White, N. J., Duparc, S., Macintyre, F., Baker, M. & Möhrle, J. J. 2016b. Antimalarial activity of artefenomel (OZ439), a novel synthetic antimalarial endoperoxide, in patients with *Plasmodium falciparum* and *Plasmodium vivax* malaria: an open-label phase 2 trial. *The lancet infectious diseases*, **16**, 61-69.

- Phyo, A. P., Nkhoma, S., Stepniewska, K., Ashley, E. A., Nair, S., McGready, R., ler Moo, C., Al-Saai, S., Dondorp, A. M., Lwin, K. M., Singhasivanon, P., Day, N. P. J., White, N. J., Anderson, T. J. C. & Nosten, F. 2012. Emergence of artemisinin-resistant malaria on the western border of Thailand: a longitudinal study. *Lancet* (London, England), **379**, 1960-1966.
- Platel, D. F., Mangou, F. & Tribouley-Duret, J. 1998. High-level chloroquine resistance of *Plasmodium berghei* is associated with multiple drug resistance and loss of reversal by calcium antagonists. *International journal for parasitology*, **28**, 641-651.
- Plowe, C. V., Cortese, J. F., Djimde, A., Nwanyanwu, O. C., Watkins, W. M., Winstanley, P. A., Estrada-Franco, J. G., Mollinedo, R. E., Avila, J. C., Cespedes, J. L., Carter, D. & Doumbo, O. K. 1997. Mutations in *Plasmodium falciparum* dihydrofolate reductase and dihydropteroate synthase and epidemiologic patterns of pyrimethamine-sulfadoxine use and resistance. *The journal of infectious diseases*, **176**, 1590-6.
- Pollitt, L. C., Huijben, S., Sim, D. G., Salathé, R. M., Jones, M. J. & Read, A. F. 2014. Rapid response to selection, competitive release and increased transmission potential of artesunate-selected *Plasmodium chabaudi* malaria parasites. *PLoS pathogens*, **10**, e1004019-e1004019.
- Ponder, E. L. & Bogyo, M. 2007. Ubiquitin-like modifiers and their deconjugating enzymes in medically important parasitic protozoa. *Eukaryotic cell*, **6**, 1943-1952.
- Pontes, J. G. M., Brasil, A. J. M., Cruz, G. C. F., de Souza, R. N. & Tasic, L. 2017. NMR-based metabolomics strategies: plants, animals and humans. *Analytical methods*, **9**, 1078-1096.
- Ponts, N., Saraf, A., Chung, D. W., Harris, A., Prudhomme, J., Washburn, M. P., Florens, L. & Le Roch, K. G. 2011. Unraveling the ubiquitome of the human malaria parasite. *The journal of biological chemistry*, **286**, 40320-30.
- Ponzi, M., Sidén-Kiamos, I., Bertuccini, L., Currà, C., Kroeze, H., Camarda, G., Pace, T., Franke-Fayard, B., Laurentino, E. C., Louis, C., Waters, A. P., Janse, C. J. & Alano, P. 2009. Egress of *Plasmodium berghei* gametes from their host erythrocyte is mediated by the MDV-1/PEG3 protein. *Cellular microbiology*, **11**, 1272-1288.
- Pouvelle, B., Buffet, P. A., Lépolard, C., Scherf, A. & Gysin, J. 2000. Cytoadhesion of *Plasmodium falciparum* ring-stage-infected erythrocytes. *Nature medicine*, **6**, 1264-8.
- Powers, K. G., Jacobs, R. L., Good, W. C. & Koontz, L. C. 1969. *Plasmodium vinckei*: production of chloroquine-resistant strain. *Experimental parasitology*, **26**, 193-202.
- Price, R. N., Uhlemann, A.-C., Brockman, A., McGready, R., Ashley, E., Phaipun, L., Patel, R., Laing, K., Looareesuwan, S., White, N. J., Nosten, F. & Krishna, S. 2004. Mefloquine resistance in *Plasmodium falciparum* and increased pfmdr1 gene copy number. *Lancet* (London, England), **364**, 438-447.

- Prudencio, M., Rodriguez, A. & Mota, M. M. 2006. The silent path to thousands of merozoites: the *Plasmodium* liver stage. *Nature reviews microbiology*, **4**, 849-856.
- Raja, A. I., Stanisic, D. I. & Good, M. F. 2017. Chemical attenuation in the development of a whole-organism malaria vaccine. *Infection and immunity*, **85**, e00062-17.
- Ranson, H. 2017. Current and future prospects for preventing malaria transmission via the use of insecticides. *Cold Spring Harbor perspectives in medicine*, **7**, a026823.
- Rathod, P. K., McErlean, T. & Lee, P. C. 1997. Variations in frequencies of drug resistance in *Plasmodium falciparum*. *Proceedings of the national academy of sciences of the USA*, **94**, 9389-9393.
- Ratner, H. K., Sampson, T. R. & Weiss, D. S. 2016. Overview of CRISPR-Cas9 biology. *Cold Spring Harbor protocols*, **2016**, pdb.top088849-pdb.top088849.
- Reininger, L., Billker, O., Tewari, R., Mukhopadhyay, A., Fennell, C., Dorin-Semlat, D., Doerig, C., Goldring, D., Harmse, L., Ranford-Cartwright, L., Packer, J. & Doerig, C. 2005. A NIMA-related protein kinase is essential for completion of the sexual cycle of malaria parasites. *The journal of biological chemistry*, **280**, 31957-64.
- Reininger, L., Tewari, R., Fennell, C., Holland, Z., Goldring, D., Ranford-Cartwright, L., Billker, O. & Doerig, C. 2009. An essential role for the *Plasmodium* Nek-2 Nima-related protein kinase in the sexual development of malaria parasites. *The journal of biological chemistry*, **284**, 20858-20868.
- Rieckmann, K. H., Beaudoin, R. L., Cassells, J. S. & Sell, K. W. 1979. Use of attenuated sporozoites in the immunization of human volunteers against *falciparum* malaria. *Bulletin of the World Health Organisation*, **57 Suppl 1**, 261-5.
- Riglar, D. T., Richard, D., Wilson, D. W., Boyle, M. J., Dekiwadia, C., Turnbull, L., Angrisano, F., Marapana, D. S., Rogers, K. L., Whitchurch, C. B., Beeson, J. G., Cowman, A. F., Ralph, S. A. & Baum, J. 2011. Super-resolution dissection of coordinated events during malaria parasite invasion of the human erythrocyte. *Cell host and microbe*, **9**, 9-20.
- Riveron, J. M., Irving, H., Ndula, M., Barnes, K. G., Ibrahim, S. S., Paine, M. J. I. & Wondji, C. S. 2013. Directionally selected cytochrome P450 alleles are driving the spread of pyrethroid resistance in the major malaria vector *Anopheles funestus*. *Proceedings of the national academy of sciences of the USA*, **110**, 252-257.
- Riveron, J. M., Yunta, C., Ibrahim, S. S., Djouaka, R., Irving, H., Menze, B. D., Ismail, H. M., Hemingway, J., Ranson, H., Albert, A. & Wondji, C. S. 2014. A single mutation in the GSTe2 gene allows tracking of metabolically based insecticide resistance in a major malaria vector. *Genome biology*, **15**, R27-R27.

- Rocamora, F., Zhu, L., Liong, K. Y., Dondorp, A., Miotto, O., Mok, S. & Bozdech, Z. 2018. Oxidative stress and protein damage responses mediate artemisinin resistance in malaria parasites. *PLoS pathogens*, **14**, e1006930-e1006930.
- Roepe, P. D. 2009. Molecular and physiologic basis of quinoline drug resistance in *Plasmodium falciparum* malaria. *Future microbiology*, **4**, 441-55.
- Rollo, I. M. 1952. Daraprim resistance in experimental malarial infections. *Nature*, **170**, 415.
- Rono, M. K., Nyonda, M. A., Simam, J. J., Ngoi, J. M., Mok, S., Kortok, M. M., Abdullah, A. S., Elfaki, M. M., Waitumbi, J. N., El-Hassan, I. M., Marsh, K., Bozdech, Z. & Mackinnon, M. J. 2018. Adaptation of *Plasmodium falciparum* to its transmission environment. *Nature ecology and evolution*, **2**, 377-387.
- Roper, C., Pearce, R., Bredenkamp, B., Gumede, J., Drakeley, C., Mosha, F., Chandramohan, D. & Sharp, B. 2003. Antifolate antimalarial resistance in Southeast Africa: a population-based analysis. *Lancet*, **361**, 1174-81.
- Rosario, V. E. 1976. Genetics of chloroquine resistance in malaria parasites. *Nature*, **261**, 585-6.
- Rottmann, M., McNamara, C., Yeung, B. K., Lee, M. C., Zou, B., Russell, B., Seitz, P., Plouffe, D. M., Dharia, N. V., Tan, J., Cohen, S. B., Spencer, K. R., Gonzalez-Paez, G. E., Lakshminarayana, S. B., Goh, A., Suwanarusk, R., Jegla, T., Schmitt, E. K., Beck, H. P., Brun, R., Nosten, F., Renia, L., Dartois, V., Keller, T. H., Fidock, D. A., Winzeler, E. A. & Diagana, T. T. 2010. Spiroindolones, a potent compound class for the treatment of malaria. *Science*, **329**, 1175-80.
- Rts, S. C. T. P. 2015. Efficacy and safety of RTS,S/AS01 malaria vaccine with or without a booster dose in infants and children in Africa: final results of a phase 3, individually randomised, controlled trial. *Lancet (London, England)*, **386**, 31-45.
- Rueden, C. T., Schindelin, J., Hiner, M. C., DeZonia, B. E., Walter, A. E., Arena, E. T. & Eliceiri, K. W. 2017. ImageJ2: ImageJ for the next generation of scientific image data. *BMC bioinformatics*, **18**, 529.
- Russo, I., Babbitt, S., Muralidharan, V., Butler, T., Oksman, A. & Goldberg, D. E. 2010. Plasmepsin V licenses *Plasmodium* proteins for export into the host erythrocyte. *Nature*, **463**, 632-636.
- Sa, J. M., Kaslow, S. R., Krause, M. A., Melendez-Muniz, V. A., Salzman, R. E., Kite, W. A., Zhang, M., Moraes Barros, R. R., Mu, J., Han, P. K., Mershon, J. P., Figan, C. E., Caleon, R. L., Rahman, R. S., Gibson, T. J., Amaratunga, C., Nishiguchi, E. P., Breglio, K. F., Engels, T. M., Velmurugan, S., Ricklefs, S., Straimer, J., Gnädig, N. F., Deng, B., Liu, A., Diouf, A., Miura, K., Tullo, G. S., Eastman, R. T., Chakravarty, S., James, E. R., Udenze, K., Li, S., Sturdevant, D. E., Gwadz, R. W., Porcella, S. F., Long, C. A., Fidock, D. A., Thomas, M. L., Fay, M. P., Sim, B. K. L., Hoffman, S. L., Adams, J. H., Fairhurst, R. M., Su, X. Z. & Wellems, T. E. 2018. Artemisinin resistance phenotypes and K13 inheritance in a *Plasmodium falciparum* cross and *Aotus* model. *Proceedings of the national academy of sciences of the USA*, **115**, 12513-12518.

- Sack, B. K., Miller, J. L., Vaughan, A. M., Douglass, A., Kaushansky, A., Mikolajczak, S., Coppi, A., Gonzalez-Aseguinolaza, G., Tsuji, M., Zavala, F., Sinnis, P. & Kappe, S. H. I. 2014. Model for *in vivo* assessment of humoral protection against malaria sporozoite challenge by passive transfer of monoclonal antibodies and immune serum. *Infection and immunity*, **82**, 808-817.
- Sanders, P. R., Gilson, P. R., Cantin, G. T., Greenbaum, D. C., Nebl, T., Carucci, D. J., McConville, M. J., Schofield, L., Hodder, A. N., Yates, J. R., 3rd & Crabb, B. S. 2005. Distinct protein classes including novel merozoite surface antigens in Raft-like membranes of *Plasmodium falciparum*. *The journal of biological chemistry*, **280**, 40169-76.
- Santos, R. L., Padilha, A., Costa, M. D., Costa, E. M., Dantas-Filho Hde, C. & Pova, M. M. 2009. Malaria vectors in two indigenous reserves of the Brazilian Amazon. *Revista de saude publica*, **43**, 859-68.
- Sanz, L. M., Crespo, B., De-Cózar, C., Ding, X. C., Llergo, J. L., Burrows, J. N., García-Bustos, J. F. & Gamo, F.-J. 2012. *P. falciparum in vitro* killing rates allow to discriminate between different antimalarial mode-of-action. *PloS one*, **7**, e30949-e30949.
- Sargeant, T. J., Marti, M., Caler, E., Carlton, J. M., Simpson, K., Speed, T. P. & Cowman, A. F. 2006. Lineage-specific expansion of proteins exported to erythrocytes in malaria parasites. *Genome biology*, **7**, R12-R12.
- Scheltema, R. A., Jankevics, A., Jansen, R. C., Swertz, M. A. & Breitling, R. 2011. PeakML/mzMatch: a file format, java library, R library, and tool-chain for mass spectrometry data analysis. *Analytical chemistry*, **83**, 2786-2793.
- Schmitz, C., Kinner, A. & Kölling, R. 2005. The deubiquitinating enzyme UBP-1 affects sorting of the ATP-binding cassette-transporter Ste6 in the endocytic pathway. *Molecular biology of the cell*, **16**, 1319-1329.
- Sebastian, S., Brochet, M., Collins, M. O., Schwach, F., Jones, M. L., Goulding, D., Rayner, J. C., Choudhary, J. S. & Billker, O. 2012. A *Plasmodium* calcium-dependent protein kinase controls zygote development and transmission by translationally activating repressed mRNAs. *Cell host and microbe*, **12**, 9-19.
- Seder, R. A., Chang, L. J., Enama, M. E., Zephir, K. L., Sarwar, U. N., Gordon, I. J., Holman, L. A., James, E. R., Billingsley, P. F., Gunasekera, A., Richman, A., Chakravarty, S., Manoj, A., Velmurugan, S., Li, M., Ruben, A. J., Li, T., Eappen, A. G., Stafford, R. E., Plummer, S. H., Hendel, C. S., Novik, L., Costner, P. J., Mendoza, F. H., Saunders, J. G., Nason, M. C., Richardson, J. H., Murphy, J., Davidson, S. A., Richie, T. L., Sedegah, M., Sutamihardja, A., Fahle, G. A., Lyke, K. E., Laurens, M. B., Roederer, M., Tewari, K., Epstein, J. E., Sim, B. K., Ledgerwood, J. E., Graham, B. S. & Hoffman, S. L. 2013. Protection against malaria by intravenous immunization with a nonreplicating sporozoite vaccine. *Science*, **341**, 1359-65.
- Shahabuddin, M., Toyoshima, T., Aikawa, M. & Kaslow, D. C. 1993. Transmission-blocking activity of a chitinase inhibitor and activation of malarial parasite chitinase by mosquito protease. *Proceedings of the national academy of sciences of the USA*, **90**, 4266-4270.

- Sherrard-Smith, E., Sala, K. A., Betancourt, M., Upton, L. M., Angrisano, F., Morin, M. J., Ghani, A. C., Churcher, T. S. & Blagborough, A. M. 2018. Synergy in anti-malarial pre-erythrocytic and transmission-blocking antibodies is achieved by reducing parasite density. *eLife*, **7**, e35213.
- Sibley, C. H., Hyde, J. E., Sims, P. F., Plowe, C. V., Kublin, J. G., Mberu, E. K., Cowman, A. F., Winstanley, P. A., Watkins, W. M. & Nzila, A. M. 2001. Pyrimethamine-sulfadoxine resistance in *Plasmodium falciparum*: what next? *Trends in parasitology*, **17**, 582-8.
- Siddiqui, F. A., Boonhok, R., Cabrera, M., Mbenda, H. G. N., Wang, M., Min, H., Liang, X., Qin, J., Zhu, X., Miao, J., Cao, Y. & Cui, L. 2020. Role of *Plasmodium falciparum* Kelch13 protein mutations in *P. falciparum* populations from Northeastern Myanmar in mediating artemisinin resistance. *mBio*, **11**, e01134-19.
- Siddiqui, F. A., Cabrera, M., Wang, M., Brashear, A., Kemirembe, K., Wang, Z., Miao, J., Chookajorn, T., Yang, Z., Cao, Y., Dong, G., Rosenthal, P. J. & Cui, L. 2018. *Plasmodium falciparum* Falcipain-2a polymorphisms in Southeast Asia and their association with artemisinin resistance. *The journal of infectious diseases*, **218**, 434-442.
- Sidhu, A. B., Sun, Q., Nkrumah, L. J., Dunne, M. W., Sacchettini, J. C. & Fidock, D. A. 2007. *In vitro* efficacy, resistance selection, and structural modeling studies implicate the malarial parasite apicoplast as the target of azithromycin. *The journal of biological chemistry*, **282**, 2494-504.
- Sidjanski, S. P., Vanderberg, J. P. & Sinnis, P. 1997. *Anopheles stephensi* salivary glands bear receptors for region I of the circumsporozoite protein of *Plasmodium falciparum*. *Molecular and biochemical parasitology*, **90**, 33-41.
- Sievers, F., Wilm, A., Dineen, D., Gibson, T. J., Karplus, K., Li, W., Lopez, R., McWilliam, H., Remmert, M., Söding, J., Thompson, J. D. & Higgins, D. G. 2011. Fast, scalable generation of high-quality protein multiple sequence alignments using Clustal Omega. *Molecular systems biology*, **7**, 539-539.
- Silvie, O., Mota, M. M., Matuschewski, K. & Prudêncio, M. 2008. Interactions of the malaria parasite and its mammalian host. *Current opinion in microbiology*, **11**, 352-359.
- Sinden, R. E., Butcher, G. A., Billker, O. & Fleck, S. L. 1996. Regulation of infectivity of *Plasmodium* to the mosquito vector. *In*: Baker, J. R., Muller, R. & Rollinson, D. (eds.) *Advances in Parasitology*. Academic Press.
- Singh, J., Ramakrishnan, S. P., Prakash, S. & Bhatnagar, V. N. 1954. Studies on *Plasmodium berghei* Vincke and Lips, 1948. XX. A physiological change observed in sulphadiazine resistant strain. *Indian journal of malariology*, **8**, 301-7.
- Singh, S., Alam, M. M., Pal-Bhowmick, I., Brzostowski, J. A. & Chitnis, C. E. 2010. Distinct external signals trigger sequential release of apical organelles during erythrocyte invasion by malaria parasites. *PLoS pathogens*, **6**, e1000746-e1000746.

- Singh, S. & Chitnis, C. E. 2017. Molecular signaling involved in entry and exit of malaria parasites from host erythrocytes. *Cold Spring Harbor perspectives in medicine*, **7**, a026815.
- Sinha, A., Hughes, K. R., Modrzynska, K. K., Otto, T. D., Pfander, C., Dickens, N. J., Religa, A. A., Bushell, E., Graham, A. L., Cameron, R., Kafsack, B. F. C., Williams, A. E., Llinas, M., Berriman, M., Billker, O. & Waters, A. P. 2014. A cascade of DNA-binding proteins for sexual commitment and development in *Plasmodium*. *Nature*, **507**, 253-257.
- Sissoko, M. S., Healy, S. A., Katile, A., Omaswa, F., Zaidi, I., Gabriel, E. E., Kamate, B., Samake, Y., Guindo, M. A., Dolo, A., Niangaly, A., Niaré, K., Zeguime, A., Sissoko, K., Diallo, H., Thera, I., Ding, K., Fay, M. P., O'Connell, E. M., Nutman, T. B., Wong-Madden, S., Murshedkar, T., Ruben, A. J., Li, M., Abebe, Y., Manoj, A., Gunasekera, A., Chakravarty, S., Sim, B. K. L., Billingsley, P. F., James, E. R., Walther, M., Richie, T. L., Hoffman, S. L., Doumbo, O. & Duffy, P. E. 2017. Safety and efficacy of PfSPZ Vaccine against *Plasmodium falciparum* via direct venous inoculation in healthy malaria-exposed adults in Mali: a randomised, double-blind phase 1 trial. *The lancet infectious diseases*, **17**, 498-509.
- Sleebs, B. E., Lopaticki, S., Marapana, D. S., O'Neill, M. T., Rajasekaran, P., Gazdik, M., Günther, S., Whitehead, L. W., Lowes, K. N., Barfod, L., Hviid, L., Shaw, P. J., Hodder, A. N., Smith, B. J., Cowman, A. F. & Boddey, J. A. 2014. Inhibition of Plasmepsin V activity demonstrates its essential role in protein export, PfEMP1 display, and survival of malaria parasites. *PLoS biology*, **12**, e1001897-e1001897.
- Smith, C. A., Want, E. J., O'Maille, G., Abagyan, R. & Siuzdak, G. 2006. XCMS: processing mass spectrometry data for metabolite profiling using nonlinear peak alignment, matching, and identification. *Analytical chemistry*, **78**, 779-87.
- Soave, C. L., Guerin, T., Liu, J. & Dou, Q. P. 2017. Targeting the ubiquitin-proteasome system for cancer treatment: discovering novel inhibitors from nature and drug repurposing. *Cancer metastasis reviews*, **36**, 717-736.
- Sologub, L., Kuehn, A., Kern, S., Przyborski, J., Schillig, R. & Pradel, G. 2011. Malaria proteases mediate inside-out egress of gametocytes from red blood cells following parasite transmission to the mosquito. *Cell microbiology*, **13**, 897-912.
- Spielmann, T. & Beck, H. P. 2000. Analysis of stage-specific transcription in *Plasmodium falciparum* reveals a set of genes exclusively transcribed in ring stage parasites. *Molecular and biochemical parasitology*, **111**, 453-8.
- Spillman, N. J., Allen, R. J. W., McNamara, C. W., Yeung, B. K. S., Winzeler, E. A., Diagana, T. T. & Kirk, K. 2013. Na(+) regulation in the malaria parasite *Plasmodium falciparum* involves the cation ATPase PfATP4 and is a target of the spiroindolone antimalarials. *Cell host and microbe*, **13**, 227-237.
- Spillman, N. J. & Kirk, K. 2015. The malaria parasite cation ATPase PfATP4 and its role in the mechanism of action of a new arsenal of antimalarial drugs. *International journal for parasitology: drugs and drug resistance*, **5**, 149-162.

- Srinivasan, P., Beatty, W. L., Diouf, A., Herrera, R., Ambroggio, X., Moch, J. K., Tyler, J. S., Narum, D. L., Pierce, S. K., Boothroyd, J. C., Haynes, J. D. & Miller, L. H. 2011. Binding of *Plasmodium* merozoite proteins RON2 and AMA1 triggers commitment to invasion. *Proceedings of the national academy of sciences of the USA*, **108**, 13275-80.
- Srivastava, A., Creek, D. J., Evans, K. J., De Souza, D., Schofield, L., Müller, S., Barrett, M. P., McConville, M. J. & Waters, A. P. 2015. Host reticulocytes provide metabolic reservoirs that can be exploited by malaria parasites. *PLoS pathogens*, **11**, e1004882-e1004882.
- Srivastava, I. K., Morrissey, J. M., Darrouzet, E., Daldal, F. & Vaidya, A. B. 1999. Resistance mutations reveal the atovaquone-binding domain of cytochrome b in malaria parasites. *Molecular microbiology*, **33**, 704-11.
- Srivastava, I. K., Rottenberg, H. & Vaidya, A. B. 1997. Atovaquone, a broad spectrum antiparasitic drug, collapses mitochondrial membrane potential in a malarial parasite. *The journal of biological chemistry*, **272**, 3961-6.
- Srivastava, I. K. & Vaidya, A. B. 1999. A mechanism for the synergistic antimalarial action of atovaquone and proguanil. *Antimicrobial agents and chemotherapy*, **43**, 1334-1339.
- St Laurent, B., Miller, B., Burton, T. A., Amaratunga, C., Men, S., Sovannaroth, S., Fay, M. P., Miotto, O., Gwadz, R. W., Anderson, J. M. & Fairhurst, R. M. 2015. Artemisinin-resistant *Plasmodium falciparum* clinical isolates can infect diverse mosquito vectors of Southeast Asia and Africa. *Nature communications*, **6**, 8614-8614.
- Stanway, R. R., Bushell, E., Chiappino-Pepe, A., Roques, M., Sanderson, T., Franke-Fayard, B., Caldelari, R., Golomingi, M., Nyonda, M., Pandey, V., Schwach, F., Chevalley, S., Ramesar, J., Metcalf, T., Herd, C., Burda, P.-C., Rayner, J. C., Soldati-Favre, D., Janse, C. J., Hatzimanikatis, V., Billker, O. & Heussler, V. T. 2019. Genome-scale identification of essential metabolic processes for targeting the *Plasmodium* liver stage. *Cell*, **179**, 1112-1128.e26.
- Stokes, B. H., Yoo, E., Murithi, J. M., Luth, M. R., Afanasyev, P., da Fonseca, P. C. A., Winzeler, E. A., Ng, C. L., Bogyo, M. & Fidock, D. A. 2019. Covalent *Plasmodium falciparum*-selective proteasome inhibitors exhibit a low propensity for generating resistance *in vitro* and synergize with multiple antimalarial agents. *PLoS pathogens*, **15**, e1007722-e1007722.
- Storm, J. & Craig, A. G. 2014. Pathogenesis of cerebral malaria—inflammation and cytoadherence. *Frontiers in cellular and infection microbiology*, **4**, 100.
- Straimer, J., Gnädig, N. F., Stokes, B. H., Ehrenberger, M., Crane, A. A. & Fidock, D. A. 2017. *Plasmodium falciparum* K13 mutations differentially impact ozonide susceptibility and parasite fitness *in vitro*. *mBio*, **8**, e00172-17.
- Straimer, J., Gnädig, N. F., Witkowski, B., Amaratunga, C., Duru, V., Ramadani, A. P., Dacheux, M., Khim, N., Zhang, L., Lam, S., Gregory, P. D., Urnov, F. D., Mercereau-Puijalon, O., Benoit-Vical, F., Fairhurst, R. M., Ménard, D. & Fidock, D. A. 2015. K13-propeller mutations confer artemisinin resistance in *Plasmodium falciparum* clinical isolates. *Science (New York, N.Y.)*, **347**, 428-431.

- Straimer, J., Lee, M. C. S., Lee, A. H., Zeitler, B., Williams, A. E., Pearl, J. R., Zhang, L., Rebar, E. J., Gregory, P. D., Llinás, M., Urnov, F. D. & Fidock, D. A. 2012. Site-specific genome editing in *Plasmodium falciparum* using engineered zinc-finger nucleases. *Nature methods*, **9**, 993-998.
- Sturm, A., Amino, R., van de Sand, C., Regen, T., Retzlaff, S., Rennenberg, A., Krueger, A., Pollok, J. M., Menard, R. & Heussler, V. T. 2006. Manipulation of host hepatocytes by the malaria parasite for delivery into liver sinusoids. *Science*, **313**, 1287-90.
- Suaréz-Cortés, P., Silvestrini, F. & Alano, P. 2014. A fast, non-invasive, quantitative staining protocol provides insights in *Plasmodium falciparum* gamete egress and in the role of osmiophilic bodies. *Malaria journal*, **13**, 389-389.
- Sultan, A. A., Thathy, V., Frevert, U., Robson, K. J., Crisanti, A., Nussenzweig, V., Nussenzweig, R. S. & Ménard, R. 1997. TRAP is necessary for gliding motility and infectivity of *Plasmodium* sporozoites. *Cell*, **90**, 511-22.
- Sumner, L. W., Amberg, A., Barrett, D., Beale, M. H., Beger, R., Daykin, C. A., Fan, T. W. M., Fiehn, O., Goodacre, R., Griffin, J. L., Hankemeier, T., Hardy, N., Harnly, J., Higashi, R., Kopka, J., Lane, A. N., Lindon, J. C., Marriott, P., Nicholls, A. W., Reily, M. D., Thaden, J. J. & Viant, M. R. 2007. Proposed minimum reporting standards for chemical analysis Chemical Analysis Working Group (CAWG) Metabolomics Standards Initiative (MSI). *Metabolomics*, **3**, 211-221.
- Sutherland, C. J., Lansdell, P., Sanders, M., Muwanguzi, J., van Schalkwyk, D. A., Kaur, H., Nolder, D., Tucker, J., Bennett, H. M., Otto, T. D., Berriman, M., Patel, T. A., Lynn, R., Gkrania-Klotsas, E. & Chiodini, P. L. 2017. pfk13-independent treatment failure in four imported cases of *Plasmodium falciparum* malaria treated with artemether-lumefantrine in the United Kingdom. *Antimicrobial agents and chemotherapy*, **61**, e02382-16.
- Syafruddin, D., Siregar, J. E. & Marzuki, S. 1999. Mutations in the cytochrome b gene of *Plasmodium berghei* conferring resistance to atovaquone. *Molecular and biochemical parasitology*, **104**, 185-94.
- Takala-Harrison, S., Jacob, C. G., Arze, C., Cummings, M. P., Silva, J. C., Dondorp, A. M., Fukuda, M. M., Hien, T. T., Mayxay, M., Noedl, H., Nosten, F., Kyaw, M. P., Nhien, N. T. T., Imwong, M., Bethell, D., Se, Y., Lon, C., Tyner, S. D., Saunders, D. L., Ariey, F., Mercereau-Puijalon, O., Menard, D., Newton, P. N., Khanthavong, M., Hongvanthong, B., Starzengruber, P., Fuehrer, H.-P., Swoboda, P., Khan, W. A., Phyo, A. P., Nyunt, M. M., Nyunt, M. H., Brown, T. S., Adams, M., Pepin, C. S., Bailey, J., Tan, J. C., Ferdig, M. T., Clark, T. G., Miotto, O., MacInnis, B., Kwiatkowski, D. P., White, N. J., Ringwald, P. & Plowe, C. V. 2015. Independent emergence of artemisinin resistance mutations among *Plasmodium falciparum* in Southeast Asia. *The journal of infectious diseases*, **211**, 670-679.
- Talman, A. M., Lacroix, C., Marques, S. R., Blagborough, A. M., Carzaniga, R., Ménard, R. & Sinden, R. E. 2011. PbGEST mediates malaria transmission to both mosquito and vertebrate host. *Molecular microbiology*, **82**, 462-74.

- Thakur, V., Asad, M., Jain, S., Hossain, M. E., Gupta, A., Kaur, I., Rathore, S., Ali, S., Khan, N. J. & Mohammed, A. 2015. Eps15 homology domain containing protein of *Plasmodium falciparum* (PfEHD) associates with endocytosis and vesicular trafficking towards neutral lipid storage site. *Biochimica et Biophysica acta*, **1853**, 2856-69.
- Tham, W. H., Healer, J. & Cowman, A. F. 2012. Erythrocyte and reticulocyte binding-like proteins of *Plasmodium falciparum*. *Trends in parasitology*, **28**, 23-30.
- Tham, W. H., Wilson, D. W., Lopaticki, S., Schmidt, C. Q., Tetteh-Quarcoo, P. B., Barlow, P. N., Richard, D., Corbin, J. E., Beeson, J. G. & Cowman, A. F. 2010. Complement receptor 1 is the host erythrocyte receptor for *Plasmodium falciparum* PfRh4 invasion ligand. *Proceedings of the national academy of sciences of the USA*, **107**, 17327-32.
- Thathy, V., Fujioka, H., Gantt, S., Nussenzweig, R., Nussenzweig, V. & Ménard, R. 2002. Levels of circumsporozoite protein in the *Plasmodium* oocyst determine sporozoite morphology. *The EMBO journal*, **21**, 1586-1596.
- Thomas, J. A., Tan, M. S. Y., Bisson, C., Borg, A., Umrekar, T. R., Hackett, F., Hale, V. L., Vizcay-Barrena, G., Fleck, R. A., Snijders, A. P., Saibil, H. R. & Blackman, M. J. 2018. A protease cascade regulates release of the human malaria parasite *Plasmodium falciparum* from host red blood cells. *Nature microbiology*, **3**, 447-455.
- Tilley, L., Straimer, J., Gnädig, N. F., Ralph, S. A. & Fidock, D. A. 2016. Artemisinin action and resistance in *Plasmodium falciparum*. *Trends in parasitology*, **32**, 682-696.
- Tomas, A. M., Margos, G., Dimopoulos, G., van Lin, L. H., de Koning-Ward, T. F., Sinha, R., Lupetti, P., Beetsma, A. L., Rodriguez, M. C., Karras, M., Hager, A., Mendoza, J., Butcher, G. A., Kafatos, F., Janse, C. J., Waters, A. P. & Sinden, R. E. 2001. P25 and P28 proteins of the malaria ookinete surface have multiple and partially redundant functions. *The EMBO journal*, **20**, 3975-3983.
- Trager, W. & Gill, G. S. 1992. Enhanced gametocyte formation in young erythrocytes by *Plasmodium falciparum* *in vitro*. *The journal of protozoology*, **39**, 429-32.
- Triglia, T., Wang, P., Sims, P. F., Hyde, J. E. & Cowman, A. F. 1998. Allelic exchange at the endogenous genomic locus in *Plasmodium falciparum* proves the role of dihydropteroate synthase in sulfadoxine-resistant malaria. *The EMBO journal*, **17**, 3807-3815.
- Tsai, Y. L., Hayward, R. E., Langer, R. C., Fidock, D. A. & Vinetz, J. M. 2001. Disruption of *Plasmodium falciparum* chitinase markedly impairs parasite invasion of mosquito midgut. *Infection and immunity*, **69**, 4048-4054.
- Tu, Y. 2011. The discovery of artemisinin (qinghaosu) and gifts from Chinese medicine. *Nature medicine*, **17**, 1217-1220.
- Tun, K. M., Imwong, M., Lwin, K. M., Win, A. A., Hlaing, T. M., Hlaing, T., Lin, K., Kyaw, M. P., Plewes, K., Faiz, M. A., Dhorda, M., Cheah, P. Y.,

- Pukrittayakamee, S., Ashley, E. A., Anderson, T. J. C., Nair, S., McDew-White, M., Flegg, J. A., Grist, E. P. M., Guerin, P., Maude, R. J., Smithuis, F., Dondorp, A. M., Day, N. P. J., Nosten, F., White, N. J. & Woodrow, C. J. 2015. Spread of artemisinin-resistant *Plasmodium falciparum* in Myanmar: a cross-sectional survey of the K13 molecular marker. *The lancet infectious diseases*, **15**, 415-421.
- Tun, K. M., Jeeyapant, A., Imwong, M., Thein, M., Aung, S. S., Hlaing, T. M., Yuentrakul, P., Promnarate, C., Dhorda, M., Woodrow, C. J., Dondorp, A. M., Ashley, E. A., Smithuis, F. M., White, N. J. & Day, N. P. 2016. Parasite clearance rates in upper Myanmar indicate a distinctive artemisinin resistance phenotype: a therapeutic efficacy study. *Malaria journal*, **15**, 185.
- Tyers, M. & Wright, G. D. 2019. Drug combinations: a strategy to extend the life of antibiotics in the 21st century. *Nature reviews microbiology*, **17**, 141-155.
- Vaid, A., Ranjan, R., Smythe, W. A., Hoppe, H. C. & Sharma, P. 2010. PfPI3K, a phosphatidylinositol-3 kinase from *Plasmodium falciparum*, is exported to the host erythrocyte and is involved in hemoglobin trafficking. *Blood*, **115**, 2500-2507.
- Vaidya, A. B. & Mather, M. W. 2000. Atovaquone resistance in malaria parasites. *Drug resistance updates*, **3**, 283-287.
- Valderramos, S. G., Valderramos, J. C., Musset, L., Purcell, L. A., Mercereau-Puijalon, O., Legrand, E. & Fidock, D. A. 2010. Identification of a mutant PfCRT-mediated chloroquine tolerance phenotype in *Plasmodium falciparum*. *PLoS pathogens*, **6**, e1000887.
- van Brummelen, A. C., Olszewski, K. L., Wilinski, D., Llinas, M., Louw, A. I. & Birkholtz, L. M. 2009. Co-inhibition of *Plasmodium falciparum* S-adenosylmethionine decarboxylase/ornithine decarboxylase reveals perturbation-specific compensatory mechanisms by transcriptome, proteome, and metabolome analyses. *The journal of biological chemistry*, **284**, 4635-46.
- van der Hooft, J. J. J., Padmanabhan, S., Burgess, K. E. V. & Barrett, M. P. 2016. Urinary antihypertensive drug metabolite screening using molecular networking coupled to high-resolution mass spectrometry fragmentation. *Metabolomics*, **12**, 125-125.
- van der Pluijm, R. W., Imwong, M., Chau, N. H., Hoa, N. T., Thuy-Nhien, N. T., Thanh, N. V., Jittamala, P., Hanboonkunupakarn, B., Chutasmit, K., Saelow, C., Runjarern, R., Kaewmok, W., Tripura, R., Peto, T. J., Yok, S., Suon, S., Sreng, S., Mao, S., Oun, S., Yen, S., Amaratunga, C., Lek, D., Huy, R., Dhorda, M., Chotivanich, K., Ashley, E. A., Mukaka, M., Waithira, N., Cheah, P. Y., Maude, R. J., Amato, R., Pearson, R. D., Gonçalves, S., Jacob, C. G., Hamilton, W. L., Fairhurst, R. M., Tarning, J., Winterberg, M., Kwiatkowski, D. P., Pukrittayakamee, S., Hien, T. T., Day, N. P., Miotto, O., White, N. J. & Dondorp, A. M. 2019. Determinants of dihydroartemisinin-piperaquine treatment failure in *Plasmodium falciparum* malaria in Cambodia, Thailand, and Vietnam: a prospective clinical, pharmacological, and genetic study. *The lancet infectious diseases*, **19**, 952-961.
- van der Wel, A. M., Tomás, A. M., Kocken, C. H., Malhotra, P., Janse, C. J., Waters, A. P. & Thomas, A. W. 1997. Transfection of the primate malaria

parasite *Plasmodium knowlesi* using entirely heterologous constructs. The journal of experimental medicine, **185**, 1499-1503.

van Dijk, M. R., Janse, C. J., Thompson, J., Waters, A. P., Braks, J. A., Dodemont, H. J., Stunnenberg, H. G., van Gemert, G. J., Sauerwein, R. W. & Eling, W. 2001. A central role for P48/45 in malaria parasite male gamete fertility. Cell, **104**, 153-64.

van Dijk, M. R., McConkey, G. A., Vinkenoog, R., Waters, A. P. & Janse, C. J. 1994. Mechanisms of pyrimethamine resistance in two different strains of *Plasmodium berghei*. Molecular and biochemical parasitology, **68**, 167-171.

van Dijk, M. R., Waters, A. P. & Janse, C. J. 1995. Stable transfection of malaria parasite blood stages. Science, **268**, 1358-62.

Van Voorhis, W. C., Adams, J. H., Adelfio, R., Ah Yong, V., Akabas, M. H., Alano, P., Alday, A., Aleman Resto, Y., Alsibaee, A., Alzualde, A., Andrews, K. T., Avery, S. V., Avery, V. M., Ayong, L., Baker, M., Baker, S., Ben Mamoun, C., Bhatia, S., Bickle, Q., Bounaadja, L., Bowling, T., Bosch, J., Boucher, L. E., Boyom, F. F., Brea, J., Brennan, M., Burton, A., Caffrey, C. R., Camarda, G., Carrasquilla, M., Carter, D., Belen Cassera, M., Chih-Chien Cheng, K., Chindaoudomsate, W., Chubb, A., Colon, B. L., Colon-Lopez, D. D., Corbett, Y., Crowther, G. J., Cowan, N., D'Alessandro, S., Le Dang, N., Delves, M., DeRisi, J. L., Du, A. Y., Duffy, S., Abd El-Salam El-Sayed, S., Ferdig, M. T., Fernandez Robledo, J. A., Fidock, D. A., Florent, I., Fokou, P. V., Galstian, A., Gamo, F. J., Gokool, S., Gold, B., Golub, T., Goldgof, G. M., Guha, R., Guiguemde, W. A., Gural, N., Guy, R. K., Hansen, M. A., Hanson, K. K., Hemphill, A., Hooft van Huijsduijnen, R., Horii, T., Horrocks, P., Hughes, T. B., Huston, C., Igarashi, I., Ingram-Sieber, K., Itoe, M. A., Jadhav, A., Naranuntarat Jensen, A., Jensen, L. T., Jiang, R. H., Kaiser, A., Keiser, J., Ketas, T., Kicka, S., Kim, S., Kirk, K., Kumar, V. P., Kyle, D. E., Lafuente, M. J., Landfear, S., Lee, N., Lee, S., Lehane, A. M., Li, F., Little, D., Liu, L., Llinas, M., Loza, M. I., Lubar, A., Lucantoni, L., Lucet, I., Maes, L., Mancama, D., et al. 2016. Open source drug discovery with the malaria box compound collection for neglected diseases and beyond. PLoS pathogens, **12**, e1005763.

Vaughan, A. M. & Kappe, S. H. I. 2017. Malaria parasite liver infection and exoerythrocytic biology. Cold Spring Harbor perspectives in medicine, **7**.

Vega-Rodríguez, J., Pastrana-Mena, R., Crespo-Lladó, K. N., Ortiz, J. G., Ferrer-Rodríguez, I. & Serrano, A. E. 2015. Implications of glutathione levels in the *Plasmodium berghei* response to chloroquine and artemisinin. PLoS one, **10**, e0128212.

Velavan, T. P., Nderu, D., Agbenyega, T., Ntoumi, F. & Kremsner, P. G. 2019. An alternative dogma on reduced artemisinin susceptibility: a new shadow from east to west. Proceedings of the national academy of sciences of the USA, **116**, 12611-12612.

Vincent, I. M., Ehmann, D. E., Mills, S. D., Perros, M. & Barrett, M. P. 2016. Untargeted metabolomics to ascertain antibiotic modes of action. Antimicrobial agents and chemotherapy, **60**, 2281-2291.

- Vinetz, J. M., Dave, S. K., Specht, C. A., Brameld, K. A., Xu, B., Hayward, R. & Fidock, D. A. 1999. The chitinase PfCMT1 from the human malaria parasite *Plasmodium falciparum* lacks proenzyme and chitin-binding domains and displays unique substrate preferences. *Proceedings of the national academy of sciences of the USA*, **96**, 14061-14066.
- Vivas, L., Rattray, L., Stewart, L. B., Robinson, B. L., Fugmann, B., Haynes, R. K., Peters, W. & Croft, S. L. 2007. Antimalarial efficacy and drug interactions of the novel semi-synthetic endoperoxide artemisone *in vitro* and *in vivo*. *Journal of antimicrobial chemotherapy*, **59**, 658-65.
- Wagner, J. C., Platt, R. J., Goldfless, S. J., Zhang, F. & Niles, J. C. 2014. Efficient CRISPR-Cas9-mediated genome editing in *Plasmodium falciparum*. *Nature methods*, **11**, 915-918.
- Walker, D. J., Pitsch, J. L., Peng, M. M., Robinson, B. L., Peters, W., Bhisutthibhan, J. & Meshnick, S. R. 2000. Mechanisms of artemisinin resistance in the rodent malaria pathogen *Plasmodium yoelii*. *Antimicrobial agents and chemotherapy*, **44**, 344-347.
- Walker, L. A. & Sullivan, D. J., Jr. 2017. Impact of extended duration of artesunate treatment on parasitological outcome in a cytotoxic murine malaria model. *Antimicrobial agents and chemotherapy*, **61**, e02499-16.
- Walliker, D., Carter, R. & Morgan, S. 1973. Genetic recombination in *Plasmodium berghei*. *Parasitology*, **66**, 309-320.
- Walliker, D., Carter, R. & Sanderson, A. 1975. Genetic studies on *Plasmodium chabaudi*: recombination between enzyme markers. *Parasitology*, **70**, 19-24.
- Wang, J., Huang, L., Li, J., Fan, Q., Long, Y., Li, Y. & Zhou, B. 2010. Artemisinin directly targets malarial mitochondria through its specific mitochondrial activation. *PLoS one*, **5**, e9582.
- Wang, J., Huang, Y., Zhao, Y., Ye, R., Zhang, D. & Pan, W. 2018. Introduction of F446I mutation in the K13 propeller gene leads to increased ring survival rates in *Plasmodium falciparum* isolates. *Malaria journal*, **17**, 248.
- Wang, J., Zhang, C.-J., Chia, W. N., Loh, C. C. Y., Li, Z., Lee, Y. M., He, Y., Yuan, L.-X., Lim, T. K., Liu, M., Liew, C. X., Lee, Y. Q., Zhang, J., Lu, N., Lim, C. T., Hua, Z.-C., Liu, B., Shen, H.-M., Tan, K. S. W. & Lin, Q. 2015a. Haem-activated promiscuous targeting of artemisinin in *Plasmodium falciparum*. *Nature communications*, **6**, 10111-10111.
- Wang, L., Delahunty, C., Fritz-Wolf, K., Rahlfs, S., Helena Prieto, J., Yates, J. R. & Becker, K. 2015b. Characterization of the 26S proteasome network in *Plasmodium falciparum*. *Scientific reports*, **5**, 17818.
- Wang, L., Nomura, Y., Du, Y., Liu, N., Zhorov, B. S. & Dong, K. 2015c. A mutation in the intracellular loop III/IV of mosquito sodium channel synergizes the effect of mutations in helix IIS6 on pyrethroid resistance. *Molecular pharmacology*, **87**, 421-429.

- Wang, P., Sims, P. F. & Hyde, J. E. 1997. A modified *in vitro* sulfadoxine susceptibility assay for *Plasmodium falciparum* suitable for investigating Fansidar resistance. *Parasitology*, **115** (Pt 3), 223-30.
- Wang, Q., Fujioka, H. & Nussenzweig, V. 2005. Exit of *Plasmodium* sporozoites from oocysts is an active process that involves the circumsporozoite protein. *PLoS pathogens*, **1**, e9-e9.
- Wang, X., Mazurkiewicz, M., Hillert, E. K., Olofsson, M. H., Pierrou, S., Hillertz, P., Gullbo, J., Selvaraju, K., Paulus, A., Akhtar, S., Bossler, F., Khan, A. C., Linder, S. & D'Arcy, P. 2016. The proteasome deubiquitinase inhibitor VLX1570 shows selectivity for ubiquitin-specific protease-14 and induces apoptosis of multiple myeloma cells. *Scientific reports*, **6**, 26979.
- Wang, Z., Wang, Y., Cabrera, M., Zhang, Y., Gupta, B., Wu, Y., Kemirembe, K., Hu, Y., Liang, X., Brashear, A., Shrestha, S., Li, X., Miao, J., Sun, X., Yang, Z. & Cui, L. 2015d. Artemisinin resistance at the China-Myanmar border and association with mutations in the K13 propeller gene. *Antimicrobial agents and chemotherapy*, **59**, 6952-9.
- Warhurst, D. C. & Killick-Kendrick, R. 1967. Spontaneous resistance to chloroquine in a strain of rodent malaria (*Plasmodium berghei yoelii*). *Nature*, **213**, 1048-1049.
- Waterhouse, A., Bertoni, M., Bienert, S., Studer, G., Tauriello, G., Gumienny, R., Heer, F. T., de Beer, T. A. P., Rempfer, C., Bordoli, L., Lepore, R. & Schwede, T. 2018. SWISS-MODEL: homology modelling of protein structures and complexes. *Nucleic acids research*, **46**, w296-w303.
- Waters, A. P. 2016. Epigenetic roulette in blood stream *Plasmodium*: gambling on sex. *PLoS pathogens*, **12**, e1005353-e1005353.
- Watkins, W. M., Sixsmith, D. G., Chulay, J. D. & Spencer, H. C. 1985. Antagonism of sulfadoxine and pyrimethamine antimalarial activity *in vitro* by p-aminobenzoic acid, p-aminobenzoylglutamic acid and folic acid. *Molecular and biochemical parasitology*, **14**, 55-61.
- Wellems, T. E., Panton, L. J., Gluzman, I. Y., do Rosario, V. E., Gwadz, R. W., Walker-Jonah, A. & Krogstad, D. J. 1990. Chloroquine resistance not linked to *mdr*-like genes in a *Plasmodium falciparum* cross. *Nature*, **345**, 253-5.
- Wells, T. N., Hooft van Huijsduijnen, R. & Van Voorhis, W. C. 2015. Malaria medicines: a glass half full? *Nature reviews drug discovery*, **14**, 424-42.
- Wells, T. N. C., Burrows, J. N. & Baird, J. K. 2010. Targeting the hypnozoite reservoir of *Plasmodium vivax*: the hidden obstacle to malaria elimination. *Trends in parasitology*, **26**, 145-151.
- White, N. J. 2008. Qinghaosu (artemisinin): the price of success. *Science*, **320**, 330-4.
- White, N. J. 2011. The parasite clearance curve. *Malaria journal*, **10**, 278.

- White, N. J., Duong, T. T., Uthaisin, C., Nosten, F., Phyo, A. P., Hanboonkunupakarn, B., Pukrittayakamee, S., Jittamala, P., Chuthasmit, K., Cheung, M. S., Feng, Y., Li, R., Magnusson, B., Sultan, M., Wieser, D., Xun, X., Zhao, R., Diagana, T. T., Pertel, P. & Leong, F. J. 2016. Antimalarial Activity of KAF156 in *falciparum* and *vivax* Malaria. The New England journal of medicine, **375**, 1152-1160.
- White, N. J., Hien, T. T. & Nosten, F. H. 2015. A brief history of Qinghaosu. Trends in parasitology, **31**, 607-610.
- White, N. J., Pukrittayakamee, S., Phyo, A. P., Rueangweerayut, R., Nosten, F., Jittamala, P., Jeeyapant, A., Jain, J. P., Lefevre, G., Li, R., Magnusson, B., Diagana, T. T. & Leong, F. J. 2014. Spiroindolone KAE609 for *falciparum* and *vivax* malaria. The New England journal of medicine, **371**, 403-10.
- WHO 2016. Malaria vaccine: WHO position paper--January 2016/Note de synthese: position de l'OMS a propos du vaccin antipaludique--janvier 2016. Weekly epidemiological record, **91**, 33+.
- WHO 2018a. Artemisinin resistance and artemisinin-based combination therapy efficacy: status report, Geneva, Switerzaland.
- WHO 2018b. Global report on insecticide resistance in malaria vectors: 2010-2016, Geneva, Switzeland.
- WHO 2018c. World Malaria Report, Geneva, Switerzaland.
- WHO 2019. World Malaria Report, Geneva, Switerzaland.
- Wickham, M. E., Rug, M., Ralph, S. A., Klonis, N., McFadden, G. I., Tilley, L. & Cowman, A. F. 2001. Trafficking and assembly of the cytoadherence complex in *Plasmodium falciparum*-infected human erythrocytes. The EMBO journal, **20**, 5636-49.
- Williams, J. L. 1999. Stimulation of *Plasmodium falciparum* gametocytogenesis by conditioned medium from parasite cultures. The American journal of tropical medicine and hygiene, **60**, 7-13.
- Wishart, D. S. 2016. Emerging applications of metabolomics in drug discovery and precision medicine. Nature reviews drug discovery, **15**, 473.
- Wishart, D. S., Tzur, D., Knox, C., Eisner, R., Guo, A. C., Young, N., Cheng, D., Jewell, K., Arndt, D., Sawhney, S., Fung, C., Nikolai, L., Lewis, M., Coutouly, M.-A., Forsythe, I., Tang, P., Shrivastava, S., Jeroncic, K., Stothard, P., Amegbey, G., Block, D., Hau, D. D., Wagner, J., Miniaci, J., Clements, M., Gebremedhin, M., Guo, N., Zhang, Y., Duggan, G. E., MacInnis, G. D., Weljie, A. M., Dowlatabadi, R., Bamforth, F., Clive, D., Greiner, R., Li, L., Marrie, T., Sykes, B. D., Vogel, H. J. & Querengesser, L. 2007. HMDB: the human metabolome database. Nucleic acids research, **35**, D521-D526.
- Witkowski, B., Amaratunga, C., Khim, N., Sreng, S., Chim, P., Kim, S., Lim, P., Mao, S., Sopha, C., Sam, B., Anderson, J. M., Duong, S., Chuor, C. M., Taylor, W. R., Suon, S., Mercereau-Puijalon, O., Fairhurst, R. M. & Menard, D. 2013. Novel phenotypic assays for the detection of artemisinin-resistant *Plasmodium*

- falciparum* malaria in Cambodia: *in-vitro* and *ex-vivo* drug-response studies. The lancet infectious diseases, **13**, 1043-9.
- Witkowski, B., Duru, V., Khim, N., Ross, L. S., Saintpierre, B., Beghain, J., Chy, S., Kim, S., Ke, S., Kloeung, N., Eam, R., Khean, C., Ken, M., Loch, K., Bouillon, A., Domergue, A., Ma, L., Bouchier, C., Leang, R., Huy, R., Nuel, G., Barale, J.-C., Legrand, E., Ringwald, P., Fidock, D. A., Mercereau-Puijalon, O., Arie, F. & Ménard, D. 2017. A surrogate marker of piperaquine-resistant *Plasmodium falciparum* malaria: a phenotype-genotype association study. The lancet infectious diseases, **17**, 174-183.
- Witkowski, B., Lelievre, J., Barragan, M. J., Laurent, V., Su, X. Z., Berry, A. & Benoit-Vical, F. 2010. Increased tolerance to artemisinin in *Plasmodium falciparum* is mediated by a quiescence mechanism. Antimicrob agents and chemotherapy, **54**, 1872-7.
- Wong, W., Bai, X.-C., Sleebs, B. E., Triglia, T., Brown, A., Thompson, J. K., Jackson, K. E., Hanssen, E., Marapana, D. S., Fernandez, I. S., Ralph, S. A., Cowman, A. F., Scheres, S. H. W. & Baum, J. 2017. Mefloquine targets the *Plasmodium falciparum* 80S ribosome to inhibit protein synthesis. Nature microbiology, **2**, 17031-17031.
- Wood, O., Hanrahan, S., Coetzee, M., Koekemoer, L. & Brooke, B. 2010. Cuticle thickening associated with pyrethroid resistance in the major malaria vector *Anopheles funestus*. Parasites and vectors, **3**, 67-67.
- Wu, Y., Kirkman, L. A. & Wellems, T. E. 1996. Transformation of *Plasmodium falciparum* malaria parasites by homologous integration of plasmids that confer resistance to pyrimethamine. Proceedings of the national academy of sciences of the USA, **93**, 1130-1134.
- Xia, J., Sinelnikov, I. V., Han, B. & Wishart, D. S. 2015. MetaboAnalyst 3.0—making metabolomics more meaningful. Nucleic acids research, **43**, W251-W257.
- Xiao, S. H., Yao, J. M., Utzinger, J., Cai, Y., Chollet, J. & Tanner, M. 2004. Selection and reversal of *Plasmodium berghei* resistance in the mouse model following repeated high doses of artemether. Parasitology research, **92**, 215-9.
- Xie, S. C., Dogovski, C., Hanssen, E., Chiu, F., Yang, T., Crespo, M. P., Stafford, C., Batinovic, S., Teguh, S., Charman, S., Klonis, N. & Tilley, L. 2016. Haemoglobin degradation underpins the sensitivity of early ring stage *Plasmodium falciparum* to artemisinins. Journal of cell science, **129**, 406-416.
- Xie, S. C., Metcalfe, R. D., Hanssen, E., Yang, T., Gillett, D. L., Leis, A. P., Morton, C. J., Kuiper, M. J., Parker, M. W., Spillman, N. J., Wong, W., Tsu, C., Dick, L. R., Griffin, M. D. W. & Tilley, L. 2019. The structure of the PA28-20S proteasome complex from *Plasmodium falciparum* and implications for proteostasis. Nature microbiology, **4**, 1990-2000.
- Xie, S. C., Ralph, S. A. & Tilley, L. 2020. K13, the cytostome, and artemisinin resistance. Trends in parasitology, **36**, 533-544.
- Yang, T., Yeoh, L. M., Tutor, M. V., Dixon, M. W., McMillan, P. J., Xie, S. C., Bridgford, J. L., Gillett, D. L., Duffy, M. F., Ralph, S. A., McConville, M. J.,

- Tilley, L. & Cobbold, S. A. 2019. Decreased K13 abundance reduces hemoglobin catabolism and proteotoxic stress, underpinning artemisinin resistance. *Cell reports*, **29**, 2917-2928.e5.
- Ye, R., Tian, Y., Huang, Y., Zhang, Y., Wang, J., Sun, X., Zhou, H., Zhang, D. & Pan, W. 2019. Genome-wide analysis of genetic diversity in *Plasmodium falciparum* isolates from China-Myanmar Border. *Frontiers in genetics*, **10**, 1065.
- Yeh, P. J., Hegreness, M. J., Aiden, A. P. & Kishony, R. 2009. Drug interactions and the evolution of antibiotic resistance. *Nature reviews microbiology*, **7**, 460-466.
- Yeoh, S., O'Donnell, R. A., Koussis, K., Dluzewski, A. R., Ansell, K. H., Osborne, S. A., Hackett, F., Withers-Martinez, C., Mitchell, G. H., Bannister, L. H., Bryans, J. S., Kettleborough, C. A. & Blackman, M. J. 2007. Subcellular discharge of a serine protease mediates release of invasive malaria parasites from host erythrocytes. *Cell*, **131**, 1072-83.
- Yoeli, M., Upmanis, R. S. & Most, H. 1969. Drug-resistance transfer among rodent *Plasmodia*. 1. Acquisition of resistance to pyrimethamine by a drug-sensitive strain of *Plasmodium berghei* in the course of its concomitant development with a pyrimethamine-resistant *P. vinckei* strain. *Parasitology*, **59**, 429-47.
- Yoo, E., Stokes, B. H., de Jong, H., Vanaerschot, M., Kumar, T., Lawrence, N., Njoroge, M., Garcia, A., Van der Westhuyzen, R., Momper, J. D., Ng, C. L., Fidock, D. A. & Bogyo, M. 2018. Defining the determinants of specificity of *Plasmodium* proteasome inhibitors. *Journal of the American chemical society*, **140**, 11424-11437.
- Yuda, M., Iwanaga, S., Shigenobu, S., Mair, G. R., Janse, C. J., Waters, A. P., Kato, T. & Kaneko, I. 2009. Identification of a transcription factor in the mosquito-invasive stage of malaria parasites. *Molecular microbiology*, **71**, 1402-14.
- Zampieri, M., Szappanos, B., Buchieri, M. V., Trauner, A., Piazza, I., Picotti, P., Gagneux, S., Borrell, S., Gicquel, B., Lelievre, J., Papp, B. & Sauer, U. 2018. High-throughput metabolomic analysis predicts mode of action of uncharacterized antimicrobial compounds. *Science translational medicine*, **10**, eaal3973
- Zeeman, A.-M. & Kocken, C. H. M. 2017. Non-human primate models and *in vitro* liver stage cultures as alternatives in malaria drug development. *Drug discovery today: disease models*, **23**, 17-23.
- Zhang, C., Xiao, B., Jiang, Y., Zhao, Y., Li, Z., Gao, H., Ling, Y., Wei, J., Li, S., Lu, M., Su, X.-Z., Cui, H. & Yuan, J. 2014. Efficient editing of malaria parasite genome using the CRISPR/Cas9 system. *mBio*, **5**, e01414.
- Zhang, M., Gallego-Delgado, J., Fernandez-Arias, C., Waters, N. C., Rodriguez, A., Tsuji, M., Wek, R. C., Nussenzweig, V. & Sullivan, W. J., Jr. 2017. Inhibiting the *Plasmodium* eIF2 α kinase PK4 prevents artemisinin-induced latency. *Cell host and microbe*, **22**, 766-776.e4.

Zhang, M., Wang, C., Otto, T. D., Oberstaller, J., Liao, X., Adapa, S. R., Udenze, K., Bronner, I. F., Casandra, D., Mayho, M., Brown, J., Li, S., Swanson, J., Rayner, J. C., Jiang, R. H. Y. & Adams, J. H. 2018. Uncovering the essential genes of the human malaria parasite *Plasmodium falciparum* by saturation mutagenesis. *Science*, **360**.

Zhu, L., Tripathi, J., Rocamora, F. M., Miotto, O., van der Pluijm, R., Voss, T. S., Mok, S., Kwiatkowski, D. P., Nosten, F., Day, N. P. J., White, N. J., Dondorp, A. M., Bozdech, Z. & Tracking Resistance to Artemisinin Collaboration, I. 2018. The origins of malaria artemisinin resistance defined by a genetic and transcriptomic background. *Nature communications*, **9**, 5158-5158.

10 Publications



Experimentally Engineered Mutations in a Ubiquitin Hydrolase, UBP-1, Modulate *In Vivo* Susceptibility to Artemisinin and Chloroquine in *Plasmodium berghei*

Nelson V. Simwela,^a Katie R. Hughes,^a A. Brett Roberts,^a Michael T. Rennie,^a Michael P. Barrett,^a  Andrew P. Waters^a

^aInstitute of Infection, Immunity and Inflammation, Wellcome Centre for Integrative Parasitology, University of Glasgow, Glasgow, Scotland, United Kingdom

ABSTRACT As resistance to artemisinins (current frontline drugs in malaria treatment) emerges in Southeast Asia, there is an urgent need to identify the genetic determinants and understand the molecular mechanisms underpinning such resistance. Such insights could lead to prospective interventions to contain resistance and prevent the eventual spread to other regions where malaria is endemic. Reduced susceptibility to artemisinin in Southeast Asia has been primarily linked to mutations in the *Plasmodium falciparum* Kelch-13 gene, which is currently widely recognized as a molecular marker of artemisinin resistance. However, two mutations in a ubiquitin hydrolase, UBP-1, have been previously associated with reduced artemisinin susceptibility in a rodent model of malaria, and some cases of UBP-1 mutation variants associated with artemisinin treatment failure have been reported in Africa and SEA. In this study, we employed CRISPR-Cas9 genome editing and preemptive drug pressures to test these artemisinin susceptibility-associated mutations in UBP-1 in *Plasmodium berghei* sensitive lines *in vivo*. Using these approaches, we show that the V2721F UBP-1 mutation results in reduced artemisinin susceptibility, while the V2752F mutation results in resistance to chloroquine (CQ) and moderately impacts tolerance to artemisinins. Genetic reversal of the V2752F mutation restored chloroquine sensitivity in these mutant lines, whereas simultaneous introduction of both mutations could not be achieved and appears to be lethal. Interestingly, these mutations carry a detrimental growth defect, which would possibly explain their lack of expansion in natural infection settings. Our work provides independent experimental evidence on the role of UBP-1 in modulating parasite responses to artemisinin and chloroquine under *in vivo* conditions.

KEYWORDS artemisinin, *Plasmodium berghei*, *Plasmodium falciparum*, drug resistance, malaria

Artemisinins (ARTs) in artemisinin combinational therapies (ACTs) remain the mainstay of malaria treatment globally and thus far remain mostly effective in sub-Saharan Africa, where most of the disease burden occurs (1). However, ART (and even ACT) resistance has emerged in Southeast Asia (SEA), with a risk of spreading that is seriously threatening recent gains achieved in malaria control (2, 3). ART resistance is thought to be primarily conferred by specific mutations in the *Plasmodium falciparum* Kelch-13 (PfKelch13) gene, and such mutations are currently almost endemic in most parts of SEA (1, 4, 5). Phenotypically, these mutations are associated with delayed parasite clearance rates *in vivo* and with reduced susceptibility of ring stage parasites *in vitro* in ring stage survival assays (RSA) (3, 6). Interestingly, the prevalence of PfKelch13 mutations remains low outside SEA (7), and the few observed PfKelch13 polymorphisms in sub-Saharan Africa are not associated with treatment failure and/or delayed parasite clearance rates (8). Moreover, large-scale genome-wide association

Citation Simwela NV, Hughes KR, Roberts AB, Rennie MT, Barrett MP, Waters AP. 2020. Experimentally engineered mutations in a ubiquitin hydrolase, UBP-1, modulate *in vivo* susceptibility to artemisinin and chloroquine in *Plasmodium berghei*. Antimicrob Agents Chemother 64:e02484-19. <https://doi.org/10.1128/AAC.02484-19>.

Copyright © 2020 Simwela et al. This is an open-access article distributed under the terms of the [Creative Commons Attribution 4.0 International license](https://creativecommons.org/licenses/by/4.0/).

Address correspondence to Andrew P. Waters, Andy.Waters@glasgow.ac.uk.

Received 12 December 2019

Returned for modification 23 January 2020

Accepted 8 April 2020

Accepted manuscript posted online 27 April 2020

Published 23 June 2020

studies have revealed that polymorphisms in other genes such as multidrug resistance protein 2, ferredoxin, and others are also associated in SEA with delayed parasite clearance rates (9). More recently, mutations in an independent gene, *P. falciparum* coronin (PfCoronin), have been shown to confer enhanced survival in ring stage parasites exposed to dihydroartemisinin (DHA) (10). Deconvoluting the geographic complexities of ART resistance, genetic determinants, and the molecular mechanism involved would thus provide an avenue to contain or rescue emergent ART resistance through efficient surveillance and/or suitable combinational therapies.

Mutations in a ubiquitin hydrolase, UBP-1 (a close homologue to HAUSP or USP7), were previously identified to modulate susceptibility to ART and chloroquine (CQ) in the rodent-infectious malaria parasite *Plasmodium chabaudi* after sequential experimental evolution and selection with a series of antimalarial drugs (11). The reported drug-resistant phenotypes emerged from *in vivo* passage and exposure of the *P. chabaudi* drug-sensitive AS line to sublethal doses of pyrimethamine, CQ, mefloquine, and ARTs (11–13). Interestingly, in these *P. chabaudi* lineages, CQ resistance at 15 mg/kg emerged first, and from this uncloned line, whole-genome sequencing revealed two UBP-1 mutations (V2697F and V2728F) that were associated with the resistance phenotype (13, 14). Further selection of this uncloned CQ-resistant line generated lines with different drug resistance profiles, as follows: (i) a line resistant to 15 mg/kg mefloquine, (ii) a line resistant to CQ at 30 mg/kg, (iii) a line resistant to up to 300 mg/kg ART, which was selected from the CQ 30 mg/kg-resistant line, and (iv) a line resistant to up to 60 mg/kg artesunate. Upon further cloning and genome sequencing of these lines, it was found that the UBP-1 V2728F mutation was common in the ART-, CQ (30 mg/kg)-, and mefloquine-resistant lines, while the V2697F mutation only fixated upon artesunate selection (11, 12, 14). Due to the complexity of the selection procedure with multiple drugs, it has been difficult to confidently associate these UBP-1 mutations with ART and CQ susceptibility in the absence of appropriate reverse genetics approaches. Recently, these mutations have been introduced into UBP-1 in *P. falciparum*, and the V2721F equivalent has been shown to associate with increased DHA RSA survival with no CQ resistance phenotype, whereas the V2728F orthologue appeared to have no ART or CQ resistance profiles (15). More interestingly, UBP-1 mutation variants have been associated with decreased effectiveness of ARTs in Africa and some parts of Asia (16–19).

In our present study, we successfully engineered UBP-1 candidate mutations in an independent rodent model of *P. berghei* infection using a CRISPR-Cas9 genome editing system. We provide a causal link to the reduced ART and CQ susceptibility profiles of these mutant lines both *in vitro* and *in vivo*. We have also characterized their relative fitness compared to that of the wild-type nonmutant parasite.

RESULTS

CRISPR-Cas9-engineered mutations in UBP-1 confer *in vivo* selective advantage to ART and CQ pressure in *Plasmodium berghei*. To experimentally demonstrate that UBP-1 mutations confer selective advantage upon ART pressure, we introduced *P. chabaudi* UBP-1 candidate mutation (V2697F and V2728F) equivalents (see Fig. S1 in the supplemental material) into the *P. berghei* 820 line using a CRISPR-Cas9 system developed and optimized in our lab (Fig. 1A). Two plasmids were initially designed to either introduce the single mutation, V2752F (V2728F *P. chabaudi* equivalent), or both mutations, V2721F (V2697F *P. chabaudi* equivalent) and V2752F, in an attempt to generate a double mutant (Fig. 1A). Silent mutations to mutate the Cas9 cleavage site and introduce a restriction site (BseYI) were also introduced to prevent retargeting of mutated loci by Cas9 for the former and diagnosis by restriction fragment length polymorphism (RFLP) for the latter (Fig. 1A and B). Transfections of these plasmids into the 820 line yielded ~0.5% mutants for the V2752F mutant line (G1807, pG945) and ~23.00% mutants for the V2721F and V2752F double-mutant line (G1808, pG946), as confirmed by RFLP analysis (BseYI digestion) of the edited UBP-1 locus (Fig. 1B). Since the efficiency was too low to clone out the mutant lines by serial dilution, we attempted a preemptive drug selection with CQ and ART of the G1807 and G1808 lines to examine

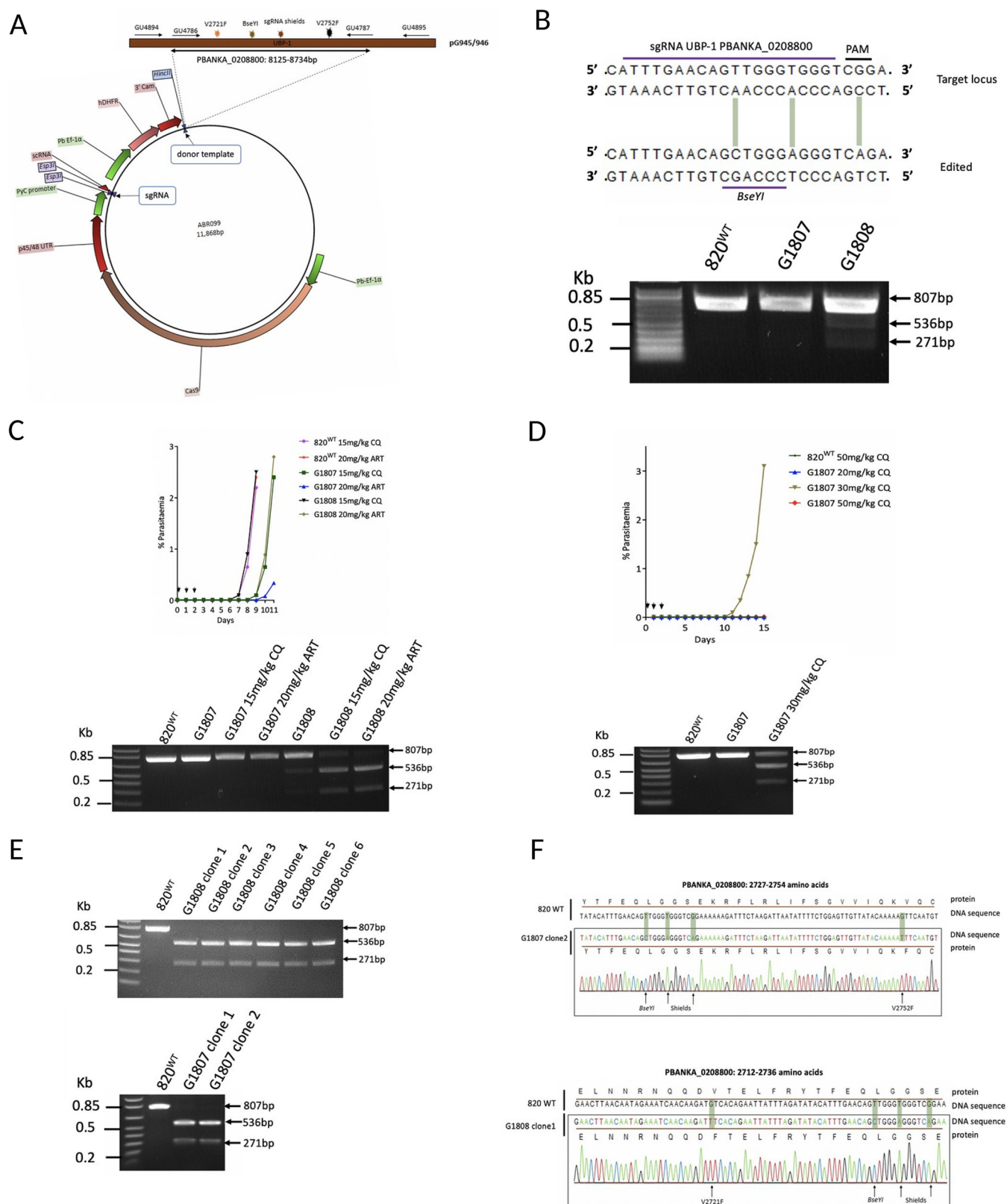


FIG 1 Introduction of UB-1 mutations in *P. berghei*. (A) Schematic plasmid constructs for the UB-1-targeted gene editing to introduce the V2721F and V2752F mutation. The plasmid contains Cas9 and *dhfr* (for pyrimethamine drug selection) under the control of the *P. berghei* EF-1 α promoter and the sgRNA expression cassettes under the control of the PyU6 promoter. A 20-bp guide RNA was designed and cloned into the sgRNA section of the illustrated vector. The donor UB-1 sequence (610 bp) is identical to that of the wild type, albeit with the desired mutations of interest (indicated by colored star symbols): V2752F (pG945), V2721F and V2752F (pG946), and silent mutations that mutate the Cas9 binding site as well as introduce the restriction site BseYI for restriction fragment length

(Continued on next page)

if selective enrichment of the mutant population could be achieved. Indeed, after infecting mice with the G1808 line and treating for three consecutive days with ART at 20 mg/kg, the recrudescence parasite population on day 9 was enriched to ~90% mutant population, as confirmed by RFLP analysis (Fig. 1C; see also Fig. S2D in the supplemental material). Meanwhile, CQ at 15 mg/kg also enriched the G1808 line to ~80%, relatively less than did ART (Fig. 1C). On the contrary, a very low-level mutant enrichment of the G1807 line (0.5% to 2.6%) was observed with CQ at 15 mg/kg, while ART did not produce any enrichment in the same line (0.5%). Interestingly, cloning of the G1808 ART-enriched lines yielded six clones that were all single mutants positive for the V2721F mutation despite coming from a plasmid with donor templates that carried both the V2721F and V2752F mutations (Fig. 1E and F). This suggests that the single V2721F mutation-carrying parasites were predominant in the G1808 line (despite resulting from transfection with a plasmid carrying both mutations) and were selectively enriched by ART. These data also suggested that introducing both mutations into the same parasite could either be lethal or result in very unfit parasites that are easily cleared by the host during early growth following transformation. Indeed, bulk DNA sequence analysis of the G1808 uncloned line revealed the absence of traces for both mutations, as only parasites carrying V2721F with silent mutations were present (Fig. S2B). Sequence analysis of the G1808 line isolated after CQ challenge at 15 mg/kg also confirmed specific enrichment for the V2721F mutation (Fig. S2D), suggesting that despite being principally enriched by ART, the V2721F mutation also modulates some resistance to CQ. Meanwhile, when we challenged the G1807 line (V2752F single mutation) with CQ at higher doses (20, 30, and 50 mg/kg), a recrudescence population was observed on day 10 with CQ 30 mg/kg (Fig. 1D). The CQ 30 mg/kg recrudescence parasites were enriched to ~61% for the mutant population (Fig. 1D, Fig. S2C) and were subsequently cloned. Sanger sequencing of G1808 ART-enriched and G1807 CQ-enriched clones confirmed the presence of the single V2721F and V2752F mutations, respectively, as well as the Cas9 cleavage silencing mutations and the silent mutations introducing the BseYI diagnostic restriction site (Fig. 1F).

The V2721F mutation confers observable reduced *in vivo* susceptibility to ARTs, while the V2752F mutation confers resistance to CQ and low-level protection against ARTs. We next quantitated the drug response profiles of the G1808^{V2721F} and G1807^{V2752F} cloned lines (first clone in each of the lines) *in vitro* and *in vivo* using DHA, ART, and CQ. In short-term *P. berghei* *in vitro* drug assays, both the G1808^{V2721F} and G1807^{V2752F} parasites showed no difference in sensitivity to DHA compared to that of the parental 820 line (Fig. 2A and B). The lack of decreased drug sensitivity of both lines is consistent with the failure of the standard 72-h drug assays to differentiate similar Kelch-13 ART-resistant parasites from sensitive lines in *P. falciparum* (3, 6). Meanwhile, a 1.8-fold increase in the half-inhibitory concentration (IC₅₀) was observed for the G1807^{V2752F} line when challenged with CQ (Fig. 2C), but not for the G1808^{V2721F} line (Fig. 2D). However, rodent malaria parasites offer the advantage of experimental drug resistance assessment *in vivo*. Therefore, we profiled the *in vivo* drug responses of the mutant lines to parental ART, which with controlled parasite inocula has been shown to effectively suppress wild-type parasites for up to 18 days following 100 mg/kg

FIG 1 Legend (Continued)

polymorphism (RFLP) analysis. (B) Illustrated 20-bp sgRNA and RFLP analysis of mutant parasites. Successful editing in the transfected parasites was observed on day 12 after transfection and pyrimethamine drug selection. RFLP (BseYI digestion) analysis of the transformed line PCR products (primers GU4894 + GU4895, 807 bp) revealed ~0.5% and ~22% efficiency for the G1807 and G1808 lines, respectively, as indicated by 2 distinct bands (536 bp and 271 bp) compared to 807-bp bands in the parent 820 line. (C) Preemptive challenge of the G1807 and G1808 lines with ART and CQ at 20 mg/kg and 15 mg/kg, respectively, and RFLP analysis of recrudescence parasites. Mice were infected intraperitoneally (i.p.) with $\sim 2 \times 10^7$ parasites on day 0. Treatment was started ~ 4 h postinfection by i.p. injection for three consecutive days. Parasitemia was monitored by microscopy analysis until recrudescence was observed. (D) Preemptive challenge of the G1807 line with higher doses of CQ and RFLP (BseYI digestion) analysis of the G1807 recrudescence population after challenge with 30 mg/kg CQ. (E) RFLP analysis of the cloned G1808 and G1807 ART- and CQ-challenged recrudescence parasites. (F) DNA sequencing confirming successful nucleotide editing for the G1807 clone 2 and G1808 clone 1 lines. The top sequence represents the wild-type 820 line (820^{WT}) unedited sequence with positions for sgRNA, protospacer adjacent motif (PAM), and V2721F or V2752F mutations indicated. The bottom sequence illustrates the nucleotide replacements at the V2721F or V2752F mutation locus and silent mutations to prevent Cas9 retargeting, as well as to introduce the BseYI restriction site for RFLP analysis in the G1807^{V2752F} and G1808^{V2721F} lines.

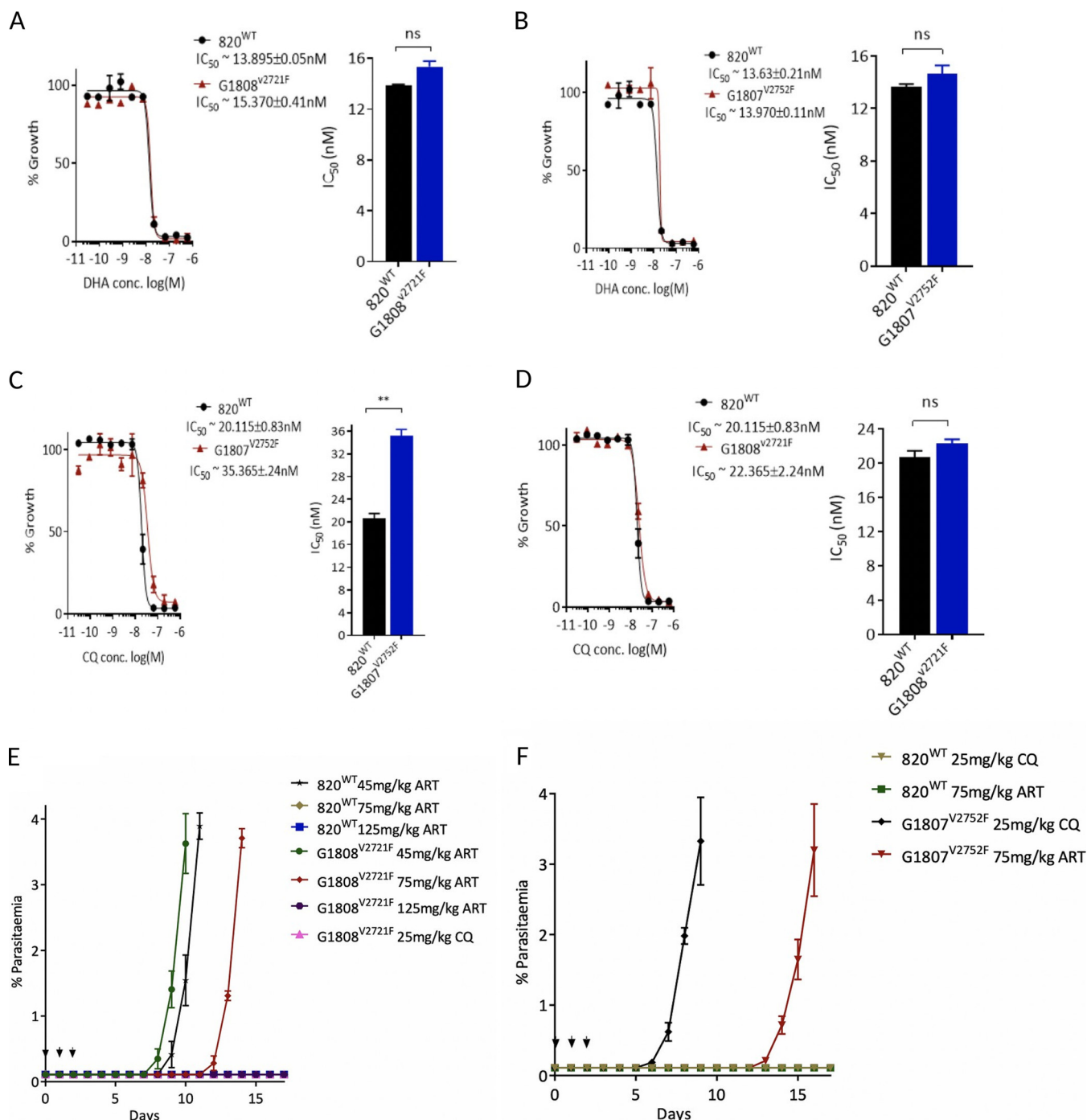


FIG 2 ART and CQ *in vitro* and *in vivo* resistance profiles of the G1807^{V2752F} and G1808^{V2721F} lines. dihydroartemisinin (DHA) dose-response curves and half-inhibitory concentration (IC_{50}) comparisons of the G1808^{V2721F} (A) and G1807^{V2752F} (B) lines relative to that of the wild-type 820 line. CQ dose-response curves and IC_{50} comparisons of the G1807^{V2752F} (C) and G1808^{V2721F} (D) lines relative to that of the wild-type 820 line. Significant differences between mean IC_{50} values or IC_{50} shifts were calculated using the paired *t* test. Error bars are standard deviations from three biological repeats. Significance is indicated with asterisks as follows: *, $P < 0.05$; **, $P < 0.01$; ***, $P < 0.001$; ****, $P < 0.0001$; ns, not significant. Modified Peters' 4-day suppressive test to monitor resistance to ART and CQ *in vivo* in the G1808^{V2721F} (E) and the G1807^{V2752F} (F) mutant lines. Groups of three mice were infected with 1×10^6 parasites on day 0. Treatment started ~1.5 h later with indicated drug doses every 24 h for three consecutive days (treatment days shown by arrows). Parasitemia was monitored by microscopy analysis of Giemsa-stained blood smears up to day 18. Error bars are standard deviations of parasitemia values from 3 mice.

dosing for three consecutive days (12). This is unlike responses to the clinically relevant ART derivative artesunate, which permits recrudescence in wild-type rodent malaria parasites at doses as high as 300 mg/kg within 14 days (20). This approach, when applied to the G1808^{V2721F} line, demonstrated that this mutation does indeed confer

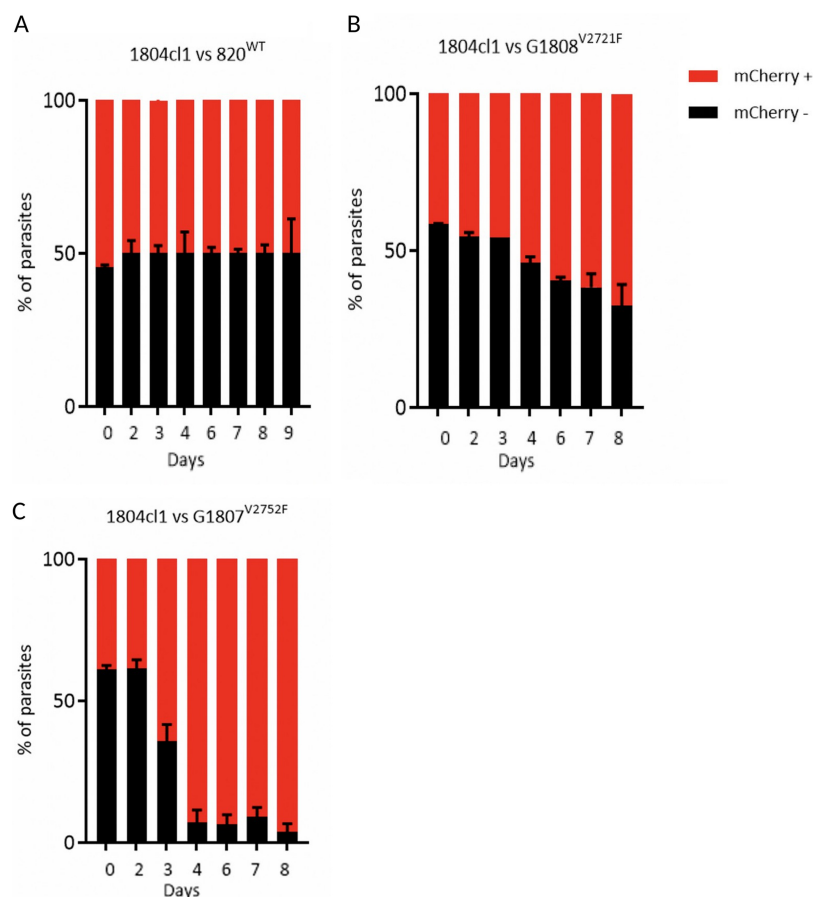


FIG 3 Growth kinetics of the 820, G1808^{V2721F}, and G1808^{V2752F} lines relative to the 1804cl1 line. The 1804cl1 line constitutively expresses mCherry under the control of the *hsp70* promoter. The 820, G1808^{V2721F}, and G1808^{V2752F} lines were mixed with the 1804cl1 line at a 1:1 ratio and injected intravenously at a parasitemia of 0.01% on day 0. Daily percentages of representative parasitemia of the 820 or mutant lines in the competition mixture were quantified by subtracting the total parasitemia based on positivity for Hoechst DNA stain from the fraction of the population that is mCherry positive (1804cl1) as determined by flow cytometry. On day 4, when parasitemia was ~5%, blood from each mouse was passaged into a new naive host, and parasitemia was monitored until day 8. Percent population changes of the mutant and wild-type lines relative to the 1804cl1 line in the 820 (A), G1808^{V2721F} (B), and G1808^{V2752F} (C) lines. Error bars are standard deviations from three biological repeats.

enhanced *in vivo* tolerance to ARTs compared to that of the parental 820 line. G1808^{V2721F} parasites survive three consecutive doses of 75 mg/kg ART, with the recrudescence population appearing on day 9 after the last dosing, whereas 820 wild-type parasites are effectively suppressed up to day 17 of follow-up (Fig. 2E). Both the G1808^{V2721F} and 820 lines survived a 45 mg/kg dose of ART, with the former having a slightly faster recrudescence rate on day 7, while the latter recrudescence a day later (Fig. 2E). Even though ART at 45 mg/kg does not significantly separate wild-type from mutant parasites, this could be due to the fitness cost that the V2721F mutation carries (Fig. 3), which would explain the recrudescence of mutant parasites at almost the same time as that for the wild type, since they would require a slightly longer time to achieve quantifiable parasitemia. Both lines remain sensitive to a 125 mg/kg ART dose, with no recrudescence observed up to day 17 (Fig. 2E). In contrast, the G1808^{V2752F} line is relatively resistant to CQ *in vivo* (Fig. 2F), surviving three consecutive doses at 25 mg/kg, with recrudescence parasites coming up on day 4 after the last dose, unlike the parental 820 line and the G1808^{V2721F} lines, which are sensitive and are effectively suppressed up to day 17. Interestingly, the G1808^{V2752F} line also displays low-level reduced susceptibility to ART at 75 mg/kg dose, with parasites coming up on day 12, later than

in the G1808^{V2721F} line (Fig. 2F). These data confirm that the V2721F mutation confers protection from ART drug challenge, while the V2752F mutation mediates resistance, primarily to CQ and, to some extent, low-level protection to ARTs. The recrudescence of the wild-type 820 and G1808^{V2721F} parasites at 45 mg/kg ART is also in agreement with our previous finding that *P. berghei* is less sensitive to ARTs, especially in the spleen and bone marrow, which could be the source of recrudescence infection at relatively lower doses (21).

Growth of parasites carrying UPB-1 V2752F and V2721F mutations is impaired.

The spread of drug resistance, as is the case in most microbial pathogens, is partly limited by detrimental fitness costs that accompany acquisition of such mutations in respective drug transporters, enzymes, or essential cellular components. The G1807 and G1808 lines carrying UPB-1 V2721F and V2752F mutations, respectively, were each grown in competition with a parental line expressing mCherry *in vivo* and were shown to be characteristically slow growing (Fig. 3A to C). In comparison, the G1807^{V2752F} line is severely impaired relative to the G1808^{V2721F} line, being completely outcompeted by day 8. These data and the earlier failure to generate the double mutant (Fig. 1) demonstrate that UPB-1 is an important (possibly essential) protein for parasite growth and that acquisition of resistance through mutation of UPB-1 confers mutation-specific fitness costs.

Reversal of the V2752F mutation restores CQ sensitivity in the G1807^{V2752F} line, while introduction of the V2721F in the same line appears to be lethal.

Drug pressure can select, in the long or short term, for mutations in sensitive parasite populations that would affect responses to the same drug. To further confirm that the phenotypes observed in our mutant lines were due to the V2721F or V2752F mutations and not to possible secondary mutations that may have been acquired during the preemptive drug pressure, we attempted to reverse the V2752F mutation in the G1807^{V2752F} line by swapping it to the V2721F genotype. This would allow us to determine if wild-type CQ phenotypes can be restored in the G1807^{V2752F} line, while at the same time assessing if the ART susceptibility profiles of the G1808^{V2721F} mutants could be reproduced in an independent line. Using a CRISPR-Cas9 editing strategy similar to the one outlined above, a single guide RNA (sgRNA) targeting a region ~50 bp upstream of the V2721F mutation was designed and cloned in the Cas9-expressing vectors (Fig. 4A). Donor DNA (698 bp; GU5189 + GU4787) containing the V2721F (for targeted mutation swap) or both the V2721F and V2752F mutations (for a forced introduction of V2721F in the G1807^{V2752F} background) was used to generate the vectors pG963 and pG962, respectively (Fig. 4A). Silent mutations mutating the proto-spacer adjacent motif (PAM) site, as well as introducing a second restriction site, SnaBI, for RFLP analysis were also included. Transfection of the G1807^{V2752F} line with pG963 and pG962 vectors successfully edited the UPB-1 locus, generating the G1918 and G1919 lines, respectively, with ~88% and ~79% efficiency as confirmed by SnaBI RFLP analysis (Fig. 4A). Cloning and sequencing of the G1918 line revealed a successful targeted mutation swap, introducing the V2721F mutation and reediting the 2752F to 2752V wild-type genotype (Fig. 4B and C). Phenotype analysis of the G1918 clone line revealed a restored *in vitro* susceptibility to CQ similar to that of the 820 wild type and a similar DHA sensitivity (Fig. 4D). Under *in vivo* conditions, the G1918cl1 line displayed a similar ART susceptibility profile at 75 mg/kg as the G1808^{V2721F} line, while CQ sensitivity was completely restored (Fig. 4E). This provided further experimental evidence that the drug susceptibility profiles observed were due to the V2721F or V2752F amino acid substitutions and not to the introduced silent mutations or secondary mutations that may have been acquired during the preemptive drug exposure. Interestingly, cloning and sequencing of the G1919 (Fig. 4B and F) line revealed successful introduction of the silent mutations (PAM mutating and SnaBI); the V2721F mutation was absent in all four clonal lines, yet the parental V2752F mutation was retained. This suggested that introduction of V2721F in the V2752F background is lethal or refractory in the parasite and further supported our failed first attempt to generate the double-mutant line (Fig. 1). Detailed sequence analysis of the transfected parasite populations

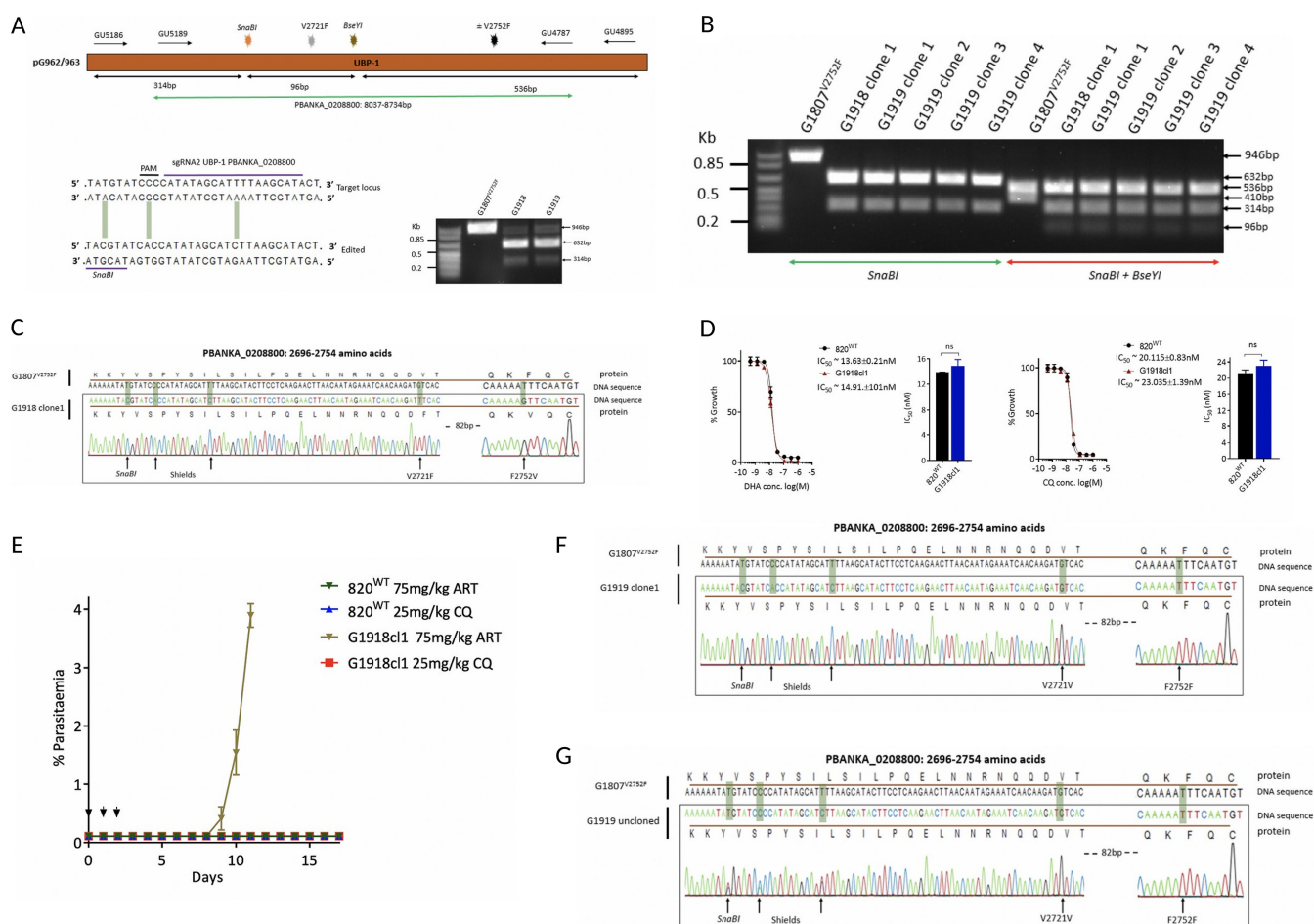


FIG 4 Swapping of the V2752F to V2721F mutations and attempted generation of a double mutant in the G1807V2752F line. (A) Schematic of the UBP-1 donor DNA in the pG962 and pG963 vectors, a 20-bp guide RNA used to target the UBP-1 region upstream of the V2721F mutation in the Cas9-expressing vectors, with introduced silent mutation sites indicated. RFLP (SnaBI digestion) analysis of PCR products (GU5186 + GU4895, 946 bp) of the G1918 and G1919 lines relative to the mutants showing successful editing by 2 distinct RFLP bands for the mutants (632 bp and 314 bp) and residual traces of the parental genotype. (B) RFLP analysis of the cloned G1918 and G1919 lines. The first six lanes to the left are RFLP analyses of G1918 and G1919 cloned line PCR products (GU5186 + GU4895, 946 bp) digested by SnaBI, showing 2 bands (632 bp and 314 bp) compared to 1 band for the parental G1807V2752F line. Six lanes to the right are the same clones digested by both SnaBI and BseYI, showing parental G1807V2752F with 2 RFLP bands (536 bp and 410 bp) as a result of digestion with BseYI only, as the SnaBI restriction site is absent, and 3 RFLP bands (536 bp, 314 bp, and 96 bp) in the G1918 and G1919 clones as a result of digestion of the PCR product by both BseYI and SnaBI. (C) Sequencing of G1918 clone 1 showing successful swapping of V2752F in the parent G1807V2752F line to the V2721F mutation. (D) *In vitro* DHA and CQ dose response curves and IC₅₀ comparisons of the G1918cl1 revertant line relative to those of the wild type, showing reversion of the CQ phenotype and similar sensitivity to DHA. Significant differences between mean IC₅₀ values or IC₅₀ shifts were calculated using a paired *t* test. Error bars are standard deviations from three biological repeats. Significance is indicated with asterisks as follows: *, *P* < 0.05; **, *P* < 0.01; ***, *P* < 0.001; ****, *P* < 0.0001; ns, not significant. (E) *in vivo* tolerance to ARTs at 75 mg/kg in the G1918cl1 line and complete restoration of CQ sensitivity. Sequence analysis of the G1919 clone1 (F) line and the G1919 uncloned (G) line, showing absence of double mutant populations.

before cloning revealed the presence of only one mutation trace in the G1919 line (despite the donor DNA containing both mutations), confirming that the double-mutant parasites do not survive or are severely growth impaired and quickly overgrown by the single-mutation parasites (Fig. 4G).

DISCUSSION

Ubiquitin hydrolases or deubiquitinating enzymes (DUBs) are essential elements of the eukaryotic ubiquitin proteasome system (UPS), which is primarily involved in maintaining cellular protein homeostasis and responding to stress. Despite the proposed involvement of *Plasmodium* DUBs in modulating susceptibility to multiple drugs, lack of conclusive experimental evidence has thus far limited studies into their detailed involvement in mode of action and/or resistance phenotypes, such as those observed with ARTs. In this study, using a CRISPR–Cas9-mediated reverse genetics approach, we

have provided experimental evidence on the direct involvement of a DUB (UBP-1) in modulating parasite responses to ART and CQ, most importantly under *in vivo* conditions. As the debate into the mechanism of action and resistance to ARTs continues, a consensus understanding is converging that ART resistance is complex, as several factors, genetic determinants, and possibly mechanisms of action appear to be involved. In *P. falciparum*, ART resistance is confined to early ring stage parasites, which has been translated in laboratory conditions to increased survival in ring stage survival assays (RSAs) (6). Mutations in Pfkelch13 and PfCoronin, as well as transient (hypothermic-hyperthermic) temperatures, have been shown to enhance ring stage parasite survival in the RSAs (10, 22, 23). More recently, characterization of Kelch-13 interacting factors has revealed that disruption of proteins that colocalize with Kelch-13, such as the parasite endocytosis proteins ESP15, UBP-1, and others of unknown function, modulate susceptibility to ARTs (24). As demonstrated in this study, reduced ART and, more, reduced CQ susceptibility can be mediated by mutations in UBP-1, underscoring a potential mechanism of cross resistance and some commonality in mode of action between CQ and ART, especially relating to hemoglobin digestion and trafficking in malaria parasites (24–26).

The UBP-1 V2728F mutation was previously designated a principle determinant of reduced ART susceptibility despite its common fixation with mefloquine and higher doses of CQ (12). Contrary to this argument, ART did not enrich this mutation (V2752F) in our study, but instead enriched the V2721F mutation, which was fixed with artesunate in *P. chabaudi*. However, enrichment of the V2752F mutation with a higher dose of CQ was achieved, showing that this mutation does indeed modulate parasite responses to CQ, while the V2721F mutation is chiefly responsible for the reduced ART susceptibility phenotype in the *P. berghei* model *in vivo*. Interestingly, drug challenge of these mutant lines *in vivo* revealed that both mutations give low-level cross-protection against both ARTs and CQ. This confirms that each of these UBP-1 mutations modulates some form of protection to both ARTs and CQ drug challenges, albeit to differing degrees, which is, therefore, in strong agreement with previous observations in *P. chabaudi* (12). This also demonstrates a plurality of pathways to resistance involving the same target. Recently, the exact equivalent UBP-1 mutations in *P. falciparum*, V3275F and V3306F, have been successfully engineered (15). In *P. falciparum* UBP-1, the V3275F mutation (V2721F *P. berghei* equivalent) shows enhanced survival to DHA in RSAs but remains sensitive to CQ. However, unlike in *P. berghei*, the V3306F (V2752F *P. berghei* equivalent) showed no enhanced survival to DHA in RSAs or resistance to CQ (15). While not entirely in agreement with the data reported here, this could be due to limitations in the ability of *in vitro* assays to fully predict actual drug responses *in vivo*, which our data highlight and which has been a concern recently with Kelch-13 mutations (27). These observations may also somewhat be confounded by species-specific differences in drug responses, pharmacodynamics, modes of action, and resistance that, in part, remain to be fully investigated. For example, previous and original linkage studies in *P. chabaudi* identified additional mutations in an amino acid transporter (*pcaat*), in tandem with UBP-1 mutations, as being strongly associated with CQ resistance phenotypes (12). Even though this could partly explain the observed *in vitro* sensitivity of *P. falciparum* V3275F mutants to CQ, our data suggest that UBP-1 mutations are sufficient to mediate quantifiable protective phenotypes to both ARTs and CQ, as the reversal of the V2752F mutation performed in this study, for example, completely restores CQ sensitivity. This provides, therefore, additional independent evidence on the direct causative role of UBP-1 mutations in modulating parasite responses not just to ARTs, but to CQ as well. The study also illustrates the potential of the *P. berghei* rodent model in proving causality to antimalarial drug resistance phenotypes under *in vivo* conditions, especially in light of recent reported discrepancies between some *in vitro* RSA resistance profiles of *P. falciparum* Kelch-13 mutants and actual *in vivo* phenotypes using the *Aotus* monkey model (27).

Interestingly, the V2721F and V2752F mutation-carrying parasites are characteristically slow growing and are easily outcompeted in the presence of nonmutants. Natural

P. falciparum UBP-1 mutations have been reportedly associated with ART treatment failure in Kenya (16, 19), SEA (18), and, more recently, in Ghana (17) (see Fig. S4 in the supplemental material). However, unlike their rodent counterparts, which are associated with reduced ART susceptibility, the reported natural E1528D and D1525E mutations occur toward the less conserved N terminus of the protein and outside the conserved, bioinformatically predicted UBP-1 catalytic domain (11) (Fig. S1). This suggests that acquisition of the mutations at the well-conserved C terminus in *P. falciparum* leads to a potential growth defect, as we observed with *P. berghei* in this study. However, as these upstream mutations are not conserved between *P. falciparum* and *P. berghei* UBP-1, we cannot test the hypothesis in this model. In fact, *P. falciparum* UBP-1 is highly polymorphic, with over 480 reported single-nucleotide polymorphisms (SNPs) (<https://plasmodb.org>), all of which are in the N-terminal region. *P. falciparum* UBP-1 has also been recently shown to be undergoing a strong positive selection in SEA (28). UBP-1 mutations could, therefore, be an independent avenue by which ART or multi-drug resistance phenotypes could emerge in regions where malaria is endemic, as has been seen in Africa (Ghana and Kenya), without actually requiring a permissive genetic background, as seems to be the current landscape with Kelch-13 mutations. However, there are constraints upon the evolution of drug resistance and UBP-1. While these data confirm that a single protein that does not transport drugs can mediate resistance to two quite distinct drug entities, it was not possible to generate a *P. berghei* line that simultaneously contained the two UBP-1 drug resistance mutations examined in this study.

In yeasts, UBP-1 localizes to the endoplasmic reticulum and plays a role in protein transport, specifically in internalization of substrates across membranes (29). Mutations in UBP-1 could, therefore, modulate endocytosis of important essential host-derived products such as hemoglobin to the digestive vacuole in a similar manner, thereby reducing exposure of the parasite to activated drug for both ARTs and CQ. Interestingly, mutations in the AP2 adaptor complex that is involved in clathrin-mediated endocytosis have also been implicated in ART resistance in rodent malaria parasites (14). One of the AP2 adaptor complex mutations (I592T) has been recently engineered in *P. falciparum* and has been shown to enhance ring stage parasite survival in RSAs (15). This further suggests that inhibition of the endocytic trafficking system is a possible generic mechanism for the parasites to survive lethal doses of drugs that require transport and activation in the digestive vacuole. This would further explain the multidrug resistance phenotype observed with the UBP-1 mutations in *P. chabaudi* and *P. berghei* in this study. Acquisition of the V2728F mutation in *P. chabaudi* was structurally predicted to reduce deubiquitination (11). In such a situation, the cellular increase in ubiquitinated proteins would be anticipated to positively feedback to the cellular machinery to rapidly degrade protein substrates at the 20S proteasome, promoting nonspecific and rapid protein turnover or impaired substrate trafficking. This would result in generally slow-growing parasites with reduced expression of, for example, multidrug resistance transporters, as well as reduced endocytosis of host-derived products like hemoglobin, which would in turn modulate parasite responses to these drugs. More recently, functional studies have revealed that PfKelch13 (a known determinant of ART resistance) localizes to the parasite cytosome and plays a role in hemoglobin trafficking (24, 26). Consequently, PfKelch13 mutations have been shown to lead to a partial loss of PfKelch13 protein function, leading to decreased hemoglobin trafficking to the parasite digestive vacuole and less DHA activation, which in turn mediates parasite survival (24, 26). Strikingly, protein pulldown at the parasite cytosomal foci where Kelch-13 localizes identified UBP-1 as a key interacting partner in the Kelch-13-mediated endocytic machinery that is involved in hemoglobin trafficking. By analyzing hemoglobin endocytosis in the ring and trophozoite stages, it has been demonstrated that partial inactivation of UBP-1 impairs hemoglobin endocytosis in both rings and trophozoites, unlike inactivation of Kelch-13, which impairs hemoglobin uptake only in ring stages of the parasites (24). This is indeed in agreement with our hypothesis on the consequences of UBP-1 mutations, and with observed *P. berghei*

phenotypes, which in a similar manner could impair trafficking of hemoglobin, leading to less activation of ARTs and CQ. Moreover, the potential role of UBP-1 in trafficking hemoglobin in both rings and trophozoites could explain the ART and CQ potential cross-resistance phenotype that we have observed with UBP-1 mutations unlike with Kelch-13 mutations, which, thus far, are known to mediate resistance to ARTs only and only in early ring stages. The experimental validation on the involvement of UBP-1 mutations in mediating potential cross-resistance to ART and CQ in malaria parasites, therefore, provides an additional understanding of drug resistance in malaria parasites, specifically for compounds that require access and/or activation in the digestive vacuole. Furthermore, the *P. berghei* model provides a useful sensitive and robust system in which to investigate the interplay and impact of simultaneous mutations of both Kelch-13 and UBP-1 *in vivo*, as well as to assess whether PfKelch13 mutations would modulate responses to CQ under *in vivo* conditions.

In conclusion, the work presented here provides further experimental evidence for the involvement of conserved mutations in a polymorphic ubiquitin hydrolase protein that serves as a nexus for resistance to two very diverse classes of drugs. The findings also underscore the potential difficulties that *in vitro* assays may have in appropriately assigning mutant parasites with appropriate phenotypes in the absence of conclusive *in vivo* measurements. *P. berghei* should therefore, be a suitable and adaptable *in vivo* model for the rapid evaluation and/or genetic engineering of mutations associated with human-infectious *Plasmodium* drug resistance observed in the field for concurrent assigning of drug resistance phenotypes under both *in vitro* and *in vivo* conditions.

MATERIALS AND METHODS

CRISPR-Cas9 generation of UBP-1 mutant lines. (i) Primary vectors. The Cas9-expressing plasmid ABR099 was used for targeted nucleotide replacement at the UBP-1 locus. ABR099 (Fig. 1A) contains the Cas9 endonuclease driven by the *P. berghei* Ef-1 α promoter, a Cas9 binding scaffold, a site for cloning the guide RNA (sgRNA) driven by the *Plasmodium yoelii* U6 promoter, an *dhfr* cassette (for pyrimethamine drug resistance selection), and a linker site for insertion of homologous repair templates. sgRNAs targeting the UBP-1 locus were designed using the Web-based eukaryotic pathogen CRISPR guide RNA/DNA design tool (<http://grna.ctegd.uga.edu/>) (30) by directly inputting the sequence of interest. Primary vectors containing the sgRNA of interest were generated by annealing the oligonucleotide pairs (GU4788+GU4789 and GU5206+GU5207; see Table S1 in the supplemental material) encoding the guide sequence and cloning them into the dual Esp3I sites upstream of the Cas9 binding domain of the vector ABR099. These plasmids were called pG944 and pG960 for the GU4788 + GU4789 and GU5206 + GU5207 annealed guides, respectively.

(ii) Mutagenesis and generation of secondary vectors. To generate the final vectors for editing the UBP-1 locus, 610 bp of UBP-1 donor DNA (PlasmoDB gene ID PBANKA_0208800) was PCR amplified using primers GU4786 and GU4787 (Table S1) designed to contain a HincII site at the 5' end. The PCR product was purified, A tailed, and cloned into the TOPO 2.1 vector using the TOPO TA cloning kit (Invitrogen) according to the manufacturer's instructions. To mutate the UBP-1 locus, 3 primer sets (Table S1) complementary to the amplified UBP-1 PCR product were designed to contain specific nucleotide substitutions, as follows: (i) a shielding primer (GU4783) containing three silent mutations mutating the sgRNA and PAM sites targeted by the GU4788 + GU4789 sgRNA (to prevent Cas9 binding the donor templates and the edited loci in the mutant parasites), as well as an introduced BseYI restriction site for restriction site fragment polymorphism (RFLP) analysis, and (ii) 2 primer sets carrying the mutations of interest, V2721F (GU4785) and V2752F (GU4784). A site-directed mutagenesis of the cloned UBP-1 PCR product in the TOPO 2.1 vector was carried out using a QuikChange multisite-directed mutagenesis kit (Agilent Technologies) using the following primer combinations: GU4783 + GU4784 for the V2752F single mutant and GU4783 + GU4784 + GU4785 for the double mutant. The resulting mutant fragments in the TOPO 2.1 vector were digested out and cloned into the linker site of the vector pG944 using the HincII restriction site to generate pG945 (single mutant) and pG946 (double mutant). For targeted mutation swapping and a second attempt to generate a double mutant line, a second sgRNA (GU5206 + GU5207) upstream of the V2721F mutation was designed and cloned into the ABR099 vector as described. Donor DNA was amplified from the G1808^{V2721F} or pG946 vector to generate single- or double-mutation templates, respectively, by using overlapping PCR as previously described (31). Briefly, internal complementary primers (GU5190 + GU5191; Table S1) carrying 3 silent mutations (2 for mutating the sgRNA and PAM of the GU5206 + GU5207 sgRNA and 1 to introduce the SnaBI restriction site for RFLP analysis) were used to amplify 2 overlapping PCR products from the G1808^{V2721F} DNA or pG946 plasmid upon linkage to HincII, introducing outer primers GU5189 and GU4787 (Table S1). After gel purification, ~50 ng of the overlapping PCR fragments was used as the template in a second round of PCR using the two outer primers (GU5189 + GU4787) to generate donor fragments with mutations of interest. The resulting fragments were subsequently cloned into the pG960 vector at the linker site using the HincII restriction site to generate the vectors pG963 (silent mutations to GU5206 + GU5207 sgRNA, V2721F mutation) and

pG962 (silent mutations to GU5206 + GU5207 sgRNA, V2721F and V2752F mutation). All PCRs were carried out using the Kapa high-fidelity PCR kit (Roche). Plasmids were verified by Sanger DNA sequencing prior to further use.

***P. berghei* animal infections.** *P. berghei* parasites were maintained in female Theiler's Original (TO) mice (Envigo) weighing between 25 and 30 g. Parasite infections were established either by intraperitoneal (i.p.) injection of ~200 μ l of cryopreserved parasite stocks or by intravenous (i.v.) injection of purified schizonts. Monitoring of parasitemia in infected mice was done by examining methanol-fixed thin blood smears stained in Giemsa (Sigma) or by flow cytometry analysis of infected blood stained with Hoechst 33342 (Invitrogen). Blood from infected mice was collected by cardiac puncture under terminal anesthesia. All animal work was performed in compliance with UK home office licensing (project reference no. P6CA91811) and with ethical approval from the University of Glasgow Animal Welfare and Ethical Review Body.

Parasite lines and transfections. An 820 line that express green fluorescent protein (GFP) and red fluorescent protein (RFP) in male and female gametocytes, respectively (32), was used for initial transfection experiments, while the 1804cl1 line, which constitutively expresses mCherry throughout the life cycle (33), was used for growth competition assays as a control. Episomal plasmid DNA (~10 μ g) from the vectors described above was transfected by mixing with Nycodenz-purified schizonts and electroporated using the Amaxa Nucleofector device II program U-033 as previously described (34). Parasites were then immediately i.v. injected into the mouse tail vein. Positive selection of transfected parasites was commenced 24 h later by inclusion of pyrimethamine (Sigma) in drinking water.

Genotype analysis of mutant lines. Blood was collected from parasite-infected mice by cardiac puncture under terminal anesthesia and lysed by resuspension in 1 \times E-lysis buffer (Thermo). Parasite genomic DNA was extracted using the Qiagen DNeasy blood and tissue kit according to manufacturer's instructions. Genotype analysis of the transfected or cloned parasite lines was conducted initially by dual PCR-RFLP. PCR using exterior primers (GU4894 + GU4895 or GU5186 + GU4895) was used to amplify fragments from the DNA of the mutant lines, followed by restriction digests with either BseYI or SnaBI restriction enzymes to verify successful editing of the UBP-1 locus. Transfection efficiencies were estimated by relative densitometric quantification of RFLP fragments by ImageJ2 (35). Further confirmation of the mutations was carried out by Sanger DNA sequencing.

***P. berghei* in vitro culture and drug susceptibility assays.** For *in vitro* maintenance of *P. berghei*, cultures were maintained for one developmental cycle using a standardized schizont culture medium containing RPMI 1640 with 25 mM hypoxanthine, 10 mM sodium bicarbonate, 20% fetal calf serum, 100 U/ml penicillin, and 100 μ g/ml streptomycin. Culture flasks were gassed for 30 s with a special gas mix of 5% CO₂, 5% O₂, and 90% N₂ and incubated for 22 to 24 h at 37°C with gentle shaking, conditions that allow for development of ring stage parasites to mature schizonts. Drug assays to determine *in vitro* growth inhibition during the intraerythrocytic stage were performed in these standard short-term cultures as previously described (36). Briefly, 1 ml of infected blood with a nonsynchronous parasitemia of 3 to 5% was collected from an infected mouse and cultured for 22 to 24 h in 120 ml of schizont culture media. Schizonts were enriched from the cultures by Nycodenz density flotation as previously described (34), followed by immediate injection into a tail vein of a naive mouse. Upon i.v. injection, schizonts immediately rupture, with the resulting merozoites invading new red blood cells within minutes to obtain synchronous *in vivo* infection containing >90% rings and a parasitemia of 1 to 2%. Blood was collected from the infected mice 2 h postinjection and mixed with serially diluted drugs in schizont culture medium in 96-well plates at a final hematocrit of 0.5% in a 200- μ l well volume. Plates were gassed and incubated overnight at 37°C. After 22 to 24 h of incubation, schizont maturation was analyzed by flow cytometry after staining the infected cells with the DNA dye Hoechst-33258. Schizonts were gated and quantified based on fluorescence intensity on an FACSCelesta or an LSRFortessa (BD Biosciences, USA). To determine growth inhibitions and calculate half-inhibitory concentrations (IC₅₀), quantified schizonts in no-drug controls were set to correspond to 100% with subsequent growth percentages in the presence of drugs, calculated accordingly. Dose-response curves were plotted in GraphPad Prism 7.

***In vivo* drug assays.** A modified Peters' 4-day suppressive test was employed to assess *in vivo* drug responses and/or resistance profiles in the wild-type and mutant lines, as previously described (37). Parasitemia was initiated by i.p. inoculation of between 10⁶ and 10⁷ parasites, followed by three daily consecutive drug doses initiated ~4 h postinoculation. CQ was prepared at 50 mg/ml in 1 \times phosphate-buffered saline (PBS) and diluted to working stock in 1 \times PBS, while ART was prepared at 12.5 mg/ml in a 1:1 mixture of dimethyl sulfoxide (DMSO) and Tween 80 (Sigma), followed by a 10-fold dilution in sterile water to an injectable working solution. All drugs were delivered by i.p. injection and were prepared fresh immediately before injection. Parasitemia was monitored daily by flow cytometry and analysis of methanol-fixed Giemsa stained smears.

***In vivo* growth competition assays.** Clonal mutant lines in the 820 background were mixed with the 1804cl1 line, which constitutively express mCherry under the control of the *hsp70* promoter, in a 1:1 mixture and injected intravenously into mice. Parasitemia in the competition mixtures was quantified by flow cytometry quantification of mCherry-positive parasites for the 1804cl1 proportional percentage and by subtracting the total parasitemia (Hoechst positive) from the mCherry-positive proportion for the 820 control and/or mutant lines. Differentiation of the mCherry-positive population from the RFP in the 820 line was carried out by applying flow compensation gating strategies (see Fig. S3 in the supplemental material).

SUPPLEMENTAL MATERIAL

Supplemental material is available online only.

SUPPLEMENTAL FILE 1, PDF file, 0.9 MB.

ACKNOWLEDGMENTS

We thank Mathias Matti for meaningful discussions and Diane Vaughan and the iii flow cytometry facility for assistance.

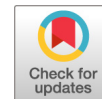
This work was supported by grants from the Wellcome Trust to A.P.W. (grants 083811/Z/07/Z and 107046/Z/15/Z). M.P.B. is funded by a Wellcome Trust core grant to the Wellcome Centre for Integrative Parasitology (grant 104111/Z/14/Z). N.V.S. is a Commonwealth Doctoral Scholar (MWCS-2017-789) funded by the UK government.

N.V.S. conceived the experiments, performed data curation, analysis, investigation, validation, visualization, and wrote the original draft. K.R.H., A.B.R., M.T.R., and M.P.B. participated in formal data analysis, investigation, validation, review, and editing. A.P.W. conceived the study, participated in planning experiments, analysis, investigation, validation, writing of the original draft, review, and editing, and performed supervision.

REFERENCES

- World Health Organization. 2018. World malaria report. World Health Organization, Geneva, Switzerland.
- Hamilton WL, Amato R, van der Pluijm RW, Jacob CG, Quang HH, Thuy-Nhien NT, Hien TT, Hongvanthong B, Chindavongsa K, Mayxay M, Huy R, Leang R, Huch C, Dysoley L, Amaratunga C, Suon S, Fairhurst RM, Tripura R, Peto TJ, Sovann Y, Jittamala P, Hanboonkunupakarn B, Pukrittayakamee S, Chau NH, Imwong M, Dhorda M, Vongpromek R, Chan XHS, Maude RJ, Pearson RD, Nguyen T, Rockett K, Drury E, Gonçalves S, White NJ, Day NP, Kwiatkowski DP, Dondorp AM, Miotto O. 2019. Evolution and expansion of multidrug-resistant malaria in southeast Asia: a genomic epidemiology study. *Lancet Infect Dis* 19:943–951. [https://doi.org/10.1016/S1473-3099\(19\)30392-5](https://doi.org/10.1016/S1473-3099(19)30392-5).
- Dondorp AM, Nosten F, Yi P, Das D, Phyto AP, Tarning J, Lwin KM, Ariey F, Hanpithakpong W, Lee SJ, Ringwald P, Silamut K, Imwong M, Chotivanich K, Lim P, Herdman T, An SS, Yeung S, Singhasivanon P, Day NPJ, Lindegardh N, Socheat D, White NJ. 2009. Artemisinin resistance in *Plasmodium falciparum* malaria. *N Engl J Med* 361:455–467. <https://doi.org/10.1056/NEJMoa0808859>.
- Mbengue A, Bhattacharjee S, Pandharkar T, Liu H, Estiu G, Stahelin RV, Rizk SS, Njimoh DL, Ryan Y, Chotivanich K, Nguon C, Ghorbal M, Lopez-Rubio JJ, Pfrender M, Emrich S, Mohandas N, Dondorp AM, Wiest O, Haldar K. 2015. A molecular mechanism of artemisinin resistance in *Plasmodium falciparum* malaria. *Nature* 520:683–687. <https://doi.org/10.1038/nature14412>.
- Ashley EA, Dhorda M, Fairhurst RM, Amaratunga C, Lim P, Suon S, Sreng S, Anderson JM, Mao S, Sam B, Sopha C, Chhor CM, Nguon C, Sovannaroeth S, Pukrittayakamee S, Jittamala P, Chotivanich K, Chutasmit K, Suchatsoonthorn C, Runchaoren R, Hien TT, Thuy-Nhien NT, Thanh NV, Phu NH, Htut Y, Han K-T, Aye KH, Mokuolu OA, Olaosebikan RR, Folaranmi OO, Mayxay M, Khanthavong M, Hongvanthong B, Newton PN, Onyamboko MA, Fanella CI, Tshetu AK, Mishra N, Valecha N, Phyto AP, Nosten F, Yi P, Tripura R, Borrmann S, Bashraheil M, Peshu J, Faiz MA, Ghose A, Hossain MA, Samad R, Rahman MR, Hasan MM, Islam A, Miotto O, Amato R, MacInnis B, Stalker J, Kwiatkowski DP, Bozdech Z, Jeeyapant A, Cheah PY, Sakulthaew T, Chalk J, Intharabut B, Silamut K, Lee SJ, Vihokhern B, Kunasol C, Imwong M, Tarning J, Taylor WJ, Yeung S, Woodrow CJ, Flegg JA, Das D, Smith J, Venkatesan M, Plowe CV, Stepniwska K, Guerin PJ, Dondorp AM, Day NP, White NJ, Tracking Resistance to Artemisinin Collaboration (TRAC). 2014. Spread of artemisinin resistance in *Plasmodium falciparum* malaria. *N Engl J Med* 371:411–423. <https://doi.org/10.1056/NEJMoa1314981>.
- Witkowski B, Amaratunga C, Khim N, Sreng S, Chim P, Kim S, Lim P, Mao S, Sopha C, Sam B, Anderson JM, Duong S, Chhor CM, Taylor WR, Suon S, Mercereau-Puijalon O, Fairhurst RM, Ménard D. 2013. Novel phenotypic assays for the detection of artemisinin-resistant *Plasmodium falciparum* malaria in Cambodia: *in-vitro* and *ex-vivo* drug-response studies. *Lancet Infect Dis* 13:1043–1049. [https://doi.org/10.1016/S1473-3099\(13\)70252-4](https://doi.org/10.1016/S1473-3099(13)70252-4).
- Ménard D, Khim N, Beghain J, Adegnik AA, Shafiu-Allah M, Amodu O, Rahim-Awab G, Barnadas C, Berry A, Boum Y, Bustos MD, Cao J, Chen J-H, Collet L, Cui L, Thakur G-D, Dieye A, Djallé D, Dorkenoo MA, Eboumbou-Moukoko CE, Espino F-E-CJ, Fandeur T, Ferreira-da-Cruz M-F, Fola AA, Fuehrer H-P, Hassan AM, Herrera S, Hongvanthong B, Houzé S, Ibrahim ML, Jahirul-Karim M, Jiang L, Kano S, Ali-Khan W, Khanthavong M, Kremsner PG, Lacerda M, Leang R, Leelawong M, Li M, Lin K, Mazarati J-B, Ménard S, Morlais I, Muhindo-Mavoko H, Musset L, Na-Bangchang K, Nambozi M, Niaré K, Noedl H, Ouédraogo J-B, Pillai DR, Pradines B, Quang-Phuc B, Ramharter M, Randrianarivelosia M, Sattabongkot J, Sheikh-Omar A, Silué KD, Sirima SB, Sutherland C, Syafruddin D, Tahar R, Tang L-H, Touré OA, Tshibangu-Wa-Tshibangu P, Vigan-Womas I, Warsame M, Wini L, Zakeri S, Kim S, Eam R, Berne L, Khean C, Chy S, Ken M, Loch K, Canier L, Duru V, Legrand E, Barale J-C, Stokes B, Straimer J, Witkowski B, Fidock DA, Rogier C, Ringwald P, Ariey F, Mercereau-Puijalon O, KARMA Consortium. 2016. A worldwide map of *Plasmodium falciparum* K13-propeller polymorphisms. *N Engl J Med* 374:2453–2464. <https://doi.org/10.1056/NEJMoa1513137>.
- Sutherland CJ, Lansdell P, Sanders M, Muwanguzi J, van Schalkwyk DA, Kaur H, Nolder D, Tucker J, Bennett HM, Otto TD, Berriman M, Patel TA, Lynn R, Gkrania-Klotsas E, Chiodini PL. 2017. *pfk13*-independent treatment failure in four imported cases of *Plasmodium falciparum* malaria treated with artemether-lumefantrine in the United Kingdom. *Antimicrob Agents Chemother* 61:e02382-16. <https://doi.org/10.1128/AAC.02382-16>.
- Miotto O, Amato R, Ashley EA, MacInnis B, Almagro-Garcia J, Amaratunga C, Lim P, Mead D, Oyola SO, Dhorda M, Imwong M, Woodrow C, Manske M, Stalker J, Drury E, Campino S, Amenga-Etego L, Thanh TN, Tran HT, Ringwald P, Bethell D, Nosten F, Phyto AP, Pukrittayakamee S, Chotivanich K, Chhor CM, Nguon C, Suon S, Sreng S, Newton PN, Mayxay M, Khanthavong M, Hongvanthong B, Htut Y, Han KT, Kyaw MP, Faiz MA, Fanella CI, Onyamboko M, Mokuolu OA, Jacob CG, Takala-Harrison S, Plowe CV, Day NP, Dondorp AM, Spencer CC, McVean G, Fairhurst RM, White NJ, Kwiatkowski DP. 2015. Genetic architecture of artemisinin-resistant *Plasmodium falciparum*. *Nat Genet* 47:226–234. <https://doi.org/10.1038/ng.3189>.
- Demas AR, Sharma AI, Wong W, Early AM, Redmond S, Bopp S, Neafsey SG, McNaie I, Cheesman S, do Rosario V, Carter R, Fidock DA, Cravo P. 2007. Gene encoding a deubiquitinating enzyme is mutated in artesunate- and chloroquine-resistant rodent malaria parasites. *Mol Microbiol* 65:27–40. <https://doi.org/10.1111/j.1365-2958.2007.05753.x>.
- Hunt P, Martinelli A, Modrzynska K, Borges S, Creasey A, Rodrigues L, Beraldi D, Loewe L, Fawcett R, Kumar S, Thomson M, Trivedi U, Otto TD, Pain A, Blaxter M, Cravo P. 2010. Experimental evolution, genetic analysis and genome re-sequencing reveal the mutation conferring artemisinin

- resistance in an isogenic lineage of malaria parasites. BMC Genomics 11:499. <https://doi.org/10.1186/1471-2164-11-499>.
13. Afonso A, Hunt P, Cheesman S, Alves AC, Cunha CV, do Rosário V, Cravo P. 2006. Malaria parasites can develop stable resistance to artemisinin but lack mutations in candidate genes *atp6* (encoding the sarcoplasmic and endoplasmic reticulum Ca^{2+} ATPase), *tctp*, *mdr1*, and *cg10*. Antimicrob Agents Chemother 50:480–489. <https://doi.org/10.1128/AAC.50.2.480-489.2006>.
 14. Henriques G, Martinelli A, Rodrigues L, Modrzynska K, Fawcett R, Houston DR, Borges ST, d'Alessandro U, Tinto H, Karema C, Hunt P, Cravo P. 2013. Artemisinin resistance in rodent malaria—mutation in the AP2 adaptor μ -chain suggests involvement of endocytosis and membrane protein trafficking. Malar J 12:118. <https://doi.org/10.1186/1475-2875-12-118>.
 15. Henrici RC, van Schalkwyk DA, Sutherland CJ. 2019. Modification of *pfap2 μ* and *pfubp1* markedly reduces ring-stage susceptibility of *Plasmodium falciparum* to artemisinin *in vitro*. Antimicrob Agents Chemother 64:e01542-19. <https://doi.org/10.1128/AAC.01542-19>.
 16. Henriques G, Hallett RL, Beshir KB, Gadalla NB, Johnson RE, Burrow R, van Schalkwyk DA, Sawa P, Omar SA, Clark TG, Bousema T, Sutherland CJ. 2014. Directional selection at the *pfmdr1*, *pfcr1*, *pfubp1*, and *pfap2 μ* loci of *Plasmodium falciparum* in Kenyan children treated with ACT. J Infect Dis 210:2001–2008. <https://doi.org/10.1093/infdis/jiu358>.
 17. Adams T, Ennison NAA, Quashie NB, Futagbi G, Matrevi S, Hagan OCK, Abuaku B, Koram KA, Duah NO. 2018. Prevalence of *Plasmodium falciparum* delayed clearance associated polymorphisms in adaptor protein complex 2 μ subunit (*pfap2 μ*) and ubiquitin specific protease 1 (*pfubp1*) genes in Ghanaian isolates. Parasit Vectors 11:175–175. <https://doi.org/10.1186/s13071-018-2762-3>.
 18. Cerqueira GC, Cheeseman IH, Schaffner SF, Nair S, McDew-White M, Phyto AP, Ashley EA, Melnikov A, Rogov P, Birren BW, Nosten F, Anderson TJ, Neafsey DE. 2017. Longitudinal genomic surveillance of *Plasmodium falciparum* malaria parasites reveals complex genomic architecture of emerging artemisinin resistance. Genome Biol 18:78–78. <https://doi.org/10.1186/s13059-017-1204-4>.
 19. Borrmann S, Straimer J, Mwai L, Abdi A, Rippert A, Okombo J, Muriithi S, Sasi P, Kortok MM, Lowe B, Campino S, Assefa S, Auburn S, Manske M, Maslen G, Peshu N, Kwiatkowski DP, Marsh K, Nzila A, Clark TG. 2013. Genome-wide screen identifies new candidate genes associated with artemisinin susceptibility in *Plasmodium falciparum* in Kenya. Sci Rep 3:3318–3318. <https://doi.org/10.1038/srep03318>.
 20. Walker LA, Sullivan DJ, Jr. 2017. Impact of extended duration of artesunate treatment on parasitological outcome in a cytotoxic murine malaria model. Antimicrob Agents Chemother 61:e02499-16. <https://doi.org/10.1128/AAC.02499-16>.
 21. Lee RS, Waters AP, Brewer JM. 2018. A cryptic cycle in haematopoietic niches promotes initiation of malaria transmission and evasion of chemotherapy. Nat Commun 9:1689. <https://doi.org/10.1038/s41467-018-04108-9>.
 22. Henrici RC, van Schalkwyk DA, Sutherland CJ. 2019. Transient temperature fluctuations severely decrease *P. falciparum* susceptibility to artemisinin *in vitro*. Int J Parasitol Drugs Drug Resist 9:23–26. <https://doi.org/10.1016/j.ijpddr.2018.12.003>.
 23. Straimer J, Gnädig NF, Witkowski B, Amaratunga C, Duru V, Ramadani AP, Dacheux M, Khim N, Zhang L, Lam S, Gregory PD, Urnov FD, Mercereau-Puijalon O, Benoit-Vical F, Fairhurst RM, Ménard D, Fidock DA. 2015. K13-propeller mutations confer artemisinin resistance in *Plasmodium falciparum* clinical isolates. Science 347:428–431. <https://doi.org/10.1126/science.1260867>.
 24. Birnbaum J, Scharf S, Schmidt S, Jonscher E, Hoeijmakers WAM, Flemming S, Toenhake CG, Schmitt M, Sabitzki R, Bergmann B, Fröhke U, Mesén-Ramírez P, Blancke Soares A, Herrmann H, Bártfai R, Spielmann T. 2020. A Kelch13-defined endocytosis pathway mediates artemisinin resistance in malaria parasites. Science 367:51–59. <https://doi.org/10.1126/science.aax4735>.
 25. Klonis N, Crespo-Ortiz MP, Bottova I, Abu-Bakar N, Kenny S, Rosenthal PJ, Tilley L. 2011. Artemisinin activity against *Plasmodium falciparum* requires hemoglobin uptake and digestion. Proc Natl Acad Sci U S A 108:11405–11410. <https://doi.org/10.1073/pnas.1104063108>.
 26. Yang T, Yeoh LM, Tutor MV, Dixon MW, McMillan PJ, Xie SC, Bridgford JL, Gillett DL, Duffy MF, Ralph SA, McConville MJ, Tilley L, Cobbold SA. 2019. Decreased K13 abundance reduces hemoglobin catabolism and proteotoxic stress, underpinning artemisinin resistance. Cell Rep 29:2917–2928.e5. <https://doi.org/10.1016/j.celrep.2019.10.095>.
 27. Sa JM, Kaslow SR, Krause MA, Melendez-Muniz VA, Salzman RE, Kite WA, Zhang M, Moraes Barros RR, Mu J, Han PK, Mershon JP, Figan CE, Caleon RL, Rahman RS, Gibson TJ, Amaratunga C, Nishiguchi EP, Breglio KF, Engels TM, Velmurugan S, Ricklefs S, Straimer J, Gnädig NF, Deng B, Liu A, Diouf A, Miura K, Tullo GS, Eastman RT, Chakravarty S, James ER, Udenze K, Li S, Sturdevant DE, Gwadz RW, Porcella SF, Long CA, Fidock DA, Thomas ML, Fay MP, Sim BKL, Hoffman SL, Adams JH, Fairhurst RM, Su XZ, Welles TE. 2018. Artemisinin resistance phenotypes and K13 inheritance in a *Plasmodium falciparum* cross and *Aotus* model. Proc Natl Acad Sci U S A 115:12513–12518. <https://doi.org/10.1073/pnas.1813386115>.
 28. Ye R, Tian Y, Huang Y, Zhang Y, Wang J, Sun X, Zhou H, Zhang D, Pan W. 2019. Genome-wide analysis of genetic diversity in *Plasmodium falciparum* isolates from China–Myanmar Border. Front Genet 10:1065. <https://doi.org/10.3389/fgene.2019.01065>.
 29. Schmitz C, Kinner A, Kölling R. 2005. The deubiquitinating enzyme Ubp1 affects sorting of the ATP-binding cassette-transporter Ste6 in the endocytic pathway. Mol Biol Cell 16:1319–1329. <https://doi.org/10.1091/mbc.e04-05-0425>.
 30. Peng D, Tarleton R. 2015. EuPaGDT: a web tool tailored to design CRISPR guide RNAs for eukaryotic pathogens. Microb Genom 1:e000033. <https://doi.org/10.1099/mgen.0.000033>.
 31. Heckman KL, Pease LR. 2007. Gene splicing and mutagenesis by PCR-driven overlap extension. Nat Protoc 2:924–932. <https://doi.org/10.1038/nprot.2007.132>.
 32. Ponzi M, Sidén-Kiamos I, Bertuccini L, Currà C, Kroeze H, Camarda G, Pace T, Franke-Fayard B, Laurentino EC, Louis C, Waters AP, Janse CJ, Alano P. 2009. Egress of *Plasmodium berghei* gametes from their host erythrocyte is mediated by the MDV-1/PEG3 protein. Cell Microbiol 11:1272–1288. <https://doi.org/10.1111/j.1462-5822.2009.01331.x>.
 33. Burda P-C, Roelli MA, Schaffner M, Khan SM, Janse CJ, Heussler VT. 2015. A *Plasmodium* phospholipase is involved in disruption of the liver stage parasitophorous vacuole membrane. PLoS Pathog 11:e1004760. <https://doi.org/10.1371/journal.ppat.1004760>.
 34. Philip N, Orr R, Waters AP. 2013. Transfection of rodent malaria parasites. Methods Mol Biol 923:99–125. https://doi.org/10.1007/978-1-62703-026-7_7.
 35. Rueden CT, Schindelin J, Hiner MC, DeZonia BE, Walter AE, Arena ET, Eliceiri KW. 2017. ImageJ2: ImageJ for the next generation of scientific image data. BMC Bioinformatics 18:529. <https://doi.org/10.1186/s12859-017-1934-z>.
 36. Franke-Fayard B, Djokovic D, Dooren MW, Ramesar J, Waters AP, Falade MO, Kranendonk M, Martinelli A, Cravo P, Janse CJ. 2008. Simple and sensitive antimalarial drug screening *in vitro* and *in vivo* using transgenic luciferase expressing *Plasmodium berghei* parasites. Int J Parasitol 38:1651–1662. <https://doi.org/10.1016/j.ijpara.2008.05.012>.
 37. Vega-Rodríguez J, Pastrana-Mena R, Crespo-Lladó KN, Ortiz JG, Ferrer-Rodríguez I, Serrano AE. 2015. Implications of glutathione levels in the *Plasmodium berghei* response to chloroquine and artemisinin. PLoS One 10:e0128212. <https://doi.org/10.1371/journal.pone.0128212>.



Plasmodium berghei K13 Mutations Mediate *In Vivo* Artemisinin Resistance That Is Reversed by Proteasome Inhibition

 Nelson V. Simwela,^a  Barbara H. Stokes,^b Dana Aghabi,^a  Matt Bogyo,^{c,d}  David A. Fidock,^{b,e}  Andrew P. Waters^a

^aInstitute of Infection, Immunity & Inflammation, Wellcome Centre for Integrative Parasitology, University of Glasgow, Glasgow, United Kingdom

^bDepartment of Microbiology and Immunology, Columbia University Irving Medical Center, New York, New York, USA

^cDepartment of Microbiology and Immunology, Stanford University School of Medicine, Stanford, California, USA

^dDepartment of Pathology, Stanford University School of Medicine, Stanford, California, USA

^eDivision of Infectious Diseases, Department of Medicine, Columbia University Irving Medical Center, New York, New York, USA

ABSTRACT The recent emergence of *Plasmodium falciparum* parasite resistance to the first line antimalarial drug artemisinin is of particular concern. Artemisinin resistance is primarily driven by mutations in the *P. falciparum* K13 protein, which enhance survival of early ring-stage parasites treated with the artemisinin active metabolite dihydroartemisinin *in vitro* and associate with delayed parasite clearance *in vivo*. However, association of K13 mutations with *in vivo* artemisinin resistance has been problematic due to the absence of a tractable model. Herein, we have employed CRISPR/Cas9 genome editing to engineer selected orthologous *P. falciparum* K13 mutations into the K13 gene of an artemisinin-sensitive *Plasmodium berghei* rodent model of malaria. Introduction of the orthologous *P. falciparum* K13 F446I, M476I, Y493H, and R539T mutations into *P. berghei* K13 yielded gene-edited parasites with reduced susceptibility to dihydroartemisinin in the standard 24-h *in vitro* assay and increased survival in an adapted *in vitro* ring-stage survival assay. Mutant *P. berghei* K13 parasites also displayed delayed clearance *in vivo* upon treatment with artesunate and achieved faster recrudescence upon treatment with artemisinin. Orthologous C580Y and I543T mutations could not be introduced into *P. berghei*, while the equivalents of the M476I and R539T mutations resulted in significant growth defects. Furthermore, a *Plasmodium*-selective proteasome inhibitor strongly synergized dihydroartemisinin action in these *P. berghei* K13 mutant lines, providing further evidence that the proteasome can be targeted to overcome artemisinin resistance. Taken together, our findings provide clear experimental evidence for the involvement of K13 polymorphisms in mediating susceptibility to artemisinins *in vitro* and, most importantly, under *in vivo* conditions.

IMPORTANCE Recent successes in malaria control have been seriously threatened by the emergence of *Plasmodium falciparum* parasite resistance to the frontline artemisinin drugs in Southeast Asia. *P. falciparum* artemisinin resistance is associated with mutations in the parasite K13 protein, which associates with a delay in the time required to clear the parasites upon drug treatment. Gene editing technologies have been used to validate the role of several candidate K13 mutations in mediating *P. falciparum* artemisinin resistance *in vitro* under laboratory conditions. Nonetheless, the causal role of these mutations under *in vivo* conditions has been a matter of debate. Here, we have used CRISPR/Cas9 gene editing to introduce K13 mutations associated with artemisinin resistance into the related rodent-infecting parasite, *Plasmodium berghei*. Phenotyping of these *P. berghei* K13 mutant parasites provides evidence of their role in mediating artemisinin resistance *in vivo*, which supports *in vitro* artemisinin resistance observations. However, we were unable to introduce

Citation Simwela NV, Stokes BH, Aghabi D, Bogyo M, Fidock DA, Waters AP. 2020. *Plasmodium berghei* K13 mutations mediate *in vivo* artemisinin resistance that is reversed by proteasome inhibition. mBio 11:e02312-20. <https://doi.org/10.1128/mBio.02312-20>.

Editor Louis H. Miller, NIAID/NIH

Copyright © 2020 Simwela et al. This is an open-access article distributed under the terms of the [Creative Commons Attribution 4.0 International license](https://creativecommons.org/licenses/by/4.0/).

Address correspondence to David A. Fidock, df2260@cumc.columbia.edu, or Andrew P. Waters, Andy.Waters@glasgow.ac.uk.

Received 17 August 2020

Accepted 8 October 2020

Published 10 November 2020

some of the *P. falciparum* K13 mutations (C580Y and I543T) into the corresponding amino acid residues, while other introduced mutations (M476I and R539T equivalents) carried pronounced fitness costs. Our study provides evidence of a clear causal role of K13 mutations in modulating susceptibility to artemisinins *in vitro* and *in vivo* using the well-characterized *P. berghei* model. We also show that inhibition of the *P. berghei* proteasome offsets parasite resistance to artemisinins in these mutant lines.

KEYWORDS malaria, *Plasmodium berghei*, *Plasmodium falciparum*, artemisinin resistance, K13, gene editing, ring-stage survival assays, parasite clearance times, proteasome, synergy

Artemisinin (ART)-based combination therapies (ACTs) have been at the forefront of globally coordinated efforts to drive down the burden of malaria. A pharmacodynamic hallmark of ARTs and their derivatives is that they are highly active and fast acting against blood stages of malaria parasites. These drugs can achieve up to 10,000-fold parasite reductions in the first replication cycle upon drug exposure (1). Such is the effectiveness of ARTs that recently reported reductions in malaria morbidity and mortality are, indeed, partly attributed to ACTs (2). The use of ARTs in combination therapies originated from early clinical trials, which showed that despite achieving faster parasite clearance, ART monotherapies resulted in recrudescence rates of up to 40% (3). ACTs deliver a pharmacological cure by taking advantage of ARTs to rapidly clear the parasite biomass in the early days of treatment while relying on the partner drug to eliminate residual parasites (4). So far, ACTs remain highly effective in Sub-Saharan Africa, the region that harbors the highest disease burden, with efficacy rates of >98% (2). Nevertheless, ACTs have been threatened by the emergence of *Plasmodium falciparum* resistance to ARTs in Southeast Asia, and resistance has the potential to spread to other regions of malaria endemicity, as has been a historical trend with earlier first-line antimalarial drugs (2, 5–7). Recently, locally derived K13 variants that are able to mediate ART resistance *in vitro* have been identified in *P. falciparum* parasites in French Guiana and in Rwanda (8, 9), further illustrating the emergent threat to ART efficacy. Moreover, an aggressive expansion of a parasite lineage carrying the genetic determinants of resistance to both ART derivatives and the ACT partner drug piper-aquine has been reported across Southeast Asia, resulting in a dramatic loss of clinical efficacy (10–13).

Clinically, *P. falciparum* resistance to ARTs manifests as reduced *in vivo* parasite clearance upon treatment with ACTs or ART monotherapies (2, 14, 15). These clearance rates are based on the Worldwide Antimalarial Resistance Network (WWARN) parasite clearance estimator (16), which quantifies relative resistance by estimating parasitemia lag phases and clearance half-lives upon treatment with artesunate (AS) or ACTs. This involves *in vivo* quantification of viable parasitemia (in patients) upon treatment with AS (2 to 4 mg/kg body weight/day) or ACTs at specified time intervals and subsequent calculation of parasite densities as a function of time (16). The parasite clearance estimator has been used to generate substantial baseline data that classify ART resistance as parasite clearance half-lives of >5.5 h and ART sensitivity as parasite clearance half-lives of <3 h (17, 18). However, interpretation of clearance half-lives can be confounded by differences in initial parasite biomass, the efficacy of the partner drug, and the level of host immunity (17, 19). Moreover, this *in vivo* phenotype does not correlate with decreased susceptibility to dihydroartemisinin (DHA) in standard growth inhibition assays where *P. falciparum* parasites (which have a ~48-h intraerythrocytic developmental cycle) are exposed to the drug for a total of 72 h (15, 20, 21). The ring-stage survival assay (RSA), where highly synchronized early-ring-stage parasites (0 to 3 h postinvasion) are exposed for a short period of time (3 to 6 h) to DHA (at the pharmacologically relevant concentration of 700 nM), provides an improved correlate for the *in vivo* delayed parasite clearance phenotype and has been the principal *in vitro* assay for determining *P. falciparum* resistance to ARTs (22, 23). At the genetic level,

polymorphisms in the *P. falciparum* K13 propeller domain have been strongly associated with ACT treatment failure (21, 24) and also correlate with delayed parasite clearance *in vivo* and increased parasite survival *in vitro* in RSAs (25–27). Reverse genetic approaches have been successfully used to show that the *P. falciparum* K13 mutations M476I, R539T, I543T, Y493H, and C580Y can confer DHA resistance *in vitro*, as defined by >1% survival in RSAs (28, 29). However, the parasite genetic background as well as underlying polymorphisms in drug resistance determinants such as *pfcr1* (*P. falciparum* chloroquine resistance transporter) and *pfmdr2* (*P. falciparum* multidrug resistance protein-2) may play a role either by modulating different levels of susceptibility to DHA or by providing a suitable biological landscape upon which these K13 mutations are more likely to arise (25, 28).

ART resistance as typified by the “delayed clearance phenotype” is, however, still classified as “partial resistance,” primarily because most patients with parasites harboring the phenotype effectively clear the infection when an effective partner drug is used or duration of monotherapy is extended (4). ART partial resistance is, therefore, confirmed or suspected when patients carry parasites with certain K13 mutations, display a parasite clearance half-life of >5.5 h, or are microscopically smear positive on day three after initiation of treatment (2, 4). The full extent to which these parameters predict subsequent ACT treatment failure or define ART resistance remains an area of continuing debate (30–35). The definition of ART resistance in these contexts would thus benefit from experimentally accessible *in vivo* models that would help interrogate ART parasite susceptibility parameters, including clearance half-lives, recrudescence rates, and treatment failures. Such models would allow for a genetic dissection of the role of K13 mutations in mediating resistance *in vivo* in the absence of confounding factors such as secondary genetic factors and/or host factors (25, 28). Currently, the K13 C580Y polymorphism is the most prevalent and dominant ART-resistant mutation in Southeast Asia (14, 36). A recent genetic cross of the K13 C580Y ART-resistant line with an *Aotus* monkey-infecting *P. falciparum* strain provided evidence, in this nonhuman primate model, that parasites carrying the C580Y mutation can display increased survival in *in vitro* RSAs with no accompanying *in vivo* ART resistance (37).

Moreover, *P. falciparum* drug resistance mutations are known to often associate with significant fitness costs that limit the prevalence and eventual propagation of resistance-conferring alleles in natural infections. For example, mutations in the *P. falciparum* chloroquine (CQ) resistance transporter (*pfcr1*) that modulate resistance to CQ massively expanded when CQ was in use in the 1970s but eventually were outcompeted and replaced with parasites carrying wild-type alleles in African high-transmission settings following withdrawal of CQ use (38, 39). Similarly, *P. falciparum* K13 mutations have been shown to carry *in vitro* fitness costs; however, the degree to which a given mutation is detrimental for growth seems to depend on the parasite genetic background (40). Relative to other K13 mutations, *P. falciparum* R539T and I543T mutant parasites that are associated with the highest RSA survival rates (23, 28) and most significant delays in parasite clearance (41) also carried the most pronounced fitness costs (40). Intriguingly, the most prevalent K13 mutation in Southeast Asia, C580Y, was fitness neutral *in vitro* when gene edited into recent Cambodian clinical isolates, whereas it displayed a significant growth defect when introduced into ART-susceptible parasites isolated before ARTs were widely deployed (40, 42). Recently, it was demonstrated that *P. falciparum* K13 localizes to the parasite cytosomes and other intracellular vesicles and plays a role in parasite hemoglobin endocytosis and trafficking to the lysosome-like digestive vacuole (43–45). K13 mutations are thought to lead to a partial loss of protein function, which subsequently impairs hemoglobin endocytic uptake, thereby lessening ART activation and conferring ART resistance (43). This has pointed toward a K13-mediated hemoglobin-centric mechanism of ART resistance, which could possibly be shared with other drugs such as CQ that act by binding to heme moieties in the digestive vacuole, following cytosome-mediated hemoglobin endocytosis (44, 46–48). Of note, mutant K13-mediated ART resistance phenotypes are

associated with upregulated cellular stress responses, which can be targeted by selective inhibition of the parasite 26S proteasome (49, 50).

Here, we report the *in vitro* and *in vivo* phenotypes of orthologous *P. falciparum* K13 mutations that were gene edited into an *in vivo* rodent model of malaria, *Plasmodium berghei*. We profiled the fitness of these *P. berghei* K13 mutant parasites relative to their isogenic wild-type counterparts as well as their sensitivity to combinations of DHA and proteasome inhibitors. Our data provide evidence that K13 mutations are causal for reduced susceptibility to ARTs in an *in vivo* model and link these mutations to *in vitro* and *ex vivo* phenotypes. Our findings also demonstrate that inhibition of the *Plasmodium* proteasome is an effective strategy to restore ART action in resistant parasites that survive treatment with ART alone.

RESULTS

CRISPR/Cas9-mediated introduction of *P. berghei* orthologous K13 mutations and *in vivo* mutant enrichment by AS. To generate *P. berghei* mutant parasites carrying orthologous *P. falciparum* K13 mutations, we attempted to introduce *P. berghei* equivalents of five *P. falciparum* K13 mutations (M476I, Y493H, R539T, I543T, and C580Y) that by reverse genetics were previously shown to confer enhanced *P. falciparum* survival in *in vitro* RSAs (28). We also introduced the equivalent of the F446I mutation that is predominant in Southern China along the Myanmar border (14). These mutations are all validated determinants of reduced *P. falciparum* susceptibility to ARTs (4). Structural homology modeling revealed that *P. berghei* and *P. falciparum* K13 (PBANKA_1356700 and PF3D7_1343700, respectively) are highly conserved (~84% sequence identity overall) at the C-terminal propeller domain, especially where resistance-conferring mutations localize (Fig. 1A). *P. berghei* K13 carries 12 extra amino acids, resulting in 738 amino acids for *P. berghei* compared to 726 for *P. falciparum*. However, modeling suggests that the extra amino acids in *P. berghei* do not change the overall propeller structure of K13 or the amino acid identity at the orthologous positions of the mutations examined in this study (Fig. 1A; see also Fig. S1A and B in the supplemental material). Using a CRISPR/Cas9 system (Fig. S2A) (46), we designed Cas9 plasmids carrying single guide RNAs (sgRNAs) to target the *P. berghei* K13 locus with corresponding homology repair templates. The repair templates carried the mutations of interest as well as silent mutations that inactivated the protospacer adjacent motif (PAM) and introduced restriction sites for restriction fragment length polymorphism (RFLP) analyses (see Table S1). Electroporation of the plasmids pG1004 (C592Y), pG1005 (I555T), and pG1006 (R551T) into the K13 wild-type *P. berghei* 1804c1 line yielded edited parasites (G2022^{C592Y.1*}, G2023^{C592Y.2*}, G2024^{I555T*} and G2025^{R551T*}) with calculated 13.4%, 18.5%, 7.7%, and 30.0% efficiencies, respectively, by RFLP analysis (see Fig. S2B; Table S1). Intriguingly, bulk DNA sequencing of these transformed parasites revealed that only the G2025^{R551T*} line carried sequence traces for the R551T amino acid substitution and accompanying silent mutations (Fig. S3A), while the rest had traces only of the silent mutations (Fig. S3B and C). Our prior studies with refractory mutations have also revealed the parasite's ability to restrict CRISPR/Cas9-mediated double-stranded break repair to the region immediately proximal to the cut site, thereby capturing the silent mutations without extending to nearby deleterious single nucleotide polymorphisms (SNPs) (46). We suspect this is a consequence of very short resection events (51). These data suggested that the C592Y and I555T mutations either result in extremely slow growing parasites or are entirely lethal in *P. berghei*. We attempted to clone the G2025^{R551T*} line by limiting dilution, but this could not be achieved, possibly due to the low mutant population (30.0%) combined with a potentially low growth rate of the mutants compared to that of wild-type parasites.

In earlier efforts to introduce UBP-1 mutations in *P. berghei*, we found that preemptive drug pressure to which the engineered mutation is anticipated to confer a protective advantage can selectively enrich for the mutant in a mixed, transfected parasite population, even when the mutant population is <1% in the mixture (46). Using this approach, we subjected a larger inoculum (2×10^7) of the G2022^{C592Y.1*},

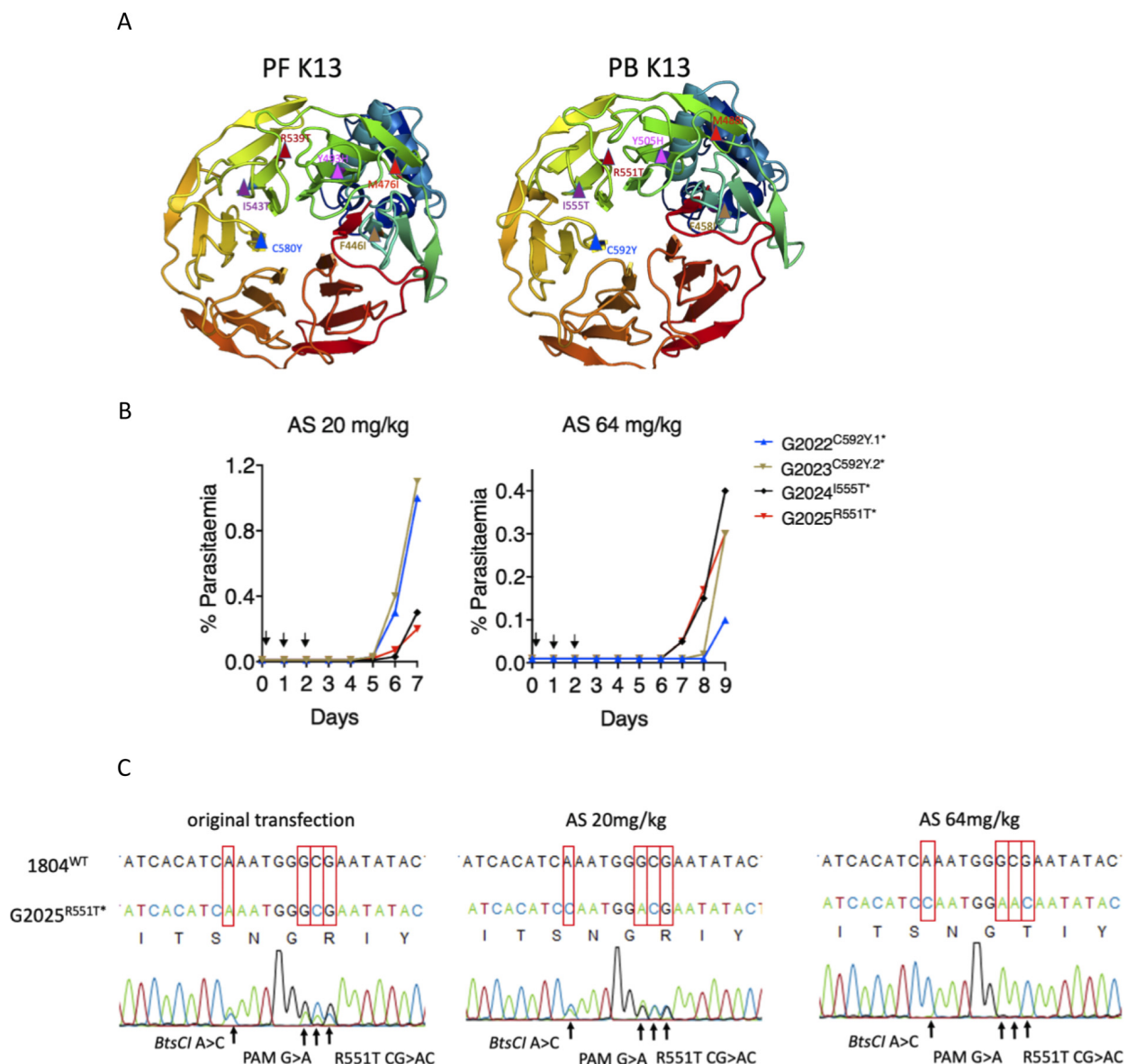


FIG 1 Introduction of orthologous K13 nucleotide substitutions in *P. berghei*. (A) Three-dimensional homology model of *P. falciparum* (PF3D7_1343700) and *P. berghei* (PBANKA_1356700) K13 for amino acid residues 350 to 726 and 362 to 738, respectively. *P. falciparum* K13 mutation sites (F446I, M476I, Y493H, R539T, I543T, and C592Y) are indicated in the structure on the left, and *P. berghei* orthologous mutation sites are modeled on the right. Models were created in SWISS-MODEL using PDB template 4zgc.1.A. Structures were visualized and annotated using PyMOL 2.3. (B) Parasitemia growth curves monitoring recrudescence of the G2022, G2023, G2024, and G2025 lines upon artesunate (AS) challenge. Mice were infected with 2×10^7 parasites by i.p. injection on day 0. Treatment with AS was commenced ~ 3 h postinfection by i.p. injection and was continued for three consecutive days as indicated by arrows. Parasitemia was monitored microscopically until recrudescence was observed. Mice were bled when the parasitemia was less than 1.5% to minimize competition from wild-type parasites in case mutants carried growth defects. (C) Sanger sequencing of bulk DNA from the G2025 R551T line showing selective enrichment of this mutation upon AS treatment at 20 or 64 mg/kg. Enrichment of this mutation was also observed in the RFLP analysis (see also Fig. S2B in the supplemental material).

G2023^{C592Y.2*}, G2024^{I555T*}, and G2025^{R551T*} lines to AS at 20 or 64 mg/kg to see if any enrichment in the recrudescence parasite populations could be achieved (Fig. 1B). Indeed, AS at both 20 and 64 mg/kg specifically enriched the R551T mutant population in the G2025^{R551T*} line from 30.0% in the initial transfection to 49.7% at AS 20 mg/kg and $>99\%$ at 64 mg/kg (Fig. 1C; Fig. S2B and Table S1). In contrast, apart from a minor enrichment that was observed for the G2024^{I555T*} line, no useful enrichments in both the G2022^{C592Y.1*} and G2023^{C592Y.2*} lines were observed by RFLP at either concentration of AS (Fig. S2B; Table S1). Furthermore, no I555T or C592Y amino acid substitution traces could be seen after population-level DNA sequencing of these lines. These data further supported the relative nonviability of *P. berghei* parasites bearing K13 C592Y

and I555T mutations. In agreement with the above-described observations, further attempts to introduce the C592Y mutation using a different sgRNA and/or different codons for the tyrosine residue in the donor template (TAT or TAC) were also unsuccessful. We did, however, observe >90% editing efficiency when introducing only silent mutations that maintained the C592C wild-type genotype in the donor template (Fig. S3 and E; Table S1). This, plus other unsuccessful attempts to generate the I555T mutant, further implies that these two K13 mutations are not viable in *P. berghei*. Meanwhile, transfection of the *P. berghei* 1804c1 line with pG983 (F458I), pG984 (Y505H), and pG1008 (M488I) successfully introduced these mutations in *P. berghei* K13, yielding the G1957^{F458I*}, G1979^{Y505H*}, and G1989^{M488I*} lines with >93% efficiencies, as confirmed by RFLP analysis (Fig. S2C; Table S1) as well as population-level DNA sequencing (Fig. S3F, G, and H). These three lines (G1957^{F458I*}, G1979^{Y505H*}, and G1989^{M488I*}) and the G2025^{R551T*} AS 64 mg/kg-challenged line were all cloned by limiting dilution. Mutations were further confirmed by RFLP analysis (Fig. S3I) and sequencing. The V2721F UBP-1 mutant line, which we previously found to mediate reduced susceptibility to ARTs in *P. berghei* (46), was also generated in the 1804c1 background and cloned (Table S1).

***P. berghei* K13 mutants display reduced susceptibility to DHA in 24-h assays and increased survival in *P. berghei*-adapted RSAs.** Unlike that for *P. falciparum*, *P. berghei* can only be maintained in one blood-stage cycle *in vitro*, which restricts drug susceptibility assays to one 24 h developmental cycle. Drug susceptibility readouts are therefore based on single-generation flow cytometry quantification of schizont maturation (46, 52, 53). Using this approach, we aimed to characterize the DHA dose-response profiles of the *P. berghei* K13 mutants compared to those of wild-type parasites or to a previously reported UBP-1 mutant with reduced ART susceptibility (46). Interestingly, in contrast to the equivalent *P. falciparum* K13 mutants, *P. berghei* M488I, R551T, and Y505H K13 mutant parasites displayed reduced susceptibility to DHA in standard growth inhibition assays with 3.3-, 1.4-, and 1.2-fold 50% inhibitory concentration (IC₅₀) increases, respectively, compared to that of isogenic K13 wild-type parasites (Fig. 2A). The *P. berghei* F458I K13 mutant displayed equal sensitivity to DHA as the wild-type and the UBP-1 V2721F mutant (Fig. 2A), in agreement with our previous observations (46). These data suggest that, despite being limited to a single-cycle 24 h exposure, the *P. berghei* standard assay can distinguish even modestly ART-resistant parasites from sensitive ones. We next investigated the DHA susceptibility of early ring-stage *P. berghei* K13 mutant parasites by adapting the *P. falciparum* RSA (22). The *P. falciparum* RSA relies on exposure of early ring-stage parasites (0 to 3 h postinvasion) to 700 nM DHA for 4 to 6 h, followed by assessment of viability in the 2nd life cycle. This protocol allows drug-exposed parasites to reinvest fresh red blood cells. With this approach, current RSA parameters define *in vitro* ART resistance as survival of ≥1% and ART sensitivity as <1% survival (22). Using a similar approach, we exposed ~1.5-h postinvasion K13 mutant *P. berghei* ring-stage parasites to DHA at 700 nM for 3 h (to accommodate for the shorter life cycle in *P. berghei*). Viability was assessed 24 h later by flow cytometry-based quantification of schizont maturation and mCherry expression. Interestingly, we observed that a significant fraction of *P. berghei* wild-type parasites survived exposure to DHA at 700 nM, with percentage survival rates of ~20.9% (Fig. 2B). This is in agreement with our previous observations that *P. berghei* is less susceptible to ARTs than *P. falciparum* (46, 54). Both the UBP-1 mutant and F458I or Y505H K13 mutant parasites had the same survival rates as the wild-type line, whereas the M488I and R551T mutants exhibited significantly higher survival rates (32.3% or 39.0%, respectively, $P < 0.001$) (Fig. 2B). This is consistent with previous reports that, in *P. falciparum*, the R539T and I543T mutations are associated with the highest rates of RSA survival (28). However, we noted inconsistencies between drug susceptibility data of the mutants in the two *in vitro* tests (standard 24-h assay and adapted *P. berghei* RSA). This might result from the inability to maintain *P. berghei* in long-term culture and extend the analysis. We therefore developed a modified *in vivo* RSA, where we injected wild-type, UBP-1 V2721F, M488I, and R551T parasites

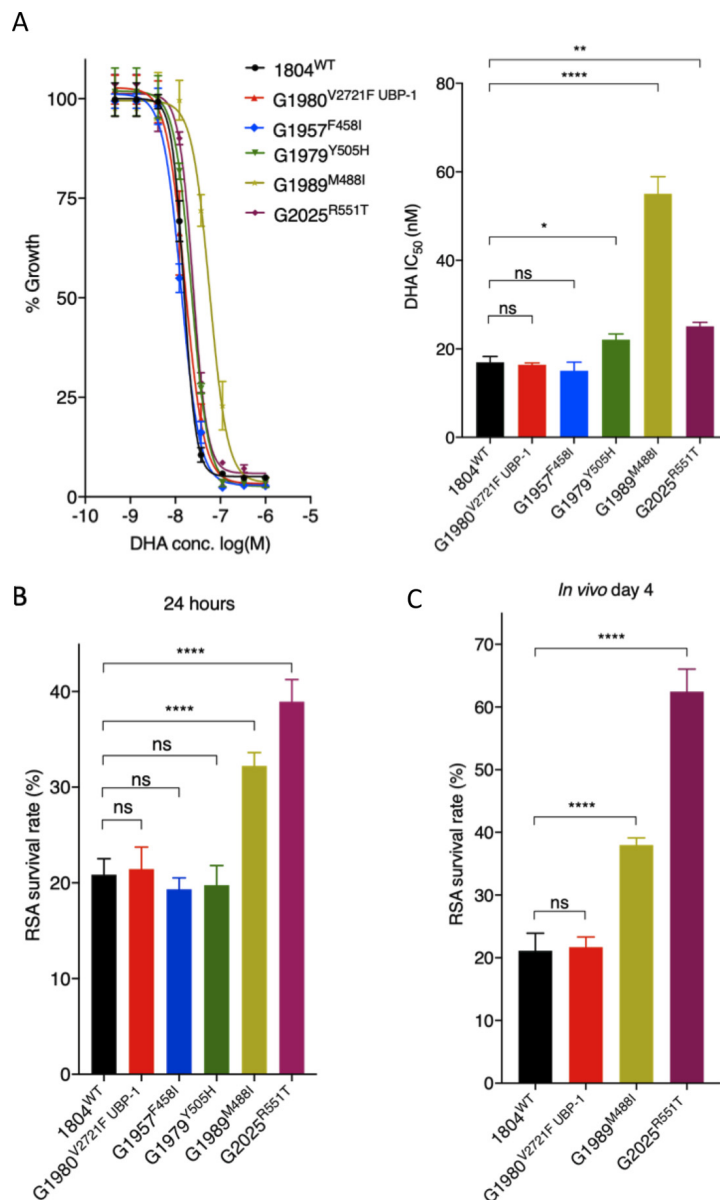


FIG 2 *In vitro* and *ex vivo* susceptibility of *P. berghei* K13 mutants to DHA. (A) DHA dose-response curves and IC₅₀ values for *P. berghei* K13 mutant lines compared to those of the wild-type 1804^{WT} and the UBP-1 G1980^{V2721F} mutant lines. (B) Survival of *P. berghei* K13 mutant lines in the *P. berghei* RSA. Results show the percentages of synchronized early ring-stage parasites (1.5-h postinvasion) that survived a 3 h exposure to 700 nM DHA relative to DMSO-treated parasites. Survival was quantified 24 h posttreatment by flow cytometry analysis based on Hoechst 33258 DNA staining and mCherry expression. (C) *In vivo* RSA survival for two K13 mutant lines (G1989^{M488I} and G2025^{R551T}) compared to that of the wild-type (1804^{WT}) and UBP-1 mutant (G1980^{V2721F}) controls. After *in vitro* exposure to DHA or DMSO as described above, parasites were i.v. injected back into mice as described in Materials and Methods. Parasitemia was quantified by flow cytometry analysis of mCherry expression on day 4 after i.v. injection, from which percentage survival rates were calculated. Error bars show standard deviations calculated from three biological repeats. Statistical significance (compared to the 1804^{WT} line) was calculated using one-way analysis of variance (ANOVA) alongside the Dunnett's multiple-comparison test. ns, not significant; *, $P < 0.05$; **, $P < 0.01$; ****, $P < 0.0001$.

back into mice 24 h after dimethyl sulfoxide (DMSO) or DHA exposure in the RSA as described above and then assessed viability by quantifying *in vivo* parasitemia on day 4. Remarkably, percentage survival in the R551T mutant parasites significantly increased from ~39.0% (24 h readout) to ~62.5%, while M488I mutant parasite survival increased from ~32.3% (24 h readout) to ~38.0% (Fig. 2C). In contrast, the percentage survival of the wild-type and UBP-1 mutant lines did not significantly

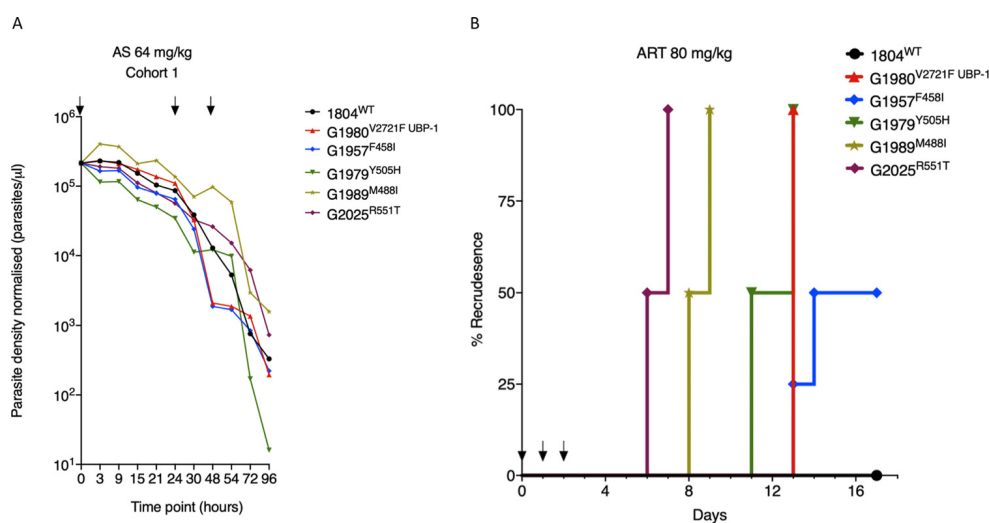


FIG 3 *In vivo* clearance and recrudescence rate of *P. berghei* K13 mutants following treatment with AS or ART. (A) Parasite clearance curves in mice infected with *P. berghei* K13 mutant lines following treatment with AS. Six mice (in each of four cohorts) were infected with 10⁵ parasites of each of the four K13 mutants, the UBP-1 mutant, and wild-type control on day 0. On day 5, at a parasitemia of ~10%, mice were dosed with AS at 64 mg/kg body weight. Day 5 was the designated 0 h time point for the dosing regimen. Parasite density per microliter of blood was quantified based on absolute counts of mCherry-positive parasites at staggered time points for each of the two cohorts, with 5 time points in the first 24 h (corresponding to at least 3 h interval coverage between the two cohorts) and at least once daily thereafter. Mice were dosed three times at 0, 24, and 48 h as indicated by arrows. Concurrent thin blood smears were prepared at each time point for microscopic analysis (Fig. S4). (B) Kaplan-Meier plots of recrudescence in wild-type and UBP-1 mutant controls compared to that of K13 mutants. A modified Peters' 4-day suppressive test was used to monitor susceptibility of the K13 mutants to 80 mg/kg ART, a dose that effectively suppresses wild-type parasites for up to 18 days. Groups of three (UBP-1 mutant, 1804^{WT}) or four mice (K13 mutants) were infected with 1 × 10⁶ parasites on day 0. ART treatment was initiated ~3 h later and continued every 24 h for three consecutive days (treatment days shown by arrows). Parasitemias were monitored by microscopic analysis of Giemsa-stained blood smears up to day 18 (Table S3). Recrudescence rates were plotted as the proportion of mice in the treatment groups that became smear positive on every individual day for the 18 days of follow-up.

change in the extended assay, despite the minor growth defect in the UBP-1 mutant, demonstrating that the *P. berghei in vitro* RSA and standard growth inhibition assays with 24-h readouts may be less robust in quantifying resistance phenotypes, especially if mutant parasites are less fit (Fig. 2C).

***P. berghei* K13 mutants mimic the delayed parasite clearance phenotype *in vivo* upon AS treatment and achieve faster recrudescence than wild-type parasites at high ART doses.** We next investigated the *in vivo* parasite clearance rates of *P. berghei* K13 mutant parasites in infected mice treated with AS. Mice were infected with a fixed inoculum of K13 and UBP-1 mutant parasites (10⁵) in four cohorts, and parasitemias were allowed to rise to ~10%. This was followed by dosing with AS at 64 mg/kg body weight, which is slightly higher than the equivalent of the maximal human clinical dose of 4 mg/kg (mouse equivalent = 49.2 mg/kg) to accommodate for the reduced ART susceptibility observed in *P. berghei* parasites. Parasitemias were quantified by flow cytometry (based on mCherry positivity) and microscopic analysis every 3 h for the first 24 h and at least once after the second and third doses at 24 and 48 h, respectively. Plotting parasite density in *P. berghei* K13 and UBP-1 mutant parasites against time revealed that in the first 24 h of sampling, parasite clearance kinetics did not sufficiently discriminate K13 or UBP-1 mutant parasites from the wild type. However, as the majority of dying parasites were being cleared by the host and mice received further doses, extended analysis revealed that *P. berghei* M488I and R551T mutant parasites consistently and significantly persisted compared to wild-type, F458I, Y505H, and UBP-1 mutant parasites (Fig. 3A; see also Fig. S4). Starting AS treatment at a high initial parasitemia (~10%) also ensured that a good proportion of parasites would be within the early ring-stage window and, therefore, would be expected to preferentially survive the first AS dose. Surviving rings were easily distinguished as viable trophozoites at

either 18-, 21-, or 24-h time points by microscopic examination of blood smears, which enabled comparisons between parasite lines. We therefore carried out concurrent collection and analysis of thin blood smears at all time points examined for flow analysis (Fig. 3A; Fig. S4). Results demonstrated that enhanced survival after the first AS dose was evident for all four *P. berghei* K13 mutant parasites as well as the UBP-1 mutant compared to wild-type parasites (see Fig. S5). Microscopy provided a more sensitive discrimination than flow cytometry-based estimation of clearance kinetics that was unable to distinguish mutant from wild-type parasites in the first 24 h. False positives could be due to the retention of mCherry positivity by dying parasites. For instance, we observed that a significant proportion of wild-type parasites remained mCherry positive and were counted as viable by flow cytometry (Fig. 3A; Fig. S4), whereas, microscopically, they were pyknotic forms (Fig. S5A and G). Remarkably, the M488I and R551T mutants remained smear positive after two consecutive AS doses (Fig. S5E, F, K, and L), whereas the wild-type, F458I, Y505H, and UBP-1 mutant parasites were cleared (microscopically smear negative) after 48 h. These data suggest that the M488I and R551T mutants meet the classical definition of ART resistance, as defined by the WHO based on day 3 (second generation) microscopy positivity, when accounting for the duration of the *P. berghei* life cycle and the dosing intervals (4). One of the four mice in the M488I treatment group remained smear positive after three consecutive AS doses (Fig. S5E). These data provide evidence that *P. berghei* K13 mutants modulate *in vivo* susceptibility to ARTs, resulting in a persister/delayed clearance phenotype under controlled conditions of initial parasite biomass and host immune status. Of note, we consistently used naive mice of same age, sex, breed, and genetic background.

Another *in vivo* marker of reduced ART susceptibility in *P. falciparum* is the rate of recrudescence upon AS treatment, which acts as a possible indicator of AS treatment failure. However, at pharmacologically safe doses in humans (2 to 4 mg/kg), ART monotherapy treatment leads to >40% recrudescence rates (1, 3), making it difficult to use this approach to separate clinically ART-sensitive from ART-resistant parasites. *P. berghei* K13 mutants, therefore, provide the opportunity to test for recrudescence rates using controlled parasite inocula as well as AS or ART dose ascendency. We treated groups of mice initially infected with 10⁶ K13 mutant, ART-resistant UBP-1 mutant, or wild-type parasites with a daily ART dose of 80 mg/kg for three consecutive days. This ART dose sufficiently suppresses the *P. berghei* wild type at equivalent parasite inocula for up to 18 days of follow-up (46). All UBP-1 mutant infections recrudescenced 11 days after the last ART dose, whereas no recrudescence (0%) was observed for the wild type (Fig. 3B; see also Table S3). These data are consistent with our previous observations (46). However, R551T mutant parasite infections achieved even faster recrudescence, namely, 50% on day 4 after the last dosing and 100% a day later, indicating a higher level of *in vivo* resistance for this K13 mutation compared to that of the UBP-1 mutant. M488I mutant parasites had a similar recrudescence profile beginning on day 6. The Y505H and F458I mutant lines both achieved recrudescence at approximately the same time as the UBP-1 mutant; however, the latter achieved only 50% recrudescence across the 18-day follow-up period (Fig. 3B; Table S3). These data further confirm that *P. berghei* K13 mutants modulate *in vivo* susceptibility to ARTs and, crucially, that recrudescence rates strongly correlate with our *in vitro* DHA RSA profiles (Fig. 2) as well as with *in vivo* clearance kinetics in established infections (Fig. 3A; Fig. S4 and S5).

***P. berghei* K13 mutants are associated with an *in vivo* fitness cost but are preferentially selected for in the presence of AS or CQ.** To assess the fitness of our *P. berghei* K13 mutants, we performed direct head-to-head competitions with wild-type parasites under *in vivo* growth conditions. *P. berghei* K13 or UBP-1 mutant lines or the parental 1804^{WT} (mCherry positive) line were mixed at a 1:1 ratio with the G159^{WT} (green fluorescent protein [GFP] positive) line and injected into mice. Changes in the proportion of GFP- or mCherry-positive parasites in the competition mixture were then quantified by flow cytometry over 9 days. These assays revealed that the F458I and Y505H mutant parasites were fitness neutral relative to the G159^{WT} line, whereas the M488I and R551T mutants carried significant fitness costs (Fig. 4A). Both the M488I and

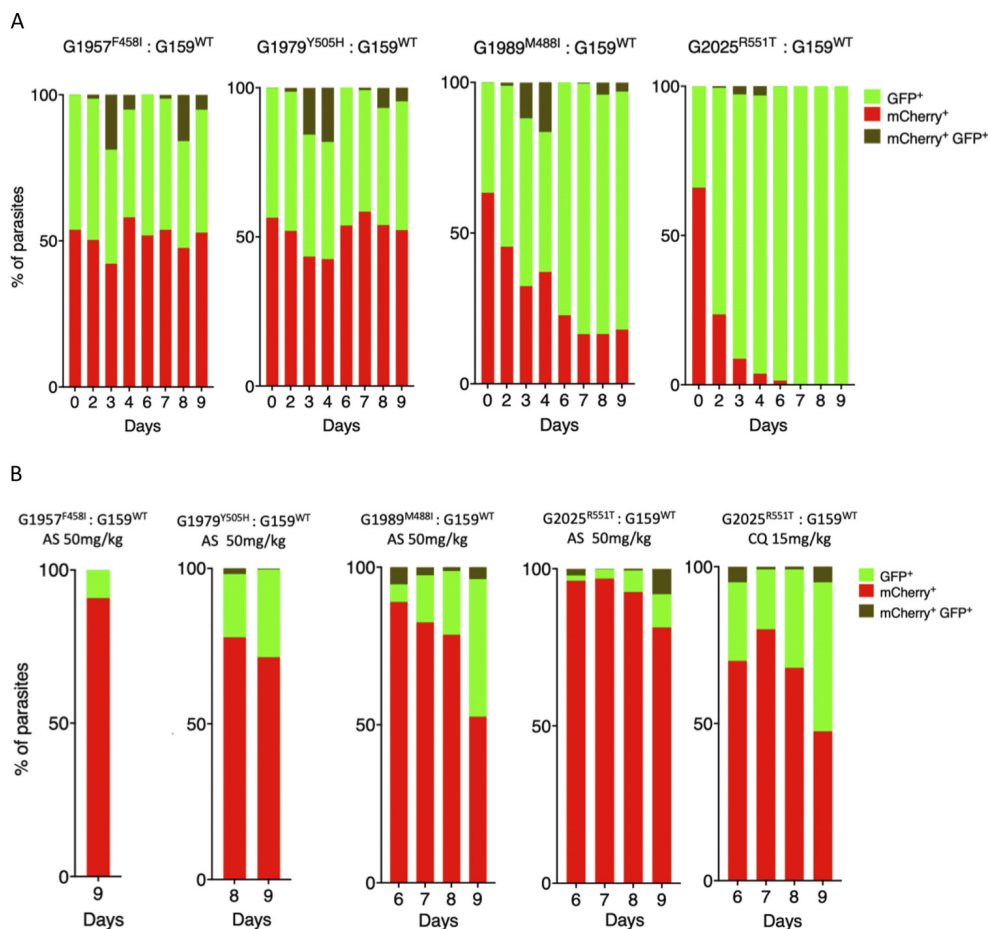


FIG 4 Relative fitness of *P. berghei* K13 mutants in presence or absence of AS or CQ. Growth competition assays with K13 mutant lines that constitutively express mCherry compared to the wild-type G159^{WT} line that constitutively expresses GFP in the presence or absence of drug pressure. The G159^{WT} line was mixed with a given mutant line at a 1:1 ratio in three groups of mice on day 0. The first group was left untreated, the second group received a dose of AS at 50 mg/kg starting from 3 h after i.p. injection for three consecutive doses, while the third group consisting of the 1804^{WT}, G1980^{V2721F}, and K13 mutant G2025^{R551T} lines received CQ at 15 mg/kg at similar dosing times as AS. Percentages of mCherry- or GFP-positive parasites were determined by flow cytometry as described in Materials and Methods. (A) Percentage population changes as measured by flow cytometry of the G1957^{F458I}, G1979^{Y505H}, G1989^{M488I}, and G2025^{R551T} mutant lines relative to that of the G159^{WT} wild-type line. (B) Proportion representation of the G159^{WT} line in mixtures with G1957^{F458I}, G1979^{Y505H}, G1989^{M488I}, and G2025^{R551T} lines on the days of recrudescence upon treatment with AS or CQ as indicated.

R551T mutations were associated with high levels of reduced susceptibility to DHA *in vitro* (Fig. 2), delayed clearance kinetics (Fig. 3A; Fig. S4), and faster recrudescence following ART treatment *in vivo* (Fig. 3B; Table S3). Comparatively, the R551T mutant parasites had a more severe growth defect than the M488I mutants and were completely outcompeted by the GFP-positive wild-type line by day 7 (Fig. 4A). This is consistent with previous observations of high *in vitro* fitness costs for the equivalent *P. falciparum* R539T mutation (40). In comparison to the G159^{WT} line, the parental wild-type line (1804^{WT}) was fitness neutral, whereas the UBP-1 V2721F mutant carried a minor growth defect as previously observed (46) (see Fig. S6A and B). We also examined the proportions of GFP-positive versus mCherry-positive parasites over time in *P. berghei* K13 mutant and wild-type parasites upon treatment with AS. Mutant parasites were mixed at 1:1 ratios with the G159^{WT} line and injected into mice that were treated with AS at 50 mg/kg beginning 3 h after infection for three consecutive days. Monitoring of recrudescence up to day 9 revealed that, upon AS treatment, the M488I and R551T mixtures recrudescenced slightly faster than the wild-type mixture and were highly enriched for the mutant population (>90%) at the time of recrudescence (Fig. 4B). The F458I and Y505H mutant mixtures recrudescenced slightly later (Fig. 4B), as

did the UBP-1 V2721F mutant (Fig. S6B), and were all significantly enriched for the mutants. In contrast, the proportions of GFP-positive versus mCherry-positive parasites in the parent 1804^{WT} and G159^{WT} competition mixture after AS treatment did not change at the time of recrudescence (Fig. S6A). These data show that mutant *P. berghei* K13 parasites are preferentially selected for upon AS treatment, despite some carrying growth defects that rendered them at a complete competitive disadvantage in the absence of drug.

With the supposed role of *P. falciparum* K13 in mediating parasite hemoglobin endocytosis (43–45), we also speculated that *P. berghei* K13 mutant parasites with strong ART resistance phenotypes might be able to modulate susceptibility to CQ (to some degree) through a similar dysregulation of the endocytic machinery. Using the *in vivo* competition assay under drug pressure as with AS as described above, the parental 1804^{WT} line, the UBP-1 V2721F line, and the K13 R551T mutant line were each mixed at 1:1 ratios with the G159^{WT} line and treated with CQ at 15 mg/kg. At the time of recrudescence, the proportion of 1804^{WT} parasites (mCherry positive) did not significantly change compared to the proportion of GFP-positive G159^{WT} parasites (Fig. S6A). In comparison, the UBP-1 V2721F mutant was enriched to ~70% (Fig. S6B), which mirrors our previous observations that this mutation can indeed be selectively enriched by CQ (46). Interestingly, upon CQ treatment, the combination of R551T mutant parasites and the G159^{WT} line achieved recrudescence at almost the same rate as that under AS pressure, with mutant parasites enriched to ~72% (Fig. 4B). These data suggest that K13 mutations can also contribute to low-level protection to CQ (43, 44).

A Plasmodium-selective proteasome inhibitor is potent against *P. berghei* wild-type and K13 mutant parasites and synergizes DHA action. An enhanced cell stress response characterized by upregulation of genes in the unfolded protein response (UPR) is a typical signature of ART-resistant parasites (50). Resistant parasites (K13 mutants) also display enhanced activity of the ubiquitin proteasome system (UPS), a conserved eukaryotic pathway that acts downstream of the UPR by degrading unfolded proteins (49, 55). UPS inhibitors are available for cancer treatment and have been shown to synergize DHA activity in wild-type and K13 mutant *P. falciparum* both *in vitro* and *in vivo*, marking them as promising agents for overcoming ART resistance (49, 56). The *Plasmodium*-selective proteasome inhibitor EY5-125 is a potent antimalarial (standard IC₅₀ against *P. falciparum* = 19 nM) that acts in synergy with ART against both ART-resistant and -sensitive *P. falciparum* strains *in vitro* (57). Here, we tested the efficacy of EY5-125 against *P. berghei* wild-type and K13 mutant parasites and examined its potential ability to synergize DHA action. *P. berghei* wild-type and the most ART-resistant K13 mutant (R551T) parasites were found to be equally sensitive to EY5-125 (Fig. 5A and B). Compared to that in *P. falciparum* (72-h IC₅₀ of ~19 nM and 1-h IC₅₀ of ~648 nM), EY5-125 is much less potent in *P. berghei* in both standard *in vitro* growth inhibition (IC₅₀ = ~700 nM) and 3-h assays (IC₅₀ = ~1,900 nM), respectively (Fig. 5A and B). These differences could be due to species-specific differences in drug sensitivity as we have observed with ARTs (46, 54) and many other drugs (58). However, combinations of DHA and EY5-125 in fixed-ratio isobologram analyses revealed a strong synergistic interaction against the *P. berghei* K13 wild-type and M488I and R551T mutant lines (Fig. 5C; see also Table S4). We also employed our *in vivo* RSA to examine whether a combination of DHA at 700 nM and EY5-125 at the equivalent 3-h IC₅₀ (1.94 μM) or 2× IC₅₀ (3.88 μM) could impact parasite survival rates. Indeed, at both the 3-h IC₅₀ and 2× IC₅₀ concentrations, EY5-125 strongly synergized with DHA (700 nM), as evidenced by significant abrogation of survival for both the wild-type and R551T mutant lines (Fig. 5D). These data demonstrate that proteasome inhibitors synergize DHA action in *P. berghei* K13 mutants equally as well as wild-type parasites both *in vitro* and *in vivo* and have the potential to be used to overcome ART resistance.

DISCUSSION

In this study, we successfully employed CRISPR/Cas9 editing to introduce four of the six targeted orthologous *P. falciparum* K13 (F446I, M476I, Y493H, and R539T) mutations

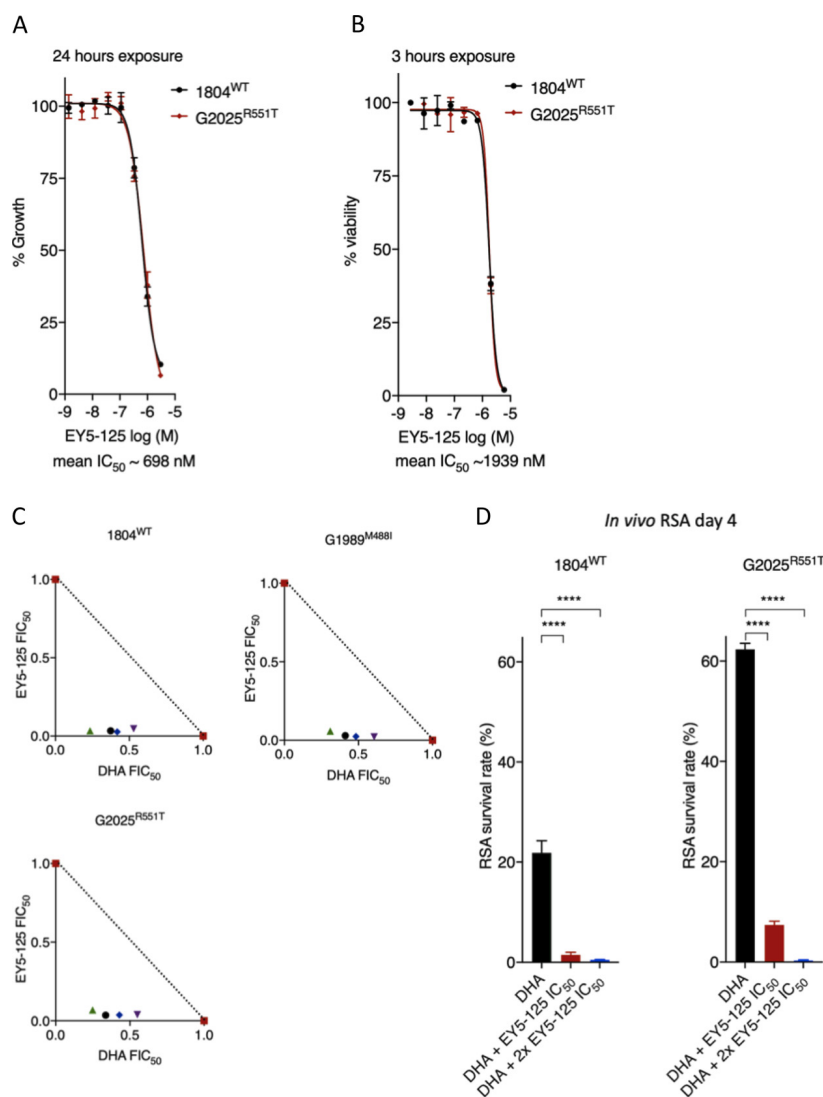


FIG 5 Activity and DHA synergy of proteasome inhibitor in *P. berghei* K13 mutants. Dose-response curves and mean IC₅₀ values for the *Plasmodium*-selective proteasome inhibitor EY5-125 for the wild-type 1804^{WT} and K13 mutant G2025^{R551T} lines in standard 24-h assays (A) or 3-h exposure assays conducted on early ring-stage parasites (B). Mean IC₅₀ is a calculated average for the two lines independently screened in three biological repeats. (C) Isobologram plots representing the interaction between DHA and EY5-125 in the wild-type 1804^{WT}, G1989^{M488I}, and G2025^{R551T} lines. Plots show mean FIC₅₀ values (Table S4) for each drug calculated from three biological repeats. (D) Synergy of EY5-125 proteasome inhibitor with DHA in the *in vivo* RSA. Parasites were exposed to DMSO or DHA at 700 nM alone or in combination with EY5-125 at 3-h IC₅₀ or 2× IC₅₀ and then injected back into mice 24 h later as described in Materials and Methods. Parasitemias in mice infected with drug or DMSO-treated parasites were determined by flow analysis of mCherry expression on day 4 after i.v. injection and were used to calculate percent survivals relative to that of DMSO-treated parasites. Error bars are standard deviations from three biological repeats. Statistical significance was calculated using one-way ANOVA alongside the Dunnett's multiple-comparison test. ****, *P* < 0.001.

into the K13 gene of the rodent model of malaria *P. berghei*. Meanwhile, introduction of two mutations (C580Y and I543T) could not be achieved. As debate continues on the role of K13 in mediating *in vivo* susceptibility to ARTs (37), phenotyping of these *P. berghei* K13 (F458I, M488I, Y505H, and R551T) mutants provides experimental evidence for the ability of mutant K13 to confer *in vivo* resistance to ARTs in a naive parasite genome background. These mutants displayed reduced *in vitro* susceptibility to DHA and phenocopied *P. falciparum* delayed clearance phenotypes upon AS treatment. Moreover, these K13 mutants achieved faster recrudescence upon ART treatment under *in vivo* growth conditions. As in *P. falciparum*, certain *P. berghei* K13 mutations were

found to cause significant growth defects, which highlights the structural and functional conservation of this protein across the two *Plasmodium* species and illustrates the fitness trade-offs that the acquisition of such mutations exerts on malaria parasite physiology.

ART resistance, principally associated with mutations in K13, is now almost endemic in Southeast Asia, with risks of global spread threatening the utility of ACTs that are at the forefront of malaria control programs (2). The *P. falciparum* C580Y K13 mutation is the most frequently observed (with >50% prevalence) and has reached fixation in most parts of Southeast Asia (25, 59). Why the *P. falciparum* C580Y mutation is so successful compared to other K13 mutations remains unclear. This mutation does not associate with high RSA survival rates compared to *P. falciparum* R539T or I543T mutant parasites, and treatment failure rates and parasite clearance rates are not more significant in C580Y-harboring parasites than those with other K13 mutations (27, 28, 60). Do fitness constraints, founder genetic landscapes, or species-specific differences between *P. berghei* and *P. falciparum* K13 explain our failed attempts to introduce the C592Y or I555T mutations in *P. berghei*? The structural homology model of the K13 propeller domain presented here demonstrates that this region is highly conserved between *P. berghei* and *P. falciparum* K13, with identical amino acids at the sites of mutations associated with ART resistance. Our unsuccessful attempts to introduce the *P. berghei* C592Y or *P. berghei* I555T mutations could therefore be more related to growth disadvantages or other deleterious effects. For example, in *P. falciparum*, the equivalent I543T and R539T mutations carry the most pronounced fitness costs (40), which could partly explain our inability to introduce the *P. berghei* I555T mutation in *P. berghei*. Moreover, *P. berghei* K13 mutations were introduced into PBANKA parasites with no history of ART exposure. These parasites might therefore be more sensitive to fitness impacts conferred by the *P. berghei* I555T or *P. berghei* C592Y substitution, as introduction of the equivalent *P. falciparum* C580Y in parasites isolated before ART was clinically introduced carried significant growth defects, as opposed to more recent Cambodian isolates where it was fitness neutral (40). A less prevalent K13 allele, *P. falciparum* R561H, that associates with significant delays in parasite clearance and peaked in prevalence in 2012 in Southeast Asia but has since declined (60) also easily outcompeted the *P. falciparum* C580Y mutation in head-to-head competitions (42). These data suggest that acquisition and propagation of certain *P. falciparum* K13 alleles, notably the C580Y substitution, might require appropriate founder genome architectures to compensate for the deleterious phenotypes. In these situations, K13 mutations (*P. falciparum* C580Y, for example), would arise in a necessary compensatory background that mitigates the deleterious growth effects leading to an initial soft sweep. In the case of ACTs, these compensatory backgrounds may also serve as general templates upon which partner drug resistance mutations might arise. This seems to be the case with the recent aggressive expansion of parasite colineages carrying the *P. falciparum* C580Y mutation and piperazine resistance determinants (10, 11).

Despite the obstacles to introducing the *P. berghei* C592Y and I555T mutations, introduction of the *P. falciparum* R539T equivalent was achieved in *P. berghei* (R551T) despite low editing efficiency in the initial transfection. We were, however, able to enrich for this mutation with AS selection applied *in vivo*, yielding almost clonal levels of the *P. berghei* R551T mutant. Similar to the *P. falciparum* R539T mutant, clonal *P. berghei* R551T mutant parasites carried the strongest DHA resistance phenotypes *in vitro* as well as the clearest AS or ART resistance profiles *in vivo*. The *P. falciparum* R539T and *P. falciparum* I543T mutations occur at relatively low frequencies in Southeast Asia, with the prevalence of both mutations ranging between 0.3% and 3.5% (36, 41, 59). This could be due to the pronounced fitness cost of these mutations (40) limiting their expansion, which we also observed with the *P. berghei* R551T mutant parasites. The combination of a naive genomic background and species-specific differences can also be invoked to explain some phenotypic differences (growth rate and level of ART resistance) seen between mutant lines of *P. falciparum* and *P. berghei* K13, as observed in this study. For example, *P. falciparum* Y493H mutants clearly associate with increased

RSA survival (23, 28) and delayed parasite clearance phenotypes (23, 41, 61), unlike the *P. berghei* counterpart (Y505H) that displayed low-level resistance to ARTs *in vitro* (in the standard assay but not in the adapted RSA) and *in vivo*. This could be due to additional underlying genetic factors in *P. falciparum* isolates providing an additive effect to the observed phenotypes, which would be absent in *P. berghei*. Nevertheless, the other *P. berghei* K13 mutations tested here appear to directly reflect the impact of the equivalent mutations in *P. falciparum*. Both *P. berghei* F458I (this study) and *P. falciparum* F446I K13 mutants are fitness neutral (62) and do not enhance RSA survival *in vitro* (62, 63) yet carry ART-protective phenotypes *in vivo* (64–66). Furthermore, *P. berghei* M488I K13 mutants display a significant growth defect that has not yet been characterized in the *P. falciparum* equivalent (M476I) and might explain its relative scarcity in Southeast Asia (67, 68).

Enhanced proteostasis is a characteristic signature of *P. falciparum* K13 ART-resistant parasites, which is typified by upregulation of genes in the UPR as well as enhanced activity of the UPS (49, 50, 55). Inhibition of the UPS by 26S proteasome inhibitors synergizes DHA action both *in vitro* and *in vivo*, which has offered a potential avenue to overcome ART resistance (49). Despite UPS inhibitors (which are clinically available for treatment of certain cancers) displaying activity in malaria parasites and synergizing DHA action, their translation into animal studies has been limited by host toxicity (69, 70). Recent structure-based design of *Plasmodium*-selective proteasome inhibitors has yielded vinyl sulfone inhibitors with a wider therapeutic window and improved host toxicity profiles (56, 57). These inhibitors not only display activity in diverse *P. falciparum* backgrounds, including those harboring K13 mutations, but also strongly synergize with DHA (71). Even though *P. berghei* proteasome structures have not been solved, functional and life cycle conservation between this parasite and *P. falciparum* is pronounced. Using EY5-125, an inhibitor selective for the *P. falciparum* proteasome (57), we demonstrate similar activity and synergy with DHA in *P. berghei* wild-type and K13 ART-resistant mutants. Importantly, we demonstrate these properties *in vivo*, which significantly strengthens the potential of these compounds in overcoming ART resistance in infected hosts.

In conclusion, our work provides robust experimental evidence that K13 mutations modulate *in vitro* and *in vivo* susceptibility to ARTs in the *P. berghei* rodent model of malaria. The cause and effect link between *P. falciparum* K13 mutations and reduced ART susceptibility is strong (23, 28). However, the reason for ART clinical failure has remained obscure because, in some cases, delayed parasite clearance phenotypes have been reported in parasites carrying wild-type K13 alleles (35, 72). This lack of clarity is further compounded by a reduced correlation between K13 mutations and parasite clearance half-lives or the frequencies of recrudescence in certain cases of ART monotherapy (35). As we demonstrate in this study, some of these observations may be attributable to fitness defects in mutant parasites that could confound the interpretation of recrudescence rates. These fitness differences might be especially relevant at the relatively low ART doses used in humans, which are already known to permit higher rates of recrudescence (3). Although a recent genetic cross between a *P. falciparum* K13 C580Y mutant parasite and an *Aotus*-infecting K13 wild-type parasite demonstrated a lack of association of this mutation with *in vivo* ART resistance metrics (recrudescence and clearance half-life) (37), we propose that this could be due to (i) the AS doses used being insufficiently high to clearly separate the lineages, (ii) the small sample sizes used, and (iii) the inherent limitation of using heterogeneous *Aotus* monkeys with various individual histories of parasite exposure and spleen status (spleen intact or splenectomized). Our *in vitro* and *in vivo* phenotypes for the *P. falciparum* F446I, M476I, Y493H, and R539T K13 mutation equivalents in *P. berghei* support their direct involvement in mediating resistance to ARTs. Our data also provide a robust immune-replete rodent host model to test for synergistic antimalarial combinations that can restore ART efficacy and overcome resistance.

MATERIALS AND METHODS

CRISPR/Cas9 generation of *P. berghei* K13 mutant lines. The Cas9 plasmid ABR099 was used to target mutations of interest into the *P. berghei* K13 locus (PlasmoDB gene identifier [ID] PBANKA_1356700) (46). To obtain *P. berghei* equivalents of *P. falciparum* ART-resistant K13 mutations (PlasmoDB gene ID PF3D7_1343700), the amino acid sequences of the two proteins were retrieved and aligned using Clustal Omega (73). To structurally align the equivalent mutations in *P. berghei* K13, three-dimensional homology models of *P. berghei* and *P. falciparum* K13 were constructed using SWISS-MODEL (PDB template 4zgc.1.A) for amino acid residues 362 to 738 for *P. berghei* and 350 to 726 for *P. falciparum*. Models were visualized using pyMol 2.3. sgRNAs designed to target a region within 0 to 30 bp of the mutation of interest within the *P. berghei* K13 locus were initially cloned into the ABR099 plasmid (see Fig. S2A in the supplemental material). Donor DNA repair templates were designed to carry the mutation of interest in addition to silent mutations that introduced restriction sites for RFLP and that inactivated the PAMs. These templates were generated by overlap extension PCR (74) and were subsequently cloned into ABR099 plasmids carrying corresponding sgRNAs at the linker sites (Fig. S2A). Generated plasmids and all corresponding sgRNAs are listed in Table S1 in the supplemental material.

Parasite lines and animal infections. This study employed two *P. berghei* ANKA-derived parasite lines, 1804cl1 and G159. The 1804cl1 (75) and G159 (Katie Hughes, unpublished) lines express mCherry and GFP, respectively, under the control of the strong constitutive *hsp70* promoter. Infections were carried out in female Theiler's Original mice (Envigo), 6 to 8 weeks old, weighing 25 to 30 g. Infections were established either by intraperitoneal (i.p.) injections of ~200 μ l of cryopreserved parasite stocks or by intravenous (i.v.) injections of purified schizonts or mixed-stage parasites diluted in phosphate-buffered saline (PBS). Parasitemias in infected mice were monitored by microscopic examination of methanol-fixed thin blood smears stained with Giemsa (Sigma) or flow cytometry-based analysis of infected blood stained with Hoechst 33342 (Invitrogen). Blood from infected mice was collected by cardiac puncture under terminal anesthesia. All animal work was performed in compliance with UK home office licensing (project reference P6CA91811) and ethical approval from the University of Glasgow animal welfare and ethical review body.

Transfections. Primary transfections were carried out in the 1804cl1 line. Approximately 10 μ g of episomal plasmid DNA from the vectors described above (Table S1) was transfected by electroporation of Nycodenz-purified schizonts using the Amaxa Nucleofector Device II program U-033, as previously described (76). Parasites were then immediately i.v. injected into mice. Positive selection of transfected parasites was commenced 24 h later by adding pyrimethamine (0.07 mg/ml; Sigma) to their drinking water.

Genotyping of transformed parasites. Parasite pellets were prepared from infected mouse blood that was lysed by resuspension in 1 \times E-lysis buffer (Thermo). Genomic DNA was extracted from the pellets using the Qiagen DNeasy blood and tissue kit according to the manufacturer's instructions. Initial analysis of the transfected or cloned parasite lines was performed using a dual PCR-RFLP approach. PCR using primers exterior to the donor templates (Table S1 and S2) was used to amplify fragments from the genomic DNA of the mutant lines, followed by restriction digests with the artificially introduced RFLP restriction enzymes. Relative transformation efficiencies were estimated by densitometric quantification of wild-type and mutant RFLP fragments by ImageJ2 (77). Mutations and initial RFLP analyses were further confirmed by Sanger DNA sequencing.

Antimalarial agents. DHA (Selleckchem) at 10 mM was diluted to a working concentration in schizont culture medium. The *Plasmodium*-selective proteasome inhibitor EY5-125, also known as compound 28 (57), was used to test for proteasome inhibitor synergy with DHA in K13 mutant and wild-type parasites. For *in vivo* drug treatment, AS (Sigma) was dissolved in 5% sodium bicarbonate prepared in 0.9% sodium chloride. CQ diphosphate (Sigma) was dissolved in 1 \times PBS. ART (Sigma) was prepared at 50 mg/ml in a 1:1 mixture of DMSO and Tween 80 (Sigma) and diluted 10-fold in sterile distilled water immediately before administration. All drugs were prepared fresh before *in vivo* administration, and drug delivery was carried out by i.p. injection.

Twenty-four-hour *P. berghei* *in vitro* culture and drug susceptibility assays. *In vitro* culture and drug susceptibility assays were carried out beginning with synchronized ring-stage parasites over 24-h schizont maturation cycles, as *P. berghei* can only be maintained for one intraerythrocytic developmental cycle *in vitro*. Parasites were cultured and exposed to drugs as previously described (46), after which schizont maturation was analyzed by flow cytometry. Infected cells were stained with the DNA dye Hoechst 33258. Schizont maturation was used as a surrogate marker of growth inhibition and was quantified based on Hoechst 33258 fluorescence intensity or mCherry expression. To determine growth inhibition and calculate half-maximal inhibitory concentrations (IC_{50} s), the percentage of schizonts in no-drug controls was set to 100% growth, and subsequent growth percentages in the presence of drugs were calculated accordingly. Dose-response curves were plotted in GraphPad Prism.

Adapted *P. berghei* ring-stage survival assays. The *P. falciparum* RSA was adapted for *P. berghei* to further assess the *in vitro* phenotypes of K13-mutant parasites based on a previously published protocol (22). Schizonts were obtained from *in vitro* cultured parasites as previously described (76) and injected i.v. into naive mice to obtain synchronous *in vivo* infections containing >90% rings at parasitemias of 0.5% to 1.5%. Approximately 1.5 h postinjection, blood was collected from the infected mice, adjusted to 0.5% hematocrit, and exposed to 700 nM DHA or 0.1% DMSO (Thermo Fisher Scientific) in 96-well plates or 10-ml culture flasks. The plates and flasks were incubated with drug under standard culture conditions for 3 h, after which, the drug was washed off at least three times. Parasites were then returned to standard culture conditions in new plates and flasks with fresh schizont medium for *in vitro* maturation. After 24 h of incubation, parasite survival was assessed by flow cytometry analysis of Hoechst

33258-stained infected cells. Viability was assessed by gating on the Hoechst 33258 DNA stain and live mCherry expression. DHA-treated samples were compared to DMSO-treated controls processed in parallel. Percent survival was calculated using the following formula: survival (%) = (viability [%] [DHA – treated]) / (viability [%] [mock DMSO – treated]).

To improve the robustness of the viability readouts beyond the 24-h flow cytometry counts, an *in vivo* expansion of the 3 h DHA- or DMSO-exposed parasites was used for selected mutants and the wild-type control. After 24 h of recovery, 2 ml of DHA- or DMSO-treated parasites was pelleted and resuspended in a 1-ml volume, from which, 200 μ l was injected i.v. into mice. *In vivo* parasitemias were quantified on day 4 postinjection, from which percentage survivals based on *in vivo* parasitemia (absolute counts of mCherry positive parasites) were calculated using the following slightly modified formula: survival (%) = (parasitemia [DHA – treated]) / (parasitemia [mock DMSO – treated]).

***In vitro* isobologram drug combinations.** DHA and EY5-125 drug interaction analyses in fixed ratios were carried out using a modified fixed-ratio interaction assay as previously described (78). DHA and EY5-125 combinations were prepared in molar concentration combination ratios of 5:0, 4:1, 3:2, 2:3, 1:4, and 0:5 and were dispensed into 96-well plates. This was followed by a 3-fold serial dilution with precalculated estimates to ensure that the test wells containing the 3-h IC_{50} s of the two drugs were located near the middle of the plate. The drug combinations were then incubated with synchronized ~1.5-h-old ring-stage wild-type or K13 mutant parasites for 3 h, after which, the drugs were washed off at least 3 times. Percent viability was quantified 24 h later by flow cytometry analysis of Hoechst 33258-stained infected cells and mCherry expression. Dose-response curves were calculated for each drug alone or in combination, from which fractional inhibitory concentrations (FIC_{50}) were obtained and summed to obtain the ΣFIC_{50} using the following formula: $\Sigma FIC_{50} = (IC_{50} \text{ of DHA in combination} / IC_{50} \text{ of drug DHA alone}) + (IC_{50} \text{ of EY5-125 in combination} / IC_{50} \text{ of EY5-125 alone})$.

An ΣFIC_{50} of >1 was used to denote antagonism, $\Sigma FIC_{50} <1$ synergism, and $\Sigma FIC_{50} = 1$ additivity. FIC_{50} values for the drug combinations were plotted to obtain isobolograms for the drug combination ratios.

***In vivo* drug assays. (i) Parasite clearance.** Parasite clearance upon treatment with AS was used to evaluate potential delayed clearance phenotypes in K13 mutant parasites. These studies were based on a modified Rane's curative test in established mice infections as previously described (79). Donor mice were infected with mutant lines and the wild-type control. Once a parasitemia of ~2% was reached, blood was obtained from the donor mice and diluted in $1 \times$ PBS. Approximately 10^5 parasites were inoculated in 4 cohorts of mice (4 mice per line) by i.p. injections on day 0, and parasitemias were allowed to rise to ~10%, typically on day 5. On day 5, at time zero, 2 μ l of blood was collected and diluted 200-fold in $1 \times$ PBS. Thin blood smears were also collected at this time. All four cohorts were then dosed with AS at 64 mg/kg at 0, 24, and 48 h. Blood sampling was performed for flow cytometry analysis, and thin blood smears were prepared five times during the first 24 h for each cohort and at least daily thereafter in a staggered manner that allowed for a 3 h life cycle coverage in the first 24 h for at least two cohorts. Parasite density at each time point was determined by absolute cell counts and mCherry expression in 0.1 μ l of whole blood diluted in PBS analyzed on a MACSQuant Analyzer 10. Thin blood smears of parasite morphologies were analyzed by microscopy. Significant viability counts in microscopy smears were based on microscopic confirmation of at least four viable parasites in a minimum of 10 fields. Clearance kinetics of normalized parasite densities versus time were plotted in GraphPad prism.

(ii) Recrudescence. A modified Peters' 4-day suppressive test was used to assess *in vivo* response profiles and recrudescence rates of wild-type and mutant lines as previously described (46, 80). Infections were initiated by i.p. inoculation of 10^6 parasites diluted from donor mice and were followed by three daily consecutive drug doses of ART at 80 mg/kg, with the first initiated ~3 h postinoculation. Parasitemia was monitored by microscopic analysis of methanol-fixed Giemsa-stained smears up to day 18 or until recrudescence was observed.

***In vivo* growth competition assays in presence or absence of drug treatment.** Mutant lines in the 1804c1 mCherry background line were mixed with the G159 GFP line at 1:1 ratios and injected i.p. (total parasite inocula of 10^6) into 3 groups of mice. The groups were either left untreated or treated with AS at 50 mg/kg for 3 consecutive days starting 3 h postinfection or CQ at 15 mg/kg. Parasitemias and fractions of mutant versus wild-type parasites were determined by flow cytometry-based quantification of mCherry- or GFP-positive parasite populations.

Reagent availability. Parasite lines and plasmids are available upon request from A. Waters.

SUPPLEMENTAL MATERIAL

Supplemental material is available online only.

FIG S1, TIF file, 2.9 MB.

FIG S2, TIF file, 2.8 MB.

FIG S3, TIF file, 2.8 MB.

FIG S4, TIF file, 2.7 MB.

FIG S5, TIF file, 2.8 MB.

FIG S6, TIF file, 2.7 MB.

TABLE S1, XLSX file, 0.1 MB.

TABLE S2, XLSX file, 0.1 MB.

TABLE S3, XLSX file, 0.1 MB.

TABLE S4, XLSX file, 0.1 MB.

ACKNOWLEDGMENTS

We thank Diane Vaughan and the University of Glasgow flow cytometry facility for assistance. We also thank Euna Yoo (Stanford University and NCI-Frederick) for providing the EY5-125 proteasome inhibitor.

This work was supported in part by grants from the Wellcome Trust to A.P.W. (083811/Z/07/Z, 107046/Z/15/Z, and 104111/Z/14/Z). Partial funding for this work was provided by the NIH (R01 AI109023 to D.A.F. and R33 AI127581 to M.B. and D.A.F.), the Department of Defense (W81XWH-19-1-0086 to D.A.F.), and the Columbia University—University of Glasgow Research Exchange Program. N.V.S. is a Commonwealth Doctoral Scholar (MWCS-2017-789), funded by the UK government. B.H.S. gratefully acknowledges earlier support from the Columbia University Graduate Training Program in Microbiology and Immunology (T32 AI106711; Program Director, D. A. Fidock).

REFERENCES

- White NJ. 2008. Qinghaosu (artemisinin): the price of success. *Science* 320:330–334. <https://doi.org/10.1126/science.1155165>.
- WHO. 2019. World malaria report. World Health Organization, Geneva, Switzerland.
- Li GQ, Arnold K, Guo XB, Jian HX, Fu LC. 1984. Randomised comparative study of mefloquine, qinghaosu, and pyrimethamine-sulfadoxine in patients with *falciparum* malaria. *Lancet* 2:1360–1361. [https://doi.org/10.1016/S0140-6736\(84\)92057-9](https://doi.org/10.1016/S0140-6736(84)92057-9).
- WHO. 2018. Artemisinin resistance and artemisinin-based combination therapy efficacy: status report. World Health Organization, Geneva, Switzerland.
- Gregson A, Plowe CV. 2005. Mechanisms of resistance of malaria parasites to antifolates. *Pharmacol Rev* 57:117–145. <https://doi.org/10.1124/pr.57.1.4>.
- Wongsrichanalai C, Pickard AL, Wernsdorfer WH, Meshnick SR. 2002. Epidemiology of drug-resistant malaria. *Lancet Infect Dis* 2:209–218. [https://doi.org/10.1016/S1473-3099\(02\)00239-6](https://doi.org/10.1016/S1473-3099(02)00239-6).
- Blasco B, Leroy D, Fidock DA. 2017. Antimalarial drug resistance: linking *Plasmodium falciparum* parasite biology to the clinic. *Nat Med* 23:917–928. <https://doi.org/10.1038/nm.4381>.
- Mathieu LC, Cox H, Early AM, Mok S, Lazrek Y, Paquet J-C, Ade M-P, Lucchi NW, Grant Q, Udhayakumar V, Alexandre JS, Demar M, Ringwald P, Neafsey DE, Fidock DA, Musset L. 2020. Local emergence in Amazonia of *Plasmodium falciparum* K13 C580Y mutants associated with *in vitro* artemisinin resistance. *eLife* 9:e51015. <https://doi.org/10.7554/eLife.51015>.
- Uwimana A, Legrand E, Stokes BH, Ndikumana JM, Warsame M, Umulisa N, Ngamije D, Munyaneza T, Mazarati JB, Munguti K, Campagne P, Crisculo A, Ariey F, Murindahabi M, Ringwald P, Fidock DA, Mbituyumuremyi A, Menard D. 2020. Emergence and clonal expansion of *in vitro* artemisinin-resistant *Plasmodium falciparum* Kelch13 R561H mutant parasites in Rwanda. *Nat Med* 26:1602–1608. <https://doi.org/10.1038/s41591-020-1005-2>.
- Hamilton WL, Amato R, van der Pluijm RW, Jacob CG, Quang HH, Thuy-Nhien NT, Hien TT, Hongvanthong B, Chindavongsa K, Mayxay M, Huy R, Leang R, Huch C, Dysoley L, Amaratunga C, Suon S, Fairhurst RM, Tripura R, Peto TJ, Sovann Y, Jittamala P, Hanboonkunupakarn B, Pukrittayakamee S, Chau NH, Imwong M, Dhorda M, Vongprommek R, Chan XHS, Maude RJ, Pearson RD, Nguyen T, Rockett K, Drury E, Gonçalves S, White NJ, Day NP, Kwiatkowski DP, Dondorp AM, Miotto O. 2019. Evolution and expansion of multidrug-resistant malaria in Southeast Asia: a genomic epidemiology study. *Lancet Infect Dis* 19:943–951. [https://doi.org/10.1016/S1473-3099\(19\)30392-5](https://doi.org/10.1016/S1473-3099(19)30392-5).
- van der Pluijm RW, Imwong M, Chau NH, Hoa NT, Thuy-Nhien NT, Thanh NV, Jittamala P, Hanboonkunupakarn B, Chutasmith K, Saelow C, Runjarern R, Kaewmook W, Tripura R, Peto TJ, Yok S, Suon S, Sreng S, Mao S, Oun S, Yen S, Amaratunga C, Lek D, Huy R, Dhorda M, Chotivanich K, Ashley EA, Mukaka M, Waithira N, Cheah PY, Maude RJ, Amato R, Pearson RD, Gonçalves S, Jacob CG, Hamilton WL, Fairhurst RM, Tarning J, Winterberg M, Kwiatkowski DP, Pukrittayakamee S, Hien TT, Day NP, Miotto O, White NJ, Dondorp AM. 2019. Determinants of dihydroartemisinin-piperaquine treatment failure in *Plasmodium falciparum* malaria in Cambodia, Thailand, and Vietnam: a prospective clinical, pharmacological, and genetic study. *Lancet Infect Dis* 19:952–961. [https://doi.org/10.1016/S1473-3099\(19\)30391-3](https://doi.org/10.1016/S1473-3099(19)30391-3).
- Imwong M, Dhorda M, Myo Tun K, Thu AM, Phyo AP, Proux S, Suwan-nasin K, Kunasol C, Srisutham S, Duanguppama J, Vongprommek R, Prom-narate C, Saejeng A, Khantikul N, Sugaram R, Thanapongpichat S, Sawangjaroen N, Sutawong K, Han KT, Htut Y, Linn K, Win AA, Hlaing TM, van der Pluijm RW, Mayxay M, Pongvongsa T, Phommasone K, Tripura R, Peto TJ, von Seidlein L, Nguon C, Lek D, Chan XHS, Rekol H, Leang R, Huch C, Kwiatkowski DP, Miotto O, Ashley EA, Kyaw MP, Pukrittayakamee S, Day NPJ, Dondorp AM, Smithuis FM, Nosten FH, White NJ. 14 July 2020. Molecular epidemiology of resistance to antimalarial drugs in the greater mekong subregion: an observational study. *Lancet Infect Dis* [https://doi.org/10.1016/S1473-3099\(20\)30228-0](https://doi.org/10.1016/S1473-3099(20)30228-0).
- Amato R, Pearson RD, Almagro-Garcia J, Amaratunga C, Lim P, Suon S, Sreng S, Drury E, Stalker J, Miotto O, Fairhurst RM, Kwiatkowski DP. 2018. Origins of the current outbreak of multidrug-resistant malaria in Southeast Asia: a retrospective genetic study. *Lancet Infect Dis* 18:337–345. [https://doi.org/10.1016/S1473-3099\(18\)30068-9](https://doi.org/10.1016/S1473-3099(18)30068-9).
- Ashley EA, Dhorda M, Fairhurst RM, Amaratunga C, Lim P, Suon S, Sreng S, Anderson JM, Mao S, Sam B, Sopha C, Chuor CM, Nguon C, Sovannaroeth S, Pukrittayakamee S, Jittamala P, Chotivanich K, Chutasmith K, Suchatsoonthorn C, Runcharoen R, Hien TT, Thuy-Nhien NT, Thanh NV, Phu NH, Htut Y, Han K-T, Aye KH, Mokuolu OA, Olaosebikan RR, Folaranmi OO, Mayxay M, Khanthavong M, Hongvanthong B, Newton PN, Onyamboko MA, Fanella CI, Tshefu AK, Mishra N, Valecha N, Phyo AP, Nosten F, Yi P, Tripura R, Borrmann S, Bashraheil M, Peshu J, Faiz MA, Ghose A, Hossain MA, Samad R, Tracking Resistance to Artemisinin Collaboration (TRAC), et al. 2014. Spread of artemisinin resistance in *Plasmodium falciparum* malaria. *N Engl J Med* 371:411–423. <https://doi.org/10.1056/NEJMoa1314981>.
- Dondorp AM, Nosten F, Yi P, Das D, Phyo AP, Tarning J, Lwin KM, Ariey F, Hanpithakpong W, Lee SJ, Ringwald P, Silamut K, Imwong M, Chotivanich K, Lim P, Herdman T, An SS, Yeung S, Singhasivanon P, Day NPJ, Lindegardh N, Socheat D, White NJ. 2009. Artemisinin resistance in *Plasmodium falciparum* malaria. *N Engl J Med* 361:455–467. <https://doi.org/10.1056/NEJMoa0808859>.
- Flegg JA, Guerin PJ, White NJ, Stepniowska K. 2011. Standardizing the measurement of parasite clearance in *falciparum* malaria: the parasite clearance estimator. *Malar J* 10:339. <https://doi.org/10.1186/1475-2875-10-339>.
- WWARN Parasite Clearance Study Group, Abdulla S, Ashley EA, Bassat Q, Bethell D, Björkman A, Borrmann S, D'Alessandro U, Dahal P, Day NP, Diakite M, Djimde AA, Dondorp AM, Duong S, Edstein MD, Fairhurst RM, Faiz MA, Falade C, Flegg JA, Fogg C, Gonzalez R, Greenwood B, Guérin PJ, Guthmann J-P, Hamed K, Hien TT, Htut Y, Juma E, Lim P, Mårtensson A, Mayxay M, Mokuolu OA, Moreira C, Newton P, Noedl H, Nosten F, Ogutu BR, Onyamboko MA, Owusu-Agyei S, Phyo AP, Premji Z, Price RN, Pukrittayakamee S, Ramharther M, Sagara I, Se Y, Suon S, Stepniowska K, Ward SA, White NJ, et al. 2015. Baseline data of parasite clearance in patients with *falciparum* malaria treated with an artemisinin derivative: an individual patient data meta-analysis. *Malar J* 14:359–359. <https://doi.org/10.1186/s12936-015-0874-1>.

18. WWARN K13 Genotype-Phenotype Study Group. 2019. Association of mutations in the *Plasmodium falciparum* Kelch13 gene (Pf3D7_1343700) with parasite clearance rates after artemisinin-based treatments—a WWARN individual patient data meta-analysis. *BMC Med* 17:1. <https://doi.org/10.1186/s12916-018-1207-3>.
19. Ataide R, Ashley EA, Powell R, Chan JA, Malloy MJ, O'Flaherty K, Takashima E, Langer C, Tsuboi T, Dondorp AM, Day NP, Dhorda M, Fairhurst RM, Lim P, Amaratunga C, Pukrittayakamee S, Hien TT, Htut Y, Mayxay M, Faiz MA, Beeson JG, Nosten F, Simpson JA, White NJ, Fowkes FJ. 2017. Host immunity to *Plasmodium falciparum* and the assessment of emerging artemisinin resistance in a multinational cohort. *Proc Natl Acad Sci U S A* 114: 3515–3520. <https://doi.org/10.1073/pnas.1615875114>.
20. Amaratunga C, Sreng S, Suon S, Phelps ES, Stepniewska K, Lim P, Zhou C, Mao S, Anderson JM, Lindegardh H, Jiang H, Song J, Su X-z, White NJ, Dondorp AM, Anderson TJC, Fay MP, Mu J, Duong S, Fairhurst RM. 2012. Artemisinin-resistant *Plasmodium falciparum* in Pursat Province, Western Cambodia: a parasite clearance rate study. *Lancet Infect Dis* 12:851–858. [https://doi.org/10.1016/S1473-3099\(12\)70181-0](https://doi.org/10.1016/S1473-3099(12)70181-0).
21. Phyto AP, Nkhoma S, Stepniewska K, Ashley EA, Nair S, McGready R, Ler Moo S, Al-Saai S, Dondorp AM, Lwin KM, Singhasivanon P, Day NPJ, White NJ, Anderson TJC, Nosten F. 2012. Emergence of artemisinin-resistant malaria on the Western border of Thailand: a longitudinal study. *Lancet* 379:1960–1966. [https://doi.org/10.1016/S0140-6736\(12\)60484-X](https://doi.org/10.1016/S0140-6736(12)60484-X).
22. Witkowski B, Amaratunga C, Khim N, Sreng S, Chim P, Kim S, Lim P, Mao S, Sopha C, Sam B, Anderson JM, Duong S, Chuor CM, Taylor WR, Suon S, Mercereau-Puijalon O, Fairhurst RM, Menard D. 2013. Novel phenotypic assays for the detection of artemisinin-resistant *Plasmodium falciparum* malaria in Cambodia: *in-vitro* and *ex-vivo* drug-response studies. *Lancet Infect Dis* 13:1043–1049. [https://doi.org/10.1016/S1473-3099\(13\)70252-4](https://doi.org/10.1016/S1473-3099(13)70252-4).
23. Arie F, Witkowski B, Amaratunga C, Beghain J, Langlois A-C, Khim N, Kim S, Duru V, Bouchier C, Ma L, Lim P, Leang R, Duong S, Sreng S, Suon S, Chuor CM, Bout DM, Ménard S, Rogers WO, Genton B, Fandeur T, Miotto O, Ringwald P, Le Bras J, Berry A, Barale J-C, Fairhurst RM, Benoit-Vical F, Mercereau-Puijalon O, Ménard D. 2014. A molecular marker of artemisinin-resistant *Plasmodium falciparum* malaria. *Nature* 505:50–55. <https://doi.org/10.1038/nature12876>.
24. Spring MD, Lin JT, Manning JE, Vanachayangkul P, Somethy S, Bun R, Se Y, Chann S, Ittivorakul M, Sia-Ngam P, Kuntawunginn W, Arsanok M, Buathong N, Chaorattanakawee S, Gosi P, Ta-Aksorn W, Chanarat N, Sundrakes S, Kong N, Heng TK, Nou S, Teja-Isavadharm P, Pichyangkul S, Phann ST, Balasubramanian S, Juliano JJ, Meshnick SR, Chour CM, Prom S, Lanteri CA, Lon C, Saunders DL. 2015. Dihydroartemisinin-piperaquine failure associated with a triple mutant including Kelch13 C580Y in Cambodia: an observational cohort study. *Lancet Infect Dis* 15:683–691. [https://doi.org/10.1016/S1473-3099\(15\)70049-6](https://doi.org/10.1016/S1473-3099(15)70049-6).
25. Miotto O, Amato R, Ashley EA, MacInnis B, Almagro-Garcia J, Amaratunga C, Lim P, Mead D, Oyola SO, Dhorda M, Imwong M, Woodrow C, Manske M, Stalker J, Drury E, Campino S, Amenga-Etego L, Thanh TN, Tran HT, Ringwald P, Bethell D, Nosten F, Phyto AP, Pukrittayakamee S, Chotivanich K, Chuor CM, Nguon C, Suon S, Sreng S, Newton PN, Mayxay M, Khanthavong M, Hongvanthong B, Htut Y, Han KT, Kyaw MP, Faiz MA, Fanelli CI, Onyamboko M, Mokuolu OA, Jacob CG, Takala-Harrison S, Plowe CV, Day NP, Dondorp AM, Spencer CC, McVean G, Fairhurst RM, White NJ, Kwiatkowski DP. 2015. Genetic architecture of artemisinin-resistant *Plasmodium falciparum*. *Nat Genet* 47:226–234. <https://doi.org/10.1038/ng.3189>.
26. Mbengue A, Bhattacharjee S, Pandharkar T, Liu H, Estiu G, Stahelin RV, Rizk SS, Njimoh DL, Ryan Y, Chotivanich K, Nguon C, Ghorbal M, Lopez-Rubio JJ, Pfender M, Emrich S, Mohandas N, Dondorp AM, Wiest O, Haldar K. 2015. A molecular mechanism of artemisinin resistance in *Plasmodium falciparum* malaria. *Nature* 520:683–687. <https://doi.org/10.1038/nature14412>.
27. Phyto AP, Ashley EA, Anderson TJC, Bozdech Z, Carrara VI, Sriprawat K, Nair S, White MM, Dziekan J, Ling C, Proux S, Konghahong K, Jeeyapant A, Woodrow CJ, Imwong M, McGready R, Lwin KM, Day NPJ, White NJ, Nosten F. 2016. Declining efficacy of artemisinin combination therapy against *P. falciparum* malaria on the Thai-Myanmar border (2003–2013): the role of parasite genetic factors. *Clin Infect Dis* 63:784–791. <https://doi.org/10.1093/cid/ciw388>.
28. Straimer J, Gnädig NF, Witkowski B, Amaratunga C, Duru V, Ramadani AP, Dacheux M, Khim N, Zhang L, Lam S, Gregory PD, Urnov FD, Mercereau-Puijalon O, Benoit-Vical F, Fairhurst RM, Menard D, Fidock DA. 2015. K13-propeller mutations confer artemisinin resistance in *Plasmodium falciparum* clinical isolates. *Science* 347:428–431. <https://doi.org/10.1126/science.1260867>.
29. Ghorbal M, Gorman M, Macpherson CR, Martins RM, Scherf A, Lopez-Rubio J-J. 2014. Genome editing in the human malaria parasite *Plasmodium falciparum* using the CRISPR-Cas9 system. *Nat Biotechnol* 32: 819–821. <https://doi.org/10.1038/nbt.2925>.
30. Krishna S, Krensner PG. 2013. Antidogmatic approaches to artemisinin resistance: reappraisal as treatment failure with artemisinin combination therapy. *Trends Parasitol* 29:313–317. <https://doi.org/10.1016/j.pt.2013.04.001>.
31. Ferreira PE, Culleton R, Gil JP, Meshnick SR. 2013. Artemisinin resistance in *Plasmodium falciparum*: what is it really? *Trends Parasitol* 29:318–320. <https://doi.org/10.1016/j.pt.2013.05.002>.
32. Hastings IM, Kay K, Hodel EM. 2016. The importance of scientific debate in the identification, containment, and control of artemisinin resistance. *Clin Infect Dis* 63:1527–1528. <https://doi.org/10.1093/cid/ciw581>.
33. Bethell D, Se Y, Lon C, Tyner S, Saunders D, Sriwichai S, Darapiseth S, Teja-Isavadharm P, Khemawoot P, Schaecher K, Rutvisuttinunt W, Lin J, Kuntawunginn W, Gosi P, Timmermans A, Smith B, Socheat D, Fukuda MM. 2011. Artesunate dose escalation for the treatment of uncomplicated malaria in a region of reported artemisinin resistance: a randomized clinical trial. *PLoS One* 6:e19283. <https://doi.org/10.1371/journal.pone.0019283>.
34. Saunders D, Khemawoot P, Vanachayangkul P, Siripokasupkul R, Bethell D, Tyner S, Se Y, Rutvisuttinunt W, Sriwichai S, Chanthap L, Lin J, Timmermans A, Socheat D, Ringwald P, Noedl H, Smith B, Fukuda M, Teja-Isavadharm P. 2012. Pharmacokinetics and pharmacodynamics of oral artesunate monotherapy in patients with uncomplicated *Plasmodium falciparum* malaria in western Cambodia. *Antimicrob Agents Chemother* 56:5484–5493. <https://doi.org/10.1128/AAC.00044-12>.
35. Kheang ST, Sovannaroeth S, Ek S, Chy S, Chhun P, Mao S, Nguon S, Lek DS, Menard D, Kak N. 2017. Prevalence of K13 mutation and day-3 positive parasitaemia in artemisinin-resistant malaria endemic area of Cambodia: a cross-sectional study. *Malar J* 16:372. <https://doi.org/10.1186/s12936-017-2024-4>.
36. MalariaGEN *Plasmodium falciparum* Community Project. 2016. Genomic epidemiology of artemisinin resistant malaria. *Elife* 5:e08714. <https://doi.org/10.7554/eLife.08714>.
37. Sa JM, Kaslow SR, Krause MA, Melendez-Muniz VA, Salzman RE, Kite WA, Zhang M, Moraes Barros RR, Mu J, Han PK, Mershon JP, Figan CE, Caleon RL, Rahman RS, Gibson TJ, Amaratunga C, Nishiguchi EP, Breglio KF, Engels TM, Velmurugan S, Ricklefs S, Straimer J, Gnädig NF, Deng B, Liu A, Diouf A, Miura K, Tullo GS, Eastman RT, Chakravarty S, James ER, Udenze K, Li S, Sturdevant DE, Gwadz RW, Porcella SF, Long CA, Fidock DA, Thomas ML, Fay MP, Sim BKL, Hoffman SL, Adams JH, Fairhurst RM, Su XZ, Wellems TE. 2018. Artemisinin resistance phenotypes and K13 inheritance in a *Plasmodium falciparum* cross and *Aotus* model. *Proc Natl Acad Sci U S A* 115:12513–12518. <https://doi.org/10.1073/pnas.1813386115>.
38. Gabrysiewicz SJ, Modchang C, Musset L, Chookajorn T, Fidock DA. 2016. Combinatorial genetic modeling of *pfprt*-mediated drug resistance evolution in *Plasmodium falciparum*. *Mol Biol Evol* 33:1554–1570. <https://doi.org/10.1093/molbev/msw037>.
39. Laufer MK, Takala-Harrison S, Dzinjalimala FK, Stine OC, Taylor TE, Plowe CV. 2010. Return of chloroquine-susceptible *falciparum* malaria in Malawi was a reexpansion of diverse susceptible parasites. *J Infect Dis* 202:801–808. <https://doi.org/10.1086/655659>.
40. Straimer J, Gnädig NF, Stokes BH, Ehrenberger M, Crane AA, Fidock DA. 2017. *Plasmodium falciparum* K13 mutations differentially impact ozone susceptibility and parasite fitness *in vitro*. *mBio* 8:e00172-17. <https://doi.org/10.1128/mBio.00172-17>.
41. Takala-Harrison S, Jacob CG, Arze C, Cummings MP, Silva JC, Dondorp AM, Fukuda MM, Hien TT, Mayxay M, Noedl H, Nosten F, Kyaw MP, Nhien NTT, Imwong M, Bethell D, Se Y, Lon C, Tyner SD, Saunders DL, Arie F, Mercereau-Puijalon O, Menard D, Newton PN, Khanthavong M, Hongvanthong B, Starzengruber P, Fuehrer H-P, Swoboda P, Khan WA, Phyto AP, Nyunt MM, Nyunt MH, Brown TS, Adams M, Pepin CS, Bailey J, Tan JC, Ferdig MT, Clark TG, Miotto O, MacInnis B, Kwiatkowski DP, White NJ, Ringwald P, Plowe CV. 2015. Independent emergence of artemisinin resistance mutations among *Plasmodium falciparum* in Southeast Asia. *J Infect Dis* 211:670–679. <https://doi.org/10.1093/infdis/jiu491>.
42. Nair S, Li X, Arya GA, McDew-White M, Ferrari M, Nosten F, Anderson TJC. 2018. Fitness costs and the rapid spread of Kelch13-C580Y substitutions

- conferring artemisinin resistance. Antimicrob Agents Chemother 62: e00605-18. <https://doi.org/10.1128/AAC.00605-18>.
43. Yang T, Yeoh LM, Tutor MV, Dixon MW, McMillan PJ, Xie SC, Bridgford JL, Gillett DL, Duffy MF, Ralph SA, McConville MJ, Tilley L, Cobbold SA. 2019. Decreased K13 abundance reduces hemoglobin catabolism and proteotoxic stress, underpinning artemisinin resistance. Cell Rep 29: 2917.e5–2928.e5. <https://doi.org/10.1016/j.celrep.2019.10.095>.
 44. Birnbaum J, Scharf S, Schmidt S, Jonscher E, Hoeijmakers WAM, Flemming S, Toenhake CG, Schmitt M, Sabitzki R, Bergmann B, Fröhle U, Mesén-Ramírez P, Blanche Soares A, Herrmann H, Bártfai R, Spielmann T. 2020. A Kelch13-defined endocytosis pathway mediates artemisinin resistance in malaria parasites. Science 367:51–59. <https://doi.org/10.1126/science.aax4735>.
 45. Gnädig NF, Stokes BH, Edwards RL, Kalantarov GF, Heimsch KC, Kuderjavy M, Crane A, Lee MCS, Strainer J, Becker K, Trakht IN, Odom John AR, Mok S, Fidock DA. 2020. Insights into the intracellular localization, protein associations and artemisinin resistance properties of *Plasmodium falciparum* K13. PLoS Pathog 16:e1008482. <https://doi.org/10.1371/journal.ppat.1008482>.
 46. Simwela NV, Hughes KR, Roberts AB, Rennie MT, Barrett MP, Waters AP. 2020. Experimentally engineered mutations in a ubiquitin hydrolase, UBP-1, modulate *in vivo* susceptibility to artemisinin and chloroquine in *Plasmodium berghei*. Antimicrob Agents Chemother 64:e02484-19. <https://doi.org/10.1128/AAC.02484-19>.
 47. Hunt P, Afonso A, Creasey A, Culleton R, Sidhu AB, Logan J, Valderramos SG, McNae I, Cheesman S, do Rosario V, Carter R, Fidock DA, Cravo P. 2007. Gene encoding a deubiquitinating enzyme is mutated in artesunate- and chloroquine-resistant rodent malaria parasites. Mol Microbiol 65:27–40. <https://doi.org/10.1111/j.1365-2958.2007.05753.x>.
 48. Henrici RC, van Schalkwyk DA, Sutherland CJ. 2019. Modification of *pfap2mu* and *pfubp1* markedly reduces ring-stage susceptibility of *Plasmodium falciparum* to artemisinin *in vitro*. Antimicrob Agents Chemother 64:e01542-19. <https://doi.org/10.1128/AAC.01542-19>.
 49. Dogovski C, Xie SC, Burgio G, Bridgford J, Mok S, McCaw JM, Chotivanich K, Kenny S, Gnädig N, Strainer J, Bozdech Z, Fidock DA, Simpson JA, Dondorp AM, Foote S, Klonis N, Tilley L. 2015. Targeting the cell stress response of *Plasmodium falciparum* to overcome artemisinin resistance. PLoS Biol 13:e1002132. <https://doi.org/10.1371/journal.pbio.1002132>.
 50. Mok S, Ashley EA, Ferreira PE, Zhu L, Lin Z, Yeo T, Chotivanich K, Imwong M, Pukrittayakamee S, Dhorda M, Nguon C, Lim P, Amaratunga C, Suon S, Hien TT, Htut Y, Faiz MA, Onyamboko MA, Mayxay M, Newton PN, Tripura R, Woodrow CJ, Miotto O, Kwiatkowski DP, Nosten F, Day NPJ, Preiser PR, White NJ, Dondorp AM, Fairhurst RM, Bozdech Z. 2015. Drug resistance. Population transcriptomics of human malaria parasites reveals the mechanism of artemisinin resistance. Science 347:431–435. <https://doi.org/10.1126/science.1260403>.
 51. Lee AH, Symington LS, Fidock DA. 2014. DNA repair mechanisms and their biological roles in the malaria parasite *Plasmodium falciparum*. Microbiol Mol Biol Rev 78:469–486. <https://doi.org/10.1128/MMBR.00059-13>.
 52. Franke-Fayard B, Djokovic D, Dooren MW, Ramesar J, Waters AP, Falade MO, Kranendonk M, Martinelli A, Cravo P, Janse CJ. 2008. Simple and sensitive antimalarial drug screening *in vitro* and *in vivo* using transgenic luciferase expressing *Plasmodium berghei* parasites. Int J Parasitol 38: 1651–1662. <https://doi.org/10.1016/j.ijpara.2008.05.012>.
 53. Janse CJ, Waters AP, Kos J, Lugt CB. 1994. Comparison of *in vivo* and *in vitro* antimalarial activity of artemisinin, dihydroartemisinin and sodium artesunate in the *Plasmodium berghei*-rodent model. Int J Parasitol 24:589–594. [https://doi.org/10.1016/0020-7519\(94\)90150-3](https://doi.org/10.1016/0020-7519(94)90150-3).
 54. Lee RS, Waters AP, Brewer JM. 2018. A cryptic cycle in haematopoietic niches promotes initiation of malaria transmission and evasion of chemotherapy. Nat Commun 9:1689. <https://doi.org/10.1038/s41467-018-04108-9>.
 55. Bridgford JL, Xie SC, Cobbold SA, Pasaje CFA, Herrmann S, Yang T, Gillett DL, Dick LR, Ralph SA, Dogovski C, Spillman NJ, Tilley L. 2018. Artemisinin kills malaria parasites by damaging proteins and inhibiting the proteasome. Nat Commun 9:3801. <https://doi.org/10.1038/s41467-018-06221-1>.
 56. Li H, O'Donoghue AJ, van der Linden WA, Xie SC, Yoo E, Foe IT, Tilley L, Craik CS, da Fonseca PCA, Bogoy M. 2016. Structure- and function-based design of *Plasmodium*-selective proteasome inhibitors. Nature 530: 233–236. <https://doi.org/10.1038/nature16936>.
 57. Yoo E, Stokes BH, de Jong H, Vanaerschot M, Kumar T, Lawrence N, Njoroge M, Garcia A, Van der Westhuyzen R, Momper JD, Ng CL, Fidock DA, Bogoy M. 2018. Defining the determinants of specificity of *Plasmodium* proteasome inhibitors. J Am Chem Soc 140:11424–11437. <https://doi.org/10.1021/jacs.8b06656>.
 58. Fidock DA, Rosenthal PJ, Croft SL, Brun R, Nwaka S. 2004. Antimalarial drug discovery: efficacy models for compound screening. Nat Rev Drug Discov 3:509–520. <https://doi.org/10.1038/nrd1416>.
 59. Ménard D, Khim N, Beghain J, Adegnika AA, Shafiu-Alam M, Amodu O, Rahim-Awab G, Barnadas C, Berry A, Boum Y, Bustos MD, Cao J, Chen J-H, Collet L, Cui L, Thakur G-D, Dieye A, Djallé D, Dorkenoo MA, Eboumbou-Moukoko CE, Espino F-E-CJ, Fandeur T, Ferreira-da-Cruz M-F, Fola AA, Fuehrer H-P, Hassan AM, Herrera S, Hongvanthong B, Houzé S, Ibrahim ML, Jahirul-Karim M, Jiang L, Kano S, Ali-Khan W, Khanthavong M, Kremsner PG, Lacerda M, Leang R, Leelawong M, Li M, Lin K, Mazarati J-B, Ménard S, Morlais I, Muhindo-Mavoko H, Musset L, Na-Bangchang K, Nambozi M, Niaré K, Noedl H, KARMA Consortium, et al. 2016. A worldwide map of *Plasmodium falciparum* K13-propeller polymorphisms. N Engl J Med 374:2453–2464. <https://doi.org/10.1056/NEJMoa1513137>.
 60. Anderson TJ, Nair S, McDew-White M, Cheeseman IH, Nkhoma S, Bilgic F, McGready R, Ashley E, Pyae Phyo A, White NJ, Nosten F. 2017. Population parameters underlying an ongoing soft sweep in Southeast Asian malaria parasites. Mol Biol Evol 34:131–144. <https://doi.org/10.1093/molbev/msw228>.
 61. Amaratunga C, Witkowski B, Dek D, Try V, Khim N, Miotto O, Ménard D, Fairhurst RM. 2014. *Plasmodium falciparum* founder populations in western Cambodia have reduced artemisinin sensitivity *in vitro*. Antimicrob Agents Chemother 58:4935–4937. <https://doi.org/10.1128/AAC.03055-14>.
 62. Siddiqui FA, Boonhok R, Cabrera M, Mbenda HGN, Wang M, Min H, Liang X, Qin J, Zhu X, Miao J, Cao Y, Cui L. 2020. Role of *Plasmodium falciparum* Kelch13 protein mutations in *P. falciparum* populations from northeastern Myanmar in mediating artemisinin resistance. mBio 11:e01134-19. <https://doi.org/10.1128/mBio.01134-19>.
 63. Wang J, Huang Y, Zhao Y, Ye R, Zhang D, Pan W. 2018. Introduction of F446I mutation in the K13 propeller gene leads to increased ring survival rates in *Plasmodium falciparum* isolates. Malar J 17:248. <https://doi.org/10.1186/s12936-018-2396-0>.
 64. Wang Z, Wang Y, Cabrera M, Zhang Y, Gupta B, Wu Y, Kemirembe K, Hu Y, Liang X, Brashear A, Shrestha S, Li X, Miao J, Sun X, Yang Z, Cui L. 2015. Artemisinin resistance at the China-Myanmar border and association with mutations in the K13 propeller gene. Antimicrob Agents Chemother 59:6952–6959. <https://doi.org/10.1128/AAC.01255-15>.
 65. Huang F, Takala-Harrison S, Jacob CG, Liu H, Sun X, Yang H, Nyunt MM, Adams M, Zhou S, Xia Z, Ringwald P, Bustos MD, Tang L, Plowe CV. 2015. A single mutation in K13 predominates in southern China and is associated with delayed clearance of *Plasmodium falciparum* following artemisinin treatment. J Infect Dis 212:1629–1635. <https://doi.org/10.1093/infdis/jiv249>.
 66. Tun KM, Jeeyapant A, Imwong M, Thein M, Aung SS, Hlaing TM, Yuen-trakul P, Promnarate C, Dhorda M, Woodrow CJ, Dondorp AM, Ashley EA, Smithuis FM, White NJ, Day NP. 2016. Parasite clearance rates in upper Myanmar indicate a distinctive artemisinin resistance phenotype: a therapeutic efficacy study. Malar J 15:185. <https://doi.org/10.1186/s12936-016-1240-7>.
 67. Tun KM, Imwong M, Lwin KM, Win AA, Hlaing TM, Hlaing T, Lin K, Kyaw MP, Plewes K, Faiz MA, Dhorda M, Cheah PY, Pukrittayakamee S, Ashley EA, Anderson TJ, Nair S, McDew-White M, Flegg JA, Grist EPM, Guerin P, Maude RJ, Smithuis F, Dondorp AM, Day NPJ, Nosten F, White NJ, Woodrow CJ. 2015. Spread of artemisinin-resistant *Plasmodium falciparum* in Myanmar: a cross-sectional survey of the K13 molecular marker. Lancet Infect Dis 15:415–421. [https://doi.org/10.1016/S1473-3099\(15\)70032-0](https://doi.org/10.1016/S1473-3099(15)70032-0).
 68. Nyunt MH, Hlaing T, Oo HW, Tin-Oo L-LK, Phway HP, Wang B, Zaw NN, Han SS, Tun T, San KK, Kyaw MP, Han E-T. 2015. Molecular assessment of artemisinin resistance markers, polymorphisms in the K13 propeller, and a multidrug-resistance gene in the eastern and western border areas of Myanmar. Clin Infect Dis 60:1208–1215. <https://doi.org/10.1093/cid/ciu1160>.
 69. Li H, Ponder EL, Verdoes M, Asbjornsdottir KH, Deu E, Edgington LE, Lee JT, Kirk CJ, Demo SD, Williamson KC, Bogoy M. 2012. Validation of the proteasome as a therapeutic target in *Plasmodium* using an epoxyketone inhibitor with parasite-specific toxicity. Chem Biol 19:1535–1545. <https://doi.org/10.1016/j.chembiol.2012.09.019>.
 70. Gantt SM, Myung JM, Briones MR, Li WD, Corey EJ, Omura S, Nussenzweig V, Sinnis P. 1998. Proteasome inhibitors block development of *Plasmodium* spp. Antimicrob Agents Chemother 42:2731–2738. <https://doi.org/10.1128/AAC.42.10.2731>.

71. Stokes BH, Yoo E, Murithi JM, Luth MR, Afanasyev P, da Fonseca PCA, Winzeler EA, Ng CL, Bogyo M, Fidock DA. 2019. Covalent *Plasmodium falciparum*-selective proteasome inhibitors exhibit a low propensity for generating resistance *in vitro* and synergize with multiple antimalarial agents. *PLoS Pathog* 15:e1007722. <https://doi.org/10.1371/journal.ppat.1007722>.
72. Mukherjee A, Bopp S, Magistrado P, Wong W, Daniels R, Demas A, Schaffner S, Amaratunga C, Lim P, Dhorda M, Miotto O, Woodrow C, Ashley EA, Dondorp AM, White NJ, Wirth D, Fairhurst R, Volkman SK. 2017. Artemisinin resistance without Pfk3 mutations in *Plasmodium falciparum* isolates from Cambodia. *Malar J* 16:195. <https://doi.org/10.1186/s12936-017-1845-5>.
73. Sievers F, Wilm A, Dineen D, Gibson TJ, Karplus K, Li W, Lopez R, McWilliam H, Remmert M, Söding J, Thompson JD, Higgins DG. 2011. Fast, scalable generation of high-quality protein multiple sequence alignments using Clustal omega. *Mol Syst Biol* 7:539–539. <https://doi.org/10.1038/msb.2011.75>.
74. Heckman KL, Pease LR. 2007. Gene splicing and mutagenesis by PCR-driven overlap extension. *Nat Protoc* 2:924–932. <https://doi.org/10.1038/nprot.2007.132>.
75. Burda P-C, Roelli MA, Schaffner M, Khan SM, Janse CJ, Heussler VT. 2015. A *Plasmodium* phospholipase is involved in disruption of the liver stage parasitophorous vacuole membrane. *PLoS Pathog* 11:e1004760. <https://doi.org/10.1371/journal.ppat.1004760>.
76. Philip N, Orr R, Waters AP. 2013. Transfection of rodent malaria parasites. *Methods Mol Biol* 923:99–125. https://doi.org/10.1007/978-1-62703-026-7_7.
77. Rueden CT, Schindelin J, Hiner MC, DeZonia BE, Walter AE, Arena ET, Eliceiri KW. 2017. ImageJ2: ImageJ for the next generation of scientific image data. *BMC Bioinformatics* 18:529. <https://doi.org/10.1186/s12859-017-1934-z>.
78. Fivelman QL, Adagu IS, Warhurst DC. 2004. Modified fixed-ratio isobologram method for studying *in vitro* interactions between atovaquone and proguanil or dihydroartemisinin against drug-resistant strains of *Plasmodium falciparum*. *Antimicrob Agents Chemother* 48:4097–4102. <https://doi.org/10.1128/AAC.48.11.4097-4102.2004>.
79. Boampong JN, Ameyaw EO, Aboagye B, Asare K, Kyei S, Donfack JH, Woode E. 2013. The curative and prophylactic effects of xylopic acid on *Plasmodium berghei* infection in mice. *J Parasitol Res* 2013:356107. <https://doi.org/10.1155/2013/356107>.
80. Vega-Rodríguez J, Pastrana-Mena R, Crespo-Lladó KN, Ortiz JG, Ferrer-Rodríguez I, Serrano AE. 2015. Implications of glutathione levels in the *Plasmodium berghei* response to chloroquine and artemisinin. *PLoS One* 10:e0128212. <https://doi.org/10.1371/journal.pone.0128212>.

Mammalian deubiquitinating enzyme inhibitors display *in vitro* and *in vivo* activity against malaria parasites and potentiate artemisinin action

Nelson V. Simwela¹, Katie R. Hughes¹, Michael T. Rennie¹, Michael P. Barrett¹, Andrew P. Waters^{1*}

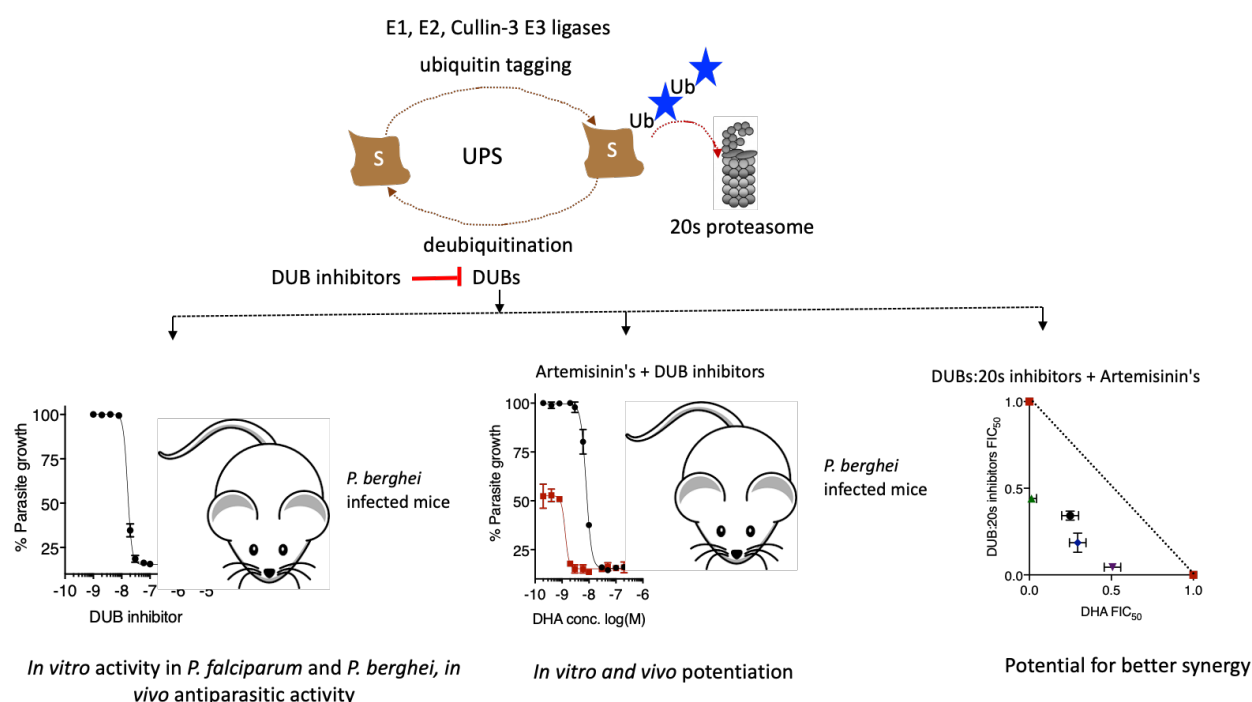
¹Institute of Infection, Immunity & Inflammation, Wellcome Centre for Integrative Parasitology,
University of Glasgow

* Corresponding author: Andrew P. Waters, email: Andy.Waters@glasgow.ac.uk

Abstract

Current malaria control efforts rely significantly on artemisinin combinational therapies which have played massive roles in alleviating the global burden of the disease. Emergence of resistance to artemisinins is therefore, not just alarming but requires immediate intervention points such as development of new antimalarial drugs or improvement of the current drugs through adjuvant or combination therapies. Artemisinin resistance is primarily conferred by Kelch13 propeller mutations which are phenotypically characterised by generalised growth quiescence, altered haemoglobin trafficking and downstream enhanced activity of the parasite stress pathways through the ubiquitin proteasome system (UPS). Previous work on artemisinin resistance selection in a rodent model of malaria, which we and others have recently validated using reverse genetics, has also shown that mutations in deubiquitinating enzymes, DUBs (upstream UPS component) modulates susceptibility of malaria parasites to both artemisinin and chloroquine. The UPS or upstream protein trafficking pathways have, therefore, been proposed to be not just potential drug targets, but also possible intervention points to overcome artemisinin resistance. Here we report the activity of small molecule inhibitors targeting mammalian DUBs in malaria parasites. We show that generic DUB inhibitors can block intraerythrocytic development of malaria parasites *in vitro* and possess antiparasitic activity *in vivo* and can be used in combination with additive effect. We also show that inhibition of these upstream components of the UPS can potentiate the activity of artemisinin *in vitro* as well as *in vivo* to the extent that ART resistance can be overcome. Combinations of DUB inhibitors anticipated to target different DUB activities and downstream 20S proteasome inhibitors are even more effective at improving the potency of artemisinins than either inhibitors alone providing proof that targeting multiple UPS activities simultaneously could be an attractive approach to overcoming artemisinin resistance. These data further validate the parasite UPS as a target to both enhance artemisinin action and potentially overcome resistance. Lastly, we confirm that DUB inhibitors can be developed into *in vivo* antimalarial drugs with promise for activity against all of human malaria and could thus further exploit their current pursuit as anticancer agents in rapid drug repurposing programs.

69 Graphical abstract



Introduction

Malaria remains the most important parasitic disease in tropical and sub-tropical regions of the world with high rates of morbidity and mortality. Despite significant gains in malaria control over the past decade, over 220 million cases and 400 000 deaths were reported in 2018, with >90% of these occurring in the WHO African region.¹ More worryingly, a global stall in malaria control has been reported with a steady increase in malaria cases being observed between 2015 and 2018.¹⁻² Caused by apicomplexan parasites of the genus *Plasmodium*, the most lethal form of human malaria is caused by *Plasmodium falciparum* which accounts for >99% of malaria cases and deaths in Sub-Saharan Africa.¹ However, human malaria caused by other *Plasmodium* spp. such as *P. vivax*, *P. ovale*, *P. malaria* and the zoonotic *P. knowlesi* remains a significant public health problem causing significant morbidity and economic impact in already poverty stricken communities.¹ The life cycle of malaria parasites comprises of multiple developmental stages between mosquito and mammalian hosts. Antimalarial drugs, which form principle components of malaria control programs, target the parasite at different life cycle stages, mostly the proliferating trophozoites and schizont stages during the intraerythrocytic development cycle of the parasites which are associated with most of the disease pathology. Artemisinins (ARTs) in ART combination therapies are the current front line drugs in malaria treatment.¹ They display fast and potent activity against virtually all blood stages of the parasites, as well as gametocytes that mediate transmission to mosquito vectors.³⁻⁴ Indeed, such is the effectiveness of ARTs, that recent gains in malaria control have been partly attributed to ART combination therapies.^{2,4} Unfortunately, *P. falciparum* (PF) resistance to ARTs has emerged in the Southeast Asia greater Mekong region and is characterised by point mutations in the Kelch13 propeller domain that associate with decreased parasite clearance rates in clinical phenotypes.^{1,4-5}

ARTs are sesquiterpene lactones derived from the Chinese herb *Artemisia annua*. Central to the activity of ARTs is the activation of the core endoperoxide bridge by haem which triggers the production of carbon centred radicals which in turn alkylate multiple and random downstream parasite targets.⁶⁻⁷ The actual events leading to ART mediated parasite death remain elusive as well as disputed. However, a promiscuous targeting of several parasite proteins by the ART generated radicals is widely accepted.⁸⁻⁹ The ART resistance- associated mutations lie in the beta propeller domain of the Kelch13 protein in PF.¹⁰ Recent work on the biological function and consequences of these Kelch13 mutations has revealed that Kelch13 localises to the parasite cytoplasmic periphery in cellular compartments called cytostomes and plays a role in haemoglobin endocytosis. ART resistance-associated mutations in Kelch13 lead to reduced abundance of this protein leading to impaired haemoglobin trafficking which lessens ART activation hence promoting parasite survival.¹¹⁻

¹² In addition, ART induced pleiotropic targeting is also known to activate ER stress and the unfolded protein response (UPR) which allow parasites to survive drug assault by rapidly turning over damaged proteins while employing cell repair mechanisms. ^{6-7, 13} ART resistant parasites (Kelch13 mutants) are indeed associated with an upregulation of genes involved in these cellular stress response pathways. ¹⁴ Meanwhile, parallel functional and localisation studies have also revealed that Kelch13 co-localises with multiple UPR components, proteins specific to the ER and mitochondria as well as intracellular vesicular trafficking Rab GTPases. ¹⁵⁻¹⁶ Central to the activity of the UPR is the ubiquitin proteasome system (UPS), a conserved eukaryotic pathway that plays a role in protein homeostasis by degrading unfolded proteins. Under ART pressure, activity of the UPS is more upregulated in Kelch13 mutant parasites compared to wild type while UPS inhibitors have been shown to synergize ART action suggesting that this pathway could be selectively targeted to overcome ART resistance. ¹⁷⁻¹⁸ Of note, Kelch13 is also predicted to play additional roles as substrate adaptor for ubiquitin E3 ligases, crucial components of the UPS; ^{7, 10} while mutations in upstream components of the UPS (ubiquitin hydrolases or deubiquitinating enzymes) also modulate susceptibility to ARTs. ¹⁹⁻²¹ Chemotherapeutic targeting of the UPS has been successfully pursued in cancers ²² and is increasingly becoming attractive in malaria parasites, ²³ even more so as potential combinatorial partners to ARTs to overcome resistance. ¹⁷⁻¹⁸

Here we report the activity of deubiquitinating enzyme (DUBs) inhibitors in both rodent and human malaria parasites. DUBs are proteases that cleave ubiquitin residues from conjugated substrate proteins in the UPS pathway. UPS targeting of proteins is initiated by ubiquitin (Ub) tagging of substrates which marks them either for specific cellular signal transduction processes like DNA repair and cell cycle progression or subsequent degradation by the 20s proteasome. ²⁴ Ub tagging is mediated by three sequential enzymes: E1, an activating enzyme; E2, a conjugating enzyme and E3, a Ub ligase for substrate specificity. The activity of these enzymes results in polyubiquitination of substrate proteins which signals for their degradation at the 20s proteasome complex depending on the number of Ub residues. DUBs reverse the activity of these downstream UPS enzymes by removing Ub from the conjugated substrates which results in diverse protein fates and cellular outcomes among which include; regulation of protein half-life, cell growth, differentiation, transcription; rescue of mis-tagged proteins as well as oncogenic and neuronal disease signalling. ²⁵ Over 100 DUBs have been identified in humans and they classify into five major families: Ub C-terminal hydrolases (UCHs), Ub specific proteases (USPs), ovarian tumour proteases (OTUs), Josephins and JAMM/MPN/MOV34. ²⁵ In malaria parasites, up to 30 DUBs have been predicted across five *Plasmodium* species (PF, *P. vivax*, *P. berghei* (PB), *P. chabaudi*, *P. yoelii*); even though their

functions remain to be fully explored.²⁶⁻²⁷ Nevertheless, *Plasmodium* DUBs seem to have intrinsic protease activity, are significantly divergent and their human orthologues are known to be important regulators of cellular pathway which makes them suitable and potential drug targets.²⁸ The role of DUBs in mediating susceptibility to standard drugs like ARTs, the diversity in the classes of DUBs and the predicted repertoire in malaria parasites would also mean an expanded chemical space for drug discovery, potential inhibitor combination for different classes as well as using DUB inhibitor combinations to overcome ART resistance. Herein, using generic mammalian DUB inhibitors that have been used as exploratory research tools as well as in clinical trials, we show that DUB inhibitors do possess *in vitro* and *in vivo* inhibitory activities against malaria parasites across two diverged *Plasmodium* species. We demonstrate that different classes of DUB inhibitors can be combined to provide greater killing efficacy as well as enhance the potency of ARTs both *in vitro* and *in vivo*. Our data demonstrate that DUB inhibition can be exploited to overcome ART resistance with similar potency as first generation proteasome inhibitors. Furthermore, inhibition of both the UPS and DUBs can be combined to further improve the potency of ARTs and negate ART resistance. These findings have the potential to be applied to the treatment of all human malaria.

Results

In vitro activity of DUB inhibitors in malaria parasites

To assay for *in vitro* activity of DUB inhibitors in malaria parasites, short term PB culture assays and PF Sybergreen I® culture assays were employed. The PB 820 and PF 3D7 lines were initially screened to determine susceptibility to inhibitors and antimalarials with known activity in malaria parasites; ART, dihydroartemisinin (DHA), chloroquine (CQ) and epoxomicin (20s proteasome inhibitor). The half-inhibitory concentrations (IC₅₀) obtained for epoxomicin, DHA, ART and CQ in both the 820 and 3D7 lines (Table 1) were all in agreement with previously published IC₅₀ values in both *Plasmodium* species.²⁹⁻³² Next, we screened seven DUB inhibitors (Table 1) in both the 820 and 3D7 line to characterise their inhibitory activity during the intraerythrocytic stages of malaria parasites. The selected compounds are DUB inhibitors being currently pursued as promising anticancer agents (Table 1) that also offered a broad coverage targeting of the 5 classes of DUBs. As shown in Table 1, activity was observed for six of the seven DUBs tested in the 820 and 3D7 lines. The activity of USP acting DUB inhibitors; b-AP15, P5091 and NSC632839 corresponds with the reported *in vitro* IC₅₀s of the compounds screened in cancer cell lines³³⁻³⁵. b-AP15 IC₅₀ also compared to previously reported IC₅₀s of 1.54 ± 0.7 µM and 1.10 ± 0.4 µM in PF CQ sensitive (3D7) and resistant (Dd2) lines respectively.³⁶ Growth inhibition was also observed for broad spectrum DUB inhibitors; PR-619 and

1,10 phenanthroline, as well as a partially selective DUB inhibitor, WP1130 (Table 1). These data suggest that DUBs are potentially essential enzymes in *Plasmodium*, and they could be pursued as potential antimalarial drug targets. Indeed, a manual curation of up to 17 of the predicted DUBs in malaria parasites²⁶⁻²⁷ shows that a majority of these (~70%, 12 of 17) are essential in either PF and PB or both (Supplementary Table 1) based on previous functional studies for selected DUBs³⁷⁻³⁸ or recent genome wide gene knockout screens.³⁹⁻⁴⁰ Strikingly, no growth inhibition was observed for TCID (IC₅₀ >100 µM), a UCH-L3 inhibitor, in both the 820 and 3D7 lines (Table 1, Supplementary Figure 1A, 1B). Among the well characterised DUBs in malaria parasites is PF UCH-L3 (PfUCH-L3, PF3D7_1460400) which was identified by activity based chemical profiling and has been shown to retain core deubiquitinating activity.⁴¹ Structural and functional characterisation of PfUCH-L3 has also shown that this enzyme is essential for parasite survival (Supplementary Table 1).³⁸ Meanwhile, in our screen, TCID, a highly selective mammalian UCH-L3 inhibitor with an IC₅₀ of 0.6 µM in mammalian cancer cell lines,⁴² displayed no activity in both the 820 and 3D7 lines (Table 1, Supplementary Figure 1A, 1B). To possibly address this (unexpected) lack of activity, we performed a phylogenetic analysis of *Plasmodium*, human and mouse UCH-L3 based on predicted protein sequences to infer their similarities which might explain the observed lack of anti-plasmodial activity of TCID. A distinct evolutionary divergence of this enzyme was observed between human, mouse and the most similar *Plasmodium* homologues (PBANKA_1324100/PF3D7_1460400) which whilst annotated as UCH-L3 shares only 33% predicted protein sequence identity with the human UCH-L3 (Supplementary Figure 1C, D). Structurally, human UCH-L3 and PfUCH-L3 have similar modes of Ub recognition and binding. However, the PfUCH-L3 Ub binding groove is structurally different from the human UCH-L3 at atomic bonding level and possesses non-conserved amino acid residues.³⁸ This lack of complete identity across active sites would perhaps further explain the observed inactivity of TCID in both PF and PB.

Different classes of DUB inhibitors can be combined to provide more effective blocking of malaria parasite growth *in vitro*.

To explore interactions between DUB inhibitors, and their potential synergy, b-AP15, a highly selective USP14 inhibitor³⁴ and the relatively most potent inhibitor of parasite growth in both PF and PB, was tested in fixed ratios with broad-spectrum DUB inhibitors; PR-619 and WP1130. Combinations at fixed ratios of 5:0, 4:1, 3:2, 1:4 and 0:5 were serially diluted and incubated with parasite cultures of the 3D7 line from which parasite growth and IC₅₀s were obtained. FIC₅₀s and ΣFIC₅₀s were calculated and isobologram interactions were plotted. A combination of b-AP15 and

PR-619 is mostly additive with a mean ΣFIC_{50} of 0.753 ± 0.23 , (Figure 2A). Meanwhile, b-AP15 and WP1130 seemingly trends towards synergy with a mean ΣFIC_{50} of 0.653 ± 0.23 , (Figure 2B) even though the interaction remains overall additive. These data suggested that DUB inhibitors, as potential antimalarial drug candidates, can be used in combination to block parasite growth presumably by simultaneously targeting several different DUB enzymatic targets.

DUB inhibitors alone or in combination can potentiate DHA action in malaria parasites *in vitro*

In order to test the hypothesis that DUB inhibitors might have a similar effect of potentiating ART activity as 20s proteasome inhibitors, we investigated the effects of DUB inhibitors on the dose response profiles of DHA *in vitro* on wild type PB and PF growth as well as their potential to synergize DHA action in fixed ratio interaction assays. The most potent DUB inhibitor b-AP15 at equivalent IC_{50} concentration improved DHA action with up to ~8-fold IC_{50} shift in wild type PB growth inhibition (Figure 2A) and up to 15-fold enhancement in the wild type PF growth inhibition (Figure 2B). The differences in potentiation between PB and PF could be due to the inherent reduced susceptibility of PB to ARTs.^{20, 43} The enhancement of DHA action by b-AP15 was also almost similar to previously reported profiles with epoxomicin, a 20s proteasome inhibitor.¹⁷ We have recently shown that experimental introduction of mutations in a DUB, UBP-1, mediated reduced susceptibility to ARTs in PB.²⁰ UBP-1 has a close human orthologue HAUSP/USP7 which is itself inhibited by P5091, a drug which in our *Plasmodium* screen was poorly potent with a relatively high micromolar IC_{50} (Table 1). Nevertheless, b-AP15 (a USP-14 inhibitor) potentiated DHA action to the same extent as in wild type ART-sensitive PB (9-11-fold) in two UBP1 mutant lines that have reduced susceptibility to ART (V2721F) or both ART and CQ (V2752F) (Supplementary Figure 2A & B). Therefore, ART (and potentially CQ) reduced susceptibility could be offset by a combinatorial drug administration approach involving DUB inhibitors through a targeted disruption of protein homeostasis most likely at the level of the UPS.

In an attempt to maximise DUB inhibitor combinations, which offered improved inhibition of parasite growth (Figure 1) as a strategy for simultaneously targeting several DUBs in the presence of DHA, we tested the effect of combining b-AP15, PR-619 and WP1130 on the dose response profile of DHA. WP1130 and PR-619 at IC_{50} concentration mildly potentiate DHA action with 1.8- and 1.4-fold improvements respectively (Supplementary Figure 3A, 3B). Meanwhile, a combination of b-AP15 and WP1130 at half IC_{50} mildly potentiated DHA action (~2-fold, Figure 2C), while all three inhibitors (b-AP15, WP1130 and PR-619) at half IC_{50} improved DHA action up to 5-fold in the ART sensitive PF (Figure 2D) and PB (Figure 2E) as well as the ART resistant PF Kelch13 C580Y mutant lines (Figure 2F).

We carried out further isobologram interaction assays for DUB inhibitor ratio combinations in an attempt to achieve improved *in vitro* killing (Figure 1) in combination with DHA. Both b-AP15 and WP1130 were essentially additive when combined with DHA in isobologram interactions with ΣFIC_{50} s of 0.967 and 1.013 respectively (Supplementary Figure 3C, 3D). However, when b-AP15 and WP1130 were mixed at a 3:2 molar concentration ratio as a cocktail and combined with DHA, a slight improvement in efficacy was observed with an ΣFIC_{50} of ~0.868 (Figure 2G) compared with 0.972 at 1:4 b-AP15 WP1130 molar concentration ratios (Figure 2H) or 0.941 at 2:3 b-AP15 WP1130 molar concentration ratio (Figure 2I). These data would suggest that optimized ratios of (improved) DUB inhibitor combinations or other proteasome inhibitors might yet achieve synergy with DHA, which would be a prerequisite to simultaneously targeting multiple DUBs or parallel pathways/enzymes in the UPS in future antimalarial combination therapies.

A combination of DUB and 20s proteasome inhibitor can synergize with DHA

An alternative approach to alleviating antimalarial resistance is combination therapies that target multiple points within known resistance mediating pathways and/or novel antimalarial drug pathways to prevent the emergence of or overcome resistance. Therefore, we explored a combination of an upstream DUB inhibitor (b-AP15) and a 20s proteasome inhibitor (epoxomicin) with DHA in fixed ratio isobologram interactions. Firstly, we tested epoxomicin in combination with DHA as well as b-AP15 and epoxomicin in fixed ratios against PF. Epoxomicin improved DHA action mildly with an ΣFIC_{50} of 0.881 (Figure 3A) which corresponds with previously reported profiles.¹⁷ Interestingly, b-AP15 and epoxomicin as a combination alone was not an improved regimen with an ΣFIC_{50} of 1.162 (Figure 3B). This failure may result from a suppression mechanism where targeting the USP14 DUB upstream by b-AP15 (Figure 3D) would potentially counteract the activity of downstream 20s proteasome inhibitor and vice versa.⁴⁴ However, a 1:1 molar ratio of b-AP15 and epoxomicin when combined with DHA, an improved interaction with DHA (ΣFIC_{50} of 0.614) was achieved (Figure 3C) than by either of the drugs alone (Figure 3A, Supplementary Figure 3C). This illustrates that targeting the UPS at several points with the optimized inhibitor concentrations can significantly improve DHA efficacy.

Pre-incubation of malaria parasites with UPS inhibitors efficiently mediates DHA potentiation

A further way to combat drug resistance in malaria, which is being explored with antibiotics⁴⁵ and has been the case with cancer neo-adjuvant therapies, would be to pre-expose parasites to lethal or sub-lethal doses of inhibitors that target the resistance pathways before the main treatment course.

A targeted inhibition of the resistance conferring pathways might then in turn improve the activity of any downstream main treatment drug. Therefore, we investigated the effect of pre-exposing malaria parasites to DUB or 20s proteasome inhibitors on the short time exposure dose response profiles to DHA in both PB and PF. The PB 507 line, which expresses a green fluorescent protein (GFP) constitutively, was used to monitor GFP intensity across the life cycle after exposure to serial concentrations of DHA for 3 hours, administration of which followed prior exposure of the parasites (1.5 hour old rings) for 3 hours to IC_{50} concentrations of b-AP15. Quantification of the GFP fluorescent signal expressed from a constitutive promoter in PB would allow us to investigate the global dynamics of protein homeostasis, recycling, unfolding and or damage which occurs in the parasites upon exposure to DHA and or UPS inhibitors. Monitoring of GFP intensity at 6, 18 and 24 hours revealed that b-AP15 pre-exposure enhances the potency of DHA as indicated by significant abrogation of GFP intensity at all the time points (Figure 4A). Additional administration of b-AP15 after DHA incubation further abrogates GFP intensity illustrating that b-AP15 compromises UPS activity in tandem with DHA, which would make them suitable partner drugs. In the PF 3D7 line, pre-incubation of ~0-3 hour old rings with b-AP15 at IC_{50} or half IC_{50} for 3 hours followed by DHA treatment for 4 hours markedly impacts parasite viability (5 and 1.6 fold respectively) compared to DMSO exposed parasites, while pre-exposing the parasites to b-AP15 at 4x IC_{50} is almost entirely lethal to the parasites (Figure 4B). Meanwhile, pre-exposure of 3D7 or an ART resistant Kelch13 C580Y line to epoxomicin at IC_{50} or 0.2x IC_{50} followed by DHA also significantly impacted parasite viability (~4.6 and ~1.4 fold respectively) as compared to DMSO (Figure 4C, 4D). Remarkably, in both the 3D7 and ART resistant Kelch13 C580Y lines, a combination of b-AP15 and epoxomicin at half IC_{50} achieved better potency with DHA (18 and 33-fold respectively) compared to either of the drugs alone at IC_{50} (Figure 4B, 4C, 4D) further illustrating that targeting multiple UPS components (Figure 3C) could be a flexible approach to overcoming ART resistance.

b-AP15 fails to block parasite growth but potentiates ART action *in vivo*

We next investigated the ability of b-AP15 to block parasite growth *in vivo* and potentially enhance ART action. An analogue of b-AP15 (itself a lead first generation DUB inhibitor), VLX1570 entered clinical trials for the treatment of multiple myeloma (Wang et al., 2016), despite being later terminated due to dose ascending toxicities (NCT02372240). b-AP15 has strong antiproliferative effects in human cancer cell lines and has displayed significant antitumor activity at 5mg/kg in *in vivo* mouse models without any side effects.³⁴ However, in a Peters' 4 day suppressive test, b-AP15 fails to clear PB parasites *in vivo* at both 1mg/kg and 5mg/kg with only minor reductions in parasite

burdens on day 4 and 5 post treatment at the latter dose which corresponds to ~70% parasite suppression on day 4 (Figure 5A, 5B, 5C). Contrary to the previous reported safety profiles of b-AP15, ³⁴ mice (Theiler's Original) treated with 5mg/kg b-AP15 started to develop toxicity signs as demonstrated by significant weight loss on day 4 and 5 post-treatment. Further treatments at 5mg/kg or higher doses were thus not pursued. To investigate the ability of b-AP15 to potentiate ART action *in vivo*, b-AP15 was administered at 1mg/kg (a safe dose that did not have any effect on parasite growth alone, Figure 5A) in combination with ART at 5mg/kg and 10mg/kg in established mice infections at a parasitaemia of 2-2.5% for three consecutive days. A combination of ART (5mg/kg) and b-AP15 (1mg/kg) did not have any significant parasite reduction as compared to ART (5mg/kg) alone, while ART at 20mg/kg cleared the parasites after three consecutive doses as expected (Figure 5D). However, a combination of ART (10mg/kg) and b-AP15 (1mg/kg) significantly abrogated parasite burden as compared to ART (10mg/kg) alone to the same extent as ART at 20mg/kg (Figure 5E). These data further showed that b-AP15 can enhance ART action *in vivo*, to a similar extent as observed *in vitro*.

Discussion

With the increasing incidence of resistance to (even combinations of) antimalarial drugs by PF and the lack of rapidly amenable drug discovery programs for related *Plasmodium* spp. such as *P. vivax*, pipelines to develop new antimalarial drugs to treat the disease as well as improve the activity of current antimalarials and tackle resistance are urgently needed. Here, we report *in vitro* and *in vivo* activity of a class of compounds targeting the parasite upstream UPS component (DUBs) in PF and PB. Antimalarial drugs are typically discovered for their activity against PF *in vitro*. Lead compounds from PF *in vitro* screens are evaluated for *in vivo* efficacy using rodent malaria parasites which have been for a long time, crucial components of these drug discovery programs. ⁴⁶ PB is the most commonly used rodent model (in what is called the Peters' four-day suppressive test) and the development of methods that allow assessment of both *in vitro* drug sensitivity and *in vivo* efficacy in this model, ⁴⁷ as we demonstrate in this study, permits easy comparisons with PF *in vitro* efficacy data. Moreover, this provides crucial *in vitro* bridging information on whether potential drug efficacy discrepancies between PF *in vitro* and PB *in vivo* are due to pharmacokinetics of the drug or intrinsic differences in drug sensitivity between the *Plasmodium* spp. As a species of *Plasmodium* that is well diverged from both PF and other human-infectious *Plasmodium*, PB drug efficacy assessment also offers a useful comparative for other non-PF human causing *Plasmodium* spp. as chemical entities

that display PF inhibitory activity *in vitro* and PB inhibitory activity *in vitro* and *in vivo* are also likely to be active against other (human infectious) *Plasmodium* species.

Herein, activity is reported for six DUB inhibitors covering most of the DUB enzyme families and include b-AP15, P5091 and NSC632839 which specifically target USPs that all displayed antimalarial activity against both rodent and human malaria parasites *in vitro*. USPs are the largest family of DUBs comprising of up to 56 individual enzymes in humans.⁴⁸ However, since less is known of USPs in malaria parasites, with their current assignments largely based on *in silico* predictions,²⁶⁻²⁷ the precise targets of these drugs remain largely obscure. Human USP14 has been demonstrated to be the target of b-AP15³⁴ and its PF orthologue PfUSP14 (PF3D7_0527200) has been recently characterised and shown to bind the parasite 20s proteasome.³⁶ Moreover, purified PfUSP14 cleaves di-ubiquitin bonds in intact polyubiquitin chains illustrating functional identity of this *Plasmodium* DUB with its human counterpart.³⁶ This provides evidence that PfUSP14 may be specifically essential in parasite proliferation during the asexual blood cycle which was supported by a whole genome piggyBac saturation mutagenesis screen in which PfUSP14 was shown to be refractory to deletion (Supplementary Table 1).³⁹ Our data also support this in both PF and PB despite the PB counterpart (PBANKA_1242000) appearing to be dispensable in a recombinase mediated genetic screen.⁴⁰ The differences in essentiality could be due to functional differences between the two *Plasmodium* spp. USP14s. as they seem to share only ~62% sequence identity (Supplementary Figure 4). The activity of b-AP15 in both PF and PB however, at almost equivalent potencies, could thus be suggestive of possible suitable compensatory effects from other DUBs upon deletion in PB which is not sufficiently compensated for when an inhibitor is used. b-AP15 may also target other DUB (or possess off target) activities in *Plasmodium* as the inhibition of purified PfUSP14 by b-AP15 is less potent than its overall parasite killing potency.³⁶ Nevertheless, the observed structural difference between human USP14 and PfUSP14 at the core catalytic domain, its possible essentiality and the activity of b-AP15 in both PF and PB *in vitro* suggests that PfUSP14 can be selectively targeted throughout the *Plasmodium* genus.³⁶ Furthermore, the observed activity of other USP inhibitors, P5091 and NSC632839 in this study suggests that their targets are essential (Supplementary Table 1) during the asexual proliferation stages of malaria parasites and can serve as useful chemical leads for more potent antimalarial discovery. More importantly, b-AP15 possesses antiparasitic activity *in vivo* achieving up to 70% parasite suppression of PB at the highest concentrations that have been tested in cancer models.³⁴ Malaria parasites have been shown to rapidly replenish proteasomes in the presence of sub-lethal doses of proteasome inhibitors⁴⁹ which would possibly explain the observed inability of b-AP15 to completely block parasite growth at this

concentration as compared to control antimalarial drugs. Whilst promising, we noted issues with the reported safety profiles of b-AP15 at 5mg/kg³⁴ where mice significantly lost weight after 4 consecutive doses. This effect could be due to the combination of a chemical inhibitor and parasite challenge making the mice more susceptible to toxic effects of b-AP15, a phenomenon which has been previously reported with carfilzomib, a 20s proteasome inhibitor.⁴⁹ Meanwhile, the *in vitro* activity of broad-spectrum DUB inhibitors, PR-619 and WP1130 as well as a zinc chelating metalloprotease inhibitor (1, 10 phenanthroline) further alludes to the promise of DUBs as drug targets in malaria parasites.

A further striking finding was the inactivity of TCID (a UCH-L3 inhibitor) in both rodent and human malaria parasites. PfUCH-L3 has been well characterised in malaria parasites and has been shown to retain core deubiquitinating activity.⁴¹ Moreover, disruption of PfUCH-L3 by experimentally replacing the native enzyme with a catalytically dead form was shown to be lethal to the parasite.³⁸ The inactivity of TCID in both rodent and human malaria parasites reported here is therefore suggestive of striking differences between mammalian and *Plasmodium* UCH-L3s. Our sequence analysis demonstrated that PfUCH-L3 shares ~33% sequence identity with human UCH-L3 consistent with previous structural and molecular docking comparisons of PfUCH-L3 and human UCH-L3 which also revealed significant differences between the enzymes especially at the ubiquitin binding groove.³⁸ This makes PfUCH-L3 an even more attractive drug target for ultra-selectivity as it is also known to possess denedylating activities which are absent in mammalian UCH-L3s.⁴¹

Targeting the *Plasmodium* UPS is an emerging interventional point, not just as a potential drug target, but now also to curb emerging ART resistance. 20s proteasome inhibitors have been shown to enhance ART action in both ART sensitive and resistant lines.¹⁷⁻¹⁸ Our data in this study also show that upstream targeting of the UPS by some but by no means all DUB inhibitors can potentiate and enhance ART action in certain cases to a similar extent as 20s proteasome inhibitors. ARTs act by targeting several (possibly random) parasite proteins upon activation⁸⁻⁹ which necessitates, among other things, an upregulated UPS mediated stress response which rapidly recycles and clears damaged proteins henceforth promoting survival in ART resistant parasites.^{6, 13, 17} As with 20s proteasome inhibitors,¹⁷⁻¹⁸ inhibition of parasite UPS by targeting single or multiple DUBs simultaneously potentiates ART or DHA action. Inhibition of parasite UPS by b-AP15, for example, would prevent the normal protein homeostasis flux through the UPS, boosting the activity of pleiotropic ARTs by blocking the parasite stress and recovery system. Indeed, despite DHA being only additive in our isobole study with b-AP15, sublethal concentrations of b-AP15 can boost DHA activity

up to 15-fold. This boost is further enhanced when 2-3 DUB inhibitors at sub-lethal concentrations are combined as they improve DHA activity more than either inhibitors alone. This suggests that carefully titrated use of current DUB inhibitors in isolation, or simultaneously in mixtures may be a means to overcome ART resistance and the rodent model deployed here could be useful tool to optimise drug dosages. Indeed, recent findings have shown that accumulation of polyubiquitinated proteins in malaria parasites either by DUB or 20s proteasome inhibition is critical in activating the stress responses and contributes to DHA lethality in malaria parasites.¹³ The observed increase in ART efficacy when combined with DUB inhibitors which is of a similar level to that achieved by inhibition of the proteasome by epoxomicin *in vitro* and Carfilzomib *in vivo*¹⁷ further alludes to the potential of DUB inhibitors for achieving similar attributes in malaria parasites.

Indeed, whilst useful as independent potential antimalarial agents, DUB inhibitors show potential for partnership and this study demonstrated that different classes of DUBs can be targeted simultaneously to achieve better parasite killing while potentially minimising the resistance emergence window. More importantly, low and safe doses of b-AP15 with no effect on parasite growth alone significantly potentiated sub-curative dose of ART to almost curative levels *in vivo* providing a proof of concept that DUB inhibitors can enhance the activity of ARTs both *in vitro* and *in vivo* making them potential adjunct drugs to enhance ART action and tackle resistance. Similarly, other potential radical ways of overcoming resistance in malaria parasites would be combining drugs with different mode of actions in complex combinations or using multiple (different) first line combinational therapies at once to raise the probability barrier of developing resistance by simultaneously targeting several pathways.⁵⁰ Our data exemplify this concept, as for example when b-AP15 and epoxomicin are combined in a fixed ratio isobole analysis, their appears to be no interaction or possibly even an antagonistic effect. This observation would be symptomatic of an antagonistic suppression mechanism where the activity of two inhibitors in the same pathway upstream or downstream negatively feeds back to the activity of the other leading to counteractive effects. However, when b-AP15 and epoxomicin are mixed in equal concentration ratios and combined with DHA, their overall activity achieves a better efficacy with DHA than either of the inhibitors alone. The optimal simultaneous exposure of the parasite UPS to DUBs and 20s proteasome inhibitors could thus act as an additional opportunity to overcome resistance to ARTs if the parasites would acquire resistance mutations to either of the UPS inhibitors. This has indeed been recently illustrated where combined inhibition of the parasite $\beta 2$ and $\beta 5$ subunits of the parasites UPS has been shown to strongly synergize DHA activity.⁵¹

In conclusion, our work confirms DUBs as potential druggable candidates in malaria parasites. Drug discovery programs take a long time, with for example a minimum of five years required to take a lead compound to a clinical candidate in malaria.⁵²⁻⁵³ The emergent resistance to ACTs, a paucity in the number of antimalarial drugs in the developmental pipeline and a lack of scalable pipelines for drug discovery in other human malaria parasites such as *P. vivax* and *P. ovale*,⁵³ all necessitates both radical as well as alternative approaches to identify new drugs and drug targets. As DUBs are already being actively explored as anticancer agents with candidate inhibitors already entering clinical trials,⁵⁴ antimalarial drug discovery programs could take advantage to structurally improve or re-purpose such entities not just as potential drug targets in malaria, but also as combinational partners to ARTs to overcome the spectre of resistance.

Materials and methods

Parasite lines

Experiments in PB were carried out in an 820 line that expresses green fluorescent protein (GFP) and red fluorescent protein (RFP) in male and female gametocytes respectively, and a 507 line that constitutively expresses GFP under the control of the Pbeef1α promoter. Generation and characterisation of the 820 and 507 lines has been previously described.⁵⁵⁻⁵⁶ Growth inhibitory experiments in PF were performed in the CQ and ART sensitive 3D7 line and the ART resistant Cambodian Kelch13 C580Y mutant line (a kind gift from D. Fidock).

Drugs and inhibitors

DHA (Selleckchem) was prepared at 1mM stock concentration in 100% DMSO and diluted to working concentration in complete (PF) or schizont media (PB). ART (Sigma) and Epoxomicin (Sigma) were dissolved in 100% DMSO to stock concentrations of 100 μM and 90μM respectively and diluted in complete culture media or schizont culture media to their respective working concentrations. CQ diphosphate (Sigma) was dissolved to stock concentration of 10 mM in 1X phosphate buffered saline (PBS) and diluted to working concentration in complete or schizont culture media. Seven different classes of DUB inhibitors (Table 1) were screened and were all obtained from Focus Biomolecules except for 1, 10 phenanthroline which was obtained from BPS biosciences. Stocks of DUB inhibitors were prepared at 10 mM in 100% DMSO and diluted in complete or schizont media to working concentrations. Testing concentrations ranged from 2000-0.01nM for epoxomicin, DHA, ART and CQ and 100-0.002μM for DUB inhibitors. All DUB inhibitors were supplied at a purity grade of >97% (Supplementary Table 2) and further analysed for chemical integrity on a High-Performance Liquid

Chromatography (HPLC) platform (Supplementary Table 3, Supplementary Figure 5) as detailed below.

HPLC analysis of DUB inhibitors

HPLC solvents were purchased from standard suppliers and used without additional purification. DUB inhibitors were analysed on a Shimadzu reverse-phase HPLC (RP-HPLC) system equipped with Shimadzu LC-20AT pumps, a SIL-20A auto sampler and a SPD-20A UV-vis detector (monitoring at 254 nm) using a Phenomenex, Aeris, 5 µm, peptide XB-C18, 150 x 4.6 mm column at a flow rate of 1 mL/min. RP-HPLC gradients were run using a solvent system consisting of solution A (H₂O + 0.1% trifluoroacetic acid) and B (acetonitrile + 0.1% trifluoroacetic acid). Further gradient analyses were run from 0% to 100% using solution B over 20 minutes. Analytical RP-HPLC data was reported as column retention time in minutes. Percentage purity was quantified by percentage peak area in relation to main peak.

PB animal infections

PB parasites were maintained in female Theiler's Original (TO) mice (Envigo) weighing between 25-30g. Parasite infections were established either by IP of ~200µl of cryopreserved parasite stocks or intravenous injections (IVs) of purified schizonts. For infections from a donor infected mouse (mechanical passage), 5-30µl of infected blood was diluted in phosphate buffered saline (PBS) followed by injections of 100-200µl by IP. Since PB preferentially invades reticulocytes,⁵⁷ mice were pre-treated with 100µl of phenylhydrazine at 12.5mg/ml in physiological saline 2 days before the infections to induce reticulocytosis for some experiments. Routine monitoring of parasitaemia in infected mice was done by monitoring methanol fixed thin blood smears stained in Giemsa (Sigma) or flow cytometry analysis of infected blood stained with Hoescht 33342 (Invitrogen). Blood from infected mice was collected by cardiac puncture under terminal anaesthesia. All animal work was approved by the University of Glasgow's Animal Welfare and Ethical Review Body and by the UK's Home Office (PPL 60/4443) and carried out by appropriately licenced individuals. The animal care and use protocol complied with the UK Animals (Scientific Procedures) Act 1986 as amended in 2012 and with European Directive 2010/63/EU on the Protection of Animals Used for Scientific Purposes.

PB *in vitro* culture and drug susceptibility assays

For *in vitro* maintenance of PB, cultures were maintained for one developmental cycle using a standardised schizont culture media containing RPMI1640 with 25mM hypoxanthine, 10mM sodium bicarbonate, 20 % fetal calf serum, 100U/ml Penicillin and 100µg/ml streptomycin. Culture flasks

were gassed for 30 seconds with a special gas mix of 5% CO₂, 5% O₂, 90% N₂ and incubated for 22-24 hours at 37°C with gentle shaking, conditions that allow for development of ring stage parasites to mature schizonts. Drug assays to determine *in vitro* growth inhibition during the intraerythrocytic stage were performed in these standard short-term cultures as previously described.²⁹⁻³⁰ Briefly, 1 ml of infected blood with a non-synchronous parasitaemia of 3-5% was collected from an infected mouse and cultured for 22-24 hours in 120 ml of schizont culture media. Schizonts were enriched from the cultures by Nycodenz density flotation as previously described⁵⁸ followed by immediate injection into a tail vein of a naive mouse. Upon IV injection of schizonts, they immediately rupture with resulting merozoites invading new red blood cells within minutes to obtain synchronous *in vivo* infection containing >90% rings and a parasitaemia of 1-2%. Blood was collected from the infected mice 2 hours post injection and mixed with serially diluted drugs in schizont culture media in 96 well plates at a final haematocrit of 0.5% in a 200µl well volume. Plates were gassed and incubated overnight at 37°C. After 22-24 hours of incubation, schizont maturation was analysed by flow cytometry after staining the infected cells with DNA dye Hoechst-33258. Schizonts were gated and quantified based on fluorescence intensity on a BD FACSCelesta or a BD LSR Fortessa (BD Biosciences, USA). To determine growth inhibitions and calculate IC₅₀, quantified schizonts in no drug controls were set to correspond to 100% with subsequent growth percentages in presence of drugs calculated accordingly. Dose response curves were plotted in Graph-pad Prism.

PF culture and the SYBR Green I® assay for parasite growth inhibition

PF 3D7 or C580Y lines were cultured and maintained at 1-5% parasitaemia in fresh group O-positive red blood cells re-suspended to a 5% haematocrit in custom reconstituted RPMI 1640 complete media (Thermo Scientific) containing 0.23% sodium bicarbonate, 0.4% D-glucose, 0.005% hypoxanthine 0.6% Hepes, 0.5% Albumax II, 0.03% L-glutamine and 25mg/L gentamicin. Culture flasks were gassed with a mixture of 1% O₂, 5% CO₂, and 94% N₂ and incubated at 37°C. Prior to the start of the experiments, asynchronous stock cultures containing mainly ring stages were synchronised with 5% sorbitol as previously described.⁵⁹ Parasitaemia was determined with drug assays performed when the parasitaemia was between 1.5-5% with >90% rings. The stock culture was diluted to a haematocrit of 4% and 0.3% parasitaemia in complete media following which 50µl was mixed with 50µl of serial diluted drugs/inhibitors in complete media pre-dispensed in black 96 well optical culture plates (Thermo scientific) for a final haematocrit of 2%. Plates were gassed and incubated at 37°C for 72 hours followed by freezing at -20°C for at least 24 hours. The plate setup also included no drug controls as well as uninfected red cells at 2% haematocrit. After 72 hours of incubation and at least overnight freezing at -20°C, plates were thawed at room temperature for ~4

hours. This was followed by addition of 100µl to each well of 1X SYBR Green I® (Invitrogen) lysis buffer containing 20 mM Tris, 5 mM EDTA, 0.008% saponin and 0.08% Triton X-100. Plate contents were mixed thoroughly by shaking at 700 rpm for 5 minutes and incubated for 1 hour at room temperature in the dark. After incubation, plates were read to quantify SYBR Green I® fluorescence intensity in each well by a PHERAstar® FSX microplate reader (BMG Labtech) with excitation and emission wavelengths of 485 and 520nm respectively. To determine growth inhibition, background fluorescence intensity from uninfected red cells was subtracted first. Fluorescence intensity of no drug controls was then set to correspond to 100% and subsequent intensity in presence of drug/inhibitor was calculated accordingly. Dose response curves and IC₅₀ concentrations were plotted in Graph-pad Prism 7. Human blood was obtained and used within the ethical remit of the Scottish National Blood Transfusion Service.

***In vitro* drug combinations**

Parasites were maintained and cultivated as described above. To determine drug interactions of DHA in combination with DUB or proteasome inhibitors, serial dilutions of DHA were mixed with fixed ratios of epoxomicin, b-AP15, PR-619 and WP1130 or their fractional combinations at their respective IC₅₀s or half IC₅₀s. The drug combinations were incubated with parasites from which parasite growth was quantified and dose response curves were plotted, for DHA alone or in combination with the fixed doses of the DUB or proteasome inhibitors. IC₅₀ values were obtained and the fold change or IC₅₀ shifts were plotted in Graph-pad Prism using the extra sum of squares F-test for statistical comparison. For drug interactions in fixed ratios, a modified fixed ratio interaction assay was employed as previously described.⁶⁰ Drug combinations were prepared in six distinct molar concentration combination ratios; 5:0, 4:1, 3:2, 2:3 1:4, 0:5 and dispensed in top wells of 96-well plates. This was followed by a 2 or 3-fold serial dilution with precisely pre-calculated estimates that made sure that the IC₅₀ of individual drugs falls to the middle of the plate. The drug combinations were then incubated with parasites from which parasite growth and dose response curves were calculated for each drug alone or in combination. Fractional inhibitory concentrations (FIC₅₀) were obtained for drugs in combination and summed to obtain the ΣFIC₅₀ using the formula below:

$$\Sigma FIC_{50} = (IC_{50} \text{ of drug A in combination} / IC_{50} \text{ of drug A alone}) + (IC_{50} \text{ of drug B in combination} / IC_{50} \text{ of drug B alone}).$$

An ΣFIC₅₀ of >4 was used to denote antagonism, ΣFIC₅₀ ≤0.5 synergism and ΣFIC₅₀ = 0.5-4 additivity.⁶¹ FIC₅₀ for the drug combinations were plotted to obtain isobolograms for the drug combination ratios.

PF viability assays

The 3D7 line was synchronised with 5% sorbitol over three life cycles followed by Nycodenz enrichment of later schizonts. Enriched schizonts were incubated with fresh red blood cells in a shaking incubator for 3 hours followed by another round of sorbitol treatment to eliminate residual late stage parasites. Resultant ring cultures were diluted to around ~1% parasitaemia and incubated with predefined drug combinations for set time periods. Drugs were washed off 3 times after the set incubation times. Parasite viability was assessed 66 hours later in cycle 2 by flow cytometry analysis of parasite cultures stained with Syber Green I and MitoTracker Deep Red dyes (Invitrogen). Flow cytometry analysis was carried on a MACSQuant® Analyzer 10.

In vivo anti-parasitic activity of DUB inhibitors

To evaluate the activity of DUB inhibitors (b-AP15) *in vivo*, the Peters' 4 day suppressive test was initially employed as previously described.⁶² Stock concentrations of b-AP15 were prepared at 3mg/ml and 1mg/ml in a 1:1 mixture of DMSO and Tween® 80 (Sigma) followed by a 10-fold dilution to stock working concentrations (5% DMSO and Tween® 80 final) in sterile distilled water. CQ was prepared at 50mg/ml in 1X PBS and diluted to working stock in 1X PBS. A donor mouse was initially infected with PB 820 line from which blood was obtained when the parasitaemia was between 2-5%. Donor blood was diluted in rich PBS following which ~10⁵ parasites were inoculated by IP into four mice groups (3 mice per group). 1-hour post infection, mice groups received drug doses by IP injection as follows: group 1 (vehicle; 5% DMSO & Tween® 80), group 2 (CQ; 20mg/kg), group 3 (b-AP15; 1mg/kg) and group 4 (5mg/kg) for 4 consecutive days. Parasitaemia was monitored daily by flow cytometry analysis of infected cells stained with Hoechst-33258 and microscopic analysis of methanol fixed Giemsa stained smears. To evaluate the potential synergy of b-AP15 and ART *in vivo*, a modified Rane's curative test in established infections was used.⁶³ Blood was obtained from a donor mouse at a parasitaemia of 2-3% and diluted in rich PBS. Seventeen mice were inoculated with ~10⁵ parasites by IP on day 0 allowing the parasitaemia to rise to ~2-2.5%, typically on day 4. Following the establishment of infection, mice were divided into five groups and received drug doses as follows: group 1 (5mg/kg ART n=3), group 2 (10mg/kg ART, n=3), group 3 (20mg/kg ART n=3), group 4 (5mg/kg ART + 1mg/kg b-AP15, n=4), group 5 (10mg/kg ART + 1mg/kg b-AP15, n=4). ART and b-AP15 were prepared at 12.5mg/ml and 1mg/ml respectively in 1:1 mixture of DMSO and Tween® 80 and diluted 10-fold (final 5% DMSO and Tween® 80) to their respective working concentrations. Parasitaemia was monitored daily by flow cytometry and analysis of methanol fixed Giemsa stained smears.

Acknowledgments

We thank Mathias Matti for meaningful discussions; Steve Ward at Liverpool School of Tropical Medicine for suggestions and carefully reading the manuscript; Diane Vaughan and the iii-flow cytometry facility for technical assistance. We also thank Amit Mahindra and Andrew Jamieson at the University of Glasgow School of Chemistry for HPLC analysis of the DUB inhibitors. This work was supported by grants from the Wellcome Trust to A.P.W (083811/Z/07/Z; 107046/Z/15/Z). M.P.B. and APW are funded by a Wellcome Trust core grant to the Wellcome Centre for Integrative Parasitology (104111/Z/14/Z). N.V.S is a Commonwealth Doctoral Scholar (MWCS-2017-789), funded by the UK government.

Author contributions

N.V.S conceived the experiments, performed data curation, analysis, investigation, validation, visualisation and writing of original draft. K.R.H, M.T.R and M.P.B participated in formal data analysis, investigation, validation, review and editing. A.P.W conceived the study, experiments, analysis, investigation, validation, writing of original draft, review, editing and supervision.

References

1. WHO 2019. World Malaria Report; World Health organisation: Geneva, Switzerland.
2. WHO 2018. World Malaria Report; World Health organisation: Geneva, Switzerland.
3. Okell, L. C.; Drakeley, C. J.; Ghani, A. C.; Bousema, T.; Sutherland, C. J., Reduction of transmission from malaria patients by artemisinin combination therapies: a pooled analysis of six randomized trials. (2008) *Malar. J.* **7**, 125-125.
4. Cui, L.; Mharakurwa, S.; Ndiaye, D.; Rathod, P. K.; Rosenthal, P. J., Antimalarial Drug Resistance: Literature Review and Activities and Findings of the ICEMR Network. (2015) *Am. J. Trop. Med. Hyg.* **93** (3 Suppl), 57-68.
5. Dondorp, A. M.; Nosten, F.; Yi, P.; Das, D.; Phyo, A. P.; Tarning, J.; Lwin, K. M.; Arie, F.; Hanpithakpong, W.; Lee, S. J.; Ringwald, P.; Silamut, K.; Imwong, M.; Chotivanich, K.; Lim, P.; Herdman, T.; An, S. S.; Yeung, S.; Singhasivanon, P.; Day, N. P. J.; Lindegardh, N.; Socheat, D.; White, N. J., Artemisinin Resistance in *Plasmodium falciparum* Malaria. (2009) *N. Engl. J. Med.* **361** (5), 455-467.
6. Tilley, L.; Straimer, J.; Gnädig, N. F.; Ralph, S. A.; Fidock, D. A., Artemisinin action and resistance in *Plasmodium falciparum*. (2016) *Trends Parasitol.* **32** (9), 682-696.
7. Haldar, K.; Bhattacharjee, S.; Safeukui, I., Drug resistance in *Plasmodium*. (2018) *Nat. Rev. Microbiol.* **16** (3), 156-170.

- 669 8. Wang, J.; Zhang, C. J.; Chia, W. N.; Loh, C. C.; Li, Z.; Lee, Y. M.; He, Y.; Yuan, L. X.; Lim, T. K.; Liu, M.;
670 Liew, C. X.; Lee, Y. Q.; Zhang, J.; Lu, N.; Lim, C. T.; Hua, Z. C.; Liu, B.; Shen, H. M.; Tan, K. S.; Lin, Q.,
671 Haem-activated promiscuous targeting of artemisinin in *Plasmodium falciparum*. (2015) Nat.
672 Commun. **6**, 10111.
- 673 9. Ismail, H. M.; Barton, V.; Phanchana, M.; Charoensutthivarakul, S.; Wong, M. H.; Hemingway, J.;
674 Biagini, G. A.; O'Neill, P. M.; Ward, S. A., Artemisinin activity-based probes identify multiple
675 molecular targets within the asexual stage of the malaria parasites *Plasmodium falciparum* 3D7.
676 (2016) Proc. Natl. Acad. Sci. U. S. A. **113** (8), 2080-5.
- 677 10. Mbengue, A.; Bhattacharjee, S.; Pandharkar, T.; Liu, H.; Estiu, G.; Stahelin, R. V.; Rizk, S. S.;
678 Njimoh, D. L.; Ryan, Y.; Chotivanich, K.; Nguon, C.; Ghorbal, M.; Lopez-Rubio, J. J.; Pfrender, M.;
679 Emrich, S.; Mohandas, N.; Dondorp, A. M.; Wiest, O.; Haldar, K., A molecular mechanism of
680 artemisinin resistance in *Plasmodium falciparum* malaria. (2015) Nature **520** (7549), 683-7.
- 681 11. Birnbaum, J.; Scharf, S.; Schmidt, S.; Jonscher, E.; Hoeijmakers, W. A. M.; Flemming, S.; Toenhake,
682 C. G.; Schmitt, M.; Sabitzki, R.; Bergmann, B.; Fröhlke, U.; Mesén-Ramírez, P.; Blancke Soares, A.;
683 Herrmann, H.; Bártfai, R.; Spielmann, T., A Kelch13-defined endocytosis pathway mediates
684 artemisinin resistance in malaria parasites. (2020) Science **367** (6473), 51.
- 685 12. Yang, T.; Yeoh, L. M.; Tutor, M. V.; Dixon, M. W.; McMillan, P. J.; Xie, S. C.; Bridgford, J. L.; Gillett,
686 D. L.; Duffy, M. F.; Ralph, S. A.; McConville, M. J.; Tilley, L.; Cobbold, S. A., Decreased K13 Abundance
687 Reduces Hemoglobin Catabolism and Proteotoxic Stress, Underpinning Artemisinin Resistance.
688 (2019) Cell Rep. **29** (9), 2917-2928.e5.
- 689 13. Bridgford, J. L.; Xie, S. C.; Cobbold, S. A.; Pasaje, C. F. A.; Herrmann, S.; Yang, T.; Gillett, D. L.; Dick,
690 L. R.; Ralph, S. A.; Dogovski, C.; Spillman, N. J.; Tilley, L., Artemisinin kills malaria parasites by
691 damaging proteins and inhibiting the proteasome. (2018) Nat. Commun. **9** (1), 3801.
- 692 14. Mok, S.; Ashley, E. A.; Ferreira, P. E.; Zhu, L.; Lin, Z.; Yeo, T.; Chotivanich, K.; Imwong, M.;
693 Pukrittayakamee, S.; Dhorda, M.; Nguon, C.; Lim, P.; Amaratunga, C.; Suon, S.; Hien, T. T.; Htut, Y.;
694 Faiz, M. A.; Onyamboko, M. A.; Mayxay, M.; Newton, P. N.; Tripura, R.; Woodrow, C. J.; Miotto, O.;
695 Kwiatkowski, D. P.; Nosten, F.; Day, N. P.; Preiser, P. R.; White, N. J.; Dondorp, A. M.; Fairhurst, R. M.;
696 Bozdech, Z., Drug resistance. Population transcriptomics of human malaria parasites reveals the
697 mechanism of artemisinin resistance. (2015) Science **347** (6220), 431-5.
- 698 15. Siddiqui, F. A.; Boonhok, R.; Cabrera, M.; Mbenda, H. G. N.; Wang, M.; Min, H.; Liang, X.; Qin, J.;
699 Zhu, X.; Miao, J.; Cao, Y.; Cui, L., Role of *Plasmodium falciparum* Kelch 13 Protein Mutations in P.
700 falciparum Populations from Northeastern Myanmar in Mediating Artemisinin Resistance. (2020)
701 mBio **11** (1), e01134-19.
- 702 16. Gnädig, N. F.; Stokes, B. H.; Edwards, R. L.; Kalantarov, G. F.; Heimsch, K. C.; Kuderjavy, M.; Crane,
703 A.; Lee, M. C. S.; Straimer, J.; Becker, K.; Trakht, I. N.; Odom John, A. R.; Mok, S.; Fidock, D. A.,
704 Insights into the intracellular localization, protein associations and artemisinin resistance properties
705 of *Plasmodium falciparum* K13. (2020) PLoS Pathog. **16** (4), e1008482-e1008482.
- 706 17. Dogovski, C.; Xie, S. C.; Burgio, G.; Bridgford, J.; Mok, S.; McCaw, J. M.; Chotivanich, K.; Kenny, S.;
707 Gnädig, N.; Straimer, J.; Bozdech, Z.; Fidock, D. A.; Simpson, J. A.; Dondorp, A. M.; Foote, S.; Klonis,
708 N.; Tilley, L., Targeting the cell stress response of *Plasmodium falciparum* to overcome artemisinin
709 resistance. (2015) PLoS Biol. **13** (4), e1002132.

- 710 18. Li, H.; O'Donoghue, A. J.; van der Linden, W. A.; Xie, S. C.; Yoo, E.; Foe, I. T.; Tilley, L.; Craik, C. S.;
711 da Fonseca, P. C. A.; Bogyo, M., Structure- and function-based design of *Plasmodium*-selective
712 proteasome inhibitors. (2016) *Nature* **530**, 233.
- 713 19. Henrici, R. C.; van Schalkwyk, D. A.; Sutherland, C. J., Modification of pfap2 μ and pfubp1
714 Markedly Reduces Ring-Stage Susceptibility of *Plasmodium falciparum* to Artemisinin *In Vitro*. (2019)
715 *Antimicrob. Agents Chemother.* **64** (1), e01542-19.
- 716 20. Simwela, N. V.; Hughes, K. R.; Roberts, A. B.; Rennie, M. T.; Barrett, M. P.; Waters, A. P.,
717 Experimentally Engineered Mutations in a Ubiquitin Hydrolase, UBP-1, Modulate *In Vivo*
718 Susceptibility to Artemisinin and Chloroquine in *Plasmodium berghei*. (2020) *Antimicrob. Agents*
719 *Chemother.* **64** (7), e02484-19.
- 720 21. Hunt, P.; Afonso, A.; Creasey, A.; Culleton, R.; Sidhu, A. B.; Logan, J.; Valderramos, S. G.; McNae,
721 I.; Cheesman, S.; do Rosario, V.; Carter, R.; Fidock, D. A.; Cravo, P., Gene encoding a deubiquitinating
722 enzyme is mutated in artesunate- and chloroquine-resistant rodent malaria parasites. (2007) *Mol.*
723 *Microbiol.* **65** (1), 27-40.
- 724 22. Soave, C. L.; Guerin, T.; Liu, J.; Dou, Q. P., Targeting the ubiquitin-proteasome system for cancer
725 treatment: discovering novel inhibitors from nature and drug repurposing. (2017) *Cancer. Metastasi*
726 *Rev.* **36** (4), 717-736.
- 727 23. Ng, C. L.; Fidock, D. A.; Bogyo, M., Protein Degradation Systems as Antimalarial Therapeutic
728 Targets. (2017) *Trends Parasitol.* **33** (9), 731-743.
- 729 24. Lecker, S. H.; Goldberg, A. L.; Mitch, W. E., Protein degradation by the ubiquitin-proteasome
730 pathway in normal and disease states. (2006) *J. Am. Soc. Nephrol.* **17** (7), 1807-19.
- 731 25. Hanpude, P.; Bhattacharya, S.; Dey, A. K.; Maiti, T. K., Deubiquitinating enzymes in cellular
732 signaling and disease regulation. (2015) *IUBMB Life* **67** (7), 544-555.
- 733 26. Ponder, E. L.; Bogyo, M., Ubiquitin-Like Modifiers and Their Deconjugating Enzymes in Medically
734 Important Parasitic Protozoa. (2007) *Eukaryotic Cell* **6** (11), 1943-1952.
- 735 27. Ponts, N.; Saraf, A.; Chung, D. W.; Harris, A.; Prudhomme, J.; Washburn, M. P.; Florens, L.; Le
736 Roch, K. G., Unraveling the ubiquitome of the human malaria parasite. (2011) *J. Biol. Chem.* **286** (46),
737 40320-30.
- 738 28. Aminake, M. N.; Arndt, H. D.; Pradel, G., The proteasome of malaria parasites: A multi-stage drug
739 target for chemotherapeutic intervention? (2012) *Int. J. Parasitol. Drugs. Drug .Resist.* **2**, 1-10.
- 740 29. Franke-Fayard, B.; Djokovic, D.; Dooren, M. W.; Ramesar, J.; Waters, A. P.; Falade, M. O.;
741 Kranendonk, M.; Martinelli, A.; Cravo, P.; Janse, C. J., Simple and sensitive antimalarial drug
742 screening *in vitro* and *in vivo* using transgenic luciferase expressing *Plasmodium berghei* parasites.
743 (2008) *Int. J. Parasitol.* **38** (14), 1651-62.
- 744 30. Janse, C. J.; Waters, A. P.; Kos, J.; Lugt, C. B., Comparison of *in vivo* and *in vitro* antimalarial
745 activity of artemisinin, dihydroartemisinin and sodium artesunate in the *Plasmodium berghei*-rodent
746 model. (1994) *Int. J. Parasitol.* **24** (4), 589-94.
- 747 31. Kreidenweiss, A.; Kremsner, P. G.; Mordmüller, B., Comprehensive study of proteasome
748 inhibitors against *Plasmodium falciparum* laboratory strains and field isolates from Gabon. (2008)
749 *Malar. J.* **7**, 187-187.

- 750 32. Bhattacharya, A.; Mishra, L. C.; Bhasin, V. K., *In vitro* activity of artemisinin in combination with
751 clotrimazole or heat-treated amphotericin B against *Plasmodium falciparum*. (2008) Am. J. Trop.
752 Med. Hyg. **78** (5), 721-8..
- 753 33. Chauhan, D.; Tian, Z.; Nicholson, B.; Kumar, K. G.; Zhou, B.; Carrasco, R.; McDermott, J. L.; Leach,
754 C. A.; Fulciniti, M.; Kodrasov, M. P.; Weinstock, J.; Kingsbury, W. D.; Hideshima, T.; Shah, P. K.;
755 Minvielle, S.; Altun, M.; Kessler, B. M.; Orlowski, R.; Richardson, P.; Munshi, N.; Anderson, K. C., A
756 small molecule inhibitor of ubiquitin-specific protease-7 induces apoptosis in multiple myeloma cells
757 and overcomes bortezomib resistance. (2012) Cancer Cell **22** (3), 345-58.
- 758 34. D'Arcy, P.; Brnjic, S.; Olofsson, M. H.; Fryknas, M.; Lindsten, K.; De Cesare, M.; Perego, P.;
759 Sadeghi, B.; Hassan, M.; Larsson, R.; Linder, S., Inhibition of proteasome deubiquitinating activity as a
760 new cancer therapy. (2011) Nat. Med. **17** (12), 1636-40.
- 761 35. Nicholson, B.; Leach, C. A.; Goldenberg, S. J.; Francis, D. M.; Kodrasov, M. P.; Tian, X.; Shanks, J.;
762 Sterner, D. E.; Bernal, A.; Mattern, M. R.; Wilkinson, K. D.; Butt, T. R., Characterization of ubiquitin
763 and ubiquitin-like-protein isopeptidase activities. (2008) Protein Sci. **17** (6), 1035-43.
- 764 36. Wang, L.; Delahunty, C.; Fritz-Wolf, K.; Rahlfs, S.; Helena Prieto, J.; Yates, J. R.; Becker, K.,
765 Characterization of the 26S proteasome network in *Plasmodium falciparum*. (2015) Sci. Rep. **5**,
766 17818.
- 767 37. Artavanis-Tsakonas, K.; Misaghi, S.; Comeaux, C. A.; Catic, A.; Spooner, E.; Duraisingh, M. T.;
768 Ploegh, H. L., Identification by functional proteomics of a deubiquitinating/deNeddylating enzyme in
769 *Plasmodium falciparum*. (2006) Mol. Microbiol. **61** (5), 1187-95.
- 770 38. Artavanis-Tsakonas, K.; Weihofen, W. A.; Antos, J. M.; Coleman, B. I.; Comeaux, C. A.; Duraisingh,
771 M. T.; Gaudet, R.; Ploegh, H. L., Characterization and Structural Studies of the *Plasmodium*
772 *falciparum* Ubiquitin and Nedd8 Hydrolase UCHL3. (2010) J. Biol. Chem. **285** (9), 6857-6866.
- 773 39. Zhang, M.; Wang, C.; Otto, T. D.; Oberstaller, J.; Liao, X.; Adapa, S. R.; Udenze, K.; Bronner, I. F.;
774 Casandra, D.; Mayho, M.; Brown, J.; Li, S.; Swanson, J.; Rayner, J. C.; Jiang, R. H. Y.; Adams, J. H.,
775 Uncovering the essential genes of the human malaria parasite *Plasmodium falciparum* by saturation
776 mutagenesis. (2018) Science **360** (6388).
- 777 40. Bushell, E.; Gomes, A. R.; Sanderson, T.; Anar, B.; Girling, G.; Herd, C.; Metcalf, T.; Modrzynska,
778 K.; Schwach, F.; Martin, R. E.; Mather, M. W.; McFadden, G. I.; Parts, L.; Rutledge, G. G.; Vaidya, A. B.;
779 Wengelnik, K.; Rayner, J. C.; Billker, O., Functional Profiling of a *Plasmodium* Genome Reveals an
780 Abundance of Essential Genes. (2017) Cell **170** (2), 260-272.e8.
- 781 41. Frickel, E. M.; Quesada, V.; Muething, L.; Gubbels, M. J.; Spooner, E.; Ploegh, H.; Artavanis-
782 Tsakonas, K., Apicomplexan UCHL3 retains dual specificity for ubiquitin and Nedd8 throughout
783 evolution. (2007) Cell. Microbiol. **9** (6), 1601-10.
- 784 42. Liu, Y.; Lashuel, H. A.; Choi, S.; Xing, X.; Case, A.; Ni, J.; Yeh, L. A.; Cuny, G. D.; Stein, R. L.;
785 Lansbury, P. T., Jr., Discovery of inhibitors that elucidate the role of UCH-L1 activity in the H1299 lung
786 cancer cell line. (2003) Chem. Biol. **10** (9), 837-46.
- 787 43. Lee, R. S.; Waters, A. P.; Brewer, J. M., A cryptic cycle in haematopoietic niches promotes
788 initiation of malaria transmission and evasion of chemotherapy. (2018) Nat. Commun. **9** (1), 1689.
- 789 44. Yeh, P. J.; Hegreness, M. J.; Aiden, A. P.; Kishony, R., Drug interactions and the evolution of
790 antibiotic resistance. (2009) Nat. Rev. Microbiol. **7** (6), 460-466.

- 791 45. Tyers, M.; Wright, G. D., Drug combinations: a strategy to extend the life of antibiotics in the 21st
792 century. (2019) Nat. Rev. Microbiol. **17** (3), 141-155.
- 793 46. Fidock, D. A.; Rosenthal, P. J.; Croft, S. L.; Brun, R.; Nwaka, S., Antimalarial drug discovery:
794 efficacy models for compound screening. (2004) Nat. Rev. Drug .Discov. **3** (6), 509-520.
- 795 47. Janse, C. J.; Waters, A. P., *Plasmodium berghei*: The application of cultivation and purification
796 techniques to molecular studies of malaria parasites. (1995) Parasitol. Today **11** (4), 138-143.
- 797 48. Davis, M. I.; Simeonov, A., Ubiquitin-Specific Proteases as Druggable Targets. (2015) Drug. Targ.
798 Rev. **2** (3), 60-64.
- 799 49. Li, H.; Ponder, E. L.; Verdoes, M.; Asbjornsdottir, K. H.; Deu, E.; Edgington, L. E.; Lee, J. T.; Kirk, C.
800 J.; Demo, S. D.; Williamson, K. C.; Bogyo, M., Validation of the proteasome as a therapeutic target in
801 *Plasmodium* using an epoxyketone inhibitor with parasite-specific toxicity. (2012) Chem. Biol. **19**
802 (12), 1535-1545.
- 803 50. Boni, M. F.; White, N. J.; Baird, J. K., The Community As the Patient in Malaria-Endemic Areas:
804 Preempting Drug Resistance with Multiple First-Line Therapies. (2016) PLoS Med. **13** (3), e1001984-
805 e1001984.
- 806 51. Kirkman, L. A.; Zhan, W.; Visone, J.; Dziedziech, A.; Singh, P. K.; Fan, H.; Tong, X.; Bruzual, I.; Hara,
807 R.; Kawasaki, M.; Imaeda, T.; Okamoto, R.; Sato, K.; Michino, M.; Alvaro, E. F.; Guiang, L. F.; Sanz, L.;
808 Mota, D. J.; Govindasamy, K.; Wang, R.; Ling, Y.; Tumwebaze, P. K.; Sukenick, G.; Shi, L.; Vendome, J.;
809 Bhanot, P.; Rosenthal, P. J.; Aso, K.; Foley, M. A.; Cooper, R. A.; Kafsack, B.; Doggett, J. S.; Nathan, C.
810 F.; Lin, G., Antimalarial proteasome inhibitor reveals collateral sensitivity from intersubunit
811 interactions and fitness cost of resistance. (2018) Proc. Natl. Acad. Sci. U. S. A. **115** (29), E6863-
812 E6870.
- 813 52. Lotharius, J.; Gamo-Benito, F. J.; Angulo-Barturen, I.; Clark, J.; Connelly, M.; Ferrer-Bazaga, S.;
814 Parkinson, T.; Viswanath, P.; Bandodkar, B.; Rautela, N.; Bharath, S.; Duffy, S.; Avery, V. M.; Möhrle,
815 J. J.; Guy, R. K.; Wells, T., Repositioning: the fast track to new anti-malarial medicines? (2014) Malar.
816 J. **13**, 143-143.
- 817 53. Wells, T. N. C.; van Huijsduijnen, R. H.; Van Voorhis, W. C., Malaria medicines: a glass half full?
818 (2015) Nat. Rev. Drug. Discov. **14** (6), 424-442.
- 819 54. Harrigan, J. A.; Jacq, X.; Martin, N. M.; Jackson, S. P., Deubiquitylating enzymes and drug
820 discovery: emerging opportunities. (2017) Nat. Rev. Drug. Discov. **17**, 57.
- 821 55. Janse, C. J.; Franke-Fayard, B.; Mair, G. R.; Ramesar, J.; Thiel, C.; Engelmann, S.; Matuschewski, K.;
822 Gemert, G. J. v.; Sauerwein, R. W.; Waters, A. P., High efficiency transfection of *Plasmodium berghei*
823 facilitates novel selection procedures. (2006) Mol. Biochem. Parasitol. **145** (1), 60-70.
- 824 56. Mair, G. R.; Lasonder, E.; Garver, L. S.; Franke-Fayard, B. M. D.; Carret, C. K.; Wiegant, J. C. A. G.;
825 Dirks, R. W.; Dimopoulos, G.; Janse, C. J.; Waters, A. P., Universal Features of Post-Transcriptional
826 Gene Regulation Are Critical for *Plasmodium* Zygote Development. (2010) PLoS Pathog. **6** (2),
827 e1000767.
- 828 57. Cromer, D.; Evans, K. J.; Schofield, L.; Davenport, M. P., Preferential invasion of reticulocytes
829 during late-stage *Plasmodium berghei* infection accounts for reduced circulating reticulocyte levels.
830 (2006) Int. J. Parasitol. **36** (13), 1389-1397.
- 831

58. Philip, N.; Orr, R.; Waters, A. P., Transfection of rodent malaria parasites. (2013) *Methods Mol. Biol.* **923**, 99-125.
59. Lambros, C.; Vanderberg, J. P., Synchronization of *Plasmodium falciparum* erythrocytic stages in culture. (1979) *J. Parasitol.* **65** (3), 418-20.
60. Fivelman, Q. L.; Adagu, I. S.; Warhurst, D. C., Modified fixed-ratio isobologram method for studying in vitro interactions between atovaquone and proguanil or dihydroartemisinin against drug-resistant strains of *Plasmodium falciparum*. (2004) *Antimicrob. Agents Chemother.* **48** (11), 4097-102.
61. Odds, F. C., Synergy, antagonism, and what the chequerboard puts between them. (2003) *J. Antimicrob. Chemother.* **52** (1), 1-1.
62. Vega-Rodríguez, J.; Pastrana-Mena, R.; Crespo-Lladó, K. N.; Ortiz, J. G.; Ferrer-Rodríguez, I.; Serrano, A. E., Implications of Glutathione Levels in the *Plasmodium berghei* Response to Chloroquine and Artemisinin. (2015) *PLoS ONE* **10** (5), e0128212.
63. Boampong, J. N.; Ameyaw, E. O.; Aboagye, B.; Asare, K.; Kyei, S.; Donfack, J. H.; Woode, E., The Curative and Prophylactic Effects of Xylopic Acid on *Plasmodium berghei* Infection in Mice. (2013) *J. Parasitol. Res.* **2013**, 356107.
64. Altun, M.; Kramer, H. B.; Willems, L. I.; McDermott, J. L.; Leach, C. A.; Goldenberg, S. J.; Kumar, K. G.; Konietzny, R.; Fischer, R.; Kogan, E.; Mackeen, M. M.; McGouran, J.; Khoronenkova, S. V.; Parsons, J. L.; Dianov, G. L.; Nicholson, B.; Kessler, B. M., Activity-based chemical proteomics accelerates inhibitor development for deubiquitylating enzymes. (2011) *Chem. Biol.* **18** (11), 1401-12.
65. Kapuria, V.; Peterson, L. F.; Fang, D.; Bornmann, W. G.; Talpaz, M.; Donato, N. J., Deubiquitinase inhibition by small-molecule WP1130 triggers aggresome formation and tumor cell apoptosis. (2010) *Cancer Res.* **70** (22), 9265-76.
66. Cooper, E. M.; Cutcliffe, C.; Kristiansen, T. Z.; Pandey, A.; Pickart, C. M.; Cohen, R. E., K63-specific deubiquitination by two JAMM/MPN+ complexes: BRISC-associated Brcc36 and proteasomal Poh1. (2009) *EMBO J.* **28** (6), 621-31.

Table and figure legends

Table 1: *In vitro* activity of DUB inhibitors in rodent and human malaria parasites. IC₅₀ values and error bars are means and standard deviations from at least 3 independent repeats.

Figure 1: *In vitro* interaction of different classes of DUB inhibitors in malaria parasites. Isobologram interaction plots and Σ FIC₅₀ values of interactions between DUB inhibitors in the PF 3D7 line. **A.** Interaction between b-AP15 and WP1130 and their raw Σ FIC₅₀ values. **B.** Interaction between b-AP15 and PR-619 and their raw Σ FIC₅₀ values. Σ FIC₅₀ values, plotted FIC₅₀s and error bars are means and standard deviations from three biological repeats.

Figure 2: *In vitro* potentiation of DHA by DUB inhibitors. **A, B.** Dose response profiles and IC₅₀ values of DHA in the presence of b-AP15 at IC₅₀ equivalent concentration (DHA δ) in the PB 820 line (**A**) and 3D7 line (**B**). **C.** Dose response profiles and IC₅₀ values of DHA in the presence of WP1130 and PR-619 at their respective half IC₅₀s (DHA $\alpha+\beta$) in the 3D7 line. **D, E.** Dose response profiles and IC₅₀ values of DHA in combination with b-AP15, WP1130 and PR-619 at half IC₅₀ (DHA $\alpha+\beta+\gamma$) in the 3D7 (**D**) and 820 line (**E**). **F** Dose response profiles and IC₅₀ values of DHA combined with b-AP15 and WP1130 at IC₅₀ (DHA δ , DHA ϵ) or b-AP15, WP1130 and PR-619 at half IC₅₀ (DHA $\alpha+\beta+\gamma$) in ART resistant Kelch13 C580Y mutant line. Dose response curves were plotted in Graph pad prism 7. Error bars are standard deviations from 3 independent biological repeats. Isobologram plots of DHA in combination with b-AP15 and WP1130 at 3:2 (**G**), 1:4 (**H**) and 2:3 (**I**) ratios and their raw Σ FIC₅₀ values. Σ FIC₅₀ values, plotted FIC₅₀s and error bars are means and standard deviations from three biological repeats.

Figure 3: A combination of DUB and 20s proteasome inhibitor improves synergy with DHA. **A-C.** Isobologram interaction between epoxomicin and DHA (**A**), b-AP15 and epoxomicin (**B**) and a mixture of b-AP15 and epoxomicin at 1:1 molar concentration ratio in combination with DHA (**C**). Σ FIC₅₀ values, plotted FIC₅₀s and error bars are means and standard deviations from three biological repeats. **D.** Illustrated figure of the UPS indicating positional scope of USP14 and 20s units of the UPS and the inhibitor targets.

Figure 4: pre-exposure of malaria parasites to UPS inhibitors alone or in combination enhances DHA action. **A** pre-treatment of the PB 507 line (1.5 hours old rings) with b-AP15 at IC₅₀ (1.5 μ M) for 3 hours followed by a wash and then DHA for another 3 hours. Median GFP intensity quantified by flow cytometry at 6 hours, 18hours and 24 hours. b-AP15 at IC₅₀ readDED after DHA wash off in one experimental condition (green plot) while b-AP15 alone used as an additional control. Results are

representative of three independent experiments. **B.** DHA dose response viability plots and lethal dose (LD₅₀) comparisons at 66 hours after pre-exposure of 0-3 hours old rings of the 3D7 line to DMSO (0.1%) or b-AP15 at half IC₅₀ (0.75µM), IC₅₀ (1.5µM) or 4X IC₅₀ (6µM) followed by DHA for 4 hours. **C, D.** DHA dose response viability plots and lethal dose (LD₅₀) comparisons at 66 hours after pre-exposure of 0-3 hours old rings of the 3D7 line (**C**) and ART resistant Kelch-13 C580Y line (**D**) to DMSO (0.1%) or epoxomicin at 0.2x IC₅₀ (2nM), IC₅₀ (12nM) or a combination of b-AP15 and epoxomicin at half IC₅₀ followed by DHA for 4 hours. Data from three independent experimental repeats. Significant differences between the conditions were calculated using one-way ANOVA alongside the Dunnet's multiple comparison test. Significance is indicated with asterisks; ****p < 0.0001.

Figure 5: *In vivo* activity of b-AP15 alone and or in combination with ART. **A** Mice (4 groups of 3 mice each) were infected with 10⁵ parasites on day 1 and treated with indicated drug doses ~1 hour post infection for four consecutive days (indicated by arrows). Parasitaemia was monitored daily by flow cytometry and analysis of Giemsa stained smears. **B, C.** Percentage suppressions on day 4 (**B**) and bar of parasitaemias on day 4 and day 5 (**C**). **D, E.** Combination of ART and b-AP15 in established mouse infections. ART at 5mg/kg (**D**) or 10mg/kg (**E**) combined with b-AP15 (1mg/kg) administered in established mice infections at a parasitaemia of 2-2.5% for three consecutive days (indicated by arrows). Parasitaemia was monitored daily. ART at 20mg/kg was used as a curative control. Significant differences were calculated using one-way ANOVA alongside the Dunnet's multiple comparison test. Significance is indicated with asterisks; *p < 0.05, **p < 0.01, ***p < 0.001, ****p < 0.0001.

938 **List of tables and figures**

939 **Table 1**

940

Inhibitor	Predicted UPS target	IC ₅₀	
		PB 820	PF 3D7
Artemisinin	-	17.23±0.4nM	6.50±0.4nM
Dihydroartemisinin	-	13.89±0.1nM	6.23±0.34nM
Epoxomicin	20s proteasome	14.20±3.0nM	11.12±0.23nM
PR-619	broad spectrum DUB inhibitor ^a	3.30±2.0μM	2.41±0.5μM
P5091	USP7 and USP47 DUBs ^b	8.38±2.10μM	Not done
TCID	UCH-L3 and UCH-L1 DUBs ^c	>100μM	>100μM
WP1130	UCH-L1, USP9X, USP14, UCH37 DUBs ^d	1.19±1.0μM	2.92±0.1μM
b-AP15	USP14 and UCH-L5 DUBs ^e	1.06±0.9μM	1.55±0.1μM
NSC-632839	USP2, USP7, SENP2 DUBs ^f	27.97±0.8μM	Not done
1,10 phenanthroline	Metalloproteases and JAMM isopeptidases ^g	0.63±0.3μM	Not done

941

942 a, ⁶⁴ b, ³³ c, ⁴² d, ⁶⁵ e, ³⁴ f, ³⁵ g. ⁶⁶

943

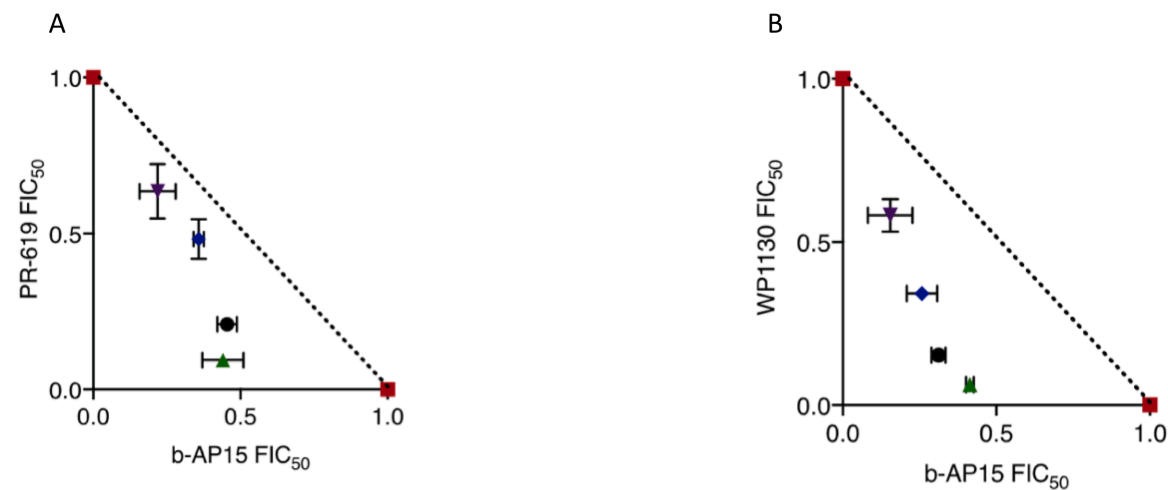
944

945

946

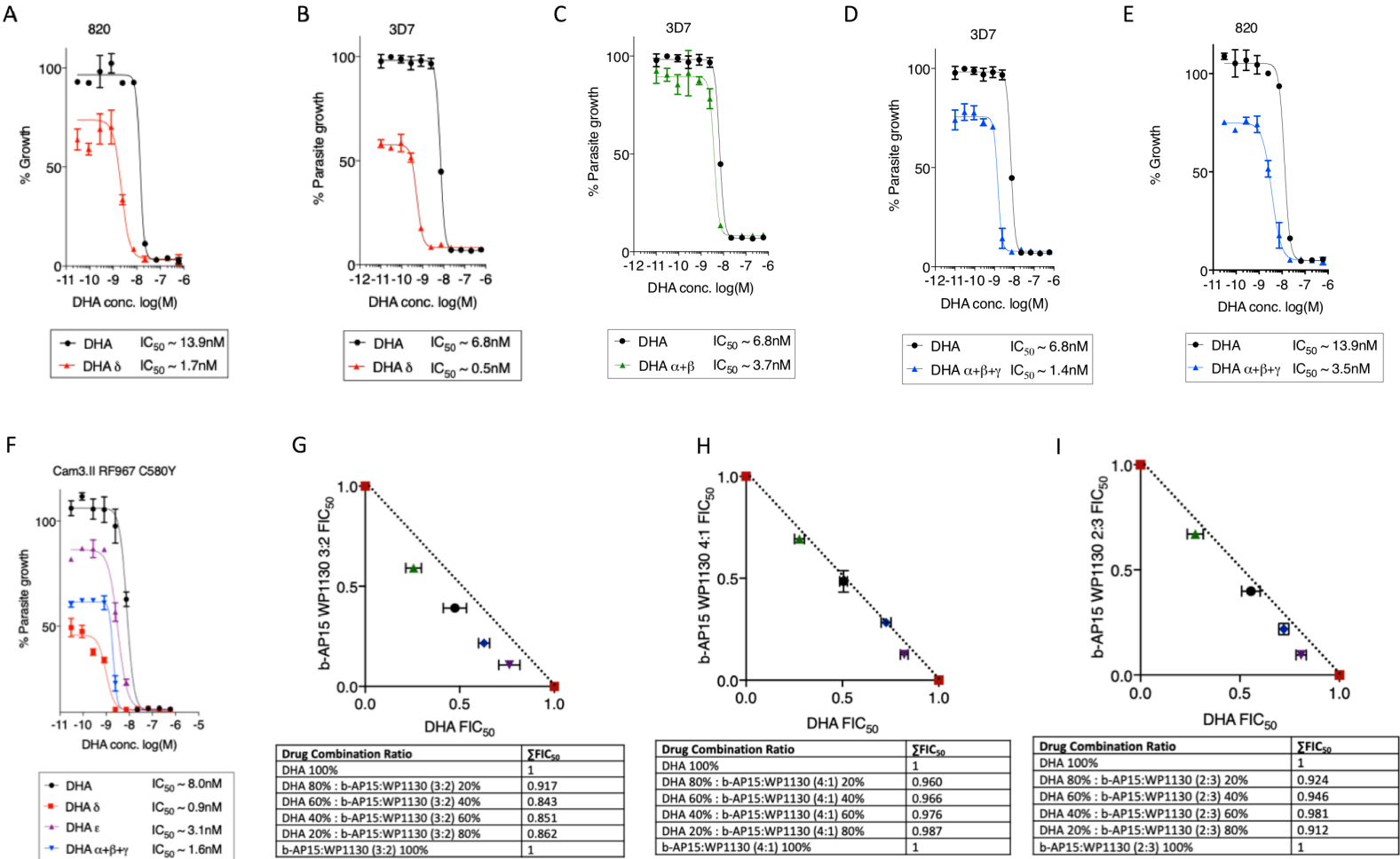
947

Figure 1

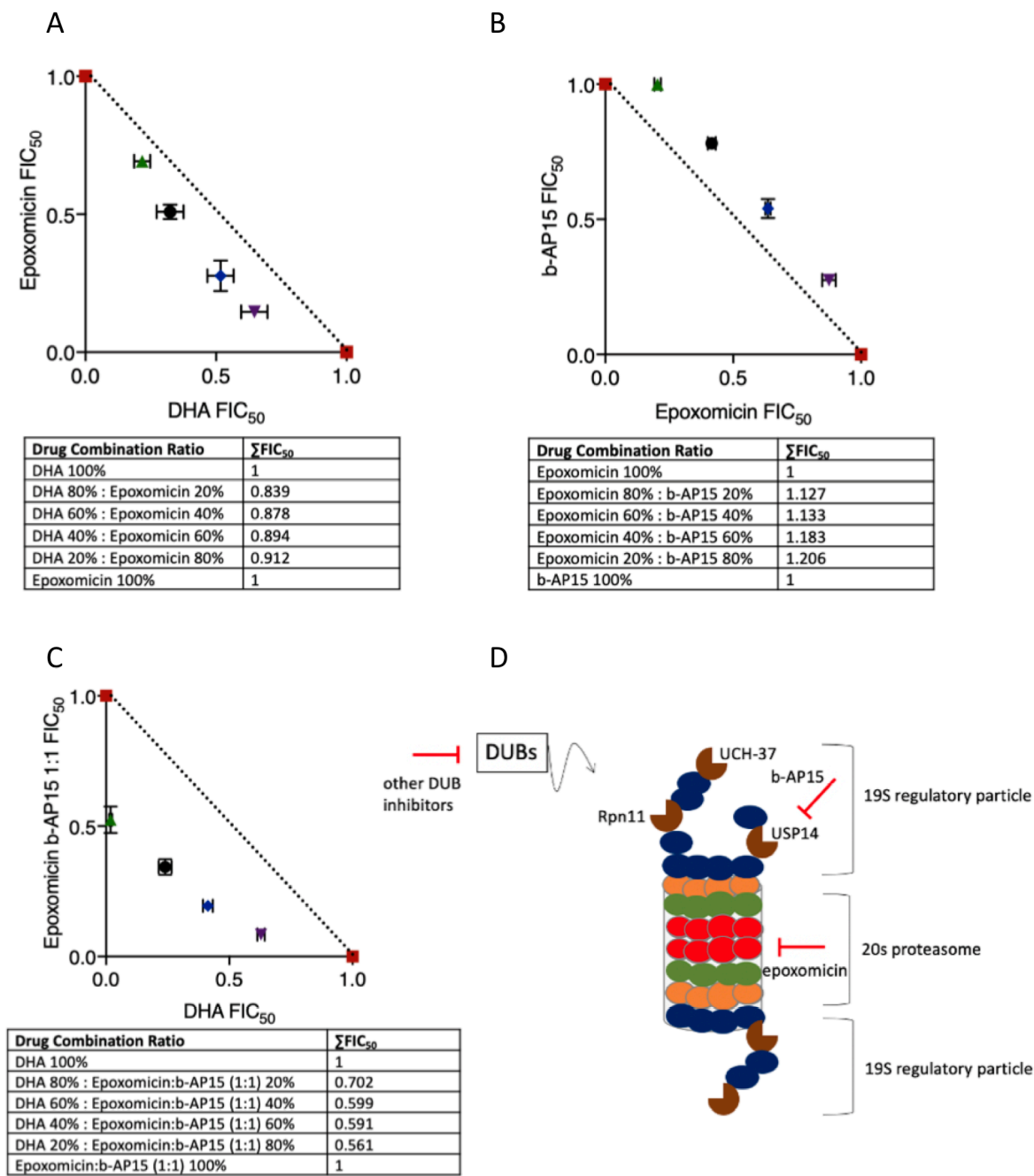


Drug Combination Ratio	ΣFIC_{50}
b-AP15 100%	1
b-AP15 80% : PR-619 20%	0.623
b-AP15 60% : PR-619 40%	0.712
b-AP15 40% : PR-619 60%	0.731
b-AP15 20% : PR-619 80%	0.896
PR-619 100%	1

Drug Combination Ratio	ΣFIC_{50}
b-AP15 100%	1
b-AP15 80% : WP1130 20%	0.478
b-AP15 60% : WP1130 40%	0.472
b-AP15 40% : WP1130 60%	0.656
b-AP15 20% : WP1130 80%	0.870
WP1130 100%	1



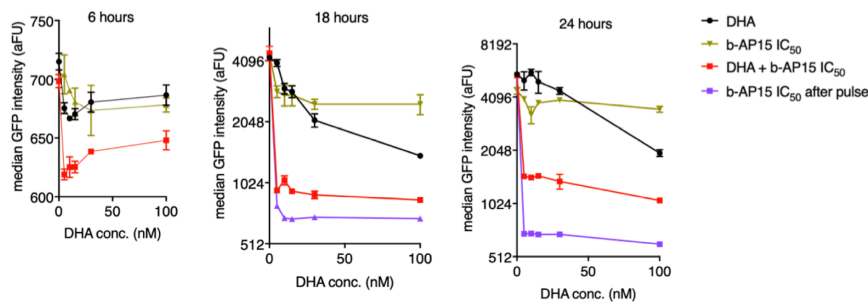
969 **Figure 3**



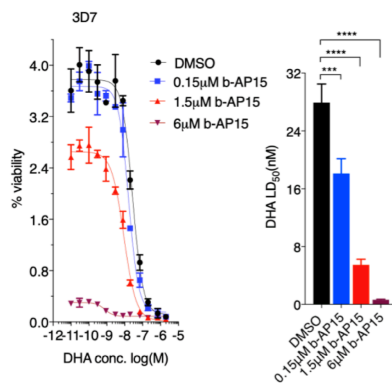
970
971
972
973
974
975
976
977

Figure 4

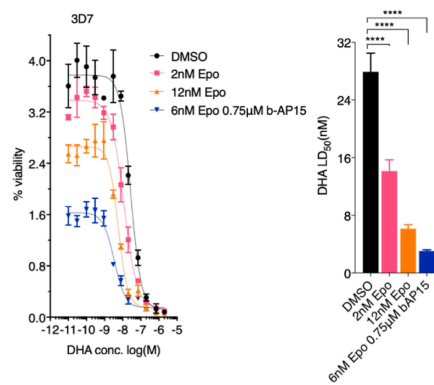
A



B



C



D

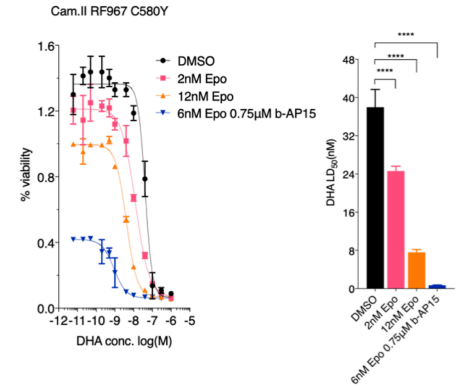


Figure 5

